

AD-A145 288

DTIC ACCESSION NUMBER

LEVEL

PHOTOGRAPH THIS SHEET

INVENTORY

Proceedings of the Seventh International Pyrotechnics Seminar of
14-18 July 1980, Volume 1

DOCUMENT IDENTIFICATION

DISTRIBUTION STATEMENT A

Approved for public release
Distribution Unlimited

DISTRIBUTION STATEMENT

ACCESSION FOR

NTIS GRA&I ☒

DTIC TAB ☐

UNANNOUNCED ☐

JUSTIFICATION

BY

DISTRIBUTION /

AVAILABILITY CODES

DIST

AVAIL AND/OR SPECIAL

A/1

DISTRIBUTION STAMP

DTIC
ELECTE
SEP 4 1984
D

DATE ACCESSIONED

DATE RETURNED

84 08 28 040

DATE RECEIVED IN DTIC

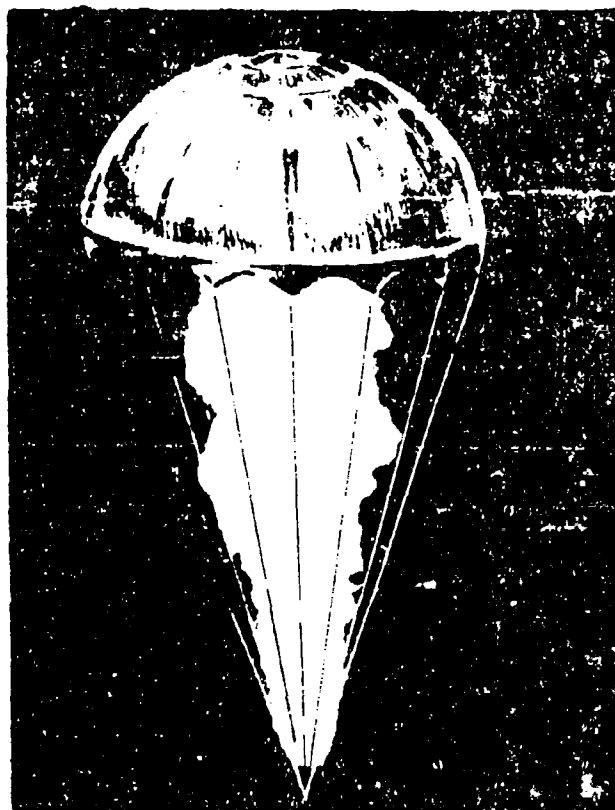
REGISTERED OR CERTIFIED NO.

PHOTOGRAPH THIS SHEET AND RETURN TO DTIC-DDAC

AD-A145 288

SEVENTH INTERNATIONAL PYROTECHNICS SEMINAR

VOLUME 1



Approved for Public Release;
Distribution Unlimited

THE LODGE AT VAIL
VAIL, COLORADO
14-19 JULY 1980

HOSTED BY
IIT RESEARCH INSTITUTE

**PROCEEDINGS
OF THE
SEVENTH INTERNATIONAL PYROTECHNICS SEMINAR**

14-18 JULY 1980

VOLUME I

STEERING COMMITTEE

**A. J. Tulis, IITRI
CHAIRMAN**

**R. M. Blunt, DRI
Chairman Emeritus**

D. H. Anderson, Sandia

D. R. Dillehay, Thiokol

B. E. Douda, NWSC

**Approved for Public Release;
Distribution Unlimited**

**IIT RESEARCH INSTITUTE
CHICAGO, ILLINOIS
60616**

Earlier Proceedings: (1) AD-679911;
(2) AD-913407; (3) AD-913408; (4) AD-A057599;
(5) AD-A087513; (6) AD-A063797.

SEVENTH SEMINAR PROCEEDINGS

Preface

This Seminar, the seventh of this biennial series to be held in the United States, continues the trend of more papers, more participants, and greater breadth of representation internationally. These Proceedings include 18 papers from 9 countries outside the US, and it appears that about 16 countries will be represented at this Seminar. This is especially encouraging at this time when we have just founded the International Pyrotechnics Society. A copy of the Constitution and By-laws of this Society is included in this Proceedings, as well as an application for membership. Please look these over and let us have your input in the form of advice, suggestions, and hopefully your participation and support by way of membership. There will be an open forum for discussion regarding this Society at this Seminar.

As most of you know, Bob Blunt has yielded the reigns of these seminars after six continuously more successful efforts. His talents have been put to good use, however, as it has been mostly his effort that has resulted in the founding of the International Pyrotechnics Society. We can be certain that Bob will remain in the forefront of pyrotechnic activity for many years to come.

We now have a Steering Committee to assure that these seminars will continue to provide the international pyrotechnics community with a forum for the interchange of technology and developments in this important area of science and engineering. As Chairman of this Steering Committee it is my desire and obligation to continue these seminars in the spirit that they were conceived, but this can only result from the continued interest and participation of the pyrotechnics community at large. I am therefore most grateful to you, the attendees, and especially to you, the authors, for making this Seminar the success it is anticipated to be. I also wish to express thanks to my fellow committee members and to the Session Chairmen for their efforts for this Seminar.

At this Seminar, for the first time we have scheduled a Poster Session. We hope that you find this alternative form of presenting new technology a refreshing experience. Please let us have your comments.

Regarding these Proceedings, it has finally become necessary to split them into two volumes. If we should need three volumes in 1982 we would gladly accommodate you. Please continue your support, particularly with the submission of papers.

Finally, I wish to thank Dr. H. Rosenwasser on behalf of the Naval Air Systems Command for their interest and support. The Navy, particularly the Naval Weapons Support Center at Crane, Indiana, spearheaded by Dr. Bernie Douda, has provided both moral and direct support in the way of attendance and papers contributions to these seminars from their inception, and in no small way has been responsible for their success.

Allen J. Tulis
Chairman
Steering Committee
International Pyrotechnics Seminars

TABLE OF CONTENTS

Volume 1

<u>Paper</u>		<u>Page</u>
69	KEYNOTE ADDRESS: --- Thoughts on Pyrotechnics. . . . <i>R. M. Blunt</i>	1
2	The Design of Progressively Burning Pyrotechnic Formulations <i>J. L. Austing and P. W. Cooper</i>	13
3	Glass Ceramics for Explosive Device Headers. <i>C. F. Ballard, R. J. Eagan and E. A. Kjeldgaard</i>	32
4	Studies of Factors Affecting Tracer Performance. . . <i>T. J. Barton and M. J. Bibby</i>	51
5	Insensitive Conducting Composition Igniters. <i>J. R. Bentley</i>	64
10	Disposal of Colored Flare Compositions <i>S. C. Chattoraj, T. A. Drehoel and C. W. Gilliam</i>	73
11	Transient Thermal Testing of an Electroexplosive Bridgewire Detonator <i>N. Chretien, C. Kassel and M. Duigou</i>	94
12	Thermal and Electrostatic Initiation of TiH_x Based Pyrotechnics <i>L. W. Collins</i>	107
14	Gauging with Penetrating Radiation for Nondestructive Testing of Pyrotechnics. <i>D. G. Costello, H. R. Lukens, L. A. Parks and A. P. Trippe</i>	118
15	Illegal Manufacture and Use of Pyrotechnics. <i>A. L. Cunn</i>	130
16	A Microcomputer System for Flare Test Analysis . . . <i>D. R. Dillehay</i>	138
17	RP Smoke Performance Modeling Using a Microcomputer. <i>D. R. Dillehay</i>	147
20	Blast Overpressures for Confined Explosions. <i>G. F. Kinney, R. G. S. Sewell and K. J. Graham</i>	153
22	Solutions for Resistance-After-Fire Problems in an Electric Match <i>A. A. Heckes and A. P. Montoya</i>	178
23	Instantaneous Smoke Screening System <i>K. O. Jacobsen</i>	193

TABLE OF CONTENTS (cont.)

Volume I

<u>Paper</u>		<u>Page</u>
24	Response of Pyrotechnic to Gaseous Discharges with the JGY-50 Electrostatic Sensitivity Tester <i>H. Kaodi</i>	201
25	Characterization Tests for Pyrotechnic Ignition and Ignition Transfer <i>R. Kelley, G. Lindsley, and N. R. Williams</i>	214
26	Hexanitrostilbene (HNS): Review of Shielded Mild Detonating Cord (SHDC) Performance Under Biased Conditions of Fabrication. <i>E. E. Kilmer</i>	233
28	Energy Output of Different Pyrotechnic Igniter Systems. <i>G. Klingenberg</i>	252
29	Use of a Jet Air Mixer for Pyrotechnic Compositions . <i>D. M. Koger</i>	274
30	Synthesis of Stable Pyrotechnic Compositions After Investigation by Calorimetric Procedures. <i>G. Krassoulia</i>	286
31	Shock Compaction of a Porous Pyrotechnic Material . . <i>L. M. Lee and A. C. Schwarz</i>	304
32	Status of Development of 2-(5-Cyanotetrazolato) Pentaamminecobalt(III) Perchlorate for DDT Devices . . . <i>M. L. Liberman and J. W. Fronabarger</i>	322
33	Visar Studies of a Reefing Line Cutter. <i>M. L. Lieberman and R. S. Wilson</i>	356
34	Certification Test for the Fluid Bed Spray Granulation Process for the Production of Colored Smoke Mixtures <i>F. L. McIntyre</i>	373
35	Flamespread Propagation Rates of Various Black Powders Using the PCRL-Flamespread Tester. <i>H. A. Messina, L. S. Ingram, M. Summerfield, and J. C. Allen</i>	388
36	Role of Surface Chemistry in the Ignition of Pyrotechnic Materials <i>W. E. Moddeman, L. W. Collins, P. S. Wang, and T. N. Wittberg</i>	408
37	Power Independent Ignition Energy Measurements. . . . <i>J. Mohler</i>	425

TABLE OF CONTENTS (cont.)

Volume 1

<u>Paper</u>		<u>Page</u>
39	Thermal Profile and Reaction Characterization - Computations and Experiments. <i>M. R. Birnbaum, C. T. Oien, C. L. Yang and A. C. Munger</i>	436
40	Electrothermal Response Testing, A Component Development Tool. <i>A. C. Munger</i>	461

Keynote Address

THOUGHTS ON PYROTECHNICS

by

Robert M. Blunt

Denver Research Institute
University of Denver
Denver, Colorado 80210

Thoughts on Pyrotechnics

Pyrotechnics is a fascinating subject for research because it sooner or later requires the investigator to apply most of the analytical tools that are available. Of course, one shouldn't overlook the appeal to the boy's love of noise and excitement that is present in much of our experimental work, whether we admit it or not. In addition to providing us with challenging problems and exciting experiments, pyro, in many cases, has afforded the only practical way to achieve the result that is desired. A special expertise is needed for the solution of the problems associated with these practical applications and the expert pyrotechnist appears to have become one of the "endangered species" in recent years. I hope the thoughts which I have presented in this paper may help to avoid his extinction. If they have any claim to merit, it is due to the people who have been my colleagues during forty years in ordnance research, which has included terminal ballistic effects, phenomena due to the detonation of explosives, missile destruct systems and incendiary ammunition functioning.

Much of my more recent experience has been with pyrotechnics, - to me, the most fascinating area of all ordnance research. In preparing this talk, I read several definitions of pyrotechnics, and would like to present them to you along with one of my own. It appears to be difficult to create a precise definition and I think it is important that we have a good one. I believe a clear definition of pyrotechnics to be a basic need if we are to attract the financial support that is needed for the conduct of research and development studies, studies that will increase our ability to design items which will function as expected, without relying so heavily on experience and testing to achieve the desired results.

After some comments on this matter of a definition of pyrotechnics, I will first discuss what I believe are some of the basic research areas on which attention should be focused, second, what I call the "image problem" of pyrotechnics and, in conclusion, the formation of an International Pyrotechnic Society.

First, let me present some definitions of pyrotechnics by the authors of several books on this subject. Brauer, in his "Handbook of Pyrotechnics", states that "Pyrotechnic means explosive devices in which explosives are burned rather than detonated". I find this definition too restricted and unimaginative because it lumps all kinds of pyrotechnics together in the category of explosives. I did not find a definition of pyrotechnics in the work by the Reverend Ronald Lancaster; the excellent quality of his work led me to ask the Reverend for his definition, which he very kindly furnished: "Explosives are reactions which perform at the highest speed and leave gaseous products. Propellants are similar to explosives, but somewhat slower. Pyrotechnics are reactions between two or more solids which produce flame or glow and which leave solid residues and gaseous products."

While Weingart does not specifically define pyrotechnics, he implies that it is the art and craft of utilizing chemical decomposition, particularly those reactions which occur at rates that produce burning or explosion. He specifically excludes detonations, except in rare cases.

Cackett in his monograph says, "Broadly speaking, pyrotechnics are employed to produce light ---, to produce smoke ---, to produce fire and incendiary effects, to measure intervals of time. They may also be required to function as propellants, igniters, and primers etc.," Although this is rather lengthy and, perhaps, more a description than a definition, I find it is close to the mark.

Shidlovsky has defined pyrotechnics as "--- the science concerning methods of production of pyrotechnic compositions and products, and of their properties". This is a circular definition, to be sure, but he goes on to say what is meant by "pyrotechnic compositions". "Pyrotechnic compositions, when ignited (or exploded), give illuminating, thermal, smoke, sound or reactive (jet) effects ---".

Ellern's definition follows a two page discussion of pyrotechnics in his treatise on Military and Civilian Pyrotechnics. He states, "Pyrotechnics is the art and science of creating and utilizing the heat effects and products from exothermically reacting, predominately solid mixtures or compounds when the reaction is, with some exceptions, non-explosive and relatively slow, self-sustaining and self-contained." A very good definition, but a bit long.

Webster's Dictionary, widely accepted as a reliable source of definitions, say "the art of making, or the manufacture and use of fireworks". This surely is an understatement and oversimplification, which is of little help. One must seek the definition of fireworks, and finds this: "Firework; a device for producing a striking display (as of light, noise, smoke) by the combustion of explosive or flammable compositions especially for exhibition, signalling or illumination, typically consisting of a paper case containing combustible material ---".

Brock provides no definition as such, although he traces the history of pyrotechnics in a most interesting presentation.

I have presented these authorities' definitions to illustrate the difficulty of arriving at a precise definition, which is evident in the variation among these. The best that can be done, I think, is to try to frame a definition that is acceptable to most pyrotechnists and that is basic enough to encompass all of the great variety of applications served by pyrotechnics. I have been rash enough to attempt this and to offer it for your consideration.

"Pyrotechnics: The science of controlled exothermic chemical reactions which are used to create timing devices, sound effects, aerosol dispersions, high pressure gas, intense heat, electromagnetic radiation, or combinations of these, and produce the maximum effect from the least volume. High explosives are excluded, but initiators are included". Your comments and improvements on this definition will be welcomed.

Next, I would like to present to you the areas of research which I believe should be pursued most assiduously. It seems that the materials of pyrotechnics have always been regarded with suspicion, fear and some awe by the general public, from the times of the alchemist in the Middle Ages until now. Knowledge of the applications of these materials in pyrotechnic devices has been restricted to a few people, and today we see the solution of production problems in military pyrotechnics hampered by the restrictions of "Security Classification", and the production of display fireworks a closely held commercial secret. As a consequence, much useful research that could be performed in university laboratories is not done, because university personnel must publish their results in the open technical literature. Besides the loss of basic information for the pyrotechnist which follows from this lack of attention, another result is the general lack of knowledge concerning pyrotechnics that prevails among those who have no experience with it. My esteemed colleagues in the chemistry and physics departments of my own university have, on occasion, referred very disparagingly to it as "dirty research" - whatever that is - or as "Oh, you mean fireworks", or "that's kid stuff". Furthermore, most university professors are unaware that many thesis subjects suitable for students who seek advanced degrees can be found in the problems now facing pyrotechnics, e.g., theses of Doua and Chazal. The advancement of pyrotechnics as a science is slowed because these subjects are not being investigated; consequently, badly needed research is not done with any plan or logic. If it is done at all, it is usually a result of the need to solve an immediate problem and not to lay a broad foundation for the future.

Why do I discuss all of this? Because I believe that today pyrotechnics is at a point of decision. If it is to grow and be recognized as one of the major subdivisions of science and engineering, to be considered on an equal footing with specialities such as perfume or polymer chemistry or explosive forming, a change in its image must be achieved. Otherwise it will continue to limp along as part black art and part experience, plus a little science. Furthermore, I think a change in the way pyrotechnics is perceived by the military is essential for its survival in the future. So long as black powder rockets could be fired a few hundred meters to terrify the enemy, or to set his haystacks on fire, the technical demands made of the pyrotechnist were rather modest. Until WW I, the demands of the military on the pyrotechnists' skills were simple; reasonably pedestrian chemistry or physics served him quite adequately and the raw materials and processing that were needed were relatively easy to obtain as standard items of commerce. That time has passed. Although the complexity of pyrotechnic devices has increased greatly in response to the growing difficulty of the problems for which they provide solutions, our understanding of the fundamental processes of pyrotechnic systems does not appear to have kept up with these demands. It is relatively easy to create a red signal flare, but it is very difficult to create an infrared decoy flare that satisfies all of the requirements of storage, safety and effectiveness as a decoy for a guided missile designed to seek the hot regions of a target. It is no longer sufficient for the pyrotechnist to mix saltpeter,

sulfur and antimony sulfide with some gum arabic solution to produce a "white" signal flare. Today, he must understand spectroscopy of the combustion process well enough to identify the emitters that create a green flame when certain mixtures which contain barium are burned and the effect of flame temperature on the purity of the color. He must understand physics and physiology well enough to compute the color purity of the green flame, and physical chemistry if he is to improve it. But this kind of information would never have been obtained by the empirical methods which characterized pyro up to about 1940, and which are still used in many cases. Information of this sort is obtained only by careful laboratory work, guided by the best available theory and the latest techniques of physical chemistry; these requirements are frequently best satisfied in the laboratories and graduate study programs of our universities. It is just this kind of study, as I mentioned earlier, that can be done as thesis research for advanced degrees - but it is very rarely done. Sometimes it is done as a part of a practical study which has some important and immediate objective that can be more quickly achieved by applying the results of a directed research study. This is usually a small ancillary research study, which generally results in supplying only one more bit of data - not the broad data base that would be a firm foundation for future problem solving. Useful, of course, but far from adequate; worse; it may very likely be available to very few persons because of publication restrictions which are usually placed on studies conducted with government funds whether they are performed at a university or a government laboratory. I am not aware of any research that is funded by the display fireworks industry, but if it exists, I'm sure that in most cases the results are kept for the sole benefit of the sponsor. As a consequence of these government and commercial restrictions, the science and technology of pyro progress very slowly. I am suggesting that there are research studies that should be done because they are of interest to everyone who is involved in pyrotechnic manufacture. The areas I believe to contain these fundamental problems of pyrotechnics which should be the subject of a continuing research program are: (1) properties of materials, (2) reaction processes, (3) flame structure. In addition, there are two areas of common need and interest which require data from laboratory investigations, and sometimes some specific testing, but which are not usually included as research subjects. These are: (4) standards and (5) safety. Finally, to support these there is a requirement for (6) formalized special education and (7) a recognized technical society to help focus our efforts.

In the materials category, I believe there is a need for research that will first define the properties which are of interest specifically for pyrotechnic uses, that is, to determine what must be quality-controlled to achieve reproducible behavior when the materials, including those used for containment, binders or sealants etc., are used for pyrotechnics. I believe this task has not received the attention it should and that it has only begun. If studies of material properties had received adequate attention and support, the matter of consistently manufacturing black powder to perform the same way in all of its applications probably would have been solved long ago, and it could be bought from any supplier anywhere, with complete confidence in its performance in the device in which it is used. Such is not the case. Neither would the manufacture of delay trains be up at by a change in the source of,

say, tungsten powder. You can surely add many examples of your own. The point of all this is simply that we do not understand the materials and the reactions of pyrotechnic compositions well enough to write good specifications for the quality control of the basic ingredients. Perhaps we can never accurately specify the quality of every ingredient, but a good research program would certainly improve many specifications and, probably, lower material costs. The specification of "Chemically pure" or "Reagent grade" material is often simply an indicator that the user is ignorant of the impurities that are really important for his purpose and he therefore takes the costly approach of minimizing every impurity.

Reaction processes are closely connected with some material properties, for example, melting and boiling points. In addition they define specific stages in reactions that must be understood before an accurate and useful model can be constructed for the purpose of predicting the changes in performance which follow changes in formulation or assembly of pyrotechnic items. As an example, consider an illuminating composition of magnesium, sodium nitrate and a binder. It is customary to speak of stoichiometric compositions of the components and to estimate the radiant output as though the combustion reactions were all proceeding in the gaseous, or at least in the liquid, phase. This is not usually the case and it leads to some highly erroneous estimates of the radiant output. If combustion really were proceeding from a stoichiometric basis, the composition of the ambient atmosphere would have no effect on the radiance of the flame. In fact, it does have an effect. When the ambient air is replaced by an inert gas, such as argon, the output may be reduced by a factor of one hundred or more. Examination of high speed motion pictures of the burning surface of the flare helps to explain this by showing what a moments' thought would predict. Even though the solid ingredients are indeed present in the proportions computed from some assumed reaction equation, they cannot react stoichiometrically because the nitrate melts and surrounds the magnesium particles, which are still solid. What is the concentration of fuel and oxidizer at this interface? What is the real oxidizer --- nitric oxide, nitrous oxide, or something else? No one knows, yet it is certainly of crucial importance to the progress of this combustion reaction. It is reaction processes in this sense that I believe should receive serious attention in a continuing pyro research program. The luminous output of the flame from this reaction is due mainly to excited sodium atoms and any process that quenches them will reduce the luminosity. Therefore, one must also include consideration of atomic processes of this nature in a good model of flame reactions.

The structure of pyrotechnic flames is of great importance to the manufacture of incendiaries, initiators, illuminating/signal/decoy flares, yet it is almost completely unknown. I will define flame structure in the context of this paper as the chemical and physical composition and the extent of the flame; that is, the spatial distribution and the nature of the chemical species in the flame and the gas/particulate velocity and temperature at every point. Years ago efforts were made by the U.S. Air Force and are currently supported by the Navy to establish data bases on specific flames to obtain data that can be used to create a theory for the prediction of radiant output as the percentage composition and the physical size are varied. As far as I know there is no continuing

effort to obtain the data that will be required for the establishment of a general flame model of practical use to pyrotechnists. Many papers and books have been published on the structure and properties of flames - but there are very few on flames from pyrotechnics. By their nature, pyro flames are transient and full of particulates - dirty flames that may be almost opaque - and therefore not attractive subjects for research when there are much simpler and easier systems to study.

But if we are ever going to acquire the ability to predict with accuracy the static and dynamic radiance of a flare from its composition and construction, continuing studies of the flame structure produced by pyrotechnic devices are required to provide the data for a model, or models with which such predictions can be made. These studies are challenging to the theoretician because of the boundary conditions and extreme temperature and composition gradients to be modelled and the reactions that must be identified. The challenge to the experimenter is equally great because of the difficulties in measuring temperatures, species, concentrations and the spatial and temporal variations of these. Studies of this complexity will require the commitment of funds to a long term program; year-by-year studies cannot conquer the problem.

There are at least two kinds of standards required by the pyrotechnist. One is a standard of measurement, or testing, so that the results from different laboratories may be compared without the question arising "are the results truly different, or is the difference due to the measurement techniques?" An outstanding example of this need for standardization is the measurement of radiation. Radiation measurements in the range from ultraviolet through infrared are among the most difficult, even when the source is a nice cooperative one with an "infinite" lifetime, such as an electric lamp. Unfortunately, our pyrotechnic sources are usually transient, unstable, and generally frustrating to work with; nevertheless, the need for good, comparable radiation measurements is of great technical and economic importance. Although there are documents of a quasi-official nature (e.g., Parish & Dinerman) which attempt to state what the measurement conditions should be, they are of very limited authority and acceptance. Unfortunately, many times it becomes necessary for those of us who are quasi-competent to make these measurements. I'm afraid much disagreement in the results from different measurements is due to this quasi-competence and to people working without the help of the experts. This help is one of the essential parts that would have been incorporated into a detailed specification of the manner in which the radiation is to be measured. Much the same comment can be made concerning burning rates, frictional and electrostatic sensitivity, impact sensitivity, chromaticity, etc. It is necessary to come to an international agreement on the meaning of terms and the methods of measurement, and then to document the test methods in sufficient detail that even the quasi-competent worker can obtain results. Perhaps then it will be possible to settle many long-standing arguments as to which device is the best.

A second form of standard is the purchasing standard, or, as it is often called in the U.S., a "Mil Spec" - a military specification of quality. As I mentioned earlier, much money can be saved by knowing what elements of a specification must be closely controlled and which

need little control. At present, there doesn't seem to be any way to write accurate specifications for purchasing such simple things as elemental tungsten powder for use in delay trains, or sodium nitrate for illuminating flare compositions, simply because the reactions in which they are used are not well understood. Perhaps, when they are, standards can be written to insure that changes in the source of supply will not cause changes in the performance of any item in which the material is used. The problem is not entirely a technical one and, probably, national rather than international committees will have to write the specifications for each country because of the political and economic factors which are different in each country and affect the decision as much as purely technical factors. Although the standards really should be based solely on good engineering practice, sometimes it will be necessary to use alternate materials because they are preferred for political or economic reasons and the specifications must be able to accommodate these nontechnical requirements.

Safety should be based on an understanding of the fundamental mechanisms which are responsible for ignition, or the initiation of an explosion. Much work has been done on these subjects which, in conjunction with the increasing concern of both industry and government over loss of life and injury to personnel, has certainly resulted in much better safety regulations than were followed some years ago. However, we still depend heavily on precautions which are the result of experience rather than the predictions of a good theory - avoid sparks, whether mechanical or electrical, impact, friction etc. Our quantization of how much friction one must avoid, or how energetic an electric spark, is rather poor - by which I mean that it is variable from one laboratory to another and from one test to another. In other words, the experimental determination of these quantities would appear to be based on a very limited understanding of the true nature of the phenomena.

I think much of the variability can be removed by improved, standard test methods which are well defined and accepted for use in all pyro laboratories and factories. Some tests we ran to determine the sensitivity of various materials to ignition by an electric spark exemplify a rather bad test method. A spark passed from a pointed tungsten electrode though a thin layer of the powder to a flat steel plate; ignition was determined by the appearance of a flame. This is a standard test method

but great variability was found in the results. Some of the variability could be assigned to the effects of changes in the relative humidity of the air, which was not controlled. My own opinion is that the varying energy in the spark not only affected the energy available to ignite the powder but also affected the dispersion of the powder because of the changing intensity of the acoustic and thermal effects in the air around the spark. Watching the tests, some of these changes could be seen with the unaided eye; as the energy supplied to the spark increased, the size of the cloud of powder it created also increased, but the increase was greater for the less dense materials. The test is simple to perform, but I think without much value as a guide to the establishment of electrical safety regulations. At present, we must often rely on data from tests such as these that are designed to meet the needs of others, such as the coal mining industry and from tests that differ in their details when performed in different

laboratories. Good, meaningful standardized tests which give consistent results in every laboratory will greatly improve the protection that can be provided for workers and plant equipment engaged in the production of pyrotechnics. It should be the objective of on-going, well funded research studies to create such tests. I would expect these studies to be useful in achieving better ignition, as well as in their primary objective of preventing it. Uniformity of safety practices would be another result of general acceptance of good test methods, especially if some effort was put forth by a generally accepted body to draft the standards to be followed.

It may appear from these comments that I am not aware of the existence of a vast literature on combustion and, I am sure, there is indeed a great deal of it with which I am not familiar. However, the bulk of the papers on combustion I have seen do not deal with pyrotechnic subjects but with propellants, or explosives, or even more general combustion systems than these. For example, there is an interesting collection of papers edited by Ingo May that has been published by the U.S. Army Ballistic Research Laboratories on the subject of ignition. The papers were prepared in response to recognition of real-world problem areas which involve ignition in an attempt to fill basic information gaps and more efficiently solve problems. The general area of concern to which these papers were addressed was propellants. Some excellent research was reported in them, but it was done on propellant compositions, not on pyrotechnic compositions. Consequently, while the material presented and the experimental techniques that were used are of considerable general interest to pyrotechnists, there are few specifics that can be employed to improve the performance of pyrotechnic devices. We should certainly borrow as much as possible from our colleagues in explosives and propellants research, but that does not avoid the necessity of doing our own work. Since black powder is an important component in pyrotechnics as well as a propellant, I will paraphrase some of the comments Ingo May and Austin Barrows made in the introduction to their work on ignition. "Black powder remains one of the great examples of the triumph of art over science. It remains an important part of many ignition trains and yet the production of it is to a large extent a "black" art. The residue is quite a serious problem in some applications; other problems are the manufacture of it in safety and with reproducible characteristics. After hundreds of years of use, the chemical and physical properties of black powder are still not adequately characterized." Much the same comment would apply to pyrotechnics in general.

While pyrotechnics can borrow much from the work in other areas of combustion, the problems are still sufficiently unique to our field as to require solution by research directed specifically to that end. I believe that a formal course in pyrotechnics could go a long way toward providing solutions to these problems. It should be taught at a university and result in the granting of Masters or Doctoral degrees in Pyrotechnic Science and Engineering. At present one becomes a pyrotechnist by chance and usually with one of the engineering or scientific disciplines as background. The novice pyrotechnist is exposed to many hazards and may soon view essential experimentation as too dangerous when, in fact, it is not. On the other hand he may ignore real dangers and injure himself and others. He is also prone to "re-invent the wheel", because

he doesn't know the history of pyrotechnics. In contrast, a graduate with his degree in Pyrotechnic Science and Engineering would be competent, safe, knowledgeable, and capable of making useful contributions to the solutions of his employer's problem soon after his employment. If there were a course like this, it would do more than provide trained professionals; it would also result in recognition of Pyrotechnic Science and Engineering as an area of professional competence, just as chemical engineering or microbiology are recognized. It would then follow that studies which would be beneficial to pyro would become a fruitful source of material for graduate research problems and the resulting work on these would soon begin to provide answers to the problems of variable material properties, reaction processes and flame structure. Furthermore, this would be a source from which one could expect the appearance of talented young workers with new ideas in commercial pyrotechnic applications. A greater commercial use of pyrotechnics would expand the market and reduce the dependence of the manufacturer on military programs for his income. The resulting stabilization in the demand for pyrotechnic products would certainly improve the stability of employment and of funding for in-house research, in contrast to the present variable need for competent personnel. The faculty that teaches the courses would be a continuing resource as a depository of the knowledge which is now kept in the memories of older pyrotechnists and lost when they leave the field. I hope you will agree that it would be beneficial to both the manufacturer of pyrotechnics and to pyro research laboratories if some university could be persuaded to take the initiative of establishing a degree in pyrotechnic science and engineering. At one time I attempted to do this at my own university and nearly succeeded, but was blocked by the tenor of the times which caused the administration to fear student reaction to programs which had military overtones; I don't believe this would be true today. Since that time the College of Engineering has been closed and I have no desire to make another attempt. If it is to happen, it will require a champion at some university to initiate the program and that champion will appear only with continuing effort by the pyrotechnics community. You must convince the university administration that a need exists, that it will continue, and that graduates will find employment. You may have to secure guarantees from government agencies who are users of pyro, that they will provide students for the first years of the degree program as a means of supporting the expense incurred by the college. In Europe the educational system differs from ours so that I cannot comment on the nature of the effort that would be needed, but I am sure that my European colleagues will know what is required in their own countries.

Perhaps the first step in the direction of establishing university degrees in pyrotechnics and solving some of the technical problems would be the creation of a group which could speak for the entire industry, as is true in the United States for societies such as the Institute of Electrical and Electronic Engineers, the Illuminating Engineering Society, the Sporting Arms & Ammunition Manufacturers Association, and the Institute of Makers of Explosives. Such an "International Pyrotechnic Society" should, I believe, supply several very much needed services to its members. It should promote and facilitate the exchange of information concerning the art and science of pyrotechnics among all interested persons. It should create and maintain an information bank which can

speed or simplify a member's search for information on a pyrotechnic material, composition, device, manufacturer or research study. It should sponsor meetings on pyrotechnics at such intervals and on such subjects as may be appropriate to further its purpose. It should encourage pyrotechnic education and educators. It should establish standards of safety, performance and quality for pyrotechnic materials, devices, manufactures and research. And, I would hope, it will publish a journal - even though at first it might appear only annually.

The group which is now responsible for presenting future International Pyrotechnic Seminars - what I am told my European colleagues call "the Denver meeting" - are also preparing the constitution and by-laws for an International Pyrotechnics Society. Those who would like to help may write to me in Denver and I will see that you receive copies of the constitution and by-laws. Your constructive comments and criticisms will be most welcome.

In conclusion, I would like to summarize by saying that a good definition of pyrotechnics seems to be essential as a means of discriminating between it and closely related subjects, such as propellants and high explosives. I am convinced that an International Pyrotechnics Society and graduate degrees in Pyrotechnic Science and Engineering are essential foundation blocks for the support of ongoing research on materials, reaction processes, flame structure and the preparation of accurate purchasing specifications. While I believe that safety is, fundamentally, an attitude or habit of thought, much can be done to protect the individual from lapses of good practice when better information becomes available from the research programs on standards. I have enjoyed my experiences with pyrotechnic research, perhaps because, like most boys, I like to hear a good loud "bang", but more because it is a challenging field that employs almost every scientific and engineering discipline.

You have been very patient, but you have listened to me for long enough, and it is time to say thank you very much for your courteous attention and for the honor of addressing you. Thank you.

Bibliography

1. Bauer, Karl O., "Handbook of Pyrotechnics," Chemical Publishing Co. Inc. New York, N.Y. 1974.
2. Lancaster, The Reverend Ronald, Takeo Shimizu, Roy E. A. Butler, Ronald G. Hall; "Fireworks, Principles and Practice," Ibid, 1972.
3. Lancaster, The Reverend Ronald, private communication, August 20, 1979.
4. Weingart, George W., "Pyrotechnics," 2nd ed., Chemical Publishing Co. Inc. New York, N.Y. 1947.
5. Cackett, J. C., "Monograph on Pyrotechnic Compositions," 1965; Ministry of Defense, (Army), Royal Armament Research and Development Establishment, Ft. Halstead, Seven Oaks, Kent, Great Britain.
6. Shidlovsky, A. A., "Principles of Pyrotechnics," Mashinostroyeniye Press, Moscow, U.S.S.R. 1965 (in Russian, 3rd ed.).
7. Ellern, Herbert, "Military and Civilian Pyrotechnics" Chemical Publishing Co. Inc. New York, N.Y. 2nd ed. 1968.
8. Webster's Seventh New Collegiate Dictionary, G.&C. Merriam Co., Springfield, Mass., 1963.
9. Brock, Alan St. H., "A History of Fireworks," P. Harrap & Co. Ltd., London, U.K., 1949.
10. "Radioactive Transfer Model of a Pyrotechnic Flame," Douda, B. E., Dept. of Chemistry, Indiana University, October, 1973; AD 769237
11. Chazal, André, "Compositions et Composants Pyrotechniques," These pour obtenir le grade de Docteur es Sciences Physiques, Université de Droit, d'Economie et des Sciences d'Aix-Marseille, Mars, 1978.
12. Parish, Wm. E., Carl E. Dinerman, "Spectral Calibration of 2.0-2.5 Micrometer Lead Sulfide Radiometer," 5 October 1978, NWSC/CR/PDTR-90 Naval Weapons Support Center, Crane, Ind. 47522.
13. Ingo W. May, Austin W. Barrows, eds., "Army Materiel Command Program, The Fundamentals of Ignition and Combustion, Vol. I: Ignition. BRL Report No. 1707, April 1974, AD919315 L, U.S. Ballistic Research Laboratories, Aberdeen Proving Ground, Maryland.
14. Ingo W. May, Austin W. Barrows, eds., "Army Materiel Command Program, The Fundamentals of Ignition and Combustion, Vol II: Combustion. BRL Report 1708, April 1974 AD919316 L, U.S. Ballistic Research Laboratories, Aberdeen Proving Ground, Maryland.

THE DESIGN AND EVALUATION OF PROGRESSIVELY BURNING PYROTECHNIC FORMULATIONS

James L. Austing
IIT Research Institute
Chicago, Illinois 60616

Paul W. Cooper
Sandia Laboratories
Albuquerque, New Mexico 87115

ABSTRACT

The design and evaluation of a pyrotechnic that burns for 2 msec and generates gas cubically with time is described. The charge is a mixture of two aluminum-plated pyrotechnics, viz., aluminum-potassium perchlorate (Al-KClO_4) and aluminum-vanadium pentoxide ($\text{Al-V}_2\text{O}_5$). The Al-KClO_4 is a gas generator, each gram of which produces 320 cc of gas referred to standard temperature and pressure; the $\text{Al-V}_2\text{O}_5$, on the other hand, is a gasless pyrotechnic. Progressive generation of gas is achieved by utilizing mixtures of two pyrotechnics in increments that are progressively richer in gas generant, over a range of 14.6% to 100% Al-KClO_4 by weight. The deflagration rate of the system is a function of the Al-KClO_4 content, and ranges from 16.2 in./msec for a mixture with 14.6% Al-KClO_4 by weight to 30.0 in./msec for pure Al-KClO_4 .

An evaluation of the pyrotechnic charge fired in air showed that the design goals were adequately achieved. The growth of the gas cloud was monitored by high speed Fastax photography. Two criteria were utilized to verify the performance: (a) a plot of gas cloud volume as a function of time on logarithmic coordinates approached and maintained the required slope of 3, and (b) a plot of cloud diameter versus time on these coordinates achieved a slope of 1. In addition, the gas specific volume maintained a consistent value of about 27,000 cc/g of reacted Al-KClO_4 throughout the 2.0-msec burning time.

INTRODUCTION

The objective of this work was to develop a progressively burning pyrotechnic formulation specifically defined as one that generates gas volume cubically with time. Mathematically, this requirement can be stated as

$$V = f(t^3) \quad (1)$$

The design specifications required a total burning time of approximately 2 msec, a total charge weight of approximately 5 grams, and a working pressure range of 15-500 psi.

A review of the burning rate data for conventional solid propellants revealed that these could not be expected to burn rapidly enough to consume a 5-gram charge in 2 msec at the above pressures. Consequently, consideration was given to pyrotechnic formulations such as aluminum-potassium perchlorate (Al-KClO_4), which for example has a burning rate of 30 in./msec and higher at ambient conditions (Ref. 1 and 2). The work of Austing, Kennedy, and Weber (Ref. 3) showed that this pyrotechnic is an effective gas generator and has a force constant in the neighborhood of 300 ft-lb_f/g_m, even though the products (Al_2O_3 and KCl) are gases at the reaction temperature but solids at ambient temperature. A charge that would generate only "temporary" gas may have desirable characteristics for some applications.

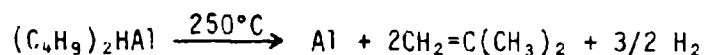
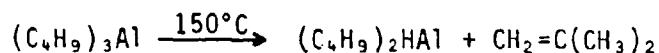
In the Second International Pyrotechnics Seminar and the Seventh Symposium on Explosives and Pyrotechnics, Austing and Remaly (Ref. 4 and 5) reported on the development of a family of aluminum-plated pyrotechnics. The plated pyrotechnic is prepared by pyrolysing a metal alkyl such as triisobutylaluminum in the presence of the oxidant powder; the end product consists of a continuous metal film or metal particles in intimate contact with the oxidant particles. Because of the improved burning characteristics of the plated pyrotechnics, in the present work aluminum-plated potassium perchlorate was considered as the gas generator, in preference to a mechanical mixture of aluminum and perchlorate powders. In order to obtain progressive generation of gas, the Al-KClO_4 could be diluted incrementally

with decreasing percentages of a non-gas-producing pyrotechnic such as aluminum-plated vanadium pentoxide ($\text{Al-V}_2\text{O}_5$), which reacts at the same temperature as the Al-KClO_4 , viz. 3370°K (Ref. 3 and 6), but produces only molten species. The goal, therefore, was to prove the feasibility of this approach by suitable design and experimental evaluation.

DESIGN OF PYROTECHNIC CHARGE

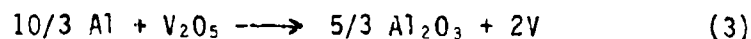
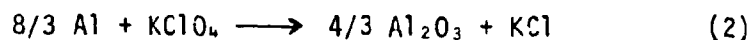
Preparation of Plated Pyrotechnics

Two plated pyrotechnic systems were required for the pyrotechnic formulation, viz. aluminum-plated potassium perchlorate and aluminum-plated vanadium pentoxide. The plating procedure is fully described in References 4 and 5, and essentially consists of pyrolysing triisobutylaluminum in a paraffin oil slurry of oxidant particles at a temperature of 250°C (Ref. 7):



The isobutylene and hydrogen are driven off, and the aluminum that remains plates itself onto the oxidant particles. After the slurry has cooled to room temperature, the product is washed several times with petroleum ether to remove the paraffin oil, filtered in a Buechner funnel, and then "dried" under vacuum for 8-16 hours.

Both plated pyrotechnics utilized in this work were stoichiometric formulations, as defined by the following reactions:



This choice was purely arbitrary, and perhaps in future work improved performance could be obtained with fuel-rich formulations. Fifty-gram batches of the stoichiometric formulations were prepared. The oxidant powders utilized for the process were ball-milled for 1.5-6 hours; as shown in

References 4 and 5, this procedure results in an average particle size of 1-2 microns. It is also shown that the aluminum film makes very little difference in the particle size distribution of the product, which indicates that the thickness of the film is small compared to the particle diameter.

Measurement of Deflagration Rate

The design of the progressively burning pyrotechnic required that the deflagration rate of $\text{Al-KClO}_4/\text{Al-V}_2\text{O}_5$ mixture be measured as a function of composition in the same configuration that would ultimately be utilized in the charge fabrication. The experimental arrangement is depicted in Figure 1. The pyrotechnic was loaded by hand into the soft aluminum tubing having an inside diameter of 0.117 inch. The charge was initiated with a mild electric detonator,* in which the total explosive charge was 97 mg of lead azide. The deflagration was monitored with two ion probes utilized in conjunction with a Tektronix oscilloscope equipped with a Polaroid camera; one probe was at the detonator-pyrotechnic interface for oscilloscope trigger, while the other was at the opposite end of the charge for determination of time-of-arrival of the reaction wave. The deflagration rate was then easily computed from the measured transit time and the known distance between the probes.

The deflagration data for the $\text{Al-KClO}_4/\text{Al-V}_2\text{O}_5$ pyrotechnic is summarized in Table 1 and plotted in Figure 2 as a function of the logarithm of weight percent Al-KClO_4 . The significance of the various weight percentages of Al-KClO_4 that were chosen will be clarified in the next section. The deflagration of the mixture containing 5.6% Al-KClO_4 appeared to be erratic and slow, and so this mixture was not utilized in subsequent charge design. The other data points almost lie on a straight line in Figure 2, and so it has been assumed that the true correlation lies on a straight line through the upper two points.

*DuPont DFP-8 Mild Electric Initiator.

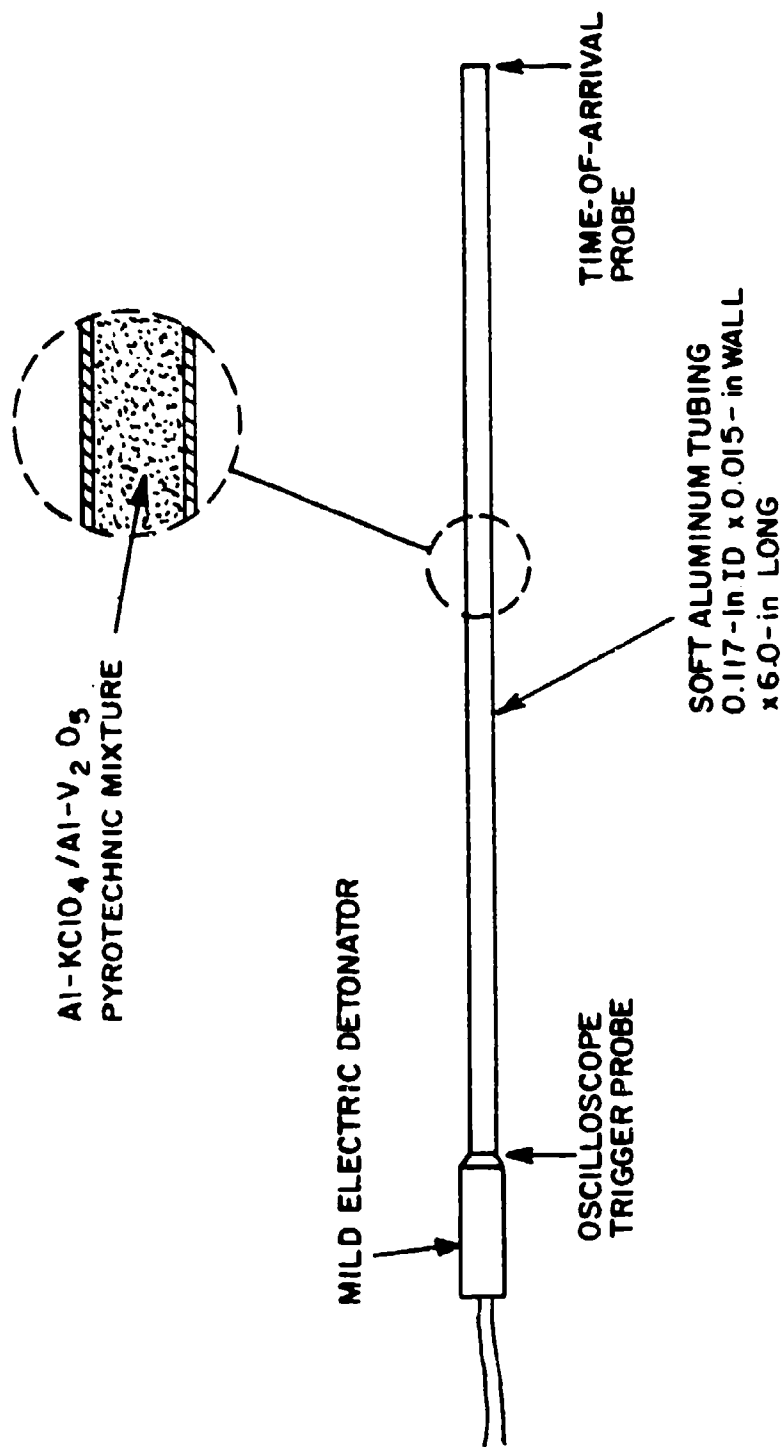


Figure 1. Experimental Arrangement for Measuring Deflagration Rate of $\text{Al-KClO}_4/\text{Al-V}_2\text{O}_5$ Mixtures

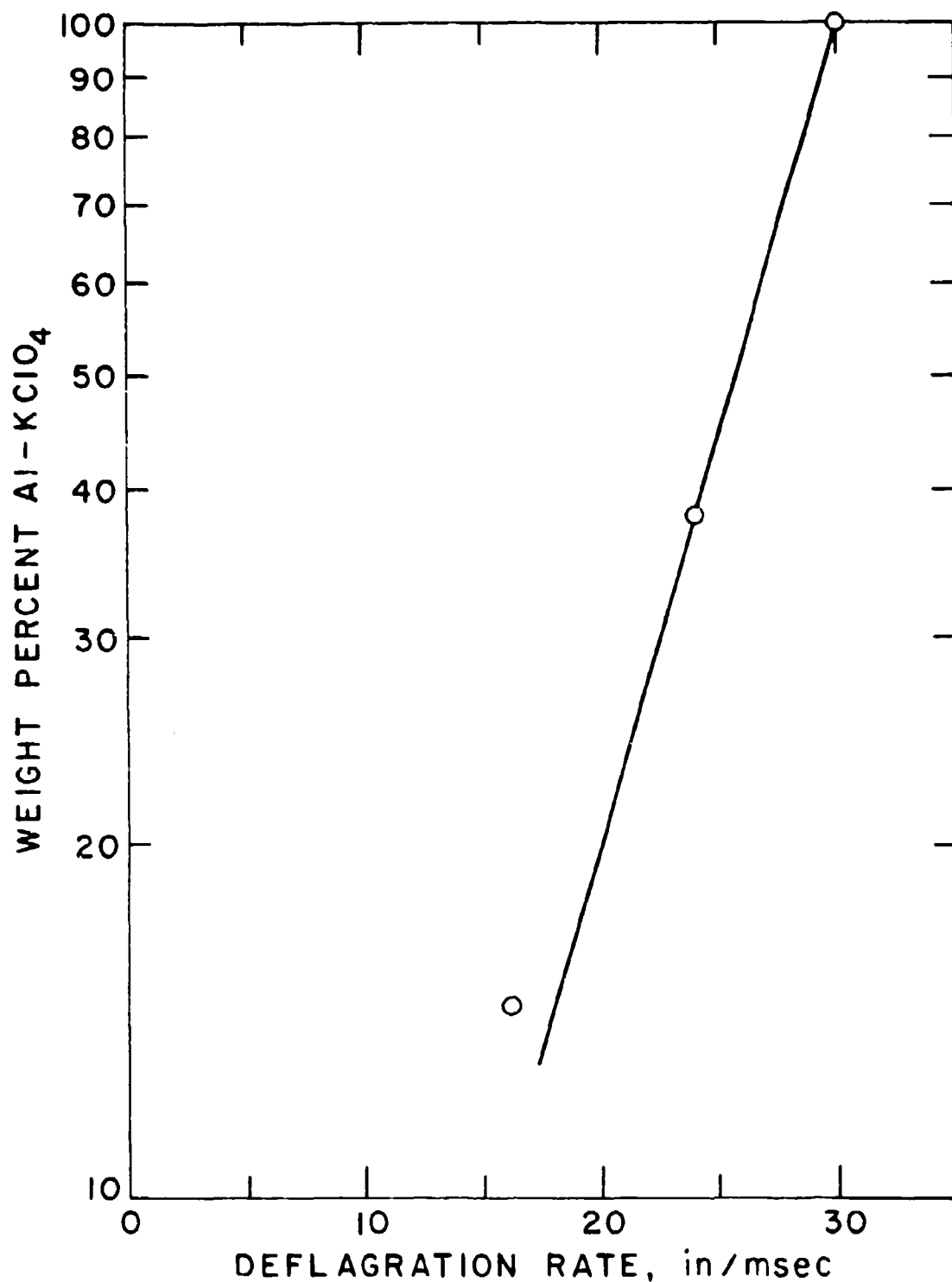


Figure 2. Deflagration Rate of Al-KClO₄/Al-V₂O₅ Pyrotechnics
As Function of Al-KClO₄ Content

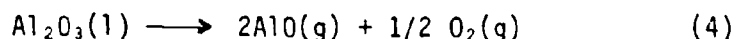
(Pyrotechnic was confined in small aluminum tube, and loading density was approximately 1.0 g/cc. Pyrotechnic was initiated by mild electric detonator.)

Table 1
 DEFLAGRATION OF $\text{Al-KClO}_4/\text{Al-V}_2\text{O}_5$ PYROTECHNIC MIXTURES
 (Experimental arrangement is depicted in Figure 1.)

Test No.	Weight Percent Al-KClO_4	Charge		Deflagration Rate, in./msec
		Weight, grams	Density, g/cc	
60	5.6	1.02	0.97	<0.6
58	14.6	1.13	1.07	16.2
61	38.1	1.02	.97	24.0
62	100.0	0.99	0.94	30.0

Gas-Generating Criterion

Thermochemical calculations show that a significant portion of the product aluminum oxide formed in the aluminum-potassium perchlorate reaction decomposes at 3770°K according to the reaction (Ref. 8):



Thus the aluminum-potassium perchlorate reaction produces three gaseous species, viz. $\text{AlO}(g)$, $\text{O}_2(g)$, and $\text{KCl}(g)$. The calculated quantity of gas represented by these three species is 0.0143 mole/g of reactant, which is equivalent to 320 cc/g at standard temperature and pressure. This volume together with the required total burning time of 2.0 msec constitutes one design point. To obtain generation of gas cubically with time, gas must be produced along a line having a slope of 3 on logarithmic coordinates and rising to the above design point. This relationship is depicted in Figure 3.

Progressively increasing amounts of gas in accordance with Figure 3 were obtained by diluting the aluminum-plated potassium perchlorate with aluminum-plated vanadium pentoxide incrementally in varying percentages. The products of the aluminum-vanadium pentoxide reaction are aluminum oxide and vanadium, both of which are in the molten state at 3770°K (ref. 6);

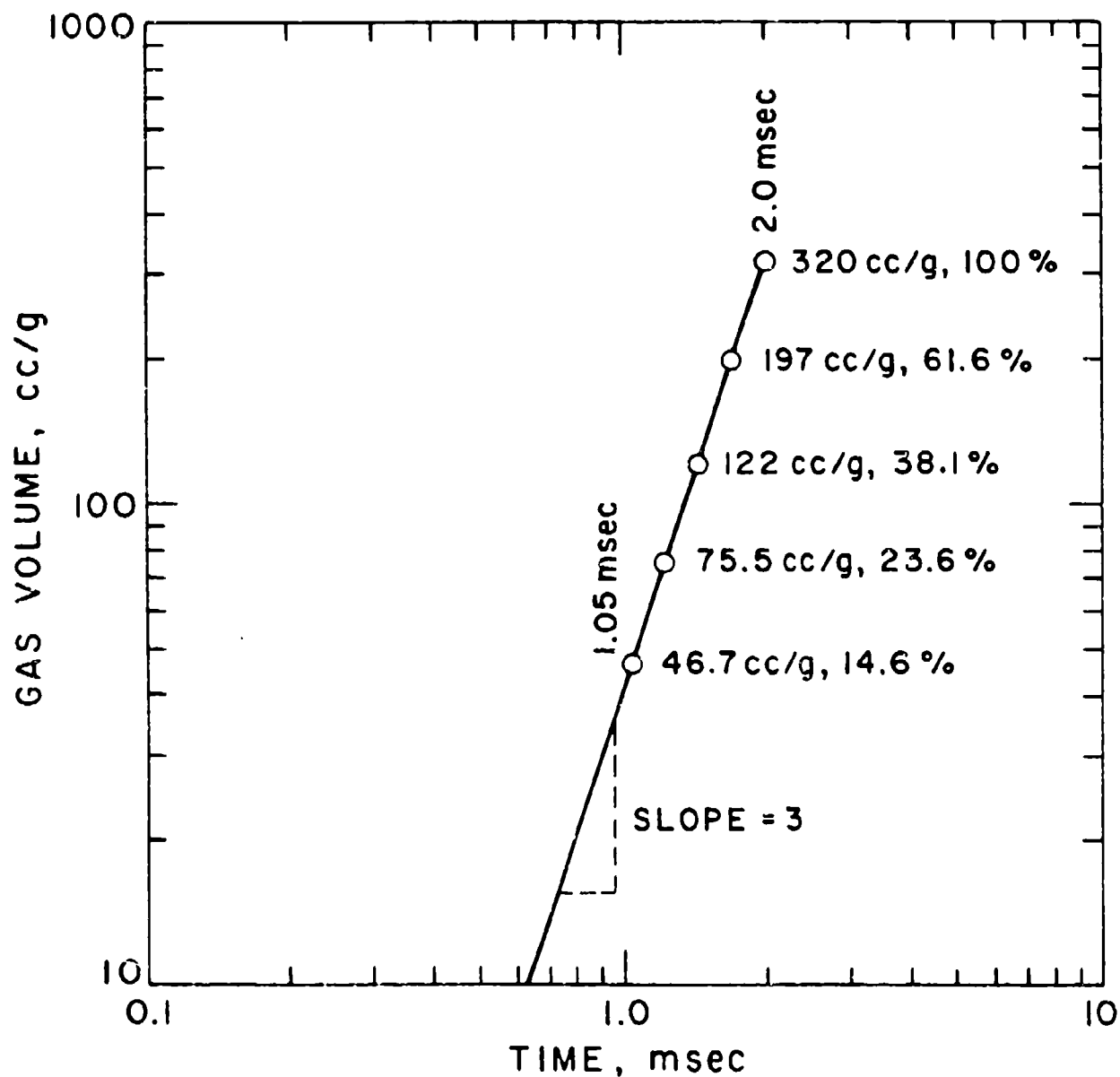


Figure 3. Relationship for Design of Pyrotechnic
To Generate Gas Cubically With Time

(Volumes are quoted at standard temperature and
pressure. Percentages refer to weight percent
Al-KClO₄.)

however, thermochemical calculations show that very little of the aluminum oxide decomposes into the gaseous species. Hence, aluminum-vanadium pentoxide is an essentially gasless pyrotechnic. The percentage shown in Figure 3 for each increment refers to the weight percentage of Al-KClO_4 , which was calculated by assuming that the amount of gas formed was directly proportional to the Al-KClO_4 content. The interval between each point on the line was arbitrarily selected as

$$\Delta \log V = 0.20875 \quad (5)$$

The corresponding times at each point were then noted; two of these times, viz. 1.05 and 2.0 msec, are shown to illustrate the graphical calculation.

Details of the Charge Design

The deflagration rate curve of Figure 2 and the gas-generating criterion of Figure 3 permit the complete design of the pyrotechnic system, the details of which are shown in Figure 4. The design calculations are straightforward, and are easily followed if the reader scans them from top to bottom. The soft aluminum tubing was identical to the 0.117-inch inside diameter configuration depicted in Figure 1, except that now the total length was 41.9 inches. Each charge increment was loaded by hand to approximately the same range of densities quoted in Table 1; a special long round ram was utilized to pack the pyrotechnic into the tubing. The length of each increment was dictated by the deflagration rate and by the criterion for generation of gas cubically with time. The calculated total pyrotechnic weight was 6.98 g, of which 3.10 g was Al-KClO_4 . Ignition was achieved by a mild electric detonator that contained only 97 mg of explosive; ignition with a detonator in lieu of a squib significantly reduced the time jitter at the initiator-pyrotechnic interface.

To achieve a more compact design package than provided by the long tube in Figure 4, after the loading had been completed the tube was coiled around a 1-inch diameter guide, with the space between each coil equal to approximately 1.5 tube diameters; the guide was then removed. In final configuration, the charge resembled a coiled spring about 4 inches high. The beginning of the tube was then inserted into a small holder in which the mild

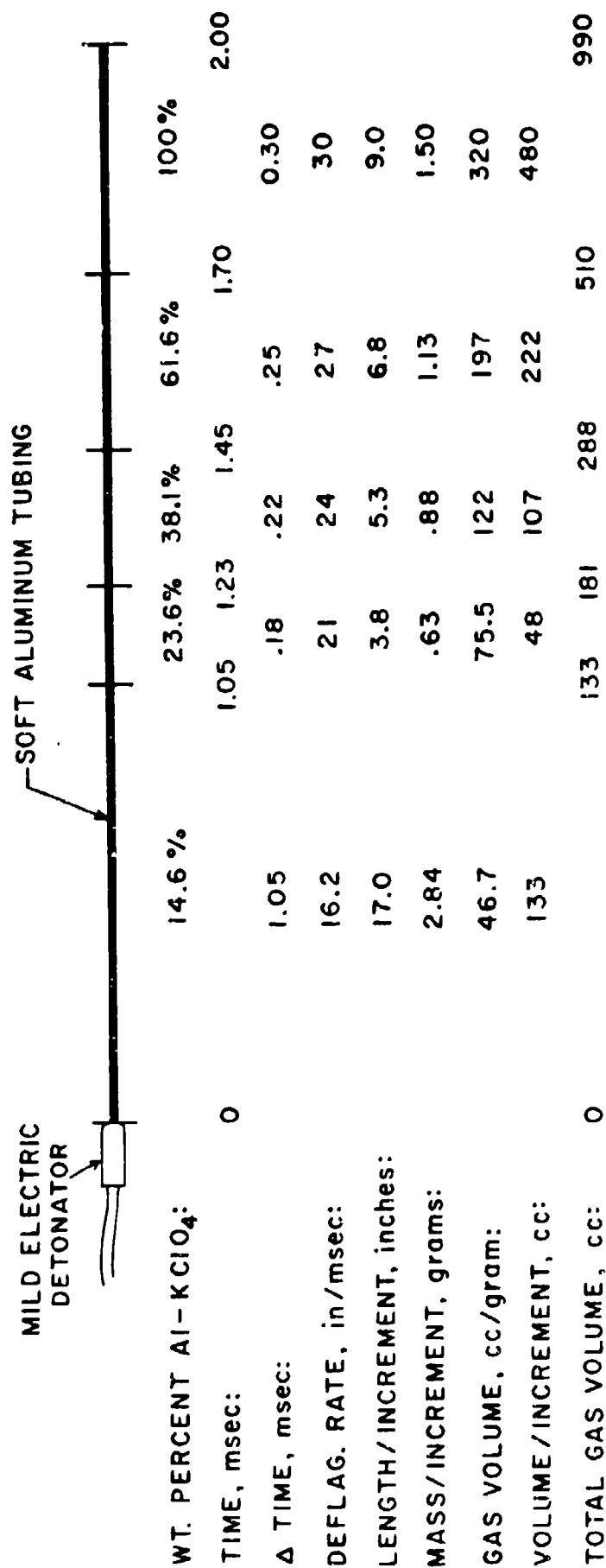


Figure 4. Complete Details of Pyrotechnic Charge Design
(Gas volumes are quoted at standard temperature and pressure.)

detonator was positioned; care was exercised to provide good interfacial contact between the detonator and pyrotechnic train.

EXPERIMENTAL EVALUATION OF THE PYROTECHNIC CHARGE

Experimental Arrangement

The pyrotechnic charge designed as described above was fired in air, and its performance was monitored by means of a 16-mm Fastax camera operated at 6 frames/msec. The essential features of the experimental arrangement can be deduced from Figure 5, which presents enlarged prints from the high speed photographic sequence. The distance between the lines on the background grid is 4 inches (10.16 cm). The coiled spring configuration for the pyrotechnic train can be discerned in the initial photograph at $t=0$; the detonator is at the bottom of the pyrotechnic charge in this experiment. In looking through the original film and through these prints, it appeared that the total burning time was very close to the specified design value of 2.0 msec, since after that time the gas cloud begins to assume an irregular shape and becomes very fuzzy in its overall contour.

Analysis of the Record

The analysis of the photographic record in Figure 5 showed that the required cubical rate of cloud growth was achieved. Table 2 shows the calculation of cloud volume at each time interval, and Figure 6 presents a plot of total gas volume as a function of time in logarithmic coordinates. It is seen that the volume growth rate approached a cubical relationship at 0.833 msec, and slightly exceeded a cubical relationship at 2.0 msec.

The procedure for calculating gas volume from the two-dimensional photographs in Figure 5 was as follows. The cross-sectional area of the cloud was determined by counting squares provided by a piece of linear graph paper superimposed over the photograph. The diameter of an equivalent circle having the same cross-sectional area as the observed gas cloud was computed from



$t = 0 \text{ msec}$



$t = 1.167 \text{ msec}$



$t = 0.167 \text{ msec}$



$t = 1.333 \text{ msec}$



$t = 0.333 \text{ msec}$



$t = 1.500 \text{ msec}$



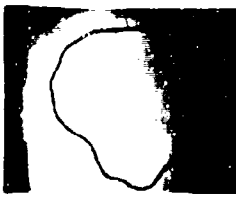
$t = 0.500 \text{ msec}$



$t = 1.667 \text{ msec}$



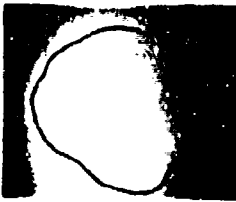
$t = 0.667 \text{ msec}$



$t = 1.833 \text{ msec}$



$t = 0.833 \text{ msec}$



$t = 2.000 \text{ msec}$



$t = 1.000 \text{ msec}$



$t = 2.167 \text{ msec}$

Figure 5. High-Speed Photographic Sequence Showing Growth of Gas Cloud in Air

(Camera operated at 6 frames/msec. Distance between lines on grid = 10.16 cm. Cloud periphery has been traced with marking pen for clarity.)

Table 2

DETERMINATION OF CLOUD GROWTH FROM HIGH-SPEED
PHOTOGRAPHIC SEQUENCE DEPICTED IN FIGURE 5

Time, msec	Cloud Cross- sectional Area, sq. cm.	Diameter of Equiv. Circle, cm	Cloud Volume, cc	Maximum Measured Diameter, cm	
				Vertical	Horizontal
0	0	0	0	0	0
.167	58	8.6	333	9	9
.333	225	16.9	2,535	20	17
.500	326	20.4	4,434	22	18
.667	391	22.3	5,913	26	22
.833	561	26.7	9,986	31	26
1.000	680	29.4	13,328	33	28
1.167	843	32.8	18,434	35	31
1.333	966	35.1	22,604	39	36
1.500	1123	37.8	28,300	44	39
1.667	1368	41.8	38,122	47	43
1.833	1626	45.5	49,322	50	49
2.000	2058	51.2	70,246	51	57

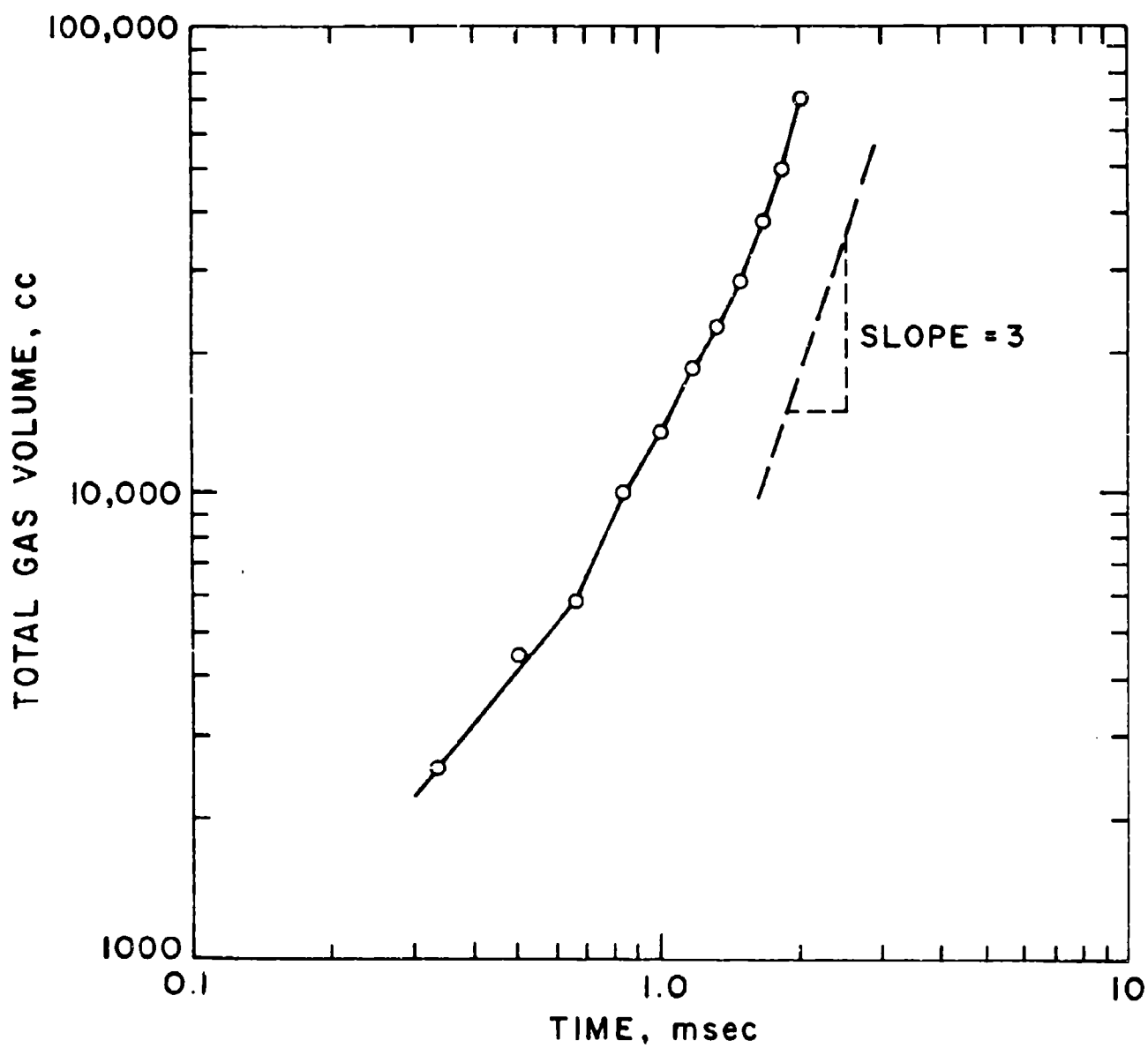


Figure 6. Gas Cloud Volume as a Function of Time

$$d_e = \left[\frac{4}{\pi} A \right]^{1/2} \quad (6)$$

where

d_e is the diameter

A is the cross-sectional area.

Values of this diameter are tabulated in the third column of Table 3. The cloud volume was then easily deduced from the formula

$$V = \frac{2}{3} A d_e \quad (7)$$

The above method for calculating cloud volume is obviously an approximation. The procedure was an expediency that was justified in the absence of three-dimension observation of the cloud growth.

If a spherical volume is increasingly cubically with time, the diameter should increase linearly with time. It is of interest, therefore, to examine the rate of growth of the cloud diameter as another test of how well the cubical rate of gas volume generation was achieved. It will be noted that three diameters are tabulated in Table 2; the diameter of the equivalent circle has already been discussed. The other two are the maximum vertical and horizontal cloud diameters measured directly from the record in Figure 5. All three diameters are plotted as a function of time on logarithmic coordinates in Figure 7, and a smooth curve has been drawn through the points by eye. It is observed that the rate of diameter increase approached and finally maintained the required linear relationship, which is equivalent to a slope of 1 on these coordinates.

Calculation of Gas Specific Volume

Another verification that the cloud growth observed in Figure 5 is real can be established by calculating the gas specific volume at each time interval. The gas specific volume is defined as the total gas volume at a given time divided by the total mass of Al-KClO_4 reacted at that time; this latter figure can be estimated from the weight percent Al-KClO_4 and the deflagration rate of each increment. The calculations are summarized in Table 3.

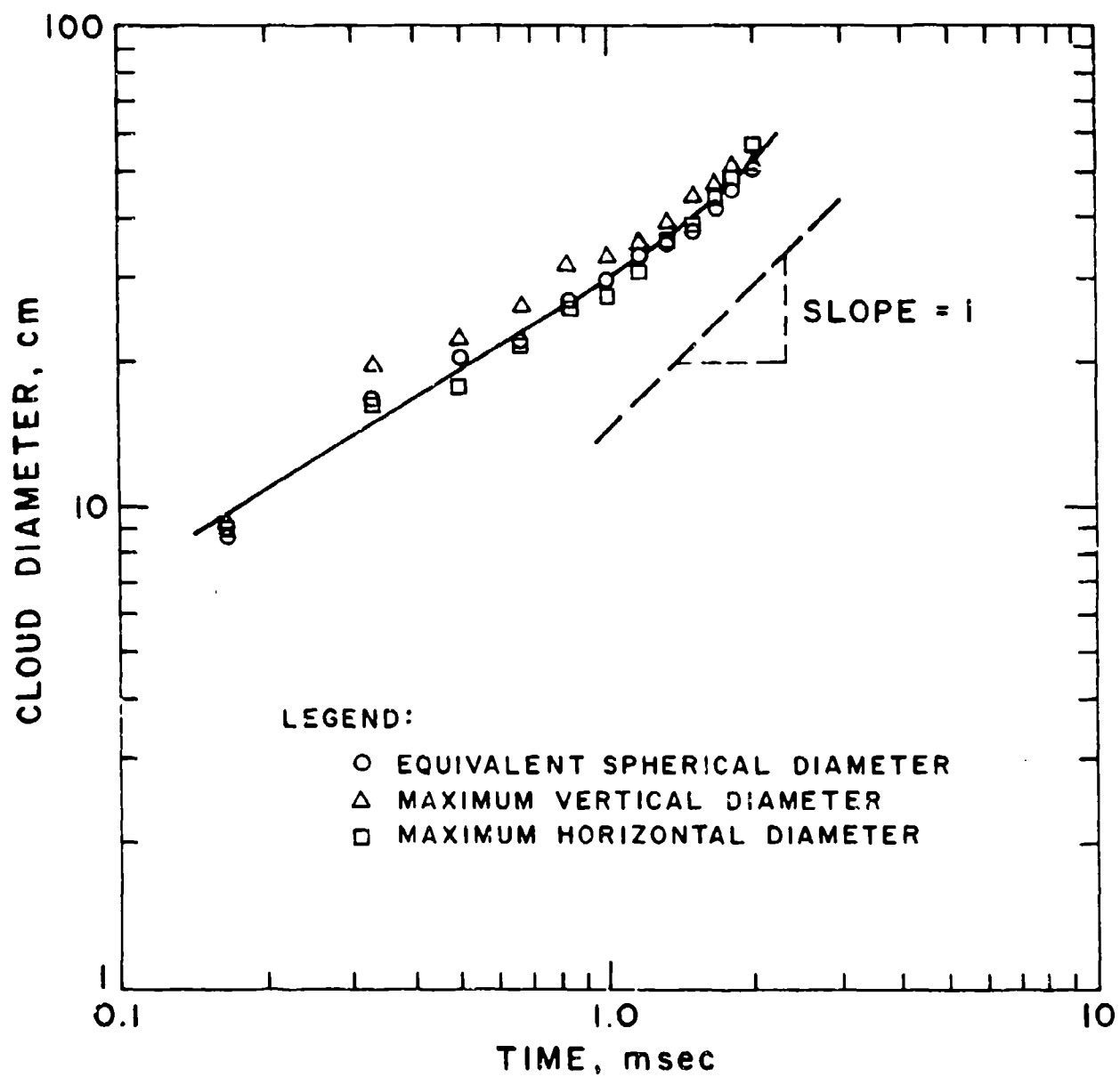


Figure 7. Gas Cloud Diameter as a function of Time

Table 3

CALCULATION OF GAS SPECIFIC VOLUME AT EACH TIME INTERVAL

Time, msec	Cloud Volume, cc	Total Mass of Al-KClO ₄ Reacted, g	Gas Specific Volume, cc/g
0.167	333	0.07	4,800
.333	2,535	.13	19,500
.500	4,434	.20	22,200
.667	5,813	.26	22,400
.833	9,986	.33	30,300
1.000	13,328	.39	34,200
1.167	18,434	.51	36,100
1.333	22,604	.72	31,400
1.500	28,300	1.04	27,200
1.667	38,122	1.50	25,400
1.833	49,322	2.17	22,700
2.000	70,246	3.10	22,700
			26,700 = Avg.*

*Average value does not include the first entry of 4,800 cc/g.

With the exception of the first entry where the pyrotechnic is just beginning to burn, the specific volume is essentially constant over the entire burning time, and all of the values agree reasonably well with the average value of 26,700 cc/g. From these observations, it can be concluded that the deflagration proceeded as predicted by the design curves, and that the pyrotechnic generated gas consistently throughout the entire 2.0-msec burning time.

SUMMARY AND CONCLUSIONS

The design, fabrication, and performance of a pyrotechnic charge that generates gas cubically with time has been demonstrated to be feasible. The Al-KClO₄ and Al-V₂O₅ plated pyrotechnics utilized in this formulation were stoichiometric systems. Perhaps better performance could be achieved by utilizing fuel-rich pyrotechnics. This parameter should be investigated more fully in future work.

The design procedures developed in this work can be extended in several directions to meet the requirements of other applications. For example, charges can be designed to generate gas at other mathematical powers with respect to time. The possibility exists that detonating explosives charges reacting in microseconds could be designed to generate gas non-linearly with time.

ACKNOWLEDGEMENTS

The authors are indebted to John Michaels and Robert Stromberg of Sandia Laboratories for their cooperation in and the direction of this work. In addition, the conscientious efforts of Mr. Douglas E. Baker in the experimental aspects of the work contributed to the success of the effort.

REFERENCES

1. J. Hershkowitz, F. Schwartz, and J.V.R. Kaufman, "Combustion in Loose Granular Mixtures of Potassium Perchlorate and Aluminum," Eighth Symposium (International) on Combustion, The Williams and Wilkins Company, Baltimore, 1962, p. 720.
2. L.D. Pitts, "Electrical Probe Technique for Measurement of Detonation and Deflagration Velocities," Proceedings Fourth Symposium (International) on Detonation, ONR Report No. ACR-126, October 1965.
3. J.L. Austing, J.E. Kennedy, and J.P. Weber, "Ignition and Output Characteristics of Pyrotechnics for EED Applications," Proceedings, First Pyrotechnics Seminar, USNAD RDTR No. 131, October 1, 1968, Crane, Indiana.
4. J.L. Austing and R.F. Remaly, "Evaluation of Aluminum-Plated Pyrotechnics as Flash Charges for Electroexplosive Devices," Proceedings, Second Pyrotechnics Seminar, Aspen, Colorado, July 20-24, 1970, Denver Research Institute, Denver, Colorado.
5. J.L. Austing and R.F. Remaly, "Properties and Performance of Aluminum-Plated Pyrotechnics for Electroexplosive Device Applications," Proceedings, Seventh Symposium on Explosives and Pyrotechnics, The Franklin Institute, Philadelphia, Pennsylvania, September 8-9, 1971.
6. J.L. Austing and J.E. Kennedy, Previously unpublished calculations.
7. K. Ziegler et al., *Agnew. Chem.*, 67, 424-425, 1955.
8. L. Brewer and A.W. Searcy, *J.A.C.S.*, 73, 5308, 1951.

GLASS CERAMICS FOR EXPLOSIVE DEVICE HEADERS

Clifford P. Ballard, Robert J. Eagan, & Edwin A. Kjeldgaard
Sandia National Laboratories
Albuquerque, New Mexico 87185

SAND80-1170C

ABSTRACT

The desired features of a header for our advanced explosive devices include small size; 700 Mpa static burst strength; corrosion resistant alloys for electrodes, bridgewire, and housing; integral charge holder; high thermal conductivity (approaching that of alumina ceramic); no braze around the electrodes; design flexibility and quick turnaround time for fabrication of development prototypes; and low cost.

1. INTRODUCTION

To meet new requirements for pyrotechnic devices which must function reliably, at high pressures, after long storage times, we have initiated a research program to develop better explosive device headers. Such headers usually use a glass or ceramic insulator to isolate electrical feedthroughs, often Niron or Kovar, from a stainless steel case. We are developing new insulators, e.g., glass ceramics, and processes for sealing them to strong, corrosion resistant super-alloys.

In this report, we summarize the desirable attributes of an explosive device header and discuss the status of our program to produce such a device.

II. DESIRABLE DESIGN FEATURES

Following is a discussion of the most desirable features an ideal header for our explosive devices would possess.

A. High Strength -- A miniature valve actuator currently under development has a 700 MPa (~ 100 kpsi) burst strength requirement. The purpose of the requirement is to ensure the integrity of the actuator in the event of a valve failure which results in no volume expansion during actuator firing, e.g., piston locking up. An actuator's survivability is tested by firing it into zero volume, i.e., pressure cube test, and measuring the output. An ideal response (Curve A of Fig. 1) is survival at a peak pressure of 700 MPa (100 kpsi). Actuators currently in production do not meet this requirement (Curve C of Fig. 1).

Specifying burst criteria for the header alone is inadequate. Static and dynamic burst pressure test results do not agree. The static burst test involves pressurizing the charge cavity of the header with a hydraulic fluid for times that are orders of magnitude longer than those observed during actual valve operation. In the static pressure test, two failure modes were observed for one of our header designs; failure in the glass, at 187 MPa ($\sigma = 16.5$ MPa); and failure in the steel housing, at 375 MPa ($\sigma = 20.7$ MPa). In the dynamic pressure test, only the housing failure mode is observed, at 549 MPa ($\sigma = 75.9$ MPa).

The observed differences are unexplained at this time. Finite element stress analysis of the header, with no rate dependent material models, predicts similar "static" and "dynamic" burst pressures.

The goal of our actuator development program is to achieve a static burst pressure of 700 MPa.

B. Corrosion Resistance -- To meet component life requirements of twenty-five years or more while using potentially corrosive pyrotechnics such as $\text{TiH}_x/\text{KClO}_4$, more corrosion resistant materials for the electrodes, bridgewire, and housing are required. Severe corrosive attack may occur with the commonly used Alloy 52 electrodes and Tophet C (nichrome) bridgewires. (See Fig. 2.) Continued use of $\text{TiH}_x/\text{KClO}_4$ is desirable since it is the only pyrotechnic that has the proper ignition and output characteristics while being spark insensitive.

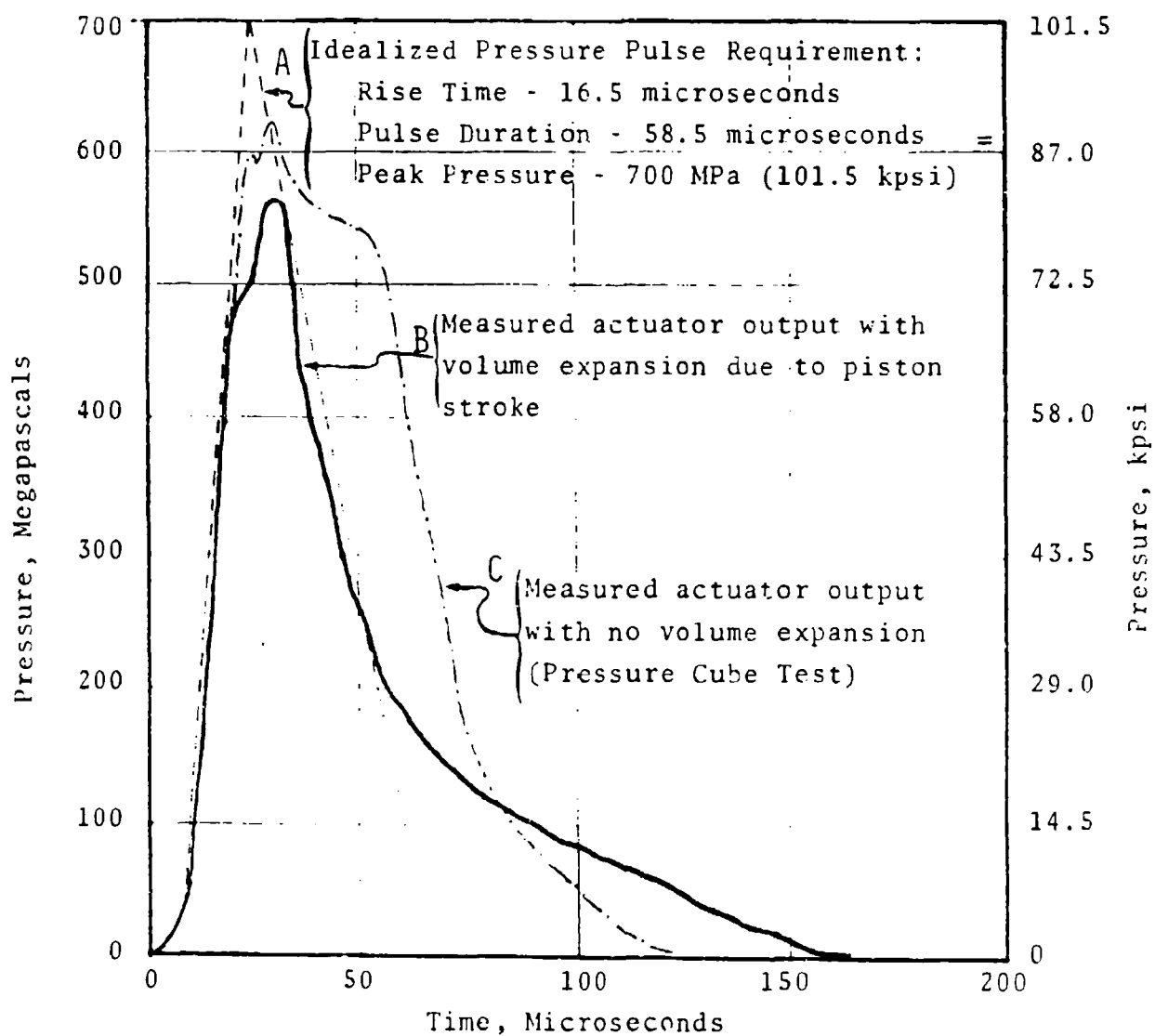
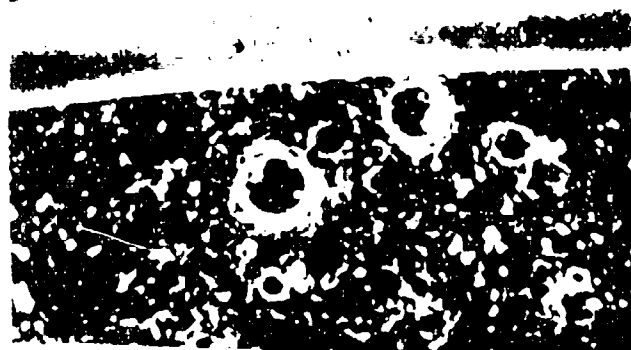
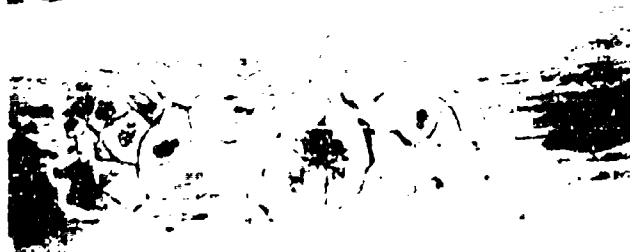
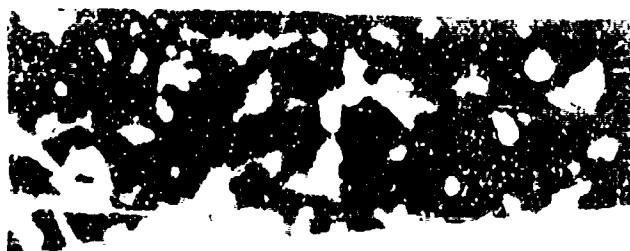
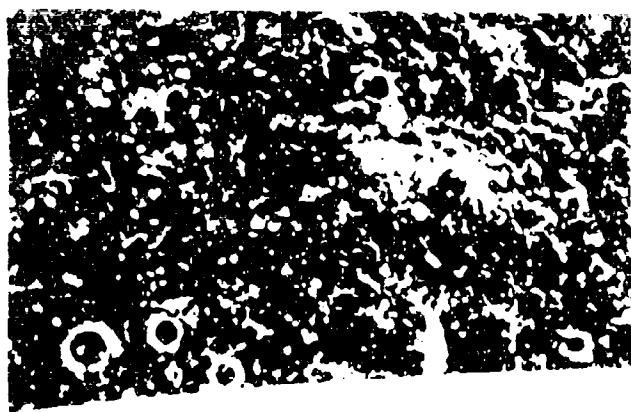
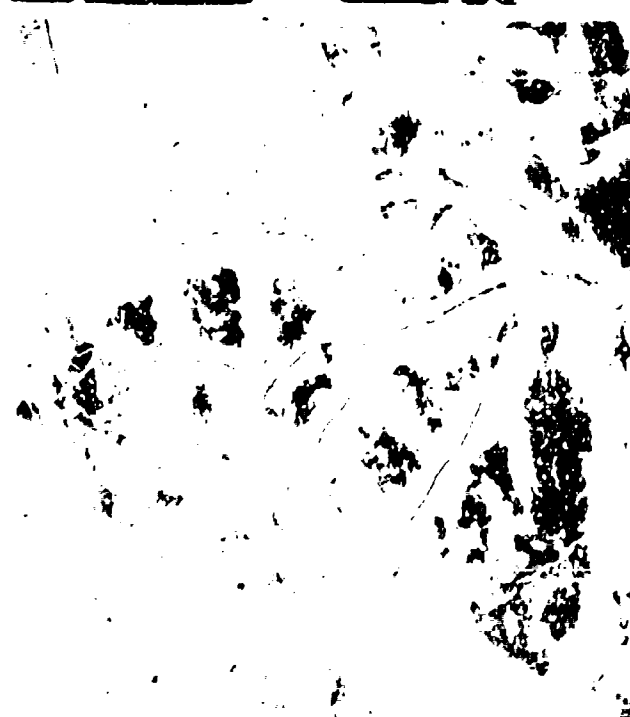
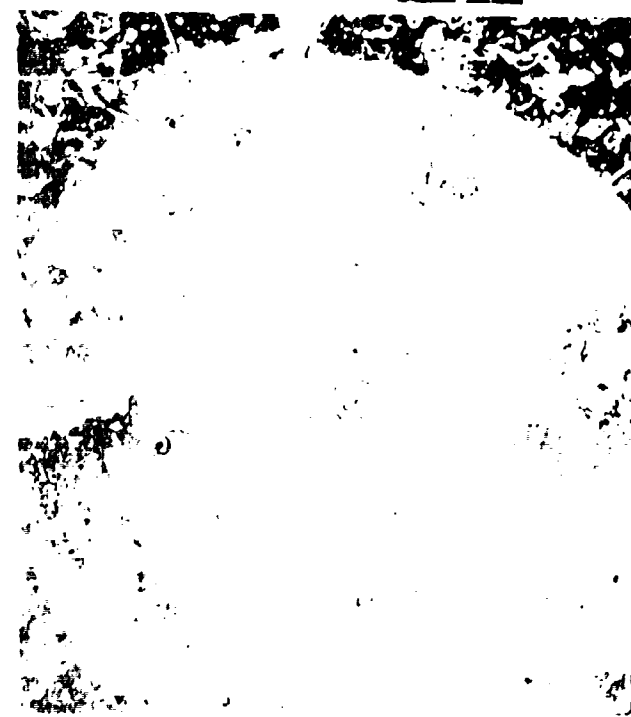


Figure 1 - VALVE ACTUATOR PRESSURE-TIME HISTORY



1000x

1000x



1000x

1000x

C. Integral Charge Holder -- An integral charge holder (see Fig. 3) is desirable for two reasons. Compatibility problems are reduced by eliminating adhesives and the gap between the charge holder and the housing (see Fig. 4) where undesirable materials could be trapped during assembly. Lower costs should result due to fewer parts and simplified processing.

D. Unbrazed Electrodes -- Brazed electrodes have three major disadvantages (see Fig. 5): 1) Precise electrode-to-electrode spacing is difficult to maintain since the electrode cannot be centered in the hole. 2) Bridgwire welding is more difficult and less reliable since it is often difficult to see the electrode/braze junction and the weld can occur on the braze material. Such a weld is not permanent and can lead to an open circuit after environmental exposure. 3) Compatibility problems are associated with the ubiquitous voids present in the braze which can trap corrosive materials to which the header is exposed during manufacture.

E. High Thermal Conductivity -- To meet a 1A, 1W no-fire requirement in a small component, the thermal conductivity of the header must be greater than commercial sealing glasses. The high thermal conductivity of alumina ceramic is a primary reason why it is used in the majority of our components.

F. Quick Development Turnaround -- A significant disadvantage of ceramic headers is the long lead times required; typical delivery time for a few hundred headers is 9-12 months. Thus the number of design iterations possible during a typical two-year development program is severely curtailed.

G. Low Cost -- Another significant disadvantage of ceramic headers is their high cost. Concern over cost is amplified in situations requiring high reliability since approximately twice as many headers are produced and destructively tested as are used, in order to provide the data for statistical assurance of quality.

H. Electrostatic Safety -- The relative insensitivity of $\text{TiH}_x/\text{KC10}_4$ pyrotechnics to spark ignition has greatly improved the handling safety of actuators during loading and use. However, another approach toward eliminating the possibility of accidental

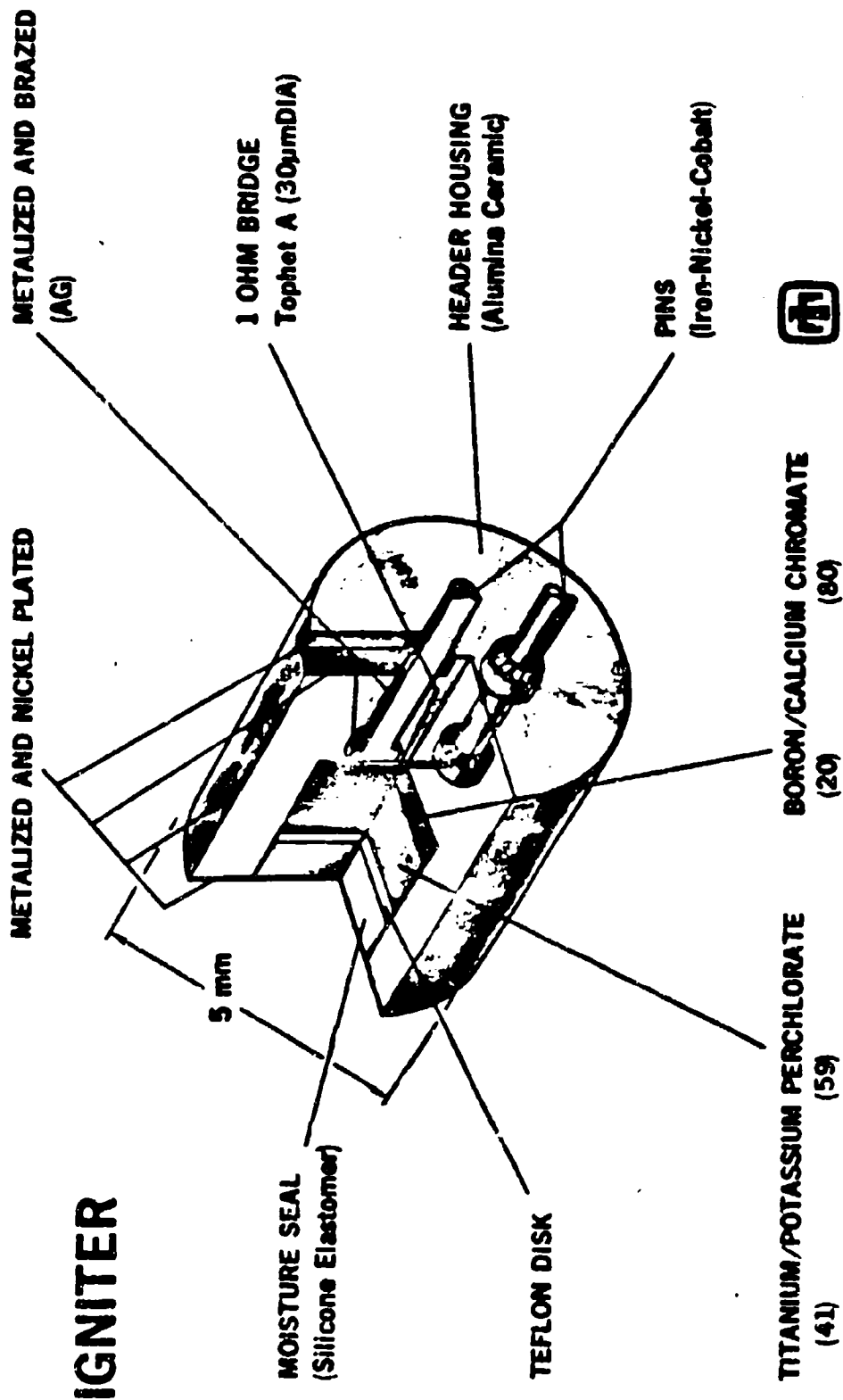


Figure 3 - ILLUSTRATION OF AN INTEGRAL CHARGE HOLDER

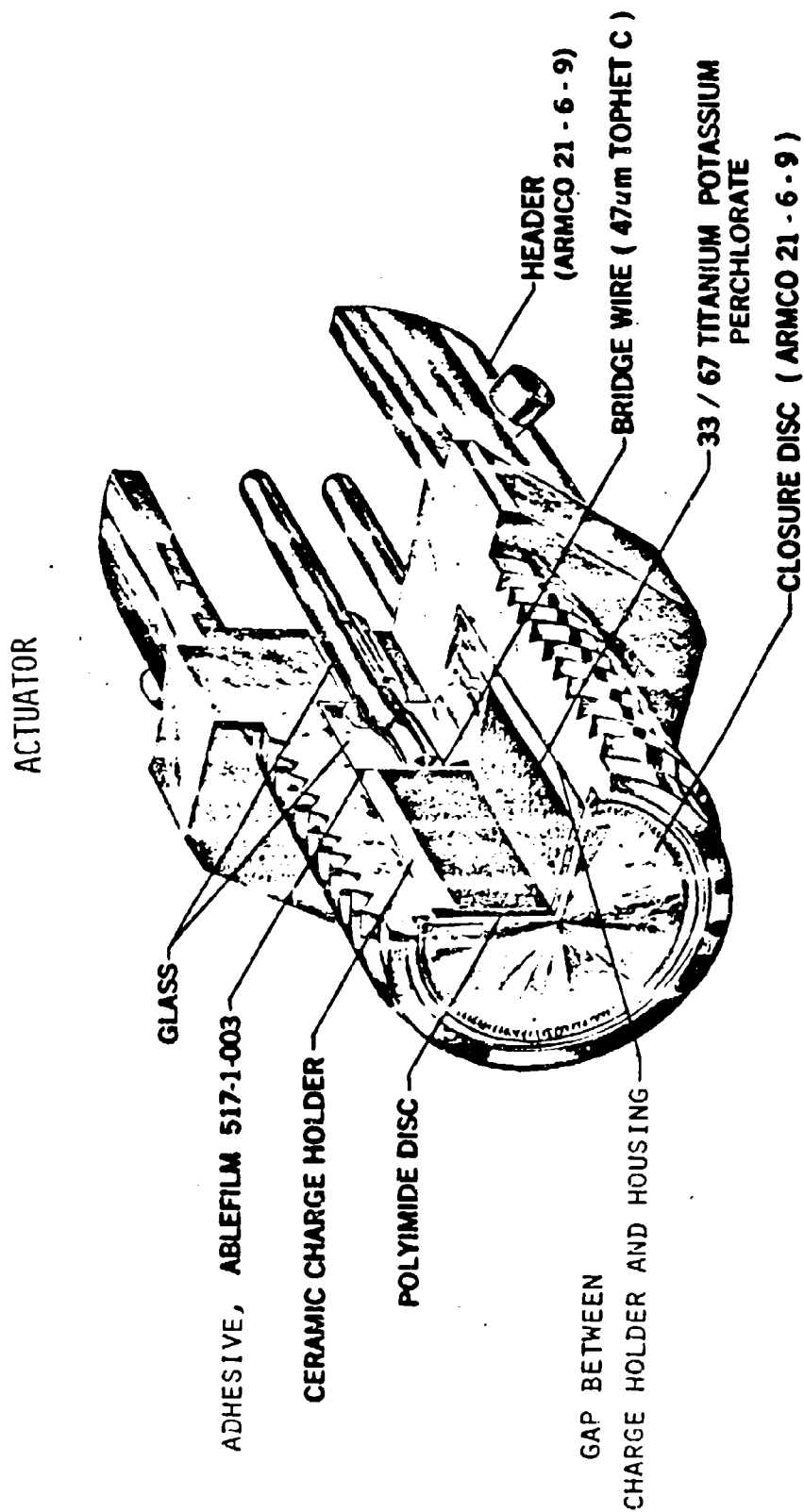


FIGURE 4 - ILLUSTRATION OF A BONDED-IN CHARGE HOLDER

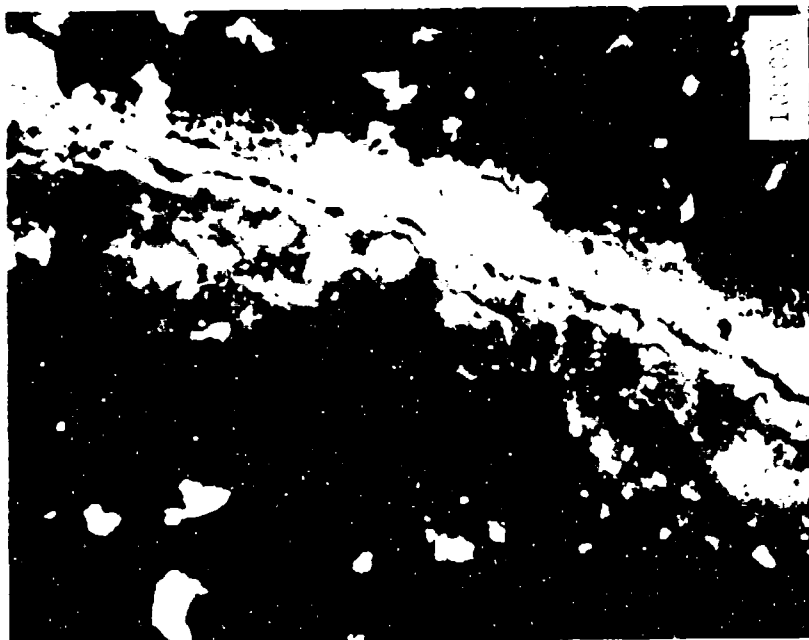
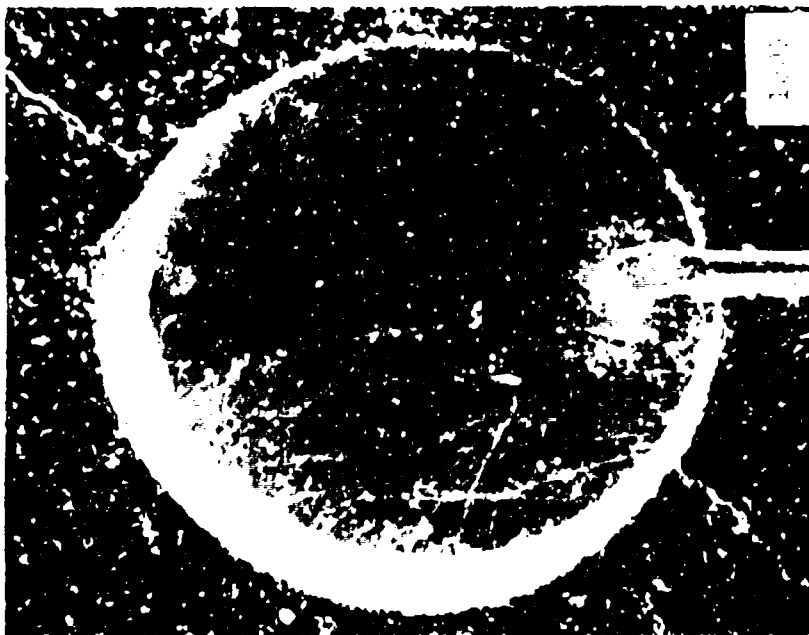


Figure 5 - KOVAR PIN BRAZED INTO A CERAMIC HEADER SHOWING OFF-CENTER PIN LOCATION, PIN/BRAZE JUNCTION AND VOID IN BRAZE AND RESULTANT ONSET OF CORROSION.

ignition (which is especially important when $\text{TiH}_x/\text{KClO}_4$ is not used) is to electrically short the electrodes and housing during exposure to dangerous levels of electrical discharge. Varistors, zinc oxide ceramics with nonlinear current/voltage characteristics, are being investigated for this application. Preliminary experiments using clip-on varistor shunts have been extremely successful. Our ultimate goal is to incorporate varistors integrally within the header design.

We assessed the feasibility of achieving these requirements on the basis of engineering design, materials availability, and fabrication technology. A model header configuration has been designed which appears to satisfy all of the design requirements. (See Fig. 6.)

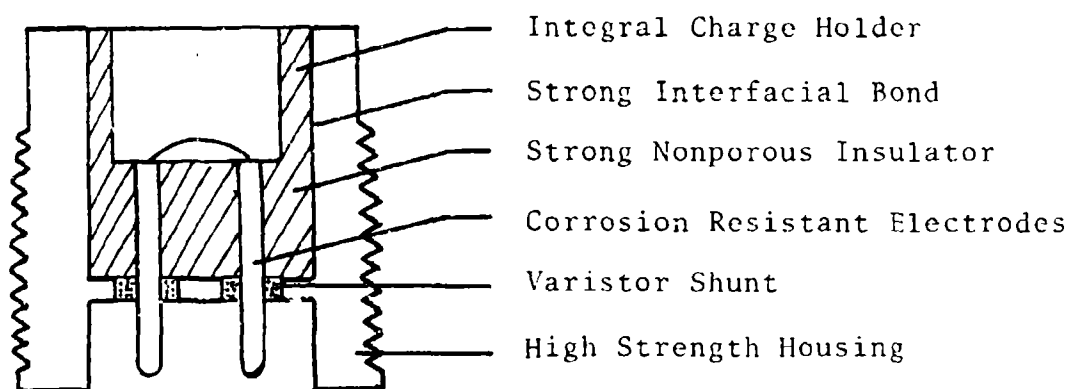


Figure 6. Model Header Configuration for Advanced Actuator

III. MATERIALS SELECTION

A survey was conducted to identify the most suitable alloys for use in headers. Five strong, corrosion-resistant alloy

candidates were selected for careful consideration (26-1 stainless steel, Inconel-718 and 625, Hastelloy C and β -C Titanium). These alloys are weldable and have moderate coefficients of thermal expansion ($\alpha = 100-160 \times 10^{-7}/^{\circ}\text{C}$). (Moderate thermal expansions improve the feasibility of hermetically sealing these alloys to insulators.)

A study was conducted to assess the relative machinability of candidate alloys for each operation used to fabricate housings: turning, boring, cutoff, facing, drilling, reaming, and threading. Large machinability differences were observed and this suggests that header requirements be divided into three cost/strength categories, i.e., low cost/moderate strength (~ 200 MPa), moderate cost/high strength (~ 500 MPa), and high cost/very high strength (~ 700 MPa). We ranked the relative machinability of Inconel-718 and 625 with metals more commonly used in header manufacture. (See Fig. 7.) Table 1 lists the alloys appropriate to each strength category.

Table 1

CANDIDATE ALLOY COMBINATIONS FOR PYROTECHNIC DEVICE HEADERS

<u>Performance</u>	<u>Housing</u>	<u>Electrodes</u>
Moderate Strength	26-1 Stainless Steel	26-1 Stainless Steel or Hastelloy C
High Strength	Inconel-625	Inconel-625 or Hastelloy C
Very High Strength	Inconel-718 or β -C Titanium	Inconel-718 or Hastelloy C

We have also investigated the feasibility of using various types of insulators in these headers. Glasses, glass-ceramics and

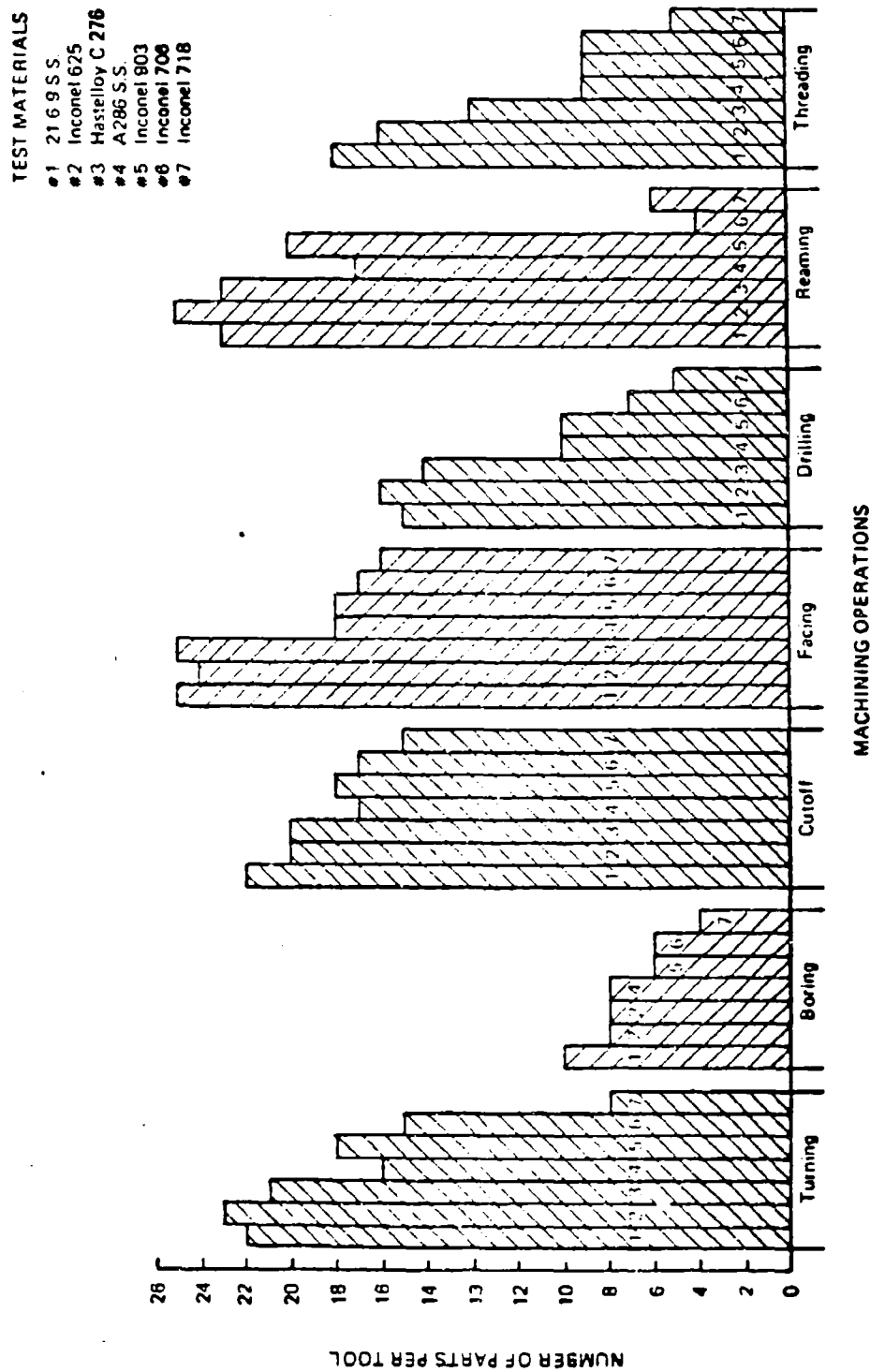


Figure 7. Machinability Test Results

brazed ceramics were evaluated on the basis of ease of fabrication, cost and technical reliability. Brazed alumina ceramic-to-metal seals are difficult to fabricate, require multiple firing operations, are expensive, and often dictate device design. To minimize stress cracking, the seal configuration must compensate for the difference in thermal expansion between the insulator and metal members. (Aluminum oxide has a low thermal expansion coefficient ($60 \times 10^{-7}/^{\circ}\text{C}$) relative to most metals used in headers.) A flow chart of the principle operations necessary to fabricate a brazed ceramic header shows that many steps are required (see Fig. 8).

Although many different glasses readily seal to metals, most commercial headers with glass-to-metal seals are fabricated using preforms of pressed and sintered glass powder. During charge cavity grinding the porous bubble structure of this material is exposed; these voids are traps for cleaning solvents and electroplating solutions. (See Fig. 9.) These contaminants can promote the corrosion of electrodes and bridgewires. In addition, most glass-to-metal seals are weak.

Glass ceramic-to-metal seals offer the greatest probability of meeting our consolidated header requirements. Glass ceramics can be molded like glass and bonded directly to oxidized metal surfaces, but they are stronger, more refractory, and have higher thermal conductivities than glasses. Another advantage of glass ceramics is that they can be made with a wide range of thermal expansion coefficients ($0-230 \times 10^{-7}/^{\circ}\text{C}$). (See Fig. 10.) Therefore, they permit great flexibility in seal design. For example, dog-logged electrodes, concentric ring electrodes and convoluted internal housing surfaces can be economically incorporated into the header design. (See Fig. 11.)

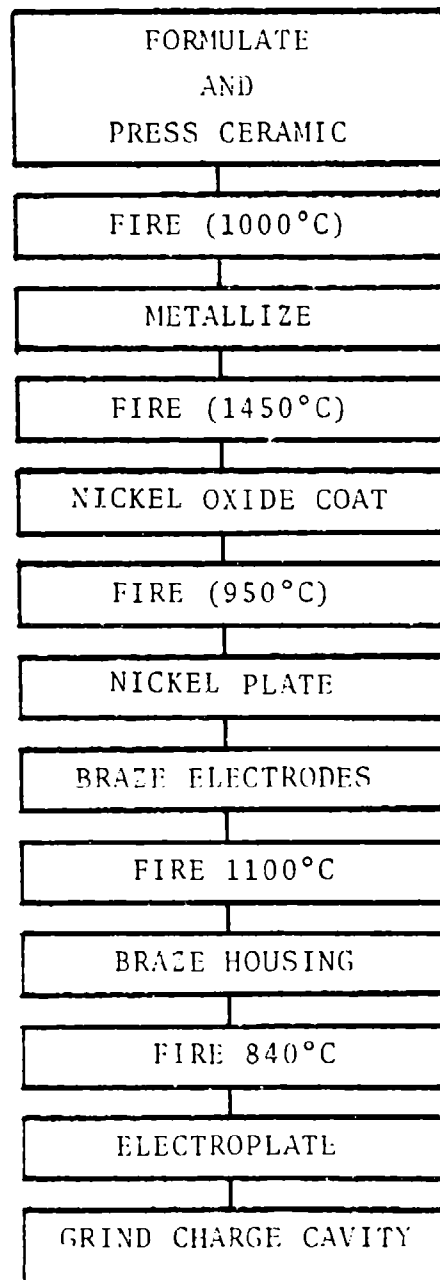


Figure 8. Typical Brazed Ceramic Header Fabrication Steps

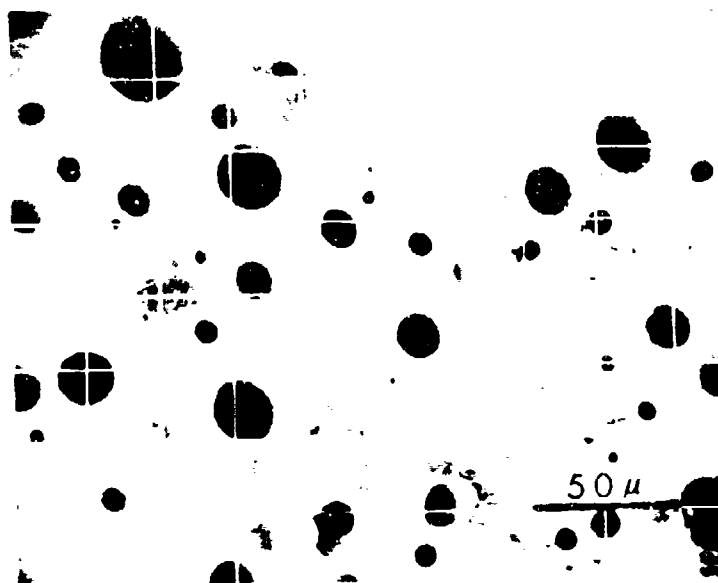
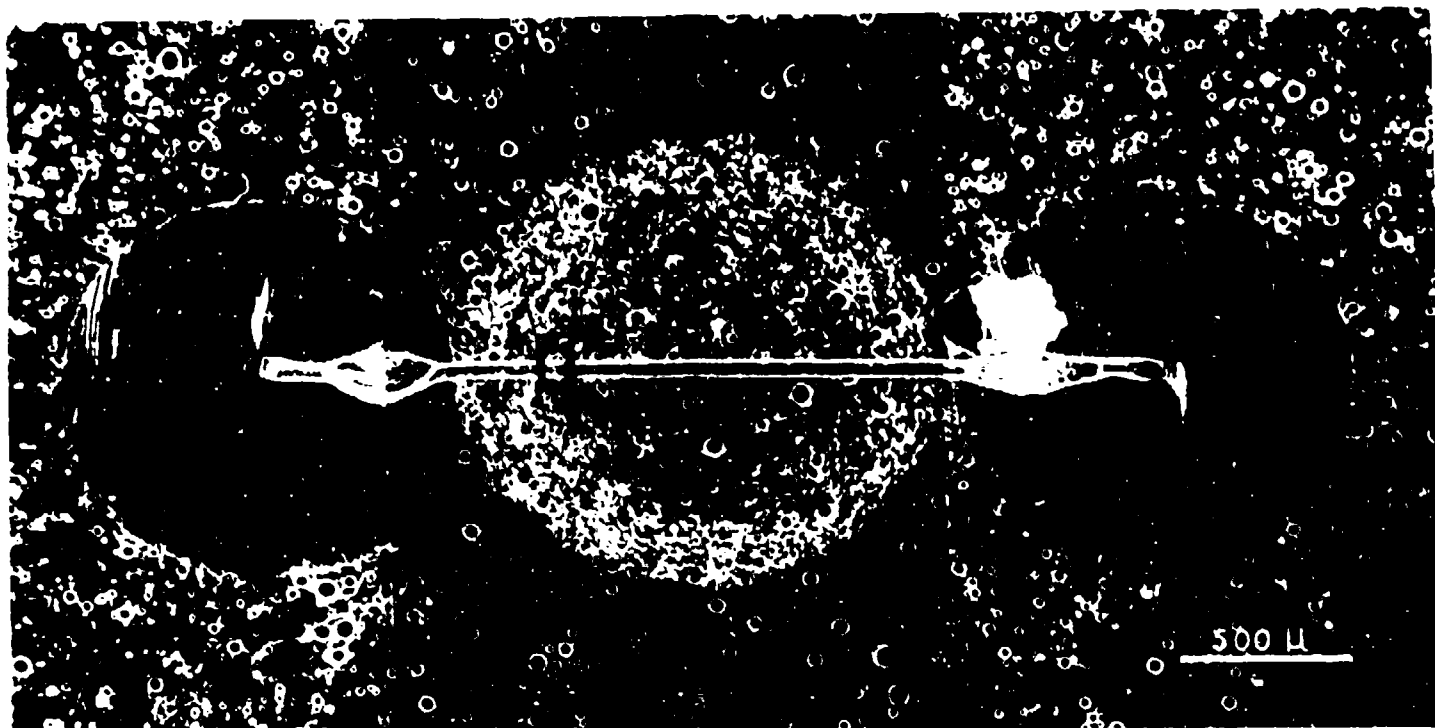


Figure 9. Typical Ground Charge Cavity Surface in a Header Fabricated with Pressed Powder Glass Preforms . (Areas noted by \square were analysed for chemical composition.)

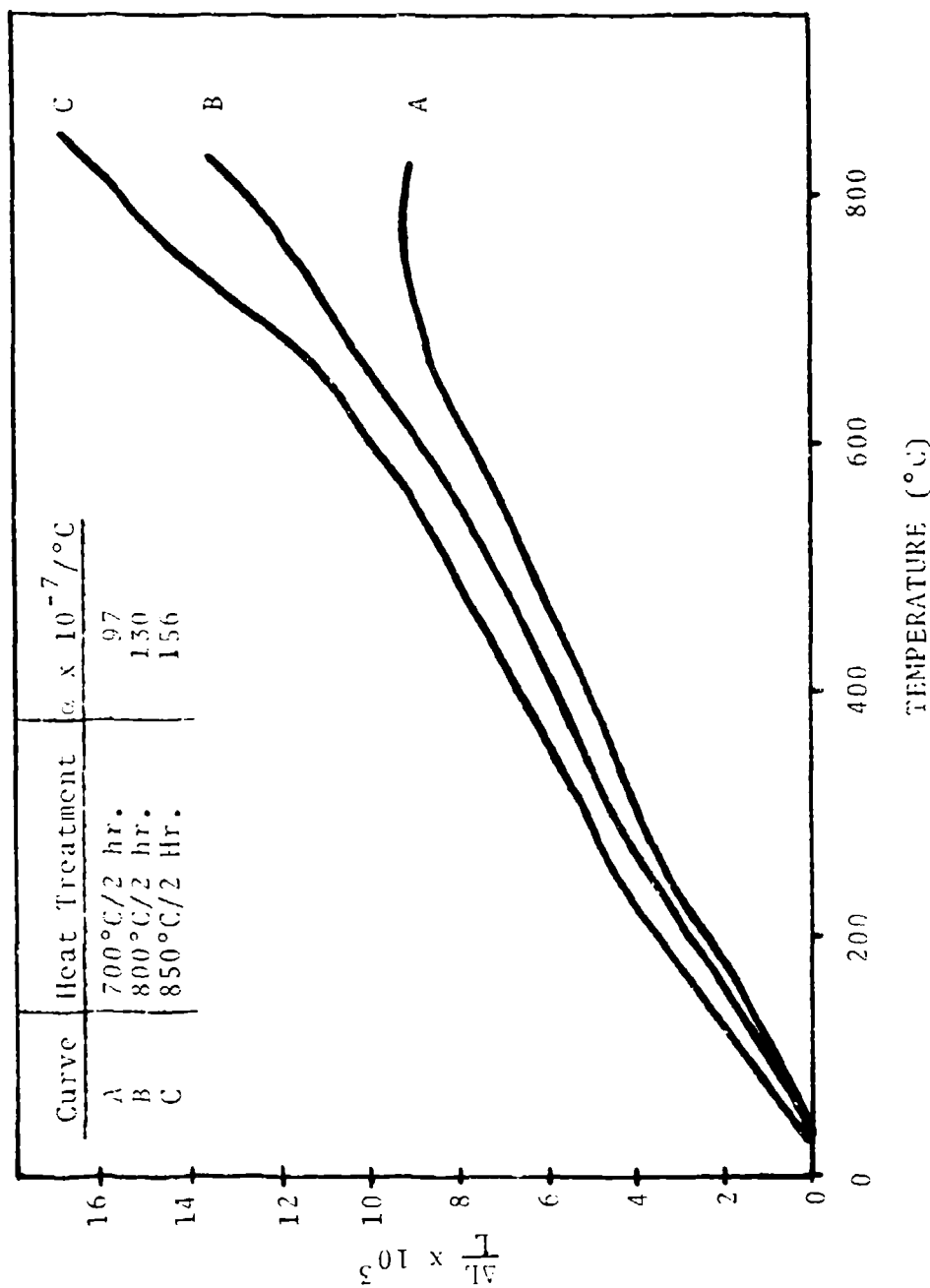


Figure 10. Crystal Phases which Develop on Heat Treatment Often Change the Thermal Expansion Characteristics of a Glass Ceramic

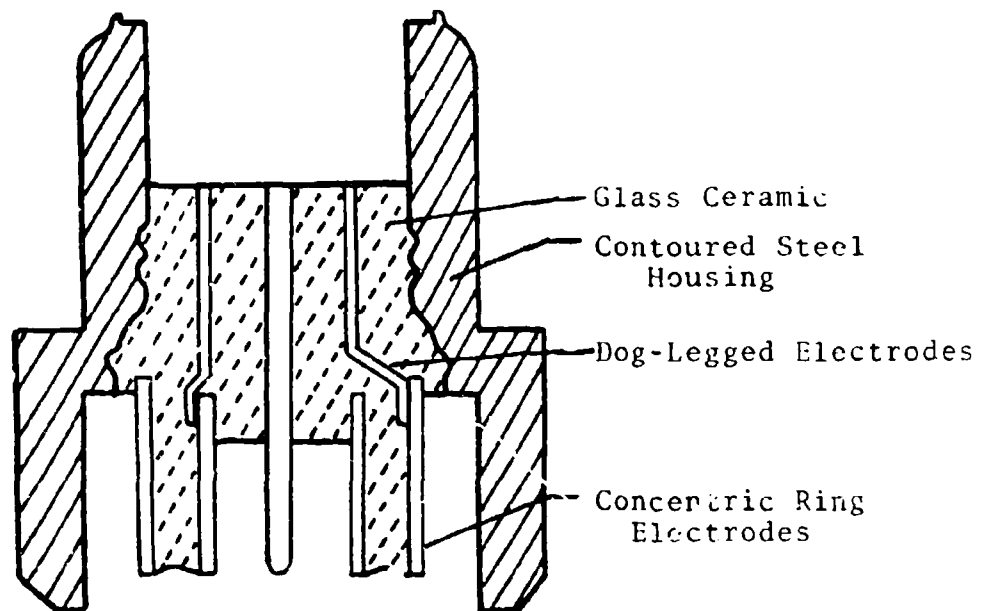


Figure 11 Glass Ceramic Seals Permit Great Internal Design Flexibility

IV. PROCESS DEVELOPMENT

At present, most glass and glass ceramic pyrotechnic headers are fabricated using preforms of sintered glass powder or solid glass tubing. The preforms and metal piece-parts are assembled on graphite or metal fixtures, then heated to melt and flow the preform. A hermetic seal is formed during this high temperature operation. Although the technique works well for most vitreous glasses, many glass ceramics tend to devitrify while heating the assembly to the sealing temperature. Viscosity increases as a

result of devitrification and often the glass ceramic does not flow and form properly. Bubble entrapment is a frequent problem. If seal temperature is raised above 1000°C, reactions between the graphite tooling, metal piece-parts, and glass impair tooling disassembly.

To address these problems, we are developing techniques for die casting hermetic seals. In this technique, a charge of molten glass ceramic (~ 1300°C) is cast directly into a heated mold (~ 450°C) containing several arrays of preoxidized metal piece-parts, e.g., electrodes and housings. (See Fig. 12.) A heated plunger is used to extrude the molten glass through runners connecting the charge cavity and the individual piece-part arrays. A hermetic seal is formed during the molding operation. After forming, the header is thermally processed to crystallize the glass ceramic. We have used this technique to fabricate several miniature pyrotechnic devices having complex internal configurations. These headers are leak-tight ($< 10^{-8}$ std cc atm/sec) after glass ceramic processing and externally appear to be bubble free. However, flat, acicular bubbles, scattered randomly along the metal/glass ceramic interface are frequently observed.

Efforts to identify and eliminate the source of gasses which cause these bubbles are underway. Attempts to degas the metal piece-parts, remove volatile constituents from the glass ceramic and engineer a process which precludes bubble formation have been unsuccessful to date.

Although our laboratory experiments utilize discontinuous, batch type fabrication operations, the use of focussed infrared heaters, hot gas jets or RF induction heaters could permit automation of this processing technique once the critical material and processing parameters are identified. We are also developing glass ceramic materials and processing techniques which permit simultaneous alloy precipitation hardening and glass ceramic crystallization.

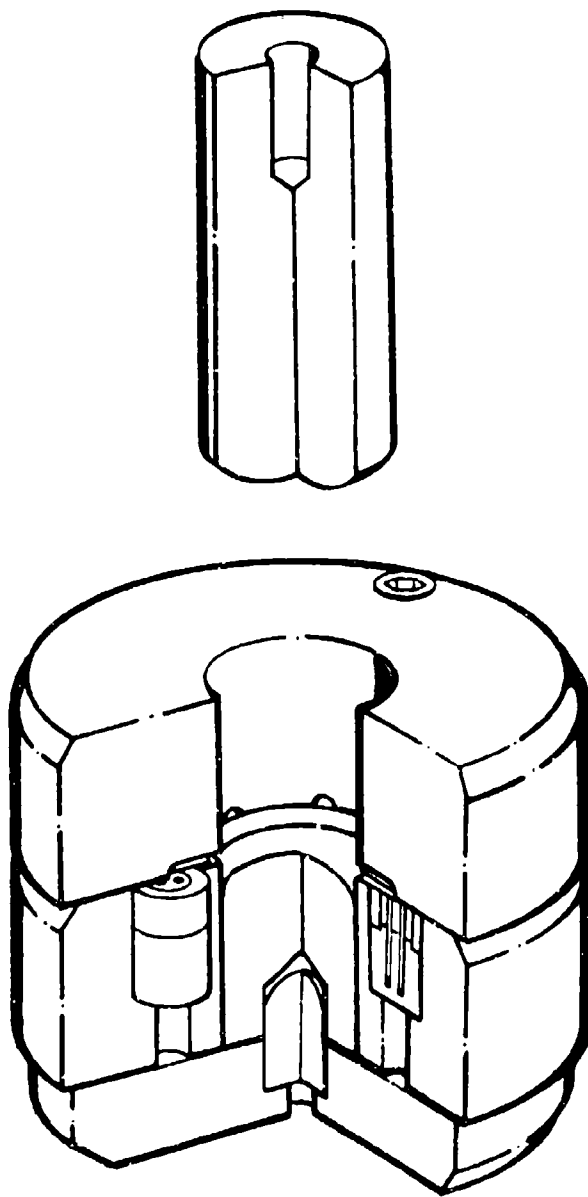


Figure 12 Cutaway of Die Casting Mold

V. SUMMARY

Although much additional experimentation is necessary we are confident that the combined efforts of our research, engineering and design programs will provide solutions compatible with our consolidated header requirements.

STUDIES OF FACTORS AFFECTING TRACER PERFORMANCE

by

T J Barton and M J Bibby

Royal Armament Research and Development Establishment

Fort Halstead Sevenoaks Kent

Abstract

Studies of the effect of spin and high velocity upon tracer performance are reported. Evidence is provided for the increase in burn rate with spin being due to the formation of a convex burning surface and consequent increased heat flow. The effect of velocity in reducing light output is shown to be due to reduced flame size. Improvements to tracer performance in high wind streams are possible by employing high magnesium content compositions, especially if pressurized by a restricting orifice. Even greater improvements in light intensity under blown conditions can be achieved with titanium fuelled compositions.

Introduction

Tracers are small pyrotechnic flares designed to provide a visible signature so that the trajectory of a projectile may be observed. To meet this requirement tracers must emit visible light (or infra-red if thermal imaging systems are employed) of sufficient intensity to be clearly observed, in bright daylight conditions, at the maximum range of the particular projectile. Figure 1 shows a typical tracer.

The range requirement for the projectile is a vital factor in tracer design since this will determine the intensity of light output that must be achieved, together with the necessary burn time.

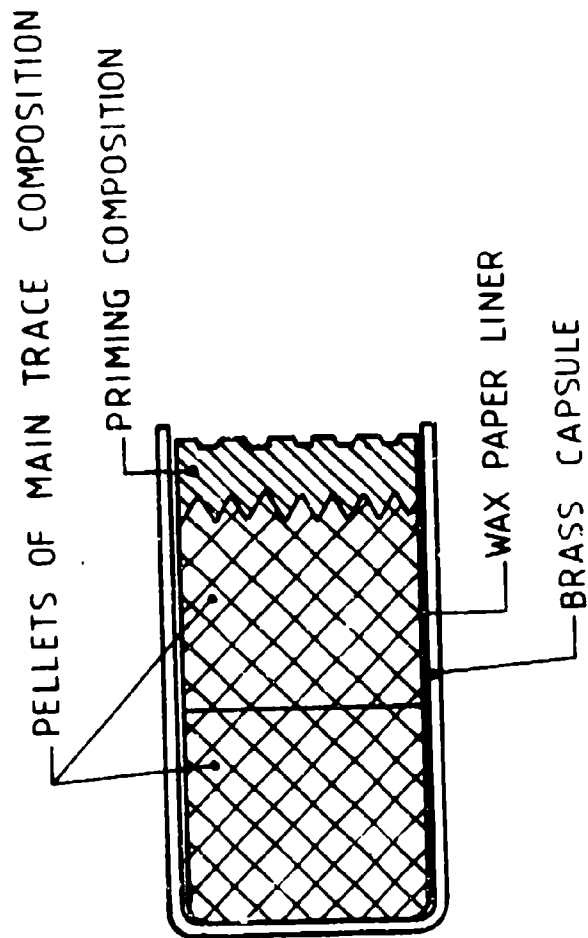


FIG.1 TYPICAL TRACER (CONSOLIDATED AT HIGH PRESSING LOADS (~ 50 tsi))]

Figure 2 shows the relationship between distance and intensity of light required for the source to be visible to the naked human eye. (1).

New technology in gun design together with new natures of ammunition have greatly increased the range requirement for tracers. Some rounds now need a tracer that is visible at ranges in excess of 3.0km(2). At the same time the rear end profile of the projectile has been dramatically decreased thereby decreasing the flame size. These new conditions have necessitated the manufacture of much brighter tracer compositions.

In addition to burning steadily to produce bright visible light tracers must withstand very adverse environments. Firstly the tracer must be readily ignited by the propellant gases, but at the same time must not be broken up, penetrated or damaged by the blast effect. Following the hot propellant blast effect the tracer experiences a violent acceleration with a consequent set back force.

When the round emerges from the barrel the tracer undergoes a very rapid change in external pressure, dropping from a value of several tons per square inch to a partial vacuum, the vacuum value depending upon the shape and velocity of the round. During the flight to target the tracer continues to experience the low pressure region at the base of the round as well as a supersonic wind stream. (3)

These in-flight conditions are shown in figure 3; their main effect upon the tracer is to contain the flame to a small region at the base of the projectile. One further factor that affects tracer functioning is the spin of the particular round of ammunition. Depending upon the design of the round a tracer may have to function at spin rates between 0 and 1500 rps.

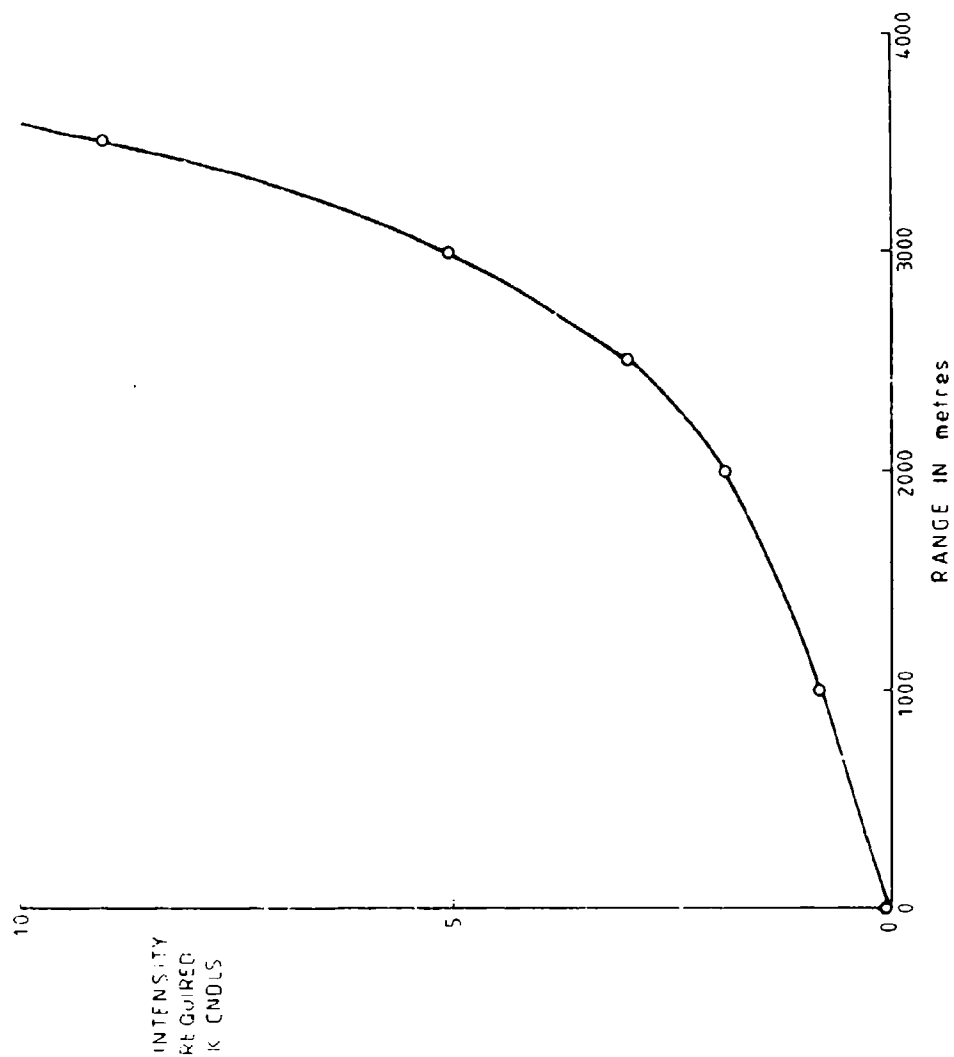


FIG. 2 INTENSITY OF POINT LIGHT SOURCE REQUIRED FOR VISIBILITY AT VARIOUS RANGES (METEOROLOGICAL VISIBILITY 10 km)

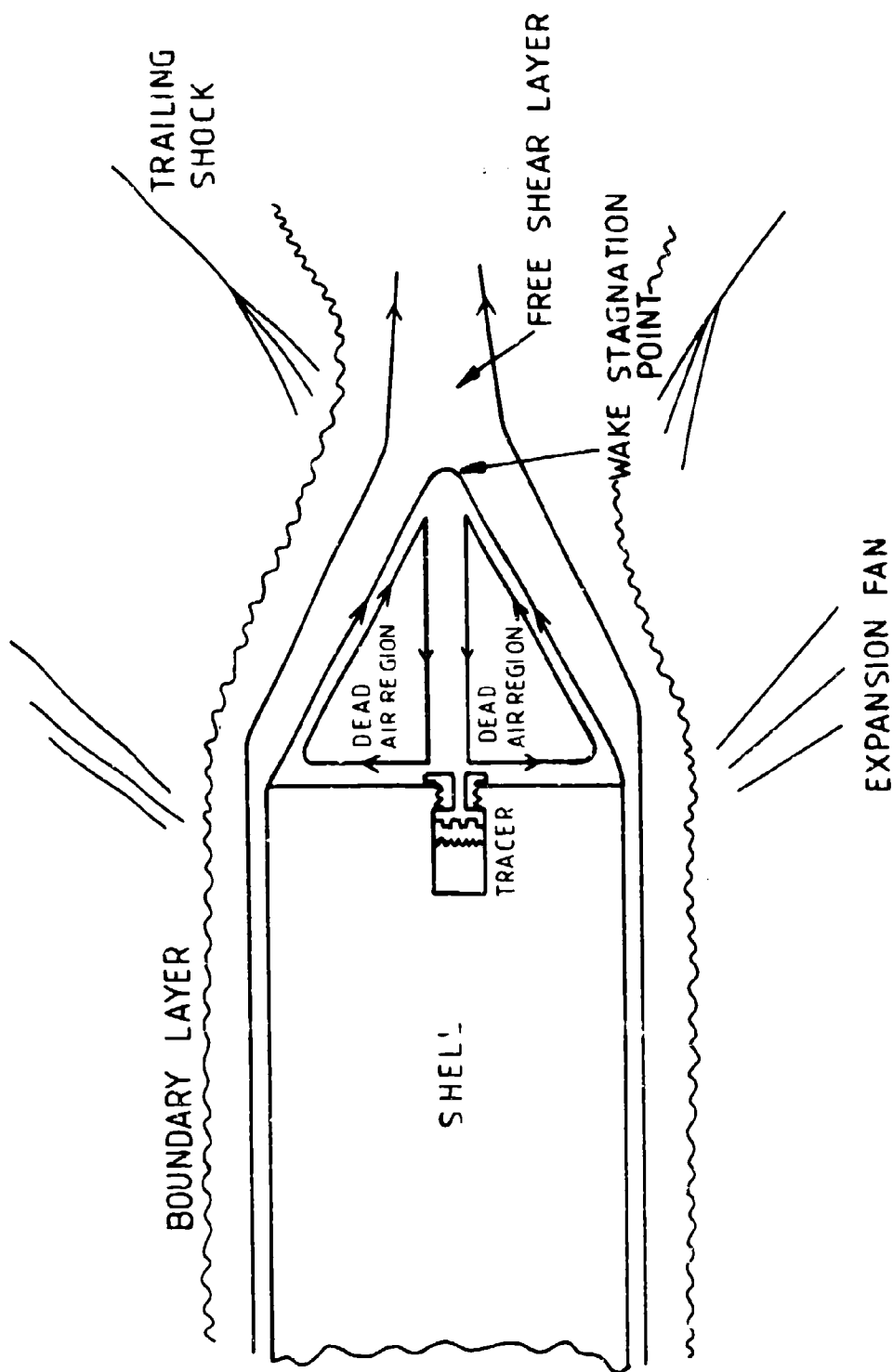


FIG. 3 CONDITIONS EXPERIENCED BY TRACER AT REAR END OF PROJECTILE

Results

To aid the tracer development programmes currently being carried out, RARDE has instigated research work to examine the effect of the various environmental factors upon tracer functioning.

Spin.

The rate of burning of many tracers is very significantly increased by high spin rates. Some previous workers have suggested that the increase in burn rate is caused by pressurisation of the burning surface by slag constricting the orifice (4). Puchalski postulated a different mechanism in which a convex burning surface is formed in the spinning tracer and this increases the heat transfer into the unreacted composition (5). However, he was not able to produce much evidence for a convex burning front. He also observed that with fuel deficient magnesium compositions the candle power was barely altered by spin whereas with stoichiometric or fuel rich compositions the light output increased with spin.

In this investigation it was shown that there was little evidence for pressurisation being responsible for the burning rate increase. The size of orifice formed by the slag was measured and it was shown that it was not small enough to cause any significant pressure rise over the burning surface. This was demonstrated by directly measuring the pressure, using a piezo gauge, created by burning tracers when constrained by steel plugs with various diameter holes in them. In addition examination of the spectra of tracers burning under spin showed no evidence for any pressure broadening of the bands.

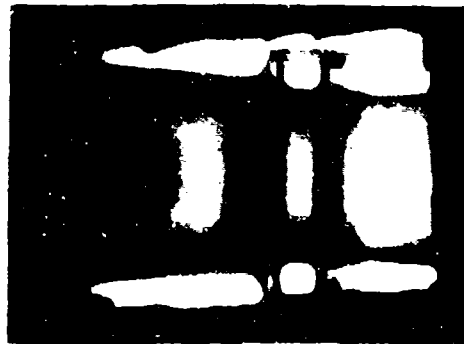
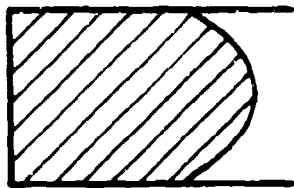
Tracers burning both statically and under spin were examined by X-ray. Statically the tracers burnt with a flat or slightly concave burning front but under spin this burning surface became

convex. These results are shown in figure 4 and confirm the previous work of Puchalski.

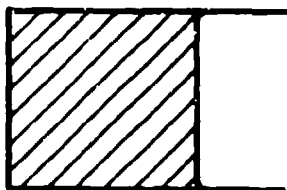
The explanation for the increase in burn rate appears to lie in an increased heat flow back into the unburnt composition. Under spin the slag produced by combustion is centrifuged to the side of the tracer capsule, or cavity, increasing the heat flow at the edge, leading to a convex burning surface. This convex surface has a larger area than a flat one and thus feeds more energy into the unburnt composition. A crude calculation shows that an increase of only 20% in heat flow could account for the maximum observed increase in burning rate.

These results outlined above were obtained from a study of existing slow burning tracer compositions; for much faster burning, high magnesium content compositions, very different behaviour was observed. Fast burning compositions showed very little change in burn rate with spin and X-ray examination indicated a virtually flat burning surface under spin. It would seem that the higher burning rate prevents the formation of the convex burning surface, possibly due to a different slag nature or simply that the slag concentration at the sides is insufficient to increase the edge heat flow at the faster burning rates.

The variation in light output with spin rate and from composition to composition was rather complicated. It was generally found that the slow burning compositions (0.07in/sec) increased their light output as the spin rate was raised from 0 to 400rps, above 400rps the light output tended to remain roughly constant. This also agrees with Puchalski's model. However changes in the particle size of the oxidant could cause a decrease in light intensity above 400rps. For the faster burning compositions (0.35in/sec) the light output usually decreased slightly between 0 and 800rps. This was beyond the range explored by Puchalski.



SPUN



STATIC

FIG. 4 SHAPE OF BURNING SURFACE STATIC AND UNDER SPIN

Wind Stream Effects

The effect of supersonic wind streams upon tracer functioning using a Mach 1.5 wind tunnel has been examined. Preliminary studies showed that projectiles with narrow cross sectional area exhibited the greatest reduction in light intensity at Mach 1.5. Consequently most of the studies were carried out on narrow projectile models. The results quoted here do not necessarily carry over to other shapes.

Traditional magnesium/strontium nitrate tracer compositions exhibited an initial increase in light output with increasing wind velocity, due to clearance of smoke. This was followed by a decrease tending to level off above Mach 1. The rate of this decrease in light intensity varied from composition to composition but was steepest for the slow burning low magnesium content formulations. For example a 38% magnesium composition had its light output reduced from 4K candelas static to 50 candelas at Mach 1.5, whilst a 59% magnesium composition was only reduced from 50K candelas static to 6K candelas at Mach 1.5. (Figure 5)

In addition to conventional magnesium based compositions, ones using titanium metal as the fuel were examined. Although titanium based tracers have a lower static light intensity they are much less susceptible to degradation of light output by velocity. Eventually titanium compositions were produced which were virtually independent of wind speed up to Mach 1.5. The light output of these very fast burning titanium compositions at Mach 1.5 was three times that of the brightest magnesium tracer.

A film study of the tracers burning in the wind tunnel revealed a correlation between flame size and light intensity. For the magnesium tracers as the wind velocity increased the flame size, due to con-

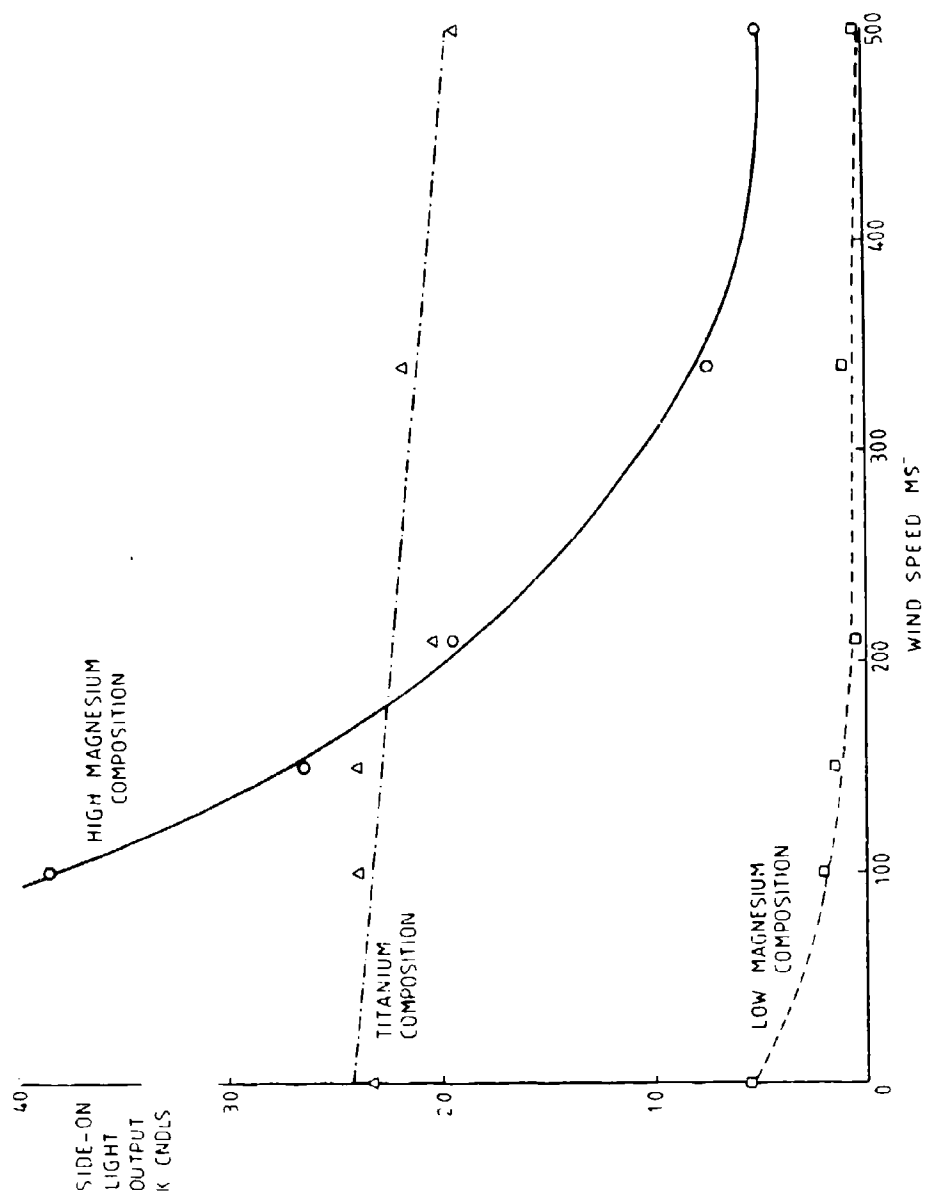


FIG 5 LIGHT OUTPUT VERSUS WIND SPEED

tainment, decreased.

Fast burning titanium compositions completely broke out of the constriction region at all wind velocities and exhibited completely independent light intensity with wind speed.

The fact that flame size seemed to be the controlling factor for light intensity, this being the main reason for the very good results obtained with titanium fuelled compositions, suggested that improvements in the performance of magnesium fuelled tracers were possible by use of flame shapers or pressurisation. When a restricted orifice plug is used with a tracer an internal pressure is generated which can cause the combustion products to be ejected at sufficient velocity to break out of the confinement region.

Experiments at Mach 1.5 with small diameter orifice retaining plugs produced very large increases in flame size and consequently light output. There was naturally a penalty in terms of severely reduced burn times. These small orifices did have the useful property of making the burning rate independent of the external pressure. This was demonstrated in vacuum tank experiments. This independence of pressure means that the tracer will not be subject to non-propagation problems caused by the partial vacuum at the base of the projectile. Figure 6 shows how the light output and burn time change with orifice area.

Conclusions

A probable explanation for the increase in burn rate with spin has been produced. It would also seem possible to improve the performance of tracers for spun ammunition by the use of higher magnesium content faster burning compositions, which will be much less effected by spin.

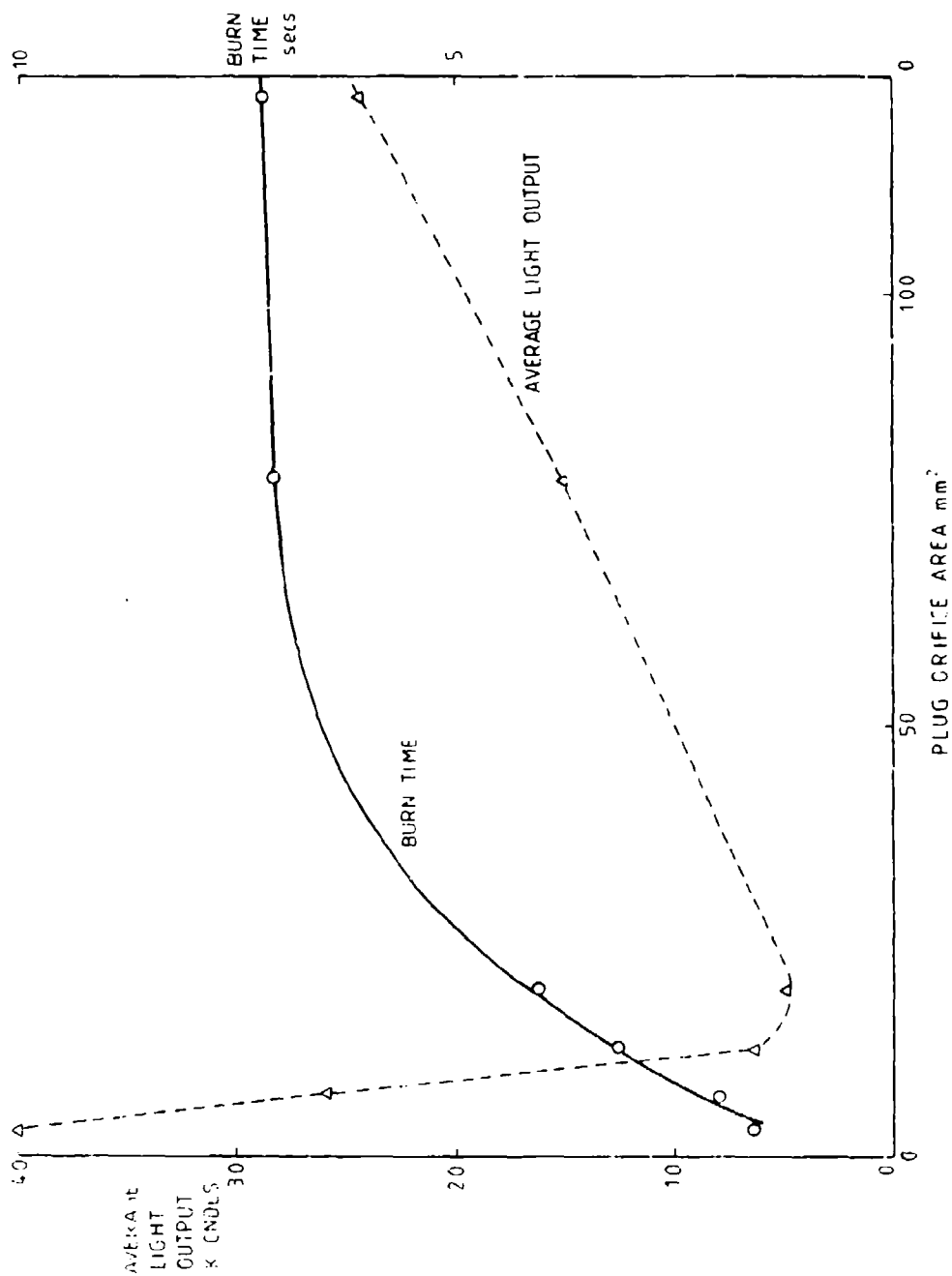


FIG. 6 BURN TIME AND AVERAGE LIGHT OUTPUT AS A FUNCTION OF PLUG ORIFICE AREA

It has been shown that light output of tracers is related to flame size and shape and consequently wind velocity, once again higher magnesium content compositions produced the best result. It was also demonstrated that titanium fuelled tracers could produce the highest light intensity under supersonic wind conditions. However improvements to magnesium based tracer performance could be achieved by pressurisation using small exit nozzles. These small orifice plugs also protected the tracer against the effects of the low pressure region at the base of the projectile.

References

- (1) W E Knowles Middleton "Vision through the atmosphere". University of Toronto Press, 1952.
- (2) International Defence Review, P259 (1976).
- (3) J E Bowman and W A Clayden. American Institute of Aeronautics and Astronautics, 5, 1524 (1967).
- (4) D C A Izod and R F Eather, "Proc 4th International Pyrotechnics Seminar", 10-1 (1974).
- (5) W J Puchalski, "Proc 4th International Pyrotechnics Seminar", 14-1 (1974)

INSENSITIVE CONDUCTING COMPOSITION IGNITERS

John R. Bentley
Materials Research Laboratories
Defence Science & Technology Organisation
P.O. Box 50, Ascot Vale, Victoria 3032, Australia

ABSTRACT

An insensitive conducting composition igniter has been developed which is particularly suited to pyrotechnic stores where electrostatic or induced electromagnetic energy could present a hazard. The igniter has been designed to not function when subjected to transients equivalent to electrostatic discharge from charged personnel and to dissipate a minimum of 1 Amp/1 Watt continuously applied to the firing pins.

Electrical initiation is one of the most common means of igniting pyrotechnic and other explosive materials. In all cases electrical energy is degraded to heat which in turn raises the temperature of a small quantity of explosive above its ignition temperature and the ensuing reaction ignites or initiates the main charge. Various systems have been used to convert the electrical energy into heat but the two most common systems are bridgewires (BW) and conducting compositions (CC). For a BW system a small metallic filament is connected across the firing electrodes; the filament is embedded in pressed or plastic bonded explosive. Passage of electric current heats the wire and so ignites the explosive. CC devices have two electrodes separated by a gap across which is pressed an explosive composition made conducting by the admixture of 3.5% graphite or metallic powder. A large number of non-uniform conducting paths are formed through the composition and, when a voltage is applied across the electrodes, current flowing through the network of paths causes localized heating of the explosive. If the current is above a threshold level, ignition will result.

The electrical characteristics of CC caps (resistance and sensitivity) are related to the pressing load, the geometric configuration of the electrodes and the percentage, particle size and shape of the graphite. The major disadvantage of CC caps is that it has proved very difficult to control these parameters. Within a batch of caps a wide range of resistances occurs and the variance of electrical sensitivity is large.

Despite this fairly major technical limitation and production problem, CC caps are widely used where their particular characteristics are required. In particular, CC caps are cheap to produce and have a fast functioning time. They can also be designed to be very sensitive and can function reliably from about 10 μ J. Their major application is thus in cartridge case primers for high rate of fire small calibre munitions and fast reaction time/limited power supply electronic fuzes.

CC caps have also been used in other applications where high sensitivity and fast reaction are not required and the N43 primer is one such example. This primer is used in Naval 4.5" ammunition and has a no fire level greater than 100 μ J. It is therefore comparable to the more sensitive bridgewire devices, e.g., T30 detonator (100 μ J all fire, functioning time 5 μ s and resistance 2.10 Ω). The resistance and threshold sensitivity of a range of CC and BW initiators are given at Table 1.

Table 1
ELECTRICAL CHARACTERISTICS OF BRIDGEWIRE
AND CC IGNITERS

<u>Bridgewire</u>			<u>Conducting Composition</u>		
R	E_t	I_t	R	E_t	V_t
0.9-1.6	2.3 mJ	0.3A	20-250	100 μ J	10
10-16	0.2 mJ	0.045A	20-250	1 μ J	4
2-2.5	1.6 mJ	0.22A	20-250	35 μ J	4
0.4-0.6	7.5 mJ	0.6A	500-2000	1 μ J	4
0.9-1.7	7.0 mJ	0.45A	15-50	100 μ J	4

E_t = Energy required for 0.1% function

I_t = Current required for 0.1% function

V_t = Voltage required for 0.1% function

For modern weapons and commercial use it is desirable to minimise the possibility of inadvertent initiation from induced currents and electrostatic discharge. Devices should therefore be as insensitive as possible commensurate with the firing supply. MIL-I-23659C is the US general design specification for electric initiators and states that devices should not fire when subjected to 1A or 1W continuous power. It has proved difficult to dissipate this amount of power from conventional bridgewires into the explosive surrounding them without exceeding the ignition temperature of the explosive. Low sensitivity BW devices can be

constructed using techniques such as lengthening the bridgewire, increasing its surface area by flattening it or increasing its diameter, bonding the bridgewire to an inert thermally conducting substrate and using high temperature of ignition or thermally conducting explosives around the wire. Usually, deposited etched bridge elements using semiconductor technology are required to meet 1A, 1W criteria.

CC devices have traditionally not been used where high levels of power dissipation are required. The aim of the work described in this paper was to develop a CC igniter which would dissipate large amounts of energy, both continuous and transient, yet maintain the advantages of low cost, ruggedness and fast functioning times associated with CC systems.

In a CC cap, the graphite forms a large number of high resistance paths between the two electrodes. These paths are not of uniform resistance but have areas of high resistance at points of contact between adjacent graphite particles. These contact points serve to concentrate the energy in a number of hot spots rather than distribute it over a well defined area as in the case for a bridgewire. The minimum firing energy for CC caps has been estimated at 1 μ J whereas the minimum hot spot energy to cause initiation is less than 10^{-5} μ J. Thus even in the most sensitive CC caps there are probably a very large number of hot spots and a large number of conducting paths. The approach used to desensitize CC caps was to increase the number of hot spots and thus divide the available energy between more ignition sites. This was achieved by increasing the percentage of graphite, which would increase the number of conducting paths, and decreasing the particle size of the graphite, which would increase the number of junctions or hot spots in each path.

In order to meet the 1A and 1W no fire criteria without excessively decreasing the sensitivity of the device the mean resistance should be close to 1 Ω . Two types of graphite were used to produce these igniters and for both types the percentage of

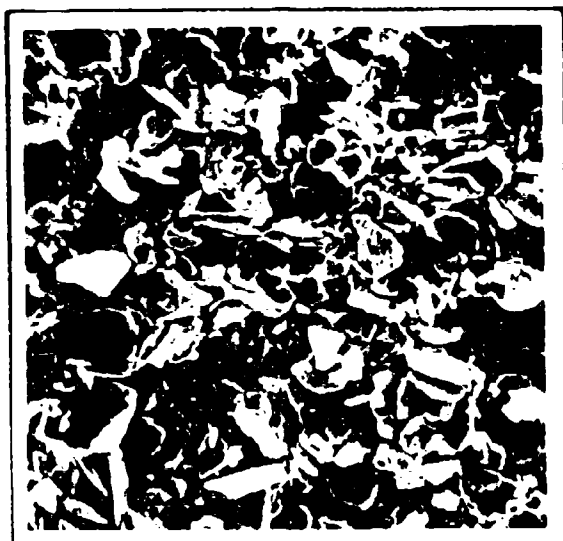
graphite was increased until the resistance of the device was close to 1 Ω . For the smaller particle sized graphite (Foliac Super Fine Flake) 7% graphite was required; for the larger particle sized material (Dohms Air Floated Graphite passing a 45 μ m sieve) 16% was required. The particle size and shape of both types of graphite were estimated from photomicrographs. These are shown at fig. 1. A composite batch using 5% Foliac and 7% DAF graphite was also tested. The explosive selected for these tests was β monobasic lead styphnate, a relatively low powered primary explosive which will not burn to detonation. It has been used widely for initiating pyrotechnic stores where very vigorous ignition can be detrimental to performance. This material was especially prepared in a fine particle size to aid mixing with the graphite. Readily available standard CC igniter bodies were used as a test vehicle and pressing was carried out using a dead load press and a pressing load of 650N. The experimental igniters are shown at fig. 2.

25 igniters of each group were produced and the resistance of each igniter was measured. The results are shown at Table 2. For each group the mean and standard deviation was calculated. The spread of resistance was similar to that normally observed in BW devices.

Table 2

RESISTANCE CHARACTERISTICS OF INSENSITIVE CC CAPS

<u>Composition</u>	<u>Mean Resistance (ohms)</u>	<u>Range (ohms)</u>	<u>Standard Deviation</u>
MBLS 93% Foliac Graphite 7%	1.54	1.23 - 1.74	0.18
MBLS 84% DAF Graphite 16%	0.78	0.63 - 0.94	0.10
MBLS 88% DAF Graphite 7% Foliac Graphite 5	0.39	0.63 - 1.45	0.17



x140

Foliac Super Fine Flake



x140

Behms Air Floated Graphite

Fig 1 : SCANNING ELECTRONMICROSCPE MICROGRAPHS

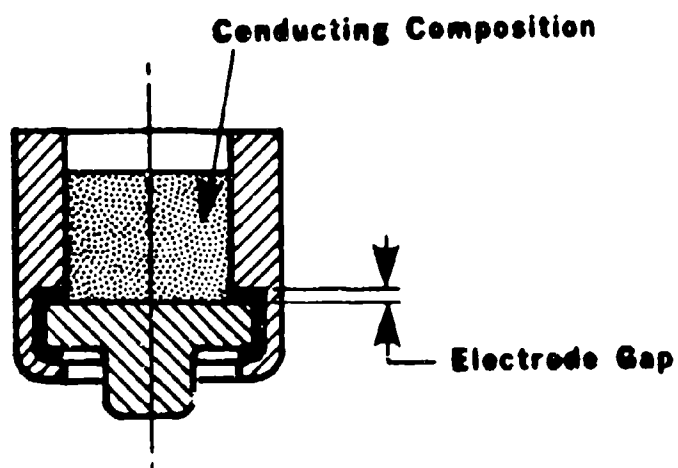


Fig 2 : TYPICAL CONDUCTING COMPOSITION CAP

NON-FUNCTIONING TESTS

Each device was subjected to a static sensitivity test. The test apparatus was designed using MIL-I-23659C as a guide. The test involves discharging through a 5 k Ω resistor a 500 μ F capacitor charged to 25 kV, connected to the firing leads and the case. This arrangement is used to simulate the worst conditions which could pertain for a charged human body. All igniters passed this test without functioning.

A 100 s, 1A DC pulse was then applied to each device. Those which had a resistance of less than 1 Ω were then subjected to a further 100 s pulse at a current determined such that 1W was applied to the devices. All igniters passed these tests without functioning.

FUNCTIONING TESTS

15 igniters from each batch were subjected to 0.5 s terminated DC pulses to determine their 50% firing current. The remaining 10 igniters were subjected to capacitor discharge firing tests to determine their 50% fire energies. The Bruceton technique was used to determine the test levels and calculate all fire and no fire current and energy. These results are summarised at Table 3.

Table 3

FUNCTIONING TESTS				
<u>Composition</u>	<u>50% Fire Current (A)</u>	<u>σ.A</u>	<u>50% Fire Energy μJ</u>	<u>σ.μJ</u>
MBLS 93% Foliac Graphite 7%	2.59	0.11	64	9 μ J
MBLS 84% DAF Graphite 16%	3.90	0.10	94	20 μ J
MBLS 88% DAF Graphite 7% Foliac Graphite 5%	3.48	0.23	63	15 μ J

These tests indicated that CC caps could be produced which met the major clauses of MIL-I-23659C but, although the power dissipation characteristics of these devices was very good, all devices tested had similar and low energy sensitivities. Other investigations at MRL have shown that ignitions by static discharge of CC devices with relatively high resistances can occur if the threshold energies are less than 100 μ J. The threshold energy for each of the devices tested indicated that they could possibly be initiated by static discharges from charged personnel.

It was considered desirable to increase the threshold energy of these devices and initially an empirical approach was used. Devices were filled using various explosives and sufficient foliac graphite to produce an igniter with a nominal resistance of 1 Ω .

This aspect will be investigated in detail at a later date, but preliminary results gained from firing a very small sample of devices are given at Table 4. The results show that devices can be produced with energy thresholds in excess of 1 mJ and are thus similar in this respect to bridgewire igniters which have an established safety record for electrostatic discharge through the firing leads.

Table 4

<u>Composition</u>	<u>T of I</u>	<u>Sensitivity to Static</u>	<u>E 50%</u>	<u>I 50%</u>
Boron/Lead Chromate Foliac Graphite 7%	> 500	0.45J ignites 0.045J no ign	1.8 mJ	4.75A
Potassium Picrate Foliac Graphite 10%	260	0.45J ignites 0.045J no ign	0.7 mJ	2.5A
Basic Lead Styphnate Foliac Graphite 7%	310	3 μ J	64 μ J	2.6A
Normal Lead Styphnate Foliac Graphite 7% Foliac Graphite 8%	280	15 μ J	72 μ J 150 μ J	2.75A

For a BW igniter most of the threshold energy is required to raise the temperature of the wire to the ignition temperature of the explosive. For an ICI type A fuze head E_t is 2.3 mJ. In excess of 1.7 mJ is required to raise the temperature of the wire to 300°C. Thus for BW devices the thermal response characteristics of the explosive are of secondary importance. These results indicate that such is not the case with CC devices and that the thermal response characteristics of the explosive is an important factor in determining threshold energy for these devices. Other explosives, particularly those which are relatively insensitive to electrostatic discharge will be tested later in an attempt to increase threshold energy.

CONCLUSIONS

This preliminary investigation indicates that insensitive CC igniters can be produced which will dissipate between 2-4 watts continuously applied to the firing leads. These devices can withstand a 25 kV transient which simulates an electrostatic discharge from a charged person even when the threshold energy of the devices is low (50 µJ).

By selecting insensitive explosives for the filling the threshold energy can be increased to in excess of 1 mJ. Future work will be aimed at increasing this threshold to approximately 5 mJ.

DISPOSAL OF COLORED FLARE COMPOSITIONS

Shib C. Chatteraj
Theresa A. Dreho¹
Clarence W. Gilliam

Applied Sciences Department
Naval Weapons Support Center
Crane, Indiana 47522

ABSTRACT

This is the final report of an exploratory development project performed on the disposal/reclamation of colored flare compositions under the pollution abatement program. The objective of this study was to develop physical and/or chemical processes on a laboratory scale for disposal of excess, obsolete or unserviceable Navy colored flare devices in an environmentally acceptable manner. The technical knowledge gained from this study is to be used in the design, construction and operation of a pilot plant for disposal of these devices and to reclaim, if possible, some of the major ingredients in the flare compositions.

A disposal/reclamation method was developed which consisted of separating the soluble material from the insoluble material in a flare composition by water dissolution. Flare compositions were dissolved in water and the insolubles separated by filtration. The aqueous solution obtained after filtration contained the salts, such as, potassium perchlorate, strontium nitrate and barium nitrate. These salts were recovered as a mixture by concentration and addition of appropriate reagents. The magnesium can be separated from the rest of the insolubles by flotation or sieving. Complete separation and reclamation of all the major components of the flare composition could not be achieved by using water alone. Explanations are given for the observed behavior.

Reactions were observed in the systems which led to the production of hydrogen and hydrogen sulfide as reaction products. Sensitivity tests on the separated mixtures show that the separated solubles and insolubles are less sensitive than the original compositions and could be safely stored or sold as the recovered mixtures.

INTRODUCTION

Almost a decade ago the Naval Sea Systems Command initiated a broad program of pollution abatement concerning pyrotechnics. To date, a number of important studies¹⁻⁶ have been made under this program. These studies include research and development of disposal methods on a laboratory scale and on a one-tenth pilot plant scale. Pilot plants for the disposal of illuminating flares and red phosphorus smoke compositions have been successfully demonstrated.^{5,6}

The objective of this study is to develop physical and/or chemical processes on a laboratory scale for disposal of excess, obsolete and/or unserviceable Navy pyrotechnic colored flare devices in an environmentally acceptable manner. Consistent with this objective, an effort has been made in this study to develop a single general approach or process applicable to all colored flare devices and to reclaim some of the chemical ingredients present in the flare compositions.

According to a recent inventory of Navy colored flare devices, there are a large number of different devices containing a total of a few thousand kilograms of flare compositions awaiting disposal. Additional quantities of scrap material are generated each year as a result of production operations.

The compositions for some representative red, yellow, green, blue and white flare devices are given in Tables 1 - 5, respectively. An analysis of Tables 1 - 5 shows that a great majority of the flare compositions contain magnesium in substantial amounts and that each composition generally contains many ingredients. In addition to the composition, each flare device will contain numerous other ingredients present in the first fire/ignition compositions, expellant charge, primer mix, delay mix, and other formulations. Needless to say, a very complex mixture must be dealt with and will undoubtedly complicate whatever approach or method might be chosen to attain the objective of this study.

TABLE 1. RED FLARE COMPOSITIONS (WEIGHT %)

	<u>Mk 66</u>	<u>Mk 13</u>		<u>Mk 1</u>	<u>Mk 2</u>
Strontium Nitrate	37	45	45	42	-
Potassium Perchlorate	15	15	25	-	-
Potassium Chlorate	-	-	-	42	64
Magnesium	29	20.4	17.5	-	-
Strontium Carbonate	-	-	-	-	18
Hexachlorobenzene	-	12	-	-	-
Polyvinyl Chloride	-	-	5	-	-
Asphaltum	14	7	7.5	-	-
Shellac	-	-	-	16	18
Binder Solution	5	-	-	-	-
Linseed Oil	-	0.3	-	-	-
Castor Oil	-	0.3	-	-	-

TABLE 2. YELLOW FLARE COMPOSITIONS (WEIGHT %)

	<u>Mk 115</u>	<u>Mk 118</u>	<u>Mk 99</u>
Barium Nitrate	32	20	53
Potassium Perchlorate	17	21	-
Sodium Oxalate	24	19.8	15
Magnesium	19	30.3	12
Hexachlorobenzene	-	-	10
Asphaltum	4	3.9	-
Laminac	-	-	10
Binder Solution	4	5	-

TABLE 3. GREEN FLARE COMPOSITIONS (WEIGHT %)

	<u>Mk 116</u>	<u>Mk 117</u>	<u>Mk 2</u>
Barium Nitrate	46.55	22.5	40
Potassium Perchlorate	21.92	32.5	-
Barium Chlorate	-	-	50
Magnesium	15.28	21	-
Copper	-	7	-
Polyvinyl Chloride	13.00	12	-
Shellac	-	-	5
Red Gum	-	-	5
Binder	3.25	5	-

TABLE 4. BLUE FLARE COMPOSITIONS (WEIGHT %)

	<u>Mk 1</u>	
Barium Nitrate	-	19.5
Potassium Perchlorate	-	39.8
Potassium Chlorate	56	-
Cupric Chloride	22	-
Cupric Oxide	13	-
Copper Ammonium Sulfate	-	-
Paris Green	-	32.6
Arsenic Trisulfide	-	-
Shellac	7	-
Stearine	2	8.1

TABLE 5. WHITE FLARE COMPOSITIONS (WEIGHT %)

	<u>Mk 2</u>
Potassium Nitrate	54
Antimony Trisulfide	18
Sulfur	13
Barium Nitrate	13
Dextrin	2

The quantity of colored flare composition available for disposal is relatively small when compared to other classes of pyrotechnics, e.g., illuminating, phosphorus, or infrared compositions. The small quantities do not negate the need for a disposal process. However, because of the relatively small quantities, the development of a sophisticated process was not considered necessary nor cost-effective at this point. This study has been limited to an investigation of a method for demilitarization and disposal that converts hazardous pyrotechnic compositions to safe, easy to handle materials that could be stored or sold as mixed metals and as mixed oxidizers. Some of the more esoteric questions about chemical reactions which occur during the disposal process are beyond the scope of the study and are left unanswered. It should be pointed out that, while these answers may be important to an understanding of the chemistry of the systems, the fact that they are unanswered in no way affects the results of this work.

In earlier work, several techniques including water dissolution, organic solvent dissolution and incineration have been investigated for the disposal of different types of pyrotechnic compositions. From these and other studies a general method has been chosen and developed in this report. This method consists of treating the flare devices with water in an attempt to separate the water-soluble ingredients, such as metal nitrates, perchlorates, etc., from the water-insoluble ingredients, such as magnesium powder, asphaltum, sulfur, charcoal, etc. Treatment with water is an attractive concept for more than one reason. In the first place, the device is immediately deactivated. The metal salt oxidizers can be dissolved in water which forms a phase separate from the water-insoluble fuel materials. The aqueous phase containing the oxidizers can then be separated from the fuel materials by filtration. The two separated and dried components are believed to be less energetic, less hazardous and, therefore, safer to handle and to store than the parent flare composition. This method is applicable to all the colored flare devices. The present study includes:

1. Experimental work on separation and recovery of soluble and insoluble ingredients from a number of flare compositions.
2. Friction, impact and electrostatic sensitivity tests of some of the separated components to determine their stability, safety in handling and storability.
3. A suggested method for disposal-reclamation of colored flare devices.

EXPERIMENTAL*

Separation of Soluble and Insoluble Products

Flare samples were obtained either from disassembled devices or from loose compositions prepared by mixing required ingredients according to specifications. A weighed amount of flare sample was treated with sufficient distilled water to dissolve the least soluble salt, such as potassium perchlorate, at room temperature. In some cases the flare pellet was broken up into pieces under water and the mixture was warmed to 50-65°C to facilitate disintegration of the sample and dissolution of the soluble components.

The aqueous mixture was filtered and the insoluble residue was washed repeatedly with 20 - 25mL of water. The combined filtrate and washings (Volume, 500 - 700mL) were evaporated almost to dryness. The resulting wet crystalline product was dried overnight in an oven at 105 - 110°C. The insoluble residue was dried in a similar manner. The water-soluble and insoluble products thus separated were weighed and stored. The

*In order to specify procedures adequately, it has been necessary occasionally to identify commercial materials and equipment in this report. In no case does such identification imply commendation or endorsement by the Navy, nor does it imply that the material or equipment identified is necessarily the best available for the purpose.

soluble products, supposed to be colorless, had a slight color because of the presence of impurities. Sensitivity tests were conducted with some of these separated products. The results of separation and recovery operations are given in Table 6 for a number of different flare types.

Purification of Recovered Magnesium Powder

Magnesium powder obtained from the sample of MK 13 Mod 0 red flare (Sample No. 1, Table 6) was collected from the bottom of the beaker after filtration. The powder, after drying, appeared black in color. The dry impure powder was purified by repeatedly washing it with small quantities of tetrahydrofuran (THF) and filtering the mixture. The black adhering impurity dissolved partly in THF, giving the filtrate a dark red-brown color.

Qualitative Experiments Tests for Strontium and Magnesium

The fraction of the black insoluble residue on filter paper obtained from the sample of MK 13 Mod 0 (Sample No. 1, Table 6) was collected and dried. Approximately 0.05g of the residue mixed with about 1mL of water was treated with a few drops of dilute nitric acid. Solid ammonium chloride and ammonium hydroxide solution were added to the filtered acid extract. The resulting alkaline solution, upon addition of potassium carbonate solution, gave no white precipitate, indicating the absence of strontium, calcium, and barium ions in the acid extract. A few drops of disodium hydrogen phosphate solution were added to this solution. A copious white crystalline precipitate appeared immediately, thus confirming the presence of magnesium ions in the acid extract of the insoluble residue.

TABLE 6: EXPERIMENTAL RESULTS OF SEPARATION AND
RECOVERY FROM COLORED FLARE COMPOSITIONS

Sample	Grams Recovered (actual/theoretical)		
	Solubles	Insolubles	Total
RED FLARES:			
(1) Mk 13 Mod 0; pressed pellet; Mg*: A-I-2; without first fire	13.3/17.4	11.0/7.5	24.3/24.9
(2) Above with first fire	15.5/16.6	9.1/7.2	24.6/23.8
(3) Above with first fire**	11.6/14.6	11.5/6.4	23.1/21.0
(4) Mk 2 Mod 0, Red; device pellet; no Mg; Quickmatch, wad, priming composition removed	8.9/8.6	4.2/4.8	13.1/13.4
GREEN FLARES:			
(5) Mk 116 Mod 1; Loose composition; Mg: III-18; composition without delay	7.9/10.3	6.7/4.7	14.6/15.0
(6) Above with delay composition	12.8/16.1	15.8/12.4	28.6/28.5
(7) Mk 2 Mod 0, Green; device pellet; no Mg; Quickmatch, wad, priming composition removed	9.8/10.7	1.9/1.2	11.7/11.9
YELLOW FLARES:			
(8) Mk 115 Mod 1; loose composition; Mg: III-18; without delay composition	9.4/14.6	10.9/5.4	20.3/20.0
(9) Mk 118 Mod 0; loose composition Mg: III-18; without first fire	8.8/12.2	11.2/7.8	20.0/20.0
WHITE FLARES:			
(10) Mk 2 Mod 0: pellet; no Mg; with Quickmatch, wad, priming composition	10.5/10.3	4.2/4.6	14.7/14.9
BLUE FLARES:			
(11) Mk 1 Mod 1; pellet; no Mg	12.4/11.9	7.3/8.2	19.7/20.1

*Mg;A-I-2 means magnesium is type I, granulation 2, and conforms to JAN-M-382.

**Prolonged contact with water and exposure to air.

Alkalinity

About 0.5g of magnesium powder (Type III, granulation 15) was added with stirring to 225mL of distilled water. The pH of the resulting mixture was measured with a Leeds & Northrup Model 7415 Research pH meter. In one and one half minutes the pH of the mixture rose from 6.0 to 9.5 units. Evolution of microbubbles of a gas (presumably hydrogen) was observed. The pH of the mixture then rose slowly to 10.7 over a period of hours and remained almost constant.

Formation of Hydrogen

The rate of evolution of microbubbles of hydrogen was observed by adding small amounts of different varieties of magnesium powder to distilled water. The following varieties of magnesium powder were used:

(1) Type I: Flaked and/or chip; Grade A: 96 percent minimum magnesium content; Granulation 2: 40 - 80 mesh size.

(2) Type III: Atomized: 98 per cent minimum magnesium content; Granulation 15: 100 - 200 mesh size.

(3) Type III: Atomized: 98 per cent minimum magnesium content; Granulation 18: 30 - 50 mesh size.

Magnesium powder of type I, grade A, granulation 2, was found to be the most reactive variety as evidenced by hydrogen bubble evolution in water at room temperature. With type III, granulation 15, bubble evolution was slower. There was little or no evolution of hydrogen microbubbles with type III, granulation 18, and water at room temperature during the first fifteen to twenty minutes. It has the slowest rate of gas evolution. It is therefore the least reactive variety while type III, granulation 15, occupies an intermediate position. The increased reactivity of type I, granulation 2 is probably a result of the increased surface area of the flaked material.

Sensitivity Tests

The following samples were submitted to the Materials Analysis and Technology Division, Weapons Quality Engineering Center at Crane for sensitivity tests:

(1) Water-soluble product from pellet with first fire; MK 13 Mod 0, Red.

(2) Water-insoluble product from loose composition; MK 116 Mod 1, Green.

RESULTS & DISCUSSION

Water-Soluble and Insoluble Products

A pyrotechnic composition with its many associated formulations is a complex mixture which contains numerous chemical ingredients in major, minor, trace and ultratrace amounts. Essentially, it is a mixture of oxidizable (fuel) and reducible (metal salt oxidizer) materials designed to undergo combustion (a combination of oxidation-reduction reactions) in the dry condition at high temperatures. When such a mixture is treated with water, it is possible that oxidation-reduction reaction(s) may occur when a very reactive ingredient, such as magnesium powder, is present. The extent of these reactions will depend on time, temperature, nature and concentrations of the chemical species involved.

Evidence of one such reaction has been found during experimentation with MK 13 Mod 0 red flare composition (Sample No. 1 - 3, Table 6) which contains magnesium powder. Evolution of hydrogen takes place upon treating this flare composition with water. This observation has led to experiments on pH measurement and reactivity of different varieties of magnesium powder. Magnesium is a reactive element. Its reactivity depends, among other factors, on the surface area (state of subdivision or particle size) and the condition of the surface. The apparent stability (decreased reactivity or non-reactivity) of magnesium stems

from the fact that an oxide film on its surface resists further penetration and corrosion by oxygen or water. Magnesium oxide is slightly soluble in water to form magnesium hydroxide which gives rise to the alkalinity of the resulting solution. As mentioned in an earlier section, a great majority of the colored flare compositions contain magnesium powder. In these compositions the possibility of hydrogen formation and other subsequent reactions exist during reclamation operations.

Table 6 shows the calculated and actually recovered amounts of water-soluble and insoluble products obtained from flare compositions. As may be seen, in most cases the actual amounts recovered differ from the theoretical amounts calculated from their respective compositions. In some cases the difference is considerable. The Mk 2 Mod 0 and Mk 1 Mod 1 compositions give results that agree with theoretically predicted amounts. The MK 13 Mod 0, Mk 116 Mod 1 and the Mk 118 Mod 0 give insolubles greater than predicted, solubles less than predicted and total quantities correct within experimental error. There are three basic differences between these two groups. The Mk 2 Mod 0 and MK 1 Mod 1 are actual device pellets removed from hardware and are at least ten years old, while the other group is composition prepared specifically for this task. The Mk 2 Mod 0 and Mk 1 Mod 1 contain no magnesium and the other group contains various particle sizes of magnesium. The Mk 2 Mod 0 and Mk 1 Mod 1 do not contain Laminac^R as the binder and the other group does (except for the Mk 13 Mod 0).

The most reasonable explanation for the observed differences in weight is that part of the soluble salts are either coated with the Laminac^R or retained by it in some other manner and are therefore not "accessible" to the water used for dissolution. Another explanation that cannot be dismissed completely is that the ingredients undergo chemical reactions while in the water that lead to products which are lighter, i.e., have lower atomic weights, than those predicted. For example, the nitrate could undergo reaction to form ammonia which would then be lost

to the atmosphere. It is evident from the changes observed in the pH of the solution and from the generation of hydrogen that some of these reactions are occurring to a limited extent. However, it seems unlikely that short-term exposure to water could result in the large discrepancies in the yields.

Several experiments were performed in an effort to explain the observed differences. The insoluble residue from the Mk 116 Mod 1 (Sample 5, Table 6) was sieved on a standard No. 140 screen. This screen will pass particles with diameters less than 105 micrometers. The granulation 18 magnesium contains no particles less than 250 micrometers. The insoluble residue could then be separated by sieving into two fractions, one of which appears to be essentially all magnesium. The recovered weight of the magnesium fraction agrees within experimental error with the theoretical magnesium weight calculated from the initial formula. Although no tests were done to determine the purity of the recovered magnesium, the close agreement between actual and theoretical magnesium weights indicates that the magnesium in the Mk 116 Mod 1 is not reacting to a large extent. This supports the argument for retention of some of the solubles by the binder.

A sample of Mk 116 Mod 1 composition was made without the binder. The solubles in this composition were separated from the insolubles in exactly the same way that the Mk 116 Mod 1 composition (Sample 5, Table 6) was separated. Temperature, stirring rate, volume of water and contact time in water were identical. In the case of the composition without binder, the actual and theoretical amounts of solubles and insolubles were identical. There was no evidence of the large discrepancies observed in the samples which contain the binder. This result also supports the argument for retention of the solubles by the binder.

The insoluble residue from the Mk 13 Mod 0 red flare composition was treated with nitric acid and qualitative tests were run for alkaline

earth metal cations. The acid extract of the insoluble residue did not contain strontium ions. This does not, of course, confirm the absence of the soluble metal salt oxidizer, strontium nitrate, in the insoluble product. The acid wash may not have extracted the strontium nitrate from the insolubles. It should also be noted that Mk 13 Mod 1 red flare does not contain the Laminac^R binder and has flaked magnesium rather than atomized magnesium. The magnesium used in the Mk 13 Mod 1 has been shown to be very reactive with water. The possibility exists that the secondary magnesium reactions may be more important in this composition than in those which contain the granulation 18 atomized magnesium. The mechanism and explanation for the discrepancies in actual and theoretical product weights may be entirely different for this class of compositions.

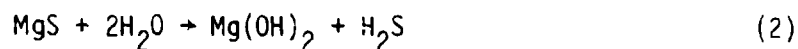
The pronounced effect of prolonged exposure to water (at room temperature and on warming) and to air is evident from the weights of products recovered from Sample Number 3, Table 6. Such undesirable experimental conditions have been avoided in obtaining the products from other samples.

Formation of Hydrogen Sulfide

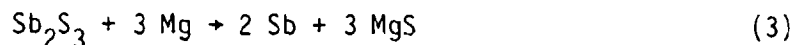
During the disintegration and dissolution processes of MK 13 Mod 0 red flare candles pressed with first fire composition (Sample Nos. 2 and 3, Table 6), hydrogen sulfide was detected by its strong odor. The odor persisted throughout the subsequent operations. The first fire composition contains, among other ingredients, black antimony trisulfide and sulfur. The flare composition has, as one of its ingredients, magnesium powder, type I, grade A, granulation 2, the most reactive variety of magnesium powder. Hydrogen sulfide is a highly toxic gas. Any proposed procedure for disposal and/or reclamation using water will have to take into account the formation and liberation of this gas.

Hydrogen sulfide may be formed in two possible ways from a MK 13 Mod 0 red flare candle pressed with a first fire composition when

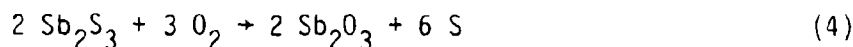
treated with water. One way is from the interactions between magnesium powder, sulfur and water. At the interface between the candle and the first fire, there is intimate contact between magnesium and sulfur particles which may form magnesium sulfide. The magnesium sulfide can then react with water to form hydrogen sulfide as shown in the following equations:



The other possible way in which hydrogen sulfide may be formed is from the interactions between antimony trisulfide, magnesium powder and water. It should be recalled here that the aqueous solution is strongly alkaline. Formation of hydrogen sulfide directly from antimony sulfide is highly unlikely. Only alkali and alkaline earth metal sulfides hydrolyze in water to form hydrogen sulfide (equation 2) and an alkaline solution. Other metal sulfides including antimony trisulfide form hydrogen sulfide only in acidic solutions. Therefore, one possible explanation for the formation of hydrogen sulfide using antimony trisulfide is that magnesium, a strong reducing agent, reacts with the trisulfide to form magnesium sulfide as shown in the following equation:



Magnesium sulfide thus formed may hydrolyze in water to form hydrogen sulfide as shown earlier in equation 2. Another plausible, much simpler explanation is that naturally occurring antimony sulfide may form free sulfur owing to partial atmospheric oxidation as shown by the following equation:



Atomic hydrogen generated by magnesium powder from water may then react with free sulfur to form hydrogen sulfide according to the following equation:



Other possible explanations may be found from a careful consideration of the chemical equilibria in solution.

Sensitivity Tests

The tests and the results for the two samples, one soluble product and the other insoluble product, are as follows:

Friction Sensitivity--No fire at 1064 ft-lbs.

Impact Sensitivity--No fire at 100cm.

Electrostatic Sensitivity--No fire at 1.0 joule.

Test data show both the samples to be insensitive to all three tests. These limited data indicate that the separated water-soluble and insoluble products are stable and can be stored.

Toxicity of Ingredients and Products

Some of the ingredients of colored flare compositions, associated formulations, and products from these materials are toxic. A few of these toxic substances are briefly mentioned below. Appropriate precautionary measures should be taken when dealing with these substances.

(1) Hydrogen Sulfide: It is a reaction product when a flare composition containing magnesium powder and a first fire composition containing antimony trisulfide and sulfur are treated with water.

(2) Antimony Trisulfide: It is present in some first fire compositions and in Mk 2 Mod 0 white flare compositions.

(3) Arsenic Trisulfide: It is present in Mk 1 Mod 1 blue flare compositions and also in orange shellac present in some flare compositions.

(4) Paris Green: $\text{Cu}(\text{C}_2\text{H}_3\text{O}_2)_2 \cdot 3\text{Cu}(\text{AsO}_2)_2$, Cupric Acetoarsenite: It is present as an ingredient in Mk 1 Mod 1 blue compositions.

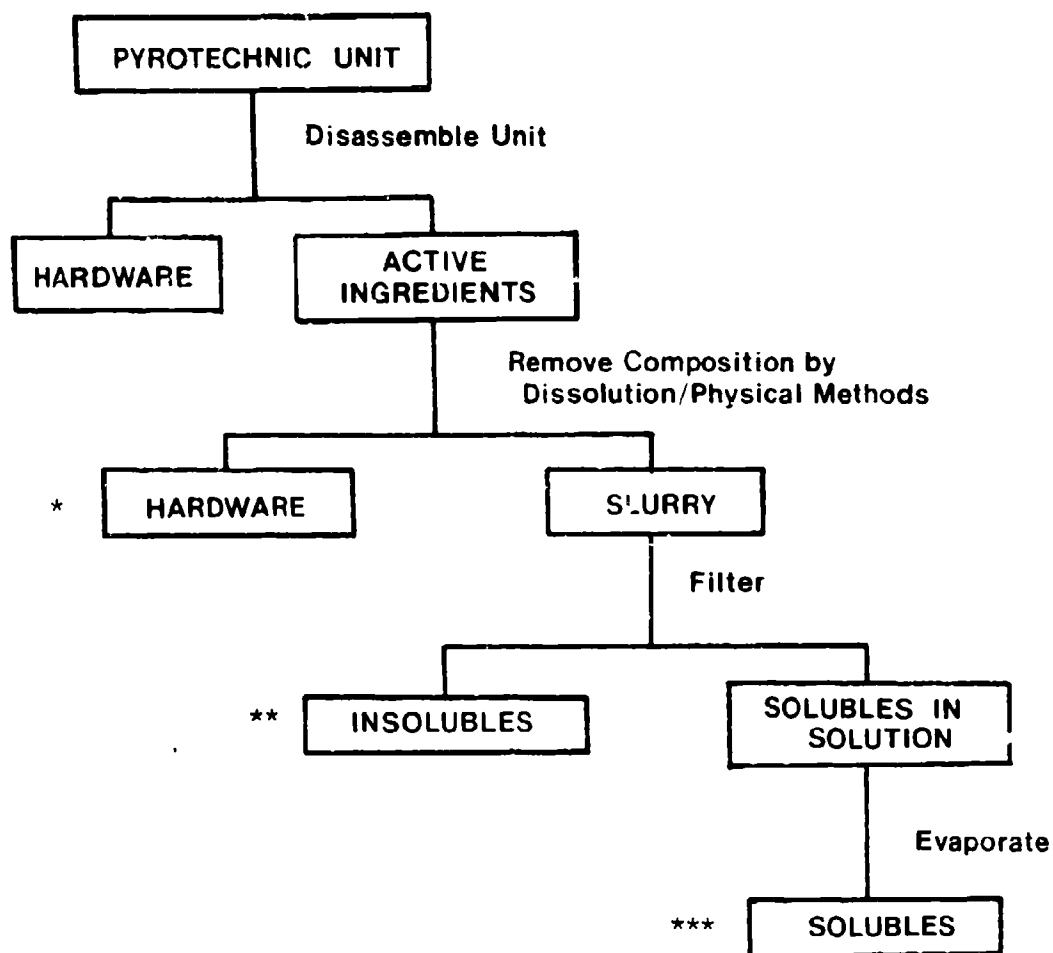
(5) Hexachlorobenzene: It is an ingredient in many red, green and yellow flare compositions.

(6) Sodium Oxalate: It is present in all yellow flare compositions.

(7) Dechlorane^R, $\text{C}_{10}\text{Cl}_{12}$: It is an ingredient in some green flare compositions. It is a suspected carcinogen. It is also used in the ignition composition of some red, yellow, and green signals.

Method of Disposal

The disposal procedure for colored flare compositions is shown schematically in Figure 1. The initial step in the process is the disassembly of the device to obtain the flare composition. Disassembly will give the flare composition either as a pressed pellet or pressed into a paper or metal container (tube or cup). The flare composition can now be treated with water. For those compositions pressed into a container, a high pressure water jet can be used to wash out the container. Alternatively, the container and composition can be crushed underwater to facilitate removal of the composition. If warm water is used, the temperature should be kept below 60°C and the contact time in either cold or warm water must be kept as short as possible (no longer than 15 minutes) to minimize the formation of gaseous products. In the



* METAL CASES, PAPER TUBES, CARDBOARD INSERTS, ETC.

** PRIMARILY METAL POWDERS, INERT INGREDIENTS, OR OTHER POTENTIALLY HAZARDOUS MATERIALS WHICH MAY BE SEPARATED FURTHER

*** TYPICALLY MIXTURES OF TWO OR MORE INORGANIC SALTS, PRIMARILY NITRATES AND PERCHLORATES, WHICH MAY BE SEPARATED FURTHER

Figure 1. Flow Chart of Disposal Method for Colored Flare Compositions

case of compositions containing magnesium powder the gaseous product is mainly hydrogen. Hydrogen gas forms an explosive mixture with oxygen in air and is highly flammable. A proper venting system should therefore be provided. Noxious and toxic gases such as hydrogen sulfide and ammonia may form in some cases. These gases may be trapped in absorbent trains.

When flare compositions are treated with water the metal salts (e.g., barium nitrate, potassium perchlorate) dissolve in the water; the magnesium settles quickly to the bottom of the container, and the remaining insoluble residue floats in the water. The simplest procedure for separating the fuels and oxidizers is filtration. This leaves a water solution of mixed salts and a mixture of insoluble fuels and additives. The filtrate can be evaporated to dryness to recover a solid mixture of salts. The separated mixed fuels and oxidizers can be stored or sold in this form. Sensitivity tests on the recovered mixtures have shown that the materials recovered from Mk 116 Mod 1 and Mk 13 Mod 0 are insensitive to the standard electrostatic, impact, and friction tests. Tests were not done on recovered products from the compositions containing metal chlorates. Since the metal chlorate compositions are typically more sensitive than compositions without the metal chlorates, it is recommended that sensitivity tests be done on these mixtures prior to storage.

The mixed salts and mixed fuels/additives can be separated further, if desired. The metals can be separated from the other insolubles (generally, additives or binders) by sieving the dry material through an appropriate screen. The metal particles are typically much larger than the additive particles and will remain on the screen. Another method of separating the metals from the additives is to float the additives away in a suitable solvent. The metal particles settle to the bottom of the container and the other insolubles can be removed by continuous addition of solvent to float away the less dense additives.

One or more of the soluble salts can be recovered from the mixture by selective precipitation. The alkaline earth metal salts can be separated

from the alkali metal salts by adding carbonate or sulfate anions to a solution of the mixed salts to precipitate the alkaline earth metal cation. The choice of reagent for selective precipitation will depend on the exact nature of the soluble salt mixture. The precipitate can be recovered by filtration and the remaining solution evaporated to dryness to recover the soluble salt(s).

These separation and recovery techniques have been demonstrated to a limited extent using the Mk 116 Mod 1 green flare composition. The techniques will have to be modified if applied to other compositions containing different species.

CONCLUSIONS

A technique has been demonstrated for separating the fuels and oxidizers in colored flare compositions. The technique consists of dissolving the soluble materials (generally, the oxidizers), filtering the mixture to separate the soluble materials from the insoluble materials (generally, fuels and additives) and recovering the soluble materials by evaporating the filtrate to dryness. In this way the hazardous pyrotechnic compositions can be converted to safe, easy to handle separate mixtures of fuels and oxidizers which can be stored or sold. General techniques for further separating the mixed fuels have been given.

Several potential problem areas have been identified. Complete separation of the soluble and insoluble components of flare compositions cannot be achieved in flares which contain an organic binder using water alone. This problem was also encountered in the illuminating flare reclamation program and was solved by the use of a methylene chloride-methanol solvent.⁶ This same solution will probably be applicable in this case.

In the flare compositions which contain the smaller magnesium particles (diameters <150 micrometers) or the flaked variety of magnesium, hydrogen is liberated when the composition is placed in

water. A hydrogen removal system must be used if the water dissolution method is used. In the flare compositions which contain sulfur, antimony trisulfide or arsenic trisulfide hydrogen sulfide can be generated when the composition is placed in water. In most cases the sulfur-containing compounds are only present in the first fire compositions. Thus, the hydrogen sulfide problem can be eliminated either by trapping the gas or by removing the first fires before the water dissolution process.

The results of this study indicate that the colored flare compositions can be demilitarized by a solvent dissolution and filtration. The general procedure is quite analagous to the illuminating flare and photoflash reclamation operations. It appears that the colored flare devices can be handled in the demilitarization facility designed for photoflash cartridges if controls for hazardous or toxic gaseous reaction products were installed.

REFERENCES

1. E. L. Hood, Evaluating A Magnesium-Ammonium Phosphate Suspension as a Fertilizer Material, RDTR No. 283, Naval Ammunition Depot, Crane, Indiana, 12 December 1974. Available DDC, AD-A010601.
2. C. W. Gilliam and J. E. Tanner, Flare, Igniter and Pyrotechnic Disposal: Red Phosphorus Smokes, RDTR No. 298, Naval Ammunition Depot, Crane, Indiana, 19 May 1975. Available DDC, AD-A013182.
3. C. E. Dinerman and C. W. Gilliam, Ecological Disposal/Reclaim of Navy Colored Smoke Compositions, NWSC/CR/RDTR-36, Naval Weapons Support Center, Crane, Indiana, 1 June 1976. Available DDC, AD-A030234.
4. C. W. Gilliam and C. E. Dinerman, Disposal of Navy Colored Smoke Compositions and Identification of Products of Combustion, NWSC/CR/RDTR-85, Naval Weapons Support Center, Crane, Indiana, 31 May 1978. Available DDC, AD-A056274.
5. F. E. Montgomery and J. E. Short, A 1/10 Scale Pilot Plant for the Ecological Demilitarization of Mk 25 Marine Location Markers/Red Phosphorus Composition, NWSC/CR/RDTR-70, Naval Weapons Support Center, Crane, Indiana, 11 November 1977. Available DDC, AD-A055440.
6. J. E. Short and F. E. Montgomery, Environmentally Acceptable Method for the Demilitarization of Mk 24 and Mk 45 Aircraft Parachute Flares in Proceedings of Sixth International Pyrotechnics Seminar held 17-21 July 1978 at Estes Park, Colorado. (Sponsored by Denver Research Institute, Denver, Colorado.), p. 537.

ACKNOWLEDGEMENTS

The support of this work by the Department of the Navy, Naval Sea Systems Command, is gratefully acknowledged.

TRANSIENT THERMAL TESTING OF AN ELECTROEXPLOSIVE BRIDGEWIRE DETONATOR

Nicole CHRETIEN - Charles KASSEL - Marcel DUIGOU

C.E.A. - B. P. N° 7 - 93270 SEVRAN - FRANCE

ABSTRACT

The transient thermal testing studied by Rosenthal has been adapted to an electroexplosive bridgewire detonator containing only secondary explosive.

This non-destructive testing consists in following the heating curve of the bridgewire due to a constant current of very short duration (0, 5 ms).

Bridgewire resistance function of the temperature increase generates a voltage variation ΔV during the constant current flow.

The voltage variation curve as a function of time $\Delta V(t)$ may be represented by a straight line whose slope allows calculation of the parameter α/C_p where α is the thermal coefficient of the bridgewire material and C_p is the equivalent heat capacity of the system.

In a preliminary study, direct measurements of wire temperature in air with an infrared microscope have been performed and perturbation thresholds have been determined for a given EBW detonator.

Different types of defaults have been manufactured and tested showing that transient thermal testing is very sensitive and allows detection of :

- welding defects of the bridgewire,
- air gaps as thin as 0,05 mm, at the wire-explosive interface,
- loading density differences of 0.10,

- voids and impurities close to the wire.

A production quality control device has been defined by taking in account all the error sources : input current, resistance spread, etc.

Thermal transient testing results concerning a batch of EBW detonators, with and without thermal cycling are compared with their functioning criterion.

1. - INTRODUCTION

Transient Thermal Testing (TTT) is a widely used method for non-destructive investigation of the quality of electroexplosive devices (EED) (réf. 1 to 13).

As far as we know, Thermal Testing has been applied to secondary explosive exploding bridgewire detonators only by CEYRAT[13], who used a constant current test.

We have adapted TTT in order to inspect the bridgewire-explosive interface of a timing EBW detonator for it is known that the quality of this interface conditions proper functioning and reliability of EBW detonators.

After a perturbation threshold study, we tried different testing methods and we have finally adopted a single square current method.

In order to investigate the limits of this control, we manufactured and tested devices with known defects (welds, air gaps, different loading densities) and we followed damage caused by thermal cycling on a batch of detonators.

II - EXPLODING BRIDGEWIRE DETONATOR

The timing detonator we want to test is represented on the following sketchplan :

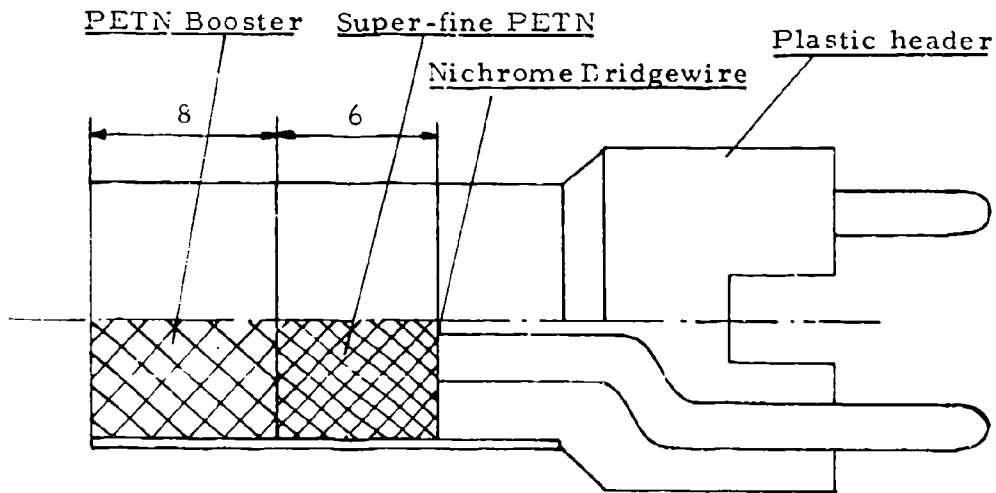


Figure 1 : EBW Detonator

The plastic header is obtained by injection molding and the bridge-wire is spot welded on the electrodes, the resistive bridgewire in Nichrome, has 0.03 mm in diameter and is in close contact with super-fine PETN whose loading density is about 0.5 of the crystal density of PETN. The booster charge is highly compressed coarse PETN.

III - THERMAL TESTING METHOD

Superfine PETN is very sensitive to temperature and partical size changes rapidly near melting point at 140°C . Thus a constant current method is limited in current and the very low thermal coefficient of the wire material (Nichrome) leads to very low voltage change across the device.

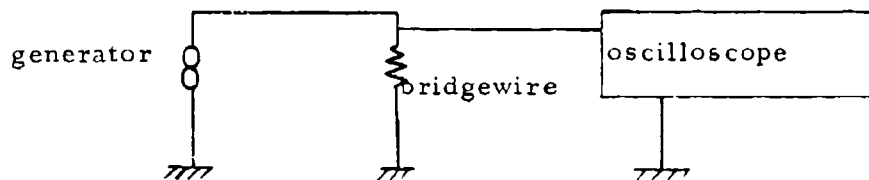
At first we used an infrared microscope to measure wire temperature in air in order to have a first evaluation of thermal characteristics of our system.

The study of the perturbing current threshold shows that very short duration impulses leading to wire temperatures highly above PETN melting point (140°C), do not alter the fonctionning characteristics of the EBW detonator.

This lead us to Transient Thermal Testing.

Our first system used a heating impulse generated by a capacitance discharge with a dynamic Wheatstone bridge to measure resistance variation. Stray current during heating limited resistance variation measurements to the cooling curve .

The use of a square voltage impulse generator enabled us to follow the heating curve by using the following diagram :



During heating wire temperature is given by the following equation :

$$\theta = \frac{R_o I_o^2}{\gamma - R_o I_o^2} \left(1 - \exp \left(-\frac{R_o I_o^2 - \gamma}{C_p} t \right) \right)$$

where : γ is the thermal conductivity,
 C_p is heat capacity.

The current impulse time is very short compared to the time constant of the system $\tau = \frac{C_p}{\gamma - R_o I_o^2}$; for our system τ is close to

10 ms ; thus a first approximation leads to :

$$\theta = \frac{R_o I_o^2}{C_p} t$$

And voltage variation across the device :

$$\Delta V \simeq \frac{R_o^2 I_o^2}{C_p} t$$

If the current and α remain constant, this gives a linear evolution of the voltage as a function of time, the slope being the followed parameter.

The generator, we used, limits the maximum current to 1 A and the perturbing threshold of the detonator tested corresponding to an amplitude of 1 A has a 4 ms duration.

We used for our test an impulse duration of 0.5 ms with an amplitude of about 1 A as shown on figure 2a.

The comparison of the voltage variation across a passive resistor, a bridgewire in air and a detonator confirmed the linear variation expected and the possibility of a non-destructive testing of our EBW detonators.

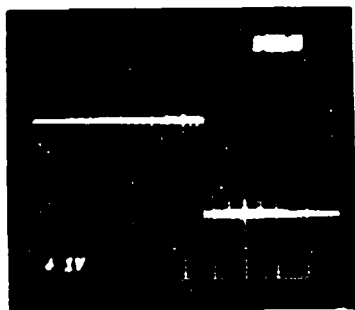


Figure 2a. Heating impulse

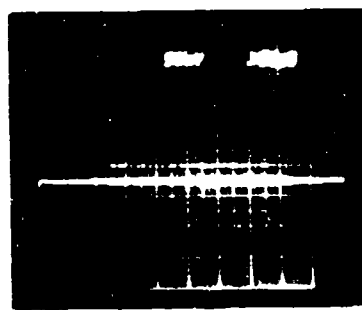


Figure 2b. Voltage variation across
a passive resistor ($\lambda = 0$)

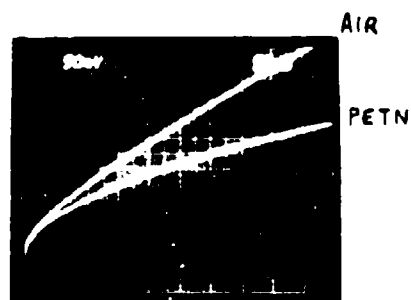
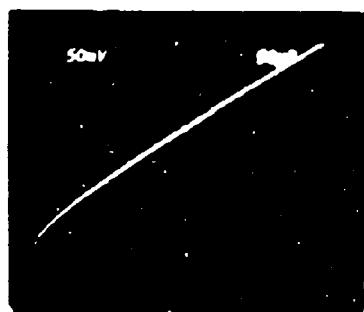


Figure 2c. Voltage variation across a bridewire in air and in a
detonator

A differential system is used to collect voltage variation across the wire and a transient sampling device allows different operations : smoothing, elimination of the non-linear part of the signal, slope measurement, integration, ect.

For our study the following experimental set up has been used.

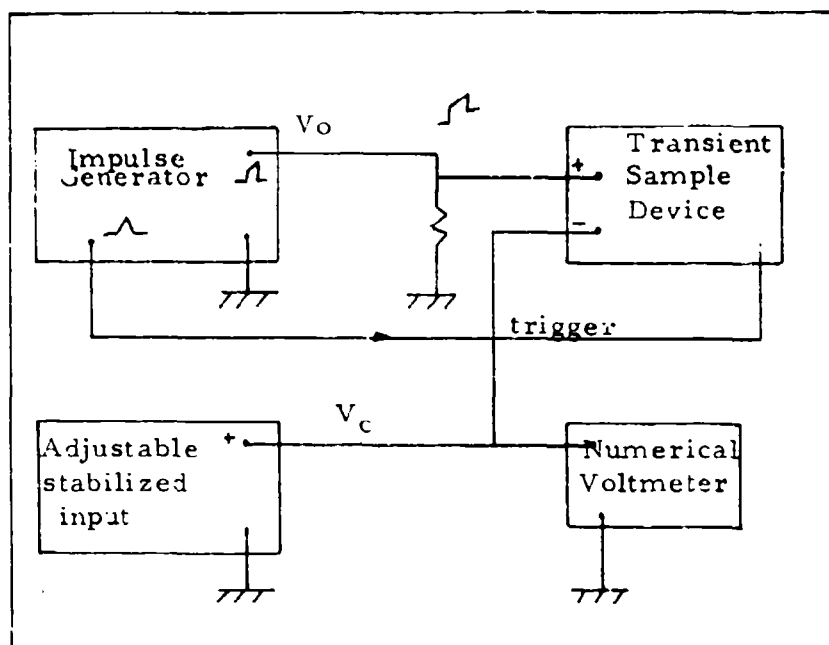


Figure 3 : Experimental set up.

IV - TEST RESULTS

We manufactured different devices including known faults defective welds, air gaps, density variations in order to evaluate the limits of the testing method.

IV. 1 - Manufactured defects

IV. 1. 1 - Welds

PETRICK (12) stated that TTT could detect solder defects, we manufacture defective welds which lead to the following diagrams :

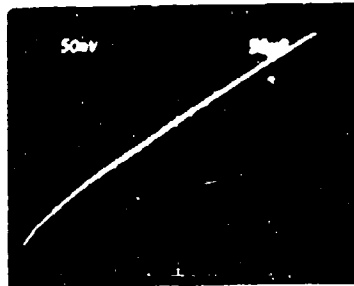


Figure 4a. Normal signal

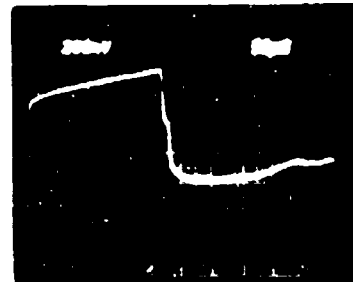


Figure 4b. Crushed weld

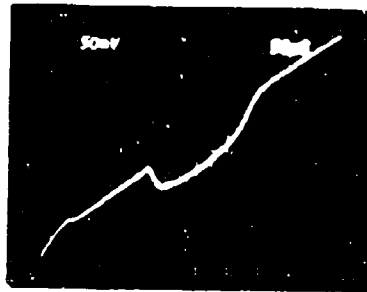


Figure 4c. Erratic contacts.

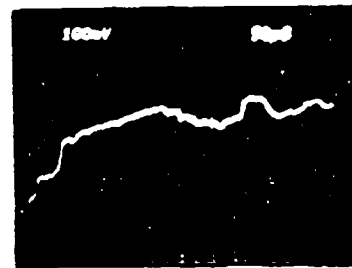


Figure 4 : Defective welds

IV. 1. 2 - Air gaps

A well known defect of EBW is the wire contact with the superfine explosive.

We tested calibrated air gaps of 0.05 , 0.1 mm and this showed that a 0.05 mm air gaps leads to the same signal a bridgewire in air ; it is thus possible to detect air gaps lower than 0.05 mm.

IV. 1. 3 - Loading density

We have tested EBW detonators with loading densities ranging from 0.75 to 0.95 the following results have been obtained.

Density	0.75	0.80	0.85	0.90	0.95
Signal slope (V/s)	64	55	49	47	45

TTT is not very sensitive to density variation.

IV. 1. 4 - PETN

We use different PETN recrystallization processes leading to superfine PETN having different physical characteristics.

One kind of superfine PETN (type E) has isometrical crystals and a specific surface of about $0.5 \text{ m}^2/\text{g}$, an other kind of superfine PETN has stick shaped crystals with a specific surface of about $3 \text{ m}^2/\text{g}$ (PETN type S).

With the same type of EBW detonator it is possible to differentiate the two types of PETN for we obtained the following values for the

signal slope : PETN E = $48 \pm 5 \text{ V/s}$
PETN S = $62 \pm 5 \text{ V/s}$.

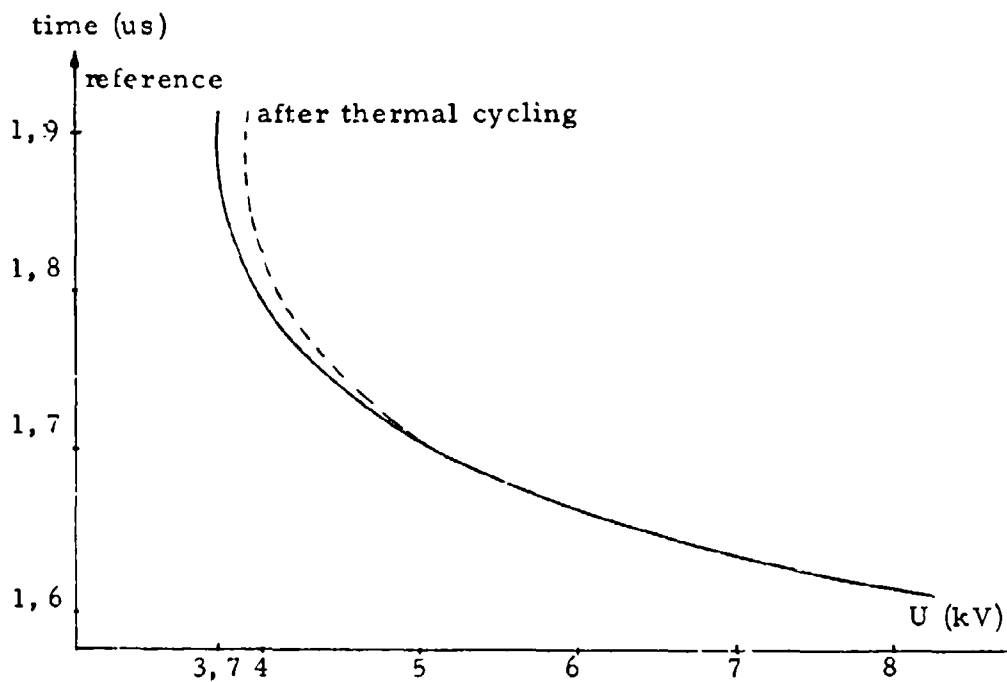


Figure 5a : Functionning time versus capacitance voltage.

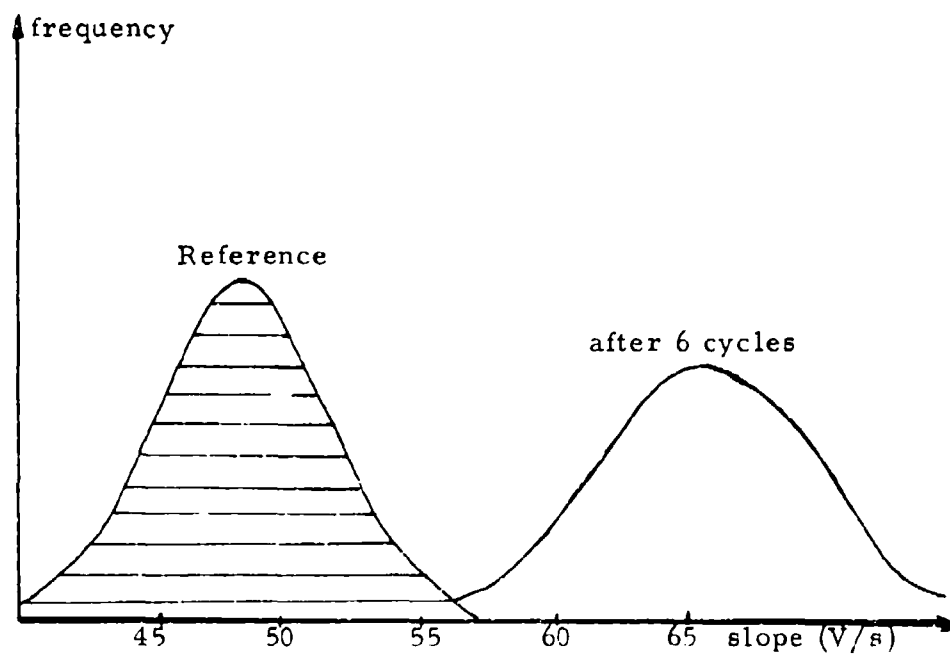


Figure 5b : Sample distribution.

The spread allows to differentiate batches of detonator but not each detonator individually.

IV.2 - Thermal cycling effects.

It is well known that EBW detonators with plastic header are sensitive to thermal cycling. A same batch of detonators has been thermally cycled and we followed the evolution of the signal slope and the functioning parameters (functioning time and dispersion). The obtained results are shown on the next diagrams. At first an evolution is observed without noticing alteration of the functioning time, after 6 cycles, functioning time is affected near threshold.

Thus Thermal Transient Testing is a very sensitive method to follow damage generated by thermal cycling on EBW detonators.

V - CONCLUSION

Thermal Transient Testing of an EBW timing detonator is possible and allows detection of air gaps lower than 0.05 mm, weld defects of the bridge wire and other defects localized close to the wire.

It allows to follow damage caused by thermal cycling before this damage is brought to evidence by the functioning characteristics of the EBW detonator.

Thermal Transient Testing is a very simple non-destructive testing that we include now in our manufacturing control process.

VI - REFERENCES

1. Rosenthal 1959, Electrothermal equations for electro-explosive devices, Navord Report, august 15, 1959.
2. Rosenthal, Menichelli 1970, Nondestructive testing of insensitive electro-explosive devices by transient techniques, Jet Propulsion Laboratory, july 15, 1970.
3. Rosenthal, Menichelli 1972, Fault determination in electro-explosive devices by nondestructive techniques, Jet Propulsion Laboratory, march 15, 1972.
4. Rosenthal, Menichelli 1972, Electrothermal follow display apparatus for electro-explosive device testing, Jet Propulsion Laboratory, march 15, 1972.
5. Rosenthal 1972, Method and apparatus for the measurement of electrothermal nonlinearity, The review of scientific instrument, november 1972.
6. Murphy, Menichelli 1972, New test for EED's, Extrait de la revue Ordnance, Strasburg A C, New methodology for transient pulse testing, nov. dec. 1972.
7. Proceedings of the 8th Symposium on explosive and pyrotechnics, The Franklin Institute Research Laboratories, february 5-7, 1974.
8. Rosenthal 1974, Heat capacity measurement method for bridge-wires, Naval Ordnance Laboratory, july 24, 1974.
9. Steele B R, Strasburg A C 1974, Transient pulse testing of electro-explosive devices, Sandia Laboratories, september 23, 1974.

10. Rosenthal, Menichelli 1975, Thermal transient test apparatus, I E E E transactions on instrumentation and measurement, june 1975.
11. Sipes W J 1976, Thermal response testing of electro-explosives devices, Proceedings of the 9th Symposium on explosives and pyrotechnics, The Franklin Institute Research Laboratories, sept. 15-16, 1976.
12. Petrick J T 1979, Advanced transient pulse analysis of electro-explosive devices, Proceedings of the 10th Symposium on explosives and pyrotechnics, San-Francisco, feb. 1979.
13. Ceyrat 1974, Contrôle non-destructif de l'interface électro-explosive des initiateurs à filament résistant, Colloque 1974 sur la fiabilité en pyrotechnie, Délégation ministérielle pour l'armement, 11-12 décembre 1974.

THERMAL AND ELECTROSTATIC INITIATION OF TiH_x BASED PYROTECHNICS

L.W. Collins
Monsanto Research Corporation
Mound Facility
Miamisburg, Ohio 45342

ABSTRACT

The thermal and electrostatic initiations of TiH_x based pyrotechnics have been investigated to determine the material properties which influence these processes. Controlled electrostatic sensitivity experiments showed that the initiation reaction for $TiH_x/KClO_4$ pyrotechnic involved a reaction of the fuel with oxygen gas and that the $KClO_4$ chemically interacts with the titanium to desensitize the material to electrostatic ignition. Other factors which influence the initiation process were also identified. As a result of these experiments, a new theory for the electrostatic initiation of TiH_x based pyrotechnics has emerged which relates the sensitivity to ignition to the chemistry of the titanium oxides which coat the metal particles.

Thermal ignition of the $TiH_x/KClO_4$ was shown to be controlled by chemical processes associated with the titanium fuel. DTA experiments were correlated with Auger spectroscopic measurements to demonstrate the role of the dissolution of the oxide coating in the thermal ignition of titanium.

*Mound Facility is operated by Monsanto Research Corporation for the U.S. Department of Energy under Contract No. DE-AC04-76-DP00053.

INTRODUCTION

Although there are several models which describe the physics of ignition for pyrotechnic materials, there has been relatively little effort to determine the chemistry of initiation processes. For example, the ignition reaction for Ti/KClO_4 pyrotechnic compositions is generally assumed to be the pyrotechnic reaction, i.e.,



While this seems to be a logical assumption, several observations related to the behavior of this material exposed to different environmental conditions raised questions that could not be adequately explained by this reaction. As a result, a number of studies were performed to resolve the chemical processes associated with the initiation of Ti/KClO_4 pyrotechnics. Thus far, the electrostatic and thermal initiation reactions have been studied and were shown to have some common characteristics while following different initiation mechanisms (Ref. 1-3). In this paper, the ignition data from these studies are reconciled with a proposed theory of initiation. The implications of this theory with respect to pyrotechnic material properties are also discussed with preliminary data which test behavior predicted by the theory.

EXPERIMENTAL

The instrumentation, experimental techniques, and material preparation and analyses have been previously reported in some detail (Ref. 1-3).

RESULTS AND DISCUSSION

The nominal electrostatic sensitivities of $\text{TiH}_x/\text{KClO}_4$ ($x = 0.15, 0.65, 1.3$) pyrotechnics in a fixed powder bed configuration were determined as a function of the oxygen concentration in the atmosphere

surrounding the sample. The sensitivities of these powders were shown to be strongly dependent on the oxygen gas concentration at low atmospheric concentration levels while independent of oxygen concentration at high levels as shown by the curves in Figure 1. The dehydriding process used to produce the lower stoichiometry subhydrides (Ref. 4) shifts the region of oxygen dependence toward lower concentration levels. If an electrostatic insensitive material is defined as one which will not be initiated by a 20 kilovolt pulse (Ref. 5), then the minimum hydride stoichiometry acceptable for a "safe" blend can be determined from the plot of hydride stoichiometry versus percent oxygen required for initiation from a 20 KV pulse. This is done by finding the hydride stoichiometry corresponding to the natural abundance of oxygen in air as shown in Figure 2. Thus, stoichiometries of about $TiH_{0.65}$ or less should be considered to be electrostatic sensitive in air while stoichiometries above this value are considered insensitive.

Two additional observations should be noted regarding the curves in Figure 1. First, the oxygen dependence of the pyrotechnic blends shows that the electrostatic initiation reaction involves the titanium fuel with oxygen gas and is not the expected pyrotechnic reaction with $KClO_4$. Secondly, the addition of $KClO_4$ to TiH_x acts to desensitize the titanium/oxygen gas reaction to electrostatic initiation as shown by the consistently lower sensitivities of the blends as compared to titanium subhydride alone at the higher oxygen concentrations.

Numerous experiments were performed to determine the nature of the desensitizing effect produced by $KClO_4$. Figure 3 shows the relationship between blend ratio and electrostatic sensitivity for titanium ($TiH_{0.15}$) blended with $KClO_4$ as compared with Ti/Al_2O_3 mixtures. These curves show that physical dilution does not seriously affect the initiation energy for the titanium/oxygen gas reaction until the titanium/diluent ratio falls below 1/10. Thus, the desensitization must be due to a chemical mechanism. Table 1 indicates that the chemical effect is not related to a particular chemical specie. There is apparently a unique property associated with $KClO_4$ and, to a lesser extent, $KClO_3$ which produces a chemical interaction with the titanium that results in a lower sensitivity to electrostatic initiation.

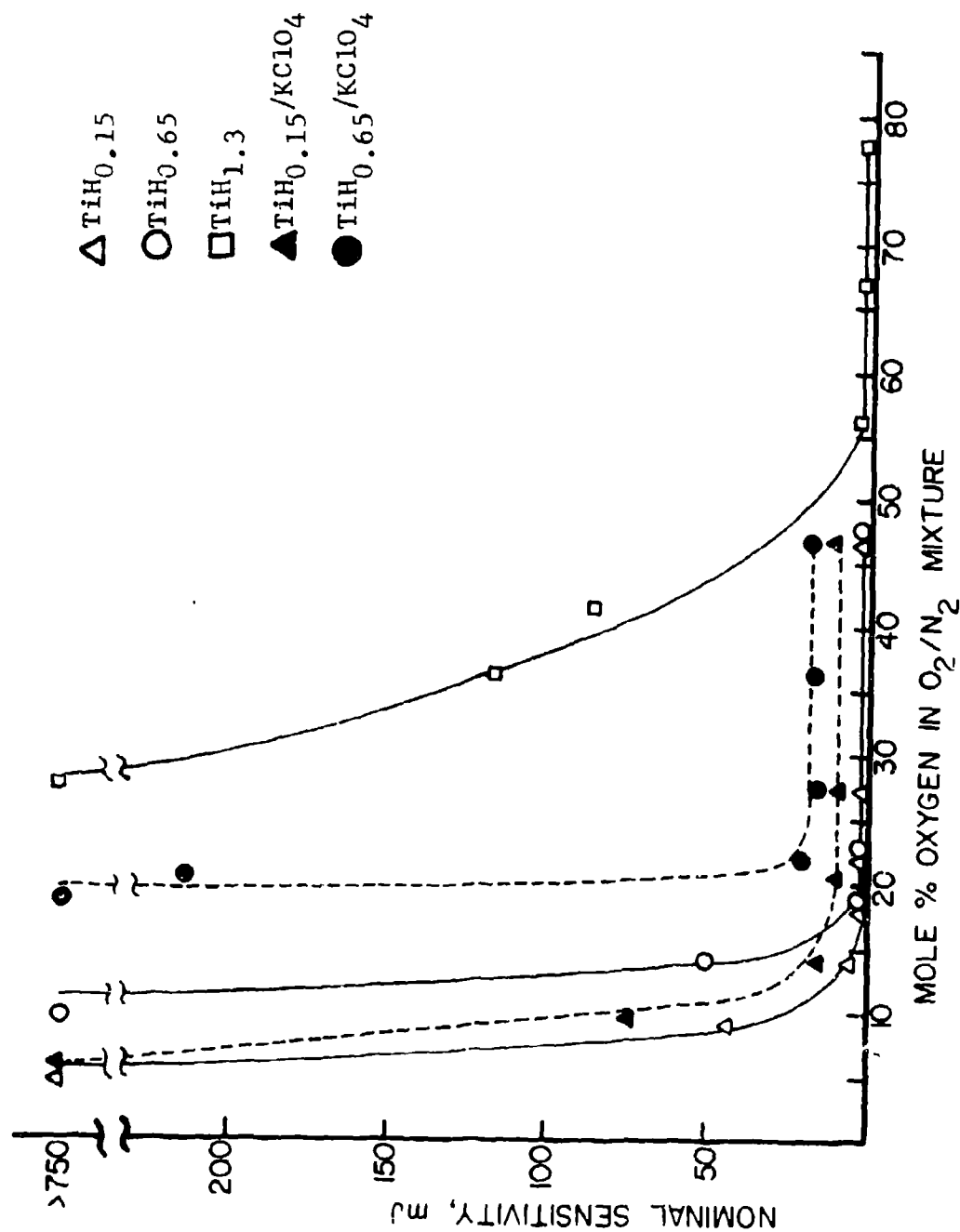


FIGURE 1. Nominal electrostatic sensitivity for TiH_x and $\text{TiH}_x/\text{KClO}_4$ blends as a function of oxygen concentration in the surrounding atmosphere.

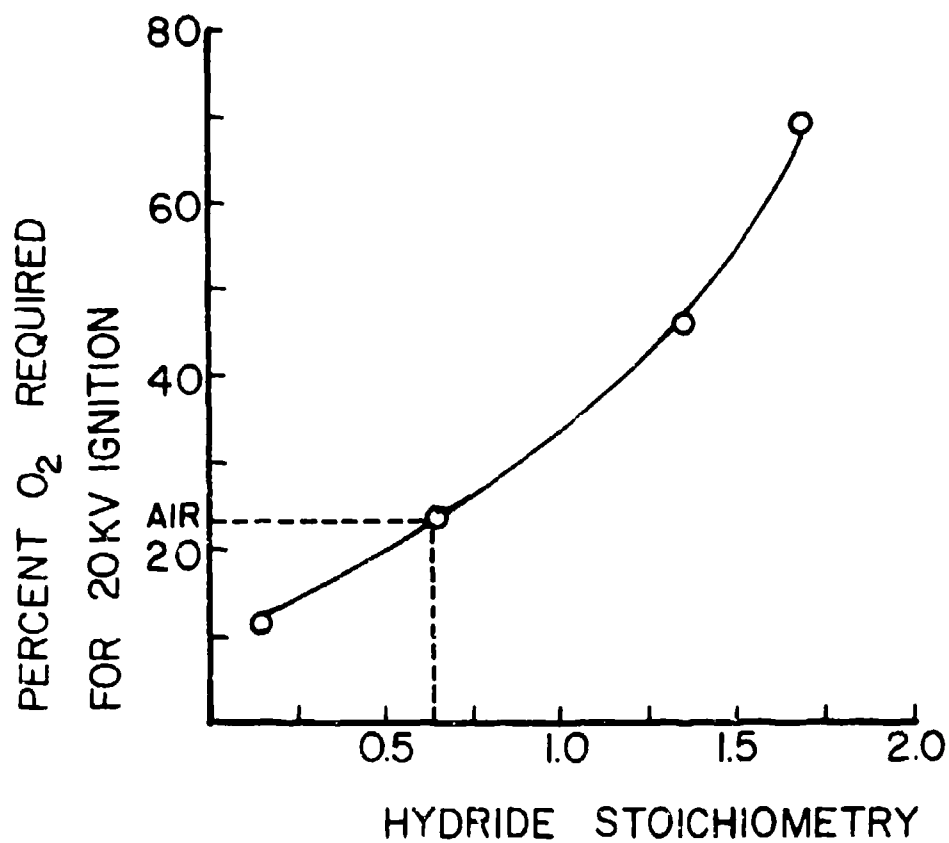


FIGURE 2. Titanium subhydride (TiH_x) stoichiometry versus oxygen concentration in surrounding atmosphere required to achieve 20kV electrostatic initiation.

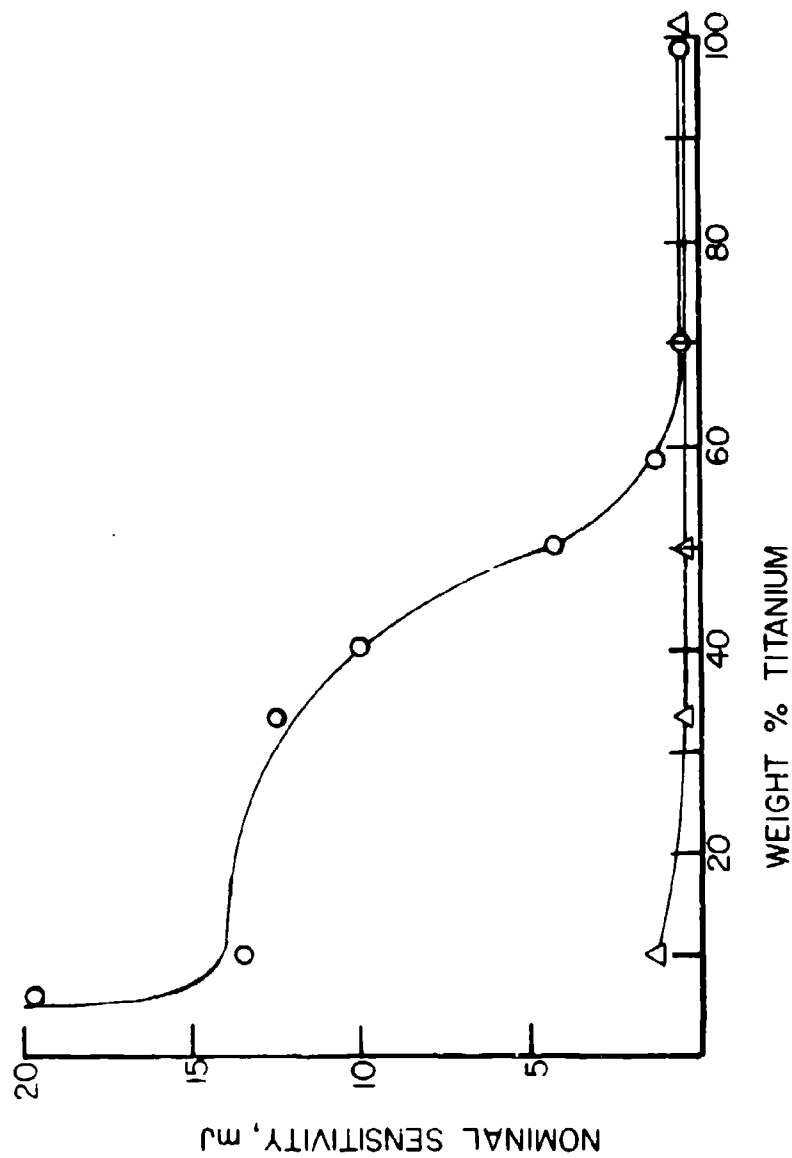


FIGURE 3. The relationship between blend ratio and the nominal electrostatic energy required for initiation of $\text{TiH}_{0.15}/\text{KClO}_4$ (O) and $\text{TiH}_{0.15}/\text{Al}_2\text{O}_3$ (Δ) blends in an atmosphere of 50% O_2 /50% Ar.

The electrostatic initiation of TiH_x and its interactions with potassium perchlorate has been explained by considering the effects of oxides in the titanium powder. The titanium powder actually consists of titanium metal covered by an oxide coating which acts to reduce its reactivity--otherwise, the material would be pyrophoric as observed when titanium powder with a fresh metal surface is exposed to air. This oxide then controls the accessibility of the titanium to the oxidizer. Thus, we postulate that the chemistry of the material is determined by the accessibility of titanium or titanium suboxides at the surface at reactive sites or regions.

Applying the proposed model to the electrostatic initiation process, the oxygen dependence at low concentrations is due to a requirement that a minimum number of the reactive sites must have oxygen in contact for sustained combustion to occur. The curves in Figures 1 and 2 then reflect the variations in reactive site density on the surface of the particle and the oxygen concentration in the atmosphere necessary to give the minimum number of oxidation points for ignition. Titanium metal must have the maximum reactive site density on the surface and therefore requires a lower oxygen concentration in the surrounding atmosphere to achieve the minimum oxidation site requirement than the higher hydrides which must have a low reactive site density. Variations in the reactive site density with respect to hydride stoichiometry could be associated with phase changes in the material or the surface could be activated by the dehydriding process.

The potassium perchlorate would also interact with the titanium oxide surface. It has been shown that titanium oxides catalyze the thermal decomposition of $KClO_4$ (Ref. 6); this suggests that at elevated temperatures, some type of intermediate complex is formed between the $KClO_4$ and titanium oxides which provides a lower energy pathway by which the decomposition can proceed. If this interaction also occurs at lower temperatures, it could produce the desensitizing effect of $KClO_4$ on the electrostatic initiation of the titanium/oxygen reaction. Table 1 shows the number of degrees by which two catalysts lower the decomposition temperature of the oxidizers which is a measure of the effectiveness of the metal oxide as a catalyst (Ref. 6). Those

TABLE 1. Electrostatic sensitivities of titanium powder blended with various oxidizers in the ratio 33 wt % fuel/67 wt % oxidizer and tested in a 50% O₂/50% Ar atmosphere. A thermogravimetric determination of the effect of two metal oxides on the thermal decomposition temperature of the oxidizers is also shown for mixtures containing 10 mole % metal oxide/90 mole % oxidizer.

Oxidizer	Nominal Sensitivity of blend with TiH _{0.15}	Effect on Decomposition Temperature, ΔT _i	
		MnO ₂	TiO ₂
Air	<1 mJ	--	--
KClO ₄	12 mJ	-120°	-40°
RbClO ₄	<1 mJ	-25°	N.D.
KIO ₄	<1 mJ	-10°	N.D.
KClO ₃	4 mJ	-85°	-22°
KNO ₃	<1 mJ	N.D.	N.D.

N.D. = not detectable

oxidizers that can be catalytically decomposed by the metal oxides are the same ones that exhibit the desensitizing effect.

Since titanium oxides are relatively poor catalysts for the decomposition process, a strong catalyst MnO_2 , was added to the pyrotechnic mixture to determine its effect on the electrostatic sensitivity. The addition of the MnO_2 lowered the electrostatic sensitivity from 12 mJ to 2 mJ. This can be explained by considering a complex interaction between the KClO_4 and titanium oxides. While this complex produces a lower activation energy for the decomposition of KClO_4 , it raises the activation energy for titanium oxides or suboxides (reactive sites) in their oxidation reactions. The addition of the strong catalyst disrupts the $\text{Ti}_x\text{O}_y\text{-KClO}_4$ complex to form the more preferred $\text{MnO}_2\text{-KClO}_4$ complex. The active Ti_xO_y regions on the surface are then free for reaction with O_2 so that the blend becomes more sensitive to electrostatic initiation.

Thermal initiation of Ti/KClO_4 pyrotechnics has also been studied and reported (Ref. 3 and 7). It was shown that thermal initiation was controlled by the dissolution of the oxide coating into the metal particle with the production of active titanium species on the surface. When the dissolution rate became fast enough, the heat produced by the rapid reoxidation reaction led to self-sustained reaction or ignition.

The titanium oxide coating on the particles then influences both the electrostatic and thermal initiation of titanium based pyrotechnics. However, the mechanisms for the two processes are different in enough respects to suggest that the electrostatic sensitivity might be altered without changing the thermal initiation characteristics. The objective of a "safe" hot wire initiated device then appears feasible if we assume that hot wire initiation is similar to the processes occurring in DTA type experiments.

Based upon the proposed theory, we would like to block the active sites to raise the electrostatic sensitivity without affecting the dissolution process which controls the thermal initiation. As an added benefit, blocking the active sites might also decrease the equilibrium water adsorbed by the material since it has been suggested that these

sites have a high affinity for water (Ref. 1). The decreased water content should then reduce the possibility of establishing an electrochemical corrosion cell within a device which could lead to ignition failures.

A batch of $\text{TiH}_{0.65}$ was treated with carbon monoxide to determine if this molecule would attach to the reactive sites to alter the surface chemistry. The electrostatic sensitivity was decreased by about 6 kilovolts due to this treatment. The moisture level for the treated material was 0.05 wt % which is below background for the untreated material.

Since the reactive regions seem to be associated with titanium suboxides, some $\text{TiH}_{0.15}$ powder was heated to 300°C in oxygen and held isothermally for a period to determine if the surface could be more fully oxidized. This treatment resulted in a decrease of about 5 kilovolts in the electrostatic sensitivity and a change in moisture content from 0.82 to 0.57 wt %. Moisture levels were determined after exposing the material to 60% RH at 22°C for five days. Thus, the preliminary data suggests that alterations in the surface chemistry can alter the electrostatic initiation and water adsorption properties of the material. DTA ignition was unchanged by the treatment.

REFERENCES

1. L. W. Collins, L. D. Haws, and A. Gibson, "The Electrostatic Initiation of Nondispersed Pyrotechnics," Combust. and Flame, In Press.
2. L. W. Collins, "Role of Potassium Perchlorate in the Desensitization of Titanium Powder to Electrostatic Ignition," Combust. and Flame, In Press.
3. L. W. Collins, "Thermal Ignition of Titanium Based Pyrotechnics," Combust. and Flame, Submitted.
4. R. S. Carlson, "Preparation of Titanium Subhydride," Seventh International Pyrotechnics Seminar, 1980.
5. T. J. Tucker, "Spark Initiation Requirements of a Secondary Explosive," Annals of the New York Academy of Sciences, 152, 643(1968).
6. L. W. Collins, Inorg. Chim. Acta, 39, 53(1980).
7. W. E. Moddeman, L. W. Collins, P. S. Wang, and T. N. Wittberg, "Role of Surface Chemistry in the Ignition of Pyrotechnic Materials," Seventh International Pyrotechnics Seminar, 1980.

GAUGING WITH PENETRATING RADIATION FOR NONDESTRUCTIVE TESTING OF PYROTECHNICS

Donald G. Costello
H. R. Lukens
Lewis A. Parks
Anthony P. Trippe

IRT Corporation
San Diego, California

ABSTRACT

Accurate measurements of thickness, density, weight, and composition of pyrotechnics can be rapidly made through the application of the principles of radiation gauging. Equipment designed for automation is performing continuous, noncontact inspections and process control functions in manufacturing and load, assemble, and pack (LAP) facilities. This paper discusses some of the considerations which influence the use of an automated penetrating radiation gauge.

The physical configurations most commonly used in radiation gauging include transmission, scattering, and backscattering arrangements. The incident energy of the penetrating radiation will depend on the material under test and the required sensitivity for the measurement. The selection of a specific type of radiation and energy spectrum can generate an inspection beam which will barely penetrate a few inches of air or will penetrate several feet of concrete. Interaction of this beam with the material in question causes energy to be removed from the beam by several physical processes. Measurement of the scattered radiation or measurement of the transmitted radiation with appropriate detectors provides the relevant inspection or process control data.

Mild detonating fuze (MDF) is a vital component in many aerospace designs. Manufacturing variations strongly alter the performance of MDF, necessitating a need for a nondestructive inspection. X-ray-based methods are primarily sensitive to the metal sheath of the MDF and are not capable of directly measuring the explosive contents. Since it is the explosive core that basically determines the

performance characteristics of the MDF, it is desirable to perform the inspection with a technique inherently sensitive to this core. Thermal neutrons exhibit a much greater sensitivity to the hydrogen, and to a lesser degree the nitrogen, in the explosive than the metal sheath. A filmless neutron gauging technique with californium-252 as the neutron source was utilized to provide an automated MDF gauge which continuously scans the MDF with a 2 percent precision at feed rates of 100 feet per minute.

The automated equipment for counting the number of igniter pellets in an ignition system component is used to illustrate the application of low energy gamma transmission techniques for 100 percent inspection of 30 mm ammunition. Another example discusses the design of a production-compatible, process control instrument to monitor the amount of black powder on a real-time basis in a hand fired simulator.

Other configurations for penetrating radiation gauges rely on measuring Compton scattered gamma rays or backscattered gamma rays to determine thickness, density, or weight. The composition of a sample can be determined in some cases by fluorescent or prompt gamma techniques. Occasionally, a difficult inspection problem can be solved through the use of dual gamma energy gauges which analyze the differential signal from a sample scanned by two beams, one low energy and one high. Dual energy gamma gauging is often effective for discriminating between elements having significant differences in their atomic numbers.

The selection of a radiation source to provide the desired sensitivity, the subsequent matching of detectors and electronics to interpret the data, and the engineering of a fully operational automated system will provide reliable, rapid inspection and process control of pyrotechnic materials and assemblies by means of penetrating radiation gauging.

1. PRINCIPLES AND TECHNIQUES

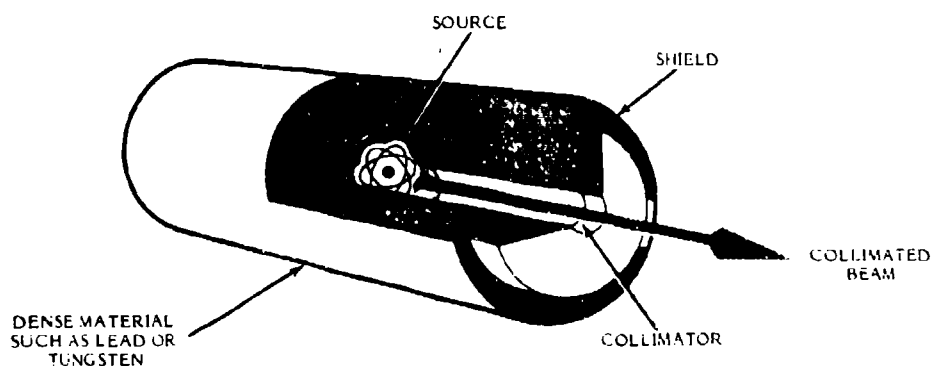
An isotopic radiation source is most commonly used for industrial gamma gauges. By selecting a specific radioisotope source, (and thereby a specific type of

radiation or specific energy spectrum), one can generate an inspection beam which will barely penetrate a few inches of air or will penetrate several feet of concrete. Other factors which effect source selection are half-life, cost, and availability. Some commonly used gamma emitting isotopes are described in Table 1. The half-life of an isotope is the time that is required for half of the atoms initially present in the source to disintegrate. The source size is often stated in units of the curie. A one curie source produces 3.7×10^{10} disintegrations per second. Some isotopes produce multiple gamma rays at each disintegration [e.g., cobalt-60 (^{60}Co) yields two gamma rays per disintegration] and therefore the source beam strength is governed by the isotope type, its size, and the solid angle of collimation. An uncollimated or unshielded isotope produces gamma rays which travel away from the source in all directions: this condition is described as a 4 radian solid angle. Commonly, restrictive collimators are fabricated from dense materials (see Figure 1) such that the gamma rays from an isotopic source form an inspection beam which is described in terms of solid angle. As shown in Figure 1, any gamma ray that does not travel in a straight line from the source to the exit of the collimator has a high probability of being absorbed in the shielding.

Table 1. Characteristics of Selected Radioisotopes

Isotope	Half-life, years	Principal gamma energies, MeV
Iron-55	2.7	0.005-0.009
Americium-241	433	0.060
Barium-133	10.8	0.05-0.38
Iridium-192	0.2	0.20-0.61
Cesium-137	30	0.660
Cobalt-60	5.26	1.17-1.33
Radium-226	1600	0.05-2.20

The interaction of the inspection beam with the material in question causes some of the gamma rays to be absorbed and some of them to be scattered. Measurement of the scattered gamma rays and/or measurement of the transmitted gamma rays with appropriate detectors provides the relevant inspection data.



RT-19187

Figure 1. A typical collimator and radioisotope source arrangement

In general, detectors convert the photons of gamma radiation into electrical signals which can be processed by conventional circuits. Two common types of detectors are an ionization chamber and a crystal scintillator coupled to a photomultiplier tube. The ionization chamber is designed to output an electrical signal generated by the flow of electrons in a wire. The gamma rays ionize the gas as they pass through the chamber. The flow of electrons through the detector is proportional to the amount of ionized gas. A crystal scintillator absorbs the gamma radiation and this excites the molecules in the crystal. As the molecules relax to their unexcited state, they emit visible light. The NaI(Tl) scintillator crystal is very efficient for converting gamma radiation into visible light and the wavelength of its resulting scintillation photons is well-matched to the spectral sensitivity of common photomultiplier tubes. The tube produces a burst of electrons for each burst of photons of visible light which impinge on its photosensitive face. An electronic circuit is used to measure this flow of electrons. In this manner, gamma rays are detected by converting the gamma ray photons into a burst of visible light photons by the crystal and then converting the light into an electrical pulse by the photomultiplier tube. An important fact, often made use of, is that proportionality is maintained throughout this chain of events so that the electrical pulse height is proportional to the gamma ray energy deposited in the

scintillator crystal. This enables gamma ray spectrometry to be performed. Other common types of gamma ray detectors are Geiger counters, proportional counters, lithium-drifted germanium counters, and photographic film.

One common penetrating radiation technique performs gamma ray transmission measurements using the typical component arrangement shown in Figure 2. This technique measures the portion of a gamma ray beam which passes through the test material. This method utilizes the fact that the gamma radiation interacts with the material in its path by scattering and/or absorption of a portion of the incident beam. The three processes of gamma absorption and scattering are (1) photoelectric absorption, (2) Compton scattering, and (3) pair production (an absorption process). The degree to which each process contributes to the total absorption is dependent upon the gamma ray energy, the atomic number of the absorber, and the amount of the absorber material. The attenuation of the gamma ray beam can be described by the simple exponential law:

$$R_T = R_0 e^{-\mu x} \quad (1)$$

where R_T = detector response to primary (unscattered) gammas with a sample in the path of the beam, R_0 = detector response to primary gammas with no sample in the path of the beam, μ = linear absorption coefficient (cm^{-1}), and x = material thickness (cm). The absorption coefficient accounts for all three absorption processes mentioned above. In many practical cases the density, ρ , (g/cm^3), of the material is often taken into account by writing the equation as:

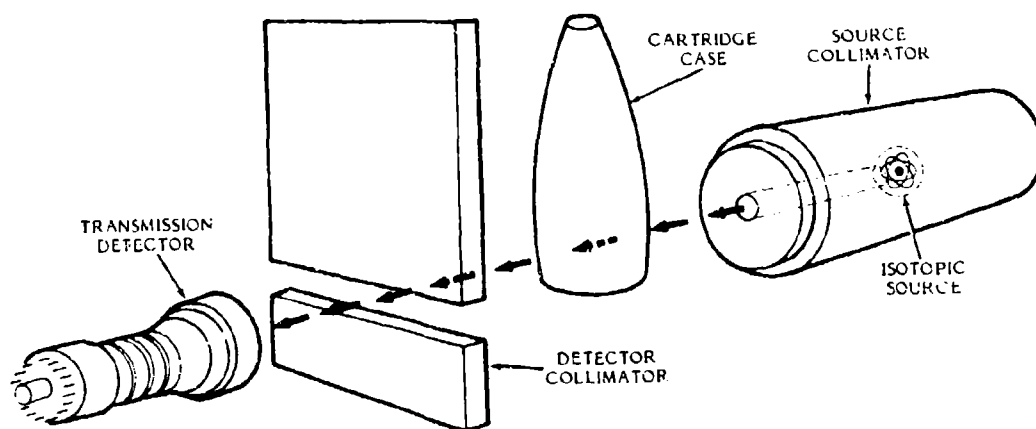
$$R_T = R_0 e^{-(\mu/\rho)\rho x} \quad (2)$$

In this case μ/ρ is called the mass absorption coefficient is expressed in cm^2/g .

In order to gauge, for example, the thickness of a sheet of steel, the source is placed on one side of the sheet and the detector on the other. If the density of the steel is $7.86 \text{ g}/\text{cm}^3$ and the mass absorption coefficient is $0.08 \text{ cm}^2/\text{g}$ (assuming that the incident beam is generated by a cesium-137 source which produces 0.66 MeV gamma rays), by rearranging equation (2) we obtain

$$-\ln R_T/R_0 = (\mu/\rho)\rho x = 0.629x \quad (3)$$

where x is the steel thickness in centimeters. If the detector measured $R_o = 10,000$ counts per second (cps) before the steel entered the gauge and then measured $R_T = 2,500$ cps after the sheet is inserted, the transmission (R_T/R_o) would be 0.25 (or 25 percent). This results in a calculated steel thickness of 2.2 centimeters (0.87 inch). This method, using an automated system with the necessary high speed electronics under computer control, can be used to gauge individual steel sheet parts as they pass or can monitor the thickness of a continuous steel strip by analyzing the variation in the transmission signal. The system can incorporate a feedback loop so that the transmission signal is used to keep the product within acceptable parameters.



RT-19126

Figure 2. Typical transmission gauge arrangement. The cartridge case shown here could be any object.

The measurement of density by the gamma transmission principle is another important application. Density measurements can be used to monitor the percent solids in a liquid slurry or the ratio of two components in a two-component liquid, solid suspension or solution, as well as in conjunction with linear flow-rate meters to obtain mass flow rates of liquids in pipes or solids on a conveyor belt.

For density measurements, the sample thickness must be fixed since the absorption and scattering in the sample are a function of density and thickness.

The measurement of average HEI (high-explosive, incendiary) density in a steel projectile is a good example of this noncontact technique. By passing the collimated beam of gamma rays through the longitudinal axis of a loaded, unfuzed projectile, a measure of R_T and R_O can again be obtained. The attenuation of the beam is described by

$$R_T = R_O \cdot e^{-\frac{\mu}{\rho_s} \rho_s x_s} \cdot e^{-\frac{\mu}{\rho_H} \rho_H x_H} \quad (4)$$

where the subscripts s and H stand for steel and HEI respectively. The first exponential term describes the beam attenuation due to the steel base material (0.25 inch) and the second describes the beam attenuation due to the HEI material (4.0 inches). The mass absorption coefficients for steel and HEI are constants as long as no drastic chemical changes occur. The density of the steel is not expected to change from projectile to projectile. The steel and HEI thicknesses are controlled to within small tolerances. Therefore, the measurement of R_O and R_T using a suitable gamma detector enables calculation of the HEI density, which is the only unknown in the equation. Absolute measurement of the average HEI density is obtained by calibrating the gauge with a standard of known density. Relative density measurements are obtained by setting an accept/reject threshold level against which the measured transmission value can be compared.

2. SPECIFIC APPLICATIONS

Mild detonating fuze (MDF) is a vital component in many aerospace designs. A usual configuration of MDF is a metallic outer sheath (0.1-0.25 inch diameter) with a high explosive inner case. One application is for signal transmission under extremely high radiation and/or electromagnetic noise environments. Manufacturing variations strongly alter the performance of MDF, necessitating a need for a nondestructive inspection. X-ray-based methods are primarily sensitive to the metal sheath of the MDF and are not capable of directly measuring the explosive contents. Since it is the explosive core that basically determines the

performance characteristics of the MDF, it is desirable to perform the inspection with a technique inherently sensitive to this core. Thermal neutrons exhibit a much greater sensitivity to the hydrogen, and to a lesser degree the nitrogen, in the explosive than to the metal sheath. A filmless neutron gauging technique was utilized to provide the real time inspection capability at high throughput rates in a fully automated, production compatible inspection process. The MDF gauge completely eliminates the need for human interpretation of the inspection results. The system is configured for maximum inspection sensitivity. Californium-252 is utilized as the neutron source. The gauge has the necessary biological shielding to accept up to 15 milligrams of ^{252}Cf . It uses a two-detector data acquisition channel which views the MDF through a precision collimation system. A continuous source monitor is utilized for an independent calibration of the system. The gauge is designed so that by simply changing the guide bushings, any size of explosive cord between 2 and 18 grains/ft can be tested. It can be operated either in a static mode (stop and count) or a dynamic continuously scanning mode. In the dynamic mode the gauge continuously scans the MDF with 2 percent precision at a 95 percent confidence level at feed rates as high as 100 feet per minute. Figure 3

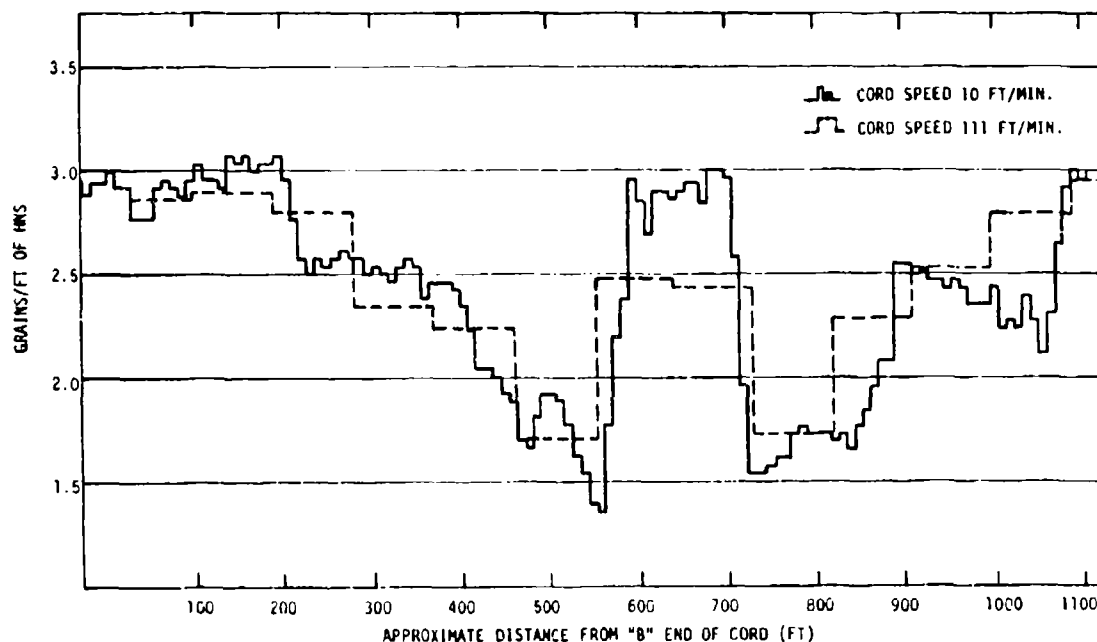


Figure 3. Data from a variable load MDF cord

shows a typical output signal displaying the grains/ft of explosive (core density) versus the distance from the end of the cord. Notice that the solid line represents the output at a scan rate of 10 feet per minute and the dotted line for 111 feet per minute.

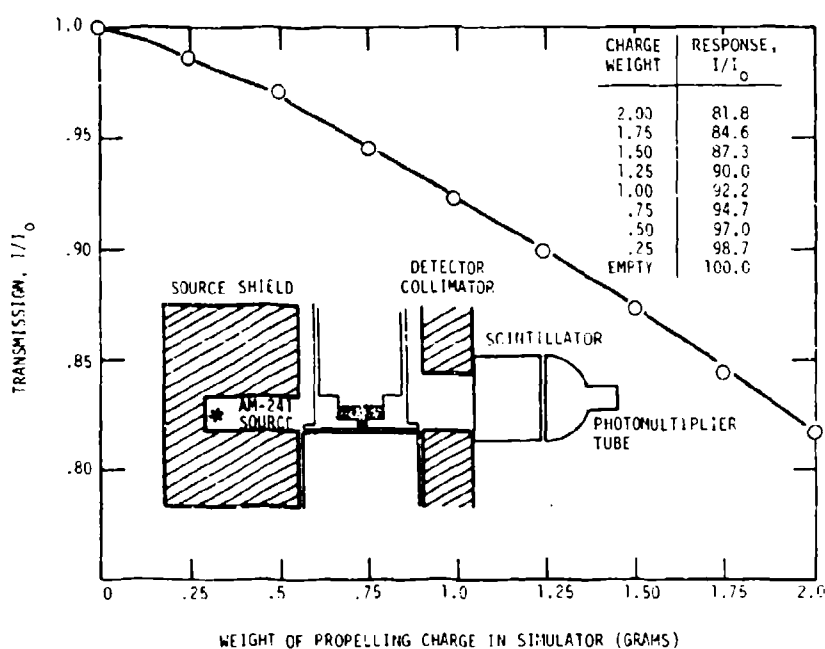
In high speed, automatic cannons (especially externally powered models) a hangfire round will function after the breach has opened and result in damage to the gun and other items close by. Therefore, it is important to correctly assemble all igniter components during the ammunition loading operations. An automatic, noncontact, penetrating radiation gauge based upon a gamma transmission configuration is currently used to count the number of igniter pellets in 30 mm ammunition cartridges. Missing IB-52 igniter pellets are detected and identified by this computer controlled gauge at a rate of 45 parts per minute. Reject cartridge cases are segregated for operator removal and disposal. Operational characteristics of the igniter pellet inspection gauge are shown in Table 2. Cartridge cases containing two pellets or less are rejected. Notice that the signal difference between the two pellet reject and the normal production (three pellet) case is approximately ten standard deviations. This separation allows for extremely reliable operation.

Table 2. Operating Characteristics for the 30 mm Igniter Pellet Gauge

	Mean Signals	Standard Deviation	Number Samples
2-pellet standard one cartridge case	2746	13	60
3-pellet standard one cartridge case	2616	10	64
Normal production	2636	13	40
Δ Counts (2-Pellet to 3-Pellet) = 130 pulses \cong 10 Standard Deviations			

A third application involves the inspection of signal and flare simulators used for training purposes. The two gram, black powder propelling charge ignites the delay on the pyrotechnic candle and launches the candle/parachute assembly from the hand held gun. If the propelling charge is lost during the loading operations, the percussion primer output gases ignite the delay element, but are insufficient to

launch the item. Subsequent functioning of the pyrotechnic in the hand gun can result in serious injury to the user. The data in Figure 4 illustrates the signal generated by a gamma transmission gauge as a function of the weight of propelling charge in the simulator. Since visual inspection of finished simulators will not detect missing or partially loaded propelling charges, a penetrating inspection technique must be utilized. Normal inspection approaches might require 100 percent x-ray radiography (film) inspection of each simulator. The use of an automated, self-calibrating, computer controlled gauge at the end of the assembly line will prove to be a more cost effective inspection procedure.



RT-19186

Figure 4. Gauge transmission response for propelling charge variations

A more complex penetrating radiation inspection system is under development to inspect the high explosive (HE) filler in artillery projectiles. The Automatic Inspection Device for Explosive Charge in Shell (AIDECS) technique scans a shell with a beam of radiation and observes the Compton scattering through a unique collimating system similar to that shown in Figure 5. The hardware consists of the

source, a beam collimator, a detector collimator, a set of radiation detectors, and a computer for system control, data collection, and analysis. During inspection, the projectile is inserted in the beam path and moved through a fixed scan pattern by a mechanical handling system. Since the amount of Compton scattered radiation is directly related to discrete density zones in the projectile, the system is capable of generating a three-dimensional data matrix representing the density of the explosive filler. Voids are identified as zones of low density and are classified according to their general shape, size, and location. On this basis, the system decides shell acceptability in accordance with military specification requirements.

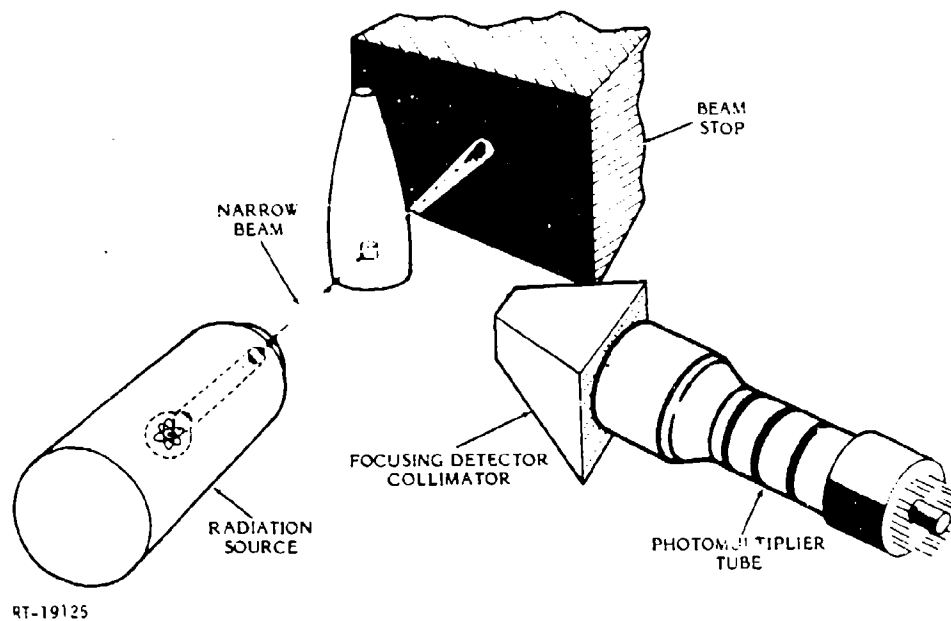


Figure 5. Typical scattering gauge arrangement

The AIDECS technique can be used in many other applications. In the one described above, it will replace an existing film radiography inspection procedure and eliminate the need for human interpretation and judgement. Thus, the AIDECS inspection of artillery projectiles will provide more consistent and reliable results at lower costs.

3. SUMMARY

Other configurations for penetrating radiation gauges besides transmission and scattering arrangements rely on backscattered gamma rays to determine thickness, density, or weight. The composition of a sample can be determined in some cases by fluorescent or prompt gamma techniques. Occasionally, a difficult inspection problem can be solved through the use of dual gamma energy gauges which analyze the differential signal from a sample scanned by two beams, one low energy and one high. Dual energy gamma gauging is often effective for discriminating between elements having significant differences in their atomic numbers. In several instances, this has proven to be a powerful inspection technique.

The measurement of neutron transmission or scattering can provide important information for certain samples. A commonly used and available isotopic source of neutrons is californium-252. IRT's portable narcotics detector is an example of neutron gauging.

The selection of a radiation source to provide the desired sensitivity, the subsequent matching of detectors and electronics to interpret the data, and the engineering of a fully operational, automated system are some of the high-technology services provided by IRT Corporation. Prototype manufacture and testing, full-scale systems fabrication, installation to existing production machines, and system maintenance are typical activities performed under the broad designation of penetrating radiation gauging.

ILLEGAL MANUFACTURE AND USE OF PYROTECHNICS

Arthur L. Cunn
Explosives Enforcement Officer
Explosives Technology Branch
Bureau of Alcohol, Tobacco and Firearms
Washington, DC 20226

ABSTRACT

This is a brief description of federal regulation and laws relating to the manufacture, storage, transportation, and sale of fireworks. A case history is presented by use of slides to show illegal manufacture in various geographical locations in the United States and the slovenly way in which the manufacturing process takes place. Also presented is a case of an accidental explosion of a residence, where illegal fireworks were made. An eyewitness account of the fire and explosion were filmed by a neighbor who had a camera in hand. This one incident involved over 4 million dollars in damage, one death, and numerous injuries. Another case history depicts the manufacturing process and storage of illegal fireworks, including the crude manufacturing process and almost non-existent safety precautions.

INTRODUCTION

The Bureau of Alcohol, Tobacco and Firearms established in 1972 is a federal bureau under the Department of Treasury. It combines law enforcement, industry regulation and tax collection. One of the Bureau of Alcohol, Tobacco and Firearms primary missions is the suppression and investigation of explosives incidents and crimes including arson.

The Bureau of Alcohol, Tobacco and Firearms assumed explosives regulations under Title XI of the Organized Crime Control Act of 1979, and published regulations which were effective February 12, 1971. The status of the pyrotechnic industry under this law was unclear. Accidental explosions and the multitude of injuries, as well as great amounts of property damage dictated that the Bureau of Alcohol, Tobacco and Firearms, enforce safe storage requirements on this industry. At about this time the Consumer Product Safety Commission and State and federal agencies notified the Bureau of Alcohol, Tobacco and Firearms of a rapid proliferation in the traffic of illegal fireworks and this is the problem I will address today.

Obviously, fireworks in general are very popular in the sense that they are desired by Americans in large numbers. Many thousands of fireworks related injuries are reported each year and the most common cause of these injuries are misuse, principally by children under 14. The federal government, specifically the Consumer Products Safety Commission conducted studies, and as a result the Child Protection Act of 1966, an amendment to the Federal Hazardous Substances Act instituted a ban on large exploding fireworks, items such as cherry bombs, silver salutes, and M-80's. Also, banned were mail order kits designed to build such fireworks. This ban on the public sale of these items were supported by the legitimate fireworks industry because of the extremely hazardous nature of the items. By 1976, other regulations were adopted to limit the powder content of "Class C" or common fireworks to less than 50 milligrams.

The Department of Transportation with the help of the fireworks industry, separated fireworks into Class B and Class C catagories. This

regulation under the Code of Federal Regulations, Part 49 for the first time set limits on the amounts of pyrotechnic composition that could be in items offered for transportation in interstate commerce.

In the State of Illinois alone a fireworks plant exploded each year between 1970 and 1973. During these years 7 persons died, 39 were injured and many millions of dollars of property damages resulted from fireworks plant explosions. This is only a small example of the magnitude of the fireworks safety problems in this country. In 1978 the criminal misuse of explosives resulted in 116 deaths, 247 injuries and more than 2 billion dollars in property loss.

With various regulations effecting the manufacturing, storage, transportation and sale of fireworks, injuries involving Class C items were reduced. Unfortunately a large illegal market in Class B fireworks was flourishing and clandestine illegal manufacturing plants were making fireworks and supplying raw material to individuals throughout the United States. This became a very significant problem in our country due to extensive accidents and injuries, as a result of both misuse and poor quality control. In 1978, several hundred persons were injured with one illegal manufacture's production of M-80 fireworks with a defective fuse. The fuse when lit had no delay and caused the firework to explode instantly before the person using it could release it from his hand. One of the illegal manufacturing plants of these devices was found to be a two story frame house with part time employees, having absolutely no training or pyrotechnic knowledge, constructing fireworks in the kitchen and living room areas. Over twenty-two (22) 55 gallon drums of flash powder were stored in the garage. An electric hot plate was used to heat coffee for the workers and a small kitchen exhaust fan was utilized to remove the explosive dust from the area. The floors and walls of the entire first floor were covered with powder and they never had an accident in the time they were in operation. None of the machinery used had explosion proof motors and ordinary concrete mixers were utilized in mixing

black powder.

This is almost typical of the type of operation that is used by the illegal manufacturer. There exists absolutely no quality control and no safety requirements involved in manufacture, storage or transportation are used.

I will now show some slides depicting some of the things I have talked about.

SLIDE 1 THROUGH 22 - SMOKE COMING FROM RESIDENCE.

On St. Patricks Day 1978, a wood frame structure valued at \$100,000 dollars located in an upper middle income community in the State of Illinois was destroyed by a fire and explosion within two minutes. Very few neighbors expected a fireworks factory to be situated in their own backyards.

The set of slides you are viewing were taken by a neighbor who was photographing his own residence when he spotted smoke coming from a house across the street. This entire sequence was captured on film in three minutes. The photographers wife called the fire department and being only a few blocks away they responded almost immediately.

Shortly after the arrival of the fire department to what first appeared to be a small smoking fire, a loud explosion occurred and the house started to breakup. Almost immediately a second explosion occurred leveling the house. At this time a burning person was seen running from the explosion. He was assisted by the firemen and removed to a hospital where he later died of burns.

The fire and explosions caused \$4 million dollars worth of damage to the area including the loss of two fire trucks and one police car.

A followup investigation disclosed that the victim, the owner of the house was manufacturing illegal fireworks in the basement and over 600 pounds of explosives consisting of perchlorate explosive powders and black powder was on the premises before the fire. The cause of the accident was determined to be a spark from a fuse cutting machine.

CASE STUDY OF ACCIDENTAL EXPLOSION OF
RESIDENCE WHERE FIREWORKS WERE MANUFACTURED

- Slide 1. Smoke observed emanating from house.
2. Fire starting to progress.
 3. Firemen arrive fro what appears to be small confined fire.
 4. First explosion occurred.
 5. This explosion injures firemen, damages fire truck and police vehicles.
 6. Second explosion follows.
 7. House starts to explode and fall apart.
 8. Fire and police personnel flee immediate area.
 9. Smoke now obsuring house.
 10. House completely devastated.
 11. New flare up of chemicals causes smoke.
 12. Fire personnel return to site to fight fire.
 13. Person seen leaving ruins and smoldering.
 14. Victim is observed by fire chief.
 15. Victim is aided by firemen and flames on cothing are smothered.
 16. Remains keep exploding and emitting dense smoke.
 17. Fire and smoke continues.
 18. Fire will not remain out, keeps relighting.
 19. More minor explosions occur.
 20. Final smoldering ruins.
 21. Aerial view of accident site.
 22. Final cleanup as water turns to ice.

CASE STUDY OF ILLEGAL FIREWORKS
FACTORY MANUFACTURING M-80 TYPE FIREWORKS

- Slide 1. Typical M-80's
2. Outer containers prior to filling.
 3. M-80 is marked as smoke.
 4. Typical illegal and dangerous storage.
 5. Sample of typical packing.
 6. Cardboard carton packaging of fireworks.
 7. Sacks of M-80's.
 8. Preparation trays for M-80's
 9. Empty cases ready for filling.
 10. Filled and sealed fireworks in storage trays.
 11. Typical work area.
 12. This scene depicts slovenly storage and work areas.
 13. Mixing machinery.
 14. Homemade mixing tub.
 15. Non-explosion proof machinery (air compressor).
 16. Fireworks ready for shipment.
 17. Storage of 55 gallon drums of perchlorate mix.
 18. Non-explosion proof hydraulic press.
 19. Dirty/contaminated work area.
 20. Cement mixer used to mix black powder.
 21. Floor used as work area.
 22. Numerous cartons filled with fireworks.
 23. Outside view of building used for manufacturing site.
 24. Picnic table used outside for assembling fireworks.
 25. An almost neat and clean work area.
 26. Flash powder covers entire inside of building.
 27. Sealer for ends of fireworks drying.
 28. Mislabeled sacks of filler material.
 29. Thousands of M-80's in drying process.
 30. Same as above (another view).
 31. Powder all over interior of building.
 32. Work bench covered with fireworks powder.

33. Fuse cutting machine without benefit of explosion proof motor.
34. Fifty-five gallon drums of fireworks mix.
35. Work bench and storage area.
36. Finished fireworks prior to packaging and shipment.
37. Filler material of corn cob grits.
38. Contaminated work area.
39. Propane torch used to melt glue for casings.

A MICROCOMPUTER SYSTEM FOR FLARE TEST ANALYSIS

by D. R. Dillehay
Thiokol Corporation
Marshall, Texas 75670

Abstract

A test system was needed to provide rapid analysis of data from flare tests. Data was being recorded in two band passes on a recording oscillograph and manually reduced to determine critical times and peaks. An inexpensive micro-computer was installed in the test tunnel and a program written to take the sensor data, store the values in the computer memory and subsequently analyze the data. Complete analysis of a flare test is now available within 10 seconds after the flare is burned. The data are formatted and printed with averages and standard deviations for distribution immediately after completion of testing. Cost savings on one program amount to over \$183,000 per year.

Background

Flare testing at Longhorn Army Ammunition Plant has traditionally been accomplished with strip charts, stop watches, electronic integrators and manual control of start and stop parameters. With the advent of more sophisticated flares, test requirements have become more stringent with data requiring millisecond resolution and more accurate determination of peak output values. In order to meet these requirements, data had to be taken with a recording oscillograph. The oscillograph traces were taken to the Documentation Group for manual reduction for the desired parameters. The traces were reduced by measuring displacements from the base line and comparing with calibration steps. Reduction of minimal data required approximately 30 minutes per test. In addition to standard lot acceptance tests, special mix qualification tests are run before a mix is consolidated which resulted in a very large workload for data reduction. The time factor for evaluation of the data necessitated much of the work to be done on overtime. Even with overtime, it frequently was the second day after testing before all the data could be analyzed, averaged, and copied onto forms for distribution.

Experimental Results

The oscillograph trace shown in Figure 1 represents a typical output versus time plot from a sensor. For this particular flare program, it is necessary to determine the time required for the output to reach a predetermined threshold level or "rise time". The time that the output remains above the threshold level is called the "action time". For Quality control purposes, it is desirable to determine the "total time". It is necessary to determine the maximum or "peak" value that occurs during the first 0.5 seconds of the

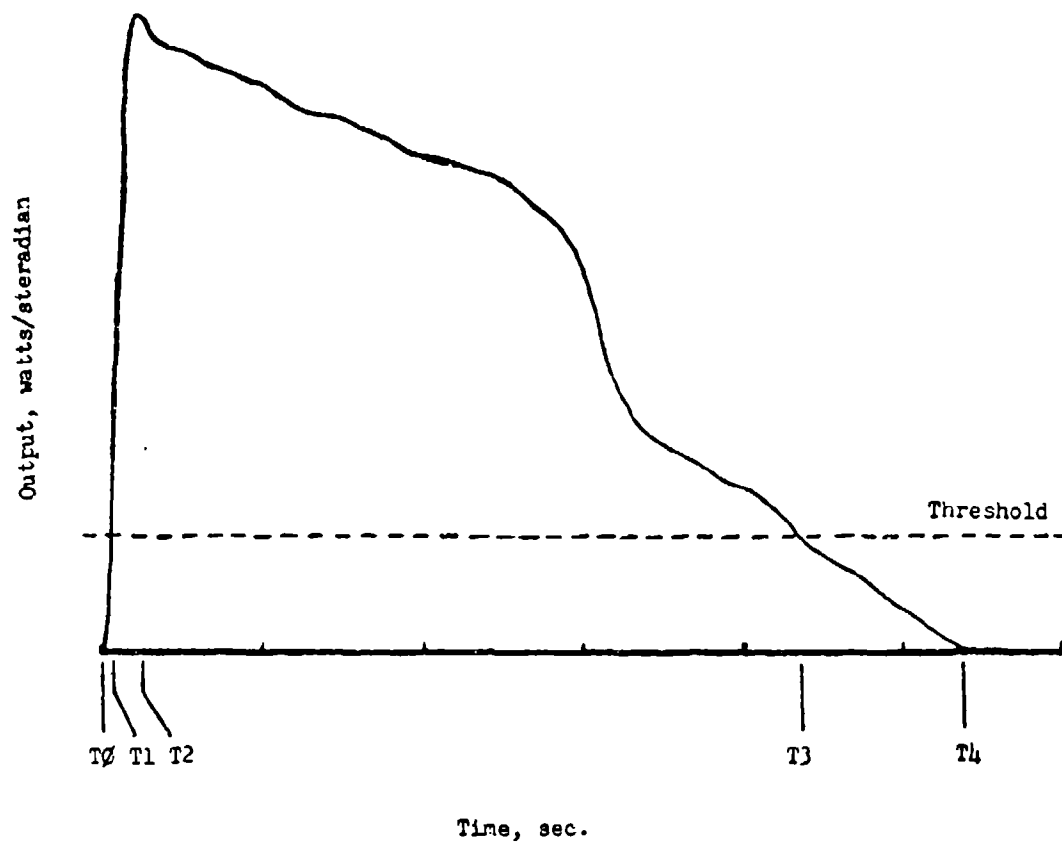


Figure 1.

test and the overall peak value during the test. It is possible for the overall peak to coincide with the peak in the first 0.5 second. The time at which the overall peak occurs must also be determined. The integral of the trace is determined to monitor the total energy output of the flare. These values are necessary for the two different channels of data on each flare tested representing information on output in two different wavelength regions.

A TRS-80 microcomputer was available and it was decided that the only practical way to take data and get immediate results for production acceptance and quality control was to use the computer in the test tunnel itself.

Telesis Laboratories custom built an 8 bit analog-to-digital converter with two channels for data acquisition. The cost was about \$400. The A/D converter used a signal from the computer to trigger a read action on both channels simultaneously. The conversion takes 800 microseconds and the values are latched for input to the computer on command.

Figures 2 and 3 show a flow chart of the desired program functions. The initialization routine clears memory and sets up arrays of the proper size to handle the data. The program then accepts input data to describe the test. These data are responses to prompts to the operator asking for the date, test identification (such as lot number), the number of mixes to be tested, the quantity of flares from each mix, and test set-up conditions. The computer program then sets up a book-keeping system to keep track of each flare by an identifying number. Using the flare number allows the operator to test the flares in random order, with the computer keeping track of the data for final formatting. Calibration involves inputting a voltage that has been calibrated against a black body to determine watts/steradian. The computer reads the voltage and calculates a calibration factor in watts/steradian/volt.

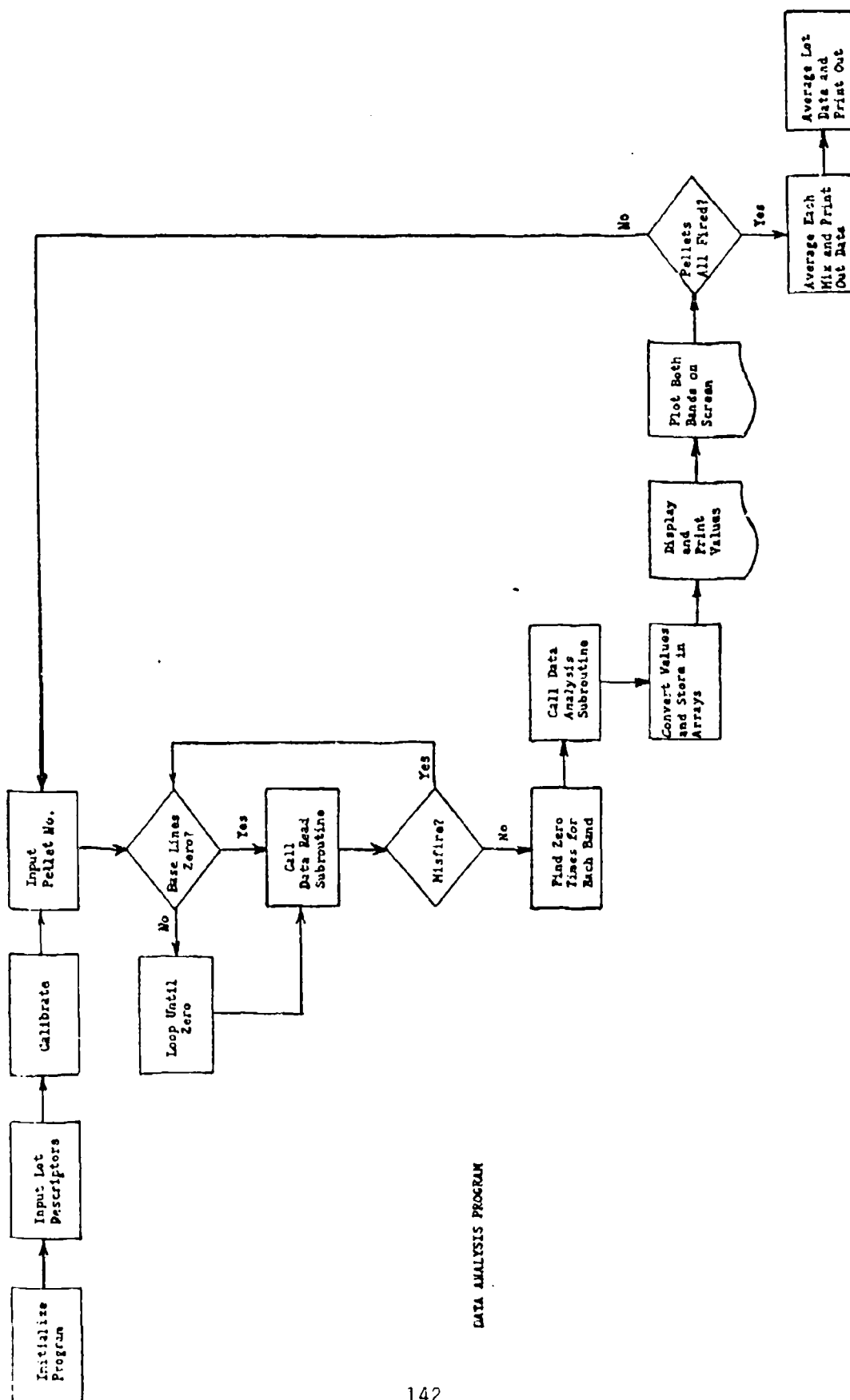


Figure 2.

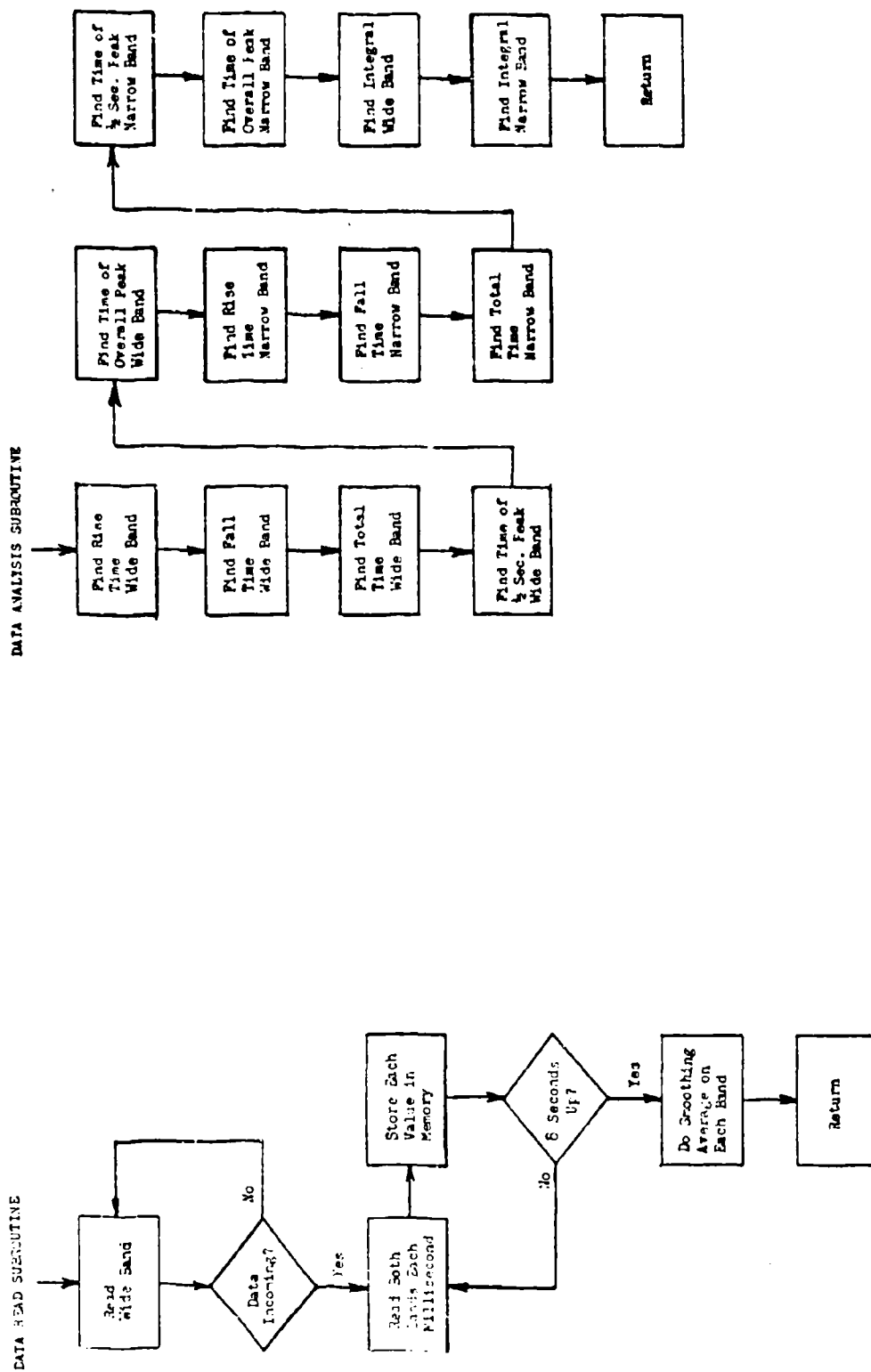


Figure 3.

Thereafter, the input voltage multiplied by the calibration factor yields the output in watts/steradian.

Using BASIC programming language, the computer could not read the input ports fast enough for millisecond resolution or reduce the data in a reasonable length of time. To solve this problem, machine language routines were written to clear blocks of memory for data storage, read the data into memory and then analyze the data. From the oscillograph traces, it was noted that some AC signal was superimposed on the input lines. While this can be smoothed out by manual data reduction, it was felt that it could lead to sizeable errors in the computer analysis. To improve the quality of the trace, a 16 sample smoothing correction was chosen. Over a 16 millisecond time period, 60 cycle noise would complete one cycle and thus the positive and negative portions will cancel. The program takes 16 values and averages them and stores the value in a temporary buffer block of memory. The program then drops one value and picks up the next value and averages the new set of 16 values. This program then moves the smoothed curve back to the original location.

Clearing the blocks of memory for data storage was simply a matter of loading each memory location with a value corresponding to zero input. To take the data, it was determined that 8 seconds was sufficient to cover the expected range of flare burn times. An 8000 byte block of memory was reserved for each channel of data and an 8000 byte buffer area was set aside to temporarily hold the smoothed curve. To conserve the 8000 bytes of memory for each channel, it was desired that data storage not begin until the flare actually started burning. To accomplish this, a loop is set up by the program to check the input from Channel 1 and to keep looping until the input value exceeds a set value.

When the set value is exceeded, the program begins to sample both channels each millisecond and store the values in memory for 8 seconds. The set value to trigger data input was chosen to be just slightly above the input noise level. When a flare ignites, the rate of rise causes the data input to begin not more than 1 millisecond after flare ignition. This is more than adequate for the current system. This technique also permits the use of slow acting igniters, such as quick-match and boron/potassium nitrate pellets, instead of the more expensive electric match igniter. At the end of 8 seconds, the program runs the smoothing average on the data from Channel 1 and then repeats the process to smooth the data recorded from Channel 2.

Once the data is recorded and smoothed, the program returns to BASIC to check the firing results for normal data and to determine the exact time that the flare started to burn. The first check is to allow for the possibility of a misfire. Occasionally, the ignition circuit fails to function. The program reads the value stored corresponding to 0.5 second. If the program happened to be triggered by any external noise pulse, and took data for 8 seconds, the data at 0.5 second would be less than some arbitrary minimum value. If the value is less, the computer program asks if it was a misfire. If "yes", control is returned to the program to test again without altering the flare number or test number. If "no", the program proceeds to analyze the data. The second check is necessary if a noise pulse triggers the system to begin reading too soon. Finding the correct zero locations for each channel is accomplished by reading values at intervals until the rise time threshold is exceeded. The program then steps backward through the input data 1 millisecond at a time until a zero reading is obtained. This memory location corresponds to the start of incoming data

At the end of testing, the program averages all the data for each mix and prints the average and standard deviation for each parameter. The data are then printed in summary form by mixes for ease of review with a final listing of the overall lot averages. A list of flares that were flagged as not being included in the averages is also printed.

The program has been implemented and has proven to be highly effective. A comparison of data values reduced manually from the traces with the computer values showed excellent agreement. The differences noted were with experimental error of the manual data reduction. Approximately 10 seconds after testing a flare, a complete analysis of both channels of data is presented for evaluation. Errors due to miscopying of the data are eliminated. The summary of the data is ready for reproduction and distribution less than 10 minutes after completion of a test. Data reduction cost savings on one program are calculated to be over \$183,000. The system will be applied to other types of flares for additional cost savings. In addition to direct savings in data reduction, the immediate availability of test data provides faster response to production problems adding incalculable savings in the production operations.

In the future, disk drives will be added to the system for storage of the computed values to permit correlations and summary reports without the necessity of re-entering the data. For reference purposes, the cost of a complete system suitable for this analysis is approximately \$4,000, not including software or program cost.

RP SMOKE PERFORMANCE MODELING USING A MICROCOMPUTER

by D. R. Dillehay
Thiokol Corporation
Marshall, Texas 75670

Abstract

The XM-803 is an experimental 155mm red phosphorus composition smoke round. It is loaded with 228 wedges of RP smoke composition and air bursts over the target. The wedges are ignited and land on the ground and generate a smoke cloud. To aid in evaluation of the burning rate of the wedges, a computer simulation was written to calculate a concentration-path length product for comparing effectiveness of the round with different burn rates for the smoke composition. The effect of wind velocity on the smoke cloud can also be studied. The computer program can also handle other smoke rounds based on phosphorus smokes.

Background

The experimental evaluation of smoke compositions is tedious, time consuming and expensive. A computer simulation was needed to allow rapid evaluation of performance under different conditions and with varying burning rates. Using this simulation, it would be possible to optimize the burning rate to give the maximum smoke obscuration for some minimum time requirement.

The CL product is the product of concentration of smoke times the path length. The CL product is used in sophisticated smoke models to determine smoke obscuration under various lighting conditions, target contrasts, and other external parameters. For the purposes at hand, the assumption was made that all other factors would remain constant and only the CL product would vary. Therefore, if the CL product is known, then obscuration would be proportional under fixed external conditions.

Experimental Results

From previous field tests and laboratory measurements, it is known that the effective CL product is 2.3 gm/m^2 for phosphorus smokes. The following listing will detail the assumptions and variables used by the computer program.

- 1) The round has an incoming angle of 60° .
- 2) Height of burst can be varied from 50 to 200 meters.
- 3) The cylindrical load of 228 wedges expands radially during descent of the wedges. The rate of expansion and descent velocity were chosen to give a 148 meter circular pattern if burst at a height of 125 meters at an incoming angle of 90° . This was related to field test patterns.
- 4) An elliptical pattern of wedges is produced on the ground due to the 60° angle. See Figure 1.

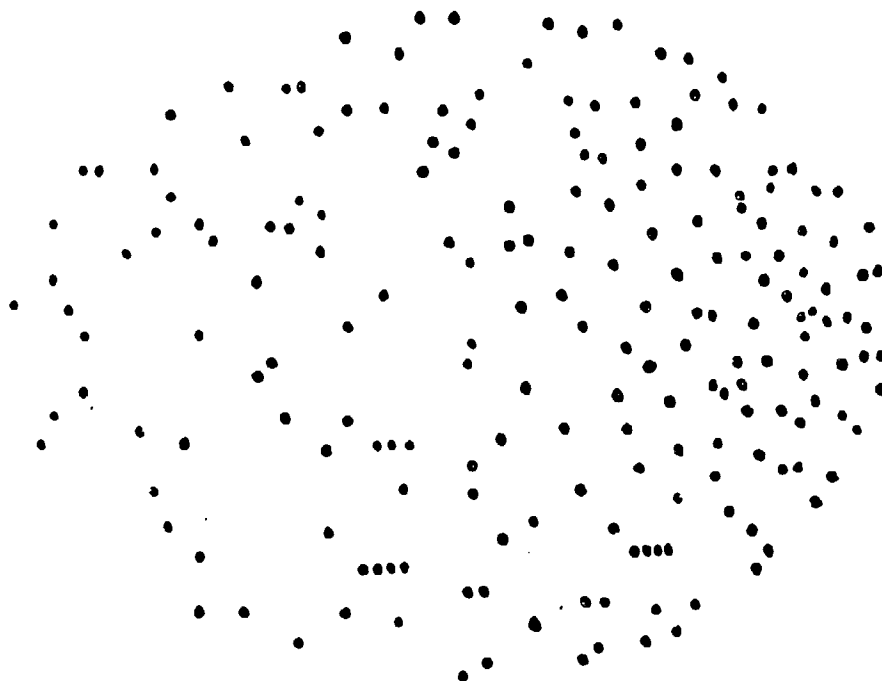


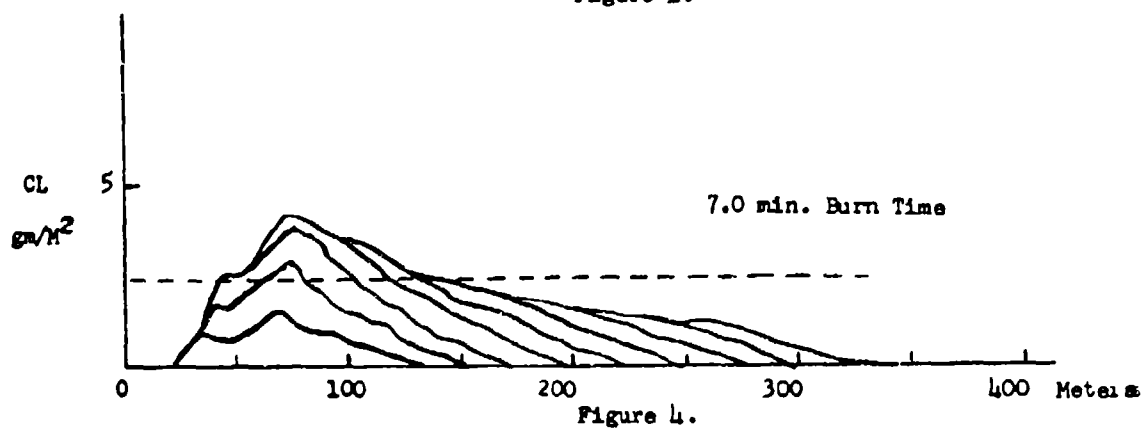
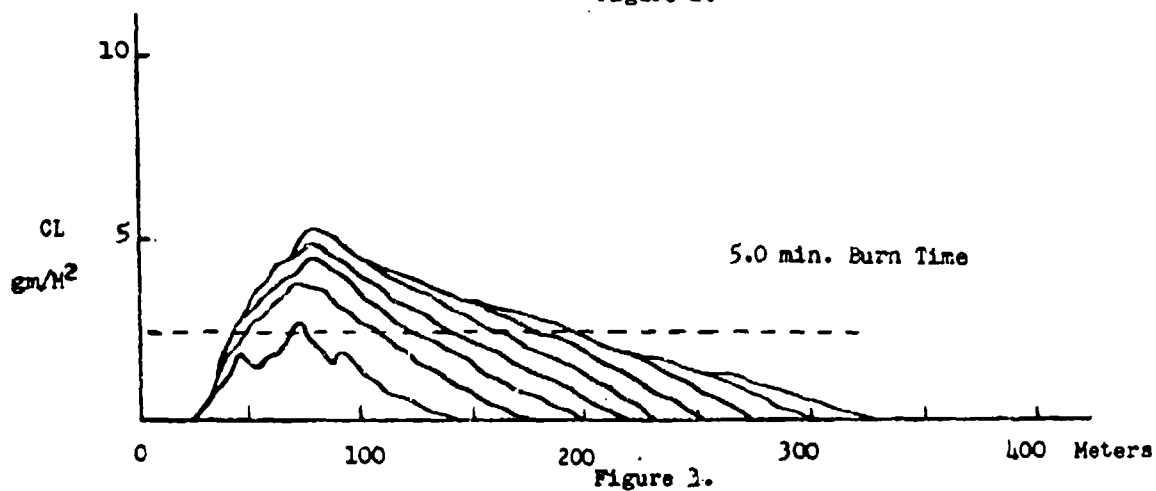
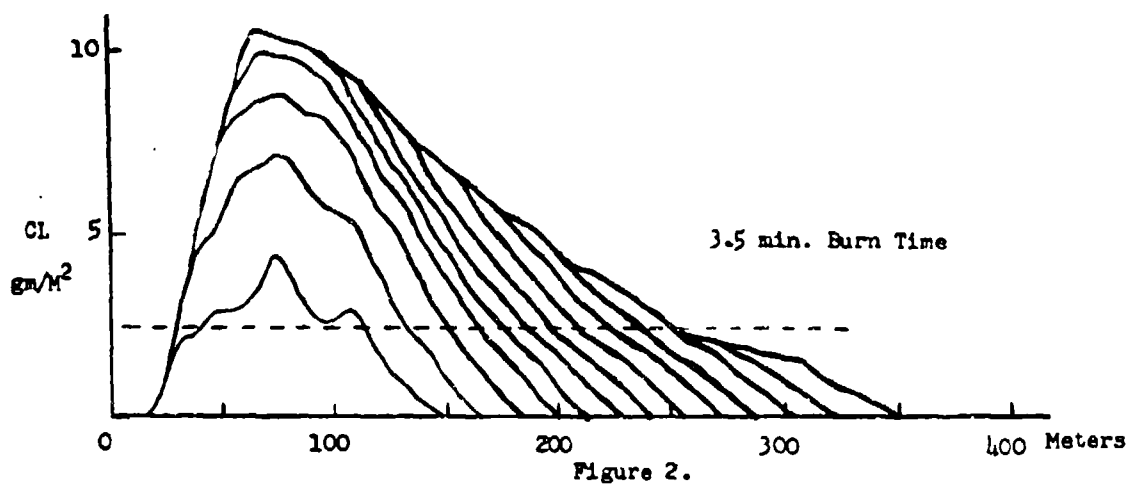
FIGURE 1.
SMOKE WEDGE GROUND PATTERN

- 5) Due to the angle and rate of expansion, the wedges are more densely distributed in the pattern towards the incoming direction.
- 6) The wedges are randomly distributed on the ground within the density boundaries.
- 7) Each wedge starts to burn at a uniform linear rate.
- 8) A cross wind of assignable velocity blows across the minor axis of the elliptical pattern.
- 9) The smoke from each wedge follows a half-cone pattern in the direction the wind is blowing.
- 10) The computer program calculates the CL product for a 2 meter line-of-sight at 10 meter intervals from the edge of the elliptical pattern out to 300 meters for each wedge and sums the values at each position at 10 second intervals.
- 11) A plot of the CL product against distance allows an evaluation of the obscuration front of the pattern at a given time.

By using several patterns, it is possible to determine the expected range of variations from rounds of a given type. This is of benefit in comparing computer data with limited field test data.

The computer used for this simulation is a TRS-80 from Radio Shack. A system capable of running the program and plotting the data can be obtained for less than \$4,000. Pending receipt of a printer-plotter, the data from the computer has been copied and manually plotted to give results comparable to Figures 2, 3, and 4. The patterns shown in Figures 2, 3, and 4 represent 3 different burning rates of the wedges. The program permits running the same ground pattern under different input conditions.

This program is just getting underway to optimize the burning rates for application to new smoke rounds



CL Versus Distance - 3 Burning Rates

utilizing red phosphorus smoke compositions. The use of an inexpensive microcomputer for simulation will reduce testing requirements and save time in program implementation.

BLAST OVERPRESSURES FOR CONFINED EXPLOSIONS

G. F. Kinney, R. G. S. Sewell, and K. J. Graham
Naval Weapons Center
China Lake, California 93555

ABSTRACT

Confined explosions of combustible and explosive fuels in grain elevators, coal mines, or ship compartments can be very damaging. The peak overpressures that such explosions can generate have been computed from first principles of conservation of mass and energy, and minimum Gibbs free energy. The amounts of the various chemical species that are present (including dissociated species) at the explosion temperature are found by iterative methods using a small tabletop computer. The peak overpressure, flame temperature, and products composition are calculated. Computer-generated overpressures agree closely with experimental observations on confined explosions of TNT in air for a three-decade range of fuel-air ratios.

The relative effectiveness of an explosive fuel in generating blast overpressure is described in terms of an internal blast yield. This is the inverse ratio of the amount of an explosive relative to some standard that is required to produce the same overpressure. Two blast yields are assigned to a given explosive--one yield for the low overpressure range and one for the high. Blast yields are presented for representative chemical explosives, and solid, liquid, and gaseous conventional combustible fuels.

CHARACTERISTICS OF INTERNAL BLAST

Blast in an internal explosion is characterized largely by its peak overpressure and duration of application. Confined air is suddenly warmed, generating a pressure rise that can be quite damaging. Examples of internal blast include blast from explosions in ship compartments, dust explosions in grain elevators or in coal mines, explosions of gasoline fumes in motorboat hulls or in refinery tanks, and natural gas explosions in

kitchens or in entire buildings. Internal blast may also account for the mysterious disappearance of an oil tanker at sea.

Maximum peak overpressures in internal explosions occur for the special case of (1) no venting effects, and (2) adiabatic conditions with no cooling effects by heat transfer to confining walls. Such maximum peak overpressures are the subject of this paper.

Internal blast from explosions with conventional fuels is a direct result of a simple combustion process. Explosive fuels, however, differ somewhat in that an initial detonation sets up a transient explosive shock, one that is quickly dissipated and can often be neglected in the overall energy effects. For explosive fuels that are also oxygen-deficient (e.g., TNT), the initial detonation is followed by combustion in an afterburn; it is the combined detonation-combustion reaction that generates internal blast. For explosive fuels that are oxygen-rich (e.g., nitroglycerin), there is no afterburn; internal blast is only a result of the warming effect of a detonation.

With conventional fuels the internal blast overpressure reaches a maximum at a fuel-air ratio that corresponds to optimum utilization of the oxygen present. Less fuel leaves unused oxygen, while more fuel does not give any increased energy release. Excess fuel serves only to increase the amount of products to be warmed, and the reduced temperature rise that results gives a decrease in developed overpressure. The characteristic maximum overpressure for conventional fuels (ca. 10 bars) contrasts with the behavior of explosive fuels that carry their own oxygen; developed overpressures for explosive fuels increase monotonically with the amount of the fuel.

In an internal explosion, after the peak overpressure is attained, a quasi-exponential pressure-decay phase is caused by cooling effects of confining walls and by gas leakage due to venting. This decay effect is relatively slow compared with rates that ordinarily occur after detonations in the unconfined atmosphere. The decay, however, causes the pressure to approach an equilibrium value that for vented explosions is also the ambient. For non-vented explosions, this equilibrium pressure can be greater than ambient if additional gas volume is created.

The slow pressure-decay rates for internal explosions lead to relatively long overpressure duration times that are perhaps as long as a major fraction of a second. The time integral of the blast overpressure is the blast impulse per unit area. Blast impulse can be an important factor in blast damage capability (Ref. 1).

THEORETICAL BACKGROUND

Efforts to describe internal blast mathematically date back to at least 1945, when the Los Alamos Scientific Laboratory (Ref. 2) suggested an empirical equation

$$\Delta P = 3000(W/V) \quad (1)$$

in then acceptable units of overpressure (ΔP) in pounds per square inch, mass of explosive (W) in pounds, and confined volume of air (V) in cubic feet. In modern metric units of bars, kilograms, and cubic metres, this can be written as

$$\Delta P = 13(W/V) \quad (2)$$

The metric pressure unit is the bar, defined in terms of SI units as 10^5 pascals (newtons per square metre), or as one-tenth of a megapascal. One bar corresponds to a pressure of 14.5 psi, approximately that of the ordinary atmosphere. The units of the term (W/V) of the equation, kilograms per cubic metre, are almost identical with ounces per cubic foot.

Overpressures computed through Equation 2 for internal explosion with TNT in air are shown in Figure 1. Also shown are experimental values for ordinary sea level conditions (Ref. 3). Rough agreement is indicated.

An equation for internal blast overpressure has been derived using the ideal gas law, but ignoring many complicating effects (Ref. 4). This equation states that for adiabatic nonvented conditions the overpressure (pounds per square inch) is

$$\Delta P = 8.8(H/V) \quad (3)$$

where the term (H/V) is the heat of combustion in kilocalories per cubic

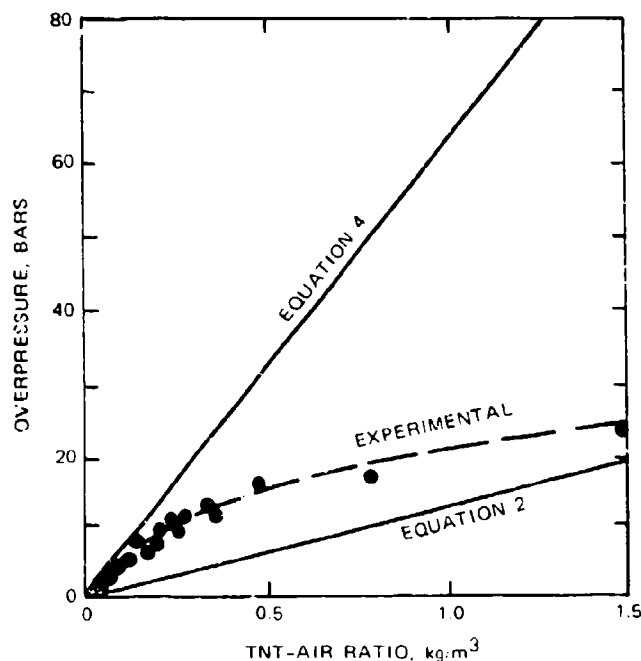


FIGURE 1. Internal Blast Overpressures for TNT-Air Explosions.

foot of product gases. In metric units of the bar and the joule per cubic metre, this equation becomes

$$\Delta P = 10^{-5}(k - 1)(H/V) \quad (4)$$

where k is the ratio of heat capacities for the confined gas (taken as 1.4, as for air at room temperature). Derivation of this equation ignores the effects of chemical dissociations in the flame, the effects of gases formed in the explosion, and the effects of temperature on heat capacity. Equation 4 may thus greatly overstate internal blast overpressures, particularly for explosions with appreciable fuel-air ratios (Figure 1).

An alternative approach to internal blast is afforded by thermodynamics. A rigorous thermodynamic analysis of internal blast takes into account the complicating effects of chemical dissociations that set an effective ceiling on both explosion temperature and blast overpressure. Combustion products at mechanical, thermal, and chemical equilibrium must be considered in this analysis.

THERMODYNAMIC CALCULATION OF INTERNAL BLAST

OVERVIEW

With internal blast, considering both conventional and explosive fuels composed of carbon, hydrogen, nitrogen, and oxygen, and including argon from the air, there are five types of atoms in the products. These products involve 12 (or more) different chemical species including unstable ones such as hydroxyl and monatomic hydrogen, monatomic oxygen, and monatomic nitrogen. To characterize 12 species, 12 independent relations are required. Five of these are provided by the law of conservation of mass, one for each type of atom. The seven additional relations are obtained through the second law of thermodynamics where the minimum Gibbs free energy restriction is utilized in the form of chemical equilibrium constants. These form 12 simultaneous nonlinear algebraic equations that can be solved by a simple heuristic method that is described below, and for which a tabletop computer is quite suitable.

To determine blast overpressure in an internal explosion it is necessary to know the explosion temperature and composition of products at that temperature. To determine explosion temperature, the conservation of energy principle is utilized. The energies involved must include both thermal energies associated with temperature and chemical energies associated with chemical composition. When these are known, the blast overpressure is computed through the ideal gas law.

CONSERVATION OF MASS RELATIONS

The conservation of mass principle is utilized in terms of individual elements. Thus all carbon in the products system is supplied by the fuel and can be expressed as the number of moles of carbon atoms, a_C . This equals the sum of the number of moles of carbon dioxide, CO_2 , and carbon monoxide, CO , in the products; i.e., $a_C = CO_2 + CO$, where a chemical formula is used to indicate the number of moles of a designated species. This type of equation is identified as a material balance. Similarly the material balance for hydrogen atoms, a_H , equals twice the number of moles of water vapor, plus twice that for molecular hydrogen, plus that for

monatomic hydrogen and hydroxyl OH. Such material balances for the five chemical elements are written as follows:

$$\text{Carbon} \quad a_C = \text{CO}_2 + \text{CO} \quad (5)$$

$$\text{Hydrogen} \quad a_H = 2\text{H}_2\text{O} + 2\text{H}_2 + \text{H} + \text{OH} \quad (6)$$

$$\text{Oxygen} \quad a_O = 2\text{CO}_2 + \text{CO} + \text{H}_2\text{O} + 2\text{O}_2 + \text{O} + \text{OH} + \text{NO} \quad (7)$$

$$\text{Nitrogen} \quad a_N = 2\text{N}_2 + \text{N} + \text{NO} \quad (8)$$

$$\text{Argon} \quad a_A = \text{Ar} \quad (9)$$

These material balances represent five of the required 12 relations; the remaining seven are obtained from free energy consideration.

GIBBS FREE ENERGY RELATIONS

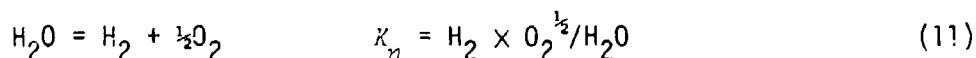
The second law of thermodynamics states that a closed system in equilibrium at uniform pressure and temperature shows a minimum in its total Gibbs free energy. The same rules apply to the quasistatic situations with internal explosions. Gibbs free energy values for particular species are conveniently expressed in alternative form as equilibrium constant of formation; data are available in sources such as the JANAF thermochemical tables (Ref. 5). These tabulated data are readily converted into conventional thermodynamic equilibrium constants, and in turn into working equilibrium constants in terms of mole numbers, K_m .

The seven mole-number relations required here and obtained by Gibbs free energy considerations are shown below. In the chemical equation to the left, a chemical formula identifies a specific component in a mixture at chemical equilibrium. In the equilibrium constant equations to the right, a chemical formula represents the number of moles of that component present in the equilibrium mixture.

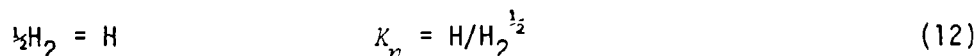
Dissociation of carbon dioxide:

$$\text{CO}_2 = \text{CO} + \frac{1}{2}\text{O}_2 \quad K_m = \text{CO} \times \text{O}_2^{1/2} / \text{CO}_2 \quad (10)$$

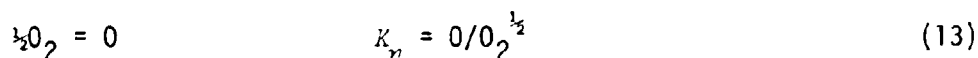
Dissociation of water vapor:



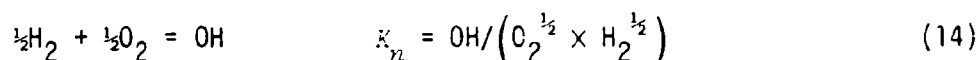
Formation of monatomic hydrogen:



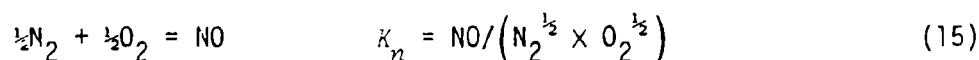
Formation of monatomic oxygen:



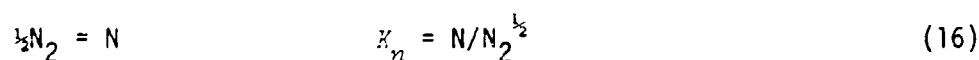
Formation of hydroxyl:



Formation of nitric oxide:



Formation of monatomic nitrogen:



Numerical values for a mole number equilibrium constant K_n depend on the species involved, the temperature, and the volume of the system. In principle such extensive equilibrium data could be stored in the memory of a large computer and utilized as required. The needed tabulations can be condensed into relatively simple algebraic equations for the (logarithm of the) equilibrium constant of formation as a function of absolute temperature T . Thus

$$\log K_f = A + B/(T+C) \quad (17)$$

where constants A and B are essentially those of the classic van't Hoff equation, and constant C , a curvature constant, provides for small discrepancies between experimental and van't Hoff values. Constants of Equation 17 are tabulated in Reference 6 for the seven chemical equilibria in the internal blast generated by C-H-N-O fuels. The temperature range for these is from 4000 K, well above the temperatures of ordinary explosions, down to 1500 K, a quench temperature below which rearrangement

reactions for explosion products are so sluggish that chemical equilibrium may not be attained.

DETERMINATION OF EQUILIBRIUM COMPOSITIONS

Twelve simultaneous equations for defining the equilibrium compositions described above (five linear material balances and seven nonlinear equilibrium expressions) are to be solved. Many methods for solution, some of them quite elegant, have been suggested. A relatively simple heuristic method of successive approximation, where each approximation seeks to improve on previous ones, is utilized here. The advantage of this method is that it can be adapted to manual solution and is also readily programmed for a small computer.

The iterative calculation begins with the nominal composition obtained through material balance considerations. Then the program computes, through equilibrium constant expressions, the amount of other species (the minor components) that would be in chemical equilibrium with these nominal species (the major components) at the assigned temperature. The amounts of major components are corrected for minor components by using the material balance equations. The minor components are then recomputed, the major components recorrected, and so on, until all requirements for equilibrium have been met as shown by identical successive results in the computation.

The iteration depends on whether the products mixture is oxygen-rich (the nominal products contain molecular oxygen) or oxygen-deficient (they contain molecular hydrogen or carbon monoxide or both). The calculations combine a material balance/equilibrium expression such as the one obtained by combining Equations 6 and 11. The number of moles of water vapor present is expressed as

$$H_2O = \frac{a'_H}{2} O_2^{1/2} / (K_n + O_2^{1/2}) \quad (18)$$

where

$$a'_H = a_H - H - OH$$

i.e., the number of hydrogen atoms available for the water vapor equilibrium. Such combined expressions have mathematical advantages because possible negative answers are avoided for amounts present. Further details are available in Reference 6.

When products composition has been determined, a blast overpressure can be computed from the known volume of the system and its assigned temperature by use of the ideal gas law. This overpressure, however, is not necessarily the maximum for that internal explosion. This maximum for non-vented explosions corresponds to adiabatic conditions where the energy of the products just equals that for the original fuel and air. Hence to ascertain this maximum, energy considerations become involved.

CONSERVATION OF ENERGY RELATIONS

The measure for energy effects in a system at a specified volume is the system's internal energy (Ref. 7), a thermodynamic item that differs from the energy item usually encountered--the enthalpy ("heat content"). Two rather different types of internal energy are involved: one thermal in nature, the other chemical. The thermal aspect is associated with temperature and heat capacity; the chemical aspect is associated with chemical composition. These two diverse aspects can, however, be combined into a single term if they relate to a common basis. The basis selected for computations is the elements in their ordinary form at a reference temperature of 25°C and pressure of the standard atmosphere (but pressure level is relatively immaterial for thermal items). On this basis, an element is assigned a chemical energy of zero, and its energy is given rather simply as the temperature integral of its heat capacity. A compound such as carbon dioxide (or an element not in its ordinary form such as monatomic oxygen) shows both this thermal aspect and an additional chemical aspect known as energy of formation. The total energy for such a material becomes the sum of these two separate aspects.

Chemical Energy

The chemical energy aspect for a constant volume system is given by the internal energy of formation, which by definition is the internal energy

change for the formation reaction. This item is not directly available for most materials. It can, however, be obtained indirectly by standard thermochemical methods from data such as heat of combustion as provided in standard sources for conventional fuels (Ref. 8) and for explosives (Ref. 9).

Tables listing internal energies of formation for many of the fuels that are important here are available in Reference 6.

Thermal Energy

The thermal component of an internal energy, the temperature integral of the heat capacity at constant volume, must relate to the selected reference temperature of 25°C. The pertinent interval for integration then becomes that from 25°C to the actual temperature for fuel, air, or explosion products, respectively.

Data on heat capacity for many fuels, particularly ones in a condensed phase, may not be readily available. Heat capacity may often be adequately approximated by the Kopp rule for additive atomic constants. These constants have been evaluated for metric units and are given in Reference 6. The values pertain to temperatures near room temperature, and within their inherent uncertainties apply to both constant volume and constant pressure conditions.

Ordinary air contains 78-mol-% nitrogen, 21-mol-% oxygen, and 1-mol-% argon. It is a diatomic ideal gas and at temperatures near 25°C its heat capacity at constant volume has the classic value of $C_v = 5/2 R$. In metric units the gas law constant R is 8.31434 J/(mol·K), so that the molar heat capacity for air at constant volume becomes

$$C_v = 5/2 \times 8.314 = 20.8 \text{ J/(mol·K)} \quad (19)$$

The number of moles of air, n , can be found by the ideal gas law with $n = PV/RT$. Since no chemical item is involved, the total internal energy for air at temperature T in kelvins and relative to the elements at 25°C is

$$E^0 = 20.8 (T - 298)n \quad (20)$$

The gaseous products from combustion-explosion reactions show heat capacities that are conveniently described by three coefficient equations (Ref. 10). These thermal items can be combined with pertinent chemical items, the internal energies of formation, to give a four-coefficient equation for the (total) internal energy for each component, relative to the elements at 25°C. Thus

$$E^{\circ} = a + bT + cT^2 + d/T \quad (21)$$

where E° is the standard internal energy per mole at temperature T and a , b , c , and d are arbitrarily selected coefficients. The four coefficients for this equation have been evaluated for the 12 components from data of the JANAF tables for the temperature range 500-4000 K (Ref. 5). These are tabulated in Reference 6. The total energy for a products mixture is then a summation of individual values per mole times the number of moles of each component present.

ADIABATIC COMBUSTIONS

The total energy of the products (sum of chemical plus thermal) just equals that for the original fuel plus air at the adiabatic flame temperature of a combustion-explosion reaction. A trial value for products temperature is assumed for computation of this flame temperature. Then by iteration, as described above, an associated equilibrium composition and internal energy of products for this assumed temperature are computed. Successive trial values for temperature are selected until the desired equality for the internal energies is found.

Given the adiabatic flame temperature, peak products pressure (for a nonvented internal explosion) can be computed by the ideal gas law $PV = (m/M)RT$ where m is the total mass of fuel plus air, and M is the apparent formula mass for the products. Blast overpressure is then obtained by subtracting the ambient atmospheric pressure.

RESULTS OF CALCULATIONS FOR INTERNAL EXPLOSIONS WITH TNT

The conventional explosive TNT (formula $C_7H_5N_3O_6$) also serves as a reference for explosives in general. In an internal explosion, TNT acts as an explosive fuel where its inherent oxygen content supplements that of the air and so may supply a substantial proportion of the oxygen for the combustion-explosion reaction. Results of calculations for internal explosions of TNT/air are reported below.

OVERPRESSURES

Overpressures generated in internal explosions with TNT are shown graphically in Figure 2 for overpressures in bars (10^5 pascals) over a three-decade range of TNT-air ratios (in kilograms of TNT per cubic metre of air at 25°C and 1 bar). Also shown are the experimental results (Ref. 3). The agreement obtained is gratifying and leads to confidence in the thermodynamic computations.

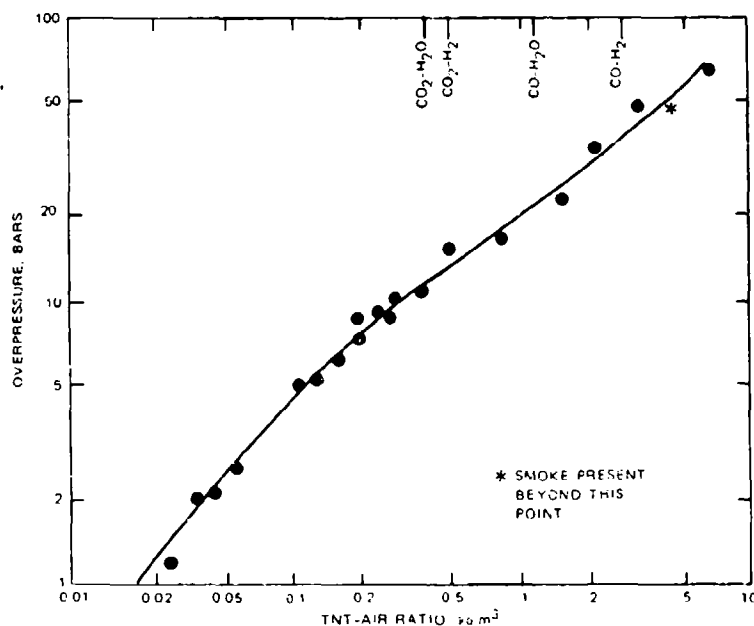


FIGURE 2. Computed (solid line) Versus Experimental (points) Overpressures for TNT-Air Internal Explosions.

Both calculated and experimental results for internal explosions with TNT show a point of inflection at an intermediate fuel-air ratio, although this was not recognized in the original report of these experiments. Beyond this point fuel-air ratios are such that the primary reaction is a detonation where increasing overpressures result largely from formation of additional gases. Below this inflection point the air provides sufficient oxygen so that combustion effects in the afterburn contribute to the overall temperature rise and resulting pressure increase.

FLAME TEMPERATURES

Computations for internal blast overpressure also allow for other characteristics of the blast. Figure 3 shows adiabatic flame temperatures for the combined combustion-explosion reaction of TNT in air at 25°C and 1 bar for a wide range of TNT-air ratios. These temperatures are appreciably higher than those for constant pressure conditions.

In contrast with pressures for internal blast with TNT, which increase monotonically with fuel-air ratio, the blast temperature curve for TNT reaches a maximum at about 3055 K at a TNT-air ratio of about 0.7 kg/m³.

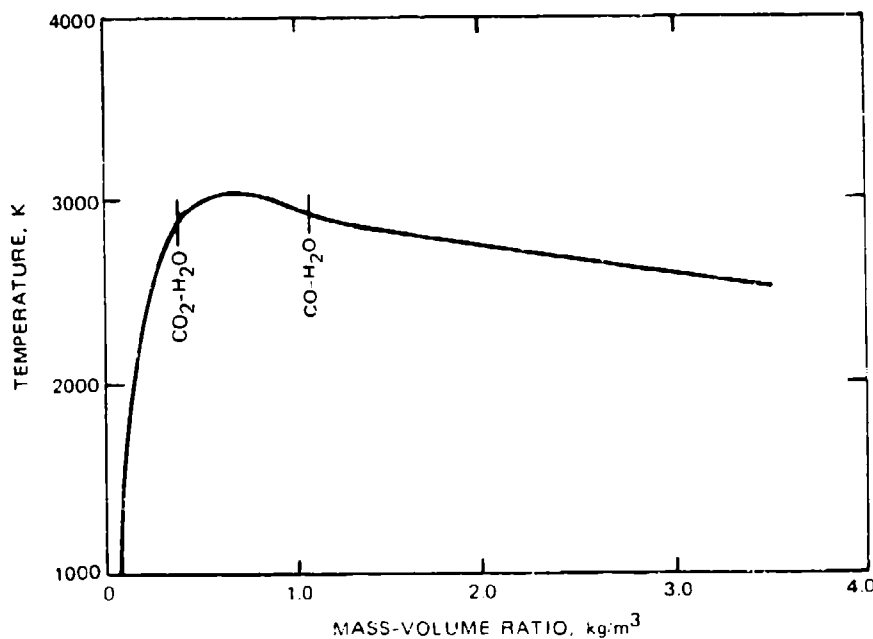


FIGURE 3. Temperatures in Internal Blast With TNT-Air Explosions.

This ratio lies between the $\text{CO}_2\text{-H}_2\text{O}$ and the $\text{CO-H}_2\text{O}$ stoichiometric reference points for TNT and is close to the fuel-air ratio at the point of inflection in the overpressure curve. This temperature maximum corresponds to a maximum utilization of oxygen in the afterburn.

PRODUCTS FORMULA MASS

Chemical dissociations at high temperatures give products such as mon-atomic oxygen and hydrogen and reduce the overall formula mass for the products mixture. The formula mass for these products decreases as much as 10% at high temperatures. The corresponding increase in the number of moles of gases present can make an appreciable contribution to blast over-pressures.

PRODUCTS COMPOSITION

The extent of chemical dissociation in the products of an internal explosion with TNT is shown in Figure 4. Composition of products versus the TNT-air ratio (logarithmic scales) is plotted. Maximum dissociation occurs in the general region of the $\text{CO}_2\text{-H}_2\text{O}$ and the $\text{CO}_2\text{-H}_2$ stoichiometric reference points and at approximately the fuel-air ratio for peak adiabatic temperature. In general any particular product of dissociation is present only in a small amount, but together these dissociations have substantial influence on products temperature because of their pronounced endothermic nature.

RESULTS OF CALCULATIONS FOR OTHER EXPLOSIVE FUELS

OVERPRESSURES

Explosive fuels generally show internal explosion overpressures similar to those for TNT--overpressures that increase monotonically with fuel-air ratio. The more highly oxygenated fuels require less oxygen from the air for complete reaction and consequently show lesser afterburn effects.

Overpressures developed in internal explosions with many explosive fuels, both oxygen-rich and oxygen-deficient, have been computed for a wide range of fuel-air ratios with air initially at 1 bar and 25°C (Tables 1 and 2). For these explosive fuels the overpressure always increases with the fuel-air ratio, but actual overpressures depend on the type of fuel. A characterization of this aspect of internal blast follows.

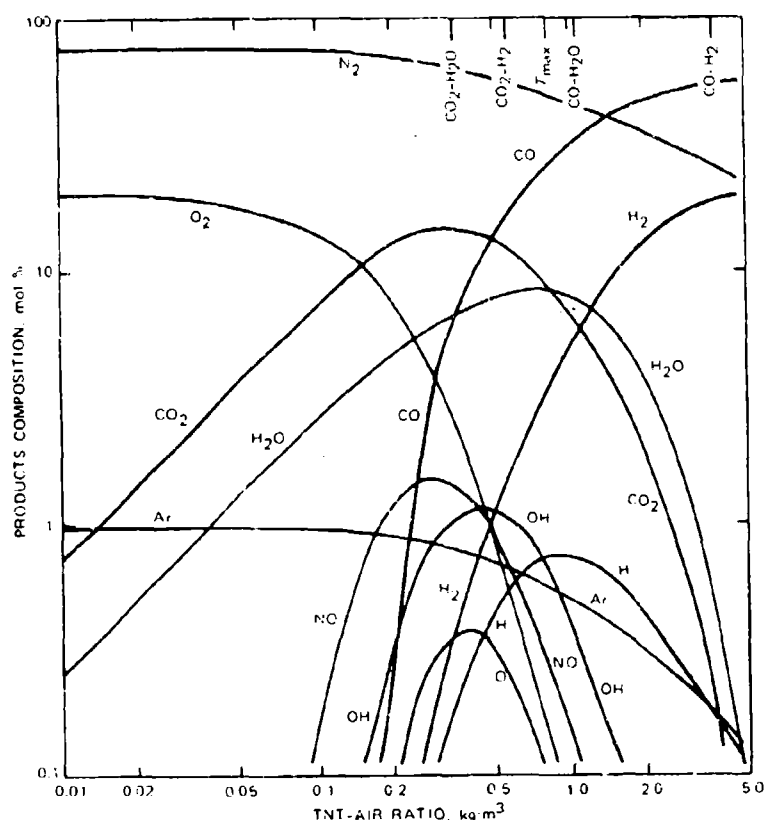


FIGURE 4. Composition of Products for Internal Explosions With TNT-Air Mixtures.

INTERNAL BLAST YIELDS

In the low overpressure range, the overpressures developed by a given fuel-air ratio of PETN are less than those for TNT. The internal blast yield for PETN is therefore defined to be less than that for TNT. Such internal blast yields are conveniently expressed relative to TNT, an explosive with a definite chemical formula and reproducible characteristics. The internal blast yield for PETN in the low overpressure range is only 52% of that for TNT on a mass basis; i.e., 52 grams of TNT give the same internal blast overpressure as 100 grams of PETN (in the low overpressure range). On a volume basis where relative density must be taken into account, the yield for PETN is 56% of that for TNT; i.e., 56 cm³ of TNT give the same internal blast as 100 cm³ of PETN (in the low overpressure range, which corresponds to explosions in a relatively large volume of air).

TABLE I. Internal Blast Overpressures (Bars) for Chemical Explosives.

Formula	Name	Fuel-air ratio, kg/m ³								
		0.05	0.10	0.30	0.50	0.80	1.0	1.4	2.0	5.0
CH ₃ NO ₂	NM, Nitromethane	2.040	3.780	9.089	12.898	17.402	20.143	25.383	32.980	70.147
CH ₉ N ₉	TAZ, Triaminoguanidine azide	2.495	4.558	11.144	15.149
C ₃ H ₅ N ₃ O ₉	NG, Nitroglycerin (glyceryl trinitrate)	1.304	2.420	6.180	9.371	13.428	15.839	20.369	26.915	59.205
C ₃ H ₆ N ₆ O ₆	RDX, Cyclonite, cyclotri- methylenetrinitramine	1.785	3.267	8.219	12.014	16.549	19.335	24.740	32.792	72.644
C ₄ H ₈ N ₈ O ₈	HMX, Cyclotetramethylene- tetranitramine	1.745	3.194	8.049	11.818	16.307	19.046	24.346	32.165	71.126
C ₅ H ₈ N ₄ O ₁₂	PETN, Pentaerythritol tetra- nitrate	1.543	2.834	7.134	10.598	14.743	17.212	21.937	28.857	63.316
C ₆ N ₆ O ₁₂	HNB, Hexanitrobenzene	1.436	2.658	6.751	10.103	14.039	16.342	20.736	27.171	59.273
C ₆ H ₅ N ₅ O ₁₀	Pentanitrobenzene	1.650	3.019	7.554	10.984	14.870	17.215	21.760	28.483	62.206
C ₆ H ₂ N ₄ O ₈	Tetranitrobenzene	1.954	3.548	8.648	12.007	15.939	18.339	23.213	30.374	66.358
C ₆ H ₃ N ₃ O ₆	TNB, 1, 3, 5-Trinitrobenzene	2.361	4.256	9.804	12.991	16.925	19.374	24.489	30.900	63.895
C ₆ H ₄ N ₂ O ₄	DNB, 1, 2-Dinitrobenzene	3.009	5.369	10.989	13.685	16.319	17.802	20.562	25.372 ^a	46.694 ^a
C ₆ H ₇ N ₃ O ₁₁ ¹ / _x	NC, Cellulose trinitrate, 14.1% nitrogen	1.701	3.106	7.690	11.131	15.060	17.418	21.958	28.622	61.634
C ₆ H ₈ N ₆ O ₁₈	Mannitol hexanitrate	1.232	2.297	4.170	8.949	12.901	15.245	19.966	25.935	56.910
C ₇ H ₅ N ₃ O ₆	TNT, 1, 3, 5-Trinitrotoluene	2.639	4.739	10.418	13.469	17.026	19.069	22.862	28.307	57.828 ^a
C ₇ H ₅ N ₅ O ₈	Tetryl, 2, 4, 6-trinitrophenyl- methylnitramine	2.223	4.019	9.523	12.887	16.992	19.570	24.586	31.943	68.051
C ₇ H ₆ N ₂ O ₄	DNT, 2, 4-Dinitrotoluene	3.287	5.834	9.398	13.101	14.583	15.368	17.862 ^a	21.774 ^a	41.704 ^a
C ₁₂ H ₄ N ₈ O ₈	TACOT, Tetranitro-1, 2, 5, 6- tetrazadibenzocycloocta- tetraene	2.691	4.836	10.569	13.738	17.653	19.978	24.255	32.292	78.819
C ₁₂ H ₆ N ₈ O ₁₂	DIPAM, 3, 3-Diamino-2, 2', 4, 4', 6, 6'-hexanitro- biphenyl	2.226	4.022	9.468	12.678	16.508	18.865	23.348	29.754	60.493

^a Smoke present.

TABLE 2. Internal Blast Overpressures (Bars) for Explosive Mixtures.

Name	Composition	Fuel-air ratio, kg/m ³								
		0.05	0.10	0.30	0.50	0.80	1.0	1.4	2.0	5.0
Comp. B-3	60% RDX, 40% TNT	2.132	3.878	9.359	12.939	17.249	19.943	25.172	32.854	70.668 ^a
Cyclotol 56/38	55% RDX, 38% TNT, 6% wax	2.449	4.422	10.244	13.708	17.887	20.414	25.209	32.146	66.123
Cyclotol 75/25	75% RDX, 25% TNT	1.989	3.620	8.909	12.593	16.968	19.687	24.982	32.783	71.426
LX-01	52% NM, 33% TNM, 15% 1-nitropropane	1.846	3.368	8.372	12.133	16.621	19.379	24.726	32.615	71.901
Octol 75/25	75% HMX, 25% TNT	1.986	3.616	8.898	12.580	16.950	19.665	24.949	32.729	71.291
PBX-9007	90% RDX, 9.1% polystyrene, 0.5% di-2-ethylhexyl- phthalate, 0.4% rosin	2.268	4.111	9.832	13.486	17.924	20.670	25.939	33.604	71.227
Pentolite 50/50	50% PETN, 50% TNT	2.198	3.975	9.454	12.900	17.112	19.771	24.972	32.667	70.929
PLX-2	50% Nitromethane, 50% acetone	3.483	6.164	11.352	12.235	12.881	13.124	13.329	16.847	34.384
PLX-3	75% Nitromethane, 25% acetone	2.624	4.710	10.593	13.021	14.845	15.900	17.871	20.666	33.773

^a Smoke present.

Internal blast yields can readily be assigned by a graphical method that utilizes plots of blast overpressure versus logarithm of the fuel-air ratio. The plots for the two materials are superimposed so that overpressures in the range of interest closely coincide. The relative internal blast yield for this range of overpressures is then given as the inverse ratio of the two corresponding fuel-air ratios.

Blast yields relative to TNT for a large number of explosive fuels are given in Table 3. Two values are included for each of these explosive fuels, one for the low overpressure range (on the order of 5 bars) and one for high overpressures (20 to 30 bars). These two values may be quite different.

In the low overpressure range, the yield includes contributions from the afterburn effect, which can be quite significant for oxygen-deficient explosives. At low overpressures an oxygen-deficient explosive fuel with substantial afterburn effects (dinitrotoluene, for example), can generate a more damaging internal explosion than an oxygen-rich explosive such as mannitol hexanitrate.

The higher overpressures generated in internal explosions with explosive fuels result primarily from detonations, and so are little influenced by the afterburn. An explosive fuel with high oxygen content does not utilize all its oxygen, and the excess oxygen is simply a diluent that reduces the yield in the higher overpressure range. Maximum internal blast yields in the high overpressure range are obtained from explosive fuels that are approximately balanced in oxygen.

RESULTS OF CALCULATIONS FOR INTERNAL EXPLOSIONS WITH CONVENTIONAL COMBUSTIBLES

OVERPRESSURES

Overpressures generated in the internal blast for three conventional fuels--benzene, JP-4 (a hydrocarbon fuel with an empirical formula, C_9H_{17}), and ethylene oxide--are plotted as a function of fuel-air ratio (Figure 5). The corresponding curve for the explosive fuel TNT is included for comparison. All the curves for three conventional combustibles show a maximum overpressure on the order of 9 to 11 bars that characteristically lies

TABLE 3. Internal Blast Yields.

Formula	Name	Yield, %TNT			
		At low overpressures		At high overpressures	
		By mass	By volume	By mass	By volume
A. Pure Explosives					
CH ₃ NO ₂	NM, Nitromethane	71	49	120	83
CH ₉ N ₉	TAZ, Triaminoguanidine azide	91	79		
C ₃ H ₅ N ₃ O ₉	NG, Nitroglycerin	40	39	97	94
C ₃ H ₆ N ₆ O ₆	RDX, Cyclonite, cyclotrimethylene-trinitramine	63	65	111	115
C ₄ H ₈ N ₈ O ₈	HMX, Cyclotetramethylenetetra-nitramine	61	70	115	132
C ₅ H ₈ N ₄ O ₁₂	PETN, Pentaerythritoltetranitrate	52	56	103	110
C ₆ N ₆ O ₁₂	HNB, Hexanitrobenzene	48	57	94	112
C ₆ HN ₅ O ₁₀	Pentanitrobenzene	55	64	107	123
C ₆ H ₂ N ₄ O ₈	Tetranitrobenzene	68	74	118	129
C ₆ H ₃ N ₃ O ₆	TNB, 1, 3, 5-Trinitrobenzene	83	85	115	118
C ₆ H ₄ N ₂ O ₄	DNB, 1, 2-Dinitrobenzene	109	103	81	78
(C ₆ H ₇ N ₃ O ₁₁) _x	NC, Cellulose trinitrate, 14.1% nitrogen	57	58	100	102
C ₆ H ₈ N ₆ O ₁₈	Mannitol hexanitrate	41	43	89	93
C ₇ H ₅ N ₃ O ₆	TNT, 2, 4, 6-Trinitrotoluene	100	100	100	100
C ₇ H ₅ N ₅ O ₈	Tetryl, 2, 4, 6-Trinitrophenylmethyl-nitramine	78	82	115	121
C ₇ H ₆ N ₂ O ₄	DNT, 2, 4-Dinitrotoluene	127	102	67	54
C ₁₂ H ₄ N ₈ O ₈	TACOT, Tetranitro-1, 2, 5, 6-tetra-zadibenzocyclooctatetraene	91	102	122	137
C ₁₂ H ₆ N ₈ O ₁₂	DIPAM, 3, 3-Diamino-2, 2', 4, 4', 6, 6'-hexanitrobiphenyl	78	85	103	112
B. Explosive Mixtures					
...	Comp. B-3	75	75	117	116
...	Cyclotol 56/38	87	89	111	113
...	Cyclotol 75/25	71	74	125	130
...	LX-01	66	49	114	132
...	Octol 75/25	69	76	120	132
...	PBX-9007	78	80	125	128

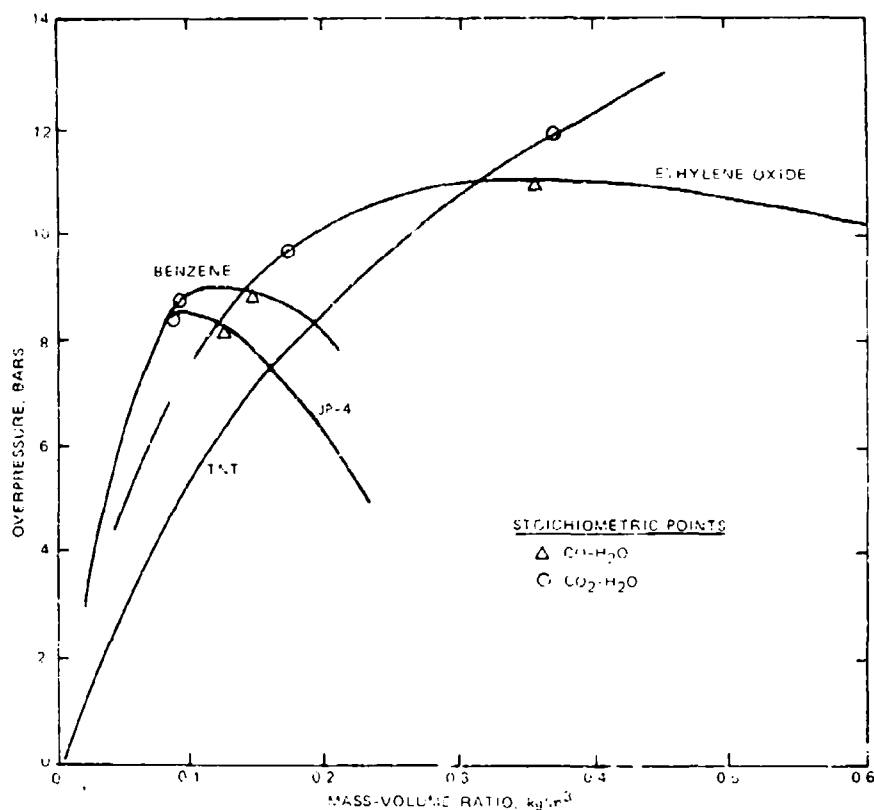


FIGURE 5. Blast Overpressures Versus Fuel-Air Ratio for Three Nonexplosive Fuels.

between the $\text{CO}_2\text{-H}_2\text{O}$ and the $\text{CO-H}_2\text{O}$ stoichiometric reference points. The two hydrocarbon fuels, benzene and JP-4, show typical behavior even though their hydrogen-carbon ratios are quite different. Ethylene oxide ($\text{C}_2\text{H}_4\text{O}$), an oxygen-containing fuel, also shows a maximum in its overpressure, but one that is broader and that occurs at an appreciably greater fuel-air ratio. This is a consequence of the diluting effect of oxygen in the molecule. For some purposes the greater mass of ethylene oxide required to achieve a maximum blast overpressure can be a disadvantage, while the broad range for high overpressures can be an advantage.

The internal blast behavior of selected conventional fuels is summarized in Tables 4 and 5 for initial conditions with air at 1 bar and 25°C . The maximum overpressure that each fuel can generate in confined air is shown along with the required fuel-air ratio. The tables also show maximum flame temperatures and the associated fuel-air ratio. In general the

TABLE 4 Internal Blast From Conventional Combustibles

Formula	Name	Maximum overpressure		Maximum temperature		Yield, % benzene	
		Bars	kg/m ²	K	kg/m ³	By mass	By volume
A. Liquids							
C ₂ H ₄ O	Ethylene oxide	10.832	0.35	2768	0.175	66	67
C ₆ H ₅ NO ₃	Nitrobenzene	10.476	25	2834	.20	60	82
C ₆ H ₆	Benzene	9.122	.12	2855	.12	100	100
C ₆ H ₁₂	Cyclohexane	9.035	.10	2646	.08	112	103
C ₆ H ₁₄	n-Hexane	9.050	.10	2651	.08	114	86
C ₉ H ₁₇	JP-4, Jet fuel	8.609	.10	2531	.10	123	112
C ₁₀ H ₁₆	THOC, tetrahydrocyclopentadiene	9.054	.10	2668	.10	101	125
C ₁₁ H ₁₀	o-Meth, o-bisulene	8.894	.10	2727	.10	104	125
C ₁₂ H ₂₀	SJ-4-I, Tetrahydromethylcyclopentadiene dimer	9.124	.10	2676	.10	101	105
C ₁₂ H ₂₂	oHF, cis-trans-Perhydrofluorene	9.119	.10	2671	.10	105	112
C ₁₄ H _{18.4}	RJ-5	9.088	0.10	2717	0.10	104	120
B. Solids							
C ₆ H ₁₀ O ₅ 1/2	Starch	7.317	0.10	2605	0.10	76	...
C ₆ H ₅ 26 NO 10CJ 55	Coal dust, bituminous	8.336	.10	2623	.10	88	...
C ₆ H ₁₀ 50 NO 10CJ 11	Coal dust, anthracite	9.656	0.20	2450	0.20	37	...

TABLE 5. Internal Blast From Gaseous Fuels.

Formula	Name	At lower explosive limit			At maximum explosive limit			At upper explosive limit			Yield, % methane	
		Vol. %	Over-pressure, bars	Flame temp., °C	Vol. %	Over-pressure, bars	Flame temp., °C	Vol. %	Over-pressure, bars	Flame temp., °C	By mass	By volume
H ₂	Hydrogen	4.0	1.54	427	74.2	12.47	3138	74.2	12.47	3138	227	29
H ₃ N	Ammonia	15.5	6.28	1770	27.0	8.75	2251	27.0	8.75	2251	39	41
H ₄ N ₂	Hydrazine	4.7	3.88	1104	10.0	7.26	1935	50.0	38	73
CO	Carbon monoxide	12.5	4.44	1413	40.0	7.69	2547	74.2	4.60	1259	19	33
C ₂ H ₂	Hydrogen cyanide	2.0	1.97	612	20.0	9.62	2706	40.0	49	83
CH ₄	Methane	5.0	5.11	1533	10.0	8.03	2336	15.0	7.35	1908	100	100
C ₂ H ₆	Methanol	6.7	5.66	1628	15.0	8.72	2264	15.8	8.69	2216	41	82
C ₂ H ₄	Cyanogen	6.0	7.59	2237	10.0	11.59	3245	32.0	40	130
C ₂ H ₂	Acetylene	2.5	4.17	1281	10.0	9.62	2768	80.0	10.81	2817	95	154
C ₂ H ₄	Ethylene	2.8	4.73	1425	10.0	8.86	2341	15.0	7.93	1786	98	170
C ₂ H ₅ NO ₂	Ethyl nitrate	3.0	5.06	1435	25.0	14.48	2188	25.0	14.48	2188	36	133
C ₂ H ₆	Ethane	3.0	5.40	1599	7.5	8.44	2247	10.0	7.73	1853	99	186
C ₂ H ₆ O	Ethanol	3.3	5.31	1540	7.9	8.81	2303	7.9	8.81	2303	55	158
C ₃ H ₆ O	Acetone	2.6	4.17	1243	7.5	8.55	2376	12.6	7.64	1765	60	217
C ₃ H ₈	Propane	2.1	5.46	1606	4.0	8.46	2347	9.3	6.94	1433	95	190
C ₄ H ₆	1,3-Butadiene	2.0	5.88	1750	5.0	9.10	2443	8.0	8.32	1866	93	314
C ₄ H ₁₀	n-Butane	1.9	6.06	1768	4.0	8.76	2312	8.4	6.30	1180	94	340
C ₄ H ₁₀ O	Diethyl ether	1.9	4.79	1406	5.0	8.94	2383	10.0	7.56	1509	68	314
C ₅ H ₁₂	n-Pentane	1.4	5.70	1667	3.0	8.83	2377	6.0	7.18	1453	88	395
C ₆ H ₁₂	Hexane	1.4	5.52	1654	4.0	8.81	2326	7.1	7.87	1639	81	395
C ₆ H ₁₄	n-Heptane	1.2	5.76	1680	2.0	8.24	2315	7.4	6.34	1153	89	480
C ₈ H ₁₈	n-Octane	1.0	5.98	1736	1.9	8.86	2397	1.9	8.86	2397	87	620

fuel-air ratio for maximum temperature is approximately that for maximum blast overpressure. This is to be expected because at lesser ratios some of the available oxygen is not utilized, while at greater ratios any excess fuel contributes only to the mass of products to be warmed and gives reduced temperature and pressure rises.

The flame temperatures given in Tables 4 and 5 for combustions at constant volume are appreciably greater than those for constant pressure conditions, since (1) the heat capacity at constant volume is less than that at constant pressure so that a given energy release produces a greater temperature rise, and (2) the chemical dissociations in the flame are partially suppressed by the higher pressure conditions of constant volume.

SUMMARY

Confined explosions such as those in grain elevators, coal mines, or ship compartments can be very damaging. The peak overpressures that such explosions can generate have been computed from first principles of conservation of mass, conservation of energy, and minimum Gibbs free energy. The amounts of the various chemical species that are present, including those resulting from chemical dissociation in the products mixture at explosion temperature, are found by using iterative methods. This iteration is readily performed on a small tabletop computer. The peak overpressure is then found by the ideal gas law from products composition and temperature. Other items such as formula mass and heat capacity for the products can also be determined. Computed overpressures agree closely with experimental observations on confined explosions of TNT in air for a three-decade range of fuel-air ratios.

Peak overpressures have been computed for a large number of confined explosions with explosive fuels, both pure chemical explosives and mixtures of these, and for a wide range of fuel-air ratios. They pertain directly to nonvented adiabatic explosions that occur so rapidly that there is little time for gas leakage or for heat transfer effects. These overpressures increase monotonically from very low values at low fuel-air ratios up to more than 70 bars at high fuel-air ratios (Tables 1 and 2).

The relative effectiveness of an explosive fuel in generating blast overpressure can be described in terms of an internal blast yield. This is the inverse ratio of the amount of an explosive relative to some standard, here taken as TNT, that is required for producing the same overpressure. These yields depend on both the type of explosive and the fuel-air ratio. Thus oxygen-deficient explosives in the low fuel-air range show pronounced afterburn effects that contribute to the pressure rise. But in the high fuel-air range, relatively less oxygen is available and afterburn is less important. Also, for oxygen-rich explosives afterburn effects are not pertinent. Considerations such as these make it possible to correlate the chemical structure of an explosive with the internal blasts it can generate. These considerations also indicate that two different internal blast yield values should be assigned to a given explosive--one yield value for the low overpressure range and one for the high. These yield pairs are given in Table 3 for representative chemical explosives and explosive mixtures.

Internal explosions with ordinary combustibles such as fuel oil, coal dust, or starch can also be important. For these explosions the maximum adiabatic overpressures attained are on the order of 8-10 bars, at a definite fuel-air ratio that characteristically lies between the $\text{CO}_2\text{-H}_2\text{O}$ and the $\text{CO-H}_2\text{O}$ stoichiometric reference points. At fuel-air ratios below the maximum overpressure there is unutilized oxygen from the air, and above it the extra fuel acts only as material to be warmed, depressing the temperature rise and associated pressure rise. Maximum adiabatic overpressures, along with associated flame temperatures and fuel-air ratios, are given for a number of liquid and solid combustibles in Table 4 and for combustible gases in Table 5. Values at the lower and upper explosive limits are also included in Table 5. Blast yields relative to benzene (for liquids and solids) or relative to methane (for gases) are also tabulated.

REFERENCES

1. R. G. S. Sewell and G. F. Kinney. "Response of Structures to Blast: A New Criterion," *Ann. N. Y. Acad. Sci.*, Vol. 152 (1968), p. 532.
2. R. W. Carlson. *Confinement of an Explosion by a Steel Vessel*. Los Alamos Scientific Report LA-390 dated 1945. Publication UNCLASSIFIED.
3. Hans R. W. Weibull. "Pressures Recorded in Partially Closed Chambers at Explosions of TNT Charges," *Ann. N. Y. Acad. Sci.*, Vol. 152 (1968), p. 357.
4. National Defense Research Committee. *Effects of Impact and Explosion*. Vol. 1. Washington, D.C., NDRC, 1946, p. 91. (Summary report of Technical Division 2, Vol. 1, publication UNCLASSIFIED.)
5. National Bureau of Standards. *JANAF Thermochemical Tables*, D. R. Stull and H. Prophet, Project Directors. Washington, D.C., NBS, 1971.
6. G. F. Kinney, R. G. S. Sewell, and K. J. Graham. *Peak Overpressures for Internal Blast*. China Lake, Calif., Naval Weapons Center, June 1979. (NWC Technical Publication 6089, publication UNCLASSIFIED.)
7. P. J. Kiefer, G. F. Kinney, and M. C. Stuart. *Principles of Engineering Thermodynamics*. New York, Wiley and Sons, 1958.
8. M. S. Kharasch. "Heats of Combustion of Organic Compounds," *J. Res. Natl. Bur. Stds.*, Vol. 2 (1929), pp. 359-430.
9. U. S. Army Materiel Command. *Properties of Explosives of Military Interest*. Washington, D.C., USAMC, 29 January 1971. (AMCP 706-177, publication UNCLASSIFIED.)
10. C. G. Maier and K. K. Kelley. "An Equation for the Representation of High-Temperature Heat Capacity Data," *J. Amer. Chem. Soc.*, Vol. 54 (1932), p. 3243.

SOLUTIONS FOR RESISTANCE-AFTER-FIRE PROBLEMS
IN AN ELECTRIC MATCH*

By

A. A. Heckes and A. P. Montoya
Initiating and Pyrotechnic Components Division
Sandia National Laboratories
Albuquerque, New Mexico

Abstract

Current leakage in an electric match after firing is a problem if it drains power that can be used elsewhere or if it induces unwanted fluctuations in other electrical circuits. This paper describes two novel techniques which significantly reduce the RAF sensitivity of a Ti/KClO_4 loaded electric match which is used to ignite the pyrotechnic materials in a thermal battery. In the first technique, a thin (less than 10 μm thick) film insulator, such as Parylene** or SiO_2 , is vapor deposited within the match cavity prior to the loading the pyrotechnic. The insulator tends to smooth the cavity surface as an aid to ejection of firing residues and to decrease the exposed metal surface area to prevent pin-to-pin short circuits. The second technique involves placing a length of heat shrinkable tubing on the match so it extends from the output end so that the shrink tubing is activated by the heat of the match and the thermal battery when fired. The shrinkage of the tubing effectively decreases the cross-sectional area for mass and heat transfer from the battery back into the match.

*This work was supported by the U. S. Department of Energy.

**Trademark of Union Carbide Corporation.

SOLUTIONS FOR RESISTANCE-AFTER-FIRE PROBLEMS IN AN ELECTRIC MATCH

I. INTRODUCTION

Electrically actuated, pyrotechnic, fire-starting devices are known by the various names of electric matches, squibs, igniters (ignitors), and initiators. All names are synonyms for the purposes of this discussion as all function through the action of electrical heating of a resistive bridgewire to ignite a pyrotechnic charge so that ignition may be subsequently transferred to other reactive materials. The bridgewire is connected between two electrical leads which are separated from each other by an insulator. The insulator is usually located at the base of the pyrotechnic charge and makes up at least part if not most of the match body.

The preferred mode of operation for the electric match is that, after ignition transfer is achieved, the bridgewire and pyrotechnic "disappear" to give an open electrical circuit which serves to indicate that the unit has functioned. If the resistance after firing, as measured between the electrical leads, is not truly infinite so that a partially open circuit exists, then the resistance should be sufficiently large that an insignificant current flows with applied voltages similar to those used to fire the match.

A problem condition of low resistance-after-fire (RAF) exists when conductive materials are retained between the match leads (pin surfaces) after the match has been fired so that a significant current continues to flow. The current that is needlessly drawn tends to deplete the energy contained in the power supply or to place demand loads on the power supply so that it cannot perform other

required functions. When the RAF problem is intermittent or noisy in character, the pulsations are capable of inducing unwanted fluctuations in other electrical components such as oscillators, amplifiers, transistors, transducers, and switches.

Techniques to decrease or eliminate RAF problems are required in order to be able to upgrade electrical matches with otherwise excellent firing characteristics but only marginal to poor RAF properties. For maximum effectiveness the technique used to improve RAF should not affect the end use and cause minimal changes in the firing characteristics of the match. Several such techniques have been investigated and found to be effective. Consequently, adaptation of these techniques may prove effective in other pyrotechnic devices with RAF problems.

II. Discussion

1. General

A low resistance RAF problem was encountered at Sandia National Laboratories where an electric match used to ignite the pyrotechnic heat source of a thermal battery gave unacceptable failure rates. The match, shown in Figure 1, gave after-fire current leakages of 10 mA or more in up to 60 percent of the battery test firing experiments and over 250 mA, which was a failure, in up to 2 percent of the experiments.

The match was loaded with 10 mg of Ti/KClO_4 pyrotechnic. A standard 1 ohm, 1 watt no-fire bridgewire was used. The lead wires were nickel plated Kovar which were silver brazed in place. The match body was composed of Al_2O_3 ceramic which had been tungsten metallized and nickel plated. Match

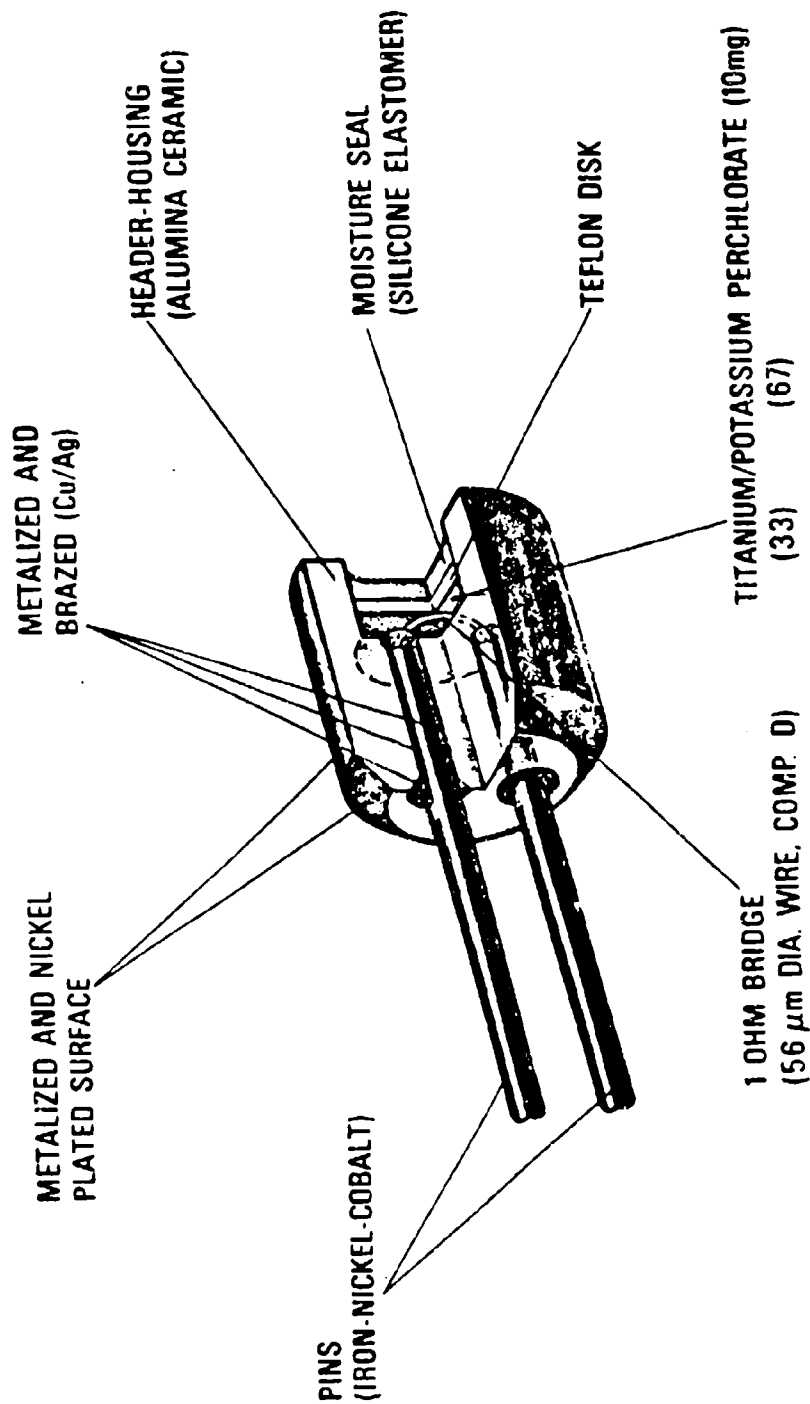


FIGURE 1. Electric Match

closure consisted of a Teflon disc pressed against the powder face and sealed with RTV silicone rubber.

The conditions that caused the RAF problem were defined by trial and error experimentation. The investigation indicated that the failures were caused by high temperatures plus the deposition of residues from both the match and the battery between the pins of the match. Initial experimentation was performed in the apparatus shown in Figure 2. It was designed with removable parts so that various volumes within the battery could be simulated. The early experiments showed that varying the degree of confinement of the output from the match did not produce RAF even when the match was fired at elevated temperatures up to 300°C which were representative of battery equilibrium temperatures. Conversely, elevated temperature battery firings had increased the severity of the RAF.

Only after the test fixture was modified so that the match ignited a quantity of the thermal battery Fe/KClO_4 pyrotechnic was any electrical conductance observed. Even then, the RAF condition was of a different character that observed in battery experiments. Finally, when small quantities of the thermal battery cell stack materials were added in the form of LiCl , LiCl/KCl electrolyte, and/or DEB (depolarizer/electrolyte/binder) material, then the RAF conditions of the battery experiments were simulated. See Figure 3. These battery simulation experiments gave conditions more severe than those in actual batteries because the failure rate was now 100 percent for unprotected matches. The principal advantages of the simulation experiments were a much lower cost than battery experiments and the high failure rate so that major RAF improvements might be better compared.

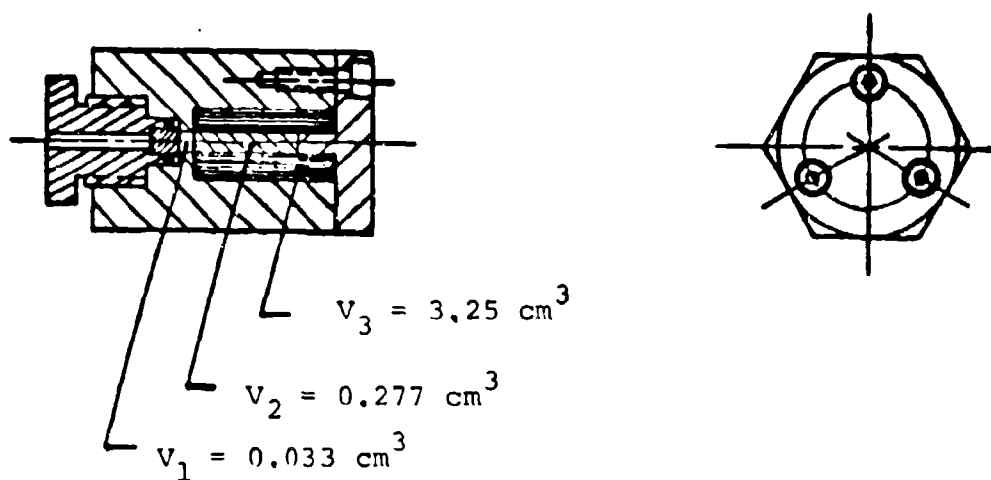


FIGURE 2. Igniter Test Fixture to Allow Changes in Confinement

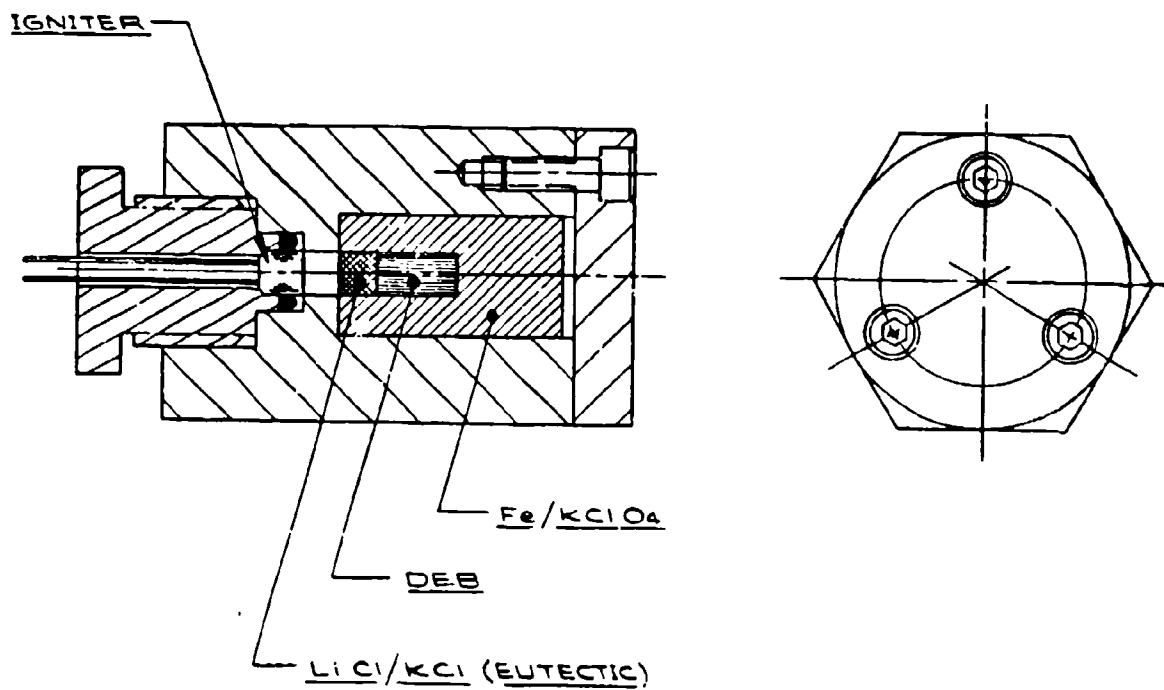


FIGURE 3. Igniter Test Fixture for Simulation of Battery Environment

2. Methods of RAF Improvement

The first successful attempts to improve RAF were those where the inner surface of the bridged but unloaded match was coated with an insulating material. Two different methods of applying the insulation were used. In one series, SiO_2 was vapor deposited to cover the exposed ends of the electrical leads in the match cavity. The other series used Parylene*, a chemically vapor deposited organic polymer, which was also deposited throughout the match cavity so that the exposed ends of the electrical leads and the bridgewire were covered. An example is shown in Figure 4. The principal differences in the materials were that SiO_2 is a high melting temperature inorganic material that is deposited line-of-sight while Parylene is an organic material with a lower decomposition temperature (but still quite thermally stable compared to other organics) that is uniformly deposited on all exposed surfaces so that it provides a completely conformal coating.

Two different thicknesses of Parylene were used, 0.34 μm and 1.2 μm . Also, two different thicknesses of SiO_2 were employed, 0.4 μm and 7 μm . Some of the bridgewires were masked to prevent deposition of SiO_2 on the center portion of the bridgewires so that the effect of coatings on the ignition characteristics could be determined. Later experiments showed that changes in ignition characteristics due to these thin coatings could be ignored but that RAF protection was significantly improved (probably due to the high dielectric strength of the materials).

*Parylene is a trademark of the Union Carbide Corporation.

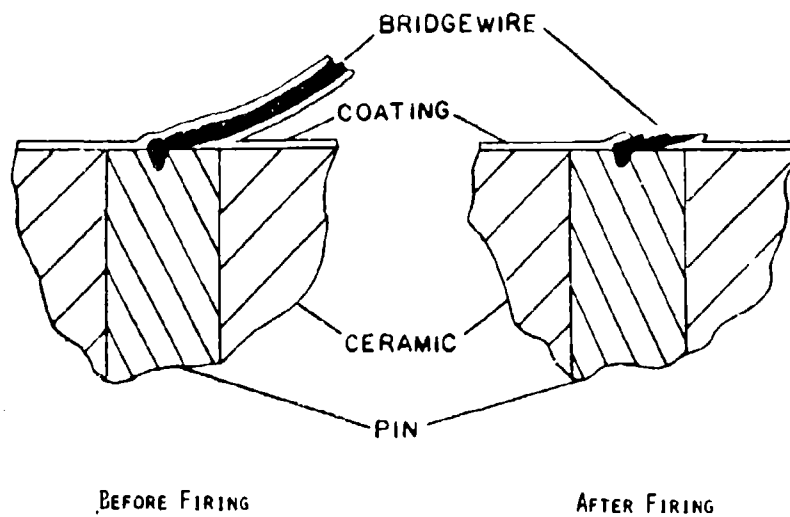


FIGURE 4. Cross-sectional Views of Pin Area of Electric Match Showing Conformal Coating

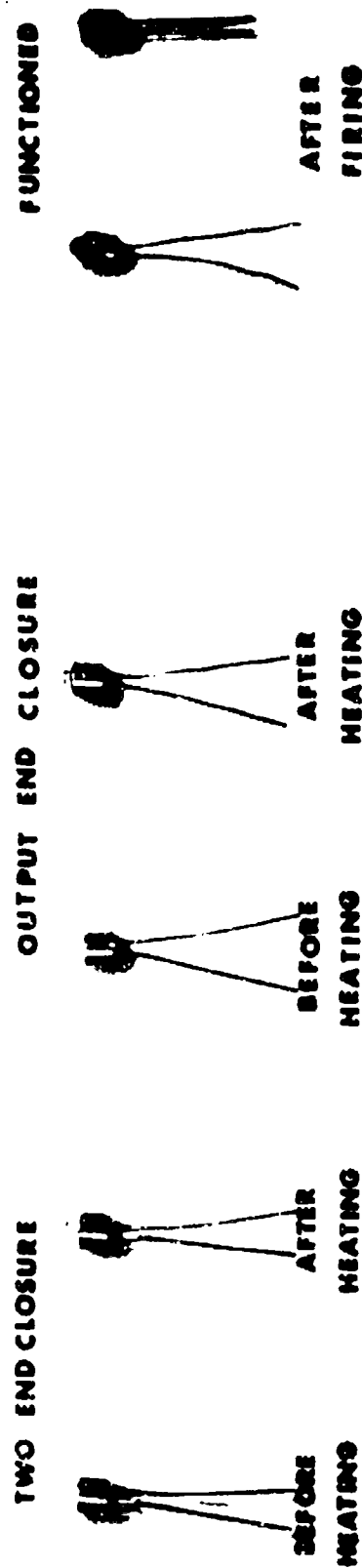
These experiments suggested that RAF could be avoided by excluding battery residues from the match cavity. Complex trap doors and other mechanical schemes were considered but discarded for a simpler technique. A piece of shrink tubing placed on the outside of the match with a short length (2 to 4 mm) extending past the match face would be activated by the heat of the match and battery to cause it to shrink and greatly reduce the area for mass transfer. The shrink tubing technique is shown in Figure 5. The idea was tried with ordinary, unimproved matches in the battery simulation apparatus. The approach was more effective than the internal coatings were for the same type of experiment.

III. Experimental Results

Electrothermal response (ETR) experiments were performed on the internally coated matches both before and after loading. A control group of matches without internal coating was also included in the ETR experiments for purposes of comparison. Matches which had shrink tubing applied to the match exterior were not placed in the ETR experiments because it was believed that no measurable changes would be observed.

The ETR results are shown in Table I. Groups 1, 2, and 3 should have had similar SiO_2 coating thicknesses but had a range of 6.2 to 7.1 μm due to run-to-run changes in the vapor deposition process. Although large changes in the thermal conductance, γ , and the temperature rise, θ , were expected because of the application of a thermal insulator to conductive metal parts which were in contact with the pyrotechnic powder, such was not the case. The changes were relatively minor, presumably due to the very thin nature of the insulating film.

SHRINK TUBING TRAP DOOR



SHRINK TUBE

FIGURE 5. Application of Shrink Tubing to Prevent RAF

TABLE I
ETR Data Summary for Electric Matches

Group	Condition	Quantity	Average Values				
			Resistance R_o Ohms	Theta θ °C	Gamma γ W/°C	C_p J/°C	Tau τ msec
1	Unloaded*	25	1.068	105.6	659	20.78	31.97
2	"	24	1.067	109.2	631	20.68	33.01
3	"	25	1.049	137.0	504	19.39	39.13
4	"	25	1.064	134.8	509	21.19	41.93
5	"	20	1.024	142.1	466	19.70	42.68
6	"	50	1.032	141.6	465	19.49	41.98
7	"	50	1.039	142.9	467	19.13	41.20
<hr/>							
1	Loaded**	25	1.085	85.0	4543	31.61	6.97
2	"	24	1.075	84.5	4527	31.13	6.88
3	"	25	1.076	80.7	4755	30.30	6.38
4	"	15	1.091	85.6	4568	29.93	6.58
5	"	20	1.033	83.2	4418	28.61	6.48
6	"	50	1.021	75.0	4834	30.51	6.32
7	"	40	1.043	87.3	4264	30.57	7.19

*Pulsed with 250 mA current for 200 msec.

**Pulsed with 600 mA current for 200 msec.

Group	Coating
1	6.8 μm SiO_2 with masked B.W.
2	7.1 μm SiO_2 with masked B.W.
3	0.4 μm SiO_2 no mask
4	6.2 μm SiO_2 no mask
5	None - Control
6	1.2 μm Parylene
7	0.34 μm Parylene

The firing characteristics of both coated and uncoated matches were determined for small samples of the matches. See Table II. Again, the changes, if any, were small enough to be within the experimental variation between samples. The difference could therefore only be determined through statistical measurements on large samples and these were unavailable.

TABLE II
Firing Characteristics of Electric Matches

Group	Average Values					Light Output
	R_o Ohm	τ_{ign} msec	E_{ign} mJ	R_{ign} Ohm	τ_{bw-brk} msec	τ msec
1	1.134	5.04	71.88	1.196	5.14	5.06
2	1.045	5.35	70.62	1.108	5.42	5.34
3	1.091	5.50	75.20	1.113	5.56	5.50
4	1.129	4.93	69.68	1.187	5.21	4.94
5	1.070	5.18	70.43	1.102	5.27	5.19
6	1.038	4.55	59.65	1.081	4.61	4.54
7	1.096	5.66	78.34	1.176	5.72	5.64

Group Code - See Table I.

Battery simulation experiments were performed with limited numbers of each match group. The shrink tubing technique was tried on matches from lots that had failed in prior battery applications and also on matches from groups 1 through 7 above. The shrink tubing technique was the only one that gave 100 percent protection in these experiments. Parylene coatings were second best. Silicon dioxide was third best. All were much better than the unprotected matches which showed 100 percent failure

rates in the battery simulation experiments. Again, it must be emphasized that the battery simulation experiments produced a much more severe environment than that found in the actual battery.

The Parylene coating was tested in 10 batteries (considered to be a minimum number to show RAF problems, if present) and was found to show no current leakage. The shrink tubing is in the process of being evaluated in battery experiments as of this writing.

Postmortem analysis of the residues in the match tend to indicate that the coatings protect the match by changing the surface so that less powder residue sticks to the area between the match pins. The shrink tubing is believed to protect the match by closing off nearly 90 percent of the area for the transfer of mass and heat from the surroundings to the cavity. Residue deposition is greatly decreased and the transfer of heat into the cavity is blocked so that the electrical conductivity of the burned residues remains low. Parylene is resistant to thermal decomposition but may also absorb some heat to keep the electrical conductivity of the residue low.

Comparison of the costs of the various techniques was made based on the small quantities produced for these experiments. The quantities ranged from 25 to 100 piece parts in each group. Production in large quantities would undoubtedly reduce the cost per piece to change the absolute numbers but probably not their relative positions. Fortunately, the most effective techniques were also cheapest. The cost of shrink tubing was estimated at 3 to 5 cents. Parylene coating, applied commercially, cost \$2.50 for each piece part. Silicon dioxide, commercially vapor deposited, cost about \$25.00 for each piece. This also included some non-recurring fixturing costs.

The compatibility of the coatings with the match components has not been measured to date. There is no obvious reason that they would not be compatible. The ability of the shrink tubing to withstand some of the battery processing and storage environments has been questioned. However, information exists which indicates that the shrink tubing has a strong chance of surviving these environments.

IV. CONCLUSIONS

1. Two techniques have been developed for protecting electric matches (squibs) from RAF problems. In the first, heat shrinkable tubing is placed on the outer match surface so that it is activated by heat from the reaction and acts as a trap door to exclude both heat and materials from the match cavity. In the second technique, the inner surface of the match is coated with an insulator to change the character of the conductive path. Parylene and SiO_2 are examples of insulators which can be applied in a sufficiently thin layer so that there is no significant change in the firing characteristics of the match.

2. The effectiveness of the materials evaluated were shrink tubing > Parylene > SiO_2 >> nothing.

3. The most effective techniques were also the cheapest. However, the cost of coatings depends on the number processed at a time and the development of the fixtures and methods of processing.

4. Compatibility of the materials in the usage environments was not evaluated, but is expected to be acceptable.

INSTANTANEOUS SMOKE SCREENING SYSTEMS

By

Kjell O. Jacobsen
A/S Raufoss Ammunisjonsfabrikker
N-2831 RAUFOSS
NORWAY

ABSTRACT

The object of this development effort was to establish a smoke for screening purposes as fast as possible, without a pillaring effect and unaffected by ground conditions such as snow, mud, water, etc.

A smoke screening system which is suitable to all types of vehicles has been developed. It is able to produce a smoke screen of 80 m extent within one second of firing.

A 76 mm instantaneous smoke grenade is developed for the smoke grenade launching system on the Leopard tank. This smoke grenade is a combination of a bursting and burning type smoke. A smoke screen is established within 1.5 sec. from firing and maintained for a period of 2 minutes.

The instantaneous smoke has also been introduced into a hand grenade.

This instantaneous smoke is adaptable to a wide variety of systems such as mortars, artillery shells, etc.

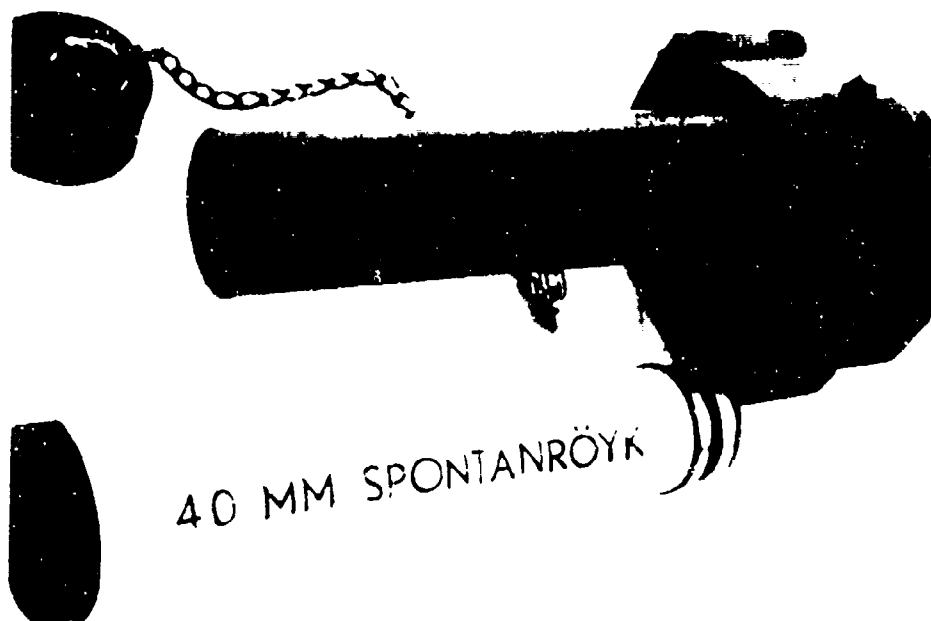
40 MM INSTANTANEOUS SMOKE SCREENING SYSTEM

Tanks and mechanized forces moving to attack must anticipate fighting through a system of integrated anti-armor defense which can start as far as 3000 m from the enemy's defensive positions. The anti-armor weapons, the light anti-tank weapons, the tank gun and wire guided missiles complement each other resulting in a high kill probability.

When employing smoke as a countermeasure against these tank-killers, it is essential that the obscuration is instantaneous rather than longlasting.

A 40 mm instantaneous smoke screening system has been developed to suit modern battlefield operations. With this system a vehicle can be screened with smoke to an extent of 80 meters within 1 sec. from firing.

The complete system consists of a launching device, firing unit and the smoke ammunition.





Employment

The smoke cartridge is inserted head-first into the launcher. The rubber protective cap must be firmly seated. This will waterproof the loading and also insure satisfactory ignition.

An electrical charge released from the command section within the vehicle fires the cartridge.

The current flows to the contact rings of the cartridge and, in turn, ignites:

- primer
- ignition/expelling charge
- smoke pellets
- pyrotechnical delay
- expelling charge for the empty cartridge.

The pressure inside the tube expels the smoke pellets with high velocity through the rubber cap. out to a distance of 30 to 40 meters. During flight, the smoke bodies are producing smoke. The spread from one tube covers an arc of approximately 45° , i.e. 5 tubes cover an arc more than 180° . The exothermic reaction while the pellets are burning, takes place in a large volume and will cause a negligible temperature rise (0.3°C). Pillaring due to high temperature is thus negligible, and the smoke screen will stay on the ground and enable the vehicle to escape to a safe position.

The duration of the smoke screen depends on the weather characteristics and vegetation, but field operations have shown that the screen lasts long enough to enable the vehicle to escape or go into new positions. The empty cartridges are ejected from the launcher 2 seconds after firing. This is accomplished by using a pyrotechnic delay system igniting an expelling charge. In this way the launcher tubes are reloadable from the hatch immediately after firing.

76 MM INSTANTANEOUS SMOKE GRENADE

This smoke ammunition was developed in accordance with German Military Requirements to suit the Leopard Smoke Launchers and has the following characteristics.

- The smoke grenade consists of an instantaneous and a slow producing smoke.
- The system establishes an instantaneous smoke screen maintained for a period of 90 seconds by a smoke producing cannister.

Besides being fired from the launching tubes, the Smoke Grenade can be thrown by hand. When functioning as a smoke handgrenade the initiation is performed by a handoperated firing device. The delay is 4.5 sec. to maintain operator safety.

The grenade can be fuzeed with either electrical or mechanical ignition systems.

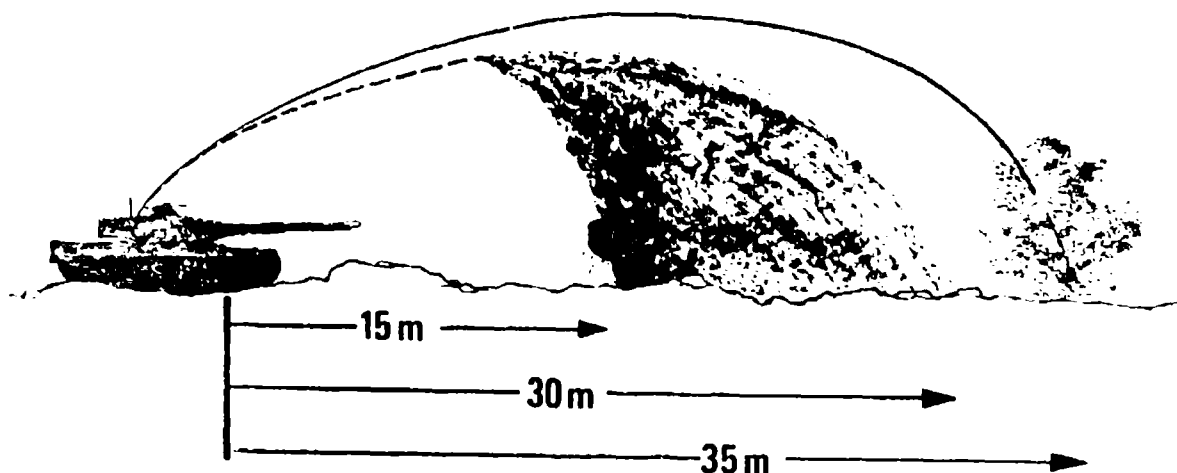
Functioning

When electrically ignited, the instantaneous smoke container is ejected from the Smoke Grenade and bursts in the air, establishing a smoke screen within 1.5 sec. from firing. After a short delay the cannister is ejected from the launcher tube. This grenade maintains the smoke screen for a period of 90 seconds.

This concept was chosen due to the 45° elevation angle of the launchers and the required delay of maximum 1.5 sec. for establishing the smoke screen.

The system is illustrated on the figure.

76 mm INSTANTANEOUS SMOKE GRENADE FUNCTIONING



SMOKE HANDGRENADE

The Norwegian Army had a requirement for a individual smoke screening system. This requirement could be met with a smoke handgrenade, if an instantaneous smoke screen could be established unaffected by ground conditions, such as snow which is a specific problem for Norway. The different parameters were established in cooperation with the Norwegian Army and the Norwegian Defence Research Establishment.

This smoke handgrenade consists of a plastic container filled with smoke pellets, a fuze with a pyrotechnic delay and an ignition/bursting charge.

Container

This is a cylindrical plastic container with screw cap. The container shall secure safe handling and storage, i.e. it shall protect the smoke bodies from the environment under severe conditions. The container also contributes to the confinement, and therefore affects the bursting.

Smoke charge

The smoke charge consists of approximately 30 smoke dics with center hole.

Fuze

The fuze body is also a plastic material. The delay column with primer and delay charge is made from brass.

A safety level is secured by a safety pin, when the safety pin is released, a spring will throw the safety lever away and move a striker with the necessary energy to ignite the primer. This in turn ignites the pyrotechnic delay charge. After a burning time of approximately 1.3 seconds the ignition/bursting charge is ignited.

Employment

On throwing, the delay column is ignited and the grenade bursts after 1.3 seconds from leaving the hand. It is important that the delay is short to ensure that the burst takes place in the air, and that the smoke screen is established as soon as possible. On bursting, the smoke bodies are ignited and spread to an extent of approximately 10 meters. The safe distance between the operator and the burst point is only 5 meters. Burst tests have shown that the smoke grenade is not dangerous at all even if it bursts less than a meter from a person.

Due to the safety aspects, this smoke handgrenade can be used for training purposes without any precautions. Toxicity is low because of the relatively low smoke concentration, but should not, of course, be used indoors.

INSTANTANEOUS SMOKE HAND GRENADE FUNCTIONING



OTHER APPLICATIONS

This smoke concept demonstrating

- Instantaneous effect
- Unaffectedness by snow or ground conditions
- No pillaring effect
- Non-toxic to personnel

has been introduced into different mortars, short range rockets and anti-aircraft projectiles.

The applicability is therefore general and could be adopted to a great variety of systems where a rapid smoke screen is more important than the duration.

An ammunition concept for the 120 mm Rheinmetal-gun will be initiated in cooperation with Germany in the near future.

The smoke screens offer adequate protection in the visible and near infra-red range of the electromagnetic spectrum. The intention in Norway is to improve the concept to include the far infra-red part of the electromagnetic spectrum as well. A cooperative effort between the Norwegian Defence Research Establishment, the Norwegian Army and Raufoss Ammunition Factory has been initiated.

RESPONSE OF PYROTECHNIC TO GASEOUS DISCHARGES WITH THE
JCY-50 ELECTROSTATIC SENSITIVITY TESTER

Engineer. Hsieh Kaodi
China's Precision Machinery Society
Beijing, China

ABSTRACT

The electrostatic spark response of some pyrotechnics to gaseous discharges were determined with the JCY-50 standardized electrostatic sensitivity tester with needle-plane electrodes configuration. The essential conditions of the spark initiation of pyrotechnics are as follows: The potential breaking down the electrode gap of the sample should be higher than its threshold voltage. The energy delivery rate should be higher than that of the losses. The duration of discharging must be long enough to give rise to propagating "hot spot", which will support a self-sustaining chemical reaction.

As for the unsymmetrical electrodes, the polarity of needle electrode played an important role. We found that the primary initiating spot produced were just near the negative electrode. The data of the electrostatic sensitivity for normal lead styphnate, yellow flare, zirconium hydride and black powder are shown, and the various factors effected on the data are discussed in this paper.

INTRODUCTION

A lot of investigations had been made on electrostatic spark sensitivity of energetic materials, several apparatus and technics had also been developed(1-5). Very often, the electrostatic sensitivity expressed as a threshold (or minimum) energy was strongly depended on the mode of discharge and the rate of energy delivery.

R.M.H Wyatt, etc. (1), and M.S. Kirshenbaum (3,4) showed that a lot of primary explosives were sensitive both to slow discharges (large series resistance) and rapid discharges (no series resistance). The least threshold energy for initiation was observed when the RC time constant was in the range of 0.1-1 ms. The optimum gap length for maximum probability of initiation was between 0.075 and 0.175 mm. Similar results have been obtained in our experiments with conventional primary explosives.

Differ from primary explosives, the mechanism of chemical reaction of pyrotechnics which composed of oxidants and fuels is more complex, and also, the longer delay period is needed when igniting. Consequently, in the experiments of electrostatic sensitivity of pyrotechnics, stimulus and sample properties must be considered together.

The object of this paper is to demonstrate the essential conditions of igniting the pyrotechnics by electrostatic discharges.

EXPERIMENTAL

1. Apparatus

The JGY-50 standardized electrostatic sensitivity tester which we used with the voltage range in 0- \pm 50KV. had a needle-plane electrode configuration. The fixed-gap of electrode assembly might be adjusted from 0-4 mm, with pre-

cision ± 0.01 mm. The values of capacitance and series resistance might be selected arbitrarily. The inductance inherent in the discharged circuit was $1.3 \mu\text{H}$.

2. Reproducibility

Fifty four series of tests, during one year, were carried out with normal lead styphnate to determine the reproducibility of the JGY-50 tester. The experimental conditions were as follows:

Capacitance, 500 pf

Gap length, 0.12 mm

Polarity of needle, negative

The 50% firing voltage V_{50} was determined by way of Bruceton method (6). The relative frequency histogram of V_{50} is shown in Figure 1. The hypothesis test had shown that the distribution of V_{50} conformed with normal distribution (sample mean, 0.93 KV; standard deviation, 0.057 KV)

The reproducibility expressed as confidence interval at 95% confidence coefficient was 0.93 ± 0.115 KV. If the polarity of needle was positive, it was 1.20 ± 0.08 KV.

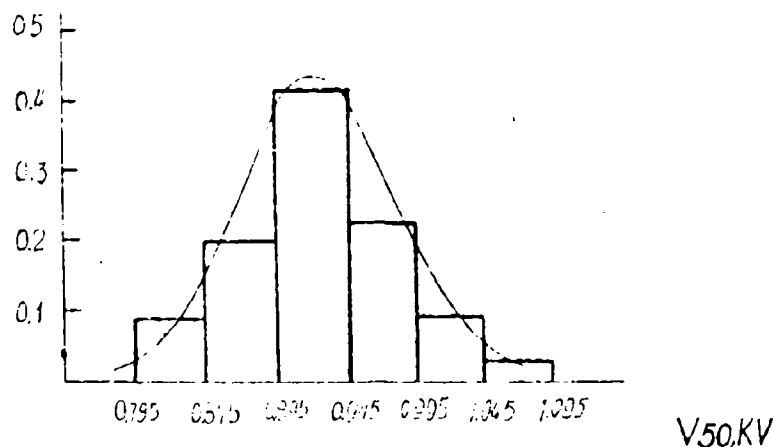


Figure 1. Relative Frequency Histogram of V_{50} of Normal lead Styphnate

3. Materials

Normal lead styphnate (standard)

Small Granular black powder (grain dimension 0.36-0.57 mm)

Yellow flare ($KClO_3$ 37%, Mg 30%, $K_2C_2O_4$ 3%, Resin 3%)

Zirconium hydride (particle size 5--10 μ)

Black powder (particle size 5--75 μ)

4. Procedure

About twenty to thirty milligrams of pyrotechnics powder were placed into a Polystyrene sample holder shown in Figure 2. The desired capacitor and resistor were connected in the firing circuit. The needle electrode was adjusted, so that a desired fixed-gap would be obtained. The polarity of needle electrode was selected. The storage capacitor, charged to the desired voltage, was discharged between the electrodes by means of a low-loss vacuum switch.

The 50% firing voltage of samples was determined by the small up-and-down method (7). After each trial a fresh sample was used. The flash or other evidence of combustion were used as ignition criterion.

The relative humidity of the testing room was maintained at 60-5%.

RESULTS

1. Dependence of Series Resistance on 50% Firing Voltage

The dependence of 50% firing voltage of small granular black powder on resistance was shown in Figure 3. The samples could not be fired when the series resistances were less than 2 $k\Omega$ (Voltage, 1--20 kV; Energy, 0.11--44 Joules), and it could be fired when the series resistances were 2.2 $k\Omega$ -- 10 $k\Omega$. When 10 $k\Omega$ resistance was used, the 50% firing voltage was approximately 10 kV, while the peak current of

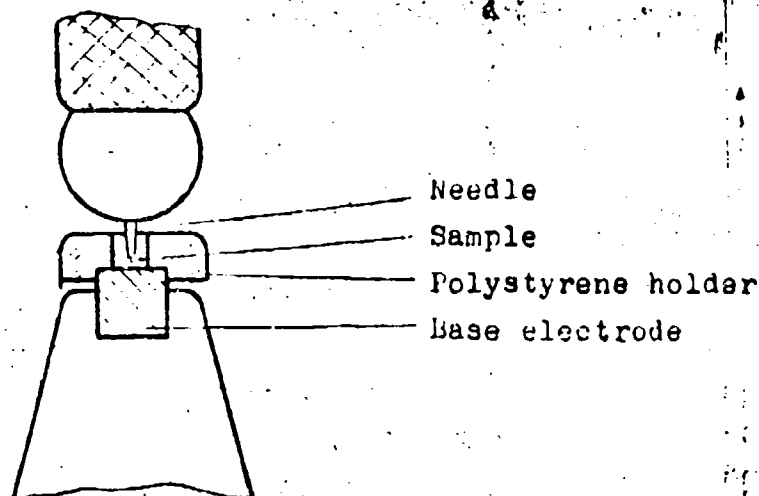


Figure 2. Needle-plane Electrode Assembly

discharge was less than 1 mA. When the polarity of the needle electrode was positive the least 50% firing voltage was obtained with 82 K Ω series resistance approximately. If the needle polarity is negative the least 0% voltage was obtained with 168 K Ω approximately. For same series resistances, the sample was more sensitive when needle electrode was negative. The series resistances were 10 K Ω -- 1 M Ω , the threshold voltage of firing was near or slightly lower than the breakdown voltage of air gap without samples (see the straight line in Figure 3).

The similar results could be obtained using various capacitances and gap lengths, as well as various pyrotechnics. Obviously, there were two limits in the series resistances. If the series resistance was less than lower limit, the samples could not be fired even when the voltage was as high as 20 KV, and the discharge was accompanied with

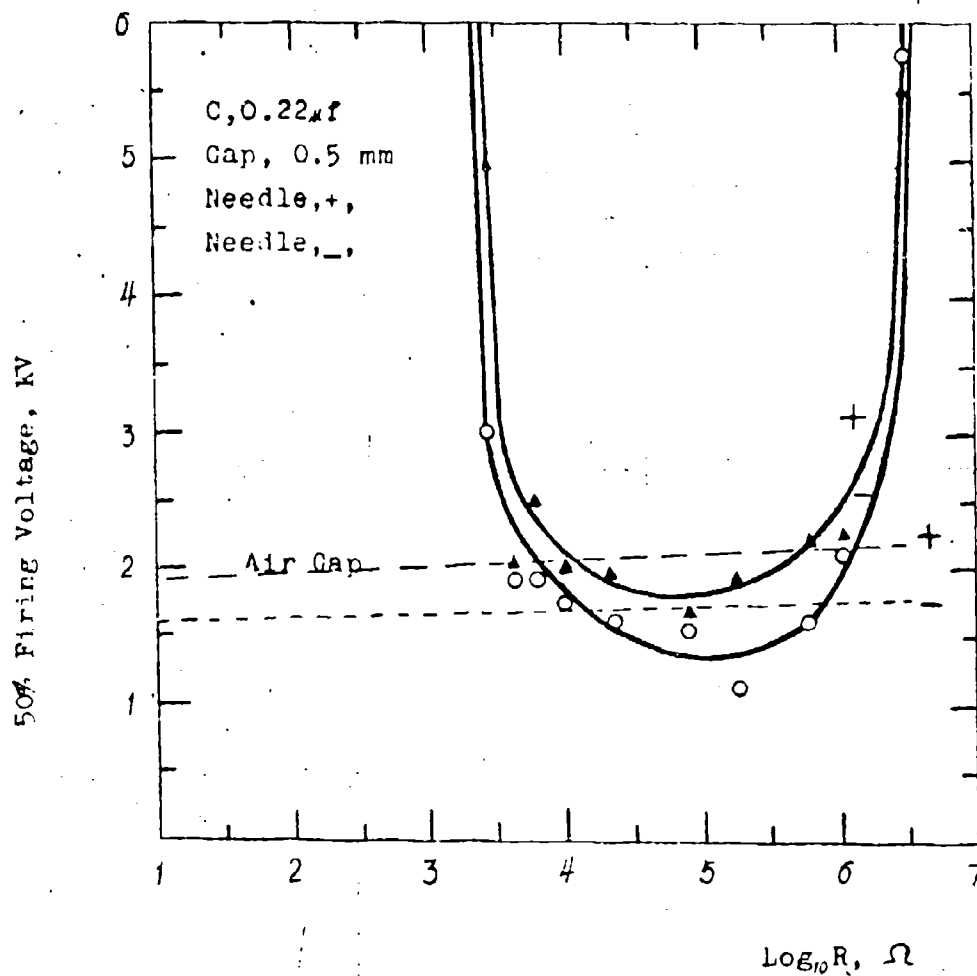


Figure 3. 50% Firing Voltage of Granular Black Powder as a Function of Resistance

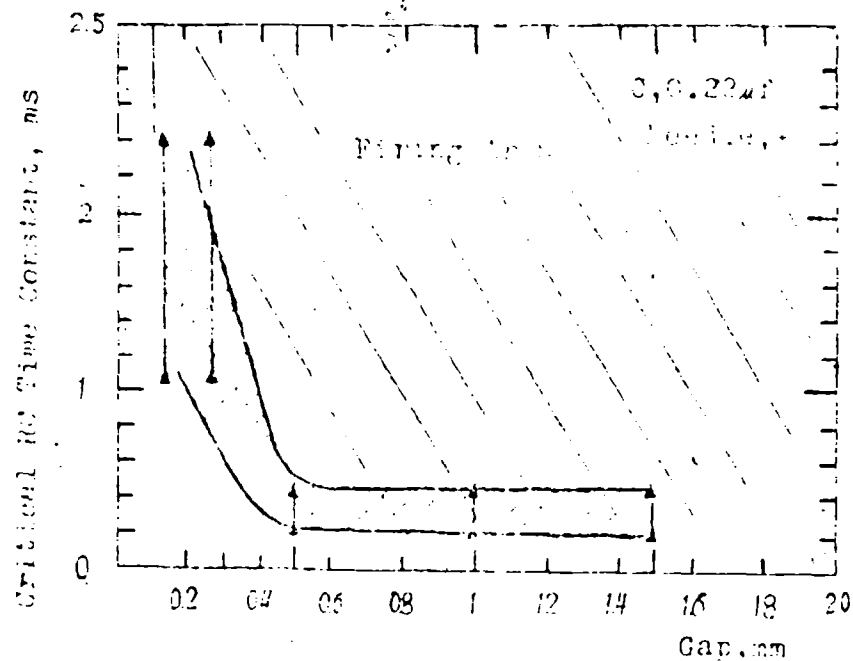


Figure 4. Critical RC Time Constant of Granular Black Powder as a Function of Gap

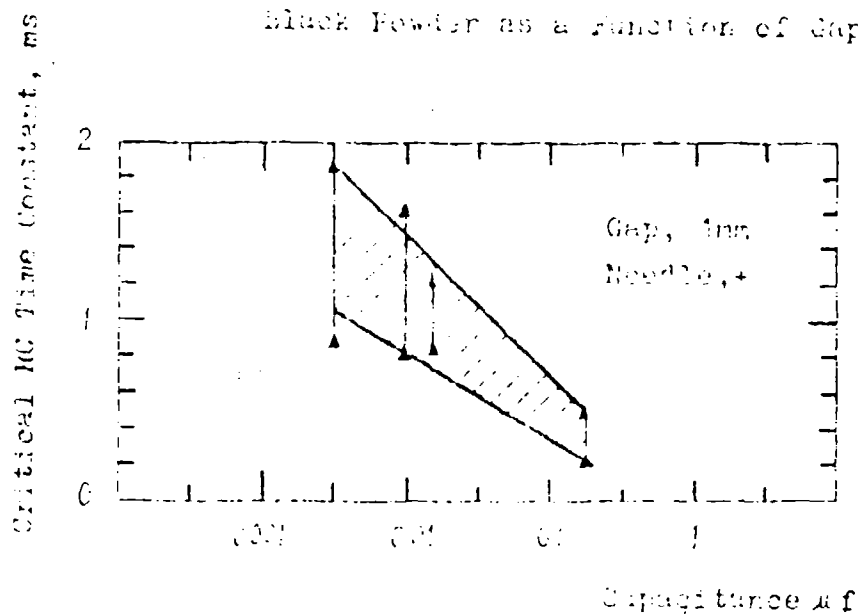


Figure 5. Critical RC Time Constant of Granular Black Powder as a Function of Capacitance

apparent sound and blue spark. The duration of discharge was depended upon the product of the lower limit resistance and the capacitance, so that the RC was defined as critical RC time constant. If the series resistance was larger than the upper limit, the samples also could not be fired at the voltage up to 20 KV, under this condition, the peak current of capacitor discharge was defined as critical current. Both critical RC time constant and critical current had statistical nature and could not be determined precisely.

2. The Factors Effecting on the Critical RC Time Constant

When the capacitance was constant, the effect of the change of gap length on the critical RC time constant was shown in Figure 4. As the gap was smaller than a particular, the critical RC time constant increased quickly. When the gap was smaller than a critical value (0.1mm) for granular black powder, the firing of the samples could not be observed with the voltage range from 0--20 KV; series resistance, 0--10 Ω . The critical RC time constant was unvarying when the gaps were 0.5--1.5 mm. It should be noted that 0.5 mm gap was just the same as maximum grain dimension of the tested granular black powder.

The effect of the capacitance on the critical RC time constant is shown in Figure 5. In the range of 0.036 μ f to 0.22 μ f, the critical RC time constant increased with the decrease of capacitance. No firings were observed for capacitance below a certain limit (1000 pf--3800pf) with granular black powder.

3. The Relationship of Critical Current and Capacitance

The relationship of critical current and capacitance is shown in Figure 6. The critical current was calculated according to the maximum series resistance required for firing below 20 KV. The resistance of spark gap was mani-

tored by an oscillograph. It was several orders of magnitude smaller than the series resistance, so that it might be disregarded for calculating the critical current. As shown in Figure 6, the critical firing currents decreased rapidly as capacitances increase.

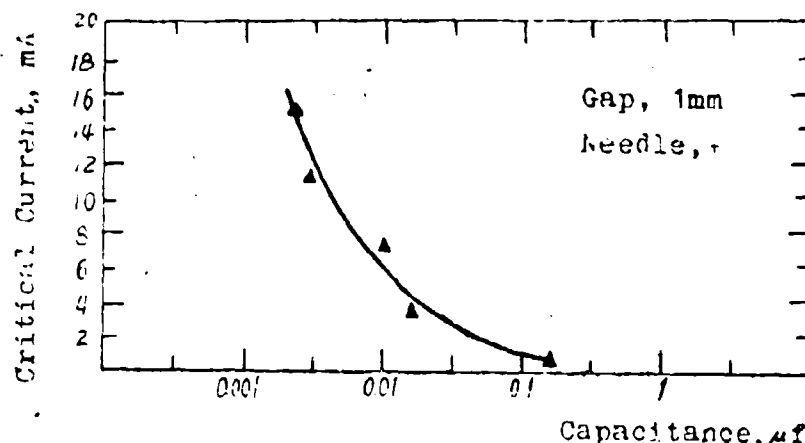


Figure 6. Critical Current as a Function of Capacitance

4. Characteristics of Polarity of Needle

R.M.F. Wyatt (5) showed that the minimum energy value of IVA lead azide decreases approximately from 2.2×10^{-4} J to 1×10^{-4} J when the polarity of the steel needle is changed from negative to positive (rubber-base electrode).

Our tests showed that all the conventional non-additive primary explosives were more sensitive with polarity of the needle negative, e.g. by using positive electrode the minimum energy value of the normal lead styphnate was 1.67 times the value obtained with negative polarity.

With the capacitance 0.22 μf, the gap length 0.5--1.5 mm, the small granular black powder was also more sensitive when the needle polarity was negative. While the gap length decreases to 0.12 mm, no firing occurred. On the contrary, firing occurred with positive needle (series resistance 10--100 KΩ). The similar results was obtained with Yellow flare.

Two photographs of the product mark remained on the

steel bases with different polarity of needle are shown in Figure 7.



Figure 7. Product Spark remained on the Steel Bases

Sample: Normal lead stynbate (no confined)

Capacitor: 500pf

Gap length: 0.12 mm

Voltage: 1.3 kV

A: Needle negative

B: Needle positive

5. Electrostatic Spark Sensitivity of Some Pyrotechnics and Materials

The electrostatic spark sensitivity of some pyrotechnics and materials are given in following table. The optimum gap, optimum series resistance and polarity of needle were selected to obtain minimum firing energy.

DISCUSSION

1. The first essential condition of the spark initiation of pyrotechnics is the potential breaching down the electrode gap of the sample should be higher than its threshold voltage. As the sample was bulk insulate material, the potential was near the threshold voltage of air-gap. But as for the pyrotechnics contained some conductive ingredients, the threshold

voltage of gap decreased. It may be one of the important factors for accident caused by electrostatic discharges.

2. The second condition is that the RC Time constant is larger than the critical value. Pyrotechnics are the mixtures of oxidants and fuels. Heat source is provided by gaseous discharges must be maintained long enough to give rise to propagating self-sustaining hot-spot in the pyrotechnics.

Otherwise, the larger part of energy of discharge would transfer to shock wave and the rapid movement of air that would blow the powder away from the electric discharge.

3. The third condition is that the energy delivery rate should be higher than that of the losses to establish the accumulation of heat for starting the oxidation-reduction of pyrotechnics. The rate of energy delivery is directly proportional to the square of instantaneous current of discharges. There must be a critical current intensity which can be approximately expressed as the peak current of capacitance discharges. When this current was lower than critical value, no firing was observed. Precise determination of critical current is of great importance for evaluating hazardous situations caused by electrostatic.

It may be generalized that the electrostatic spark sensitiveness of pyrotechnics not only expressed by minimum energy, but also by breakdown voltage, critical RC time constant, critical current and arcing fraction.

Table

Electrostatic Spark Sensitivity of Pyrotechnics and Materials

Pyrotechnics	Capacitance (μ f)	Polarity of Needle	Gap length (cm)	Tc ^a (ms)	Ic ^b (mA)	Ro ^c (K Ω)	V ₅₀ ^d (KV)	E ₅₀ ^e (mJ)
Granular Black Powder (unconfined)	0.022	+	1.0	4.8-11.2	<1	1000	5.5	332
Granular Black Powder	0.022	-	1.0	0.8-1.2	<3.5	168	2.7	80
Black Powder	0.22	-	0.5	0.2-0.4	<1	168	1.15	145
Black Powder	0.01	+	1.5			168	3.0	45
Yellow Flame	0.033	+	1.25	2.7-3.8	<0.8	183	7.0	716
GrHz (unconfined)	485 pf	-	1	2.1-2.6 μ s		183	1.7	0.70

^aTc, Critical RC Time Constant;^bIc, Critical Current;^cRo, Optimal Series Resistance;^dV₅₀, 50% Firing Voltage;^eE₅₀, 50% Firing Energy.

REFERENCES

1. R.M.H. Wyatt, P.W. Moore, C.K. Adams, J.F. Sumes, The Ignition of Primary Explosives by Electric Discharges, Proc. Roy. Soc. A, Vol 246, 1958
2. C.R. Westgate, L.D. Fallock, M.R. Kirshenbaum, Electrostatic Sensitivity Testing for Explosives, Techn.Rept. 4319, Picatinny Arsenal, Dover, N.J., 1973
3. M.S. Kirshenbaum, Response of Lead Azide to Spark Discharges Via a New Parallel--Plate Electrostatic Sensitivity Apparatus, Techn. Rept. 4559, Picatinny Arsenal, Dover, N.J., 1973
4. M.S. Kirshenbaum, Response of Primary Explosives to Gaseous Discharges in an Improved Approaching--Electrode Electrostatic Sensitivity Apparatus, Techn. Rept. 4955, Picatinny Arsenal, Dover, N.J., 1976
5. H.D. Fair, R.F. Walker, Energetic Materials, Plenum Press, New York and London, 1977
6. W.J. Dixon, A.M. Mood, A Method for Obtaining and Analyzing Sensitivity Data, J.A.S.A, Vol. 43, 1948
7. W.J. Dixon, The Up-and-Down Method for Small Samples, J.A.S.A, Vol. 60, 1955

CHARACTERIZATION TESTS FOR PYROTECHNIC IGNITION
AND IGNITION TRANSFER

R Kelly
G L Lindsley
N R Williams
Foyal Armament Research and Development Establishment
Fort Halstead, Sevenoaks, Kent, UK

ABSTRACT

Little is known about the relative importance of heat shock and particles in determining the ignition processes which ultimately lead to combustion of pyrotechnic compositions. For example it is impossible to predict, on the basis of thermochemical, transport or other data, how easily a composition will ignite and which compositions will ignite each other. A number of tests have therefore been devised to characterize the ability of pyrotechnic and initiatory explosive compositions to ignite and transfer ignition to other similar compositions. The results of such tests can be used to rank compositions in terms of their ignitability for a particular environment and geometry and hence provide data to assist the designers of pyrotechnic stores and to test theoretical models for ignition and ignition sensitiveness.

Ignitability has been assessed directly by means of a standard gap test and indirectly by measuring times to ignition of pellets of composition dropped into a preheated furnace at various temperatures. Pressure-time profiles obtained from combustion of pyrotechnic compositions in small pressure vessels have been used to characterize and compare post ignition behaviour.

Ignition transfer has been assessed by means of flash tubes in which hot gases, shock and particles from the pyrotechnic or initiatory explosive donor composition are channelled through small diameter metal tubes to ignite similar acceptor compositions. Thermal transfer of energy across a metal barrier (through barrier initiation) has also been studied from temperature-time profiles measured by a radiometric technique.

INTRODUCTION

Recently RARDE has considerably expanded both its intramural and extramural effort on military pyrotechnics research and development under 3 broad headings. These are:

- a. Ignition Studies
- b. Solid State Propagation Studies
- c. Gas Phase Studies.

Inevitably there is considerable overlap between studies carried out under these 3 headings reflecting the fact that pyrotechnic reactions involve complex interactions between the above processes. For example the light emitted from the gas phase species present in small amounts in the plume of a tracer or flare composition is greatly affected by the combustion reactions in the condensed phases. In general one can learn a lot about the characteristics of igniter materials under heading (a) and of delay and incendiary compositions under headings (a) and (b). However, a comprehensive understanding of tracers, flares, other illuminants and infra-red decoys requires extensive studies under each of the headings (a), (b) and (c).

A fourth heading:

- d. Supporting Thermal Studies

provides valuable quantitative data in support of work carried out under the 3 main headings (a) to (c).

The work described in the present paper deals with heading (a) - Ignition Studies - and in particular with characterization tests which have been developed with the aim of providing information of practical use to designers of pyrotechnic devices. A persistent cause of problems in such devices is the uncertainty of the ignition process and, although fundamental work is being done in this area at Leeds University and elsewhere, the ignition and combustion process for each individual composition is complex, the number of compositions in use is large and the number of situations and configurations in which pyrotechnic compositions are used is even larger. For these reasons the choice of pyrotechnic composition for a particular application is usually made on empirical rather than scientific grounds.

A common method of determining the closeness to failure of a pyrotechnic process is to test its operation at extremes of temperature and pressure but this requires large numbers of tests specific to that single situation. Whilst it is not possible to devise general experiments which give information of direct use in specific design situations, trends can be established by means of simple experiments and large numbers of compositions can be dealt with.

COMPOSITIONS

Details of the compositions used in the present work are given in Table 1. These vary from composition F, a gas producing initiatory explosive commonly

Table 1

Composition Details

<u>Composition</u>	<u>Formulation (Weight %)</u>
A	Boron 30, Potassium nitrate 70
B	Boron 20, Potassium nitrate 70, Silicon 10
C	Gunpowder G40
D	Silicon 50, Potassium nitrate 50
E	Silicon 40, Potassium nitrate 40, SMP*20
F	Potassium dinitrobenzfuroxan (KDNBF)
G	Boron 10, Bismuth oxide 90

* SMP = sulphurless mealed powder

used in explosive actuators, to composition G, a thermitic material which is relatively gasless but produces a heat retentive slag.

IGNITABILITY

Two main techniques are described for assessing the ignitability of pyrotechnic compositions. First a gap test, in which a 5mm diameter cylindrical donor pellet, consisting of 100mg of pressed composition, is ignited opposite a similarly pressed pellet of acceptor composition. The distance between them is adjusted using a Bruceton staircase method for obtaining and analysing the data. A mean ignition distance, defined as the separation which corresponds to 50% probability of ignition of the acceptor composition, is determined from 30 to 40 separate tests. The donor pellet is ignited from the rear surface so that the mean ignition distance is not

dependent on the time of burning or the burning rate of different compositions. Rear surface ignition also corresponds to the common configuration in an explosive train, for example where a composition is pressed onto a delay column to ensure transfer of ignition to the remainder of the system. Typical mean ignition distances in the gap test, obtained with some of the compositions identified in Table 1, are given in Table 2.

Table 2

Mean Ignition Distances from the Gap Test		
Donor Composition	Acceptor Composition	Mean Ignition Distance (mm)
A	A	52
A	B	44
A	C	83
A	D	19
A	E	63

It is interesting to note from Table 2 that gunpowder (black powder) is easily the most ignitable composition under the conditions of this experiment. Secondly, addition of only 20% of sulphurless mealed powder to the least ignitable composition (D-silicon/potassium nitrate) has the effect of increasing the mean ignition distance by a factor greater than 3. By extending this test in future work to embrace a wider range of compositions it is intended to rank pyrotechnic compositions in their ability to ignite particular acceptor compositions and vice versa.

The quality and quantity of combustion products from the donor composition can be assessed in a parallel experiment by using a constant speed rotating disc of filter paper set up at a fixed distance from the donor composition. A deposit or smear of combustion products on the filter paper gives a measure of the reaction time and product distribution characteristic of the donor composition and its manner of ignition. These smears of combustion products are photographed (Figure 1) to give an additional series of performance characteristics. The common practice of using pellets with perforations or conical indentations in the donor surface can also be investigated by this technique to support their frequent use to enhance the ignition process.

The second main technique for assessing ignitability is the measurement of times to ignition of pellets of composition heated in a furnace. A hot-stage microscope, described by Charsley and Tolhurst (1), has been used in these experiments. The unit is brought to a steady temperature and a 50mg pellet of composition is dropped into an inconel crucible positioned on the temperature measuring thermocouple. On insertion of the sample the temperature registered by the thermocouple falls but quickly rises until ignition occurs when there is a rapid temperature rise. Typical temperature-time curves are illustrated in Figure 2.

The isothermal temperature of the hot-stage microscope unit is varied over a range in which ignition occurs for each particular composition. It is found that the measured temperature of ignition increases as the temperature of the unit is raised, as shown in Table 3 for composition B. This

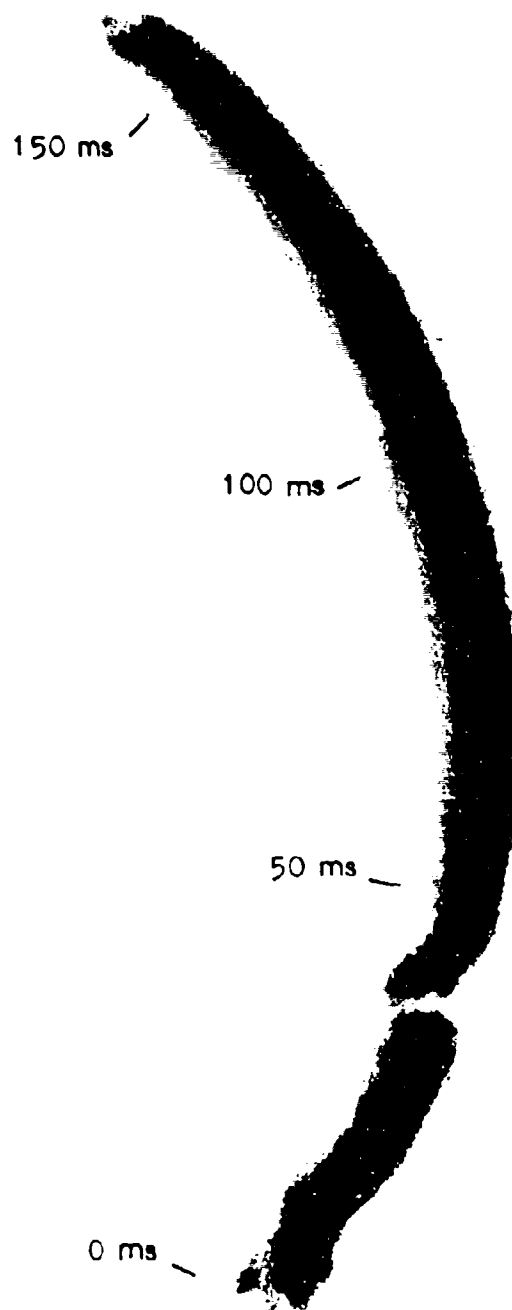
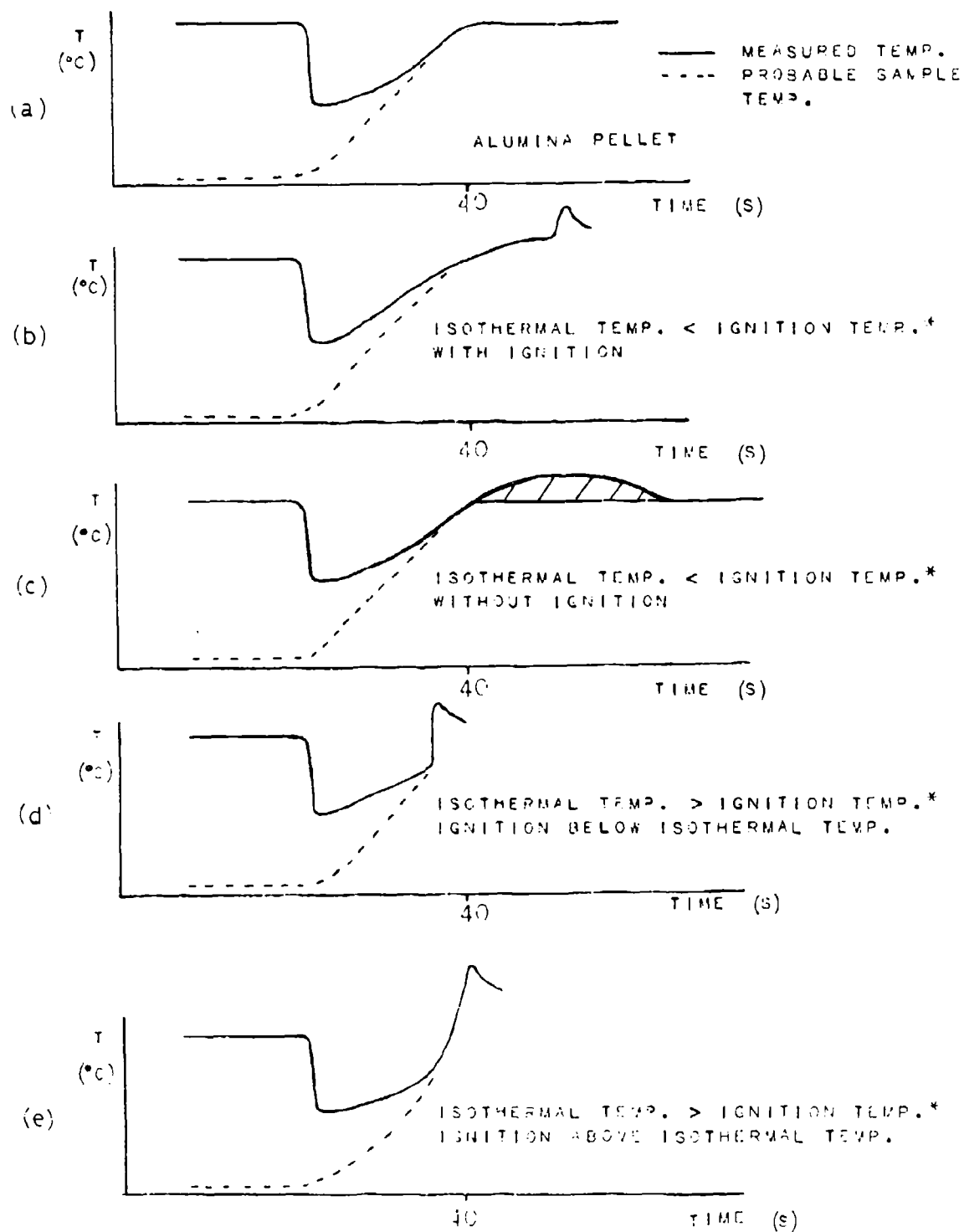


FIG 1. DEPOSIT FROM COMPOSITION A ON ROTATING DISC



* IGNITION TEMP. AS DETERMINED BY DTA

FIG. 2. TYPICAL TEMPERATURE - TIME CURVES FOR TIME TO IGNITION TEST

Table 3

Time to Ignition Results for Composition B

Temp °C	Time to ignition (sec)	Measured Ignition Temp °C
475	-	non-ignition
485	-	non-ignition
490	43±0	510±10
500	39±5	502±3
525	32±6	528±10
550	24±5	539±6
575	22±1	547±2
600	16±2	556±9

effect is thought to rise from the sample temperature lagging behind the measured temperature, especially for the shorter ignition times. For example after 10 seconds the sample is about 40°C below the measured temperature indicated by the thermocouple. Nevertheless it is apparent that times to ignition can vary over a wide range and that a carefully designed furnace of high heat capacity will be required in future work to minimise this temperature lag. A thermocouple embedded in the pellet of composition is also highly desirable to monitor the sample temperature and to detect any self-heating caused by exothermic reactions below the ignition temperature. Measurements made with standardised equipment would indicate the lowest temperature at which ignition occurs and the time required to ignite at various temperatures.

Results from this type of experiment have been reported (2,3) in which times to ignition of more than 6 minutes have been measured, for example for oxidant - phenolformaldehyde castings (3). Only gunpowder in the current

work ignites in times as long as 2 minutes and this is believed to be due to the slow oxidation of carbon which builds up heat in the sample until ignition finally occurs. The results from these studies are being compared with those from thermal analysis techniques (DTA, TGA and DSC) carried out at much lower heating rates.

POST IGNITION

Pressure vessels of nominally 2, 5 and 10ml capacity are used to generate pressure-time curves characteristic of electric fuzeheads and pyrotechnic compositions. The pressure changes are followed using a Kistler type 601H piezoelectric pressure transducer, Kistler type 5001 charge amplifier and Gould 4100 digital storage oscilloscope. A single sweep of the oscilloscope is triggered by the firing current and a pre-trigger section of 25% of the full sweep allows an accurate baseline to be recorded.

The small 2ml vessel is used to assess the performance of both existing and experimental fuzeheads. Fuzeheads which give consistent output are used to ignite and study pyrotechnic compositions in the larger 5 and 10ml vessels.

Pressure-time curves are often analysed by evaluating the peak pressure and time to peak pressure. However it can be difficult to determine the peak pressure and the exact location where the pressure rises from the baseline. A curve of dp/dt against t can help to overcome this problem. Typical p against t and dp/dt against t curves for 300mg of loose powdered composition B in the 5ml vessel are shown in Figures 3 and 4 respectively. Figure 5 shows a graph of peak pressure, corrected for the volume occupied by the sample, against sample weight for composition B in the 5ml vessel. A linear relationship is observed up to 0.5g of composition but at higher sample weights the pressure increase is greater, presumably as a result of

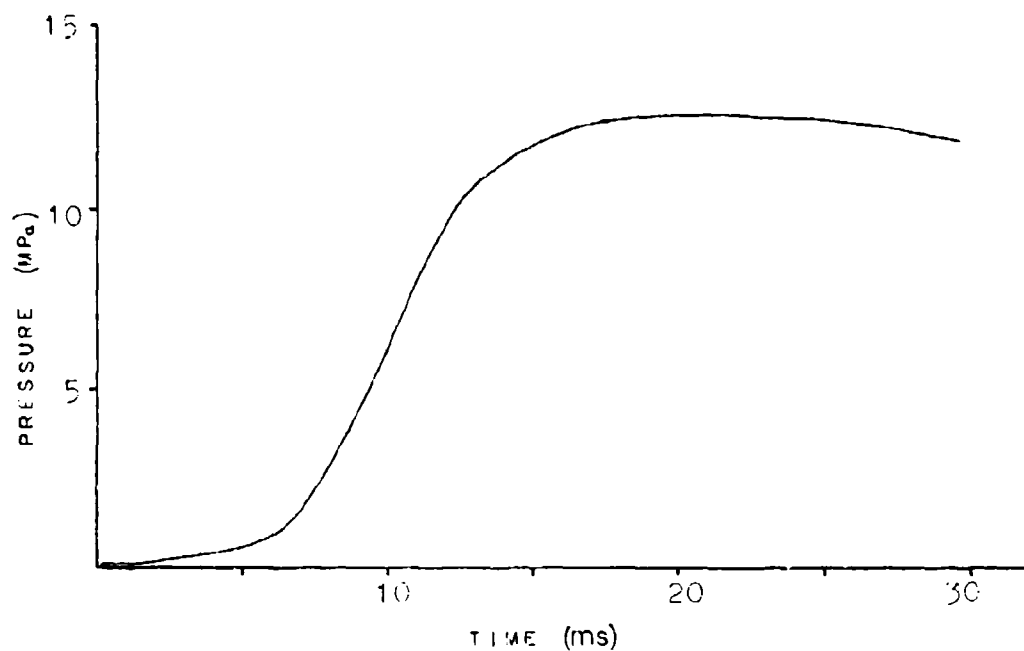


FIG 3. PRESSURE - TIME CURVES FOR COMPOSITION 3

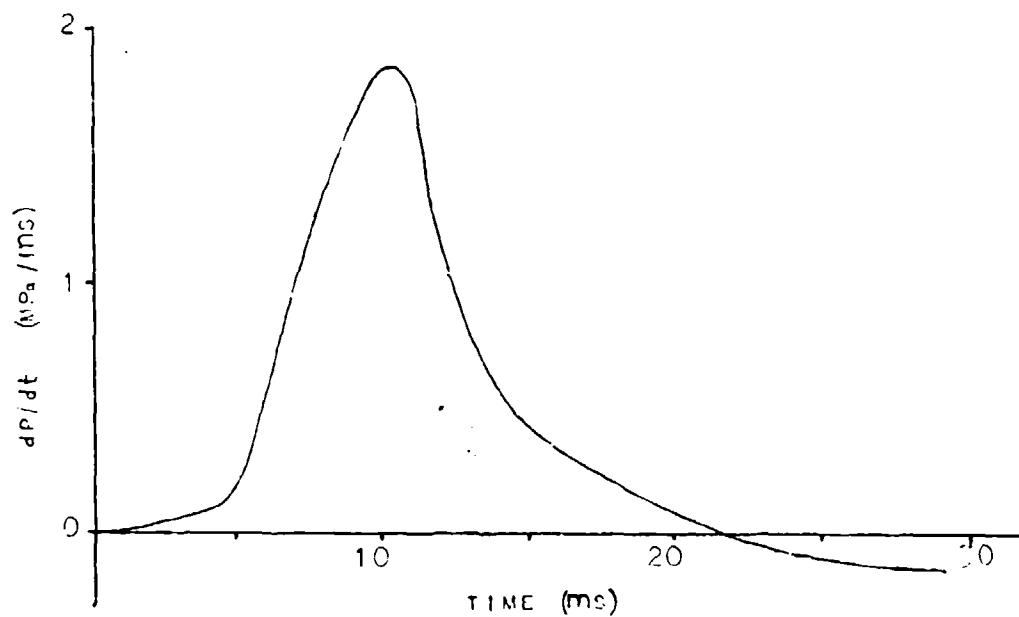


FIG 4. DIFFERENTIAL PRESSURE - TIME CURVES FOR COMPOSITION 3

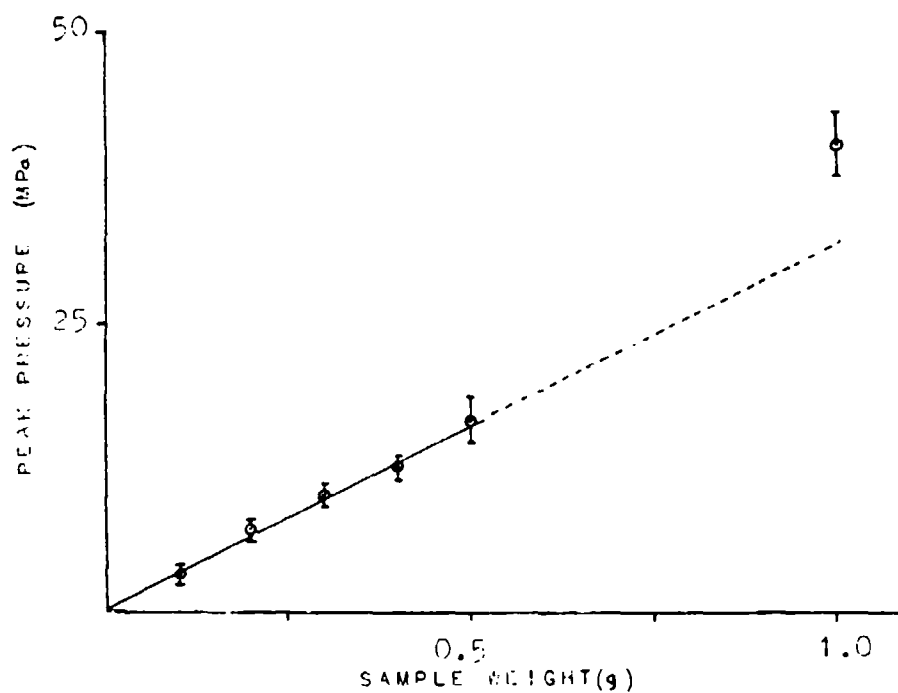


FIG 5. PEAK PRESSURE AGAINST WEIGHT OF COMPOSITION B

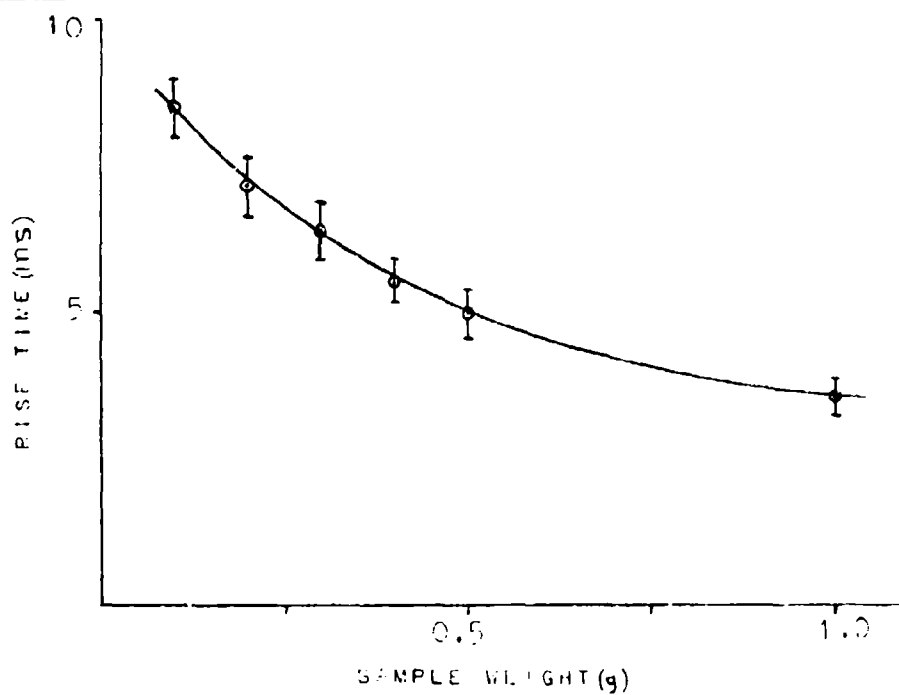


FIG 6. RISE TIME AGAINST WEIGHT OF COMPOSITION B

increased gas phase temperature. A plot of rise time, defined as peak pressure divided by the maximum slope, against sample weight is shown in Figure 6 from which the burning rate can be seen to increase with increasing weight of sample.

IGNITION TRANSFER

An ignition stimulus can be transferred over surprisingly long distances by channelling the products of combustion (hot gases, shock and particles) from a pyrotechnic or initiatory explosive donor composition through small diameter metal tubes called flash tubes. For the experiments described here composition F (KDNBF) has been used as both donor and acceptor compositions and these are connected by stainless steel flash tubes with internal diameters varying in the range 0.6-2.5mm. The pressed donor composition is sealed into one end of the tube, ignited by means of a bridgewire, and the acceptor end is left unsealed. This experimental arrangement is shown in Figure 7.

The critical length of tube for successful ignition of the acceptor composition, ie above which ignition transfer does not occur, has been determined for each internal diameter tube. The results are shown in Figure 8 for the experiments carried out at atmospheric pressure, from which the critical length can be seen to increase with increasing internal diameter up to 2.0mm and then to decrease to 2.5mm diameter. The maximum critical length is greater than 1m. Reducing the pressure further increases the critical length indicating that energy transfer is more efficient under these conditions. For example at a pressure of 100mPa the critical length exceeds 1m for flash tube internal diameters greater than 1mm.

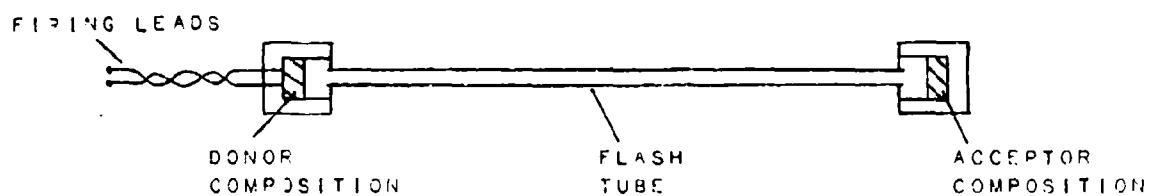


FIG 7. FLASH TUBE ARRANGEMENT

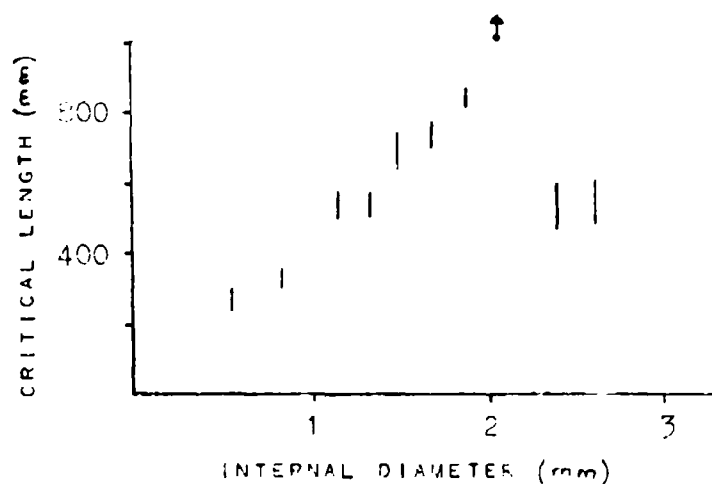


FIG 8. CRITICAL LENGTH AGAINST FLASH TUBE INTERNAL DIAMETER

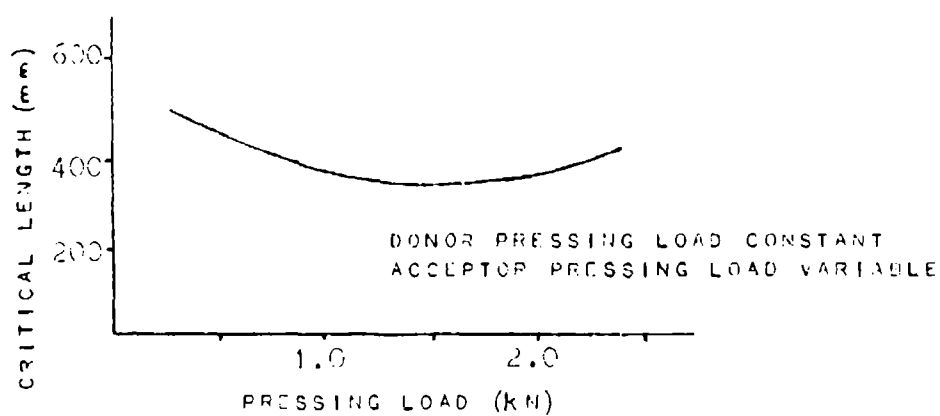


FIG 9. CRITICAL LENGTH AGAINST PRESSING LOAD OF ACCEPTOR

Using composition F (KDNBF) in flash tube experiments at atmospheric pressure the critical length does not vary with the mass of the donor composition when this exceeds 10mg. The critical length is however dependent upon the pressing stress on the acceptor composition, as shown in Figure 9. Not surprisingly bends in a flash tube reduce the critical length. One way of studying this effect is to determine a critical radius of curvature for a specific length of flash tube with a 180° bend in it.

A standardised flash tube arrangement can be used to evaluate the effectiveness of compositions, both donors and acceptors, in this mode of ignition transfer by measuring critical lengths. For example at atmospheric pressure and with composition F (KDNBF) as acceptor and a tube of 1.78mm id, a critical length of 780mm is obtained with composition F as donor while a much smaller critical length of 70mm is obtained with the relatively gasless composition G as donor.

Flash tubes can themselves be evaluated using standard compositions to compare different flash tube materials and forms of tube. For these experiments the choice of compositions can be based on gap test, rotating disc or pressure vessel assessments.

Finally ignition transfer across a metal barrier acting as a pressure bulk-head (through barrier initiation) is being studied using a Barnes Spectral-master model 12-55 Infra-Red Radiometer. This instrument has a Cassegrain optical system giving a field of view of 2.5mR which permits focusing onto a 3mm diameter thermal septum at the acceptor end of the through barrier initiation device shown in Figure 10. The rise time of the radiometer, being less than 100µs, is sufficiently fast to enable temperature-time profiles, generated by ignition of pyrotechnic donor compositions, to be measured on the acceptor side of the barrier.

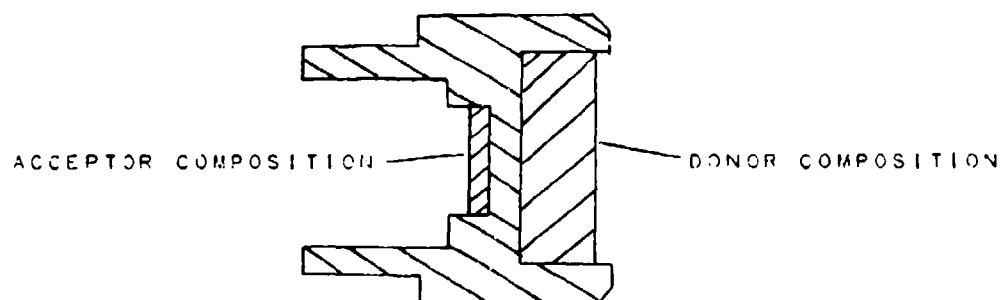


FIG 10. TYPICAL THROUGH BARRIER INITIATION (TBI) DEVICE

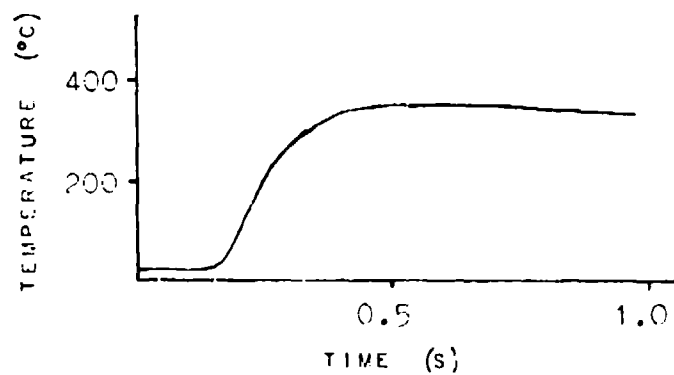


FIG 11. TYPICAL TEMPERATURE - TIME PROFILE FOR TBI DEVICE

Figure 11 shows a typical temperature-time profile which indicates that, in the arrangement shown in Figure 10, peak temperatures of about 350°C are achieved in 0.4 second. Numerous experiments of this type have shown that the ideal composition for this mode of ignition transfer should have a relatively high heat of combustion and produce a solid, heat retentive slag with very little gas evolution, to ensure good thermal contact with the metal barrier. This technique of measuring temperature-time profiles with a radiometer provides a direct means of assessing the characteristics of compositions for use in this particular environment. Data is also generated necessary for the correct choice of acceptor composition, the post ignition characteristics of which will depend on the function which it is required to perform.

CONCLUSIONS AND RECOMMENDATIONS

The various tests described in this paper have proved useful in initial studies to characterize the ability of pyrotechnic and initiatory explosive compositions to ignite and transfer ignition to other compositions in an explosive train. Each test produces results which are strictly only applicable to the particular geometry and environment of each test. The results of different tests, however, provide interesting comparisons between different types of pyrotechnic composition. For example the results from the gap test and flash tube experiments using gunpowder and KDNBF respectively have given quantitative support to the long held view among pyrotechnists that reliable ignition between compositions not in direct contact is favoured by using gassy donor compositions to transfer heat and particles to the acceptor compositions. Similarly radiometric studies of through barrier initiatory devices have confirmed the role of gasless, heat retentive compositions in producing efficient heat transfer across metal barriers.

The present range of tests needs to be extended in future work to add further information on the effectiveness of a composition in its action in an explosive train. At the same time important parameters such as ignition time, burning time, length of flame and flame temperature need to be properly evaluated.

REFERENCES

1. E L Charsley and D E Tolhurst, The Application of Hot Stage Microscopy to the Study of Pyrotechnic Systems. Proceedings of Pyrochem International, University of Surrey, Guildford, UK, 1975.
2. H Henkin and R McGill, Indust and Eng Chem, 44 1391 (1952).
3. H L Girdhar and A J Arora, Combustion and Flame 28 109 (1977) and 31 245 (1978).

HEXANITROSTILBENE (HNS): REVIEW OF SHIELDED MILD
DETONATING CORD (SMDC) PERFORMANCE UNDER BIASED
CONDITIONS OF FABRICATION

E. Eugene Kilmer
Naval Surface Weapons Center, W.O.
Silver Spring, Maryland 20910

ABSTRACT

The performance of explosives and explosive systems can be determined by many different methods. The efforts of this task, have been directed towards applying the results of High Performance Liquid Chromotography (HPLC) to better understand the variability of the purity of explosives in their bulk condition and after loading into hardware. The performance of Shielded Mild Detonating Cords (SMDC) was studied after exposure to elevated temperatures to determine what affect impurities have on performance of the explosive.

The performance of the cords subjected to elevated temperatures of 218°C (425°F), 260°C (500°F) and 282°C (540°F) is discussed. Hexanitrostilbene produced in the United States and England were compared with respect to particle geometry and purity.

The variability in the particle size and geometry of the HNS-I being produced raised the question of possible variable sensitivity to explosive shock and fragment impact initiation. The results of certain tests indicate sufficiency of explosive initiation with respect to HNS-I variable particle geometry.

All of the HNS samples were acceptable in the design except for one sample which assayed high in acid content before being subjected to elevated temperatures.

INTRODUCTION

The objective of this work was to determine if the variability in the particle size and geometry of the HNS-I currently produced by industry would affect its response to an explosive shock stimulus. The test vehicle chosen for this study was the standard Shielded Mild Detonating Cord (SMDC) end booster. A cutaway view of this piece of ordnance is shown in Figure 1.

A number of bulk HNS samples obtained from various manufacturers were sent to the McDonnell Douglas Corporation at St. Louis, Missouri for testing by the QUEST method.^{1,2} The first group of explosives loaded and tested are listed in Table 1. The explosives selected were typical samples of the production lots that each vendor produces according to his own proprietary techniques. Scanning electron photomicrographs (SEM) taken of each sample are shown in Figures 2 through 9 to document the morphology of the crystalline explosive.

SMDC Sensitivity To Fragment Initiation

The test technique used to determine the sensitivity of the explosives to fragment impact was originally developed as part of the study by Schimmel in 1973. Sketches of the hardware arrangement are shown in Figure 10. The data collected in this study was obtained using two test configurations for the SMDC end boosters: end-to-end and side-to-end. The end-to-end (donor-to-acceptor) hardware, laboratory set-up, was arranged with a constant one-half inch air-gap. The test variable was the thickness of the steel shim placed between the donor and acceptor end booster. The side-to-end configuration was arranged with a constant one-tenth inch air-gap test increment. Side-to-end initiation is always more difficult than end-to-end initiation and therefore requires a reduced air-gap to accomplish detonation transfer.

-
1. Schimmel, M. L. "Quantitative Understanding of Explosives Stimulus Transfer," NASA CR2341, December 1973.
 2. Schimmel, M. L., "Measurement of Explosive Output," Report E206, McDonnell Aircraft Corp., 15 November 1965.

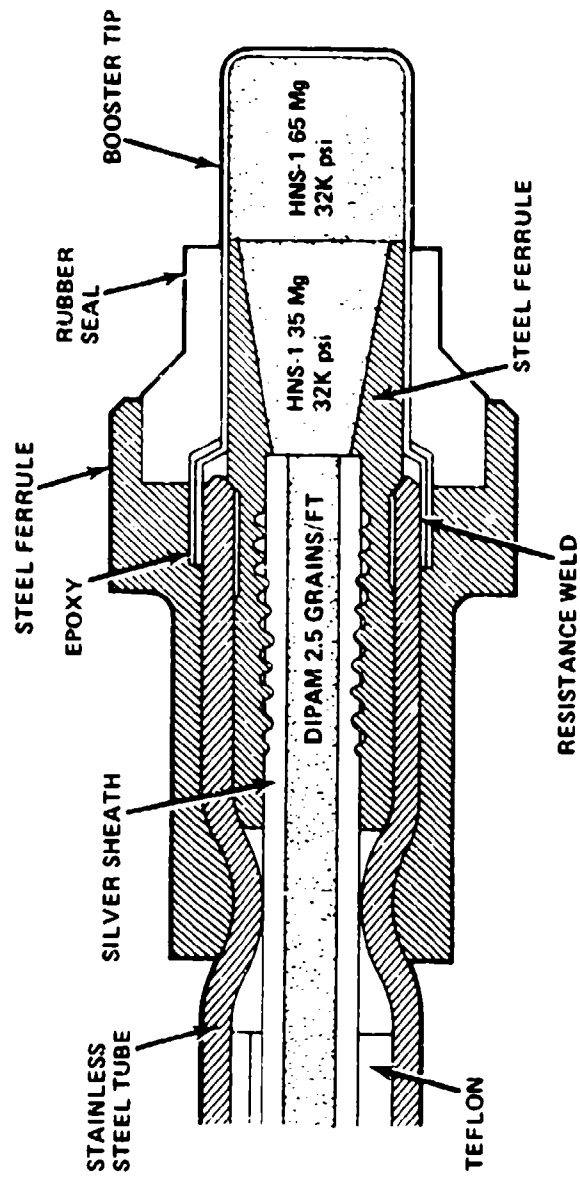


FIGURE 1 SMDC END TIP HARDWARE (MCDONNELL DOUGLAS CORP.)

Table 1. Explosives/Vendor Identification (HNS)

<u>NSWC Identification</u>	<u>Vendor Identification (lot)</u>	<u>Type</u>
2232	British PERME 343	I
2417	British PERME 553	I
2297	United Tech Inc. 3	I
2413	United Tech Inc. 8	I
2282	Chemtronics 114-11	I
2087	Chemtronics 64-19	I
2247	NSWC 96-8433-48#2	I
2407	Silas Mason Hanger 7157-07C-011	I
2132	Tel McC Selph 1014	I
2130/2134	Tel McC Selph 1125	I
1479	Del Mar Engr 250-7	II
2299	Silas Mason Hanger 6348-07H-001	II
2323	Ensign Bickford 30	II

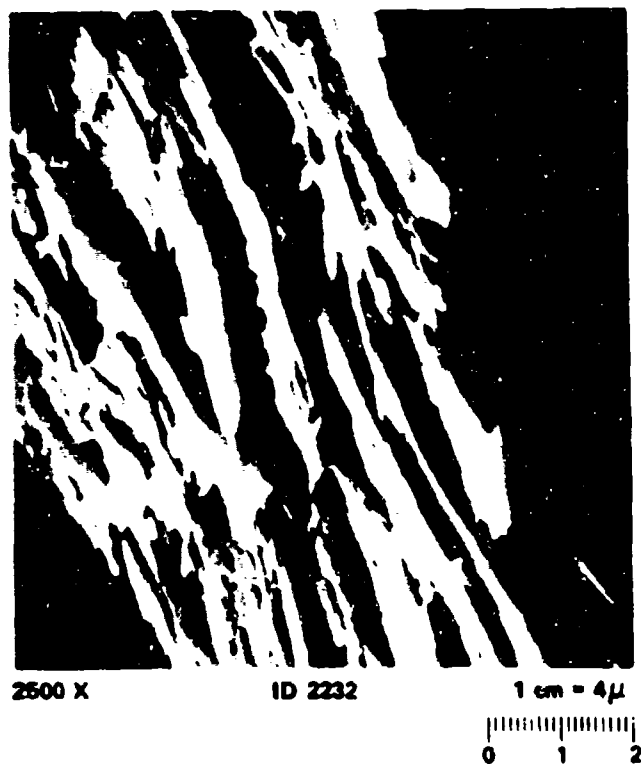


FIGURE 2 HEXANITROSTILEBENE: BRITISH PERME 343 (ID2232)



FIGURE 3 HEXANITROSTILBENE: NSWC 96-8433-48-2 (ID2247)



FIGURE 4 HEXANITROSTILBENE: UNITED TECH. INC. 3 (ID2297)



FIGURE 5 HEXANITROSTILBENE: CHEMTRONICS 64-19 (ID2087)



FIGURE 6 HEXANITROSTILBENE: TEL/McC/S 1125 (ID2134)



FIGURE 7 HEXANITROSTILBENE: DEL MAR ENG. 250-7 (ID1479)



100 X

ID 2299

1 cm = 100 μ



FIGURE 8 HEXANITROSTILBENE: SILAS MASON HANGER 6348-07H-001 (ID2299)



50 X

ID 2323

1 cm = 200 μ



FIGURE 9 HEXANITROSTILBENE: ENSIGN BICKFORD 30 (ID2323)

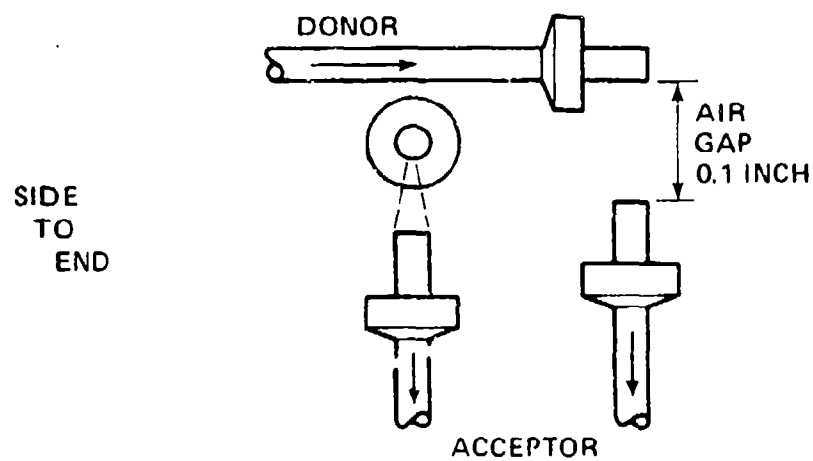
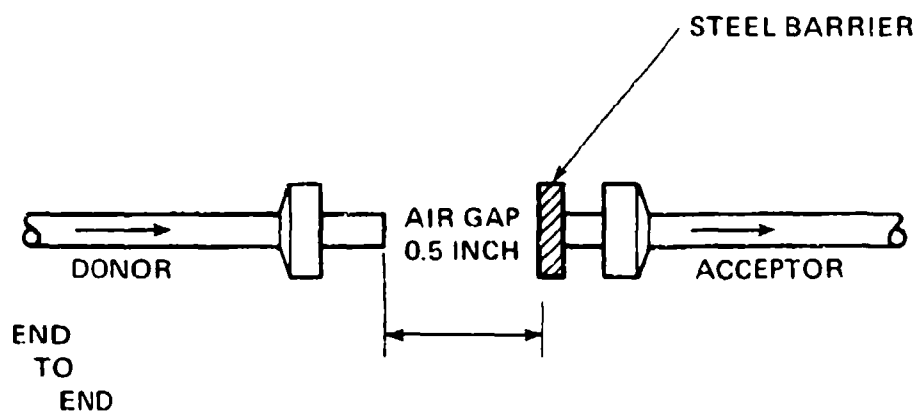


FIGURE 10 DETONATION TRANSFER ARRANGEMENT (MCDONNELL DOUGLAS CORP.)

It should be pointed out that the test results in reference 1 show that HNS-I is more sensitive to fragment initiation than HNS-II. In addition, the samples tested in that study show that at the 50% response level of the acceptor-closure thickness of shim, the shim was approximately twice as thick for the HNS-I (NSWC ID 537) as for the HNS-II (NSWC ID 528).

The data collected by McDonnell Douglas Corporation using the QUEST method is summarized in Table 2. End-to-end configuration testing shows the approximate 50% response level for the acceptor-closure thickness, for HNS-I, to be 0.20-inch. One exception is NSWC ID 2087 which was 0.017. The results show HNS-II to be about 0.10-inch for a 50% response level in this configuration. These test results not only confirm the sensitivity difference between HNS-I and HNS-II, as measured in reference 1, but also show that the test will distinguish between the sensitivity of HNS-I samples with grossly different particle sizes. This test however is not sensitive enough to differentiate sensitivity between samples of comparable particle size. As is shown in Figure 5, ID 2087, this HNS-I was larger in particle size than the HNS-I explosives in Figures 2, 3, 4, and 6. HNS sample ID 2087 was found to be less sensitive to fragment initiation than the other smaller sized HNS-I particles as is shown in Table 2. However, this conclusion was drawn from a small sample population and should be expanded statistically for a more definitive answer.

If one considers the purity of the explosive, i.e., the percentage of hexanitrobibenzyl and other materials in the HNS, then a review of the chemical assays and fragment sensitivity will indicate the reaction or sensitivity to fragment initiation is not a function of the purity of the material (Table 2). Further, a comparison of the surface areas of the HNS shows the more sensitive HNS-I to have a much greater surface area than the HNS-II. The only sample in which deviates in sensitivity is the single sample of HNS-I (ID 2087) which has been measured by a high speed surface analyzer and found to have about half the surface area of the standard HNS-I (ID 2297, 2232). These results suggest that there is no significant improvement to fragment initiation when the surface area exceeds $27,000 \text{ cm}^2/\text{cm}^3$. This can be seen in a plot of the steel barrier thickness vs the surface area in Figure 11. In

Table 2. Summary of Fragment Sensitivity,
Chemical Assay and Surface Area Analysis for HNS

NSWC ID #	HNS Type	Approx. 50%-Fire Acceptor Closure Thickness (in)	HPLC Assay		% TNB	Surface Area Analysis* cm ² /cm ³
			% HNS	% HNBiB		
2247	I	0.020	99.5	0.5	None	128,336
2130/2134	I	0.020	93.0	6.7	None	67,297
2232	I	0.020	97.6	1.9	0.3	52,165
2297	I	0.020	94.5	4.6	0.1	47,929
2087	I	0.017	99.2	0.6	Trace	26,818
1479	II	0.010	99.5	0.2	None	8,996
2299	II	0.010	99.6	None	None	8,996
2323	II	0.010	98.7	None	None	7,612

* - Surface area measurements consisted of an average value determined from two test runs on a Micrometrics High Speed Surface Analyzer Model 2205. Accuracy is within 3%.

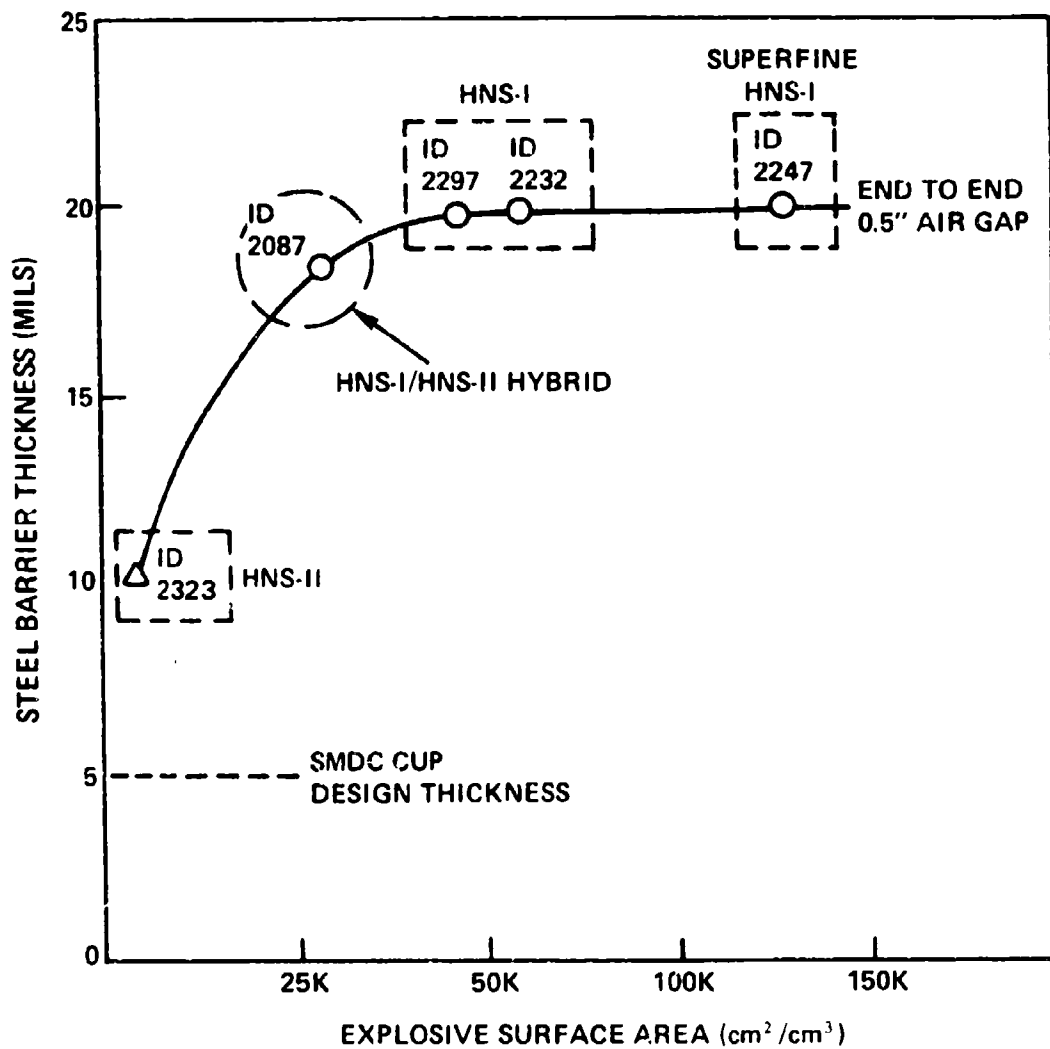


FIGURE 11 HEXANITROSTILBENE - FRAGMENT INITIATION SENSITIVITY AT A 50% FIRE RESPONSE WITH STEEL BARRIER THICKNESS VS EXPLOSIVE SURFACE AREA AT THE 0", 500 AIR GAP. (END TO END CONFIGURATION)

addition, a comparison of barrier thicknesses reveals that HNS-II is too insensitive to be used in the end cup of the SMDC end booster. The data in Figure 12 indicates HNS-II will not initiate in a side-to-end configuration at a steel thickness greater than 3 mils (50% fire response). The implication here is the stainless steel cup used to enclose the end booster on a standard SMDC tip measures 5 mils thick and would therefore cause reliability problems in the side-to-end configuration.

Acceptability of HNS-I in SMDC Hardware

The acceptability of various lots of HNS-I, produced by different manufacturers, was to be accomplished by measuring their performance in doing work by incorporating the materials into Shielded Mild Detonating Cords (SMDC). This work was done concurrently with (a) sensitivity-to-fragment initiation and (b) particle size analysis of several lots of HNS-I.

The test method and equipment selected for this task was the McDonnell Douglas Corporation Energy Sensor.² It utilizes precalibrated aluminum honeycomb as a crushable element with the output energy of the end booster determined in units of inch-pounds. The SMDC line was assembled into the energy sensor as shown in Figure 13 where it is initiated by a blasting cap. A piston is propelled forward from the explosion of the tip of the SMDC. The measurement of energy output is determined from length of honeycomb crushed in that fixture. Each honeycomb element is precalibrated to determine the crush strength as a function of distance. This force multiplied by the distance (length of honeycomb crushed) yields the effective energy (in inch-pounds) of the explosion used to do work. This test was used during development qualification and is still used for the acceptance testing of F-111 aircraft SMDC hardware. As a result many thousands of test firings that have been made, the average energy output and variation of output are well established.

The explosives tested were selected from a representative production lot of HNS-I produced by each of several vendors. All of these vendors were the primary producers of HNS-I in the United States except for one vendor in England. The object of the selection was to determine

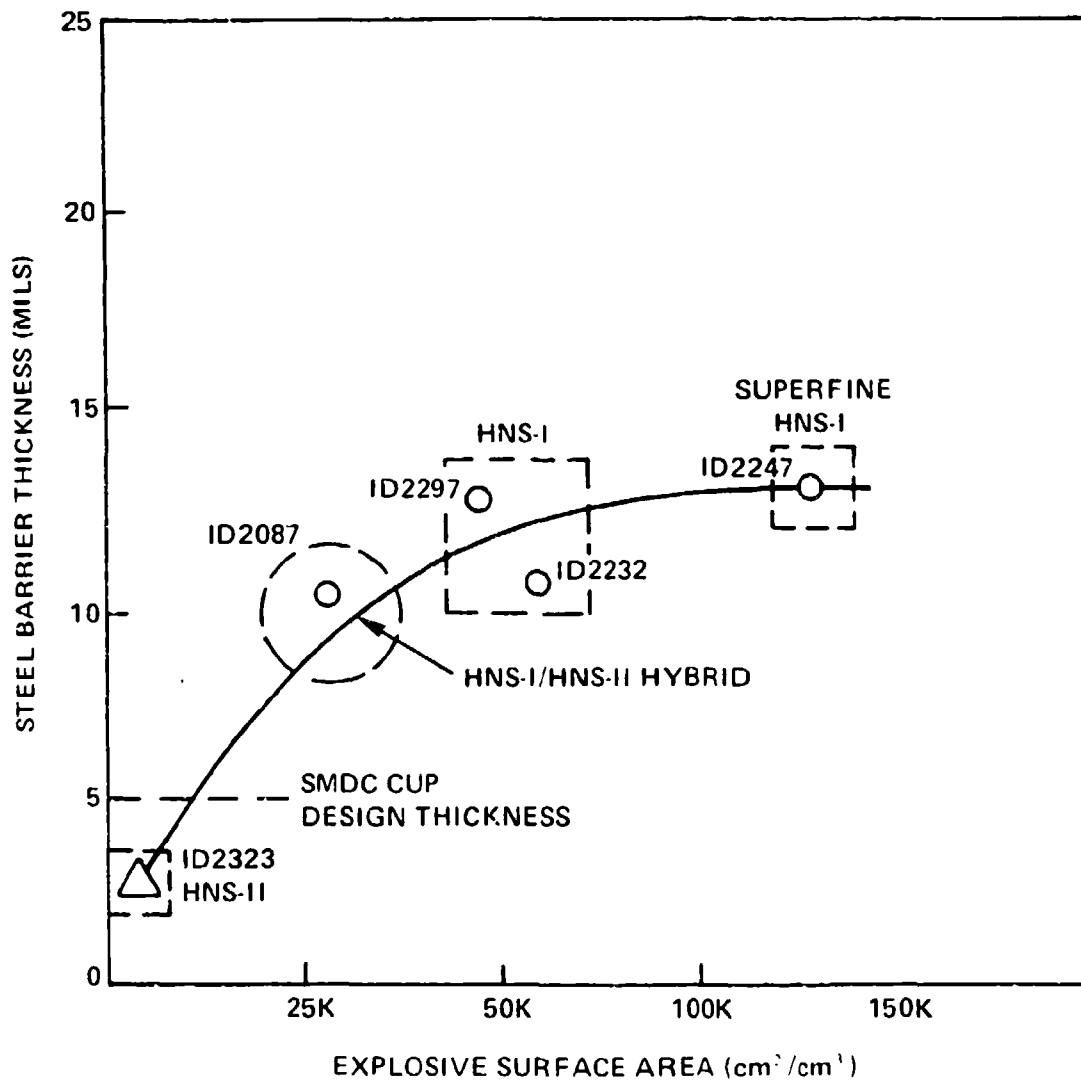


FIGURE 12 HEXANITROSTILBENE - FRAGMENT INITIATION SENSITIVITY AT A 50% FIRE RESPONSE WITH STEEL BARRIER THICKNESS VS EXPLOSIVE SURFACE AREA AT THE 0". 100 AIR GAP. (SIDE TO END CONFIGURATION)

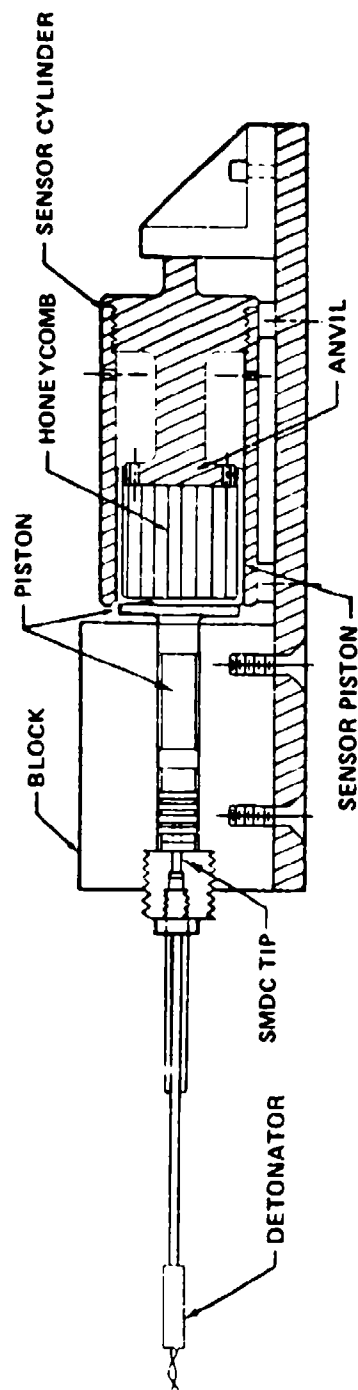


FIGURE 13 SMDC OUTPUT TEST FIXTURE (MCDONNELL DOUGLAS CORP.)

if HNS-I, as a production explosive, would show any variable output when used in the SMDC vehicle. The Naval Surface Weapons Center (NSWC) and vendor lot identifications are shown in Table 1. The energy sensor is identified as a MCAIR P/N 12K016-07 Initiator Output Test Fixture. The standard for the tests were the F-111 SMDC end tips furnished by MCAIR. SMDC lines were loaded with explosive from the various vendors and fabricated by Explosives Technology.

A total of eighty-four (84) SMDC-end tip energy output tests were made at ambient temperature. In addition to the seventy (70) tests with the NSWC-supplied end tips, fourteen (14) tests were performed with the F-111 end tips for control data. Initially, six (6) F-111 end tips were fired to verify proper functioning of the energy sensor; then eight (8) more F-111 end tip firings were interspersed throughout the tests of the NSWC-supplied end tips.

The test pattern used with the NSWC-supplied end tips where the first thirty-five (35) NSWC-supplied end tips were tested was as follows: Five (5) end tips from one of the seven lots were fired before proceeding to five from the next lot, etc. With the last thirty-five (35) NSWC-supplied end tips tested, one end tip from the first lot was fired followed by one from the second lot, etc., rotating through the seven lots sequentially five times.

The results obtained from the F-111 end tip control firings are tabulated in Table 3. The results obtained from the NSWC-supplied end tip test firings are tabulated in Table 4.

CONCLUSIONS AND RECOMMENDATIONS

1. The testing of HNS-I and HNS-II by the McDonnell "QUEST METHOD" resulted in differentiating between both materials but it is not sensitive enough to distinguish differences between HNS-I samples.
2. All materials tested from vendors in the United States and England were determined to be acceptable for use in SMDC hardware from the viewpoint of explosive initiation sensitivity.
3. Comparison of surface area analyses and sensitivity to fragment initiation reveals that the HNS-I minimum surface area should be greater than $27,000 \text{ cm}^2/\text{cm}^3$ (approximately $1.55 \text{ m}^2/\text{g}$).

Table 3. Measured Energy Output of NSWC-Supplied Tips
and F-111 Control Tips

Pantex Lot 7157-07C-0001 No. 2407	UTC Lot 8 No. 2413	Brit. PERME 553 No. 2417	Expl. Tech./ McDonnell Douglas F-111 Control Tips
Energy (In-Lb)	Energy (In-Lb)	Energy (In-Lb)	(In-Lb)
414	440	331	405
572	420	402	347
412	393	386	353
406	459	418	362
443	378	336	398
246*	322	336	342
467	384	467	340
216*	480	462	346
436	346	376	444
437	184*	354	481
Total: 3587	3622	3934	5679
Average: 448	402	393	406

* - Inaccurate (low) value not included in column total and average. The flagged values occurred during tests in which explosive-generated gas leaked past or expelled the reused aluminum nut holding the SMDC-tip in the test-fixture adapter.

Table 4. Measured Energy Output of NSWC-Supplied Tips

T/M/C Lot 1014 NSWC ID No. 2132 Energy (In-Lb)	Brit. PERME 343 No. 2232 Energy (In-LB)	Chem. Lot 114-11 No. 2282 Energy (In-Lb)	UTC Lot 3 No. 2297 Energy (In-Lb)
341	242	297	222 *
319	230 *	294	313
316	305	302	322
329	378	443	286
281	445	338	316
443	428	431	396
395	314	266	311
477	439	420	409
433	444	355	469
346	331	389	373
Total: 3680	3326	3535	3195
Average: 368	370	354	355

* - Inaccurate (low) value not included in column total and average. These flagged values occurred during tests in which explosive-generated gas leaked past or expelled the reused aluminum nut holding the SMDC-tip in the test-fixture adapter.

4. HNS-II is not recommended for use in SMDC end booster design (this remark does not imply the detonating cord). Marginal performance is expected since test results indicate 3 mils of steel barrier will yield a 50% fire response to other SMDC tips.

5. Within the limitations of the energy sensor capability, there is no significant energy output difference among the seven HNS lots tested, since each lot produced an average energy value within the 400 ± 50 in-lb range. Also, none of the test lots shows much statistical difference from the results obtained with the F-111 end tips, which averaged 406 in-lb. Finally, all of the data obtained during this test program is comparable to that obtained over past years from acceptance tests with new F-111 and F-15 SMDC-end tips.

6. It has been shown that HNS-I manufactured throughout the United States and England will perform in the SMDC vehicle.

ENERGY OUTPUT OF DIFFERENT PYROTECHNIC IGNITER SYSTEMS

GUENTER KLINGENBERG
FRAUNHOFER-INSTITUT FUER KURZZEITDYNAMIK
ERNST-MACH-INSTITUT
ABTEILUNG FUR BALLISTIK (EMI-AFB)
HAUPTSTRASSE 18, 7858, WEIL AM RHEIN, WEST GERMANY

ABSTRACT

A special igniter case designed by Dynamit Nobel AG was used for measuring the energy output of four different igniter formulations in terms of gas pressure, flame temperature, and gas velocity in order to study the performance of pyrotechnic igniter systems, and to evaluate the energy efflux at the igniter vent. Four igniter systems were defined which consisted of (A) B-KNO₃, (B) black powder, (C) nitrocellulose, and (D) mixtures of nitrocellulose with black powder. Open air firings were carried out with these igniters to obtain their general characteristics. Peak values of (A) 5 MPa, 2000°K, 1200 m/sec; (B) 5 MPa, 1600°K, 1300 m/sec; (C) 12 MPa, 2500°K, 1400 m/sec; and (D) 4 MPa, 1600°K, 1300 m/sec were measured at the igniter vent. From these data mass and energy flux were evaluated. The compositions of nitrocellulose and B-KNO₃ both had higher energy output than the black powder formulation. Due to condensation reactions, B-KNO₃ generated an extremely high particle concentration while the nitrocellulose composition produced extremely low particle concentration in the gas outflow. However, due to the confinement conditions, the nitrocellulose was only partly combusted. Results that will be presented will include flow visualization through the use of shadowgraph and schlieren photography, flame spectra and pressure measurements, gas velocity by means of Laser-Doppler-Velocimeter, and spectroscopic temperature measurements at the igniter vent.

INTRODUCTION

Since the effect of pyrotechnic propellant charge igniters on ignition and combustion is still poorly understood, a panel of scientists was assembled in Germany from ballistic institutes, universities, and private industries to study basic ignition processes (Ref. 1). A fundamental program was formulated with each group performing specific projects. These projects include the (a) construction and development of a special igniter system with different igniter compositions, (b) investigations of the processes occurring inside the igniter and at the igniter vent, (c) studies on the effect of the igniter on the propellant bed, and (d) ignition modeling. Initially, these studies were focused on the design of the igniter system including the selection of suitable igniter formulations and on the igniter performance measuring the vent characteristics. One of the tasks of EMI-AFB was to determine the energy output of these igniters in terms of gas pressure, flame temperature, and gas velocities employing optical and pressure measurement techniques, radiative emission-absorption techniques, and a Laser-Doppler-Velocimeter (Ref. 1). Prior to describing the experiments which have been conducted, the igniter-chamber design is discussed and the selected igniter formulations are reviewed in light of the requirements.

A schematic of the special igniter case designed by Dynamit Nobel A.G. (Ref. 2) (DNAG) is shown in Fig. 1. The general objective was (a) to control the internal combustion by means of the flow channels in order to obtain a better defined outflow at the igniter vent, and (b) to load the igniter case with four different igniter compositions. An electrical device first ignites the initial igniter producing hot gases which initiate subsequently the igniter composition contained in the igniter case. The combustion gases pass through the transverse flow channels, merge in the conical part of the nozzle, and escape at the cylindrical igniter vent expanding into the surroundings. However, as revealed by these studies, there are some negative features associated with this system (Ref. 1). Due to the inadequate confinement, part of the gases produced by the initial igniter escape through the transverse flow

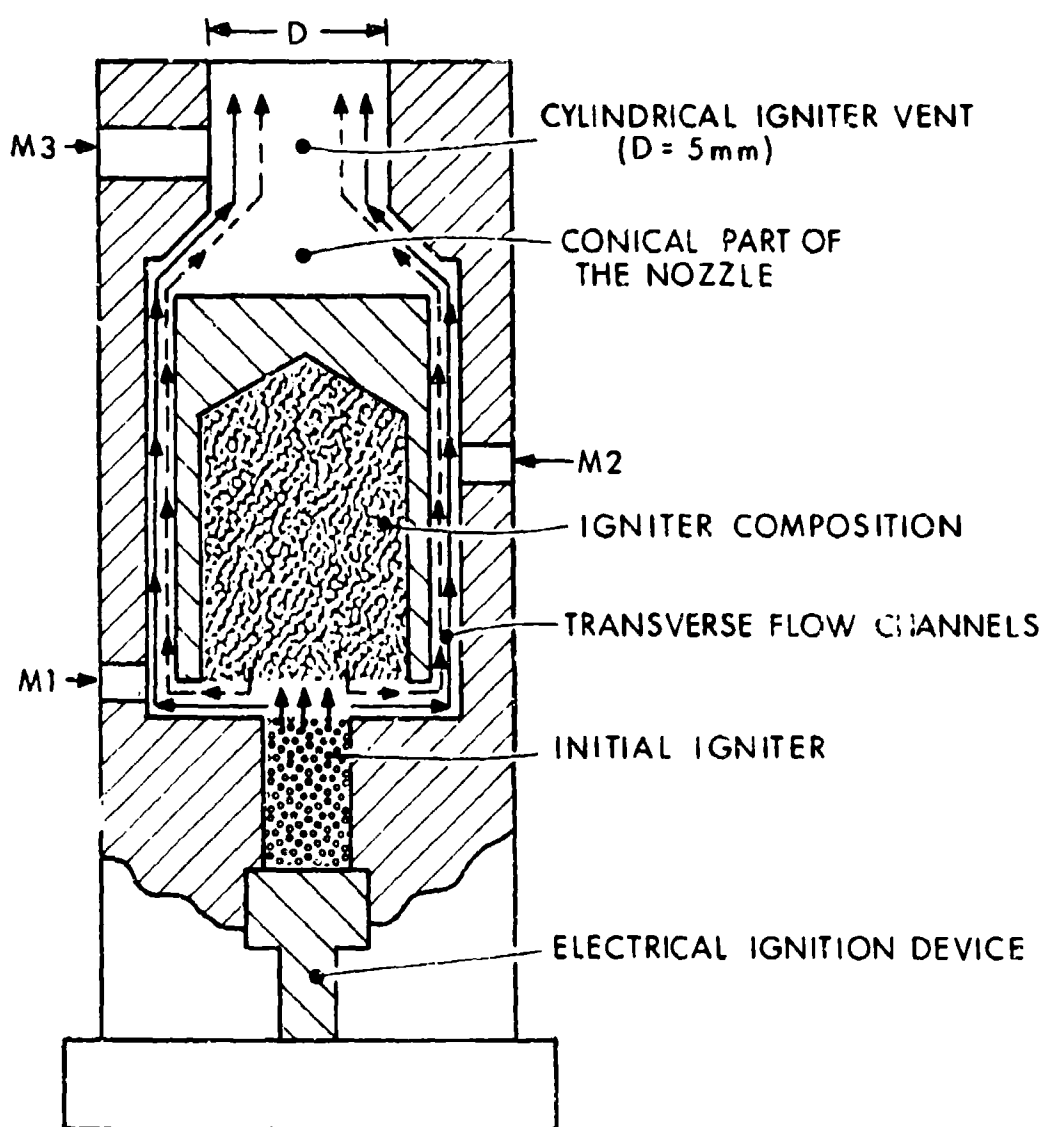


Fig. 1. Electrical Igniter System Indicating Location of Pressure Measuring Ports (M1, M2, M3) and Flow Path for Igniter Gases.

channels forming a precursor flow at the igniter vent, as indicated in Fig. 1. In addition, the cone-shaped part of the nozzle causes rapid flow expansion within the igniter system enhancing possible condensation reactions which may increase the internal energy. Consequently, the energy output at the igniter vent is dependent on the internal flow development.

The criteria for selecting four different igniter formulations as defined by the ignition panel were to obtain the following igniter vent characteristics:

1. hot, gas-poor
2. cold, gas-poor
3. hot, gas-rich
4. cold, gas-rich

In addition, the objective was to obtain one extremely particle-poor and one particle-rich outflow in order to study both the gas and gas-particle ignition. The question of characterizing the igniter formulations was further discussed by the ignition panel. Of the possible parameters, i.e., heat of explosion, activation energy, reaction energy, and reaction enthalpy, the heat of explosion was chosen since it can easily be determined experimentally by a calorimeter. Therefore, it was decided to load the igniter so as to have equal heats of explosion for all four igniter formulations taking into account different loading densities (Ref. 1).

To match these requirements the DNAG selected the following four igniter compositions:

- | | |
|--|-------------------|
| 1. Boron-Potassium Nitrate (B-KNO ₃) | - Code: AZM 953-1 |
| 2. Black Powder (S-C-KNO ₃) | - Code: Y593 |
| 3. Nitrocellulose (Nc) | - Code: MV 7308 |
| 4. Nitrocellulose-Sulfurless-Black Powder (Nc-C-KNO ₃) | - Code: NKP-S-536 |

as listed in Table 1.

Table 1
FOUR IGNITER COMPOSITIONS

CODE NO.	NAME	QUALITY	MAIN CONTENTS	LOADING DENSITY	HEAT OF EXPLOSION (J)
AZM 953-1	Boron-Potassium Nitrate	Hot, Gas-Poor	70.7% KNO_3 23.7% B	0.45 g/cm ³	793
Y 593	Black Powder	Cold, Gas-Poor	75% KNO_3 10% S 15% C	0.90	793
MV7308	NC-Powder	Hot, Gas-Rich	98% NC	0.65	793
NKP-S 536	NC Sulfurless Black Powder Mixture	Cold, Gas-Rich	39% NC 47% KNO_3 12% C	0.85	792

To obtain equal heat of explosion of 793 joules for all four igniter formulations required rather drastic deviations in the loading densities from 0.9 to 0.45. Experimental determinations of the specific heat of explosion and the activation energy by Brede (Ref. 2) and Krien (Ref. 3) are shown in Table 2.

Table 2
EXPERIMENTALLY DETERMINED PROPERTIES OF IGNITER MIXTURES

CODE NO.	IGNITION TEMPERATURE (K)	GAS VOLUME (CM ³)	HEAT OF EXPLOSION (J/g)	ACTIVATION-ENERGY (kJ/mol)
AZM 953-1 B- KNO_3	848	194	6612	105
Y 593 S-C- KNO_3	696	208	3051	61.9
MV7308 NC	495	617	4288	251
NKP-S 536 NC-C- KNO_3	554	375	3298	77

Kuthe (Ref. 4) calculated the thermodynamic data of the four igniter formulations by a thermochemical model using the ideal gas equation. In addition, he assumed an expansion ratio of 200:1, and an isentropic expansion in order to evaluate the influence of condensation reactions by a parametric study. Some of the results are shown in Fig. 2 and Fig. 3, which display the concentration of condensation products and the reaction enthalpy vs. temperature at constant pressure $p = 20$ MPa. For B-KNO₃ with the cooling of the igniter gases a dramatic change of the condensation products occurs with a corresponding change of the reaction enthalpy for temperatures below 2400°K. Apparently, the condensation reactions release energy increasing the internal energy of the flow. Since, for the B-KNO₃ composition AZM 953-1, one of the main combustion products is boron oxide (Ref. 1), a high concentration of condensation products is found to occur with the cooling of the igniter gases during expansion which is associated with an increase of reaction enthalpy. The nitrocellulose composition MV 7308 for a flame temperature above 1800°K shows no formation of condensation products. However, due to the formation of soot particles an increase of the condensation products and a corresponding small change of the reaction enthalpy was found for temperatures below 1800°K, Fig. 2 and Fig. 3.

According to the simple approximations made, this analysis is only capable of predicting the general tendency of the reacting gas-particle flow. A more detailed description of the unsteady flow inside of and at the exit plane of the igniter case awaits the development of a 2-D-2-phase gas dynamic model including the chemistry. Nevertheless, it became obvious that due to the expected flow expansion within the conical part of the igniter nozzle, the igniter vent characteristics will be partly dependent on internal condensation reactions. Furthermore, when firing into open air data on the energy output in terms of pressure, flame temperatures, and gas velocities should be measured in the vicinity of the exit plane of the igniter vent to avoid additional effects caused by the rapid flow expansion in front of the nozzle (Ref. 1).

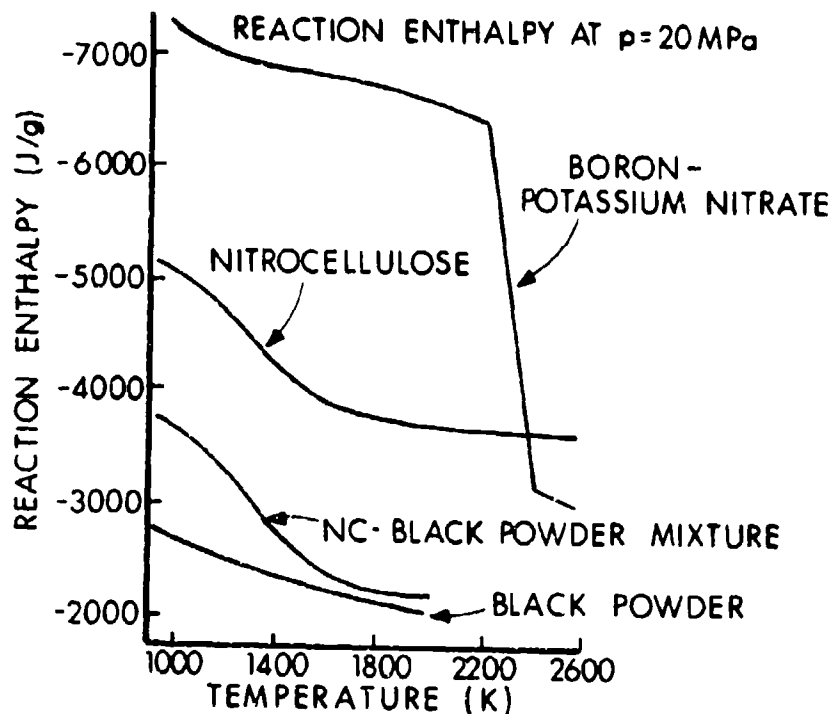


Fig. 2. Thermochemical Calculation at Constant Pressure of Condensed Products in the Four Igniter Formulations

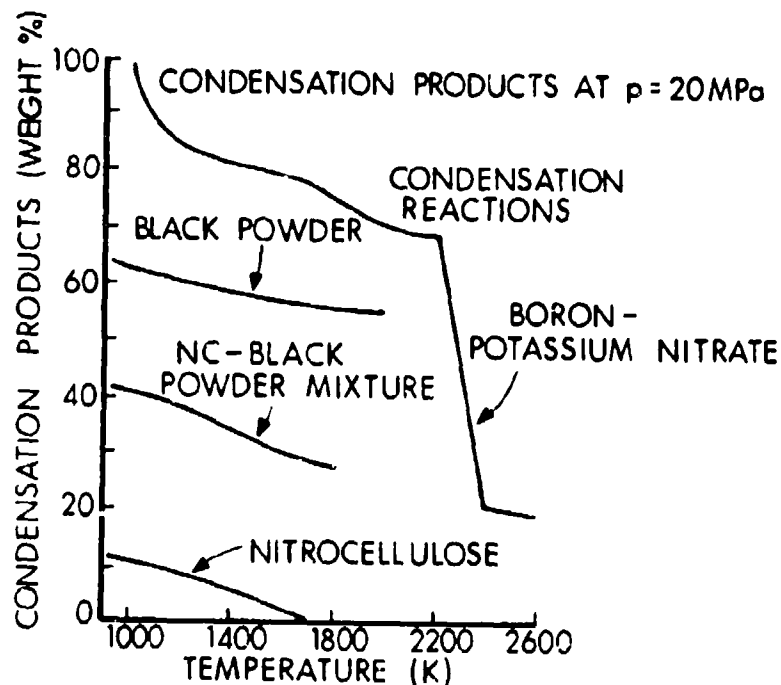


Fig. 3. Thermochemical Calculation of Reaction Enthalpy at Constant Pressure ($p = 20 \text{ MPa}$) for the Four Igniter Formulations

EXPERIMENTAL

Experiments were performed when firing the four different igniters into open air using a special fixture to permit recordings of the igniter output (Ref. 1). About 100 μ sec after the electrical ignition pulse the first gases arrive at the igniter vent. The jitter of the time between electrical pulse and arrival of the gases was measured to be less than 20 μ sec. Time zero in these experiments is the arrival of the gases at the igniter vent, i.e., about 100 μ sec after electrical ignition.

In order to study the igniter vent characteristics the following experiments were performed (Ref. 1):

1. Flow visualization through use of shadowgraph and schlieren photography employing multiple exposure techniques (24 spark sources).
2. Investigation of the formation of flames and particles by means of still pictures and time-resolved drum camera recordings.
3. Recording of the visible and near infrared spectrum of the flames through use of spectrographs.
4. Pressure measurements using a KISTLER gage (603B) at location M3 (see Fig. 1), i.e., in-case measurements 2 mm from the end of the igniter nozzle.
5. Spectroscopic temperature measurements employing a modified line reversal technique at position X = 2.5 mm in front of the igniter vent, i.e., in the center of the so-called primary flash.
6. Gas velocity measurements by means of a new Laser-Doppler-Velocimeter (Ref. 8) within the gas outflow 2.5 mm in front of the igniter vent.

The employed experimental techniques for flow and flame visualization, flame spectra recordings, spectroscopic temperature and pressure measurements as well as gas velocity measurements are well established and were used in the field of ballistic studies. They are thoroughly documented in References 5 to 9. No further detail will be given here except to mention that a special setup was employed for the modified reversal method to record the radiation flux from the primary flash with and without superimposed radiation of a calibrated tungsten ribbon lamp simultaneously by separating the imaged radiation through light pipes, see Fig. 4.

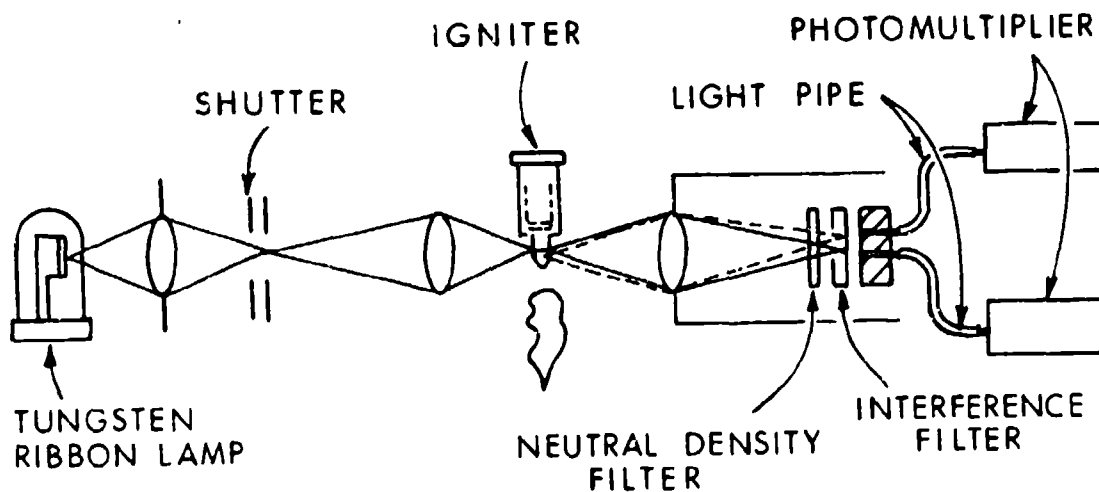


Fig. 4. Scheme of Set-up for Spectroscopic Temperature Measurements

From the measured flow parameters at the igniter vent, the energy flux at the igniter vent can be calculated using the equation given by Celmins (Ref. 10) for a cylindrical nozzle:

$$\frac{dE}{dt} = \dot{E} = \dot{m} (c_v T_e + \frac{1}{2} u_e^2) \quad (1)$$

$$\frac{dm}{dt} = \dot{m} = A \rho_e u_e \quad (2)$$

where $A = \pi r^2$ denotes the area of the vent, ρ_e , T_e , and u_e the vent characteristics ($\rho_e = f(p)$), and c_v the specific heat for $p = \text{const.}$ Since the pressure, temperature, and gas velocity histories p_e , T_e , u_e vs. time are known from experiment, and c_v can be derived from thermochemical calculations (Ref. 4) the energy efflux \dot{E} can be evaluated. However, one has to be cautious about interpreting the results. Even if the real measured data are used including effects of condensation reactions the role of the gas-particle flows is neglected since Equation (1) was derived from gas phase calculations. Therefore, particle-rich flows as generated by the K-BNO₃ composition AZM 953-1 can lead to an underestimation of the energy efflux neglecting the energy content of the boron oxide particles. Nevertheless, Equation (1) was used to calculate the energy efflux of the igniter vent.

RESULTS

In case measurements of pressure histories at locations M1, M2, and M3 (see Fig. 1) performed by DNAG and EMI-AFB, reveal that a drastic pressure decrease occurs from location M1/M2 (transverse flow channels) to M3 (igniter vent) indicating the rapid flow expansion in the conical part of the nozzle. Table 3 summarizes the results for average peak values of pressure.

Table 3
PRESSURE MEASUREMENTS IN IGNITER
(SEE FIGURE 1)

MAXIMUM GAS PRESSURE OBTAINED ALONG TRANS- VERSE CHANNELS AND NOZZLE VENTS	DNAG M_1/M_2	EMI-AFB M_3	PRESSURE DECREASE TO IGNITER FROM $M_{1,2}$ to M_3
AZM 953-1 (B-KNO ₃)	24.8 MPa	4.8 MPa	1/5
Y 593 (Black Powder)	13.7 MPa	4.8 MPa	1/3
MV7308 (Nc)	46.6 MPa	11.0 MPa	1/4
NKP-S536 (Nc-Black Powder)	27.0 MPa	3.7 MPa	1/7

Consequently, an effect on the vent characteristics is to be expected, especially in the case of the B-KNO₃ composition AZM 953-1, consistent with the thermochemical calculations, mentioned above. Characteristic blast fields are generated by firing the four igniters, as shown in the case of the nitrocellulose composition MV7308, Fig. 5. Fig. 6 shows time integrated pictures of the flames occurring after discharge of the four igniters.

Due to the high gas pressure ratio of $P_e/P_\infty \geq 37$, where P_∞ denotes the pressure of the surrounding atmosphere, the gases issuing from the igniter vent form a blast field characterized by (a) a highly underexpanded supersonic flow area terminated by inner shocks, (b) a turbulent accumulated gas zone which surrounds toroidally the underexpanded flow area, and (c) an outer strong blast wave containing the flow which propagates into the atmosphere in a nearly spherical manner, Fig. 7. The blast field is associated with an intense flash of light in distinct areas of the flow field, i.e., the primary flash at the igniter vent, the intermediate flash in front of the mach disk, and the secondary flash in the outer turbulent layers (Ref. 1), Fig. 7. These flow and flash phenomena correspond

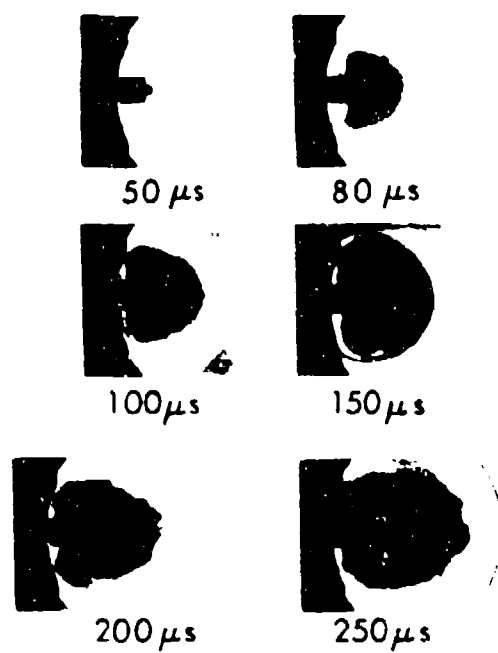


Fig. 5. Sequence of Multiple Spark Shadowgraph Displaying the Development of Igniter Blast Fields



AZM 953-1

BOKUN - POTASSIUM NITRATE



BLACK POWDER



NITROCELLULOSE (NC)



NC - BLACK POWDER MIXTURE

Fig. 6. Time-Integrated Flame Pictures of Igniter Gases

to the unsteady flow expansion generated by gun firings, and are investigated in details in References 5, 7, 11, and 12. Of importance is that the primary flash can be seen as simply an extension of the hot compressed gas column inside the igniter nozzle (Ref. 7). Thus, spectroscopic temperature and gas velocity measurements within the center of the primary flash give the initial condition at the igniter vent.

The still pictures of Fig. 6 further display traces of hot, luminous particles produced by condensation during expansion; especially in the case of the B-KNO₃ composition AZM 953-1. Apparently, the B-KNO₃ composition produces particle-rich flows while the nitrocellulose composition MV7308 produces extremely low particle density gas flow in agreement with the thermochemical calculations, see Fig. 2. However, due to the high expansion ratio at the igniter vent, condensation reactions are more effective in the gas flow expanding in front of the nozzle. In order to study the effect of in-case expansions occurring in the conical part of the igniter nozzle, the "primary flash" at the exit plane of the igniter vent was investigated spectroscopically. Fig. 8 shows the time integrated recorded spectrum of the B-KNO₃ igniter gases, with identified boron oxide emission. A more detailed analysis of the particles produced by the four igniter compositions was most recently performed by Trinks and Schilf, and Mach (Ref. 13 and 14) applying mass spectrometry and scattering techniques. Besides the BO-bands for B-KNO₃, the spectrum of the primary flash for the four igniter compositions contains both spectral lines and a strong background of continuum radiation (Ref. 1). The emitted lines in particular Na- and K-resonance lines stemming from the additives to the igniter compositions, are excited because of the high flame temperature. Therefore, line reversal was applied at wavelength 589 nm (Na-D-line) and 769 nm (K-line) both giving the same temperatures.

The results of pressure, temperature, and gas velocity measurements at the igniter vent are shown in Fig. 9 and Fig. 10. Since the precursor gases stemming from the initial igniter output arrive first at the igniter vent for $t_0 < t < 30 \mu\text{sec}$, the same vent characteristics were obtained

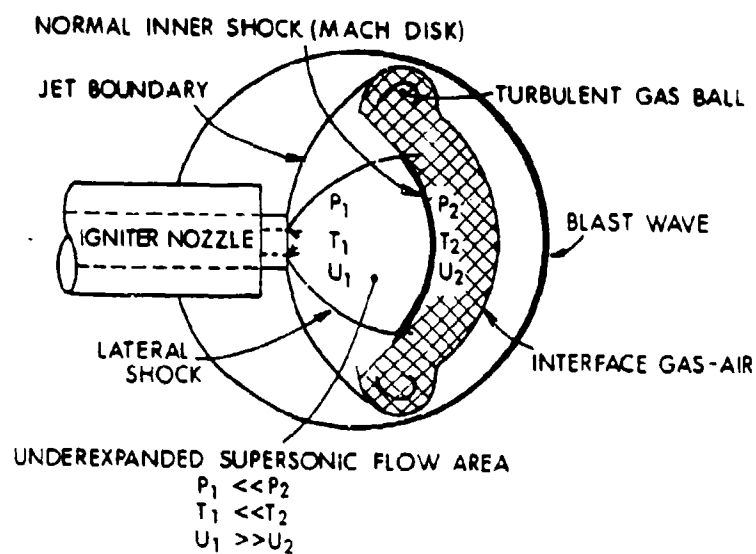
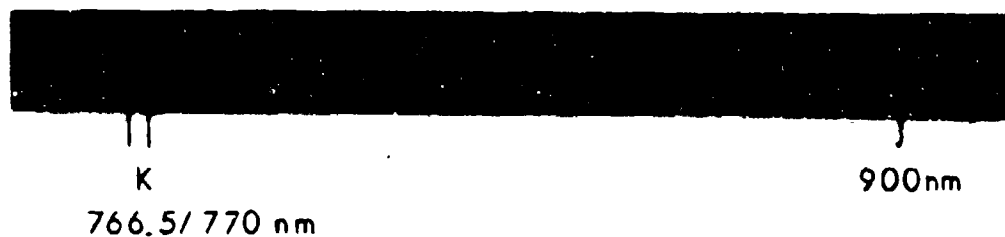
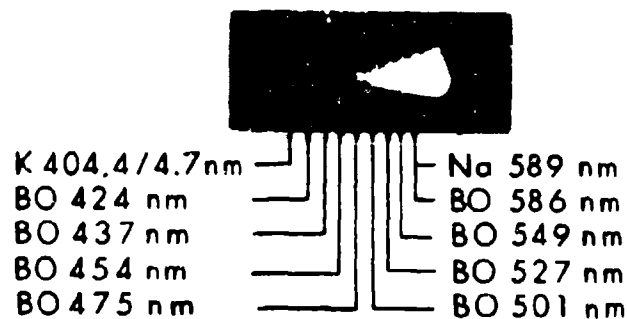


Fig. 7. Schematic Representation of Igniter Vent Blast/Field



FILM: KODAK HIGH SPEED INFRARED 2481



FILM: KODAK RECORDING 2475

Fig. 8. Spectrum of the $B-KNO_3$ Igniter Gases at the Igniter Vent

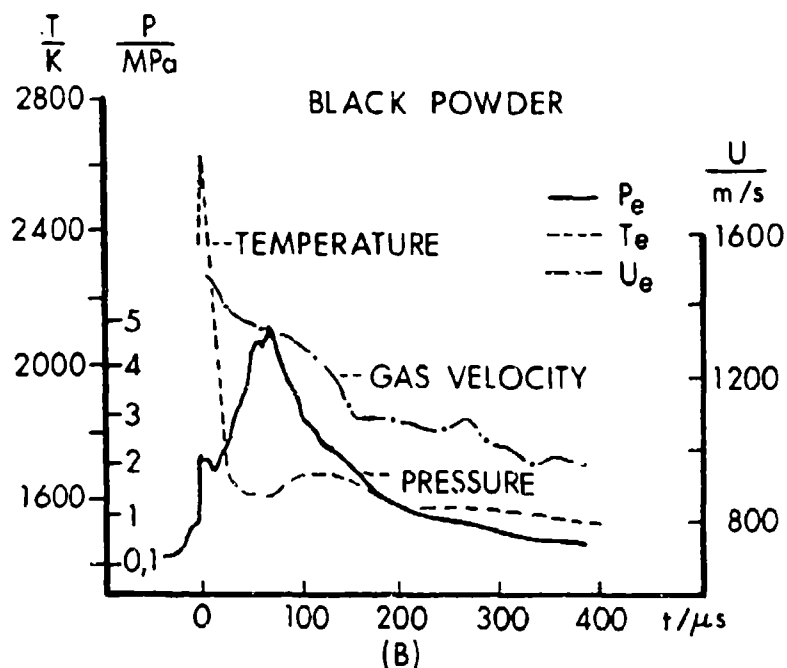
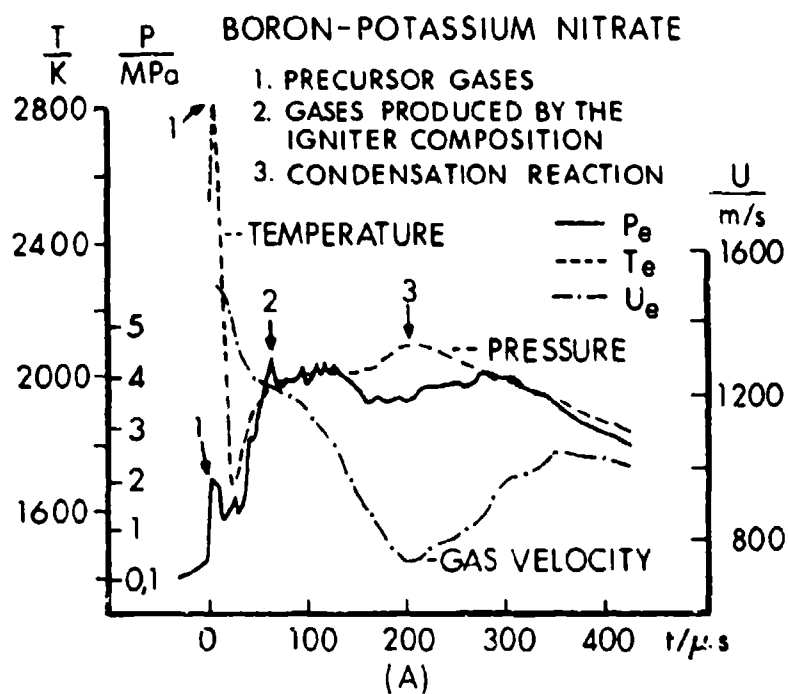


Fig. 9 (A) & (B). Igniter Exit Pressure, Temperature, and Velocity as a function of Time for (A) Boron-Potassium Nitrate (AZM 953-1) and (B) Black Powder (Y-593).

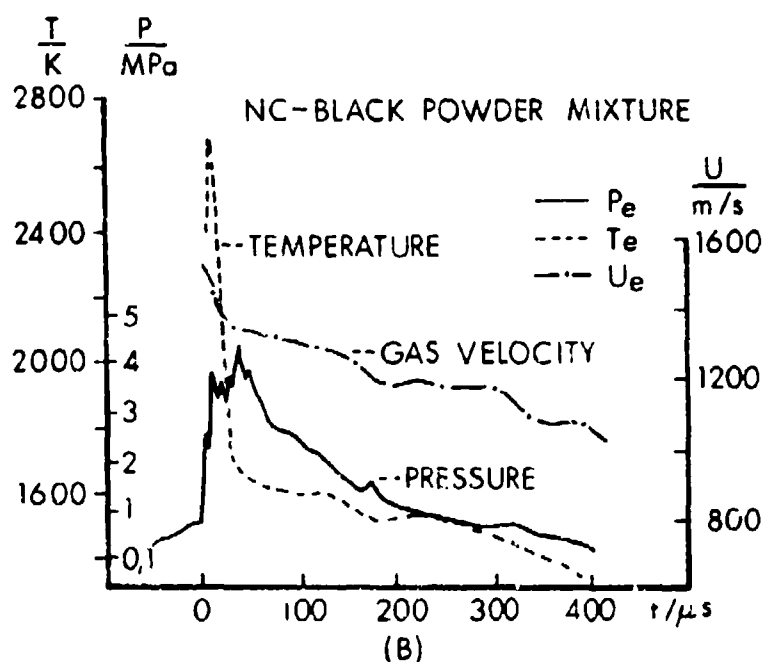
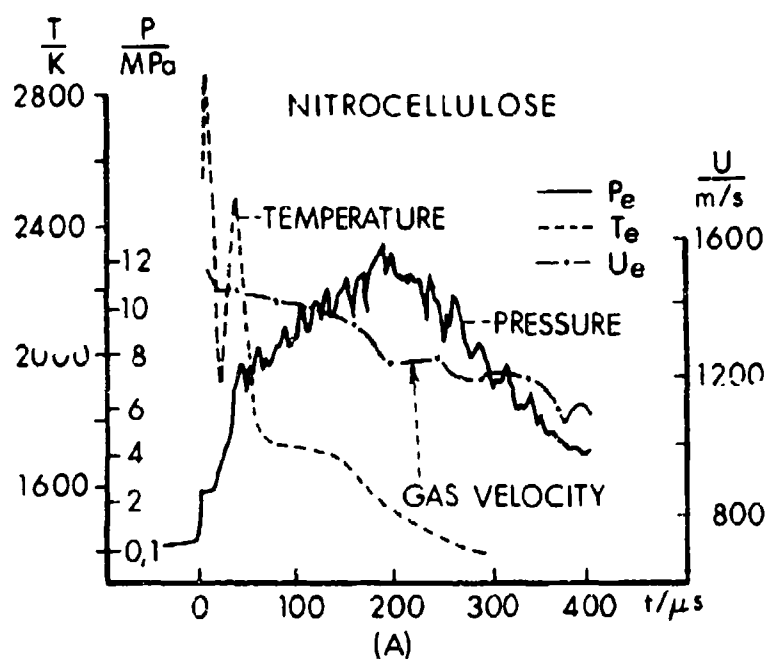


Fig. 10 (A) & (B). Igniter Exit Pressure, Temperature, and Velocity as a Function of Time for (A) NC (MV7309) and (B) NC-Sulfurless Black Powder (Star-S).

with peak values of $p = 2$ MPa, $T = 2800$ K, and $V = 1600$ m/sec for all four igniter formulations indicating the effect of the initial igniter gases.

The second pressure increase is associated with the arrival of the igniter composition gases at the igniter vent at $t \geq 30$ μ sec. Fig. 9a displays further the effect of condensation reaction occurring inside of the igniter case. About $t = 200$ μ sec after t_0 a maximum occurs in the temperature-time history associated with the minima of pressure and gas velocity. This shows the effect of condensation of boron oxide on the flow. Small effects of the condensation reactions were also found in the case of the black powder formulations Y593 and the Nc-black powder mixture NKP-S, while the nitrocellulose produced very little particulate matter during expansion.

A different behavior is displayed in the p , T , u - curves of the nitrocellulose composition MV7308 (Fig. 10a) indicating that the internal combustion is not complete. The second temperature peak at $t = 40$ μ sec first approaches the calculated maximum flame temperature of 2600 K. However, a rapid decrease of T follows, associated with a relatively slow pressure increase and a rapid decrease of gas velocity. The first layer of the previous nitrocellulose is fully ignited and reaches the flame temperature. Due to inadequate confinement the grains (0.3 to 0.4 mm diameter) move into the flow passage which becomes clogged with individual grains (Fig. 11) causing a quenching of the reactions.

The calculated energy efflux for $30 \leq t \leq 400$ μ sec is shown in Figure 12. Considering the restrictions discussed above, the "hot" igniter compositions nitrocellulose and B-KNO₃ are found to produce higher energy output than the "cold" black powder formulations. Comparable results were obtained by Bragg (Ref. 2) using the interrupted ignition technique. The data in Fig. 12 does not include the effect of the precursor flow coming from the initial igniter device. Table 4 compares the precursor energy (E_{pr}) with the igniter energy (E_{ig}). These were obtained by a time integration of the data in Fig. 12. The igniter energy



Fig. 11. Post Firing Section of Nitrocellulose (MV7308) Igniter
(Note the Unburned NC-Grains in the Chamber and Flow Channels)

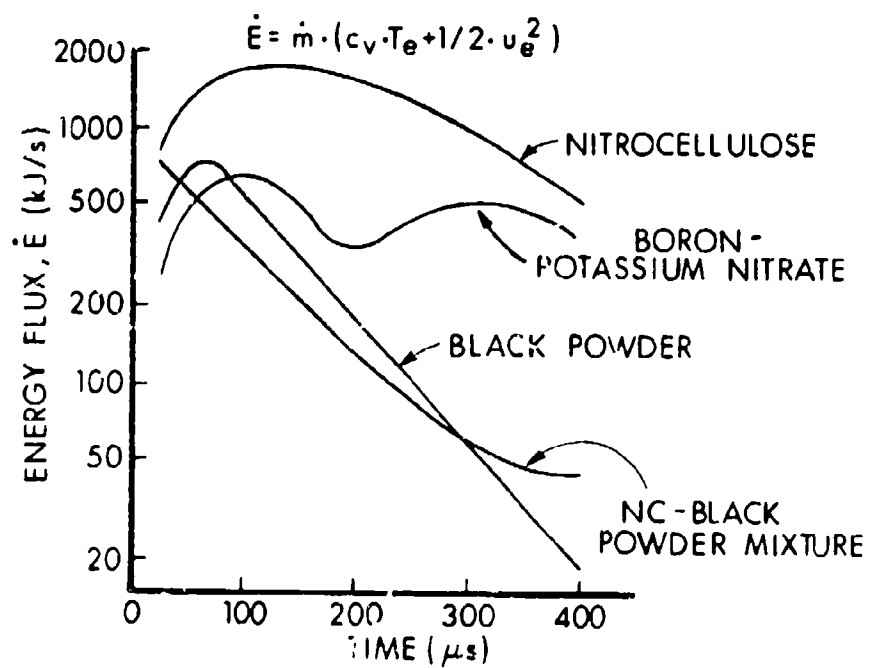


Fig. 12. Energy Flux at the Igniter Vent for $30 \leq t \leq 400 \mu\text{sec}$
(Particulate Matter is not Considered)

(Eig) is also compared with the total energy calculated from the thermochemical model (Ec). The effect of the precursor (5 joules) is small compared to the high energy output of the igniter composition gases.

Table 4
EXPERIMENTAL AND THEORETICAL VALUES FOR IGNITER OUTPUT ENERGIES

	PRECURSOR FLOW (INITIAL IGNITION DEVICES)		IGNITER FLOW (IGNITER COMPOSITIONS)		
	Epr (JOULES)	Epr/Eig (%)	Eig (JOULES)	Ec (JOULES)	Eig/Ec (%)
B-KNO ₃ (AZM 953-1)	5	2.8	178	540	33
Black Powder (Y 593)	5	5.7	88	580	15
Nitrocellulose (MV7308)	5	1.1	458	720	64
Nitrocellulose- (NKP-S) Black Powder	5	7.3	68	565	12

CONCLUSIONS

1. Due to the inadequate confinement, a precursor flow is formed so that only part of the initial igniter gases interact with the igniter compositions. A confinement should be implemented to improve the performance.
2. The nitrocellulose composition is only partly combusted. Reduction of nozzle diameter can improve the reaction.
3. During the flow inside of the igniter case, flow expansion occurs associated with condensation reactions changing the igniter vent characteristics.
4. The nitrocellulose composition produces extremely low particle density gas flow and represents the gas ignition type.

5. The $B-KNO_3$ composition produces particle-rich flows due to condensation reactions during free in-case flow expansion and represents the gas-particle ignition type.
6. The "hot" compositions nitrocellulose and $B-KNO_3$ generate higher energy output than the "cold" black powder formulations.

ACKNOWLEDGEMENTS

The author is indebted to Mr. O. Wieland for laboratory assistance, to Dr. G. Smeets and Mr. H. Mach (ISL) for assistance in performing the gas velocity measurements, to Dr. Kuthe (DNAG) for the thermochemical calculations, and to Mr. J. Knaption, Mr. R. Comer, and Dr. K. White (BRL) for reviewing the paper and discussing the thermochemical aspects.

REFERENCES

1. G. Klingenberg, O. Wieland, "Untersuchungen der Eigenschaften von vier Experimentier-Treibladnugsanzuendern beim Abfeuern in den freien Raum", EMI-AFB-Report No. V9179, 1979
2. U. Brede, "Confrontation of Ignition Behavior of Different Compositions According to the Method of Interrupted Ignition Techniques", Fifth International Symposium on Ballistics, Toulouse, France, 16-18 April 1980
3. G. Krien, "Physikalisch-chemische Kenndaten von Auzuendmischungen", Bundesinstitut fuer chemische Technik, BICT, Heimerzheim, BICT-Notiz 3.0-3/4369/77, 1977
4. R. Kuthe, "Thermodynamische Berechnungen der Auzuendmischungen", DNAG-Report, 1977
5. G. Klingenberg, H. Mach, "Investigation of Combustion Phenomena Associated with the Flow of Hot Propellant Gases - I: Spectroscopic Temperature Measurements Inside the Muzzle Flash of a Rifle", Combustion and Flame 27, 163-176 (1976)

6. G. Klingenberg, H. Mach, "Experimental Study of Non-Steady Phenomena Associated with the Combustion of Solid Gun Propellants", Proceedings of the Sixteenth (International) Symposium on Combustion, The Combustion Institute, pp. 1193-1200 (1976)
7. G. Klingenberg, "Investigation of Combustion Phenomena Associated with the Flow of Hot Propellant Gases" - III: Experimental Survey of the Formation and Decay of Muzzle Flow Fields and of Pressure Measurements", Combustion and Flame 29, 289-309 (1977)
8. G. Smeets, A. George, "Instantaneous Laser Doppler Velocimeter Using a Fast Wavelength Tracking Michelson Interferometer", Rev. Sci. Instrum. 49 (11), November 1978
9. G. Klingenberg, H. Mach, "In-Bore Measurements of Gas Velocity and of Radial Gas Temperature Distributions", Proceedings of the Fourth International Symposium on Ballistics, 17-19 October 1978, Naval Postgraduate School, Monterey, California
10. A. Celmins, "Theoretical Basis of the Recoilless Rifle Interior Ballistic Code "REGRIFF"", Ballistic Research Laboratory, ARADCOM, Aberdeen Proving Ground, MD 21005, BRL-Report No. 1931, 1976
11. G. Klingenberg, G.A. Schroeder, "Investigation of Combustion Phenomena Associated with the Flow of Hot Propellant Gases - II: Gas Velocity Measurements by Laser-Induced Gas Breakdown", Combustion and Flame 27, 177-187 (1976)
12. G. Klingenberg, "Analysis of Gun Muzzle Flash Phenomena", Proceedings of the Fourth International Symposium on Ballistics, 17-19 October 1978, Monterey, California
13. H. Trinks, N. Schilf, "Investigation About Ignition Processes by Short-Time Photography, Multichannel Mass Spectrometry and Condensate Analysis", Proceedings of the Fifth International Symposium on Ballistics, Toulouse, France, 16-17 April 1980
14. H. Mach, "Optical Techniques Applied to the Analysis of Particulate Matter in Flames and Gas Flows", German-French Research Institute (ISL), St. Louis, France, ISL-Rep. 1980 to be published

USE OF A JET AIR MIXER FOR PYROTECHNIC COMPOSITIONS

by

D. M. Koger

U. S. Army ARRADCOM
ARRADCOM Resident Operations Office
NASA National Space Technology Laboratories
NSTL Station, MS 39529

ABSTRACT

Continuous flow techniques for material handling in the explosive and chemical industry are replacing conventional batch methods because of inherent advantages in terms of cost, efficiency, and safety. The Jet Airmix Blender® is a component of the proposed Continuous Flow Process (CFP) for pyrotechnics, and represents a new method in the production of dry pyrotechnic compositions. The Jet Airmix blender is pneumatically operated, and has a working capacity of 2170 pounds with a blending cycle of less than one minute.

The application of pneumatic mixing to pyrotechnic composition is relatively new. Associated hazards include: surface charge due to triboelectrification, various amounts of dust suspension at different concentrations, high impingement velocities of particles, and large masses of pyrotechnic materials due to larger batch sizes. Because of those inherent conditions a detailed analysis was undertaken to determine the hazards associated with this blending concept, and whether the degrees of those hazards are within acceptable limits for fullscale production.

The results of this study indicate no risk or hazards attached to charging, blending, or discharging the Jet Airmix blender during production of up to 2170 pounds of pyrotechnic compositions as formulated by Pine Bluff Arsenal, Pine Bluff, Ark., using dry air as the carrier medium. The full spectrum of potential hazards concerning the complete continuous flow process (CFP) was not within the scope of this study; rather, specific worst-case situations were analyzed.

INTRODUCTION

BACKGROUND

Pyrotechnic compositions are usually blended by one of two methods: wet or dry. Dry blending is accomplished in a tumble device such as a ball mill, double-cone blender, a Vee blender, a motionless mixer or a pneumatic mixer. Wet blending is accomplished in various types of mixers that range from dough type planetary blenders to highly complex liquid mixing systems. Wet mixing is accomplished by adding a volatile liquid carrier to the mix to form a paste-like substance or, as in some cases, as much as 50% by weight to form a highly viscous composition.

Mixing in general is performed in small batches ranging from several hundred grams to a maximum of 45.5 kg (100 lb) depending upon the type of mix and the quantity required. For most mixing processes the 45.4-kg (100-lb) limit is imposed because all pyrotechnic compositions are considered to be a DoD Class 7 (U. N. 1.1) during mixing, granulating, drying and loading operations. Only after consolidation can the pyrotechnic composition be considered to be less sensitive or DoD Class 2 (U. N. 1.3) when appropriate test data indicate.

Problems associated with mixing are many, ranging from agglomeration of constituents to stratification and incomplete mixtures. Generally, the oxidizers are hygroscopic and in the raw form they may be chunky or in a solid block, and milled in a hammer mill or in an attrition mill to obtain the desired particle size. So that the fuel and oxidizer do not come into intimate contact with one another, either the fuel or oxidizer may be premixed with the diluent before the final mixing of all ingredients. Some of the fuels also pose problems in that they may have to be coated with an oil to make them less hazardous to use. Sieving and screening operations of all constituents are required prior to mixing and in the case of most wet blends after drying, the composition is broken up and screened prior to loading. If no diluent is added to the formula, then the

fuel and oxidizer are carefully loaded in layers with either the fuel or oxidizer loaded first and alternate layers of constituents added. Another technique is to add constituents to the mixture of specified intervals of time during the mixing cycle. The mixing cycle varies from 10 minutes to an hour, with some blending operations taking longer. In all cases, mixing of pyrotechnics should be performed remotely.

Dry blend is accomplished in several different types of apparatus. Regardless of the actual device, specific tasks should be accomplished prior to loading the ingredients. A simplified flow diagram depicting these steps is shown in figure 1. In almost all cases, a pyrotechnic formulation is based upon a percentage of ingredients by weight. Weighing of the constituents, while fundamental, is critical and these percentages are often held to less than 0.5%. Milling may be accomplished in a hammer mill or an attrition mill. All ingredients are screened or sieved to meet the specified particle size and the oxidizer and additive may be premixed. This is an important step which, besides diluting the oxidizer, prevents agglomeration from reoccurring. Then all ingredients are added to the blender in a specified sequence. Dry blending is usually accomplished in approximately 30 minutes. If the mixing cycle is too long, stratification or separation of the ingredients may occur or if too short, an intimate mixture may not be obtained.

Wet blending is accomplished in various types of devices where the mixture is wetted by a volatile to form a paste-like substance, or it may be wetted sufficiently to acquire the consistency of a cake dough. A planetary dough mixer may be used or a Muller type mixer may also be used. The mixing bowl and blade for the planetary mixer are made of nonsparking stainless steel; in the Muller type all tools, mullers and pan are also constructed of stainless steel. The weighing, sieving, and milling operations are similar for wet blending as for dry blending. The ingredients are placed in the pan or bowl and the liquid carrier is added in sufficient quantity to form a thick paste. The planetary blade and/or the mullers were previously adjusted so as not to touch the bottom

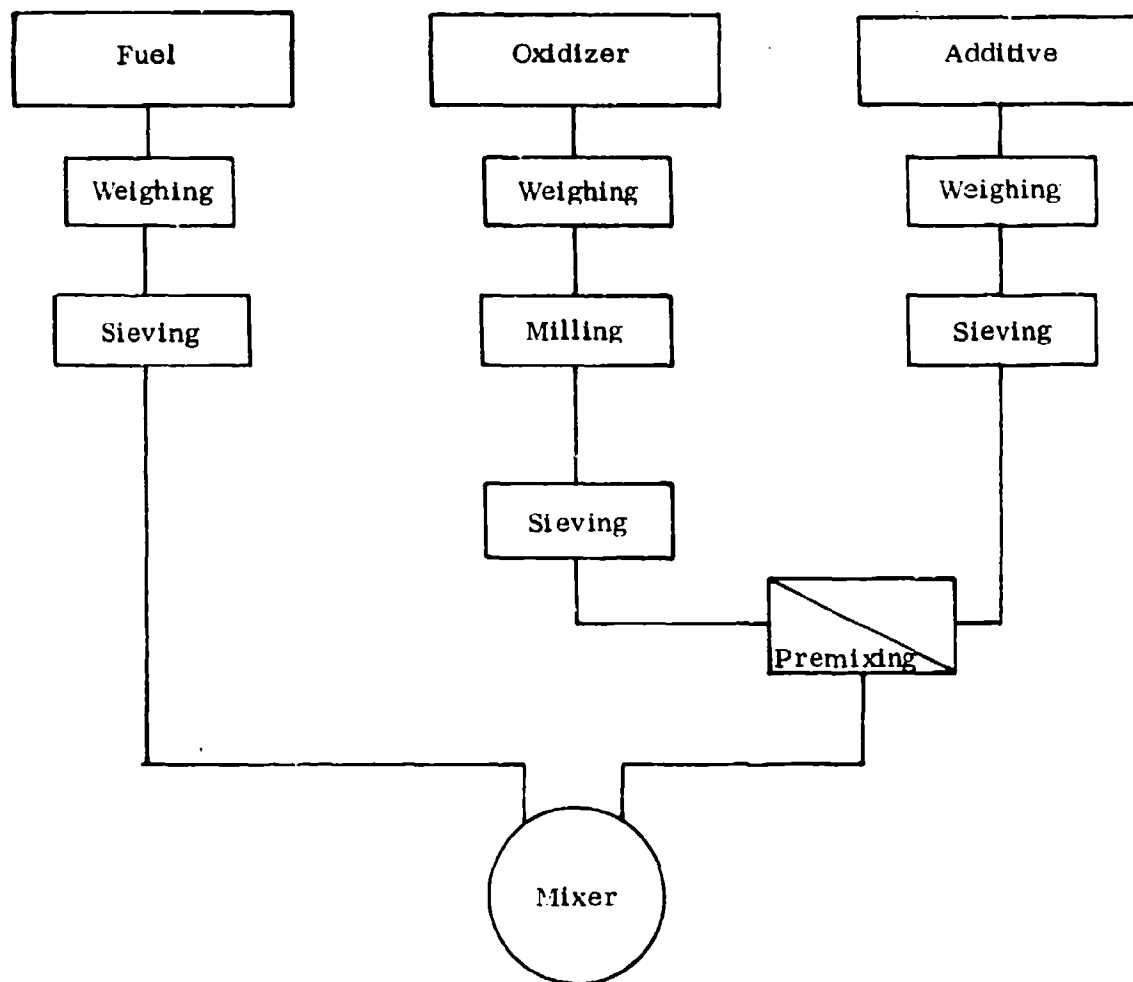


Figure 1. Simple Flow Diagram of Prepreparation for Dry Blending

or the side of the pan or bowl. The mixer is operated remotely but stopped periodically to allow for scrape down of the sides of the bowl or pan. If additional liquid is needed to maintain consistency, it is usually added at this time. The mixing cycle ranges from 20 minutes to 2 hours. The mixture is then granulated by screen and the mix is dried. It may be loaded in the granular form or broken up into smaller particle size prior to loading. A typical planetary type mixer is shown in figure 2.

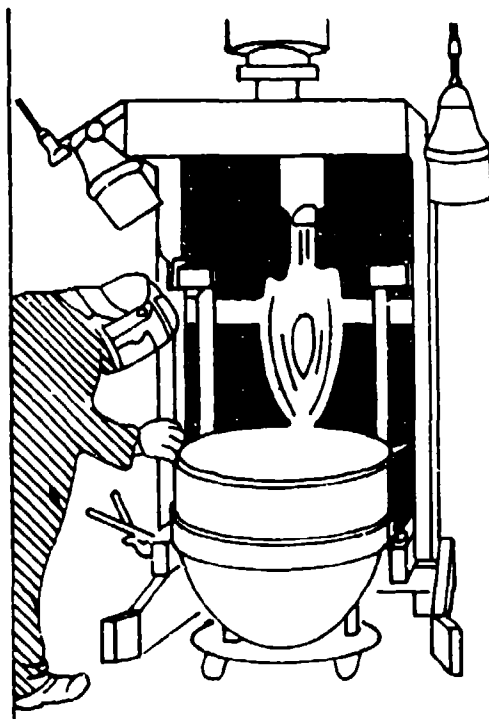


Figure 2. A Typical Hobart Planetary Dough Mixer

The Muller type mixer or planetary blender for wet mixes and double-cone or ball mill devices have been utilized almost exclusively from the early days of manufacturing until the present. Large batch sizes are obtained by operating many mixers to blend small quantities and then cross-blend to achieve an acceptable batch size for loading operations. With the advent of the arsenal modernization programs, new types of blending techniques and larger batch sizes have begun to find their way into the manufacturing process. Because of this, beginning in 1973 an extensive investigation was made of several types of blenders or mixers that utilized new technology and mixed large quantities, up to 907 kg (2000 lb), in a single operation. The purpose of the investigation was to determine: 1) the hazards associated with large quantities; 2) what type of mixers were available, and the problems associated with the new mixing systems.

A candidate blender known as the Jet Airmix® blender was selected for this program (Ref. 1 and 2).

OBJECTIVE

The objective of this study was to generate empirical safety data from tests performed to evaluate the potential hazards associated with full-scale blending.

TEST PLAN

Pneumatic mixing as in a jet Airmix device was new. The Airmix device has a working capacity of 984 kg (2170 lb) with a blending cycle of less than one minute. A pulse of air with a duration of 2 to 5 seconds is passed through 36 de Laval nozzles at a preset angle. This lifts the ingredients up the total height of the column. This is followed by a pause of 5 seconds allowing the ingredients to come to full rest; then the pulse cycle is repeated until 5 full pulse-and-pause cycles have occurred. After these cycles the composition is completely mixed. The hazards associated with pneumatic mixing were thought to include: 1) surface charge due to triboelectrification, 2) dust suspension at different concentrations, 3) high impingement velocities of particles and (4) mass effects from such a large quantity of mixture. Particular emphasis was placed on the measurement of the surface charge and the determination of initiation levels for various pyrotechnic compositions. At present, only smoke compositions have been tested in the Airmix blender. Initially, tests were conducted in a one liter bench model Airmix blender shown in figure 3. Each constituent

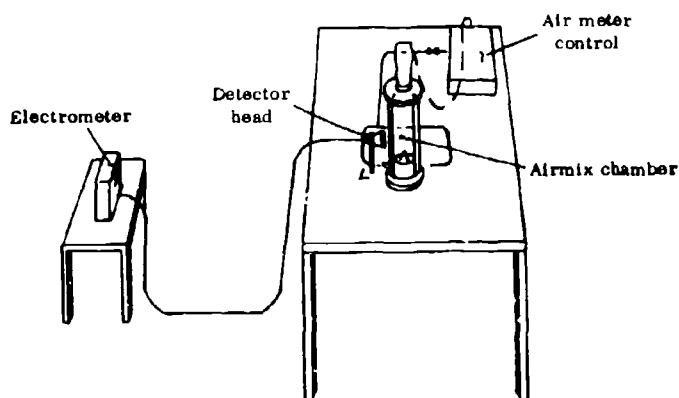


Figure 3. One-Liter Airmix Blender Set Up

was placed in the one-liter model and a series of measurements were obtained; then mixing of several constituents such as diluent and fuel, diluent/oxidizer, dye fuel/dye oxidizer and fuel/oxidizer were tested. The ultimate tests were conducted on all complete formulations in the 1-m³ (35-ft³) model in 454-kg (1000-lb) quantities for colored smoke and 984-kg (2170-lb) quantities for HC white smoke. Figure 4 shows the 1-m³ (35-ft³) jet Airmix test configuration. Over 3000 different electrostatic measurements were obtained on colored smokes and screening smoke in various scaled models to full-size production models. Full-scale thermal ignition tests were then conducted to determine if the hazards associated with large masses of pyrotechnic compositions were thermal or explosive in nature. In these tests 454 to 984 kg (1000 to 2170 lb) of signaling smoke and screening smoke mixtures were thermally initiated under static and dynamic mixing conditions in the full scale jet airmix blender.

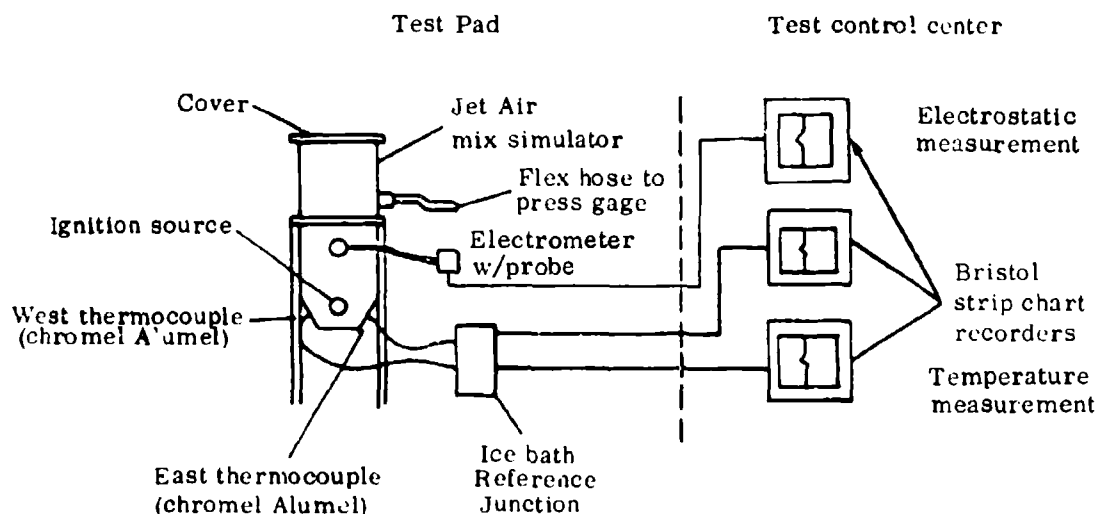


Figure 4. Test Set Up for Electrostatic Measurements and Full-Scale Thermal Initiation Test

RESULTS

DATA ANALYSIS

The mixing vessels for the purposes of these analysis represent a solid cylindrical capacitor and each has a specific charge density for each configuration. The total electrostatic charge generated within the mixing vessel was measured with an electrometer. These measurements were monitored continuously and recorded every 5 seconds. The highest value obtained during each period was also recorded. All values were then reduced by a computer program and the values for each point were determined. The high, low and mean values were reported for each significant operation.

Data analysis of the full scale burn tests included temperature and pressure measurements. Only the peak values were reported. Visual observation and motion picture coverage aided the determination of the overall reaction.

TESTS RESULTS

Results of the scale model test for the constituents of HC white smoke and violet smoke in the scale model tests are shown in table 1. The surface charge values for the individual constituents and combination of constituents for the HC smoke mixture were generally less than the complete mix. The electrostatic charge was found to be in the microjoule range. The reported initiation value for HC smoke mixture is 0.122 joules for electrical spark initiation and $>50K$ joules in a dust cloud. (Refs. 3, 4, and 5). The surface charge values for violet smoke constituents and their combinations were found to be higher than the completed mix. This was opposite of the findings for the HC smoke mixture. Still, in all cases the measured values were significantly less than reported initiation values (Ref. 6). Results indicate that the surface charge due to triboelectrification was minimal.

Table 1

ELECTROSTATIC MEASUREMENTS OF CONSTITUENTS AND COMPLETE

Sample material and charging sequence	Energy level Joules		$E = \frac{Q^2}{2c}$
	High	Low	
Zinc oxide	2×10^{-8}	2×10^{-9}	1×10^{-9}
Hexachloroethane	3×10^{-8}	1×10^{-9}	9×10^{-9}
Aluminum	3×10^{-9}	1×10^{-11}	5×10^{-10}
Hexachloroethane/zinc oxide	3×10^{-7}	3×10^{-9}	1.5×10^{-7}
Hexachloroethane/aluminum	2×10^{-9}	4×10^{-10}	1×10^{-9}
Zinc oxide/aluminum	1×10^{-8}	4×10^{-9}	7×10^{-9}
Hexachloroethane/zinc oxide/ aluminum	9×10^{-7}	1×10^{-7}	5×10^{-7}
Sodium bicarbonate/sulfur	3.52×10^{-7}	6.95×10^{-10}	5.87×10^{-8}
Sodium bicarbonate/potassium chlorate	5.45×10^{-9}	3.64×10^{-10}	5.78×10^{-10}
Sodium bicarbonate/violet dye	1.28×10^{-9}	2.05×10^{-10}	4.37×10^{-10}
Sulfur/violet dye	1.68×10^{-9}	9.75×10^{-10}	3.17×10^{-10}
Potassium chlorate/violet dye	2.77×10^{-9}	2.05×10^{-10}	4.32×10^{-10}
Potassium chlorate	9.33×10^{-7}	7.2×10^{-8}	4.88×10^{-7}
Sulfur	1.54×10^{-6}	1.29×10^{-7}	2.83×10^{-7}
Sodium bicarbonate	4.63×10^{-6}	6.30×10^{-8}	4.86×10^{-7}
Violet dye	4.56×10^{-6}	1.15×10^{-7}	2.67×10^{-7}
Sodium bicarbonate/ dye/sulfur	1.86×10^{-8}	2.06×10^{-10}	4.14×10^{-10}
Sodium bicarbonate/ dye/potassium chlorate	3.30×10^{-9}	2.06×10^{-10}	3.05×10^{-10}
Sodium bicarbonate/ sulfur/potassium chlorate	2.07×10^{-9}	3.64×10^{-10}	5.51×10^{-10}
**Sodium bicarbonate/ sulfur/dye potassium chlorate	1.28×10^{-9}	3.64×10^{-10}	5.25×10^{-10}

**Complete mix

Results of the electrostatic surface charge measurement for full scale production are shown in table 2. The electrostatic values for the HC white smoke were similar to those found in the small scale tests. However, the measured values for the violet smoke were significantly higher than those found in

Table 2
FULL-SCALE BLENDING TEST ENERGY LEVELS

Composition	Weight kilograms (pounds)	Energy level Joules		
		High	Low	Mean
HC white smoke mixture	984 (2170)	7.86×10^{-6}	1.12×10^{-6}	2.91×10^{-6}
Preblend* (violet smoke)	340 (750)	1.24×10^{-2}	5.57×10^{-3}	9.54×10^{-3}
Final blend (violet smoke)	454 (1000)	8.66×10^{-3}	4.88×10^{-3}	6.98×10^{-3}

*Without the oxidizer

the small scale apparatus. Still, the results are several orders of magnitude less than that being reported for initiation in a dust cloud or by electrical sparks. The higher readings were attributed to the ambient humidity and temperature for the open-field test. The environment for the laboratory tests was humidity and temperature controlled.

The results of the full-scale thermal ignition tests are given in Table 3. Test results show that the burn times ranged from a low of 110 seconds for

Table 3
RESULTS OF FULL-SCALE BURN TESTS

Material	Weight kg (lb)	Total burn time (sec)	Gross reaction rate kg/sec	Maximum temperature °C °F	Quasi-static pressure kPa (psig)
HC white smoke jet Airmix (static)	984 (2170)	564	1.74	(1740)	34.5 (5)
Violet smoke jet Airmix (static)	454 (1000)	110	4.13	154 (309)	34.5 (5)
Violet smoke jet Airmix (dynamic)	454 (1000)	175	2.23	334 (633)	8.27 (1.2)

violet smoke in the static state (initiation occurred when the material was at rest) to a high of 564 seconds for HC smoke. The gross reaction rates are quite slow when compared to burning of propellants or explosives in similar quantities. The static pressure measurements are indicative of a slow reaction as well and remained constant while burning as venting through the top occurred. The venting function was an additional requirement of the test series to simulate manufacturing conditions. It was shown from these tests in both dynamic (ignition during the fluidized state) and static conditions that the potential hazards were thermal in nature versus an explosive hazard.

CONCLUSIONS

1. The hazards associated with pneumatic mixing are no greater than conventional dry or wet blending.
2. Pneumatic mixing may be safer in that actual mixing time is significantly less than conventional methods, thereby reducing exposure time.
3. Mixing large quantities of pyrotechnic is feasible.
4. The hazards associated with mixing large quantities of certain types of pyrotechnic mixtures (in this case, smoke mixtures) are primarily thermal in nature.
5. Electrostatic hazards due to triboelectrification are extremely low.

REFERENCES

1. McIntyre, F. L., Identification and Evaluation of Hazards Associated with Blending of HC White Smoke Mix by Jet Airmix Process, Contractor Final Report, Edgewood Arsenal EA-FR-EA4021, January 1974.
2. McIntyre, F. L., Identification and Evaluation of Hazards Associated with Blending of Violet Smoke Mix by Jet Airmix Process, Edgewood Arsenal Contractor Report EM-CR-75001-EA4D91, March 1975.

3. King, P. V., and Koger, D. M., Pyrotechnic Hazards Classification and Evaluation Program Phase III, Segments 1-4, Investigation of Sensitivity Test Methods and Procedures for Pyrotechnic Hazards Evaluation and Classification, GE-MTSD-R-059, April 1971.
4. Wilcox, W. R., Pyrotechnic Dust Sensitivity Testing Program, Edgewood Arsenal, Contractor Final Report, EA-FR-IDOX, June 1973.
5. Morris, L. T., Preliminary Hazards Fault Tree for HC White Smoke Grenade Manufacturing Process, Edgewood Arsenal Contractor Report, EA-5100C, May 1975.
6. McIntyre, F. L., A Compilation of Hazards Test Data for Pyrotechnic Compositions ARRADCOM Preliminary Report, February 1980.

SYNTHESIS OF STABLE PYROTECHNIC COMPOSITIONS AFTER
INVESTIGATION BY CALORIMETRIC PROCEDURES

Author : G. KRASSOULIA
SOCIETE EUROPEENNE DE PROPULSION - B.P. n° 37
33160 - ST-MEDARD-EN-JALLES - FRANCE

ABSTRACT : Calorimetry applies to the various pyrotechnic substances and can be used to facilitate the research and synthesis of pyrotechnic compositions for specified purposes.

This paper deals with the utilized equipment and the recommended methods to achieve pyrotechnic operation answering a pressure-time law.

The case of a small gas generator squib is given as an example of application.

KEYWORDS : Calorimetry - Programmed differential calorimetry - Heat of combustion - Pyrotechnics - Pyrotechnic compositions - Energetic composite materials - Initiator - Squibs - Gas generator.

1. INTRODUCTION

Basic pyrotechnic substances are fairly well catalogued by the specialists as well as their uses in recent [1], [2], [3] and less recent [4], [5] formulations.

Our purpose in this account is to show how the measurement facilities, mainly assigned to laboratory work, can be used to the development of composite pyrotechnic materials capable of answering a functional law dictated by a specification.

Our purpose further is to show pyrotechnists who do not always have the research facilities of advanced industries at their disposal,

that they can however apply to such facilities at an advanced stage of pragmatically acquired data, when they are bound to bring about a guarantee of the validity of their development work and of the resulting hardware construction, to their contracting authorities.

As a matter of fact the recording of the stability or thermal history of pyrotechnic components and compositions subjected to programmed differential calorimetry ("CDP") [6] corresponds to an identity card that gives a most valuable guarantee as to the reproducibility of their effects.

Hereafter in this account we shall deal with in succession :

- the calorimetric equipment implemented and the corresponding measuring methods of the parameters characterizing the pyrotechnic substances and their mixtures, with the purpose of ascertaining the formulation of a pyrotechnic composition (reminder of the stability criteria).
- the description of the results obtained during the development of a gas micro-generator in accordance with the previously established principles.

Through this process we shall bring a continuation to our previous publication, namely :

"The advantages offered by programmed differential calorimetry ("CDP") make it an efficient tool in terms of : research, characterization and control of power generating substances at every stages of their development, fabrication and utilization".

2. EQUIPMENT

2.1. - Summary description of the equipment :

Of industrial production design, and used in programmed differential calorimetry for other purposes, (fig. 1) the equipment

(DSC 111 from SETARAM - fig. 1) is comprised of five major parts :

- the calorimetric sensor
- the electronic unit
- the gas atmosphere control unit
- the recorder
- the sample-holder crucibles.

A computer may be added to eliminate manual integration of the curves data.

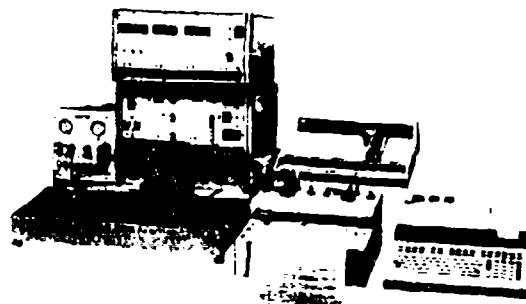


fig. 1

2.1.1. - Calorimetric sensor (fig. 2) :

The heat of the calorimeter is a programmable block, arranged in an external enclosure at ambient temperature. Thin refractory tubes pass throughout the enclosure and the block : their mid-part serves as the test chamber. Such mid-part is largely covered with a thermocouple calorimetric fluxmeter which connects it up directly with the reference block through the

TIAN-CALVET process. The arrangement is fully symmetrical. Quick cooling down of the calorimetric block is achieved by built-in gas circulation.

2.1.2. - Electronic unit : It is comprises of three housings :

- temperature programming, enabling working under dynamic conditions (minimum speed 1 K/hr, maximum speed 30 K/mn) or under static conditions.
- derived integral proportionally acting (P.I.D.) control.
- amplification enabling to work in various sensitivity ranges (25 μ V to 100 mV full scale).

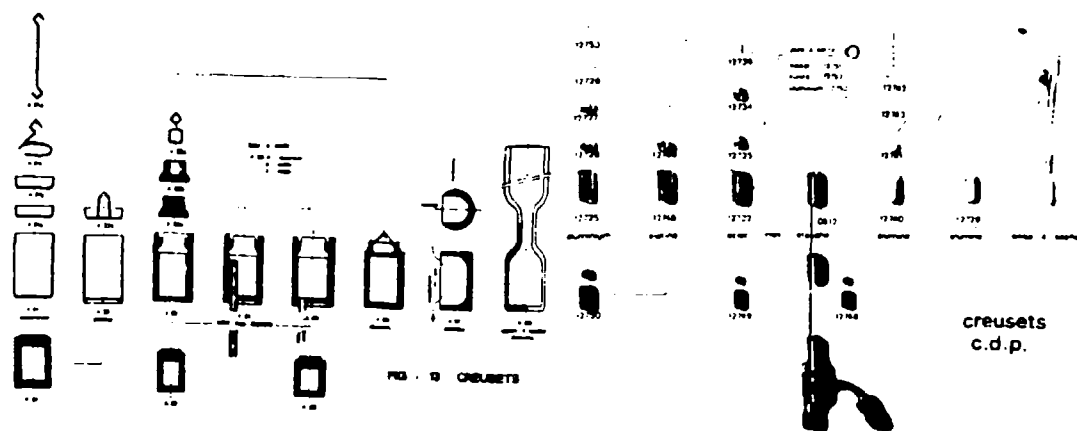
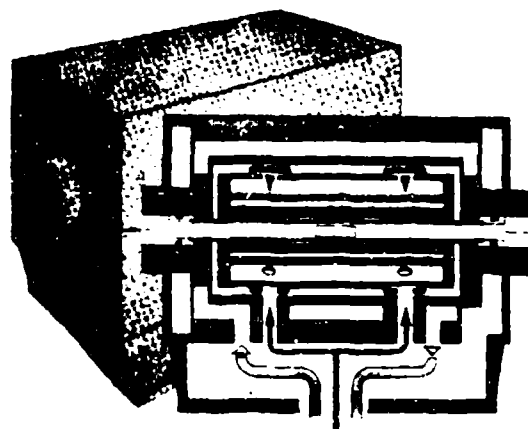


fig. 2

2.1.3. - Gas atmosphere control : Two possibilities are offered :

- scanning of the samples under any atmosphere.
- working under pressure by using special type crucibles (withstanding 100 bar under 350°C).

2.1.4. - Recorder :

It allows recording the generated calorimetric signal, namely the variation of heat power versus time or temperature.

2.1.5. - Sample holder crucibles (fig. 2 bis) :

They are of most varied types according to the work to be carried out ; their maximum capacity is 0.3 cm^3 , which corresponds to a test sample capability close to 100 mg.

2.2. - Principle of operation (fig. 3) :

When a heat effect develops, heat exchange occurs between the cell enclosing the sample and the reference block. The heat flux that builds up is measured directly by a thermoelectric cell. In fact, two thermoelectric cells located on the test

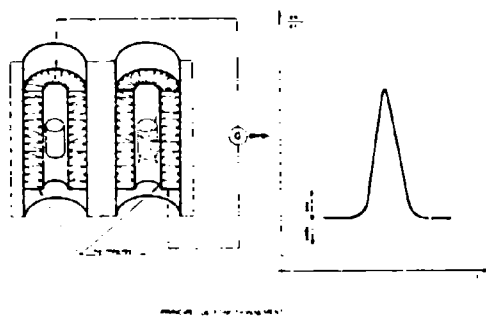


fig. 3

tube and on the reference tube are mounted opposite to each other, in order to get free from secondary thermal effects, and continuously compare the transmitted electromotive forces.

2.3. - Interpretation of the curves :

The unbalance occurring between the two thermoelectric cells as a thermal effect develops, is amplified and recorded on a potentiometric recorder. According as this will be an exothermic or endothermic effect, the obtained signal shall produce on the recorder a deflection in one direction or in the other.

Previous calibration of the equipment either through joule's effect or through measurement of the melting heat of pure products allows determination of the electromotive force/delivered power ratio, which gives the sensitivity of the equipment.

It varies with temperature but remains close to 10 $\mu\text{V}/\text{mW}$.

The obtained curve therefore represents the heat amount delivered per unit time $\frac{dH}{dT}$ versus temperature or versus time.

Integration of this curve thereby leads to direct measurement of the power.

3. MEASURED CRITERIA OF STABILITY

The stability of the components is revealed in programmed differential calorimetry ("CDP") by the temperature rise through which all the transitions related to state changes appear on the thermograph (sublimation, evaporation, loss of crystallization water, melting, etc ...) [77] [87].

In the selection that he has to make between preselected components, the pyrotechnist attempts to eliminate the component that exhibits changes below a temperature level stipulated by a specification. The compatibility between thus selected components is verified, according to the same criterium, on binary mixtures of equal weights or equal volumes.

The compatibility and stability of the component mixtures systematically appeals to change of state calorimetry.

Reaction calorimetry reflects the transient contact reactions that sometimes correspond, in the course of what some call "sterelization" [9] [10] to intergranular stabilization reactions which may sometimes be deliberately introduced on an a priori basis.

The total decomposition of the components corresponds to a sudden change that is reflected on the thermograph by a maximum heat release. The change is particularly marked where the involved components are known for their affinity and their tendency to interchange their atoms, with a significant heat release in agreement with the data in the thermochemical tables [11] [12].

The chemical kinetics of such a reaction is indicated on the thermograph by the steepness of the plot of the heat release. A pyrotechnic composition considered to be stable and reliable, shows the start of the reaction at a high temperature level (self-ignition or flash point) and unvarying heat release profile (see thermograph fig. 9 n° 5).

Taking the above considerations into account we have designed a number of measuring methods adapted to the capabilities of "CDP" (Programmed Differential Calorimetry) such as the determination of the self-ignition point of a pyrotechnic composition, of the energy transmitted, etc ... [13].

Originally the numerous preliminary tests that we conducted, using "CDP", by igniting a composition through temperature programming, even at high rates showed that the energy values obtained were most dispersed and quite far from the values given in the literature.

This result was easily explained by the fact that gradual rise of temperature causes a thermal change or decomposition before the self-ignition temperature is reached, which leads to a much incomplete reaction (fig. 4).

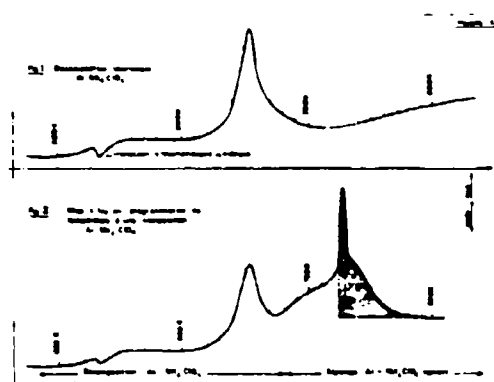


fig. 4

Ignition through temperature programming from ambient temperature therefore does not allow determining through this process the heat of combustion of the composition but allows accurate determination of their self-ignition point.

The knowledge of the self-ignition point makes possible the measurement of the heat of combustion by carrying out ignition at constant temperature by introducing the sample in the sensor already placed at a temperature slightly higher than the self-ignition point. The temperature rise is then extremely fast, and changes have no time to

occur, since the self-ignition temperature is reached as through hot wire initiation. Such quickness of ignition no longer allows differential measurement because the response time of the calorimeter is too long. The recommended method is to use a single tube and proceed as follows : (fig. 5).

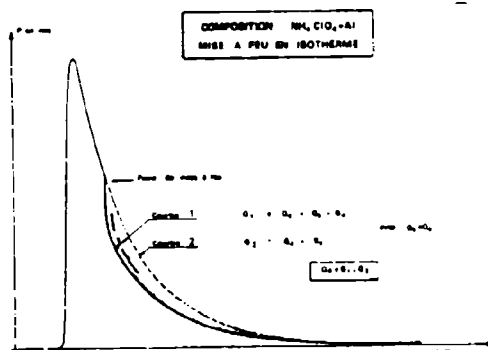


fig. 5

- the sample (about 5 mg) is placed into a stainless steel crucible crimped with a nickel joint, and located in the active part of the calorimeter. The obtained signal Q_1 is the summation of three factors :

$$Q_1 = Q_C + Q_E + Q_R$$

Q_C = heat amount required to bring the crucible from ambient temperature to working temperature.

Q_E = heat amount required to bring the sample from ambient temperature to working temperature.

Q_R = heat amount generated by the reaction.

That first step, which takes about 5 minutes being completed, the crucible is removed from the sensor, cooled down to ambient temperature, and placed again in the calorimeter.

The obtained signal Q_2 now is represented by :

$$Q_2 = Q_C + Q_E,$$

It will be considered, given the low weight of the test sample and disregarding the heat capacity change of the sample prior to and after combustion, that :

$$Q_E = Q_E,$$

The difference between the two curves therefore allows finding the value of the heat of combustion within about fifteen minutes.

The use of "CDP" visualizes, explicits and complements the chemical and physicochemical knowledge of the pyrotechnist who is thereby in a position to extend his research to new synthesis compounds, either organic, inorganic, metallic or organometallic, according to the assigned purpose, and whatever the final function : generation of gas, heat, smoke, or radiation, for optimum reaction efficiency.

It allows eliminating the sacred fear of the enemy named moisture, through systematic early detection and controlled selection of the components : non hygroscopic ones treated not to contain water or naturally hydrophobic.

It allows, as we shall see, to eliminate any substance that exhibit a transition point below a prescribed temperature level.

The formulation of a pyrotechnic composition basically is governed by rules pertaining to the chemistry of oxidations and combustions

[14] [15] mainly with regard to the reactions in the condensed phase, it should take into account the chemical and physical nature of the combined substances. To build up a stable construction from every viewpoints, it involves the elements of its functional specificity that are active mostly in the flame or in the gaseous phase depending on the sought for prevailing effect.

The contribution requested of "CDP" in the establishment of a pyrotechnic formulation is temporarily restricted to the selection of the components and the definition of the basic reaction regarded as the major source of heat power of which the functional action is known.

The determination of the parameters related to the effects of the reaction products requires other means that we have attempted to obtain by adaptation of a micro-calorimetric bomb (fig. 6) appropriately modified to measure :

- . peak pressure
- . residual pressure
- . maximum reaction temperature,

with the assistance of an associated electronic system.

The diagrams of the figure annexed hereto, illustrate two views, one of them corresponding to the conventional version of the bomb that allows calibration, and the other one corresponding to the modified version.

Without going into further details on this type of calorimeter, we would like to emphasize the number and simultaneity of the measurements that it makes possible.

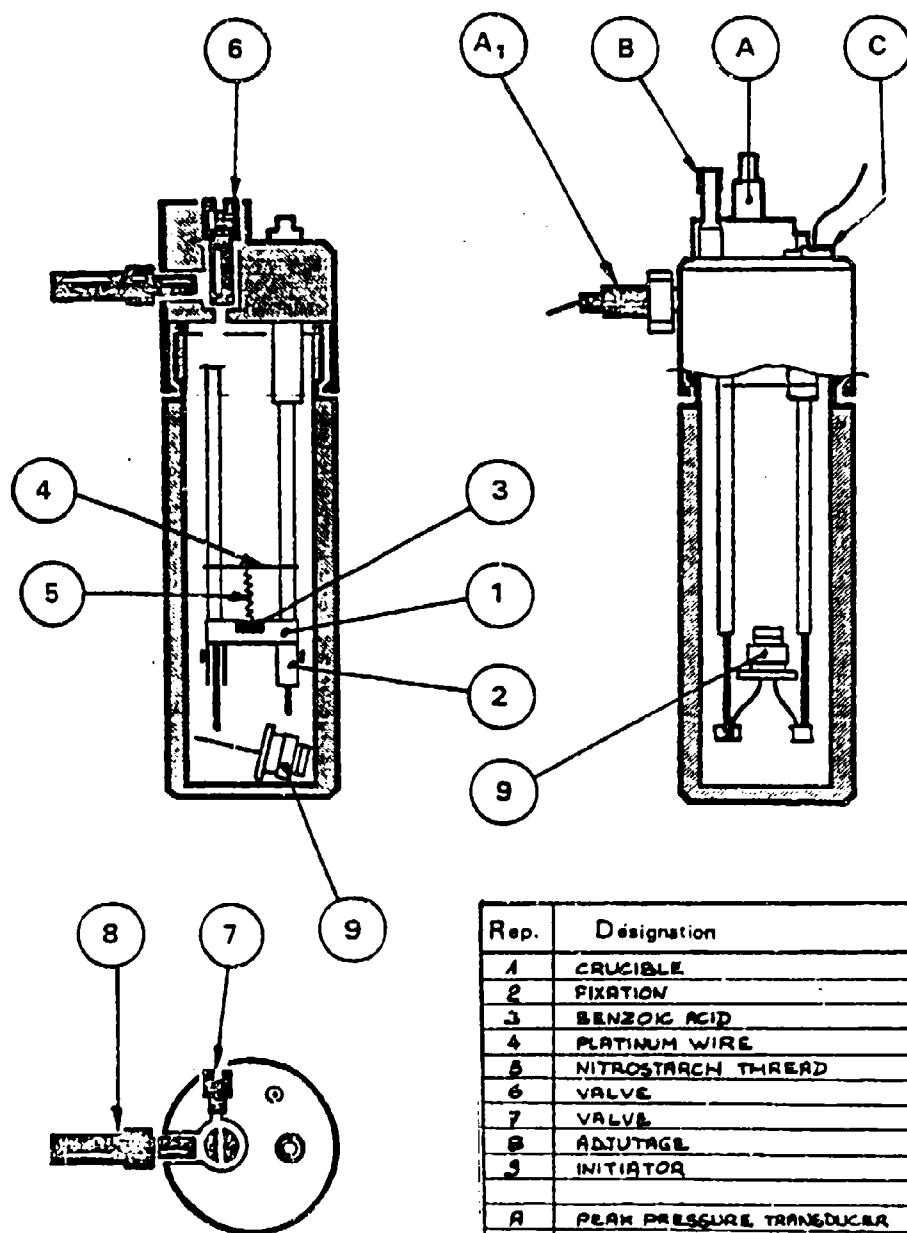


Fig. 6

Rep.	Designation
1	CRUCIBLE
2	FIXATION
3	BENZONIC ACID
4	PLATINUM WIRE
5	NITROCELLULOSE THREAD
6	VALVE
7	VALVE
8	ADJUSTAGE
9	INITIATOR
A	PEAK PRESSURE TRANSDUCER
B	THERMO. TRANSDUCER
C	PHOTO-CELL
A ₁	FINAL PRESSURE TRANSDUCER

4. APPLICATIONS : DEVELOPMENT OF A GAS MICRO-GENERATOR

The component, shown on fig. 7 annexed hereto, represents a gas generating squib intended to comply with a pressure-time law (peak pressure and residual pressure) illustrated on fig. 8. This component is a small size squib comprising :

- 1 A - 1 W 5 mn Initiator (1) with double resisting elements, equipped with four 90° elbowed pins for electric power input purposes.
- attachment nut.
- body (4) enclosing the functional charge.

The general specification that should be complied with by this device is the one applying to space vehicles.

- The problem was solved through the following procedure :
 - . Adjustment of the charge of the initiator acting as the igniter.
 - . Adjustment of the primer located on the functional charge to comply with the pressure-time law of the peak pressure.
 - . Adjustment of the functional charge to comply with the residual pressure required at the end of the operation after return to ambient temperature.
- The major constraints originated from :
 - . The confinement dictated by the very small dimensions of the device.
 - . The stringent environmental conditions laid upon equipment intended for space applications.

By applying the principles as stated under paragraph 3 hereabove, various compositions and their respective substances have been investigated.

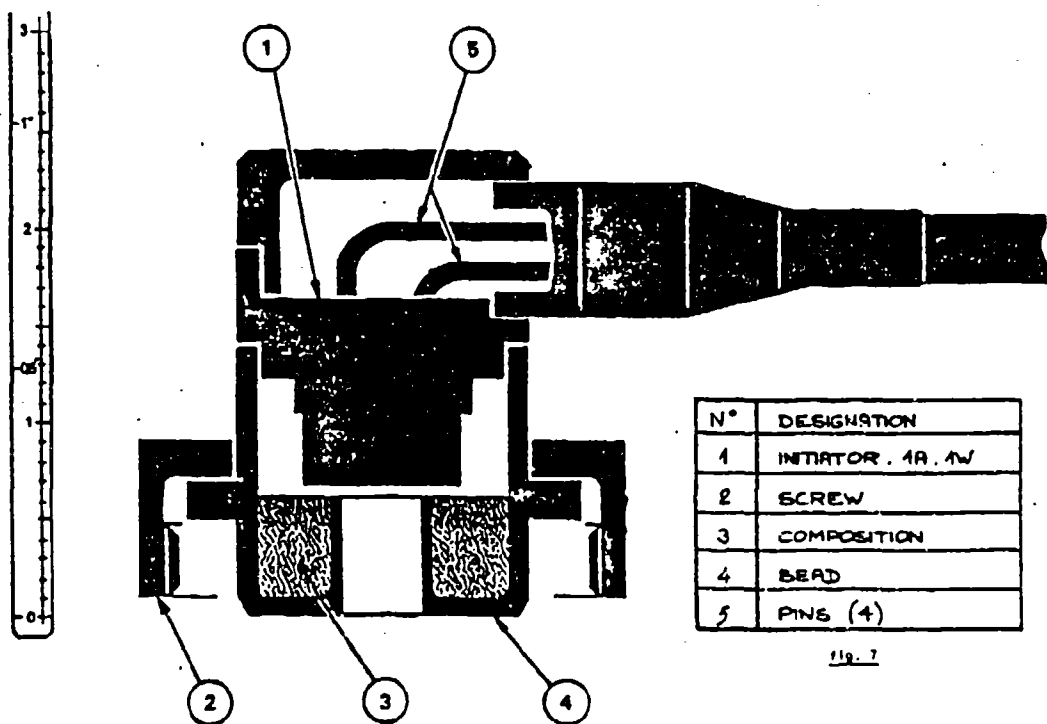


fig. 7

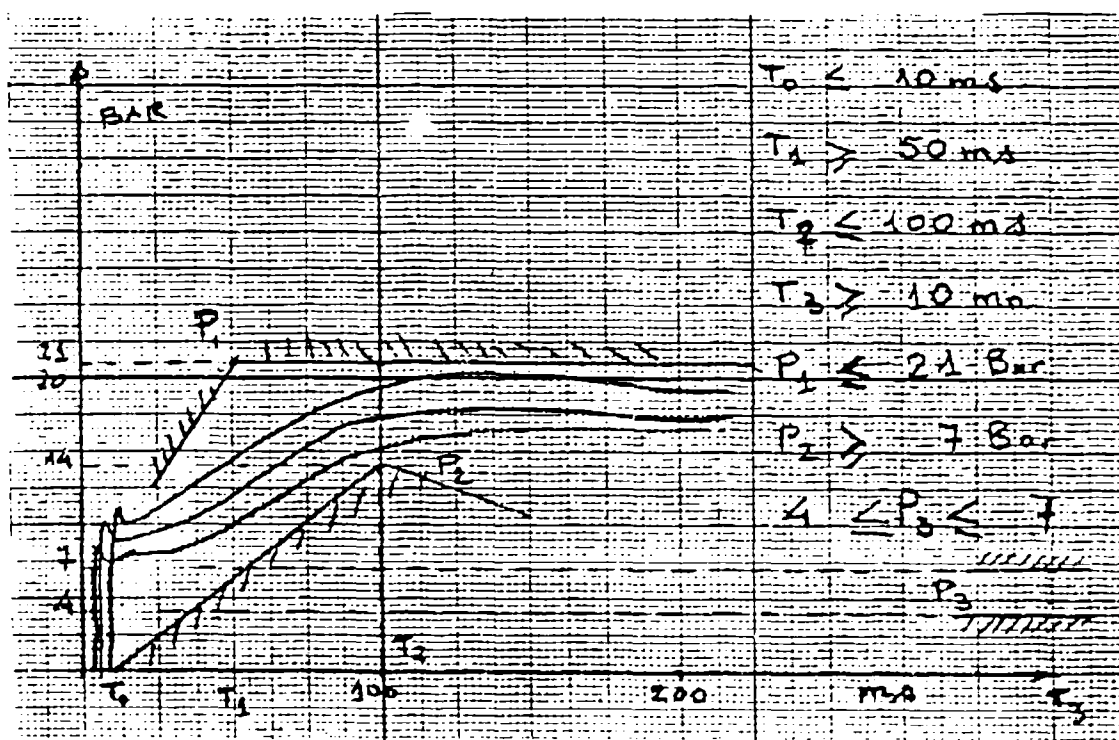


fig. 8

- The thermograph on fig. 9 represent :

- . the initiating composition of the 1 A - 1 W initiator (n° 5).
- . the igniting composition of the functional charge (n° 6).
- . the priming mixture of the functional charge (n° 7).
- . the basic composition modified by a regulation additive (n° 8).

Fig. 9 shows thermographs of a number of substances among which the regulation additive was selected to comply with the stability and function of the composition of the functional charge (n° 1 to 4).

Finally, fig. 8 shows the pressure recording taken as the device was mounted in a 35 cm³ test bomb.

5. CONCLUSION

The extent of the subject matter did not allow dealing further, as would have been advisable, into more cases of application, the main point being to know that calorimetry and programmed differential calorimetry are in fact a valuable tool in pyrotechnics, applying to corroborate the syntheses conducted by the pyrotechnist and avoid wastes of time.

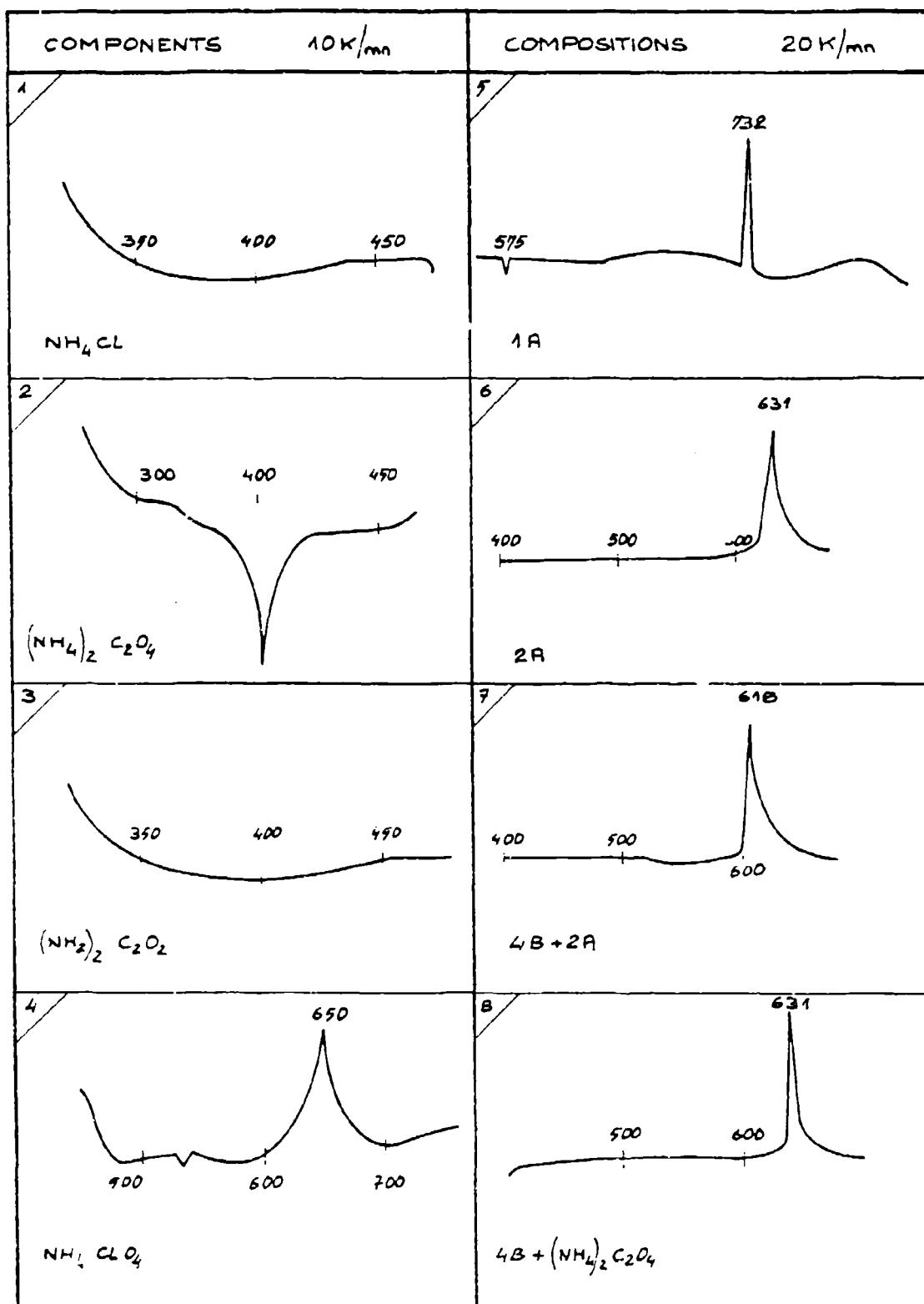


fig. 9

BIBLIOGRAPHY

- [1] AEROSPACE ORDNANCE HANBOOK
by FRANK B. POLLARD - JACK H. ARNOLD, JR.
- [2] MILITARY AND CIVILIAN PYROTECHNICS
by DR. HERBERT ELLERN.
- [3] ENCYCLOPEDIA OF EXPLOSIVES AND RELATED ITEMS
by FEDOROFF AND ALL.
- [4] PYROTECHNICS
by C.W. WEINGART.
- [5] PIRO. NIA E FUOCHI ARTIFICIALI
by ATTILIO IZZO.
- [6] MESURE DES ENERGIES DE COMBUSTION DES COMPOSITIONS PYROTECH-
NIQUES PAR CALORIMETRIE DIFFERENTIELLE PROGRAMMEE
COLLOQUE TOULOUSE - ESA SP 144 - JANVIER 1979.
- [7] THERMAL ANALYSIS OF EXPLOSIVES AND PROPELLANT INGREDIENTS
by J. NORMAN MAYCOCK.
- [8] KINETICS AND MECANIS OF THE THERMAL DECOMPOSITION OF METAL
CHLORITES, CHLORATES, AND PERCHLORATES
by F. SOLYMOSI.
- [9] EXPLOSIVE AND PYROTECHNIC AGING DEMONSTRATION
by LAWRENCE L. ROUCH AND J. NORMAN MAYCOCK
REPORT NASA N° CR-2622 FEB. 1976.

[10] EXPLOSIVES AND PYROTECHNIC PROPELLANTS FOR USE IN LONG
TERM DEEP SPACE MISSIONS
by CARL S. GORZYNSKI, JR AND J. NORMAN MAYCOCK
NASA CR 132373 - 1974.

[11] TABLES THERMOCHIMIQUES
by M.L. MEDARD.

[12] JANAF THERMOCHEMICAL TABLES
by STULL, DR - PROPHET, H.
NSRDS - NBS - 37.

[13] NOTE SEP - REF : DCQ/B N° 62358/79.

[14] COMBUSTION
by J. SURUGUE - M. BARRERE.

[15] OXYDATIONS ET COMBUSTIONS
by A. VAN TIGGELEN AND ALL.

SHOCK COMPACTION OF A POROUS PYROTECHNIC MATERIAL

L. M. Lee
Ktech Corporation
Albuquerque, New Mexico 87110

A. C. Schwarz
Sandia Laboratories
Albuquerque, New Mexico 87115

ABSTRACT

The results of an experimental program to generate Hugoniot data for an unreacted pyrotechnic material are discussed and the data presented. The program included both sample fabrication and experimental determination of stress-particle velocity Hugoniot data for the pyrotechnic, titanium hydride—potassium perchlorate ($\text{TiH}_2\text{-KClO}_4$), at two densities. The $\text{TiH}_2\text{-KClO}_4$, which was supplied as a powder mixture, was pressed to the desired bulk sample density and size using a ram and die technique. Samples were produced with nominal 2.02 or 2.27 g/cm³ densities. Hugoniot data were generated on the porous pyrotechnic samples using standard flat plate impact techniques.

The experimental program provided information defining the shock compaction behavior of porous $\text{TiH}_2\text{-KClO}_4$ up to 70 kbar. The Hugoniot data for both sample densities indicated full compaction was achieved in the 15 to 20 kbar stress range.

INTRODUCTION

Pyrotechnic materials are utilized in a number of system and component applications. Effective design and performance analyses of systems employing pyrotechnic materials are dependent upon proper modeling of the materials' thermodynamic behavior. A complete thermodynamic equation of state is based on numerous types of material properties data, including the shock response or Hugoniot of the unreacted pyrotechnic. The primary purpose of the study reported here was to experimentally determine the shock loading behavior of a specific unreacted pyrotechnic material at two densities, and provide information to support equation-of-state modeling efforts.

The pyrotechnic studied was titanium hydride—potassium perchlorate ($\text{TiH}_2\text{-KClO}_4$) supplied in powder form. A sample fabrication technique was developed to make reproducible, high quality samples that could be used to determine dynamic material properties data. The development effort resulted in a ram and die sample pressing apparatus that made it possible to fabricate free-standing reproducible, porous pyrotechnic samples with controlled bulk densities. Two sets of $\text{TiH}_2\text{-KClO}_4$ samples were made, with one set having a nominal bulk density of 2.02 g/cm^3 and the other set having an average density of 2.27 g/cm^3 . Theoretical solid density of the $\text{TiH}_2\text{-KClO}_4$ mixture was calculated to be 2.85 g/cm^3 . No binder was used in the sample, which resulted in minimal sample structural integrity.

The experimental program provided Hugoniot data for both the 2.02 and 2.27 g/cm^3 density $\text{TiH}_2\text{-KClO}_4$, using gas gun impact techniques. The dynamic response of the porous, unreacted $\text{TiH}_2\text{-KClO}_4$ was determined under conditions of uniaxial-strain shock loading. The shock loading characteristics of the pyrotechnic material were obtained from plate-impact experiments performed with a 102-mm bore compressed gas gun. The basic experimental configuration used to generate the Hugoniot data employed a piezoelectric transducer mounted in the projectile to measure stress. The projectile-mounted transducer design was adopted so that

the pyrotechnic sample could be placed in the target and not subjected to any acceleration loads. Previous experience indicated that pressed pyrotechnic and explosive samples cannot be mounted on projectiles and directly impacted into targets successfully because of their limited structural integrity.

The pyrotechnic sample was impacted with a tungsten carbide (WC) plate backed with a shunted quartz gauge to make the stress measurement. Higher impact stresses were attainable for a given impact velocity using the WC impactor plate rather than impacting with quartz directly because of the higher mechanical impedance of WC. The WC plate also separated the quartz gauge from the porous pyrotechnic sample, which helped to minimize gauge failure caused by local discontinuities at the gauge front electrode.

The experimental program provided information defining the shock compaction behavior of porous $\text{TiH}_2\text{-KClO}_4$ up to 70 kbar. The Hugoniot data for both sample densities indicated full compaction was achieved in the 15 to 20 kbar stress range. The stress-particle velocity data were transformed to the stress-specific volume and shock velocity-particle velocity planes using the Hugoniot equations to facilitate utilization of the experimental results.

MATERIAL AND SAMPLE FABRICATION DESCRIPTION

The Pyrotechnic investigated was a mixture of 33 weight percent TiH_2 powder and 67 weight percent KClO_4 powder supplied by Sandia Laboratories, Albuquerque, NM. The crystalline density of the pyrotechnic powder, which was very fine, was calculated from the simple mixture law:

$$\frac{1}{\rho_{12}} = \frac{x}{\rho_1} + \frac{1-x}{\rho_2}$$

where ρ_{12} is the mixture density, ρ_1 and ρ_2 are the two constituent densities and x is the weight fraction of constituent one. The solid densities used in the calculation were 3.90 g/cm^3 for the TiH_2 and

2.52 g/cm³ for the KClO₄ (Ref. 1, 2), with the resulting solid mixture density being 2.85 g/cm³.

The fabrication technique developed for making the pyrotechnic samples was guided by a number of factors, ranging from safety to ease of operation. One of the first decisions made was to attempt to fabricate a free-standing pressed sample from the pyrotechnic powder. A free-standing sample (i.e., not in a retaining ring or cup) facilitated making bulk density measurements, as well as sample flatness and parallelism measurements. Based on these factors, and discussions with people experienced in the field^{*}, a ram and die pressing apparatus was designed and fabricated. The ram and die approach made it possible to completely remove the sample from the die and inspect it prior to use in the impact experiment.

The fabrication apparatus used in making the pyrotechnic samples is shown schematically in Figure 1. The ram and die were designed to make a constant volume sample (30.48-mm diameter and 2.80-mm thick) by pressing to a fixed position (shown in the enlarged view in Figure 1) and holding the load for 5 minutes. Consequently, the bulk density of the sample was controlled by the mass of the pyrotechnic powder placed in the die. The sample was placed on a flat plate upon removal from the die and weight and linear sample measurements were made. The sample bulk density was calculated from the dimensional and mass measurements. The finished sample had limited structural strength because no binder was used in the pressing and, consequently, was easily broken during handling.

A backer plate of plexiglass was attached to the pyrotechnic sample following the sample density determination to alleviate the breakage problem. The backer plate and pyrotechnic sample were bonded together using 5-minute cure epoxy[†] that was initially applied to the circumference of the recess in the backer plate (Figure 2). A minimum amount of

^{*} Matson, P. E., Sandia Laboratories, and Harrell, D., Pantex Div. of Mason & Hanger, Amarillo, TX (Private Communication).

[†] Devcon "5 Minute" Epoxy, S/N 14250, Devcon Corp., Danvers, MA 01923.

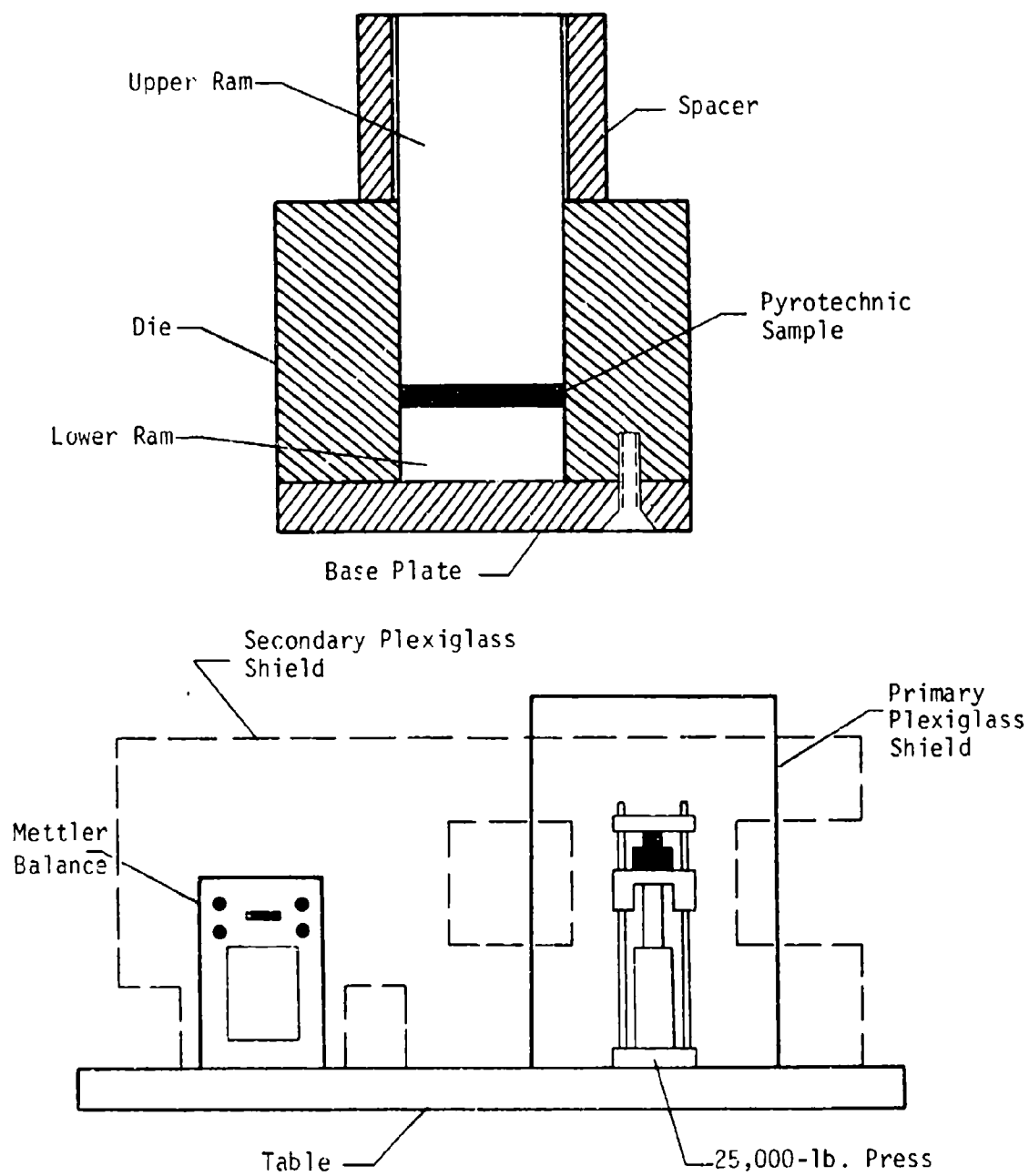


Figure 1. Schematic of Pyrotechnic Sample Fabrication Apparatus.

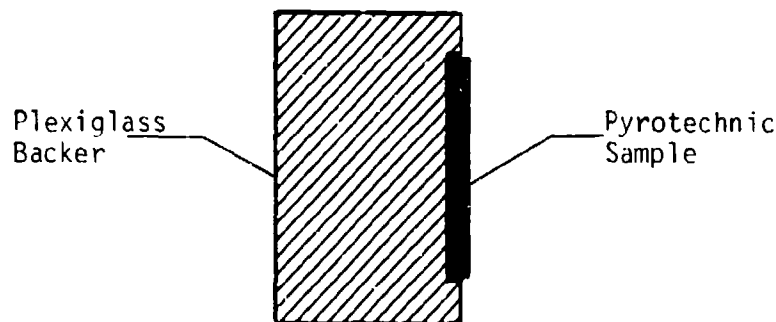


Figure 2. Schematic of Pyrotechnic Sample and Plexiglass Backer Used to Hold the Sample.

epoxy was used on the circumference and only a thin film was applied to the flat surface that was in contact with the sample. The small amount and location of epoxy used in mounting the sample did not influence the Hugoniot measurements. The backer plate provided a convenient way for mounting the samples in the targets and also minimized sample breakage due to handling.

The low density pyrotechnic samples were fabricated by pressing to a stop. However, the load applied to the ram was also monitored during fabrication and compared with previously determined pressure vs. sample density data. Slight sample distortion was observed when the lower density pyrotechnic samples were removed from the die. The final sample thickness was approximately 7.5 percent larger than the design thickness based on ram, die, and spacer dimensions. The increase in sample thickness was attributed to material spring-back after load removal. The diameter of the sample also expanded slightly upon removal from the die (approximately 0.5 percent). The pressing technique was used to produce fifteen samples with an average density of 2.02 g/cm^3 and a range of $\pm 0.03 \text{ g/cm}^3$. The mass of the powder used in each sample was well controlled, which was a major factor in producing the high quality samples. All of the powder handling and sample pressing was conducted behind plexiglass shields, as shown in Figure 1.

The high density pyrotechnic samples used in the Hugoniot experiments were fabricated in the same manner as previously described with one exception. The load required to compress the powder and force the ram down to the spacer position could not be achieved with the hydraulic press available. Consequently, these samples were fabricated by pressing to a known ram load of 1.43 kbar, and not to a known volume. Nine of the eleven density samples were held at load for 5 minutes. The load for two samples was held for 30 minutes, with a 2.5 percent increase in bulk density being observed. These results indicated that the final pressing density was somewhat time-dependent, but not a strong function of time at load. The higher density samples had an average density of $2.27 \pm 0.05 \text{ g/cm}^3$ and proved to be as reproducible as the lower density samples which were fabricated by pressing to a known volume.

EXPERIMENTAL PROCEDURES AND ANALYSIS

The dynamic response of the porous, unreacted $\text{TiH}_2\text{-KClO}_4$ was determined under conditions of uniaxial-strain shock loading. The shock loading characteristics of the pyrotechnic material were obtained from plate-impact experiments performed with a 102-mm bore compressed gas gun (Ref. 3). Analysis of the shock loading data employed the Rankine-Hugoniot jump equations, which assume steady wave behavior and thermodynamic equilibrium behind the shock front (Ref. 4).

1. HUGONIOT EXPERIMENTS

The basic experimental configuration used to generate essentially all of the Hugoniot data is shown schematically in Figure 3. In this configuration the piezoelectric transducer used to measure stress was mounted in the projectile rather than the target. The projectile-mounted transducer design was adopted so that the pyrotechnic sample could be placed in the target and not subjected to any acceleration loads. Previous experience indicated that pressed pyrotechnic and explosive samples

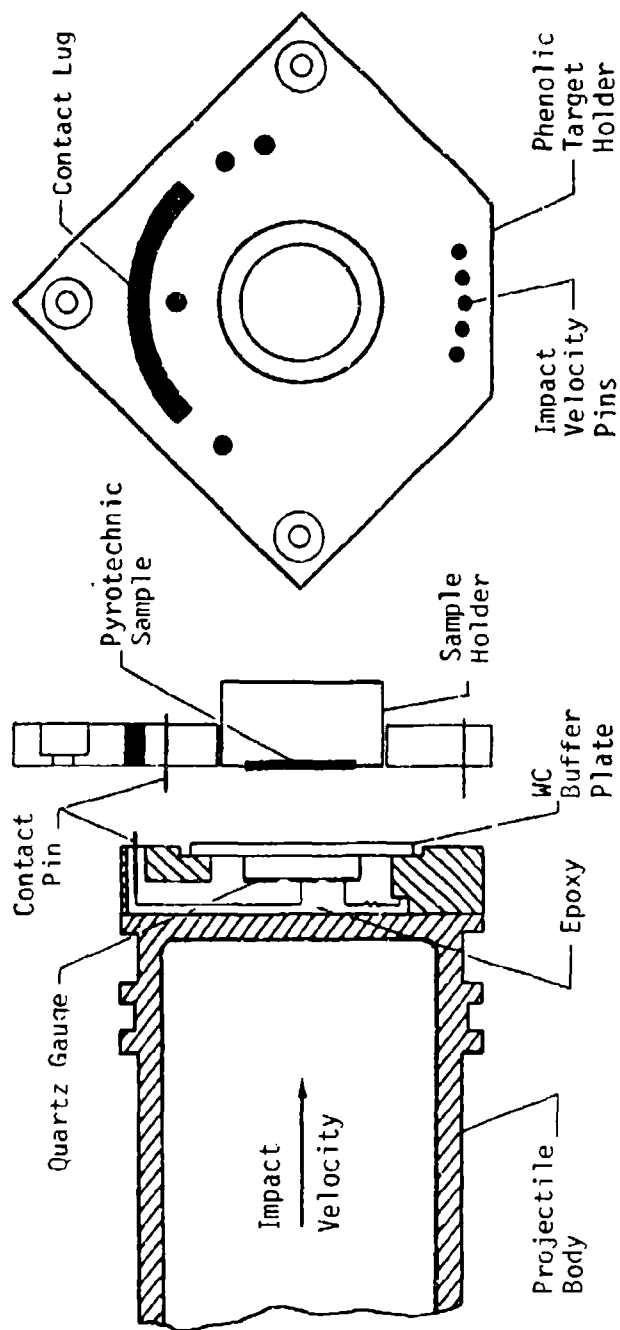


Figure 3. Schematic of the Projectile and Target Configuration Used to Generate the Pyrotechnic Hugoniot Data.

cannot be mounted on projectiles and directly impacted into targets successfully because of their limited structural integrity*.

The pyrotechnic sample was impacted with a tungsten carbide (WC)⁺ plate backed with a shunted quartz gauge (Ref. 5) to make the stress measurement. Higher impact stresses were attainable for a given impact velocity using the WC impactor plate rather than impacting with quartz directly because of the higher mechanical impedance of WC. The WC plate also separated the quartz gauge from the porous pyrotechnic sample, which helped to minimize gauge failure caused by local discontinuities at the gauge front electrode. The thicknesses of the sample, WC buffer plate, and quartz gauge were designed such that the initial stress wave generated at impact could propagate into the quartz gauge without being influenced by side or edge rarefaction waves. The measured experimental quantities included impact velocity and the time resolved current output of the quartz gauge as measured by the voltage across a 50-ohm termination resistor. Impact velocity was determined from time interval readings obtained from three 10-nsec counters triggered by charged pins with known distance intervals. Impact velocity was calculated from these data with an estimated maximum error of ± 0.4 percent. The maximum experimental error associated with the quartz gauge measurements was estimated to be ± 3 percent.

2. DATA ANALYSIS

The buffer plate experiments yielded stress-particle velocity data directly, as shown schematically in Figure 4. Continuity of stress and particle velocity across the WC-pyrotechnic sample interface requires:

$$\Delta\sigma_s = \Delta\sigma_b$$

and

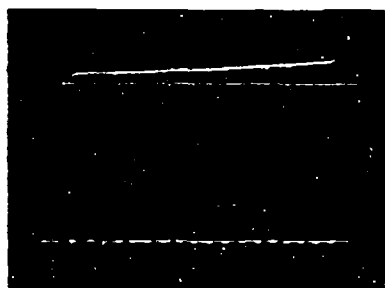
$$\Delta u_s = IV - \Delta u_b$$

where $\Delta\sigma_s$ and $\Delta\sigma_b$ are the stress changes in sample and buffer plate, respectively, and Δu_s and Δu_b are the particle velocity changes in the

* Mitchell, D. E., Sandia Laboratories, Private Communication.

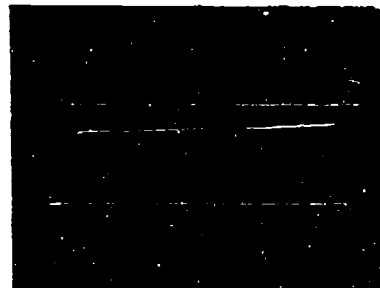
+ Type K-68, Kennametal Inc., Latrobe, PA.

Shot 808
Impact Velocity = 0.412 mm/ μ s



0.05 μ s/Time Mark
1.70 Volts Cal.

Shot 796
Impact Velocity = 0.739 mm/ μ s



0.05 μ s/Time Mark
6.50 Volts Cal.

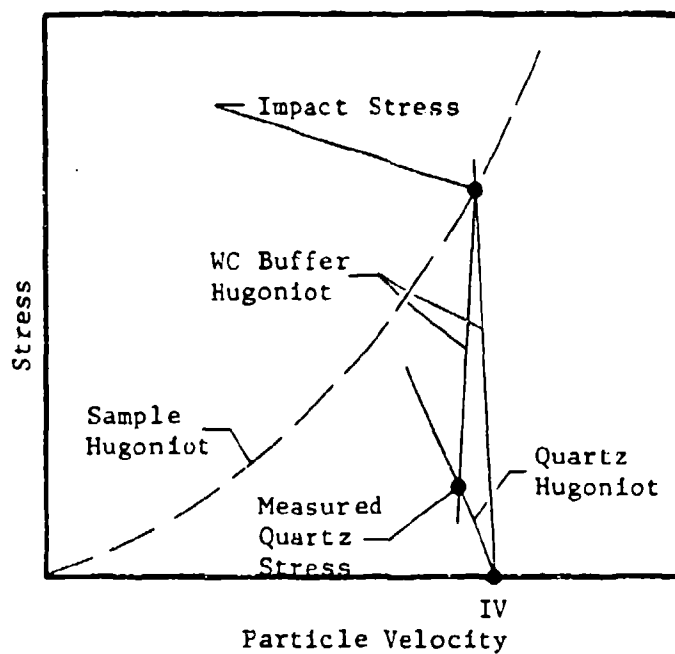


Figure 4. Representative Quartz Gauge Records from Pyrotechnic Hugoniot Shots and Schematic Diagram of Data Analysis Technique.

sample and buffer plate, respectively. Impact velocity is denoted V . The stress and particle velocity state reached in the buffer after impact was calculated from the measured quartz gauge stress amplitude σ_q and the known Hugoniot for the WC* buffer material and quartz crystal (Ref. 5). These experiments do not provide explicit information on stress wave shape or the loading path followed by the porous pyrotechnic. Measurements of the wave profile after it has propagated through the unreacted material are necessary to suitably define this portion of material response. The pressure-particle velocity data from the buffer plate experiments were transformed to the shock velocity-particle velocity and stress-specific volume plane by using the Hugoniot equations.

EXPERIMENTAL RESULTS AND DISCUSSION

The experimental program provided information defining the shock compaction behavior of porous $\text{TiH}_2\text{-KClO}_4$ up to 70 kbar, as well as a technique to fabricate free-standing pyrotechnic samples. The impact testing portion of the program was broken into three phases: (1) system check shots; (2) low density pyrotechnic Hugoniot shots; and (3) high density pyrotechnic shots. The system check shots were fired to verify the experimental design and to check all recording systems. Two experiments were performed with $\text{TiH}_2\text{-KClO}_4$ samples mounted on projectiles. Acceptable data were recorded on the first of these two tests (Shot 801) but anomalous results were recorded on the second test (Shot 802). The limited data recovery from these two shots was attributed to sample break up due to acceleration loads.

The results of the Hugoniot experiments on the 2.02 and 2.27 g/cm³ $\text{TiH}_2\text{-KClO}_4$ samples are given in Tables 1 and 2, respectively. The initial sample condition and type of experiment used to generate the data are also listed. The stress-particle velocity data are plotted in Figure 5 for both densities of material. Also shown in Figure 5 are polynomial fits to the data determined using a least squares technique and

* Karnes, C. H., Sandia Laboratories, Private Communication.

Table 1
SUMMARY OF HUGONIOT DATA FOR LOW DENSITY PYROTECHNIC ($\text{TiH}_2\text{-KClO}_4$)

Shot No.	Type of Experiment	Initial Conditions				Hugoniot Data			
		Impact Velocity (mm/ μs)	Sample Number	Sample Thick. (mm)	Sample Density (g/cm ³)	Stress (kbar)	Particle Velocity (mm/ μs)	Shock Velocity (mm/ μs)	Specific Volume (cm ³ /g)
794	XQ/WC \rightarrow Pyro	0.517	2	3.05	2.00	16.9	0.501	1.675	0.3480
796	XQ/WC \rightarrow Pyro	0.739	3	3.01	2.01	29.8	0.710	2.056	0.3210
797	XQ/WC \rightarrow Pyro	1.010	4	3.01	2.01	50.0	0.961	2.555	0.3067
800	XQ/WC \rightarrow Pyro	0.880	7	3.02	2.01	39.4	0.842	2.334	0.3186
801	Pyro \rightarrow WC/XQ	1.274	8	3.03	2.00	73.7	1.200	3.060	0.3032
808	XQ/WC \rightarrow Pyro	0.412	10	2.95	2.07	11.6	0.400	1.406	0.3458
810	XQ/WC \rightarrow Pyro	0.246	11	2.97	2.05	5.4	0.241	1.098	0.3812

Table 2
SUMMARY OF HUGONIOT DATA FOR HIGH-DENSITY PYROTECHNIC (TiH₂-KC10₄)

Shot No.	Type of Experiment	Initial Conditions			Hugoniot Data				
		Impact Velocity (mm/ μ s)	Sample Number	Sample Thick. (mm)	Sample Density (g/cm ³)	Stress (kbar)	Particle Velocity (mm/ μ s)	Shock Velocity (mm/ μ s)	Specific Volume (cm ³ /g)
803	XQ/WC \rightarrow Pyro	0.519	B	3.37	2.25	22.0	0.498	1.946	0.3300
804	XQ/WC \rightarrow Pyro	0.775	C	3.31	2.25	40.5	0.735	2.445	0.3108
809	XQ/SC \rightarrow Pyro	0.245	E	3.30	2.29	8.0	0.237	1.478	0.3673
811	XQ/WC \rightarrow Pyro	0.409	F	3.36	2.26	16.0	0.397	1.805	0.3465
812	XQ/WC \rightarrow Pyro	0.695	G	3.35	2.27	35.7	0.660	2.386	0.3188
814	XQ/WC \rightarrow Pyro	0.903	H	3.33	2.28	54.9	0.850	2.835	0.3073
817	XQ/WC \rightarrow Pyro	0.993	J	3.28	2.32	64.3	0.930	2.981	0.2967

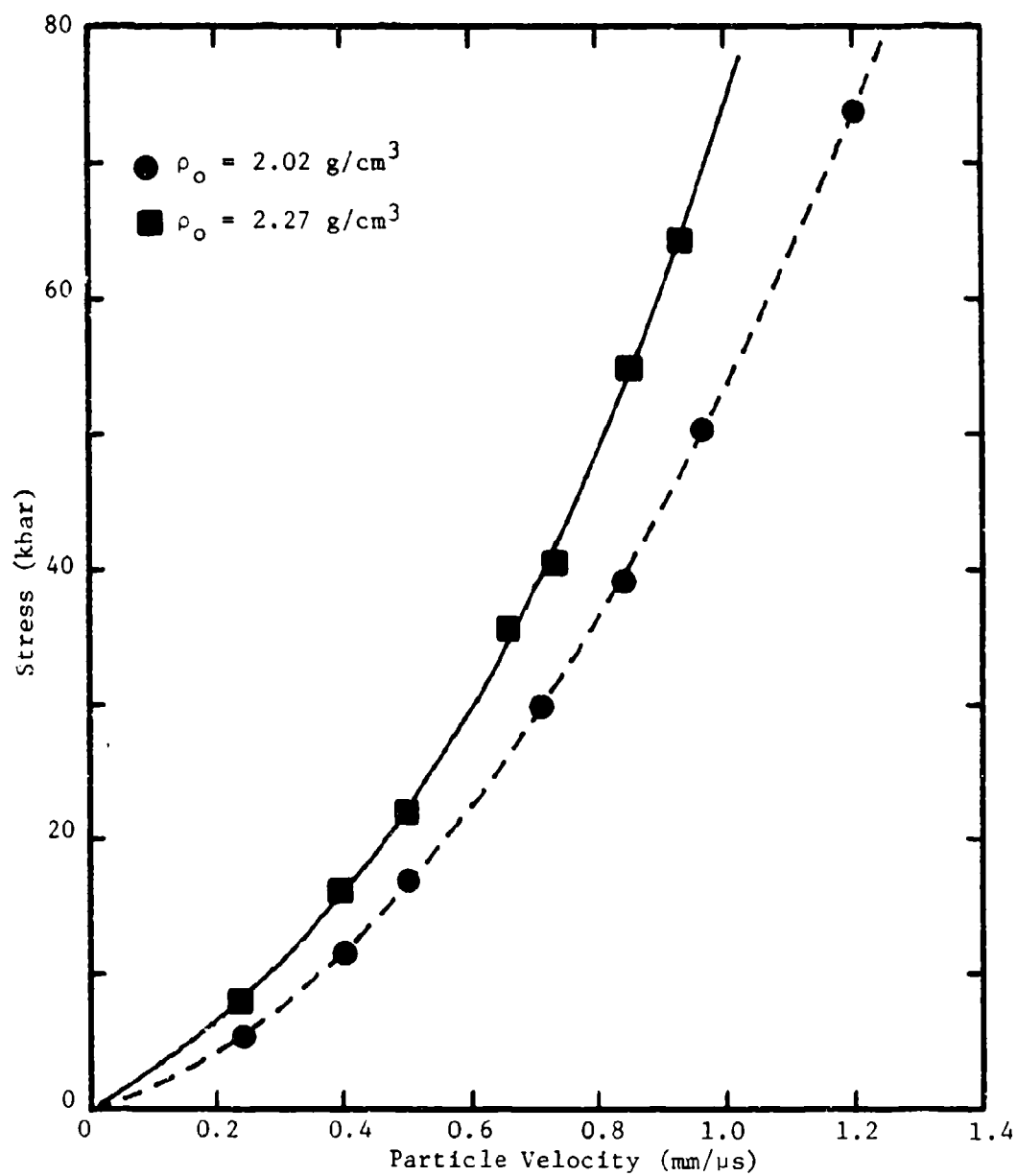


Figure 5. Stress-Particle Velocity Hugoniot Data for Porous Titanium Hydride-Potassium Perchlorate.

constraining the fit through the origin. The relations derived in this manner are:

$$\sigma = 12.84u + 41.31u^2 - 0.69u^3$$

for the 2.02 g/cm³ density material, and

$$\sigma = 28.01u + 20.00u^2 + 26.21u^3$$

for the 2.27 g/cm³ density material, where stress σ is kbar and particle velocity u is mm/ μ s.

The stress-particle velocity data were transformed to the shock velocity-particle velocity plane by using the Hugoniot jump equation. Shock velocity was calculated from:

$$U_1 = \frac{\Delta\sigma_1}{\Delta u_1 \rho_0}$$

where U_1 is shock velocity, $\Delta\sigma_1$ is the change in stress, Δu_1 is the change in particle velocity, and ρ_0 is the initial sample density. Linear fits to the two sets of data were obtained, as shown in Figure 6, with the relations being:

$$U = 0.61 + 2.04u$$

for the 2.02 g/cm³ density material, and

$$U = 0.92 + 2.19u$$

for the 2.27 g/cm³ density material, where U and u are mm/ μ s. The data were also transformed to the stress-specific volume plane using the Hugoniot equation:

$$\rho_1 = \frac{\rho_0}{1 - \frac{\Delta u_1}{U_1}}$$

where ρ_1 is the material density at shock state 1. Both densities of pyrotechnic material displayed essentially the same compaction response above 20 kbar as shown in Figure 7.

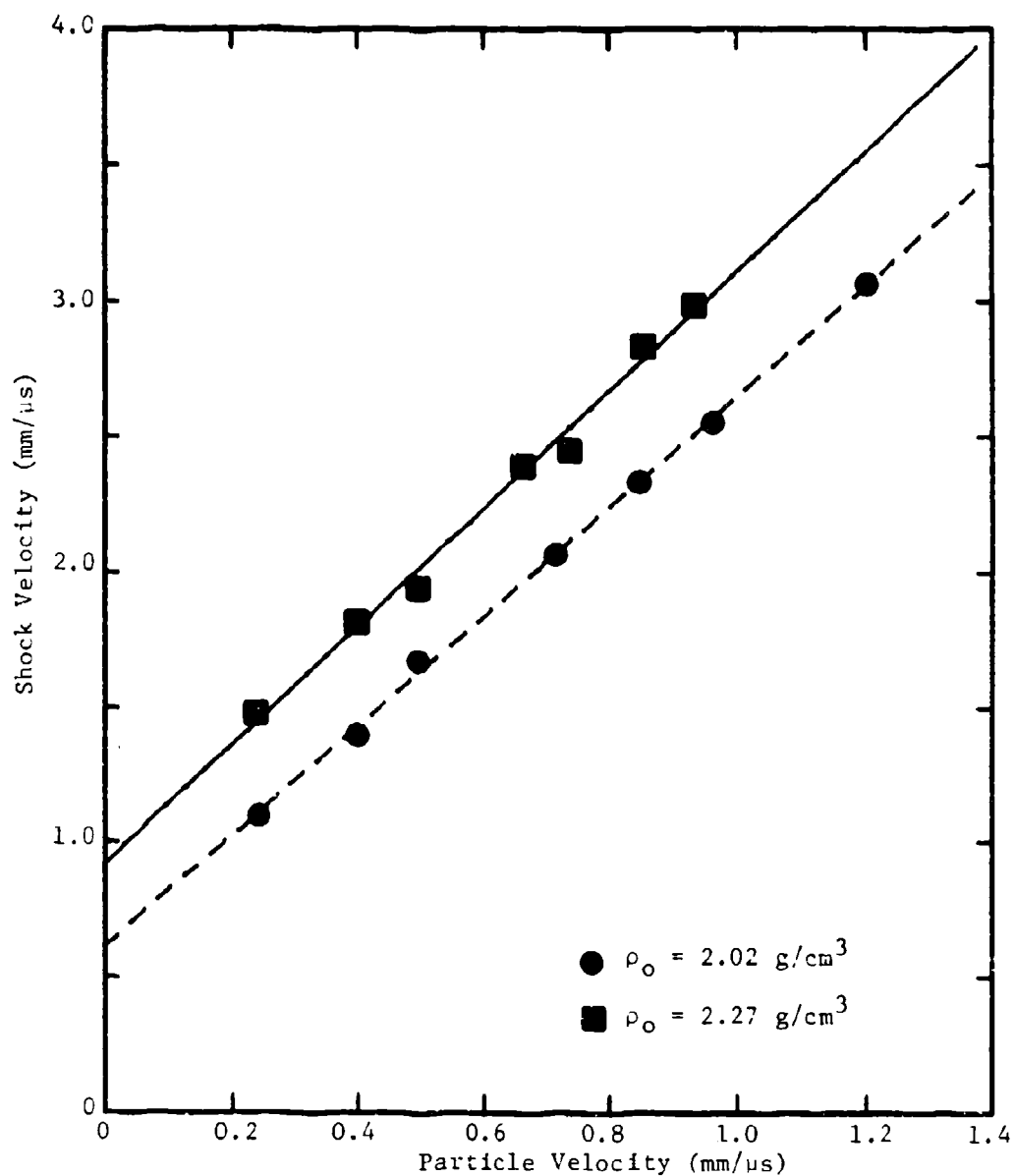


Figure 6. Shock Velocity-Particle Velocity Hugoniot Data for Porous Titanium Hydride-Potassium Perchlorate.

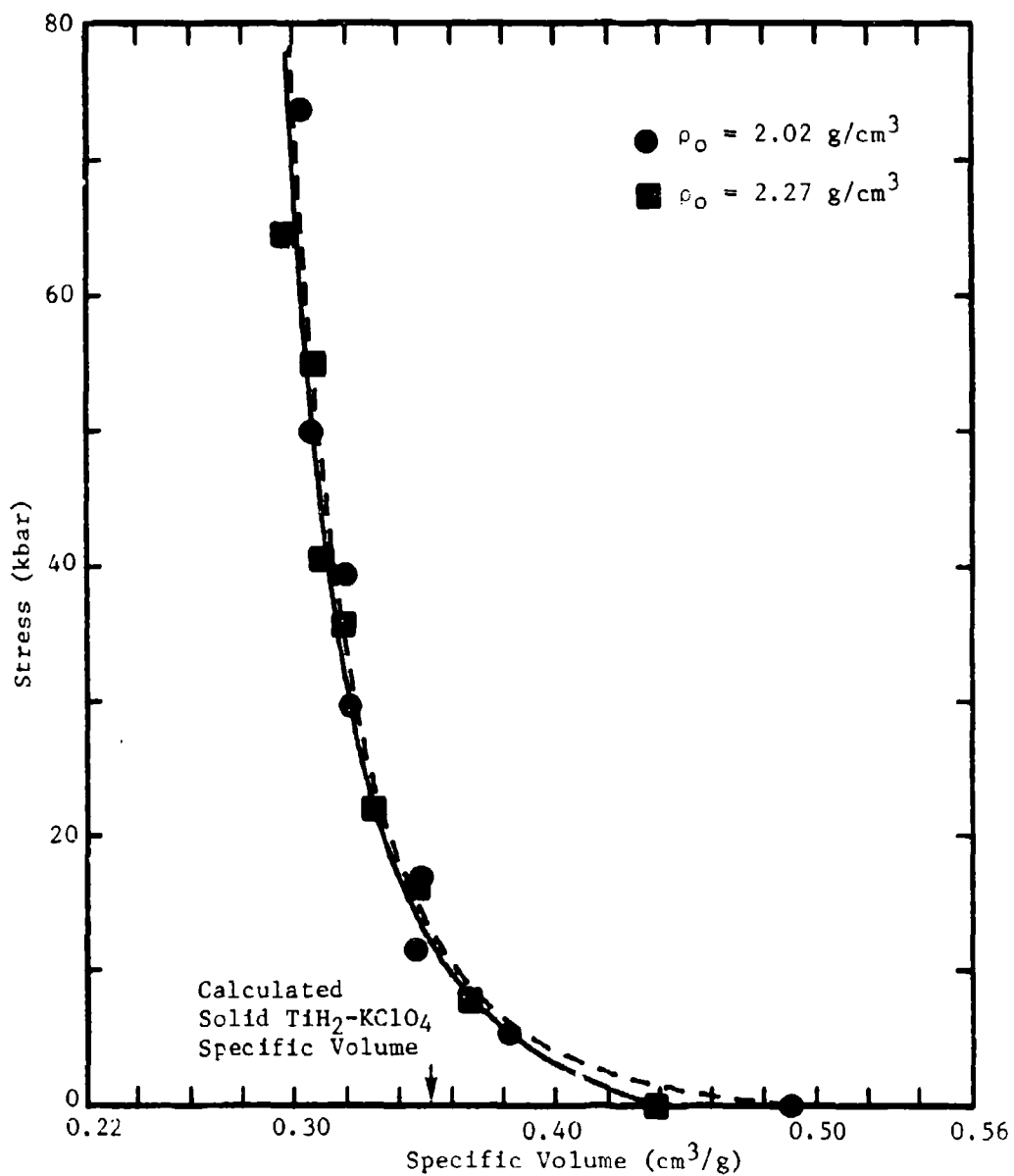


Figure 7. Stress-Specific Volume Hugoniot Data for Porous Titanium Hydride-Potassium Perchlorate.

REFERENCES

1. C.R.C. Handbook of Chemistry and Physics, R. C. Weast, Ed., Chemical Rubber Co., Cleveland, OH, 52 Edition, 1971-1972.
2. Handbook of Chemistry, Land, Ed., Handbook Publishing Co., Sandusky, OH, 17th Edition, 1947.
3. Lee, L. M., Operation of the Air Force Weapons Laboratory Material Response Impact Facility, AFWL-TR-75-287, Air Force Weapons Laboratory, Kirtland AFB, NM, March 1976.
4. Rice, M. H., McQueen, R. G., and Walsh, J. M., in Solid State Physics, "Compression of Solids by Strong Shock Waves," F. Seitz and D. Turnbull, Eds., Academic Press, New York, 1958, Vol. 6, pp. 1-63.
5. Graham, R. A., Neilson, F. W., and Benedick, W. B., "Piezoelectric Current from Shock-Loaded Quartz--A Submicrosecond Stress Gauge," J. Appl. Phys., 36, No. 4, 1965, pp. 1775-1783.

STATUS OF THE DEVELOPMENT OF
2-(5-CYANOTETRAZOLATO)PENTAAMMINECOBALT(III)
PERCHLORATE FOR DDT DEVICES

By

Morton L. Lieberman
Sandia National Laboratories
Albuquerque, NM 87185

and

John W. Fronabarger
Unidynamics Phoenix, Inc.
Phoenix, AZ 85062

ABSTRACT

The inorganic explosive 2-(5-cyanotetrazolato)pentaamminecobalt(III) perchlorate has been the subject of an ongoing development program. This material, designated CP, is of interest for low-voltage, hot-wire detonator applications. Synthesis of CP is accomplished by conventional coordination chemistry preparative methods. Its structure has been established via ^{15}N NMR spectroscopy and x-ray diffraction techniques. Impurities have been identified and characterized. Procedures for qualification of the powder for detonator use have been established. Investigations of thermal properties are under way and no corrosion or compatibility problems have been determined under normal detonator environments. The physics of deflagration-to-detonation transition (DDT) of CP is being addressed. Studies are in progress to determine the shock characteristics of unreacted material, detonation parameters, equation of state of the reaction products, and characteristics of the transition to detonation. Engineering considerations have included measurements relating CP particle size, compaction behavior, spark sensitivity, shock sensitivity, thermal ignition sensitivity, growth-to-detonation in device hardware, and output.

I. INTRODUCTION

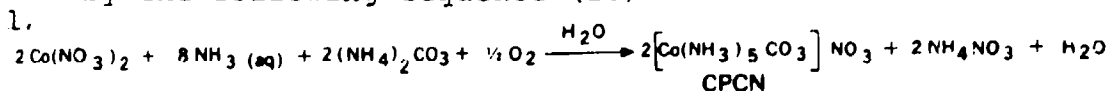
Inorganic explosive materials have been of interest to Sandia Laboratories for low-voltage, hot-wire detonator applications because of their relatively high thermal stability, ease of ignition, and good explosive output. A major objective of our studies has been the development of a safe material which can be readily ignited from a bridgewire with a low energy input, and which can rapidly grow from deflagration to detonation in a short distance.

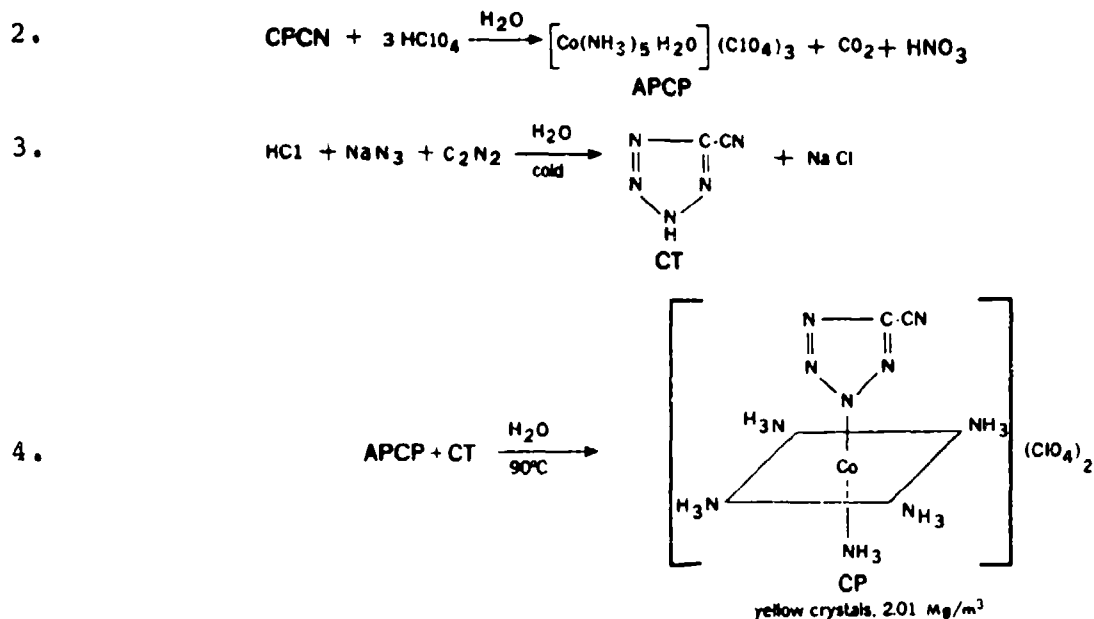
Sandia activities in high energy cobalt coordination compounds have been performed primarily in-house and at Unidynamics under contract since 1961. A variety of these chemical compounds have been shown to exhibit attractive properties. Little of this information, however, has been reported in the open literature. One material of particular interest for detonator applications is 2-(5-cyanotetrazolato)-pentaamminecobalt(III) perchlorate, designated CP. This compound was initially examined in 1969 (1) and has been the subject of an extensive ongoing development program since 1975 (2-19). It is currently being incorporated in detonators for weapons applications. Many results of unpublished studies have been included in quarterly reports of the Sandia Deflagration-to-Detonation Transition (DDT) Project (13-17).

II. CHEMISTRY

A. Preparation

The synthesis of CP is accomplished by conventional coordination chemistry preparative methods as depicted by the following sequence (10):





Steps 1 and 2 are well known and are described in a variety of literature sources. The APCP is purified by recrystallization from an excess of aqueous perchloric acid. 5-Cyanotetrazole (CT), step 3, is prepared essentially by the method of Henry (2) which involves the addition of one mole of azide at low temperature (5-10°C) to the activated cyano group of cyanogen. The CP is prepared by a typical anation reaction of CT (approx. 35 percent excess) and the aquo complex (APCP) in aqueous media (90°C, 3 hours). Cooling of the reaction mixture to 25°C provides a crude product containing about ten percent of a hydrolytic impurity 5-carboxamido-tetrazolatopentaamminecobalt(III) perchlorate ("amide complex").

The crude is recrystallized from slightly acidified (HClO₄) aqueous solution containing ammonium perchlorate. The purified material contains 2-3 percent of "amide complex" and is of rather large particle size. In order to arrive at a particle size suitable for detonator

applications, the purified material is reprecipitated from slightly acidified (HClO_4) aqueous solution by controlled addition to chilled stirring isopropyl alcohol. After air drying, the product is sieved through a USS-ASTM 140 mesh stainless steel screen. Overall, 3200g APCP yields about 1200g of yellow-orange screened CP.

B. Structure

The chemical structure of CP was arrived at via a series of analytical treatments, each succeeding technique providing a clearer concept of the true structure. Initially, the compound was quantitatively analyzed for perchlorate and cobalt content. Subsequently, the electronic (UV-visible) and infrared spectra were obtained (1). Also, the proton and carbon-13 natural abundance NMR shifts were determined (21). All the data generated supported the original concept of the CP structure. The spectral characteristics and assignments are summarized in Table 1.

The remaining uncertainty was the specific position of cobalt substitution on the tetrazole ring. This was determined by the appropriate nitrogen-15 labeling of CP (1) and determination of the ^{15}N NMR shifts of CT and the corresponding CP samples (21). The ^{15}N labeling of CT in two modes is as follows:

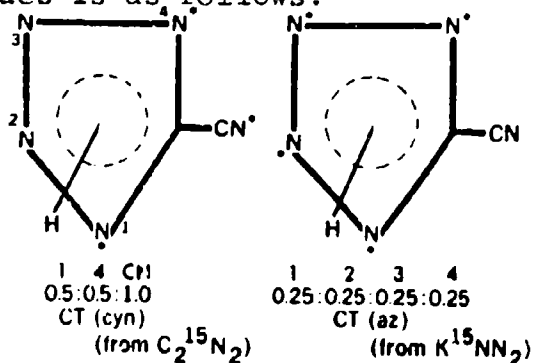


TABLE 1

SPECTRAL CHARACTERIZATION

NMR

Proton

cis NH_3 3.65-3.71 ppm

trans NH_3 3.50 ppm

^{13}C

CN 111.6 ppm

C-CN 141.1 ppm

IR

$\nu(\text{NH}_3)$ 3230 cm^{-1}

$\nu(\text{CN})$ 2266 cm^{-1}

$\delta(\text{NH}_3)$ 1625, 1330, 830 cm^{-1}

$\nu_d(\text{ClO}_4^-)$ 1080-1145 cm^{-1}

$\nu_s(\text{ClO}_4^-)$ 942 cm^{-1}

$\delta_d(\text{ClO}_4^-)$ 630 cm^{-1}

Tetrazole ring 1430, 1040 cm^{-1}
(also 1295 and 1170 cm^{-1} but not apparent due to ClO_4^-)

TLC

R_f

.75-.79

UV/VIS

$^1\text{T}_{2g} \longleftrightarrow ^1\text{A}_{1g}$	λ, nm	$\epsilon, (\text{moles/l})^{-1}$
	334	60
$^1\text{T}_{1g} \longleftrightarrow ^1\text{A}_{1g}$		
	464	60

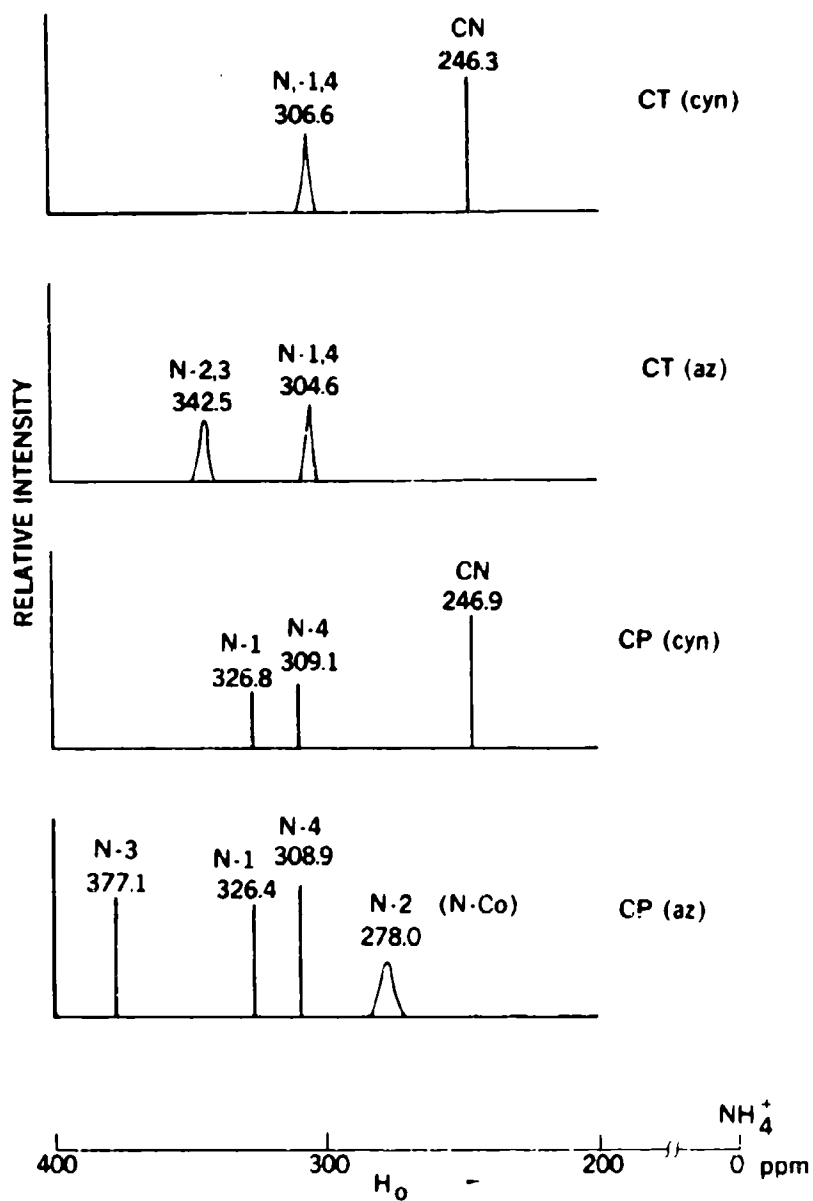
The ^{15}N NMR spectra of the two labeled CT forms and their corresponding CP forms are illustrated in Figure 1. Analysis of these data resulted in assignment of the tetrazole ring substitution by cobalt as N-2 as shown in Step 4 of the synthesis sequence (Section II, A).

Briefly, the arguments are as follows:

1. Previous studies have shown that direct attachment of a group to a tetrazole ring nitrogen results in a downfield shift of that nitrogen. Ring nitrogens adjacent to the substituted nitrogens are shifted upfield.
2. For CP ($\text{C}_2^{15}\text{N}_2$) N-1 and N-4 are no longer equivalent as in CT ($\text{C}_2^{15}\text{N}_2$). N-1 is shifted upfield.
3. For CP (K^{15}NN_2) N-1 is shifted as in item 2. N-3 is shifted upfield relative to N-3 in CT (K^{15}NN_2). N-2 is shifted downfield relative to N-2 in CT (K^{15}NN_2). Note that N-1, N-4 and N-2, N-3 are magnetically equivalent pairs in CT (K^{15}NN_2).
4. Further evidence for N-2 substitution is broadening of the N-2 peak in CP (K^{15}NN_2).

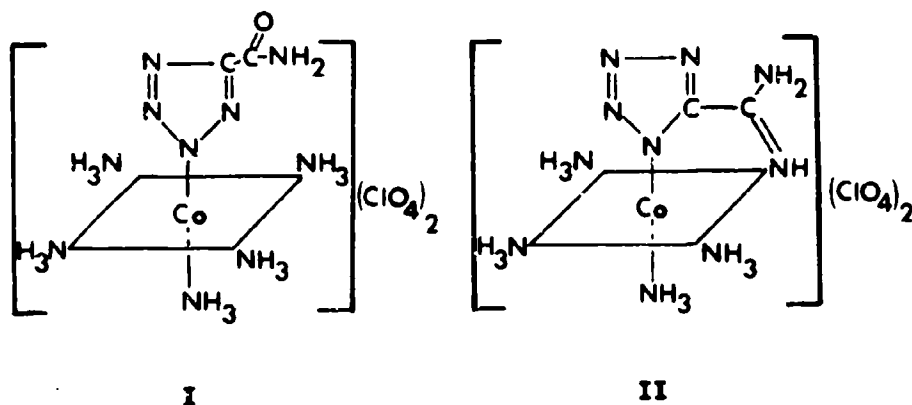
The complete structure of CP was determined by Graeber and Morosin (4) via single crystal x-ray diffraction analysis. Crystals are monoclinic, $\text{P2}_1/\text{a}$, with $a = 24.777(9)$, $b = 7.673(3)$, $c = 7.884(3)\text{\AA}$, $\alpha = 90.0$, $\beta = 101.20(1)$, $\gamma = 90.0^\circ$, and $Z = 4$. The calculated density is 1.974 Mg/m^3 compared to Marchi's (16) experimental determination by helium pycnometry of 1.96_5 Mg/m^3 . The tetrazole ring is N-2 bonded, in agreement with the NMR results, and is a slightly distorted pentagon with mean bond length of 1.34\AA . One perchlorate group of the unit cell is disordered.

Figure 1. ^{15}N NMR Spectra



- Establishes Cobalt bonding to N-2 of cyanotetrazole

As previously mentioned, the major impurity in purified CP is the "amide complex" (2-3 percent). This impurity is quite difficult to remove completely (<1 percent) which is surprising in view of its relatively high water solubility. Although no in-depth structural studies have been performed, it is assumed the material has the structure shown by structure I below.



An additional impurity is formed in the preparation of CP and is depicted by structure II. This compound is referred to as the "amidine chelate" and its structure has been proven by ¹⁵N NMR (22) and single crystal x-ray diffraction (12) studies much in the same manner as CP. In purifying CP, it is recalled that acid media is always employed. Neutral or basic conditions result in the formation of both "amide complex" and amidine chelate as shown in Figure 2 (1).

C. Analytical Qualification

The qualification of CP powder for detonator applications involves a number of tests as indicated in Table 2. Several of these techniques were based on those utilized in the previously discussed structure proof.

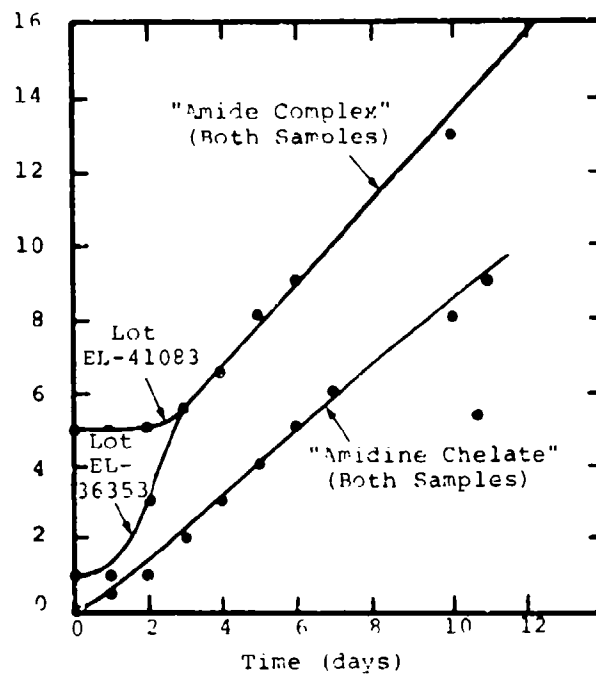


Figure 2. CP Decomposition in Water

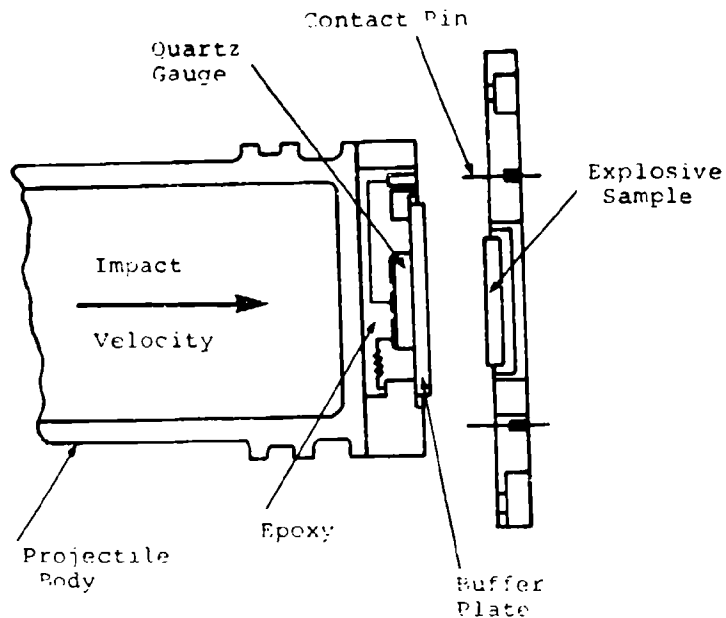


Figure 3. Schematic of the projectile and target configuration used to generate the explosive Hugoniot data.

TABLE 2. ANALYTICAL QUALIFICATION TESTS

1. Moisture content
2. Water uptake at 98 percent humidity
3. pH of a 1 percent standard CP solution
4. Chloride ion content
5. Perchlorate content
6. Cobalt content
7. 5-carboxamidotetrazolatopentaamminecobalt(III) perchlorate content ("amide complex")
8. Ammonium ion content
9. Functionality tests in detonator hardware
10. Surface area analysis by low temperature Krypton absorption (BET technique)
11. Nitrate ion content
12. Free cyanide ion content
13. Trace metal content
14. Infrared and UV-Visible spectrum
15. Sensitivity
16. Differential Scanning Calorimetry (DSC)
17. Microscopy

The last seven tests in this list are for information only, and no specified limits have been established. Typical analysis values for CP are provided in Table 3. Data for items 9, 15, 16, and 17 are not given but are discussed in subsequent sections of this document.

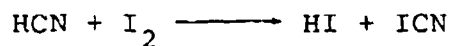
Most of the analytical procedures are relatively straightforward. Moisture content (test 1) is actually weight loss on drying, and water uptake at 98 percent humidity (test 2) is determined by weight gain of the same sample dried in test 1. The chloride (test 4) and ammonium ion (test 8) concentrations are determined using specific ion electrodes (3). Perchlorate (test 5) is determined gravimetrically as tetrapentylammonium perchlorate (23). Cobalt (test 6) is determined by the classical method of electrolytic deposition of metal (24) after digestion of the sample in sulfuric acid.

Jungst and Peterson established a method for the determination of "amide complex" (test 7) based on deuteration of the coordinated ammonias by D_2O (5). This shifts the degenerate deformation NH_3 band thus permitting unobscured observation of the "amide complex" carbonyl at approximately 1700 cm^{-1} by IR spectroscopy. A reasonable estimate of "amide complex" content can be made using thin layer chromatography (1); however, the method does not give precise results. Efforts are currently in progress to develop simpler and more reliable methods for this determination. The surface area (test 10) is determined by low temperature krypton absorption (BET technique), and a specified requirement exists. However, the surface area requirement can be waived if the detonator functionality test is satisfactory. Nitrate ion (test 11) is determined by a calorimetric method using diphenylbenzidine (25). Cyanide (test 12) is determined

TABLE 3. TYPICAL ANALYSIS VALUES FOR CP

Test	Requirements	Typical Results
Perchlorate	45.54 \pm 0.3%	45.3 - 45.6
Amide Complex	<5.0%	1.5 - 2.5
Cobalt	13.44 \pm 0.3%	13.6 - 13.7
pH	>4.5	5.6
Chloride	<100 ppm	not detected (30 ppm)
Ammonium	<100 ppm	30-75 ppm
Nitrate	--	250 ppm max (range 70-250 ppm)
Cyanide	--	not detected
Trace Metals	--	obtained (no metal greater than 0.02%)
Ultraviolet-visible and Infrared Spectra	--	obtained
Moisture, content	<0.1%	0.02
uptake	<0.2%	0.12 - 0.27
Surface area	0.4 - 0.6 m ² /g	0.4 - 0.6

by a titrametric method based on the following reaction (3):



Starch indicator is used to detect the disappearance of iodine. Trace metals (test 13) are determined spectrographically after the sample has been digested in a mixture of nitric and sulfuric acids.

CP of acceptable purity and particle size for use in detonators can be produced in 1 kg size lots. The process has been developed and documented (1, 10) to the extent that good reproducibility can be expected for subsequent lots. Total elapsed time for the preparation and qualification of a lot of CP is 6-8 weeks exclusive of functionality tests.

III. THERMAL PROPERTIES

Searcy and Shanahan (7) have examined the thermal decomposition of CP by means of thermal analysis, gas chromatography, mass spectroscopy, and chemical analysis by the techniques developed by Merrill (3, 18). Their data show that decomposition occurs via a three-stage process. The first stage is endothermic and commences with the evolution of ammonia. Cobalt(III) is reduced to cobalt(II) and cleavage of the tetrazole group occurs producing nitrogen. The second stage is exothermic and commences at 286°C. Reaction of perchlorate ion with ammonia and partial oxidation of the cyanotetrazole occur. This stage occurs in parallel with the first stage. In the final stage, additional undetermined redox reactions, consecutive to those in the other stages, take place.

Aging and compatibility studies have been in progress for 3 years. Massis and coworkers (19) have shown that, over that time period, the formation of Co(II) at or below 80°C is nominally ≤ 800 ppm and is not significantly greater than that obtained at room temperature. Storage at 120°C, however, has resulted in ~ 2.5 percent conversion. Typical materials of igniter construction (alumina, kovar, and nichrome) have shown no evidence of corrosive attack when examined via scanning electron microscopy.

Physical thermal properties are also under investigation. Collins (16) has determined the heat capacity of CP via differential scanning calorimetry. Over the temperature range 80-180°C, it is given by the equation

$$C_p = 0.1545 + 0.0003T \quad ,$$

where T is the Kelvin temperature and C_p is the heat capacity in cal/g-K. The coefficient of thermal expansion has been determined by Massis (16) via thermal mechanical analysis of pressed pellets. Values range from 52×10^{-6} mm/mm-°C for the range -50 to -25°C up to 66×10^{-6} mm/mm-°C for the range 100 to 125°C. The room temperature value is 60×10^{-6} mm/mm-°C.

IV. DDT PHYSICS

A. Goals

To understand the behavior of CP as a DDT material, a number of theoretical and experimental studies have been undertaken. The ultimate objective is to develop a model capable of estimating growth to detonation behavior for specified configurations, densities and initiation stimuli. To support this modeling effort, experiments are

being conducted with CP to measure 1) the shock characteristics of unreacted material, 2) the detonation parameters, 3) the equation of state for the reaction products, and 4) the characteristics of the transition to detonation. In the following sections, the results of these studies are discussed.

B. DDT Modeling

Krier and Gokhale (26) have developed a model based on a reacting, two-phase flow. The model was originally developed for study of growth to detonation in granular propellants. The solid material is treated as a compressible porous bed through which the hot gaseous reaction products can flow. Thus, energy is transferred ahead to the unburned region by convection and by mechanical deformation. Arrhenius kinetics are assumed and accelerating reactions are predicted. Present work is directed toward incorporation of this model into an existing wave propagation computer code.

C. Shock Hugoniot for Unreacted CP

As part of the input to the model, it is necessary to provide the shock compression characteristics of the unreacted material. These characteristics have been obtained by Lee (27) in a series of controlled, planar impact experiments (see Figure 3). The projectile contained a quartz stress gauge to monitor the stress at the impact interface. The initial jump in stress upon impact, the measured impact velocity, and the known characteristics of the impactor buffer material permit computation of a point on the Hugoniot for the explosive sample. Subsequent output from the gauge revealed induction time to initiation for step input stress to the CP sample.

The experiments were performed using porous CP samples at 72 and 82 percent TMD. The resulting Hugoniot information is summarized in Figure 4 which shows the data plotted in the stress-particle velocity plane. The corresponding shock velocity-particle velocity relationship are

$$u_s = 0.49 + 2.26 u_p \quad (u_p < 0.5)$$

for an initial density of 1.47 Mg/m^3 , and

$$u_s = 0.54 + 3.57 u_p \quad (u_p < 0.7)$$

for an initial density of 1.66 Mg/m^3 .

u_s and u_p are shock velocity and particle velocity, respectively, in km/s. For stresses above about 2-3 GPa, initiation was so prompt that unreacted Hugoniot data could not be observed.

Substantial effects due to initial porosity were expected and observed. Shock loading of porous materials has been studied extensively (28, 29) in inert materials and found to result in much larger internal energies than for non-porous samples of the same materials, compacted at the same pressure. The excess internal energy was considered by Hayes and Mitchell (30) to be concentrated in the vicinity of the initial pores. These regions then become the "hot spots" where ignition occurs. The porous material description developed by Sheffield and coworkers (31) for HNS is being applied to develop the mechanical description of CP.

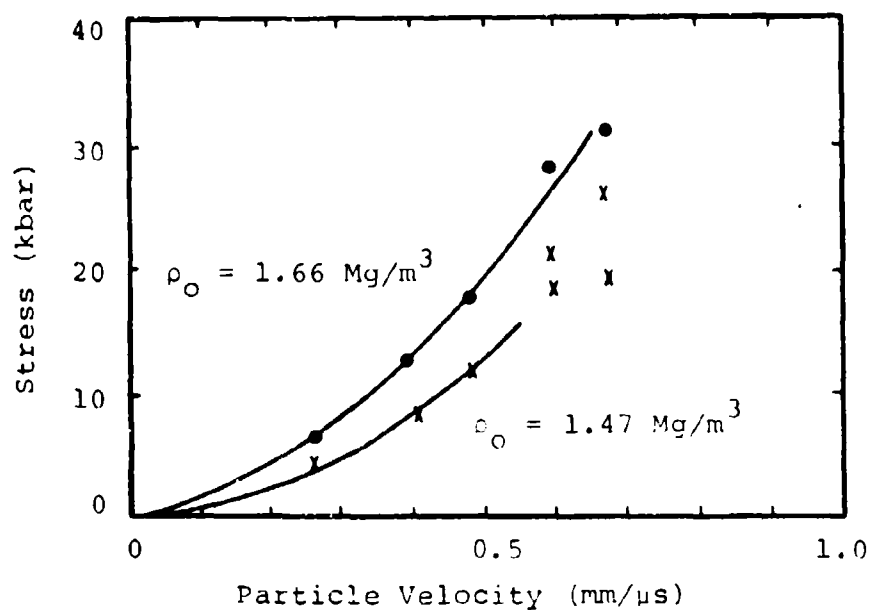


Figure 4. Stress-particle velocity Hugoniot data for porous CP explosive.

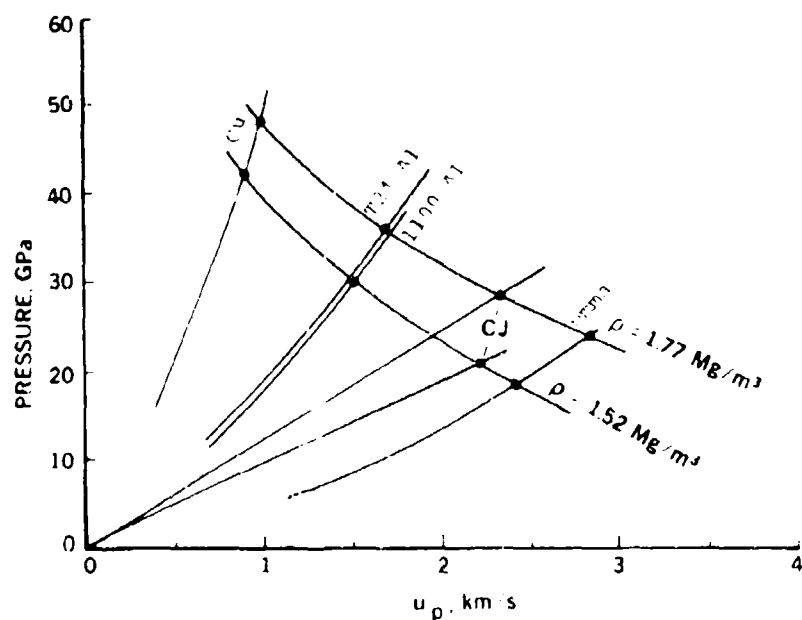


Figure 5. Reshock Hugoniot and release adiabat data for CP to obtain CJ pressure.

D. Detonation Parameters

The detonation velocity and pressure of CP have been measured in several independent tests. The detonation velocity in a confined, 6.35 mm diameter sample is given by West (32) as

$$D^* = 0.868 + 3.608 \rho_0$$

where velocity is in km/s and ρ_0 is CP initial density in Mg/m^3 .

The detonation pressure has been obtained by Stanton (33) using VISAR (34) velocity interferometric techniques to measure the particle velocity imparted to thin samples of aluminum, copper, and polymethyl methacrylate. Those results, shown in Figure 5, yield the release adiabat below, and the recompression Hugoniot above, the CJ point for two initial densities of CP. A straight line from the origin having slope $\rho_0 D^*$ intersects the curve at the CJ point. Indicated CJ pressures are about 28 GPa and 21 GPa for initial densities of 1.77 and 1.52 Mg/m^3 , respectively.

E. Reaction Product Equation of State

Cylinder expansion tests by West (32) give the measured velocity of a thin copper cylinder wall as a function of time after a detonation sweeps down the explosive charge contained in the cylinder. The data will be fit to a model from which the parameters for the reaction products will be obtained.

These tests indicate that CP is intermediate in strength in terms of its Gurney energy (35) or ability to accelerate metal. At TMD, the Gurney energy would be

about 3 MJ/kg, which compares with 4.44 and 2.81 MJ/kg for HMX and TNT, respectively.

F. Characteristics of the Transition to Detonation

The transition from deflagration to low order detonation and on to high order detonation occurs very rapidly in CP. Streak camera techniques have been used by Igel (17) to observe the transition in samples loaded into transparent assemblies in both flat disc and long cylinder configurations. Ignited from a hot wire, the deflagration phase, if present at all, lasts only a few microseconds. A rapid transition to low velocity detonation occurs for samples in the density range of 1.3 Mg/m³ and greater. The low velocity detonation proceeds at velocities in the range of 0.75 to 1.2 km/s, with the higher velocities obtained in higher density samples.

The low velocity detonation abruptly transitions to high velocity detonation after a run distance which varies with initial density. At a density of 1.3 Mg/m³, the run distance is only 2-3 mm. At a density of 1.5 Mg/m³, the run distance is thought to be in excess of 15 mm. Further work is in progress to define these transitions as a function of density.

V. ENGINEERING CONSIDERATIONS

A. Design Factors

A schematic illustration of a detonator is given in Figure 6. The igniter is attached to a steel housing. The explosive CP is loaded in the igniter, transfer column, and output regions in a series of increments. Different loading pressures and/or particle sizes may be utilized in the three regions to affect performance

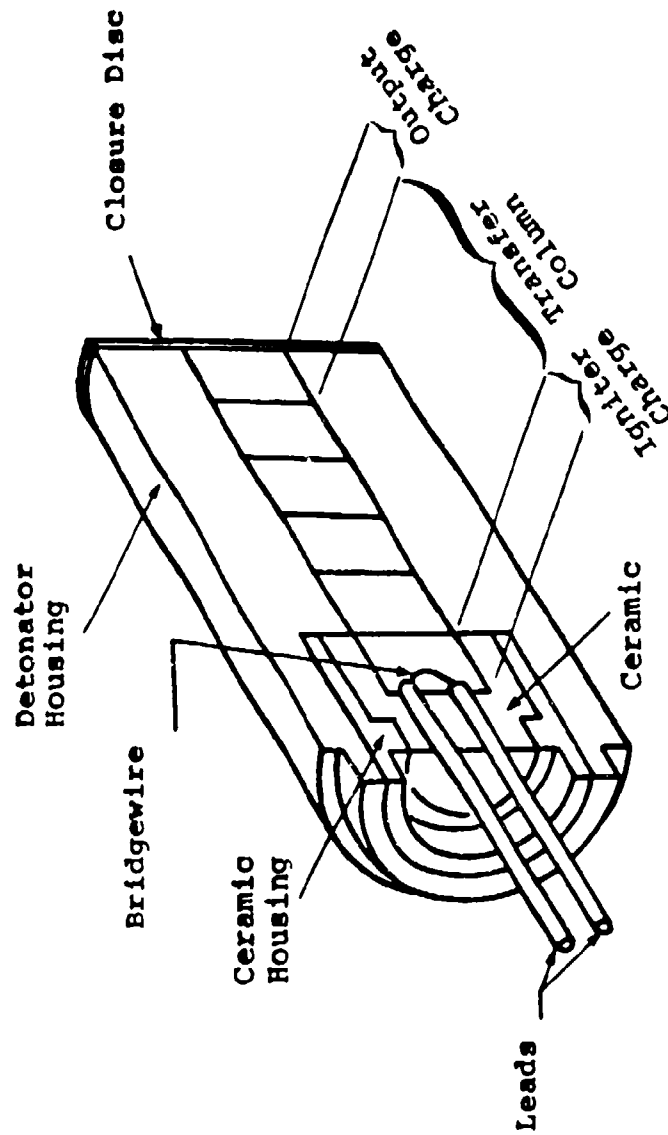


Figure 6. Generalized CP Detonator Design

characteristics. Loading conditions in the igniter are selected to provide satisfactory ignition characteristics. Those in the transfer column are chosen to produce reliable transition from deflagration to detonation. An output charge loaded to greater density than that of the transfer column may exist in detonators which require an increased detonation output.

B. CP Lots

Because the CP synthesis process (10) includes a final particle size adjustment step, considerable variation in particle size distribution can be deliberately introduced. Figure 7 shows optical photomicrographs that illustrate the extent of variation obtained. Lot A is typical of those lots being incorporated in production detonators. The individual particles consist of agglomerates of many smaller crystals. Data for CP properties and performance presented in the report have been determined with such material except where otherwise noted.

C. Loading

The relationship between loading pressure and resultant density in smooth metal sleeves as determined by Laib (36) and by Munger and Seubert (37) is given in Figure 8. Using scanning electron microscopy, Colman has shown that at low loading pressures (5 kpsi, 34 MPa) the agglomerates are broken with minor breakage of individual crystals (38), while at a pressure of 10 kpsi major fracturing of individual crystals occurs (16). No significant increase in fracturing is observed at pressures up to 40 kpsi.

Figure 7. Photomicrographs of CP lots.



LOT A



LOT B



LOT C



LOT D



LOT E



LOT F

MAGNIFICATION 100X SCALE --- 100 μ

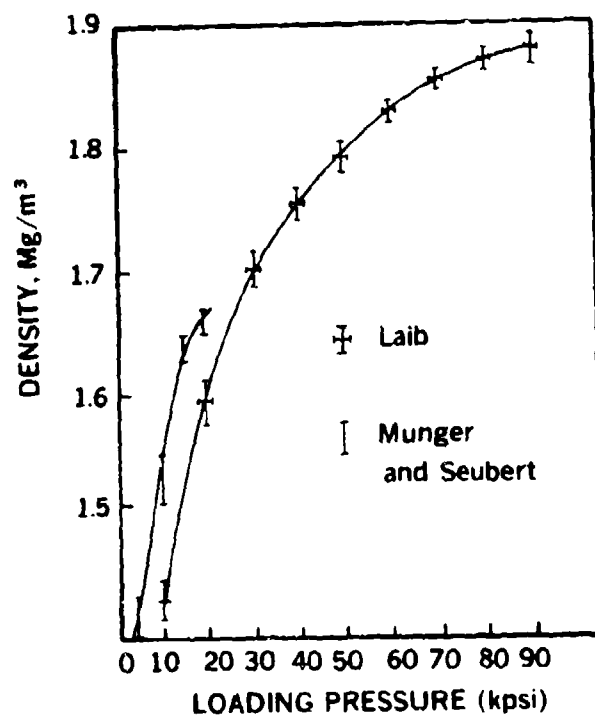


Figure 8. Density of CP in metal sleeves as a function of loading pressure.

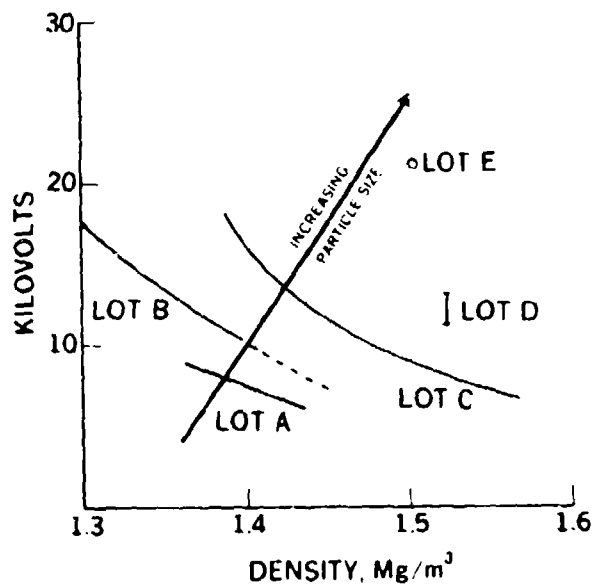


Figure 9. Electrostatic discharge sensitivity of CP as a function of particle size.

D. Electrostatic Discharge

The determination of ignition sensitivity to electrostatic discharge (ESD) is determined by discharging a 600 pF capacitor charged to a preselected voltage through a 500 ohm resistor in series with the test material. Loose powder and unconfined pellets of CP are not ignited by the human body equivalent electrostatic discharge (20 kV, 600 pF, 500Ω). For pellets confined in a metal sleeve, however, the ignition sensitivity to ESD has been found to initially increase (decreasing voltage) sharply with increasing density and decreasing particle size (Figure 9) (9, 15). Fronabarger and Heckes have shown that various degrees of densensitizing can be achieved through the use of additives (8). Recent work given in Figure 10 establishes that the sensitivity of CP initially increases but then decreases as the density is increased (1). Figures 9 and 10 coupled with the microscopy obtained as a function of loading pressure (Section V. C) suggest that the initial increase in sensitivity with increasing density is simply due to a decreasing particle size effect. The subsequent decrease in sensitivity with further increases in density is surmised to reflect the increasing effect of the dielectric strength of the explosive. The U-shaped sensitivity curve (Figure 10) is the net result of these two independent effects.

E. Shock Sensitivity

One measure of the impact sensitivity of an explosive is the run distance to detonation after a sample is subjected to step shock. This run distance depends upon the amplitude of the shock. Lee (27) has measured step shock response for two densities of CP and the results

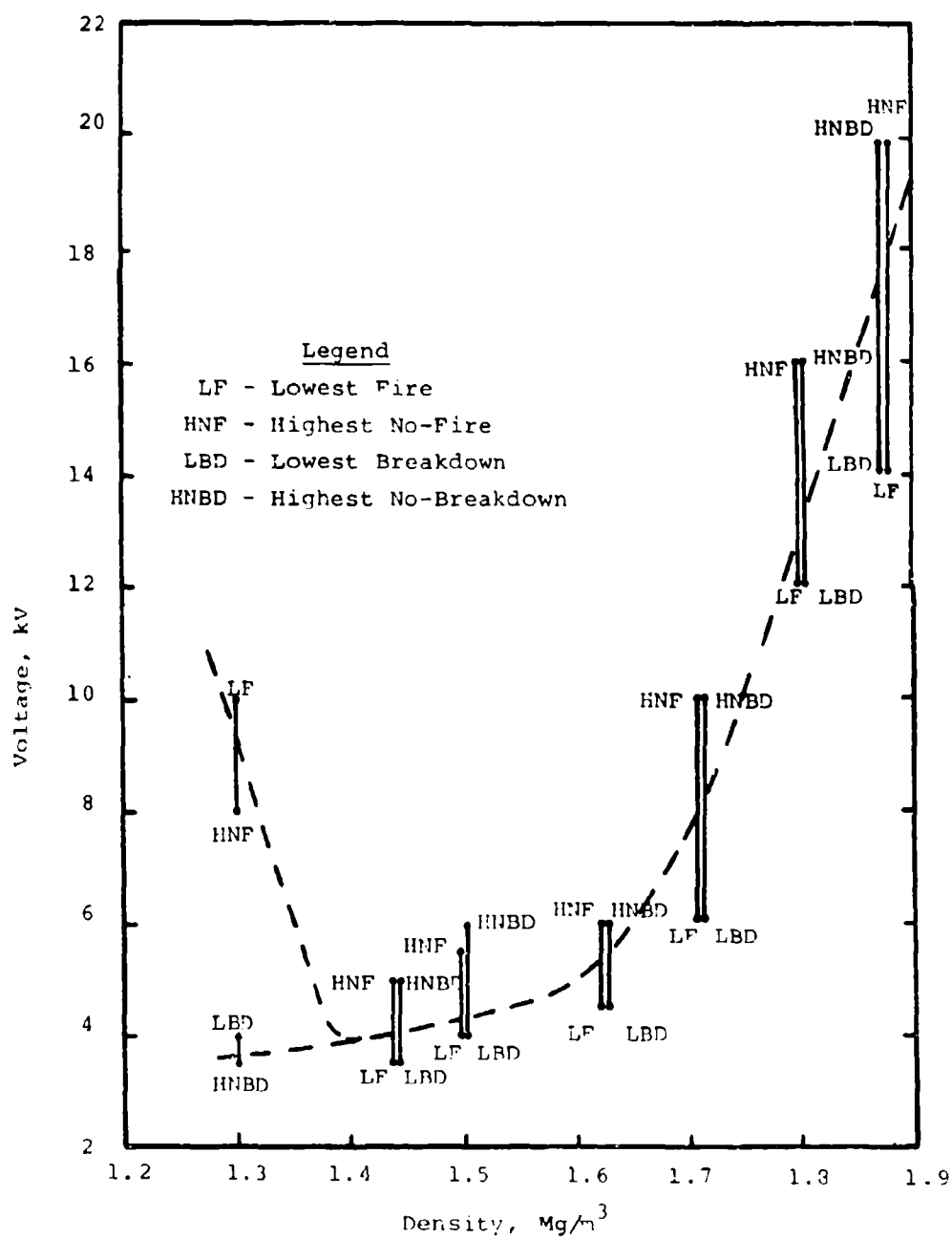


Figure 10. Electrostatic discharge sensitivity of CF as a function of density.

are shown in Figure 11 in comparison with some other common explosives. Based on this measure, CP is comparable in shock sensitivity to PETN.

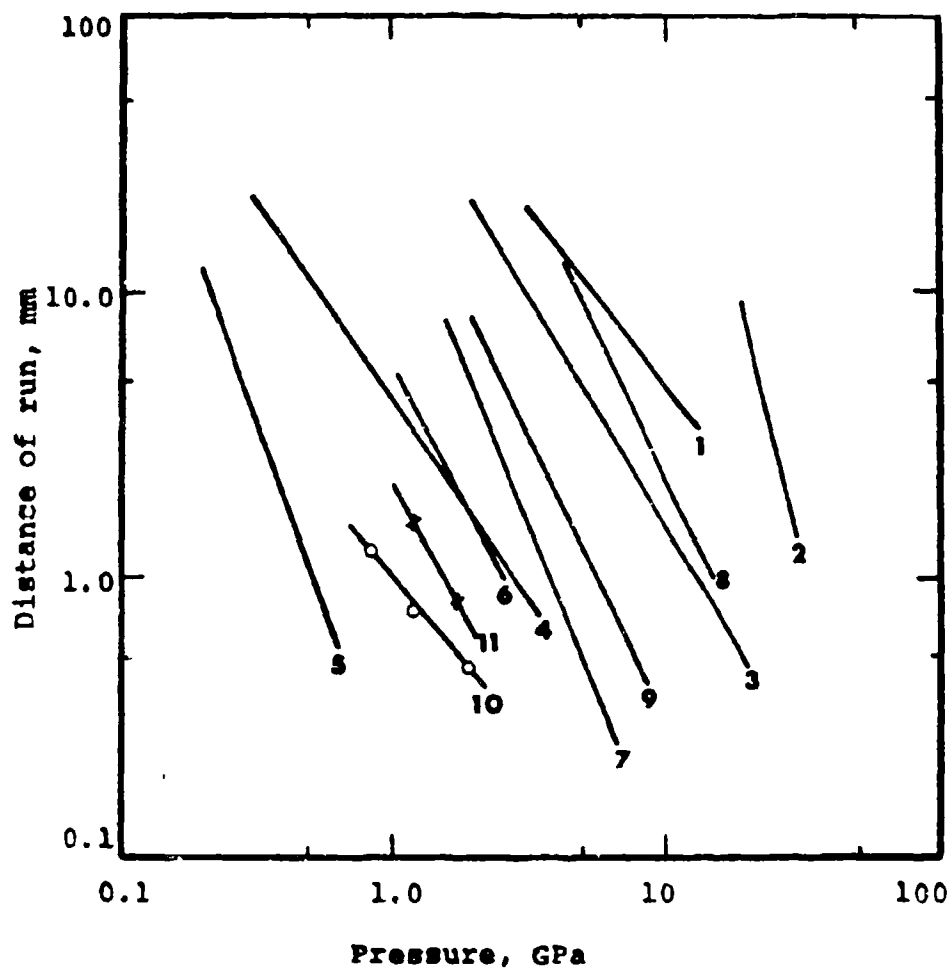
F. Thermal Ignition

Ignition of CP in detonators is performed via hot wires. The effect of powder particle size on the energy required for ignition is shown in Figure 12. These data show that reliable ignition at low energy is favored by small particle size and relatively high density. While the particle size used in a given detonator is normally held constant, the density in the igniter is maintained at a high value relative to that in the transfer column. A typical igniter (1 Ω , 0.051 mm diameter Tophet A bridgewire) sensitivity curve is shown in Figure 13.

Laser initiation of CP has also been investigated. With a ruby laser, a 50 percent initiation threshold was obtained at 0.03 J/mm² and the no-fire level was 0.01 J/mm². Davies (39) obtained an initiation threshold of 0.25 J/mm² (1.0 mm diameter, 630 μ s pulse) with a neodymium laser.

G. Empirical DDT and Output Studies

Leslie, Dietzel and Searcy (2) examined the DDT characteristics of an early lot of CP. Results of their studies, Figure 14, established that growth to detonation occurs readily at relatively low densities (<1.5 Mg/m³) and that it does not occur under comparable conditions at higher powder densities (>1.7 Mg/m³). An ongoing study by Schaeffer (40) has confirmed that current production-type CP lots behave similarly. As a result, detonators are designed to have transition charges of 1.5 Mg/m³ density.



Curve No.	Explosive	ρ (Mg/m ³)
1	Comp B	1.72
2	NQ	1.69
3	PBX-9404	1.83
4	PBX-9407	1.60
5	PETN	1.0
6	PETN	1.60
7	PETN	1.72
8	TNT	1.63
9	XTX-8003	1.53
10	CP	1.44
11	CP	1.65

Figure 11. Log-Log plots of distance of run to detonation vs. initial shock pressure of various explosives. Data for materials other than CP are from the compilation of Dobratz (42).

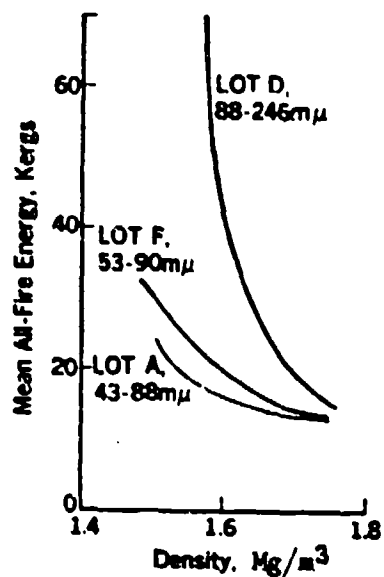


Figure 12. Hot wire ignition sensitivity of CP as a function of density.

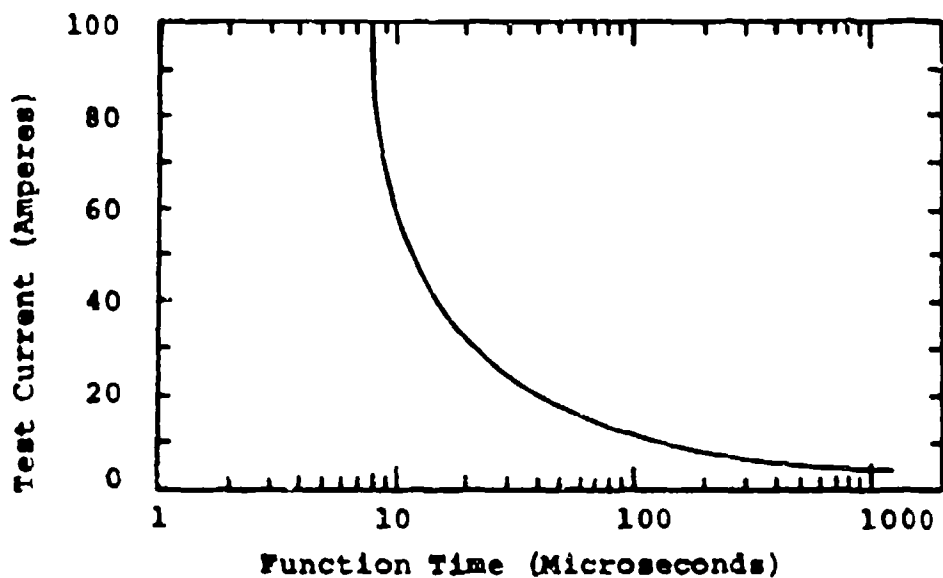
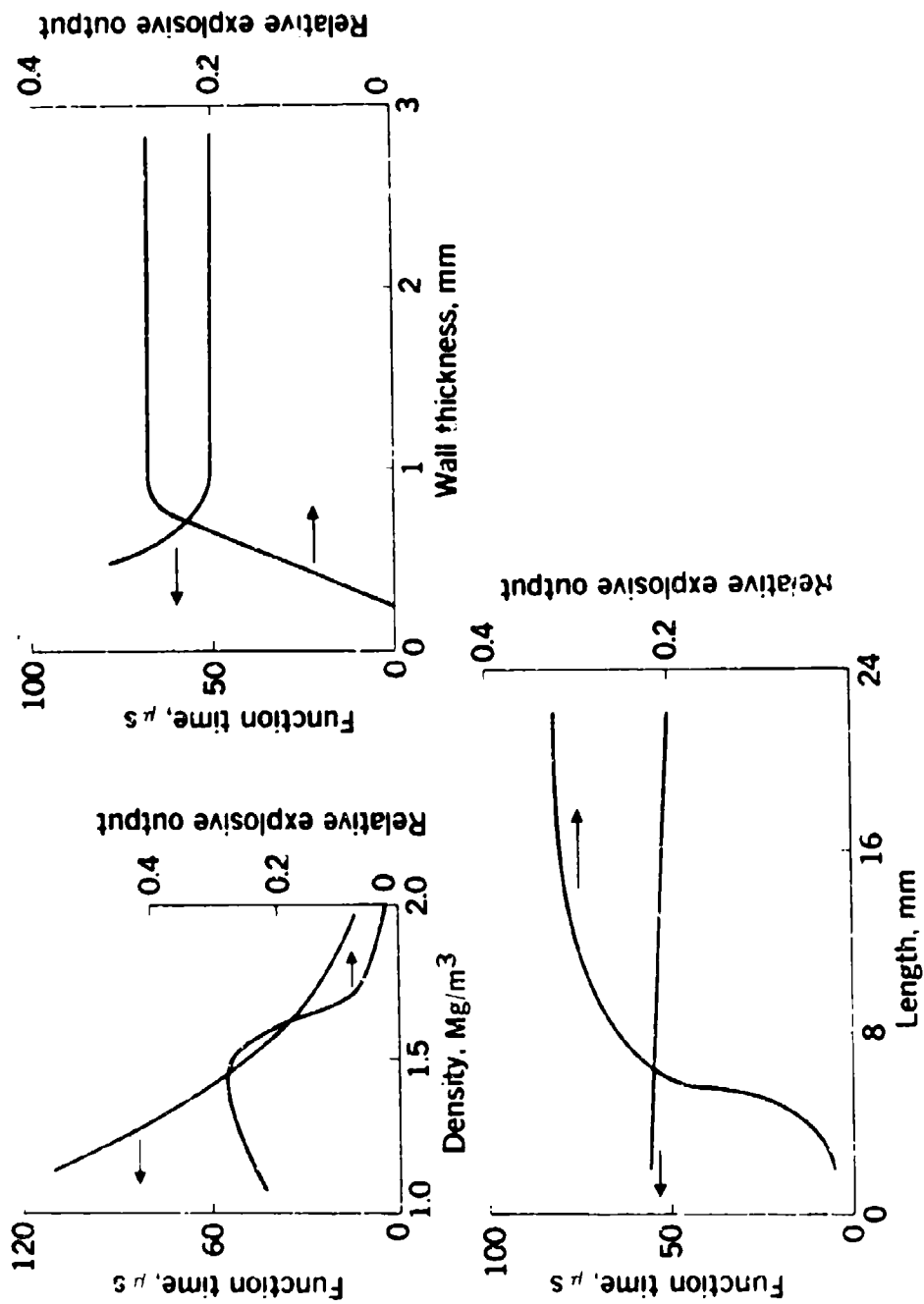


Figure 13. Typical hot wire ignition sensitivity as a function of applied constant current.

FIGURE 14
TYPICAL PERFORMANCE CHARACTERISTICS
10A Firing Signal



The study by Leslie, et al (2) also examined the effects of confinement and column length on output for a powder density of 1.4 Mg/m^3 . They found that some minimal confinement is required to grow from deflagration to detonation and that a column length of $\sim 10 \text{ mm}$ is appropriate in the 1.9 mm diameter test units. A detonation subsequently developed by Lieberman, Villa, and Lause (41) incorporated a 5.97 mm transfer column of 2.95 mm diameter and 1.5 Mg/m^3 powder density which followed an igniter loaded to higher density. They also showed that increasing the density of the output column following the transfer column increased the resultant output.

An ongoing study of other high energy cobalt inorganic coordination compounds (17) has shown that DDT can be enhanced (shorter run distance) through the use of larger particle size material. Additional work is in progress to determine the particle size, density, and column lengths required to achieve a CP detonator of minimal size.

VI. SUMMARY

The status of the development of the explosive CP for DDT devices has been reviewed. A variety of studies dealing with the chemistry, thermal properties, DDT physics, and component engineering have been completed, while others are currently in progress.

VII. REFERENCES

1. J. W. Fronabarger, unpublished work performed at Uni-dynamics Phoenix, Inc. under Sandia Laboratories contracts.
2. W. B. Leslie, R. W. Dietzel, and J. Q. Searcy, "A New Inherently Safe Explosive for Low Voltage Detonator Applications", Sixth Symposium (International) on Detonation, San Diego, CA, August 1976.
3. R. M. Merrill, "Chemical Analysis Technique for the Determination of Chloride, Ammonium, and Cyanide in the Explosive, 5-Cyanotetrazolatopentaamminecobalt(III) Perchlorate (CP)", Sandia Laboratories Report SAND77-1899, March 1978.
4. E. J. Graeber and B. Morosin, "Secondary Explosive, 5-Cyanotetrazolatopentaamminecobalt(III) Perchlorate", presented at the Am. Cryst. Assn., U. of Oklahoma, Norman, Oklahoma, March 19-24, 1978.
5. R. G. Jungst and P. K. Peterson, "Analysis of Amide Complex Impurity in CP Explosive by Infrared Spectroscopy", Sandia Laboratories Report SAND78-1395, August 1978.
6. H. S. Schuldt, "CP Compatibility/Reliability: Part I March 1977", Sandia Laboratories Report SAND77-1420, August 1978.
7. J. Q. Searcy and K. L. Shanahan, "Thermal Decomposition of the New Explosive 2-(5-Cyanotetrazolato)pentaamminecobalt(III) Perchlorate", Sandia Laboratories Report SAND78-0466, August 1978.
8. J. W. Fronabarger and A. A. Heckes, "Summary Report on Desensitizing CP Explosive to Electrostatic Discharge via Additives", Sandia Laboratories Report SAND77-2133, October 1978.
9. M. L. Lieberman and J. W. Fronabarger, "An Overview of the Development of the Explosive 2-(5-Cyanotetrazolato)pentaamminecobalt(III) Perchlorate", presented at the ACS/CJS Chemical Congress, Honolulu, Hawaii, April 1-6, 1979.

10. W. Fleming, J. W. Fronabarger, and J. Q. Searcy, "Preparation of 2-(5-Cyanotetrazolato)pentaamminecobalt(III) Perchlorate, CP, A New Material for Detonator Applications", Am. Def. Prep. Assn. Mtg., Materials and Processing Division, Albuquerque, NM, May 15-17, 1979.
11. K. E. Bullock, A. R. Burke, and D. M. Colman, "Photo-acoustic Spectroscopy Applied to Problems in Explosives", presented at the Federation of Analytical Chemistry and Spectroscopy Societies Annual Meeting, Philadelphia, PA, September 1979.
12. E. J. Graeber and B. Morosin, "Crystal and Molecular Structure of an Amidine Chelate, 5- Amidinotetrazolato-tetraamminecobalt(III) Bromide", presented at the Am. Cryst. Assn., U. of Alabama, Eufala, Alabama, March 17-31, 1980.
13. M. L. Lieberman, ed., "Activities of the Deflagration-to-Detonation Transition Project: Quarterly Report for the Period September Through November 1978", Sandia Laboratories Report SAND79-0837, April 1979.
14. M. L. Lieberman, ed., "The Deflagration-to-Detonation Transition Project: Quarterly Report for the Period December 1978 Through February 1979", Sandia Laboratories Report SAND79-1267, June 1979.
15. M. L. Lieberman, ed., "The Deflagration-to-Detonation Transition Project: Quarterly Report for the Period March 1979 Through May 1979", Sandia Laboratories Report SAND79-1952, October 1979.
16. M. L. Lieberman, ed., "The Deflagration-to-Detonation Transition Project: Quarterly Report for the Period June Through August 1979", Sandia Laboratories Report SAND80-0230/1, January 1980.
17. M. L. Lieberman, ed., "The Deflagration-to-Detonation Transition Project: Quarterly Report for the Period September Through November 1979" Sandia Laboratories Report SAND80-1157, to be published.
18. R. M. Merrill, "Spectrophotometric Determination of Co(II) in the Presence of the Coordination Compound, 2-5-Cyanotetrazolato-Pentaamminecobalt(III) Perchlorate (CP)", Sandia Laboratories Report SAND79-0653, to be published.

19. T. M. Massis, P. K. Morenus, D. H. Huskisson, and R. M. Merrill, "Stability and Compatibility Studies with the Inorganic Explosive 2-(5-Cyanotetrazolato)pentaamminecobalt(III) Perchlorate (CP)", to be presented at the Am. Def. Prep. Assn. Joint Symp., ADPA Chemicals and Plastics Section of the Materials and Processes Division, Radford Arsenal, Radford, VA, October 14-16, 1980.
20. R. A. Henry, Naval Weapons Center, China Lake, CA 93555, private communication.
21. L. L. Gerchman, unpublished work performed at SRI International under Sandia Laboratories contract.
22. L. Carey, unpublished work performed at SRI International under Sandia Laboratories contract.
23. R. G. Dosch, "Determination of Perchlorate by Precipitation with Tetra-n-pentylammonium Bromide", Anal. Chem. 40, (4) 829 (1968).
24. A. I. Vogel, "Quantitative Inorganic Analysis", Longmans, Green and Co., New York (1951), p. 524.
25. F. Feigl, "Spot Tests in Inorganic Analysis", Elsevier Publishing Co., New York (1958), p. 328.
26. H. Krier and S. S. Gokhale, "Modeling of Convective Mode Combustion Through Granulated Propellant to Predict Detonation Transition", AIAA Journal, 16, 1978, pp. 177-183.
27. L. M. Lee, unpublished work performed at Ktech Corporation under Sandia Laboratories contract.
28. K. K. Krupnikov, M. I. Brazhnik, and V. P. Krupnikova, "Shock Compression of Porous Tungsten", Soviet Physics/JETP, 15, 470 (1962).
29. W. Hermann, "On the Dynamic Compaction of Initially Heated Porous Materials", Sandia Laboratories Report SC-DR-68-865, April 1969.
30. D. B. Hayes and D. E. Mitchell, "Shock Sensitivity of Porous HNS Explosive", Sandia Laboratories Report SAND77-1363, December 1977.

31. S. A. Sheffield, D. E. Mitchell, and D. B. Hayes, "The Equation of State and Chemical Kinetics for Hexanitrostilbene (HNS) Explosive", Proceedings of Sixth Symposium (International) on Detonation, Coronado, California, August 1976.
32. G. T. West, unpublished work performed at Pantex under Sandia Laboratories contract.
33. P. L. Stanton, unpublished work performed at Sandia Laboratories.
34. L. M. Barker and R. E. Hollenbach, "Laser Interferometer for Measuring High Velocities of Any Reflecting Surface", J. Appl. Phys. 43, 11, 4669-4675, November 1972.
35. J. E. Kennedy, "Gurney Energy of Explosives: Estimation of the Velocity and Impulse Imparted to Driven Metal", Sandia Laboratories Report SC-RR-70-790, December 1970.
36. G. R. Laib, unpublished work performed at Naval Surface Weapons Center.
37. A. C. Munger and N. J. Seubert, unpublished work performed at Mound Facility.
38. D. M. Colman, unpublished work performed at Mound Facility.
39. F. W. Davies, the Boeing Company, private communication.
40. D. R. Schaeffer, unpublished work performed at Mound Facility.
41. M. L. Lieberman, F. J. Villa, and A. Lause, unpublished work performed at Sandia Laboratories and at Unidynamics Phoenix, Inc., under Sandia contract.
42. B. Dobratz, "Properties of Chemical Explosives and Explosive Simulants", Lawrence Livermore Laboratory Report UCRL-51319, Rev. 1, July 31, 1974.

VISAR STUDIES OF A REEFING LINE CUTTER

By

Morton L. Lieberman
Sandia National Laboratories
Albuquerque, NM 87185

and

Russell S. Wilson
Systems, Science and Software
P. O. Box 1620
La Jolla, CA 92038

ABSTRACT

The VISAR has been used to study the output performance of a pyrotechnic-driven reefing line cutter. Velocity-time and displacement-time profiles were obtained during blade motion, both with and without the reefing line present. The data yielded measures of the utilization of the blade's momentum and kinetic energy. Units of two different designs were tested. Those that leaked gas yielded considerably lower kinetic energy and momentum values. The VISAR data also showed evidence that gas leakage in such units occurs prior to, or during, the initial several millimeters of blade displacement.

INTRODUCTION

Since the development of the Velocity Interferometer System for Any Reflector (VISAR) (1), the instrument has found considerable application in studies of the performance of pyrotechnic devices (2-8). Generally, these studies have addressed the development of valve actuators. This report describes the application of VISAR measurements to the development of a pyrotechnic-driven reefing line cutter.

EXPERIMENTAL

The reefing line cutter is illustrated in Figure 1. The actuator is loaded with boron/calcium chromate against the bridgewire, followed by titanium subhydride/potassium perchlorate (nominally 83 mg). The mass of the steel cutter blade is nominally 21 g. It is positioned over the actuator and the O-ring is designed to act as a gas seal during motion of the blade. Some free volume exists in the cavity between the actuator and the blade. A shear pin extends into the blade to prevent premature motion. During travel, the blade must completely cut the Kevlar reefing line and its confining two Teflon centering spacers.

Routine measurements performed during component development include time of initial blade motion (t_0), time of blade flight (t_f), and depth of dent in the aluminum back-up block (D). Values of t_0 and t_f are determined by breaking a pencil lead switch located in the hole of the body near the tip of the blade and by cutting a wire switch located between the reefing line and the aluminum block, respectively. The depth of dent provides a measure of output at the end of the stroke.

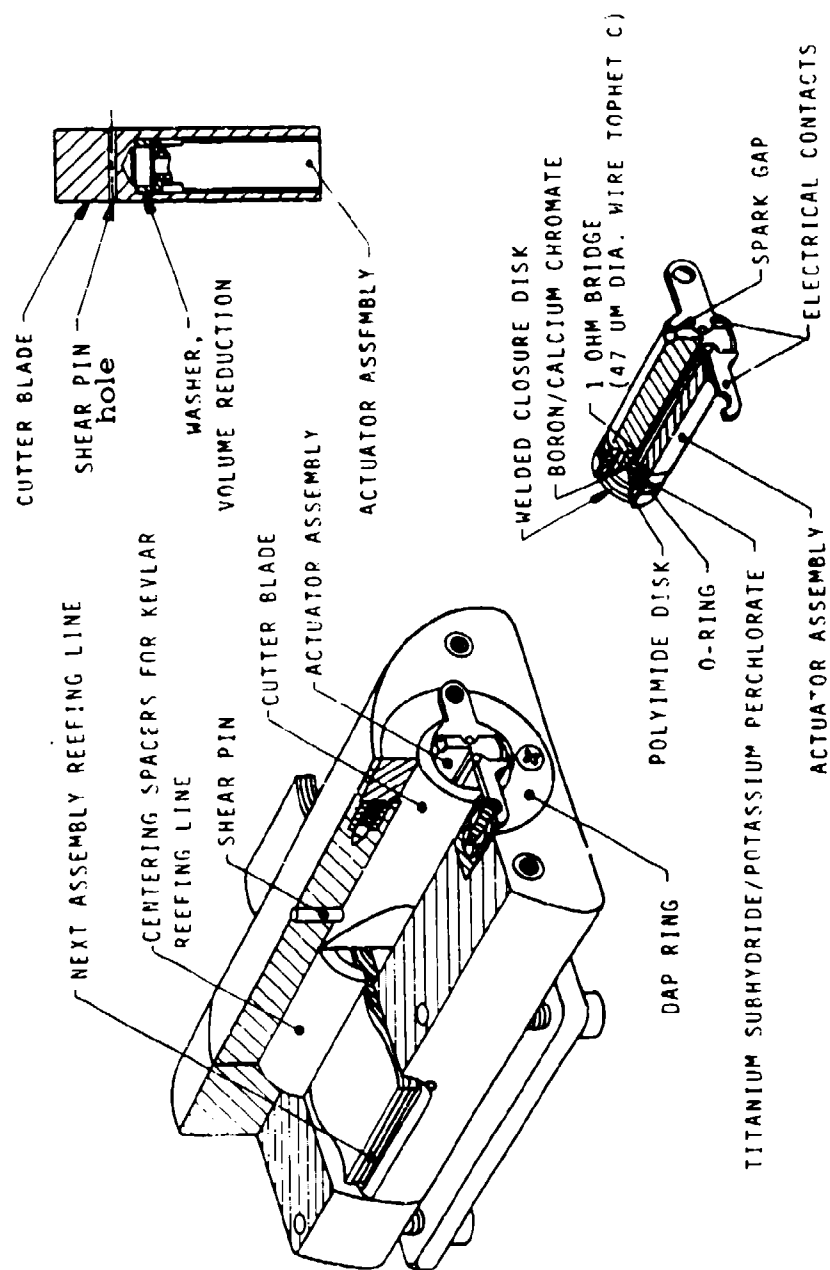


Figure 1. Reefing line cutter.

In order to perform VISAR measurements, units were specially modified. As shown schematically in Figure 2, a small hole was drilled in the wall of the blade for attachment by welding or brazing of a small diameter (1.0 mm), long (66.0 mm) kovar rod. The plastic connector that is attached behind the actuator and blade (not shown in Figure 1) was machined to accommodate the rod and minimize oscillations during motion. The opposite end of the rod was threaded so that a sandblasted, flat, aluminum part could be attached. The latter provided a diffuse surface for reflection of the VISAR laser beam during blade motion. The length of the rod extending beyond the plastic connector was sufficiently long to permit measurement of complete blade motion.

All tests of the specially modified units were performed at low temperature. Assembled units (without the diffuse reflectors) were conditioned at approximately -54°C for a nominal period of 2 hours prior to firing. The VISAR was pre-focused with a dummy unit. Then the test unit was removed from the temperature-controlled chamber, the reflector was attached, electrical connections were made, final focusing was performed, and the unit was fired. The reflector was not refrigerated in order to avoid condensation on the reflecting surface. The time elapsed between removal of the test unit from the temperature-controlled chamber and firing was nominally 5 minutes. For comparison purposes, tests were performed both with and without the reefing line and centering spacers present.

Two different designs of the reefing line cutter were tested. The first was that shown in Figure 1 with an O-ring lubricant of Dow-Corning No. 55 but without the shown volume reduction washer. The latter employed the soft silicone rubber volume reduction washer in the cavity between the actuator

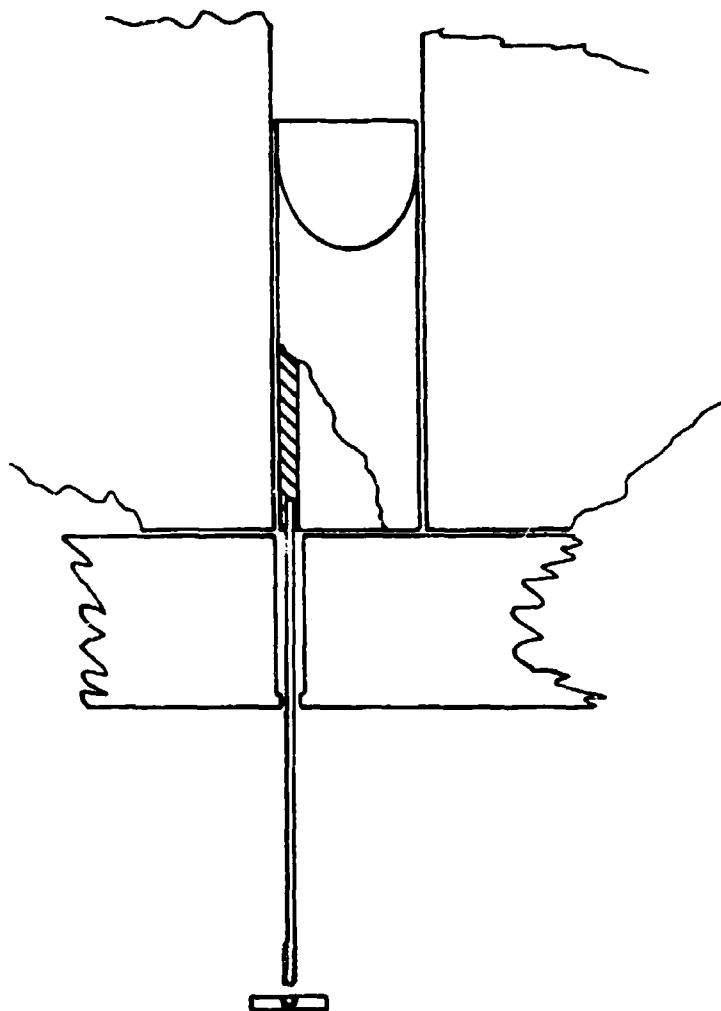


Figure 2. Cutaway drawing of modified reefing line cutter.

and the blade. This reduced the free volume by $\sim 70 \text{ mm}^3$ (~ 40 percent). In addition, this design incorporated a Super-O-Lube lubricant.

A VISAR has a sensitivity which is readily adjustable by means of a time delay built into the system. The original VISAR design used solid quartz etalons to provide the delay and was limited to sensitivities of approximately 100 m/s per fringe. The velocity of the reefing line cutter was less than this value and therefore a greater delay was required for adequate resolution. For this work, the VISAR was operated with a delay in air, a type which may readily be extended an order of magnitude longer than the delay available with an etalon. Two slightly different sensitivities were used. Tests of units of the first design were performed with a fringe constant of 29.2 m/s per fringe and for tests of the second design, 24.1 m/s per fringe. The necessary imaging in the delay leg of the interferometer was accomplished with a pair of identical lenses whose focal lengths were 330 mm for the initial tests and 400 mm for the later experiments. The velocity resolution obtained with these sensitivities is approximately 0.5 m/s.

The VISAR provided three channels of data: two velocity channels in quadrature (90° out of phase) and a beam intensity monitor to record variations in the light received by the VISAR from the moving target. The two quadrature channels are required to eliminate ambiguity in the sign of the acceleration which would otherwise exist at each maximum and minimum of the interference signal. This ability was essential for deciphering the oscillatory velocity data produced by the blade. An additional benefit of the quadrature technique is that it increases the average velocity resolution by providing continuous coverage with the high sensitivity

portion of the fringe signals, between the maximum and minimum, thereby eliminating the need to read data from the less sensitive region of the peaks.

The pulsed photo detectors normally used with the VISAR were replaced with continuous detectors to provide a recording window sufficiently long to capture data from the entire transit of the blade. This also eliminated the need to trigger the detectors, which would have been difficult to do with precision given the significant scatter seen in the function times.

All VISAR data were recorded on digital oscilloscopes having pre-trigger recording capability. The trigger signal was obtained from the breakage of a pencil lead placed directly in front of the blade. Since the detectors were continuously on, the pre-trigger feature permitted recording the initial motion of the blade while the shear pin was being cut. This was found to be a significant feature since the initial motion of the blade preceded the breakage of the pencil lead by a much longer time than expected.

A lens of 750 mm focal length was used to focus the laser beam on the target attached to the piston. This lens was moved 13 mm away from the target after the optics of the VISAR had been aligned, thereby minimizing the defocusing of the system as the blade moved through its approximately 26 mm long stroke. After the target moves back through the position of optimum focus there is a continuous reduction in the amplitude of the VISAR signals. Velocity data were obtained as long as the signal amplitude was great enough to provide an unambiguous record. This generally extended past the time of impact of the blade on the aluminum back-up block of the reefing line cutter housing so the velocity history

includes the deceleration of the blade and frequently its rebound from the end plate.

The displacement data were obtained from a numerical integration of the velocity data. In addition to providing a continuous position-versus-time record, these data also permit an independent check of the VISAR results to be obtained by comparing the measured displacement at the time of the wire fiducial with the known position of the wire.

RESULTS

Figure 3 shows VISAR data obtained for units of the first design (no volume reduction washer) both with and without the reefing line present during blade motion. In these and subsequent plots, the upper curve is the blade velocity (m/s) versus time (μ s) plot and the lower curve is the displacement (mm) versus time plot. The effect of the reefing line on the velocity profile is apparent. In its absence, the velocity increases smoothly in a near-exponential manner to a maximum value of 63 m/s. Some additional displacement of the blade occurs beyond the velocity maximum as it cuts into the aluminum block and comes to rest. With the reefing line present, a broad velocity maximum is observed. This is followed by a decreasing velocity during the latter portions of the blade motion. The maximum velocity is 46 m/s and the value at the surface of the aluminum block is only \sim 25 m/s. Clearly, a considerable decrease in the blade's velocity occurs as a result of cutting the reefing line. Kinetic energy of the blade is expended during the cutting process.

The velocity profiles of Figure 3 both exhibit peaks within the first millimeter of displacement. This phenomenon has been observed in all of the tests and is believed to be

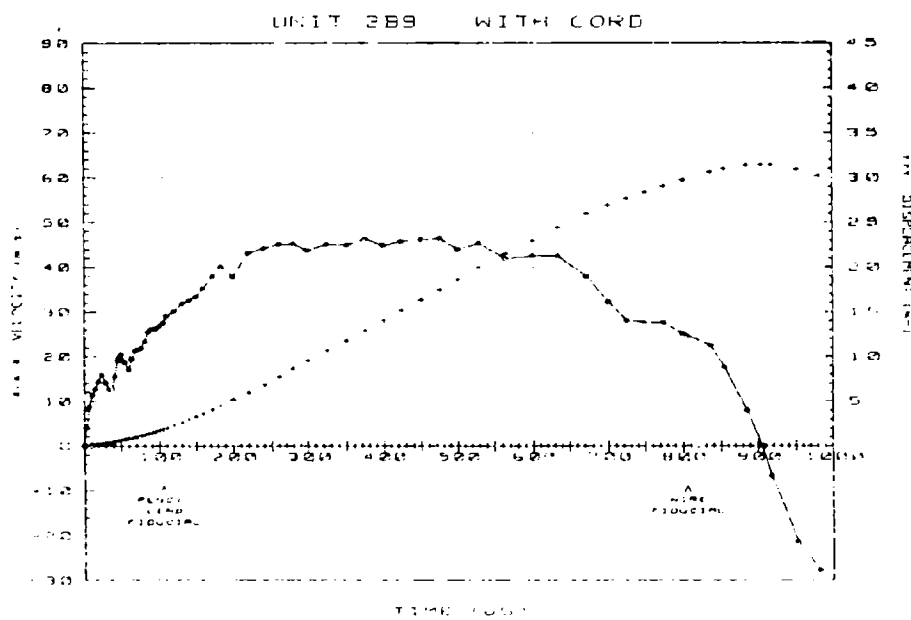
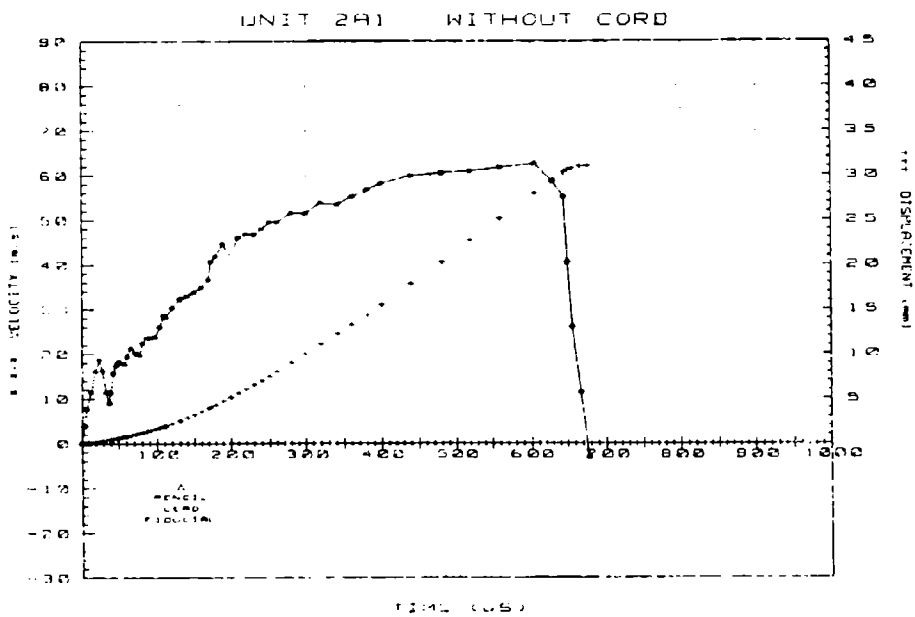


Figure 3. VISAR data from units of first design. Unit 2A1 without reefing line; Unit 2B9 with reefing line.

associated with cutting of the shear pin (diameter = 1.59 mm). Thus, the shear pin apparently limits early motion and has a measurable effect on the velocity profile.

Figure 3 also shows the fiducials associated with breaking the pencil lead and cutting the wire. Note that the VISAR-measured motion commences over 100 μ s prior to breakage of the pencil lead, which had previously been defined as the time of initial blade motion. The displacement profiles show that the blade travels a relatively short distance during this early period, i.e., the velocity, or slope of the curves, is relatively low in this period. Comparison of the profiles obtained with and without reefing lines also shows that the presence of the cord increases the time of blade motion by ~ 150 μ s.

Reefing line cutters of the first design were regarded as marginally satisfactory because of tests in which only slight dents were obtained in the aluminum block. Evidence existed that the O-ring seal did not prevent gas leakage. The second design (with changes in tolerances and assembly procedures) was adopted to alleviate that condition.

Figure 4 shows data obtained in two tests performed without the reefing line. The oscillations in the data are believed to be due to vibrational motion of the laser target superimposed on the net translational motion of the blade. Accordingly, these peaks are believed to represent only the motion of the target, not the motion of the overall blade. The profiles are virtually identical. Total blade motion occurs in 500 μ s compared to over 600 μ s in the first design. Final blade velocity is ~ 80 m/s compared to 63 m/s in the earlier case. Breakage of the pencil lead occurs after only 20 μ s compared to over 100 μ s in the first design.

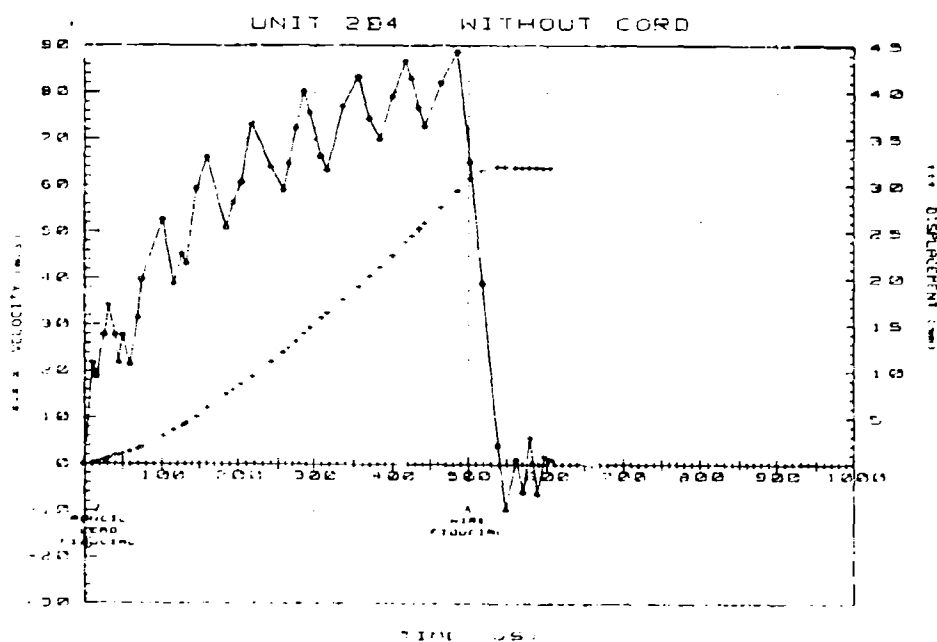
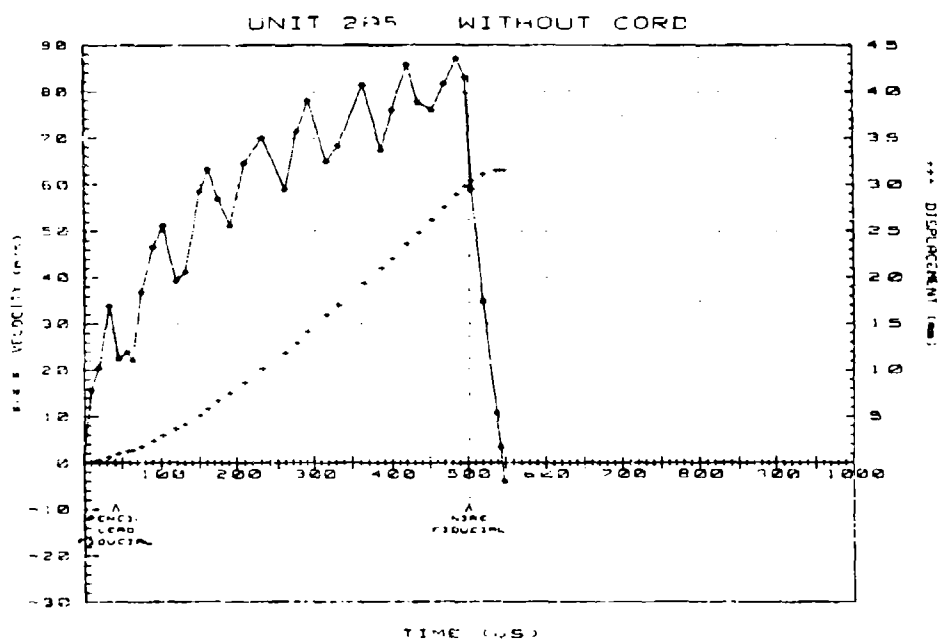


Figure 4. VISAR data from units of second design without reefing line.

Figure 5 shows VISAR data obtained in four tests performed with the reefing line present. The data are highly reproducible. A broad velocity maximum of ~ 60 m/s occurs in each case. Final velocities are nominally 40-50 m/s and total blade motion takes 530-610 μ s. All of these values exhibit output improvements over those obtained from the first design. Unlike units of the first design, none of later devices showed any evidence of gas leakage (i.e., displaced O-rings or smoke deposits on the exterior of the actuator).

Output comparisons for the eight tests are given in Figure 6. In (a)-(c) the circles and stars symbols represent tests of the first and second design, respectively. The parameters used are defined as follows:

- D = depth of dent in aluminum block,
- v_f = velocity of blade at time of wire fiducial,
- d = displacement of blade from initial position, and
- v_d = velocity of blade at displacement d.

The superscript zero is used to designate the value of a parameter obtained when the test was performed in the absence of the reefing line.

Figure (6a) shows the relationship between v_f and D. The curve is smooth and non-linear. The three greatest dents are for the tests performed without reefing lines. Note, however, that the units of the first design clearly produce outputs (v_f and D) that are considerably lower than those of comparable units of the second design. Good reproducibility of units in the latter group is again apparent from the dent values. The marginal nature of the first design is indicated by the extrapolation which suggests that a 20 percent reduction of v_f would yield no dent. This is shown further in

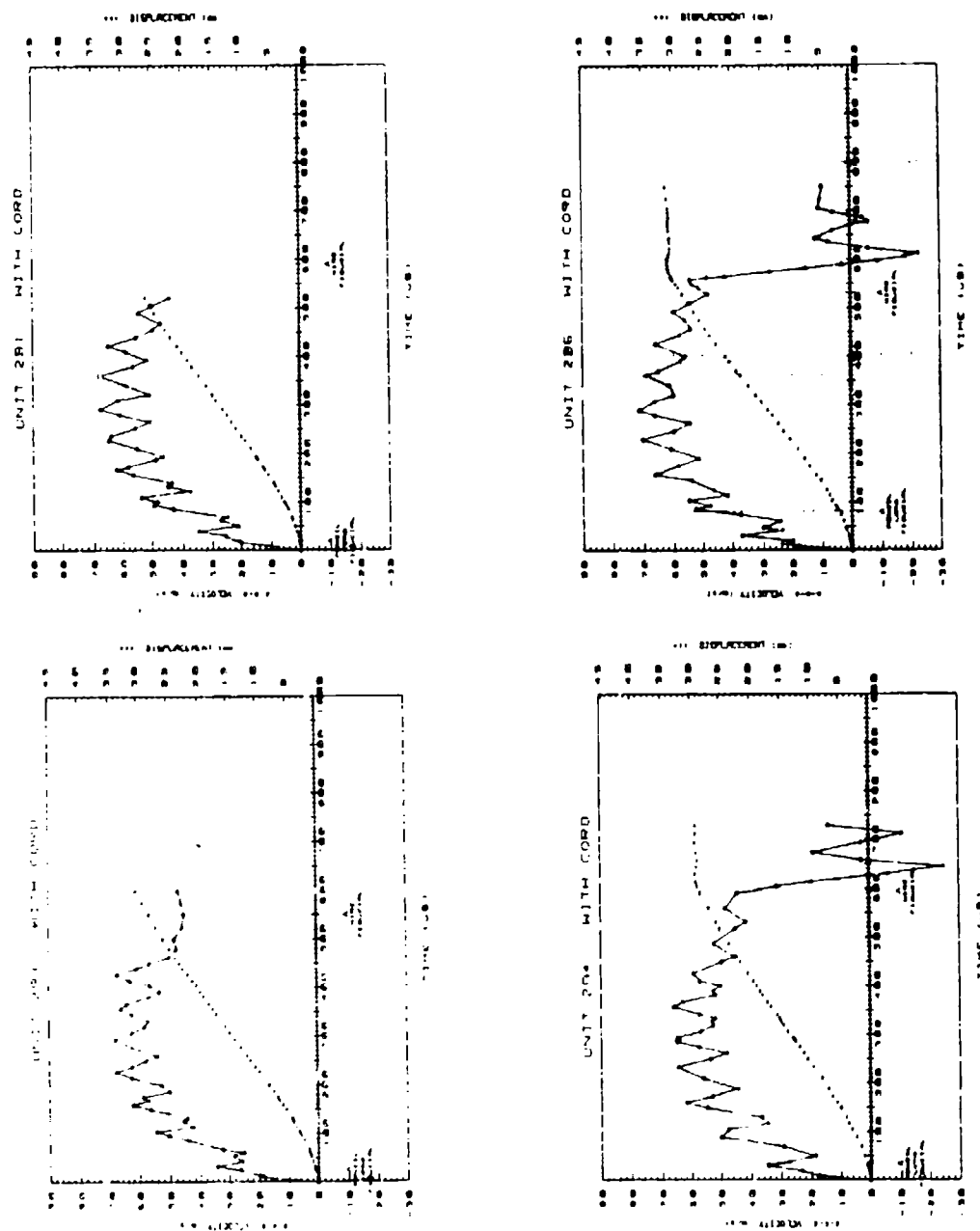


Figure 5. VISAR data from units of second design with reefing line.

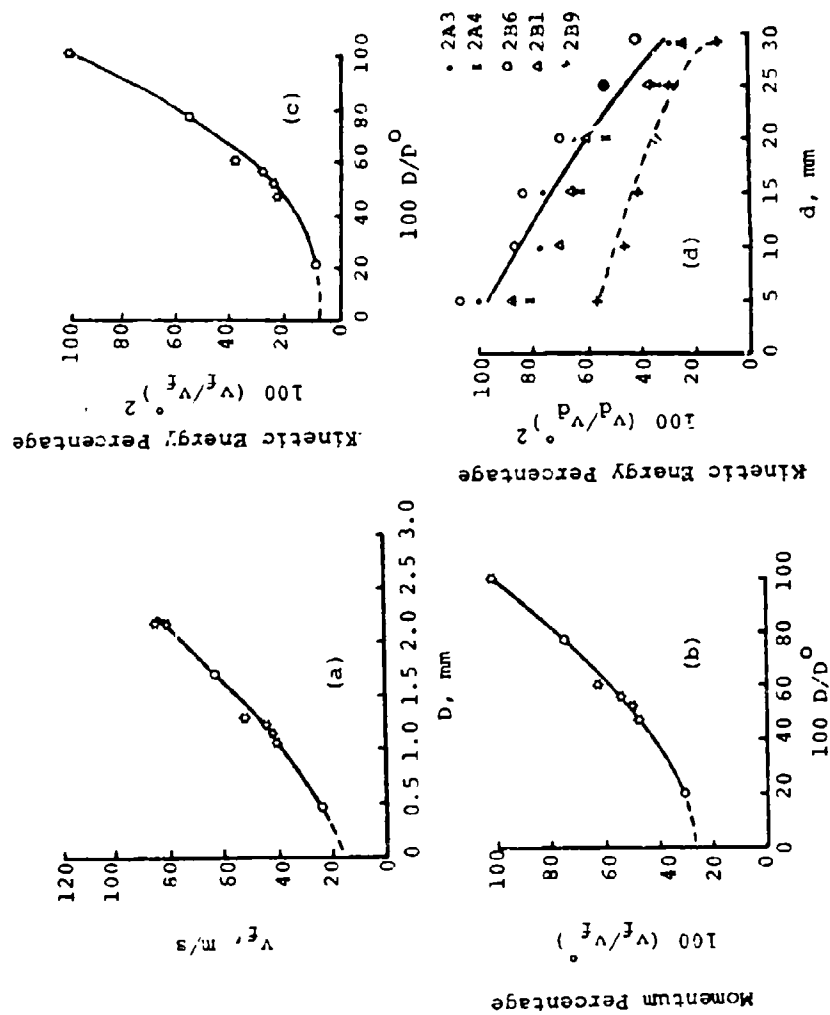


Figure 6. Output comparisons for the eight tests. In (b)-(d) velocities and dents are shown relative to the second design no-cord condition.

(b) and (c), where the percentages of momentum and kinetic energy, respectively, are plotted against the percentage of dent, all relative to the second design no-cord condition. From the latter curve it can be seen that the unit of the first design possessed only ~10 percent of the kinetic energy available from the actuator at the end of the stroke.

Figure (6d) shows the effect of displacement during cutting on the decrease in kinetic energy. Units of the second design are reasonably reproducible. The kinetic energy decreases in a smooth, possibly linear manner after the first 5 mm of displacement. The unit of the first design also shows a relatively linear relationship, except possibly at the end of the displacement. In this case, however, the kinetic energy values are considerably lower than those of the second design for all displacement values. This observation suggests that venting of units of the first design occurs prior to much, if any, motion. The previously noted relatively long elapsed times between VISAR-detected motion and breakage of the pencil lead for such units further supports this conclusion.

Previous work (7) has shown that for such actuators the motion of a projectile is given by the relation

$$P_{\max} = \frac{2Mv_a}{t_a A},$$

where P_{\max} = maximum gas pressure,

M = mass of projectile,

v_a = velocity of projectile at zero acceleration,

t_a = flight time corresponding to v_a , and

A = area over which the gas is driving the projectile.

For units of the second design, Figure 4 yields values of v_a and t_a . With the known hardware parameters of M and A, one finds that the maximum gas pressure is 97MPa (14 kpsi).

SUMMARY

A VISAR has been used to study the performance of pyrotechnic-driven reefing line cutters. Differences in design of the cutter have shown considerable differences in a variety of measured parameters. The detection of early motion by the VISAR suggests that major differences in performance result from gas leakage during that period.

ACKNOWLEDGEMENTS

The authors wish to acknowledge the support of D. L. Marchi and F. J. Villa of Sandia and D. Foltz of Unidynamics Phoenix, Inc., in designing, procuring, and fabricating the modified reefing line cutters.

REFERENCES

1. L. M. Barker and R. E. Hollenbach, "Laser Interferometer for Measuring High Velocities of Any Reflector Surface", J. Appl. Phys. 43, November 1972, p. 4669.
2. R. Ng, "VISAR Measurements of Velocities in Explosive Values", Sandia Laboratories Report SAND76-8048, December 1976.
3. R. Ng, "Measurement of Pressure Output Histories of Electroexplosive Devices", Proc. 9th Symp. on Explosives and Pyro., September 15-16, 1976, Franklin Institute, Philadelphia, PA.
4. M. L. Lieberman and K. M. Haskell, "Pyrotechnic Output of $TiH_x/KClO_4$ Actuators from Velocity Measurements", Proc. 6th Int'l Pyro. Seminar, July 17-21, 1978, Estes Park, CO.

5. R. Ng, "Experimental Determination of the Equation of State of Explosives and Pyrotechnics used in Explosive Actuators", Proc. 6th Int'l Pyro. Seminar, July 17-21, 1978, Estes Park, CO.
6. M. L. Lieberman and K. M. Haskell, "Pyrotechnic Output of $TiH_x/KClO_4$ Actuators: I. Analysis of VISAR Data", Sandia^xLaboratories Report SAND78-1687, September 1978.
7. M. L. Lieberman, "Pyrotechnic Output of $TiH_x/KClO_4$ Actuators: IV. Modelling of $TiH_x/KClO_4$ Actuator Pyrotechnic Output", Sandia Laboratories Report SAND79-0027, February 1979.
8. R. Ng, "Variable Explosive Chamber Test Results", Proc. 10th Symp. on Explosives and Pyro., February 14-16, 1979, Franklin Institute, San Francisco, CA.

CERTIFICATION TEST FOR THE FLUID BED SPRAY GRANULATION
PROCESS FOR THE PRODUCTION OF COLORED SMOKE MIXTURES

by

F. L. McIntyre

Computer Sciences Corporation
NASA National Space Technology Laboratories
NSTL Station, MS 39529

ABSTRACT

Violet smoke, red smoke and CS pyrotechnic mixtures were tested in accordance with Army Technical Pulletin 700-2 for both bulk and end-item configurations. The results of these tests indicate that they are a **probable Class 1.3** (formerly DoD Class 2). These same mixtures were tested during the manufacturing process in a new type mixing device known as the Fluid Bed Spray Granulation Process and found to generate minimal amounts of electrostatic energy during the mixing, graulation or drying process. Full-scale simulation tests utilizing mass quantities, 336 and 426 kg (740 and 940 lb), indicated that there were no mass detonation hazards during dynamic mixing conditions. There is no apparent difference in the degree of hazards as associated with large quantities of pyrotechnic mixtures using the fluid bed spray graunlation process. In fact, due to less handling requirements the hazards may be less than older conventional methods.

INTRODUCTION

BACKGROUND

Pine Bluff Arsenal (PBA) is a primary source of colored smoke signaling and screening devices for the Department of Defense (DoD). At the present time safety constraints limit the amount of pyrotechnic that can be blended in a single mixer to 45.4 kg (100 lb) because it is considered a hazardous material with a classification of 1.1 (formerly DoD class 7) during mixing and prior to consolidation in an end item. A daily production run requires approximately 907 kg (2000 lb) per day for each specific smoke device. To meet production requirements, it is necessary to use multiple blenders and then cross-blend so that appropriate batch sizes for daily production requirements can be met. PBA requested through the ARRADCOM Resident Operations Office at NSTL, MS, that a series of studies be conducted to investigate the use of new and improved mixing equipment, allowing the increase of batch sizes from 45.4 kg to 907 kg (100 lb to 2000 lb). Such studies (Ref. 1, 2, 3, 4 and 5) were undertaken over a period of several years and the results indicated that it was feasible to blend large quantities of colored and screening smoke without any increase in hazards. The quantity distance requirement based upon classification was changed from a 1.1 to a 1.3 (formerly DoD class 7 to 2). As a result of these studies, certification of 907-kg (2000-lb) batch sizes for HC smoke mixture and 454-kg (1000-lb) batch sizes for colored smoke were granted when blending was accomplished in the jet Airmix* blender.

During this same period, PBA was in the process of screening new and improved equipment to be utilized in the blending process that would further reduce potential hazards from dust and excess handling and reduce the number

*Trade name of Sprout-Waldron Company for a unit produced under a patent purchase from Grun, Lissberg, Germany.

of rejected batches. Pine Bluff Arsenal selected a new process known as the Fluid Bed Spray Granulation Process in which approximate batch sizes of 336 kg (740 lb) of colored smokes and CS pyrotechnic mixture could be blended, granulated and dried in a single process that would reduce dust hazards and allow for a reduction of personnel on the load assembly and pack (LAP) line. This system required the same certification tests that were conducted on the Jet Airmix system.

OBJECTIVE

The objective of this study was to determine the potential hazards associated with the Fluid Bed Spray Granulation Process (FBSGP) and determine if the process was safe for blending large quantities of colored smoke mixtures. However, formula changes were required in this process and these new formulas were to be classified in accordance with TB 700-2 on both the bulk mixtures and end-item munitions.

EXPERIMENTAL METHODS

MATERIALS

The mixtures considered for the certification program were: 1) M18 violet smoke, drawing no. B143-5-1 with a chemical composition of violet-dye 42%, sodium bicarbonate 24%, potassium chlorate 25%, and sulfur 9%; 2) 40mm red smoke, drawing no. B143-3-1 consisting of dye red 40.2%, potassium chlorate 31.3%, sulfur 12.3%, and sodium bicarbonate 14.3%; and 3) CS pyrotechnic mixture, drawing no. B143-14-7 consisting of CS agent 41.2%, potassium chlorate 27.8%, sugar 18.5%, and magnesium carbonate 12.3%. The binder solution consisted of approximately 85/15% water/dextrin which is added to the mixture once blending has occurred.

The mixtures were first blended in a pilot plant model, then bulk classification tests were conducted and, finally, the same formulations were blended in the full-scale production model for the full-scale simulation and end-item tests.

TEST PLAN

Bulk quantities of each of the pyrotechnic mixtures were tested in accordance with chapter 3, U.S. Army TB 700-2 which provides the requirements to assign hazards classification for bulk materials. These tests are designed to determine the ease of initiation and stability and include: 1) card gap test, 2) detonation test, 3) ignition and unconfined burning test, 4) impact sensitivity and 5) thermal stability tests.

End-item tests of each type of pyrotechnic device were tested in accordance with chapter 4 of U.S. Army Technical Bulletin 700-2 (Ref. 6) which provides for the requirement to assign hazards classification for end items. These tests include: 1) detonation test A, 2) detonation test B, and 3) external test C.

Mixing in the fluid bed spray granulation process (FBSGP) is accomplished by placing the desired quantity of constituents into the hopper, then positioning it over the lower air duct and pneumatically sealing it with the upper chamber. The ingredients are then blended in a fluidized bed for a specified time, followed by a shaking cycle to clean the filter bags and then a repeat of the blending cycle. Once the blending cycle is completed, the binder solution, water, is added at a specified rate until granulation is achieved. Drying is accomplished by blowing heated air, 65°C (150°F) for approximately 30-40 minutes. The hazards associated with this type of mixing were thought to include: 1) surface charge due to triboelectrification, 2) dust suspension at different concentrations, 3) high impingement velocities, 4) increased surface area for burning in this fluidized state and 5) mass effects of large quantities.

Electrostatic measurements were obtained in the WSG15 pilot model shown in figure 1 using 9.07 kg (20 lb) quantities and in the WSG300 full scale production model shown in figure 2, using 290 kg (640-lb) quantities. These measurements determined the amount of electrostatic energy generated during blending, wetting and drying cycles.

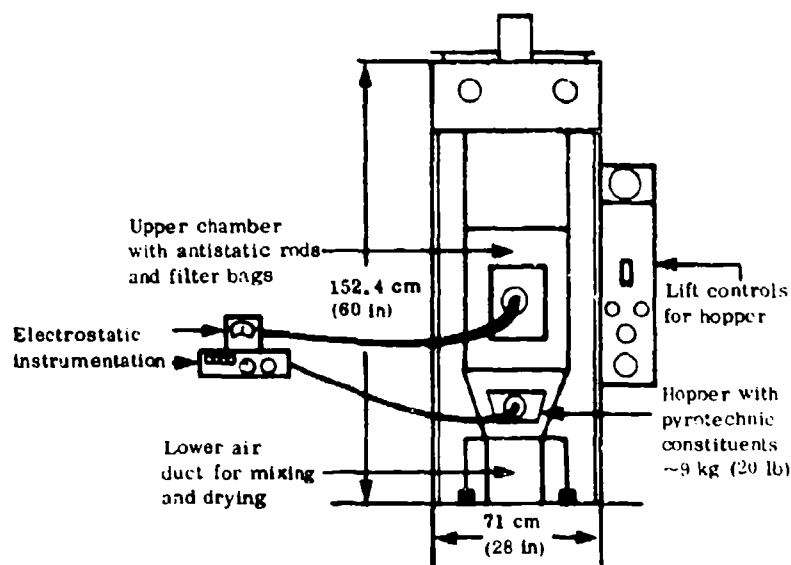


Figure 1. Plan View of WSG15 Pilot Plant Fluid Bed Spray Granulator

Full-scale simulation tests were performed to determine if mass detonation would occur during the blending cycle under dynamic conditions. The premixed compositions in 318-kg (700-lb) quantities were placed inside the simulator and ignited by a single hot spot ignition source while the mixture was being fluidized. The test setup is shown in figure 3.

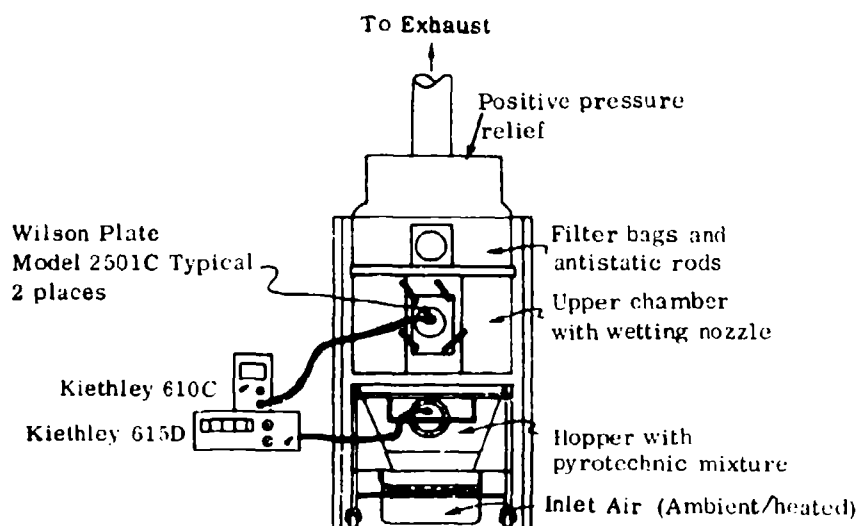


Figure 2. Full-Scale WSG300 Fluid Bed Spray Granulator

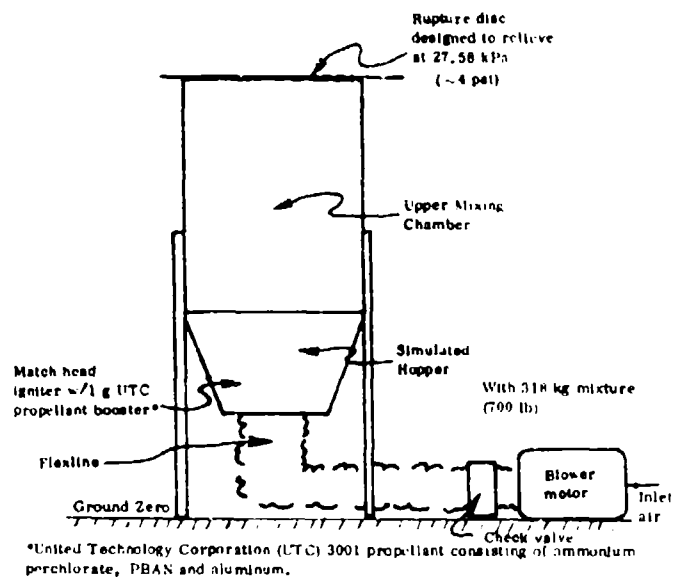


Figure 3. Full-Scale Blending Simulation Test Setup

INSTRUMENTATION

Electrostatic measurements were obtained using Model 610C and Model 615D Keithley electrometers. Each unit was attached to the surface of both the pilot model and the full-scale FBSG at the viewing port with a 7.62-cm (3-in) Wilson plate static detector. A typical electrical equivalent circuit is shown in figure 4.

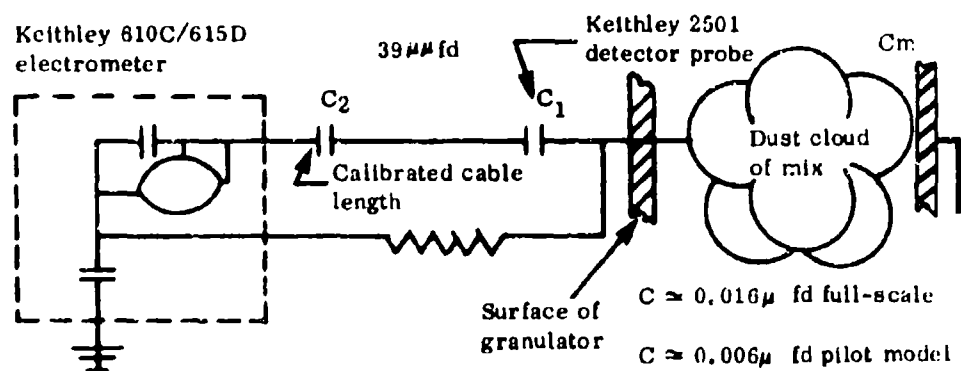


Figure 4. Equivalent Circuit of the Electrometer for Measuring the Electrostatic Charge (Coulombs)

The electrometers were read remotely at specified intervals via closed circuit television and were recorded directly. The highest value for each specified time was recorded, not the average value.

Temperature measurements for the pilot and full-scale tests were standard measurements as specified by the supplier which include inlet and outlet temperatures. No direct contact measurements were made of the various mixtures. As previous studies (Ref. 3, 4, 5) had indicated, there was no increase in temperature due to blending of colored smoke mixtures.

RESULTS

DATA ANALYSIS

Electrostatic measurements were obtained remotely using an electrometer affixed to the surface of the test articles. Measurements were monitored continuously and recorded manually every 30 seconds. The highest value obtained during each measuring period was the recorded value. All values were then placed into a computer and the calculations for each point were made, then the high, low, and mean values were reported for each significant operation.

Data analysis of the bulk and end-item classification tests are based upon the go/no-go results of the prescribed tests as outlined in chapter 3 and 4 of TB 700-2. Interpretation of the results for DoT and DoD purposes leads to the following designations:

DoT Forbidden - if the results from the thermal stability test indicate either an explosion, burning, or marked decomposition of the sample.

DoT Restricted - if the impact sensitivity tests result in an explosion at a drop height of less than 10.16 cm (4 in).

DoT Class A (U. N. Class 1.1) - if one or more of the following occur:

(1) the detonation test indicates sensitivity to a No. 8 blasting cap by mushrooming the lead block; (2) the card gap test indicates a sensitivity value greater than 70 or more cards; (3) the impact sensitivity test produces an

explosion above 10.16 cm (4 in) and (4) the ignition and unconfined burning test produces a detonation.

DoT Class C (U. N. Class 1.3) - if all of the following occur: (1) the ignition and unconfined burning test does not result in an explosion; (2) the thermal stability test does not result in an explosion, burning or marked decomposition; (3) the detonation test does not result in an explosion and (4) the card gap test results in a sensitivity of less than 70 cards or no reaction at zero cards.

This is shown diagrammatically in figure 5.

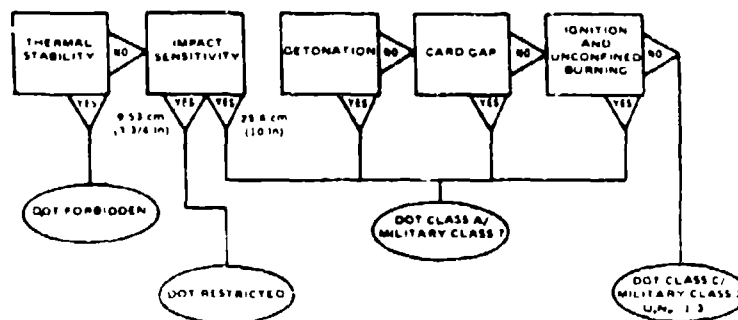


Figure 5. Interpretation of Test Results per TB 700-2, Change 1

Interpretation of end-item test results are shown in figure 6 and leads to the following designation:

DoT Class A (U. N. Class 1.1) - if an explosion results from the detonation test A, detonation test B and external heat test C and/or fragments dispersion.

DoT Class C (U. N. Class 1.3) - if there were no explosions in detonation test A and external heat test C and fragment dispersion is minimal.

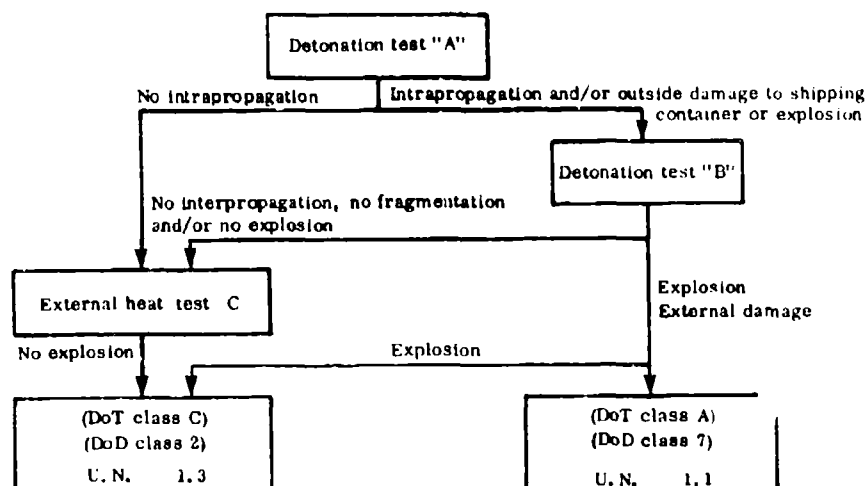


Figure 6. Interpretation of End-Item Test Results in Accordance with TB 700-2

TEST RESULTS

The results of the bulk tests in accordance with chapter 3 of TB 700-2 are given in table 1. None of the pyrotechnics exhibited characteristics of an explosion as the results of detonation tests, card gap tests or ignition and unconfined burning tests. There was no weight loss or change in configuration due to elevated storage temperature for a 48-hour period as outlined in the thermal stability test. From interpretation of results in accordance with chapter 3 paragraph 13, subparagraphs a, b and c, a Class C, (DoD Class 2) U.N. Class 1.3 was assigned to these bulk mixtures.

TABLE 1. BULK CLASSIFICATION TEST RESULTS

Sample material	Detonation test	Ignition and unconfined burning	Impact sensitivity test*	Thermal stability	Card gap test
Violet Smoke Mixture Dwg. # B143-5-1	No detonation	No explosion	0 at 9.43 cm 1 at 25.4 cm	No explosion no wt. loss	No detonation
Red Smoke Mixture Dwg. # B143-3-1	No detonation	No explosion	0 at 9.53 cm 2 at 25.4 cm	No explosion no wt. loss	No detonation
CS Pyrotechnic Mixture Dwg. # B143-14-7	No detonation	No explosion	0 at 9.53 cm 0 at 25.4 cm	No explosion no wt. loss	no detonation

* indicates number of explosions at each drop height.

End-item test results indicate that there was no variation of previously reported results (Ref. 7) due to a formula change. None of the pyrotechnic end items propagated within the container or caused outside damage to the packing container in the detonation test A configuration. Therefore, detonation test B was not performed. There was no explosion and minimal fragmentation for the M18 grenade and M47 riot control grenade from the external heat test C. Fragmentation was limited to sporadic ejection of components individually. During the total burning of the pyre there were no explosions. Results are shown in table 2.

TABLE 2. SUMMARY OF RESULTS END ITEM CLASSIFICATION

Material	Detonation test A results	Detonation test B results	External heat test C		
			Explosion	Fragmentation	Maximum fragmentation dist.
Grenade, Hand Smoke, Violet, M18 Dwg. # D 13-19-17	No propagation	N/A*	None	None	0
40 mm Projectile Red Marker Dwg. # D 9323253	No propagation	N/A*	None	Yes	45.7 m (150 ft)
Grenade, Hand, Riot CS, M47 Dwg. # D 13-25-70	No propagation	N/A*	None	None	0

* Not performed due to detonation test A results.

Summaries of the electrostatic data as measured during the pilot plant production of colored smokes and CS pyrotechnic mixture are given in table 3. Data given are taken from an average of 90 measurements each throughout the blending, granulation, and drying cycles. The amount of electrostatic energy generated during any given phase is several orders of magnitude less than the minimum energy required for initiation by electrical spark. Figure 7 shows the initiation level of the pyrotechnic mixture and the capacitance of the WSG15 pilot model. It can be seen that less than 100 volts is being generated during any given operating cycle. Based upon test results, electrostatic energy does not constitute a hazard due to mixing, wetting, and/or drying of these pyrotechnic mixtures.

TABLE 3. PILOT MODEL WSG15 BLENDING ELECTROSTATIC CHARGE GENERATION

Formulation	Weight kg (lb)	Operation Time (min)	Energy level (Joules) $E = \frac{1}{2} \frac{Q^2}{C}$		
			High	Low	Mean
Violet Smoke Mixture IV Dwg. # B143-5-1	13.6 (30)	Mixing 2	2.13×10^{-8}	5.92×10^{-10}	4.79×10^{-11}
		Wetting 8	9.43×10^{-7}	4.4×10^{-8}	6.6×10^{-7}
		Drying 21	2.13×10^{-6}	9.01×10^{-7}	1.55×10^{-6}
Red Smoke Mixture III Dwg. # B143-3-1	9.07 (20)	Mixing 3	1.89×10^{-5}	1.71×10^{-7}	7.77×10^{-6}
		Wetting 21	3.19×10^{-5}	1.06×10^{-5}	1.42×10^{-5}
		Drying 34.5	1.03×10^{-5}	7.26×10^{-7}	4.55×10^{-6}
CS Pyrotechnic Mixture Dwg. # B143-14-7	9.07 (20)	Mixing 3	2.49×10^{-5}	9.48×10^{-9}	1.3×10^{-7}
		Wetting 25	9.01×10^{-7}	1.16×10^{-7}	3.04×10^{-7}
		Drying 25	2.61×10^{-7}	5.93×10^{-10}	9.64×10^{-8}

A summary of electrostatic data as measured during full-scale plant production of colored smokes and CS pyrotechnic mixtures is given in table 4. The

TABLE 4. FULL-SCALE MODEL WSG300 BLENDING ELECTROSTATIC CHARGE GENERATION (AVERAGE CHARGE GENERATED FOR TWO BLENDING CYCLES)

Formulation	Weight kg (lb)	Operation Time (min)	Energy level (Joules) $E = \frac{1}{2} \frac{Q^2}{C}$		
			High	Low	Mean
Violet Smoke Mixture IV Dwg. # B143-5-1	299 (660)	Mixing 7.5	5.58×10^{-7}	1.99×10^{-9}	1.66×10^{-7}
		Wetting 38.5	3.2×10^{-6}	3.46×10^{-6}	1.31×10^{-6}
		Drying 59	2.04×10^{-6}	2.06×10^{-11}	4.38×10^{-7}
Red Smoke Mixture III Dwg. # B143-3-1	299 (660)	Mixing 5.5	3.31×10^{-6}	1.3×10^{-6}	2.55×10^{-6}
		Wetting 54	3.23×10^{-6}	8.32×10^{-13}	5.61×10^{-7}
		Drying 60	3.32×10^{-6}	5.74×10^{-11}	1.43×10^{-6}
CS Pyrotechnic Mixture Dwg. # B143-14-7	290 (640)	Mixing 22	7.04×10^{-7}	1.87×10^{-8}	1.44×10^{-7}
		Wetting 23	5.87×10^{-5}	3.67×10^{-8}	4.3×10^{-7}
		Drying 84	1.14×10^{-7}	4.32×10^{-11}	2.02×10^{-7}

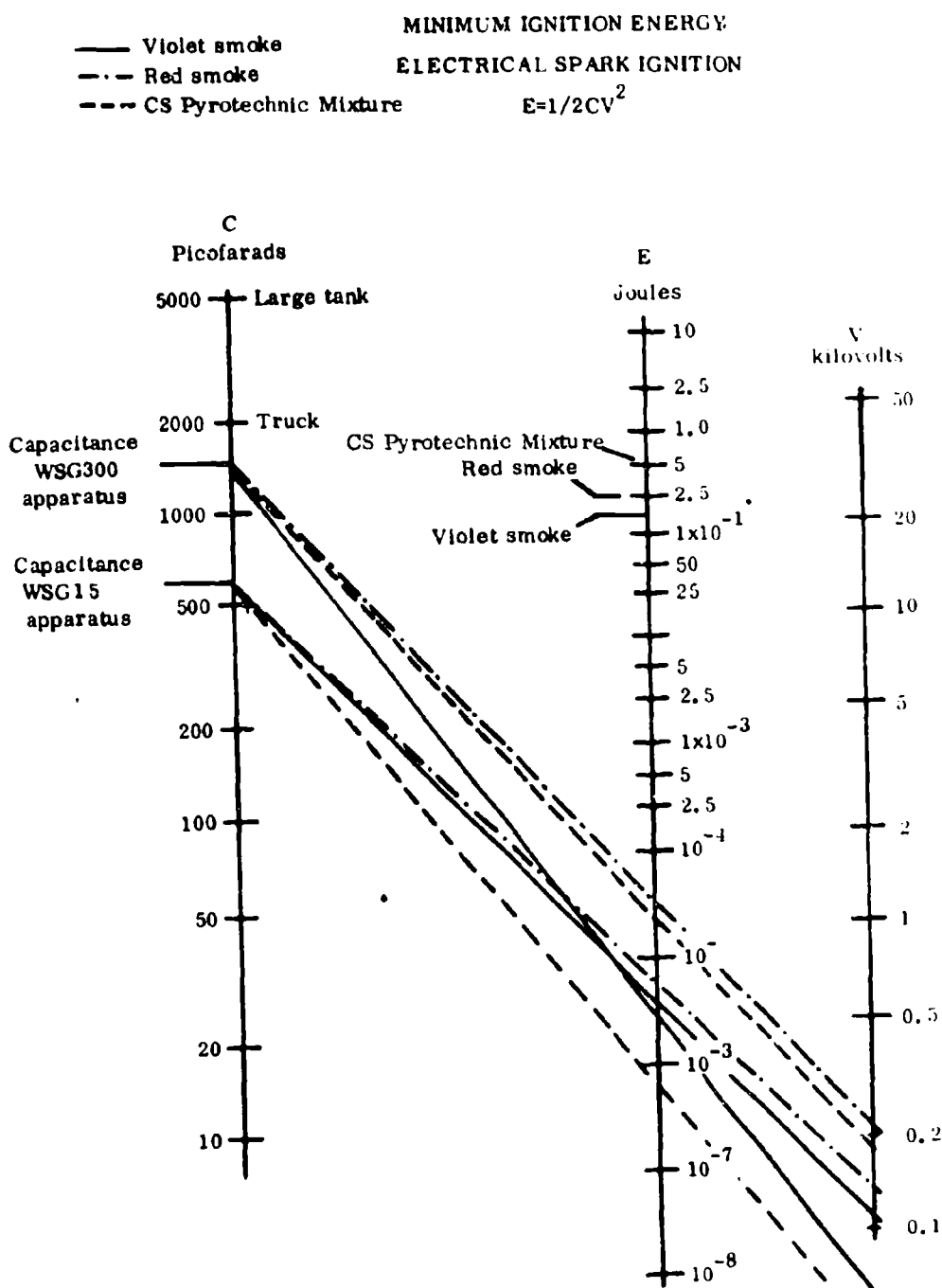


Figure 7. Nomograph of Electrostatic Charge Generation During Mixing, Granulating and Drying in Pilot and Full-Scale Fluid Bed Spray Granulation Process.

data for the full-scale tests are on the same order of magnitude as the pilot plant tests. There are no apparent hazards due to electrostatic charge buildup during the mixing, granulating or drying cycle.

A summary of the full-scale simulation tests is given in table 5. None of the mixtures exhibited characteristics of an explosion. The burn time of each mixture varied from a low of 44 seconds for red smoke to a high of 320 seconds for CS pyrotechnic mixture. The measured surface temperatures ranged from a low of 318°C to a high of 468°C. There was no measurable pressure external to the simulation vessel.

TABLE 5. SUMMARY OF RESULTS OF FULL-SCALE SIMULATION TESTS

Test material	Weight kg (lb)	Burn Time Sec	Maximum temperature °C	Maximum external pressure	Maximum internal pressure
Violet smoke Dwg. # B143-5-1	336 (740)	126	365	No external pressure recorded	34.5 kPa (5 psi)
Red smoke Dwg. # B143-3-1	336 (740)	44	318	No external pressure recorded	34.5 kPa (5 psi)
Chemical agent Dwg. # B143-14-7	435 (960)	369	463	No external pressure recorded	13.8 kPa (2 psi)

There was no damage internally or externally to the vessel due to blast pressure; however, there was some damage to the external ducting due to the fire. The same simulator was utilized for all test series.

The use of the fluid bed spray granulation process to manufacture pyrotechnics has several advantages over conventional mixing methods in that mixing, wetting, kneading, granulating, drying, breaking-up, admixing and sieving of fines that were formerly accomplished in separate steps can now all be accomplished in a single apparatus. Because of this, the normal hazards associated with handling are minimized to a single loading operation of constituents and discharging of

the finished product. The apparatus itself has no impact points due to no moving parts; there is no friction other than moving particles of the mix which do not constitute any hazard. The binder added to the mix is nonvolatile which also minimizes hazards. There is no pressure-type stimulus associated with the operation. Electrical component and switching are remote from the mixing operation. Electrostatic hazards are at a minimum and the temperature of the air used for drying 60-80°C (140-175°F) is significantly below the autoignition or decomposition temperature of the pyromixes. This apparatus then affords the minimum number of possible stimuli under normal operation conditions and further reduces potential hazards sources. In the event of an accidental initiation, no matter how remote, the system has a built-in relief system that should preclude the hazards of an explosion by automatic relieving with a minimal pressure buildup. The mixing cubicle at Pine Bluff Arsenal utilizes an ultraviolet fire detection and suppression system that, in the event of such an incident, provides sufficient corrective action from a water deluge system to lessen any potential damage to equipment or facility. Results of the "worse case" scenario tests conducted during the course of this investigation indicate that explosive hazards associated with manufacturing large quantities 300-400 kg (660-880 lb) of colored smoke and CS pyrotechnic mixtures are at a minimum and that the fluid bed spray granulation process affords the least hazardous method of production.

CONCLUSIONS

1. None of the colored smoke or CS pyrotechnic mixtures indicate that there are any apparent hazards due to electrostatic charge buildup during the mixing, wetting and drying cycles in either pilot or full-scale production in the fluid bed spray granulation process.
2. None of the colored smoke or CS pyrotechnic mixture exhibit characteristics of mass detonation in 371-454-kg (700-1000-lb) quantities due to initiation during a "worse case" scenario under dynamic mixing conditions.
3. Based upon interpretation of bulk materials test results in accordance with

TB 700-2 chapter 3, all of the colored smokes and CS pyrotechnic mixture would constitute a probable DoT Class C, (DoD Class 2), U.N. 1.3.

4. Based upon interpretation of end-item test results in accordance with TB 700-2 chapter 4, the probable classification of the end-items tested would warrant a DoT Class C, (DoD Class 2), U.N. 1.3.
5. Under all conditions of tests in various configurations of pyrotechnic mixtures ranging from 371-454 kg (700-1000 lb) quantities, the hazards associated with these pyrotechnic mixtures are a probable en masse fire hazard only, as there is no tendency for any of these mixtures to mass detonate.

REFERENCES

1. McIntyre, F. L., Identification and Evaluation of Hazards Associated with Blending of HC White Smoke Mix by Jet Airmix Process, Final Report EA-FR-4D21, January 1974.
2. McIntyre, F. L., Identification and Evaluation of Hazards Associated with Blending of Violet Smoke by Jet Airmix Process, Edgewood Arsenal Contractor Report EM-CR-75001, March 1975.
3. McIntyre, F. L., Engineering Study of Jet Airmix Fire Suppression, Edgewood Arsenal Contractor Report EM-CR-76012, August 1975.
4. McIntyre, F. L., Evaluation of Violet Smoke Initiation Under Dynamic Conditions in the Jet Airmix Blender, Edgewood Arsenal Contractor Report EM-CR-77008, November 1976.
5. Wilcox, W. R. and McIntyre, F. L., Identifications and Evaluations of Hazards Associated with Blending of Violet Smoke Mix by Double Cone Process, Edgewood Arsenal Contractor Report EA-27R1, April 1977.
6. Army Technical Bulletin 700-2 Change 1, Explosives Hazards Classification Procedure, January 1968.
7. King, P. V., Koger, D. M., Pyrotechnic Hazards Classification and Evaluation Program Phase I, GE-MTSD-R-035, May 1970.

FLAMESPREAD PROPAGATION RATES OF VARIOUS BLACK
POWDERS USING THE PCRL-FLAMESPREAD TESTER

N.A. Messina, L.S. Ingram, and H. Summerfield
Princeton Combustion Research Laboratories, Inc.
Princeton, New Jersey 08540

and

J.C. Allen
U.S. Army Armament Research and Development Command
Dover, New Jersey 07801

ABSTRACT

Princeton Combustion Research Laboratories, Inc. has utilized its Flamespread Tester, developed for ARRADCOM, Product Assurance Directorate, Dover as an end-of-line quality assurance technique for continuous-line product Class 1 Black Powder, for determination of flamespread properties of various granulated and pelletized Black Powder-base formulations. The purpose is to evaluate each formulation as a possible candidate for artillery primer applications. The underlying proposition of this new test method is that the main function of Black Powder primers in guns or howitzers is to spread the ignition flame in a controlled manner through the propulsive charge. Therefore flamespread propagation velocity is chosen as the quantity to be measured in the rating procedure. The PCRL-Flamespread Tester measures the flame front propagation through a packed bed of sample Black Powder by means of the timewise response of three equidistant phototransistor light sensor assemblies. Further, combustor pressure-time history is monitored for determination of peak pressures, ignition delays, and pressurization characteristics.

INTRODUCTION

The particular combustor configuration selected for flamespread velocity determination was adapted from the configuration of a cased 105 mm howitzer round. In actual use, the M28B2 primer of the field round is loaded partially with a specified mass of Class 1 Black Powder (mesh size between 4 and 8 per inch). The pyrotechnic initiator starts combustion at one end, which then spreads along the tube in a few milliseconds, shooting flame gases radially outward into the packed propellant bed of the cartridge chamber. These flame gases initiate and help spread the combustion wave through the propellant bed in a prescribed manner. Recent ballistic research has disclosed a correlation between such flamespreading in the propellant charge and phenomena such as chamber pressure waves and breech pressure spikes, which suggests that flamespreading rate in the primer tube may have an important effect on internal ballistic characteristics.

The apparatus designed for the flamespread tests in this project is shown schematically in Figure 1. Figure 2 displays photographs of the Flamespread Tester in the disassembled and assembled states. In addition to the obvious "boiler plate" nature of the design, several significant changes were made from the standard M28B2 primer:

(i) To assure more reproducible flamespread rates, although admittedly slower than in the actual primer, the Sample tube was packed as fully as possible, e.g. nominally 25 g Class 1 Black Powder granules. This gave a fixed and predictable porosity.

(ii) To avoid erratic flamespread behavior due to occasional plugging of the orifices by granules or pellets of Black Powder, the orifices were made into narrow slots of the same vent area per unit length of Sample Tube as the M28B2 primer. Experience showed that such vent slots could not be plugged by the powder granules or pellets. Experience showed also that this change improved the uniformity of the measured flamespread rate data.

(iii) To assure more reproducible start-up at ignition (commercial squibs were found to be erratic), an "integrating chamber" was placed between the squib igniter and the bed of Black Powder, which served to

collect the gases from the squib and release them into the Black Powder bed at a controlled rate (exhaust time about $\frac{1}{2}$ millisecond). It has been suggested by us that this "integrating chamber" technique could have useful application not only to a test apparatus like this one but also to bayonet primers of actual artillery in order to improve ballistic reproducibility.

(iv) To provide a directly detectable means of tracking the advance of the flame front in the Sample Tube, phototransistor light sensors were designed into the tube with thin glass light pipes to convey the radiation from the tube to the light sensors.

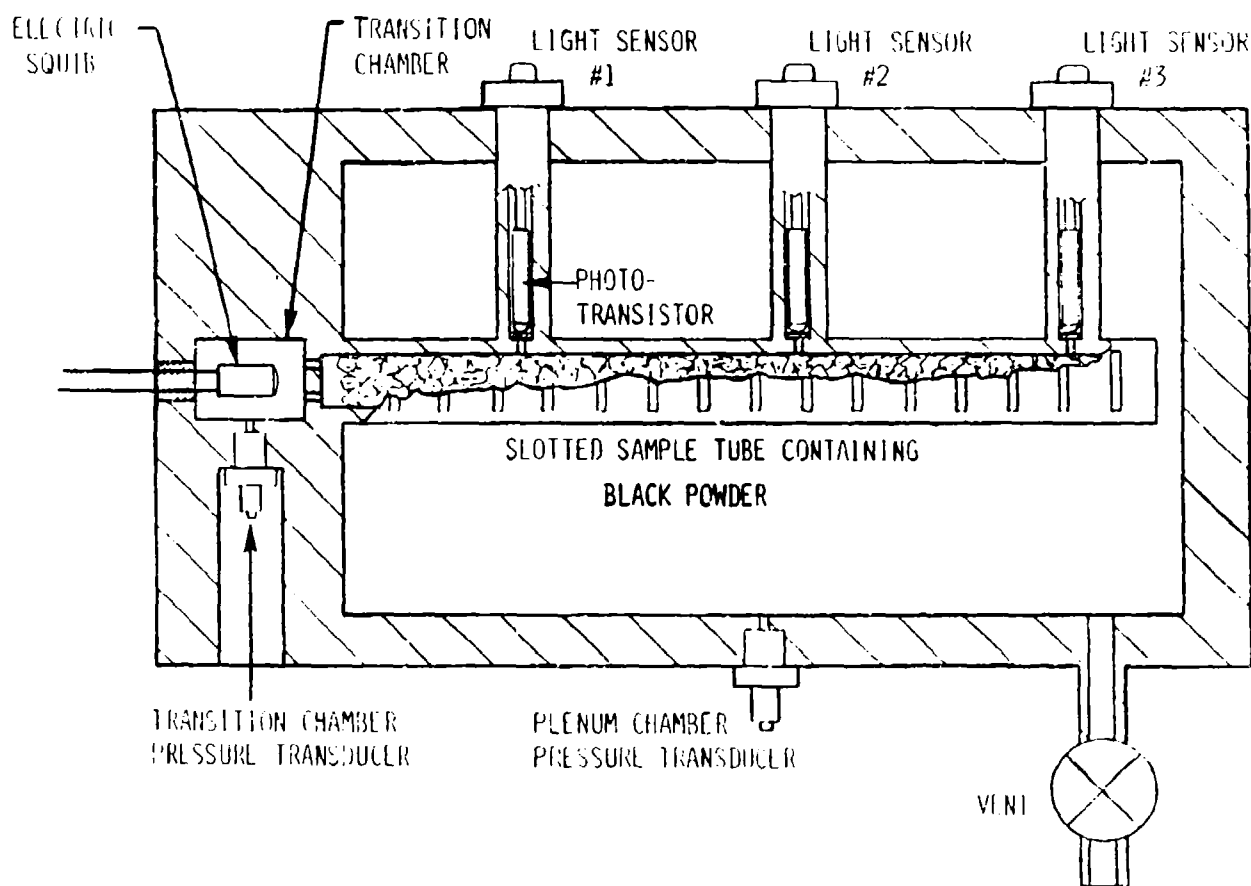
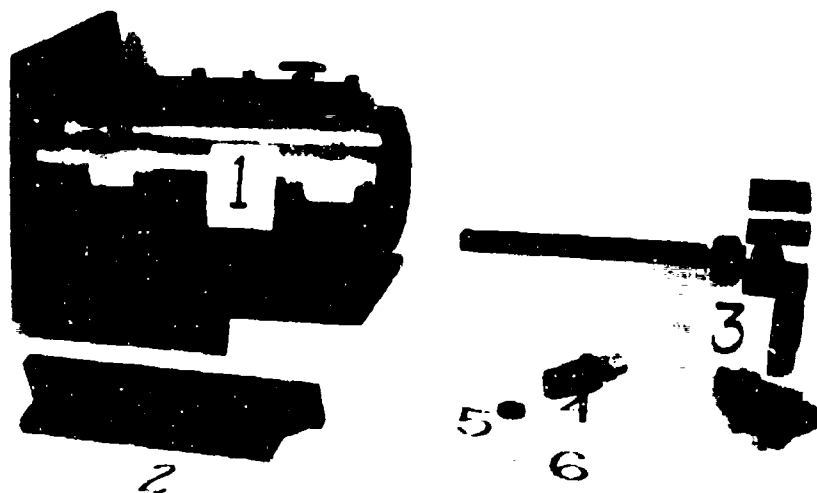
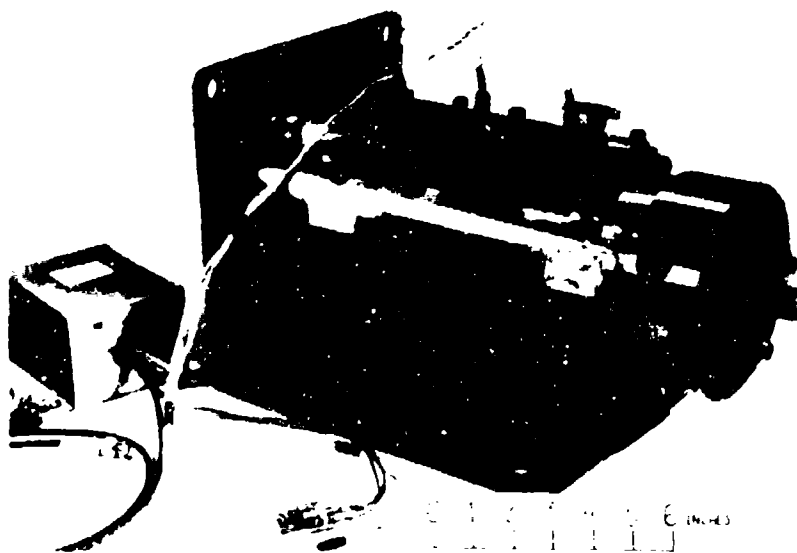


Figure 1. Schematic Drawing of Flamespread Tester.



- a. DISASSEMBLED FLAMESPREAD TESTER: (1) Flamespread Tester Chamber; (2) Light Sensor System; (3) Slotted Sample Tube mounted onto Variable L* Igniter Head; (4) Transition Chamber Assembly and Conax Gland; (5) Igniter Orifice Plate; and (6) CAD Electric Squib.



- b. ASSEMBLED FLAMESPREAD TESTER (In Laboratory Configuration).

Figure 2. Photographs of the PCRL-Black Powder Flamespread Tester

As diagnostic aids for evaluation of candidate Black Powders, pressure measurements were made in the plenum chamber that simulated the empty cartridge chamber. The plenum chamber was provided with a vent valve as shown, and a vent duct to discharge the combustion gases to an appropriately harmless collection system. Solid residues were found deposited after each firing, in the tube and in the plenum chamber, but they could be removed rather easily in preparation for the next firing.

Another approach to qualifying Black Powder for primer applications would be to measure the conventional relative quickness and/or induction time in a closed bomb type firing. Flamespread rate can be related to powder ignitability, as measured by induction time, and to burning rate as measured by relative quickness, so there is some logic to adopting this approach. In fact, Black Powders that burn fast also display rapid flamespread rates. However, although the techniques are well established, the closed bomb measurement is no more simple to operate than the present flamespread system. Moreover, it is not clear that an apparatus that was really designed to measure mainly burning rate and not flamespread directly is suitable for use in qualifying Black Powders for its proper function in a gun. After all, Black Powder is not the propelling charge of the gun, and so a device that measures relative quickness may not be reporting the correct functional property. Thus, it is conceivable that a particular powder sample that, for some reason, has a slow burning coating on the granules but a fast burning interior would show a slow flamespread rate but a high relative quickness. The result of the closed bomb test might therefore be misleading.

DISCUSSION

The following describes an evaluation of the sensitivity of the PCRL Flamespread Tester for determining variations in flamespread rate associated with deviations in Class 1 granulation Black Powder specification.

A series of ten deviant Black Powder lots (Class 1) was prepared by ARRADCOM for the purpose of evaluating the sensitivity of the test

apparatus to off-specification deviations by comparing flamespread propagation velocities with that obtained for a "Standard" Lot G0E 75-44. Identification of the Deviant Lots are presented in Table 1.

TABLE 1
Identification of Deviant Class 1 granulation Black Powder Lots.

TEN (10) BLACK POWDER LOTS ARE TO BE MANUFACTURED IN THE PILOT PLANT. EACH LOT WILL HAVE A SPECIFIC MANUFACTURED DEFECT AS LISTED BELOW.

LOT 1 - HIGH KNO_3 : KNO_3 -78.01% C-11.95% S-8.50%
LOT 2 - LOW KNO_3 : KNO_3 -73% C-16.3% S-10.4%
LOT 3 - POOR AGGLOMERATION (POOR BLENDING HOMOGENEITY)
LOT 4 - HIGH DENSITY POWDER (ABOVE 1.80 gm/cc)
LOT 5 - LOW DENSITY POWDER (1.60-1.70 gm/cc)
LOT 6 - NON-STANDARD GLAZE (0.2% GRAPHITE vs. 0.1%)
LOT 7 - CHARCOAL WITH HIGH CARBON CONTENT (67.8%)
LOT 8 - CHARCOAL WITH LOW CARBON CONTENT (52.58%)
LOT 9 - LARGE PARTICLE SIZE INGREDIENT (JET MILL PRODUCT)
LOT 10 - SMALL PARTICLE SIZE INGREDIENT (JET MILL PRODUCT)
LOT 11 - G.O.E. "GREEN GRAIN" (UNGLAZED) BLACK POWDER GLAZED WITH NON-SPECIFICATION DIXON GRAPHITE (HIGH ASH CONTENT) IN A HARPERIZER

THESE LOTS WILL BE PROCESSED THROUGH AN INTENSIFIED BLENDER, THE JET MILL, AND PRESSED INTO CAKES WITH THE DENSITY BEING MONITORED. THE CAKES WILL BE PROCESSED THROUGH THE PREBREAKER, GRANULATOR, SCREENED, AND THEN DRIED. POLISHING AND GLAZING WILL BE DONE IN THE HARPERIZER.

Various Black Powder-base compacted pellets were prepared at ARRADCOM, Dover with different weight percent of nitrocellulose included in the formulation. Tables 2 through 6 present the formulation of the compacted pellets and the associated pellet density. In each case the relative weight percent of charcoal (and carbon black), sulfur, and potassium nitrate is nominally equal that of Class 1 granulation Black Powder, Standard Lot. The weight percent of nitrocellulose in these compacted pellets ranges from zero to 67 percent. Table 7 presents the mass loading and packing density of each of the pelletized mixes.

Initial flamespread tests performed with Class 1 granulation Black Powders were conducted with the combustor continuously venting to atmosphere through a 0.18-inch diameter vent orifice. Flamespread rates for each lot of Class 1 granular Black Powder were remarkably

TABLE 2

FORMULATION OF TYPE C PELLETS ($\rho = 1.56 \text{ g/cc}$)

CONSTITUENT	PERCENT BY WEIGHT	
Peerless 155 Carbon Black (Cities Service)	2.5	
Charcoal, Roseville, fines	2.5	
Sulfur, amor.	3.33	
Pptd. KNO_3 *	25.0	
NC Fluid Ball Powder* (12.6% N)	1.67	
NC Fluid Ball Powder*	65.0	
	100.	
Thermoplastic Polyurethane, Estane 5702 (B.F. Goodrich)	1.33	ADDED
n50 hydrophobic silica	0.5	ADDED
*14 pre-coated		

TABLE 3

FORMULATION OF TYPE I PELLETS ($\rho = 1.637 \text{ g/cc}$)

CONSTITUENT	PERCENT BY WEIGHT	
Peerless 155 Carbon Black (Cities Service)	4.5	
Charcoal Airofloat F (IAAP)	4.5	
Sulfur, amor.	6.24	
Pptd. KNO_3	45.0	
NC Fluid Ball Powder	40.0	
	100.24	
Coatings, Binder	1.90	ADDED

TABLE 4

FORMULATION OF TYPE J PELLETS ($\rho = 1.564 \text{ g/cc}$)

CONSTITUENT	PERCENT BY WEIGHT	
Peerless 155 Carbon Black (Cities Service)	2.5	
Charcoal	2.5	
Sulfur, amor.	3.47	
Pptd. KNO_3	25.0	
NC Fluid Ball Powder	66.67	
	100.14	
Resorcinol	1.0	ADDED
KNO_3	6.25	ADDED
Boron, amor.	1.67	ADDED
	109.06	
Coatings, Binder	0.98	ADDED

TABLE 5

FORMULATION OF MODIFIED BLACK POWDER PELLETS
($\rho = 1.52 \text{ g/cc}$)

<u>CONSTITUENT</u>	<u>PERCENT BY WEIGHT</u>	
Pptd. KNO ₃ with 1% polypropylene, 0.1% PVP	75.0	
Peerless 155 Carbon Black (Cities Service)	7.5	
Powdered Charcoal, Maple (IAAP)	7.5	
Sublimed Sulfur (J.T. Baker)	10.0	
	<u>100.</u>	
Thermoplastic polyurethane, Estane 5702 (B.F. Goodrich)	1.33	ADDED

TABLE 6

"BASELINE" GRADE A5
(CLASS 7) BLACK POWDER DUP-32-2, 10/3/63
($\rho = 1.906 \text{ g/cc}$)
Coatings, Binder 0.72 Percent by Weight

TABLE 7

MASS LOADING AND PACKING DENSITY OF VARIOUS BLACK POWDER-BASE FORMULATIONS

<u>DESIGNATION</u>	<u>MASS LOADING (g)</u>	<u>PACKING DENSITY $\bar{\rho}$ (g/cc)</u>
TYPE C PELLET	19.36	0.87
TYPE I PELLET	21.20	0.96
TYPE J PELLET	19.60	0.88
MODIFIED B.P. PELLET	18.11	0.82
CLASS 7 B.P. PELLET	24.75	1.12
CLASS 1 B.P. GRANULE	24.64	1.11

consistent. Five firings were made in most cases, and the indicated error bars in Figure 3 embrace all five of the firing measurements.

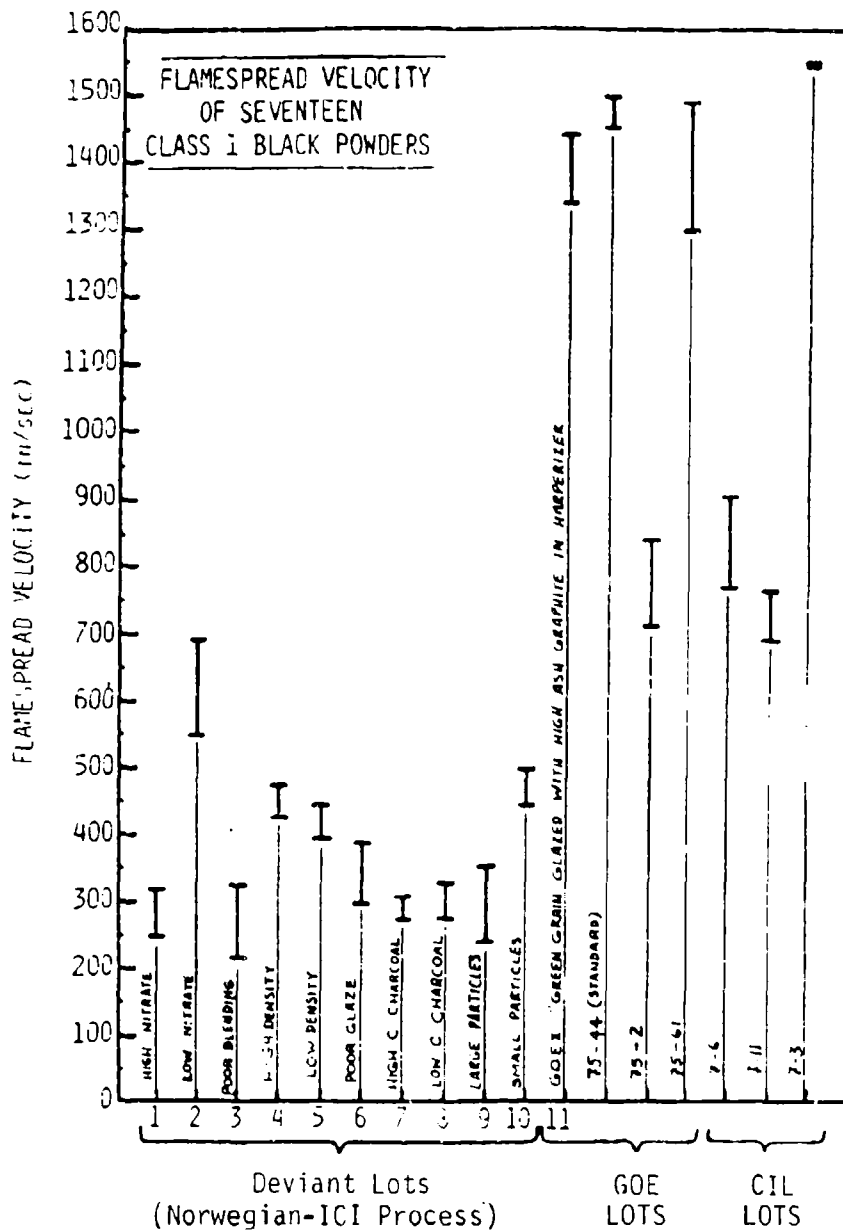


Figure 3. Flamespread Velocity Data of Seventeen Class 1 Black Powders Using the PCRL-Flamespread Tester.

In general, the differences in the composition and in physical make-up within the series of ten Class 1 granulation deviant Black Powder lots leads to definite differences in flamespreading rates that could be detected without ambiguity.

It is apparent that the flamespread propagation velocity of Deviant Lot 11 (GOE 75-44, green grain glazed with non-specification high ash content Dixon graphite in "Harperizer") is not much different from that associated with the Standard Lot, GOE 75-44, both being in the range of 1300-1500 in/sec. Flamespread propagation velocities of most other Deviant Lots are a factor of 3.5-6 times slower than the GOE 75-44 Standard. Flamespread tests of Deviant Lot 2 (low KNO_3 content) resulted in propagation velocities a factor of 2-3 times slower than the GOE 75-44 Standard.

It is interesting to note that the flamespread propagation velocity of lot GOE 75-2 and lots CIL-7-6 and CIL-7-11 are a factor of 2 times slower than the GOE 75-44 Standard. Similar observations have been noted in closed bomb RQ measurements of these particular lots, performed at ARRADCOM, Large Caliber Weapon Systems Laboratory, Dover, in which the observed RQ is only 60-70% of that for the GOE 75-44 Standard.¹

It should be pointed out that a hang-fire occurred with the M203 igniter system (combination base pad and center core system employed in the top-zone bagged charge which is used in the 155 mm howitzer). The origin of this problem was traced to the igniter and specific lot of Class 1 granulation Black Powder used, that being CIL-7-11.² PCRL flamespread tests of this Black Powder indicate a 50% performance factor when compared to Standard Lot GOE 75-44. Further, M483 and M549 projectile tests at -60°F with CIL-7-11 resulted in ignition delays (time from initiation of percussion primer to ignition of center core) 1.5-2 times more severe as that obtained for the Standard Lot.³

The results of the PCRL flamespread tests for the Deviant Lots are compared with other ballistic firing test evaluation methods in Figure 4. This is a summary plot of data from ARRADCOM, Large Caliber Weapon Systems Laboratory, Dover closed bomb firings⁴, (inverse induction

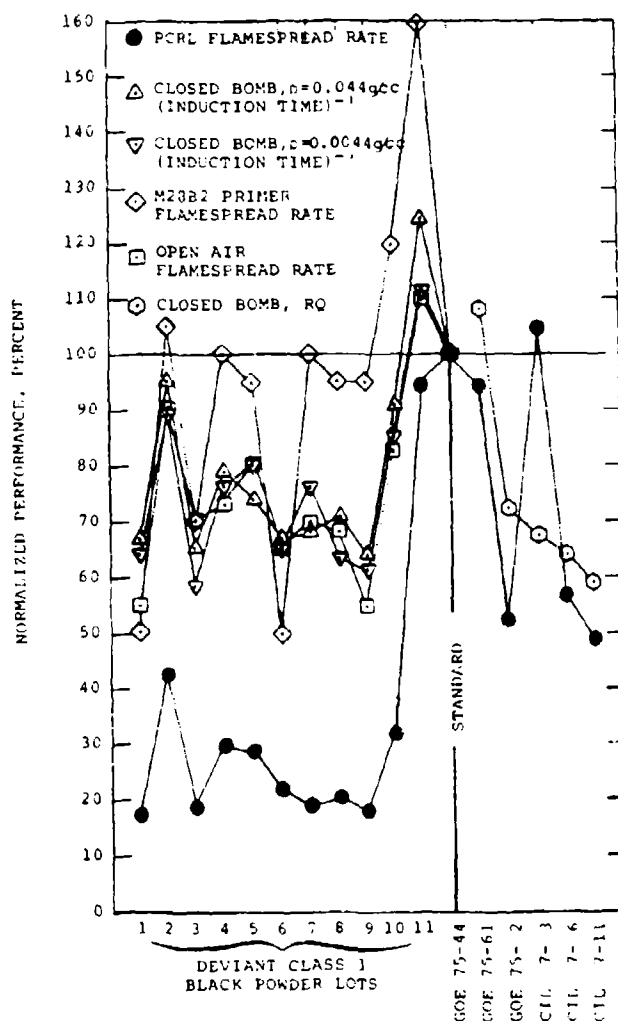


Figure 4. Normalized Flamespread Performance Data of Various Class 1 Black Powders.

time for two different closed bomb loading densities); the open air flamespread tests performed by ARRADCOM, Ballistic Research Laboratory⁵; and the M28B2 bayonet primer flamespread tests performed by ARRADCOM, BRL.⁵ Normalized performance of the various Class 1 Black Powder lots is reported, the normalizing factor being the test data associated with Standard Lot GOE 75-44. Note that the performance data of the

various flamespread velocity tests for the Deviant Lots are compared with inverse induction time performance data of closed bomb tests rather than conventional relative quickness data, RQ, since flamespread rate is a measure of grain-to-grain ignitability in the bed rather than rate of pressurization of the bed.

Table 8 summarizes the conditions and results of the various flamespread tests of Class 1 Black Powders.

TABLE 8

COMPARISON OF VARIOUS FLAMESPREAD MEASUREMENTS FOR CLASS 1 BLACK POWDER LOTS

<u>TYPE</u>	<u>NOMINAL VOID FRACTION</u>	<u>PRESSURE, KPSI (MPa)</u>	<u>FLAMESPREAD VELOCITY RANGE, IN/S (M/S)</u>
PCRL FLAMESPREAD TESTER, REF. 7	0.41	0.5-1.45 (3.5-10.)	315-1575 (8-40)
M28B2 PRIMER, REF. 5	0.54	1.45 (10.)	1180-3940 (30-100)
OPEN AIR FLAMESPREAD, REF. 5	N/A	0.015 (0.1)	11-28 (0.3-0.7)

Flamespread propagation velocities of Black Powder in open air are considerably less than those obtained when the bed is confined in a tube, as is to be expected. In fact, recent observations of Black Powder flamespread rate as a function pre-pressurization level in the PCRL Flamespread Tester indicate a strong dependence of flamespread rate on pressurization level of the environment into which the Black Powder combustion products exhaust.^{6,8}

Furthermore, the flamespread rate as determined from M28B2 primer tube tests⁵, is 2-3 times that obtained in the PCRL Flamespread Tester. This might be attributed to rather large differences in void fraction of the M28B2 primer tube vs. the PCRL Sample Tube. In order to obtain flamespread propagation rates with minimal data variation in the PCRL Flamespread Tester, extreme care was exercised to achieve maximum reproducible loadings, i.e., minimal void fraction, in the Sample Tube. The nominal void fraction achievable in the PCRL Sample Tube is 0.41. The larger void fraction in the BRL M28B2 primer tube, 0.54, is representative of a looser bed packing which may permit a more rapid flamespread rate. Inspection of the normalized performance results for the Deviant Class 1 Black Powder Lots obtained from BRL M28B2

primer tube flamespread measurements reveals that 6 of the 11 Deviant Lots perform within $\pm 5\%$ of the GOE 75-44 Standard Lot. It is our belief that this is a result of the large void fraction in the M28B2 primer tube tests. This is further suggested by the observation that 10 of the 11 Deviant Lots produce flamespread rates in the PCRL Flamespread Tester less than 50% of the Standard GOE 75-44 Lot.

Normalized performance based on inverse induction time of Closed Bomb firings of the Class 1 Black Powder lots at two different loading densities indicate trends similar to the flamespread rate results of the PCRL Flamespread Tester although the magnitude of the performance factor for the Deviant Lots is approximately 40% larger for the Closed Bomb firings. Note that all the Deviant Lots except Lot 11 underperform the Standard GOE 75-44 Lot in the Closed Bomb tests.

A final point should be made regarding the comparisons of normalized performance of Figure 4. The void fraction in the M28B2 primer flamespread tests most nearly duplicates that of the bayonet primer in the 105-mm Howitzer. Therefore, the propagation rates reported in these experiments may be typical of nominal values achievable in actual operation of the M28B2 primer in the artillery round. However, the sensitivity and reproducibility of the flamespread measurement data in the PCRL Flamespread Tester to variations in Black Powder formulations and to intra-class and interclass size variations make the device attractive for use as a laboratory simulator for comparative analysis of various primer formulations and igniter trains for artillery applications.

The vented chamber mode of operation of the Flamespread Tester proved unacceptable for flamespread determination of compacted pellet formulations with nitrocellulose added because of the fizz-burn or dark zone burning characteristics below approximately 7-10 atm

(100-150 psi). No discernible flamespread rate can be extracted from the oscillograph records of light sensor outputs vs. time, since the precise point of departure of the light sensor responses from baseline cannot be identified. As shown in Figure 5, oscillograph records

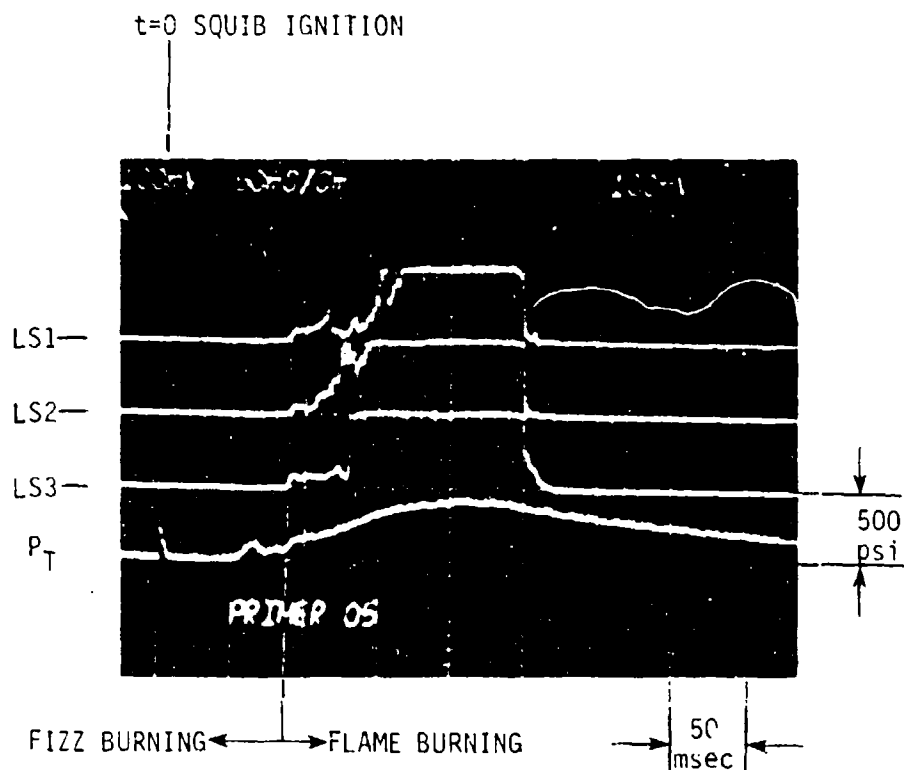


Figure 5. Oscillograph records of initial flamespread test performed with TYPE C pellets indicating low pressure dark zone burning characteristics resulting in non-detectable flamespread through the packed pellet bed.

of TYPE C pellet (67% NC), all light sensors appear to respond at approximately the same time, that being 90 msec after squib ignition. Note that the onset of pressurization in the Sample Tube associated with the burning process occurs 40 msec prior to the detection of radiation from the combustion zone. Note also that the departure of the light sensor responses from their respective baselines occurs at a pressure of approximately 100 psig. What is being observed is the non-luminous fizz-burn regime for NC formulations.

In order to obtain flamespread propagation rates for these Black

Powder-base pellets with NC added, the dark zone burn regime must be bypassed. This is achieved by operating the Flamespread Tester in the closed chamber mode (removal of vent) and pre-pressurizing the combustor to 50 psig prior to firing. This pre-pressurization level was chosen for all flamespread rate tests of pelletized Black Powder-base formulations. A typical oscillograph record of flamespread test performed with TYPE C pellet at a chamber pre-pressurization of 50 psig is shown in Figure 6. The light sensor responses indicate that flaming times,

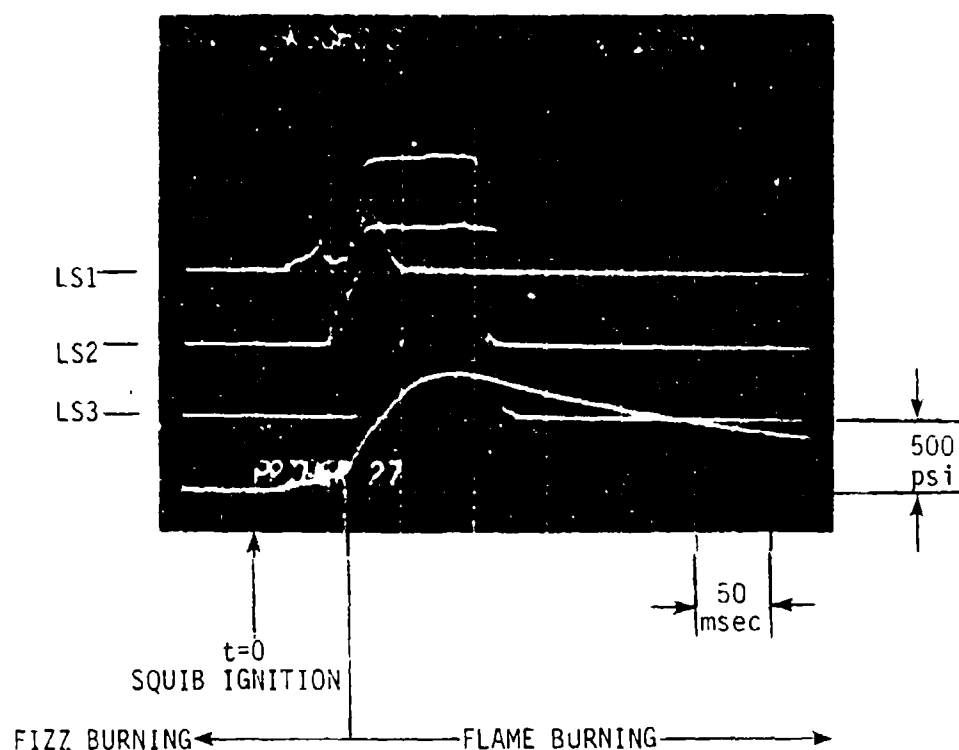


Figure 6. Oscillograph Record of Flamespread Test performed with TYPE C pellets at pre-pressurization of 50 psig.

i.e., propagation velocities, are indeed measurable. For comparison purposes, additional flamespread tests were performed with Class 1 granulation Standard Lot G0E 75-44 at a pre-pressurization level of 50 psig.

Figure 7 displays the timewise evolution of chamber pressure for the various compacted pellets, including Class 1 granulation Standard

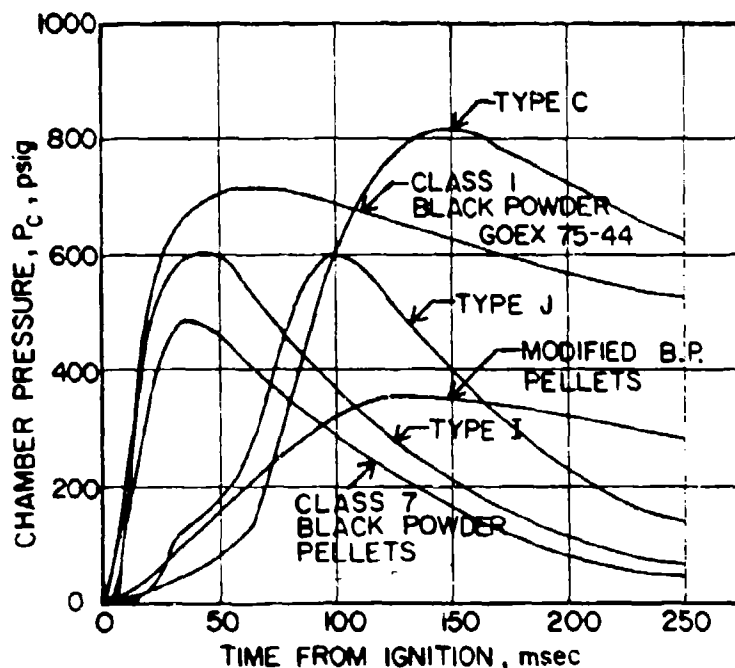


Figure 7. Temporal Development of Chamber Pressure for Various Black Powder-base formulations.

Lot Black Powder. Several observations are noted insofar as plenum chamber history is concerned:

1. The chamber pressurization associated with Black Powder-base compacted pellets TYPE C, TYPE J, and Modified Black Powder (B.P.) is considerably slower than that produced by Class 1 granulation Black Powder.
2. Both TYPE I pellet (40% NC, 60% BP equiv.) and Class 7 Black Powder pellet (manufactured from Lot DUP-32-2 with less than one percent by weight of binder added) each produce a chamber start-up pressurization rate approximately equal that of Class 1 Black Powder granules, although the peak pressures attained are somewhat less. Peak chamber pressure for Class 1 granulation Black Powder is approximately 700 psig. That attained for TYPE I pellet is 600 psig, while Class 7 B.P. pellets produce $p_{c_{max}} \sim 500$ psig. It should be pointed out that the $p_{c_{max}}$ produced by these various mixes is not only a function of the gas-producing constituents of the formulation but a combined effect of gas evolution and rate of water vapor condensation and inherent heat

loss to the chamber walls.

3. TYPE J and TYPE C pellets, both containing a large percentage of nitrocellulose in their respective formulations (in excess of 60% by weight), show a transitional behavior in the p_c -t history, occurring at $p_c \sim 150$ psia. This is indicative of the transition from fizz-burning to flaming for these NC-added formulations. Apparently, for an NC-added formulation with $NC \leq 40\%$, rapid chamber pressurization occurs with no transition evident, e.g., TYPE I pellet.

4. Modified B.P. pellets, manufactured from basic ingredients (KNO_3 , carbon black, charcoal, sulfur), produce peak chamber pressure approximately 125 msec after squib ignition compared to 35 msec when the pellet is formed from Class 7 granulation Black Powder. Inspection of the Modified B.P. pellets indicated a poor homogeneity of the mix resulting in poor pressurization performance. A pronounced effect on flamespread propagation velocity is also obtained, as will be seen in Fig. 8.

Flamespread propagation rates of the various compacted pellets are shown in Figure 8. These flamespread rates are average rates based

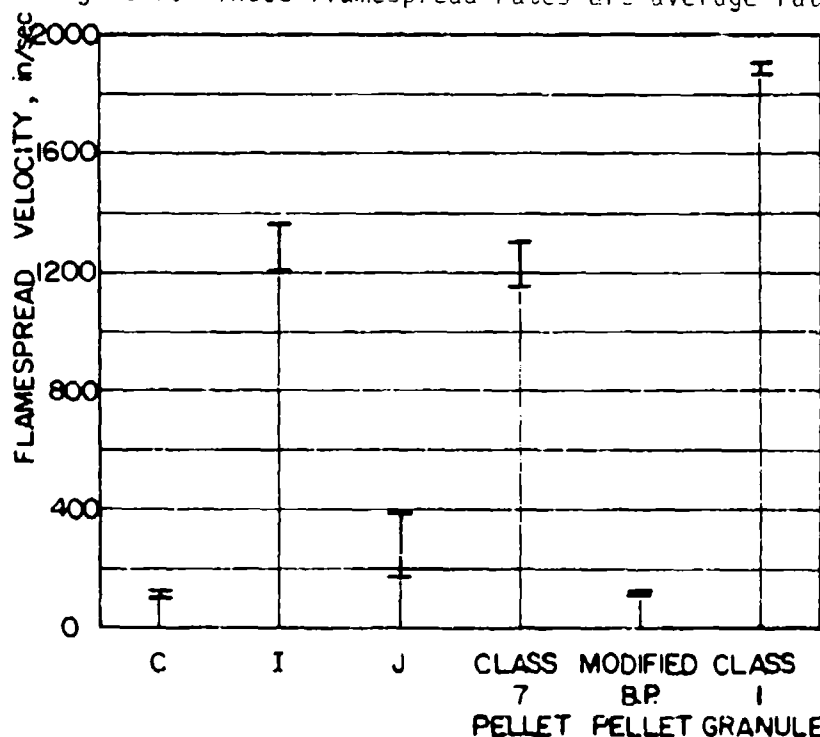


Figure 8. Flamespread Velocity Data for Black Powder-base Compacted Pellets.

on the flaming time between the first and third light sensors (LS1 and LS3). The "I-beams" indicate run-to-run variation in extracted flame-spread velocity in the interval LS1 - LS3. The flamespread rate for Standard Lot GOE 75-44 is shown for comparison purposes. The propagation velocity of the Standard Lot is approximately 1900 in/sec. It should be remembered that this series of flamespread measurements was performed with a combustor pre-pressurization of 50 psig, while the flamespread rates displayed in Figure 3 are for a continuously vented chamber with no pre-pressurization.

The following observations are noted:

1. Both TYPE C pellet and TYPE J pellet display a considerable shortfall in achievable flamespread rates compared to the Standard Lot. A 20% performance factor is obtained for these high percentage NC-added pellets. This is commensurate with the chamber pressurization histories of both mixes, as seen in Figure 7.

2. The flamespread velocity of Modified B.P. pellets is only 5% of that obtained for the Standard Lot. However, if the pellet is formed from Class 7 granulation Black Powder, the flamespread rate increases dramatically to approximately 1200 in/sec. Although the basic ingredients of both pellets are nearly identical, structural differences in the resulting pellets, due to different ways of manufacture, produce large variations in achievable flamespread rates. It is suggested that better control of the homogeneity of the mix of Modified B.P. pellets will increase the performance of these pellets.

3. TYPE I pellet produces propagation velocities of approximately 1300 in/sec, only a 25% shortfall from Standard Lot rates. Thus, from the standpoint of pressure production and flamespread propagation performance, TYPE I pellet compares favorably with Standard Lot Class 1 granulation Black Powder.

4. The flamespread performance of TYPE C, TYPE J, and Modified B.P. pellets is no better than the flamespread characteristics obtained for the majority of Class 1 granular Deviant Lot Black Powders.

CONCLUSIONS

In general, comparisons of flamespread propagation velocities of Deviant Class 1 Black Powder Lots with corresponding measurements for Standard Lot GOE 75-44 indicate a significant reduction in flamespread performance for the majority of the Deviant Lots. Similar trends have been noted in closed bomb firings performed at ARRADCOM, Dover, in which inverse induction time is considered the relevant performance parameter for comparison with flamespread velocities.⁴ In those instances where anomolous behavior of an actual gun firing has been traced to a specific lot of Black Powder, flamespread tests of that powder indicate anomolous propagation velocities.

The results of experimental flamespread performance tests with TYPE I pellet, an NC-added, Black Powder-base formulation, lend merit to the application of this compacted pellet for artillery primers. Of course, vast improvements in performance may be achieved by considering such structural variations as the pellet length-to-diameter ratio, pellet packing density, and optimization of constituent weight percentages.

The flamespread tests of Class 7 Black Powder pellets demonstrate that a pelletized rather than a granular formulation of Black Powder may have useful applications for artillery primers, especially from the standpoint of manufacture. It remains to be established whether a modified Black Powder pellet can be manufactured from basic ingredients which produce flamespread propagation rates and chamber pressurization characteristics equivalent to either Class 7 Black Powder pellets or Class 1 Black Powder granules.

It is premature to speculate at this time as to the effects of these various Black Powders on the ballistics of artillery. The relationship between flamespread rate in the primer tube and in the packed propellant bed of the charge assembly must be established in order to provide the link between the flamespread rates as obtained by the PCRL Flamespread Tester and acceptable gun firing performance.

Only after study of the correlations between muzzle velocity, breech pressure, ignition perturbations if any, etc., for each of the Black Powders and the measured flamespread rates would it be possible to draw final conclusions as to the full implications of new primer formulations. However, the sensitivity and reproducibility of the flamespread measurement data obtained with the PCRL Flamespread Tester to variations in Black Powder formulations make the device quite attractive for use as a laboratory simulator for comparative analysis of new primer applications and ignition trains for artillery applications.

REFERENCES

1. Shulman, L., Private Communication, ARRADCOM, Dover, NJ, May 1978.
2. Guess, B., "Product Improvement Test of M203E1 Propelling Charge, 155MM", U.S. Jefferson Proving Ground, Report No. 78-440, May 1978.
3. Allen, J.C., Private Communication, ARRADCOM, Dover, NJ, January 1980.
4. Lenschitz, C., Private Communication, ARRADCOM, Dover, NJ January 1978.
5. White, K.J., Holmes, H.E., and Kelso, J.R., "Effect of Black Powder Combustion on High and Low Pressure Igniter Systems", 16th JANNAF Combustion Meeting, Monterey, CA, September 1979.
6. Messina, N.A., Ingram, L.S., Apostolico, K.A., and Summerfield, M., "Flamespread Measurements of Pelletized Primer Mixes", Princeton Combustion Research Laboratories, Inc. Final Report No. PCRL-FR-79-006, October, 1979.
7. Messina, N.A., Ingram, L.S., and Summerfield, M., "Black Powder Quality Assurance Flamespread Tester", Princeton Combustion Research Laboratories, Inc. Final Report No. PCRL-TR-78-101, December, 1978.
8. Messina, N.A., Ingram, L.S., Apostolico, K.A., and Summerfield, M., "Further Studies of Flamespread Measurements of Pelletized Primer Mixes", Princeton Combustion Research Laboratories, Inc. Final Report No. PCRL-FR-80-003, March 1980.

ROLE OF SURFACE CHEMISTRY IN THE IGNITION OF PYROTECHNIC MATERIALS

W. E. Moddeman, L. W. Collins and P. S. Wang
Monsanto Research Corporation
Mound Facility*
Miamisburg, Ohio 45342

and

T. N. Wittberg
University of Dayton Research Institute
Dayton, Ohio

ABSTRACT

Due to the interaction of fresh metal surfaces with oxygen of the atmosphere, native oxides always form on reactive metals, such as titanium and aluminum. In this paper, the chemistry of the native oxide will be discussed in light of its role in pyrotechnic (Ti/KClO_4) and thermite ($\text{Al/Cu}_2\text{O}$) reactions. Auger electron spectroscopy (AES) and x-ray photoelectron spectroscopy (XPS) were used to characterize the surface chemistry of the native oxide at ambient (25°C) and at elevated ($<1000^\circ\text{C}$) temperatures. From the AES data it was concluded that the oxide on titanium began dissolving at 300°C , and above 350°C the data showed the presence of "free" metal on the surface. XPS data showed the dissolution process to proceed through the formation of titanium suboxides. Similar AES data recorded on the native oxide of aluminum indicated that no dissolution occurs over the temperature range of 25°C to $>660^\circ\text{C}$ (the melting point of aluminum metal). However, AES analysis of $\text{Al/Cu}_2\text{O}$ pellets revealed the presence of an interfacial reaction zone between the aluminum fuel and the Cu_2O particles. These AES and XPS results were found to complement the thermal property measurements, such as DSC and DTA, on the Ti/KClO_4 pyrotechnic and $\text{Al/Cu}_2\text{O}$ thermite mixtures. A reaction mechanism is presented for the Ti/KClO_4 pyrotechnic mixture illustrating the role of the surface oxide in the ignition process. A model is also presented for $\text{Al/Cu}_2\text{O}$ ignition.

*Mound Facility is operated by Monsanto Research Corporation for the U.S. Department of Energy under Contract No. DE-AC04-76-DP00053.

INTRODUCTION

The basic chemical mechanisms which control the thermal ignition of pyrotechnic materials are not well known. A series of studies to determine these mechanisms for a limited number of pyrotechnic blends is presently underway at the Mound Facility. As part of this effort, a study of the surface chemistry of $TiH_x/KClO_4$ ($0.15 \leq x \leq 1.9$) pyrotechnic compositions began in 1975 followed by studies on Al/Cu_2O thermites a year later (Ref. 1 to 7). Early results established that the titanium subhydride particles are coated with thin layers of titanium oxide, suboxide, and/or hydroxides with Ti^{+4} as the primary oxidation state. Also, a contaminant layer of carbon was always present on the fuel surface. In more recent studies, it was shown that simply mixing titanium powder with the $KClO_4$ oxidizer lowered the surface concentration of titanium suboxides (or hydroxides). The surface oxides were shown to dissolve upon heating through a process which increased the surface concentration of the suboxides followed by an increase in free titanium metal at the surface at higher temperatures. These surface processes have been related to the electrostatic and thermal initiation mechanisms for the $TiH_x/KClO_4$ system (Ref. 8 and 9).

The surface chemistry of aluminum fuel, Cu_2O oxidizer, and both powdered and compacted Al/Cu_2O thermites has been investigated at the Mound Facility (Ref. 3 to 7). The native oxide coating on the Al powders as received from the manufacturer was found to increase by approximately 20% after mixing with the Cu_2O oxidizer at room temperature. Pressing the mixture for 15 minutes at $425^\circ C$ doubled the thickness of the aluminum oxide coating on the fuel. It was also shown that the surface of the Cu_2O contained small concentrations of CuO that disappeared upon heating.

For most applications, the Al/Cu_2O thermites are pressed at elevated temperatures and pressures to form special shapes and densities required to meet specific needs. This hot pressing utilizes temperatures of 425° to $500^\circ C$ and pressures in excess of 10,000 psi. These conditions plastically deform the fuel so that a matrix of Cu_2O oxidizer is

established in a continuum of aluminum. An interfacial region of at least 100 Å between the Al and Cu₂O is produced by the pelletizing process which was examined by scanning Auger microscopy (Ref. 7).

In this study, the surface chemistries of Ti/KClO₄ and Al/Cu₂O are related to thermal data for these systems. Mechanisms to explain the roles of the surface oxides in the ignition of these pyrotechnics are proposed for each system.

EXPERIMENTAL

The titanium based pyrotechnic materials used in this study have previously been described in some detail (Ref. 8 and 9). Polycrystalline titanium and aluminum foils were used for both the AES and XPS experiments to minimize the influence of surface roughness on the measurements.

Theoretically stoichiometric thermite mixtures (11 wt % Al and 89 wt % Cu₂O) were produced by dry mixing Reynolds XD28 aluminum flake and Cerac "Pure" cuprous oxide in a V-blender for one hour (Ref. 10). Aluminum flake was used as received while Cu₂O powders were sieved through a 400 mesh screen prior to blending. Thermite pellets about 6 mm in diameter, 2 mm in height, and at 90% of theoretical density were pressed from powders with preheated graphite dies under dry nitrogen at 425°C and 12,000 psi for 15 minutes (Ref. 12).

Thermal data were generated with a DuPont 990 thermoanalyzer using the 1200° high temperature DTA cell, the DSC cell and the 951 thermogravimetric analyzer. A Varian Auger spectrometer (Model 981-2707) having a maximum electron beam energy of 10 keV and a minimum spot size of 5 μm was used for the AES measurements. A beam energy of 5 keV and a beam current density of 20 mA/cm² (2 μA beam rastered over 10⁴ μm²) was selected. The XPS data were obtained with an extensively modified AEI ES-100 photoelectron spectrometer. Modifications to this instrument include the addition of a 220 l/sec turbomolecular pump and a 110 l/sec ion pump for evacuation of the sample chamber. The heater assembly in the AES and XPS systems has been used in cathode studies

and is described elsewhere (Ref. 11). In both cases, the temperature of the foil was measured using a chromel-alumel thermocouple which was spot-welded directly to the foil.

RESULTS AND DISCUSSION

1. Titanium

Unprotected titanium metal powder is pyrophoric; that is, a fresh metal surface of titanium can ignite spontaneously in air at room temperature. However, if the metal powder is passivated, e.g., with its native oxide, oxidation rates become negligible so that the powder is stabilized to temperatures in excess of 500°C. Figure 1 illustrates the DTA curves for titanium powder ($\text{TiH}_{0.15}$) and for the $\text{TiH}_{0.15}$ mixed with KClO_4 , KIO_4 , KClO_3 , or RbClO_4 oxidizers. The exothermic oxidation reactions for these pyrotechnic systems were relatively slow until the temperature exceeded 500° where the reactions became self-sustaining, i.e., ignition occurred. All of the major features in these curves below 500° can be attributed to processes associated with the oxidizers; for example, the strong endothermic peak at 300° in the curve for $\text{TiH}_{0.15}/\text{KClO}_4$ is due to a rhombic to cubic phase transition in the KClO_4 . Thus, the DTA thermal data establish that thermal ignition of titanium based pyrotechnics is controlled by processes associated with the fuel and is relatively independent of the oxidizer.

Auger electron spectroscopy (AES) is a well-documented surface characterization technique capable of probing the top nanometers of material. AES surface scans were recorded for a passivated titanium foil sample as a function of temperature and the ratio of the intensity of the L-MM 418 eV line of titanium to the K-LL 509 eV line of oxygen was calculated. This ratio is shown as a function of temperature in Figure 2. The increase in the Ti/O ratio beginning just below 300°C is characteristic of the dissolution of the oxides of titanium into the metal substrate. This is indicative of an increase in surface reactivity due to increased availability of unoxidized titanium metal.

While AES clearly indicates the dissolution process, it cannot provide direct evidence for changes in the oxidation state of titanium

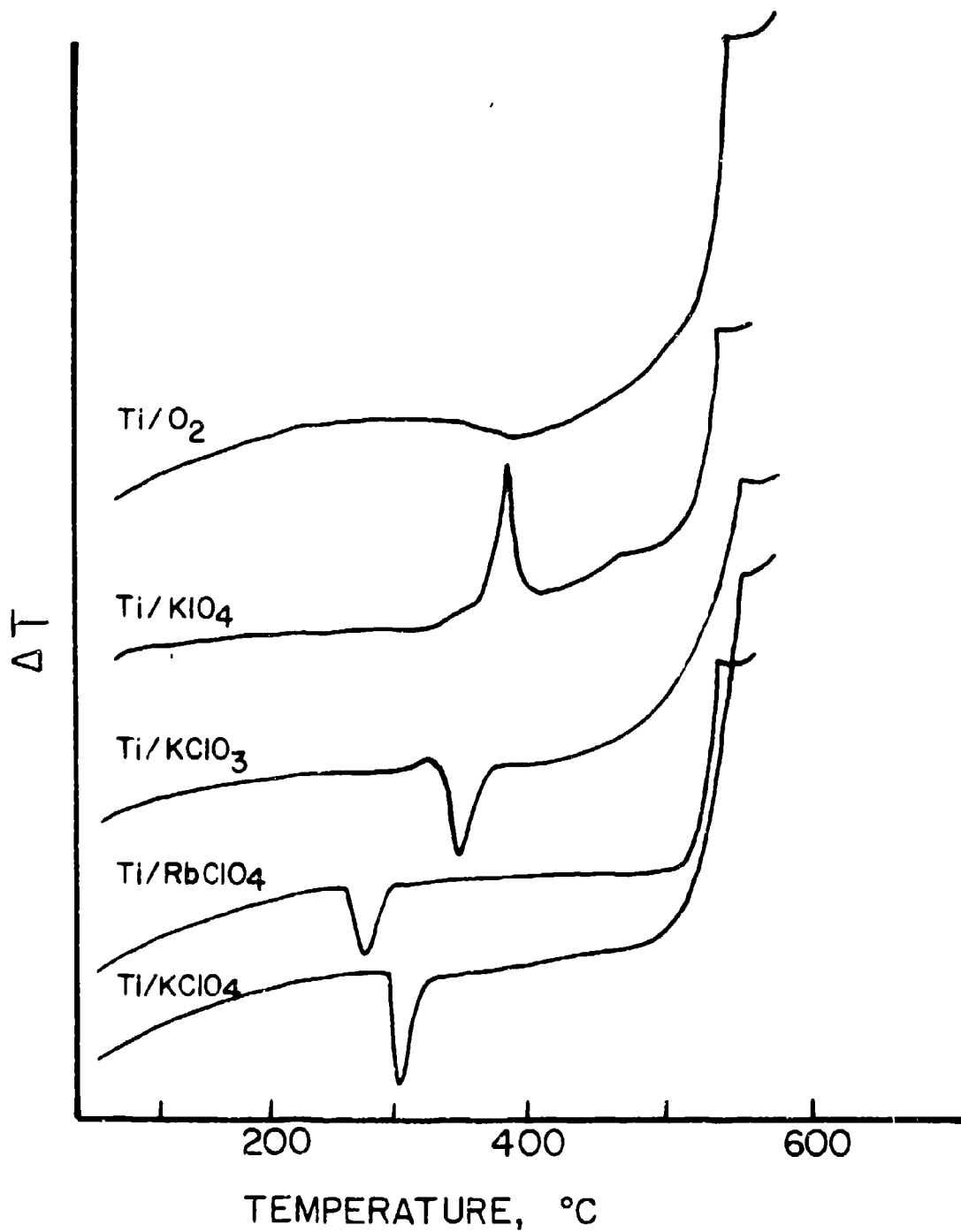


FIGURE 1. DTA curves for $\text{TiH}_{0.15}$ powder and $\text{TiH}_{0.15}$ /oxidizer pyrotechnic blends.

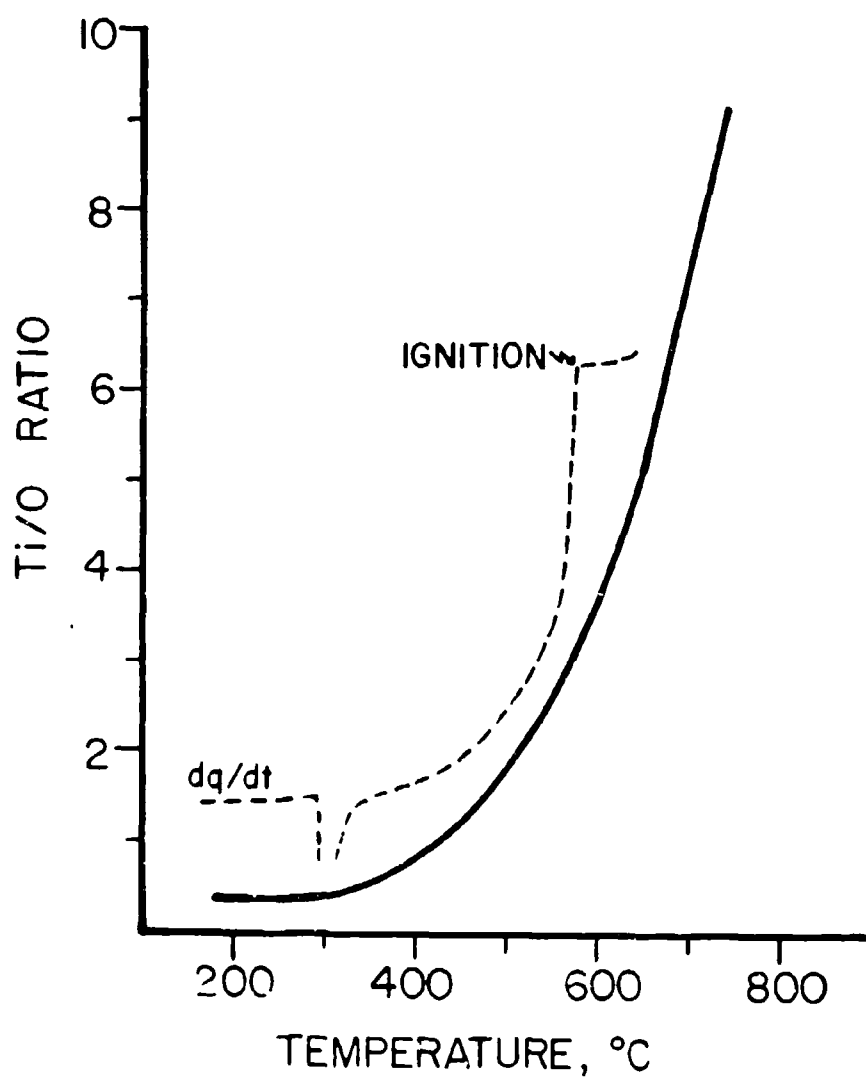


FIGURE 2. Ratio of Ti L-MM Auger (418 eV) line to O K-LI (510 eV) line as a function of temperature.

which would be expected to accompany this process. It has previously been shown that it is possible to detect lower oxidation states of titanium such as TiO , Ti_2O_3 , and Ti_3O_5 within the passive TiO_2 film by using XPS (Ref. 12). Therefore, the $O\ 1s$ and $Ti\ 2p$ spectra were recorded at eight different temperatures in order to study changes in the surface chemistry during dissolution. Peak deconvolutions were carried out using a DuPont 310 Curve Resolver under the assumption that titanium was bound as Ti^0 , Ti^{+4} , or Ti^{+n} where $0 < n < 4$. The total counts-per-second under each titanium peak was then ratioed to the total counts-per-second under the O^{-2} portion of the $O\ 1s$ spectrum and plotted as a function of temperature. This plot, shown in Figure 3, shows that the Ti^0/O^{-2} ratio begins to increase at $\sim 350^\circ$ which is in good agreement with the AES data. The Ti^{+4}/O^{-2} ratio begins to decline at $\sim 300^\circ C$ coincident with the increase in Ti^0/O^{-2} and Ti^{+n}/O^{-2} ratios. Interestingly, the Ti^{+n}/O^{-2} ratio does not peak until a temperature of 450° is attained. Thus, we conclude from the XPS data that the dissolution process proceeds through the formation of lower titanium oxides.

It should be noted that ultra high vacuums were used in generating the AES and XPS data. In normal oxidizing environments such as those used in generating the thermoanalytical data and in pyrotechnic blends, the replacement of the native oxide is sufficiently rapid between 300° and 500° to keep the active titanium surface concentration very low. This reoxidation of the surface is indicated by DSC as a weak exotherm which we have superimposed on the Auger data in Figure 2.

These data then provide a basis for understanding the chemical processes associated with the thermal ignition of titanium based pyrotechnics. The rapid oxidation reaction necessary to generate sufficient heat for self-sustained reaction is controlled by the availability of reactive titanium at the surface of the fuel particles. At temperatures below 500° , the dissolution reaction that generates the active specie at the surface was relatively slow so that there was insufficient fuel available for sustained oxidation in the DTA sample configuration. At temperatures in excess of 500° , the dissolution became rapid enough that the oxidation reaction which mirrors it generated sufficient heat for ignition. Thus, the ignition process seems to be kinetically

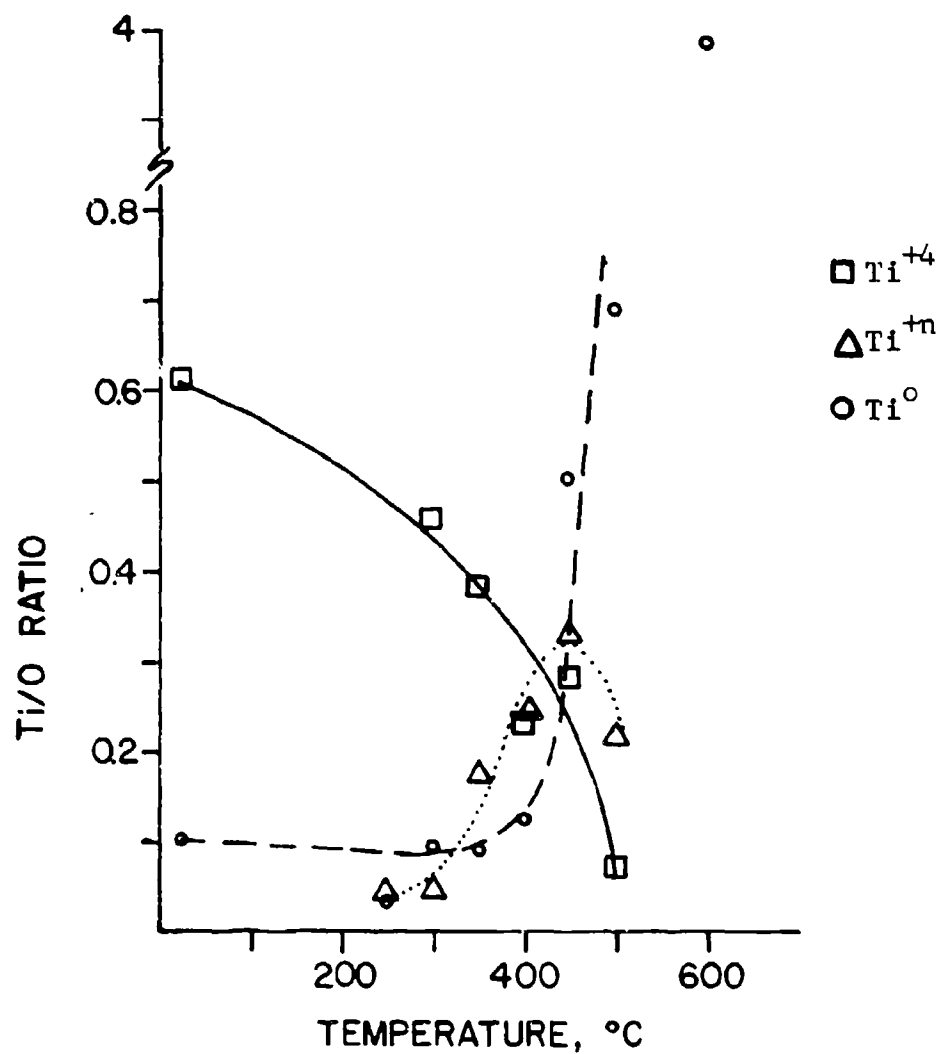


FIGURE 3. Ratio of the titanium $2p_{3/2}$ line to the oxygen $1s$ line for O^{-2} as a function of temperature.

controlled by the dissolution of the titanium oxides with the concomitant production of reactive titanium on the surface. The diffusion controlled reaction with oxygen gas at the inner titanium-titanium oxide boundary also occurs but has been shown to be slow as compared to the surface oxidation process (Ref. 2).

2. Aluminum

Aluminum, like titanium, has an oxide coating which stabilizes the very reactive metal against further oxidation until relatively high temperatures. The oxidation process is again controlled by the availability of reactive metal on the surface. When the unoxidized aluminum is exposed to even trace quantities of oxygen, it rapidly reacts as shown by the thermogravimetric curves in Figure 4. A gain in mass is shown for the spherical aluminum powder beginning at about 600° regardless of the atmosphere surrounding the sample; the high affinity of the free metal for oxygen removes trace contaminants of oxygen from the "inert" atmospheres. For the spherical aluminum which has a nominal particle size of 10 μm , the increase in oxide thickness represented by the weight gain shown in Figure 4 is of the order of 4000 Å.

The oxidation of aluminum powder at about 600°C is also shown by the DTA curves in Figure 5. Again, the exotherm is relatively independent of the atmosphere surrounding the sample. The endotherm corresponding to the fusion of aluminum at 660° is very weak or completely absent due to the coincident oxidation process which is much more energetic. However, after the powder has once been heated through this region, the increased oxide layer slows the oxidation process so that the exotherm disappears and the fusion endotherm is well resolved. It should also be noted that the oxide coating appears to remain intact through heating cycles to temperatures of 1000°C; the powder remains unchanged in appearance after heating whereas other metal powders such as the titanium flow together upon melting.

The oxidation process occurring at about 600° that is indicated by the thermoanalytical techniques corresponds to an increase in the concentration of unreacted aluminum at the surface of the particles. This increase in concentration is shown directly by the increase in the Al/O

SPHERICAL ALUMINUM

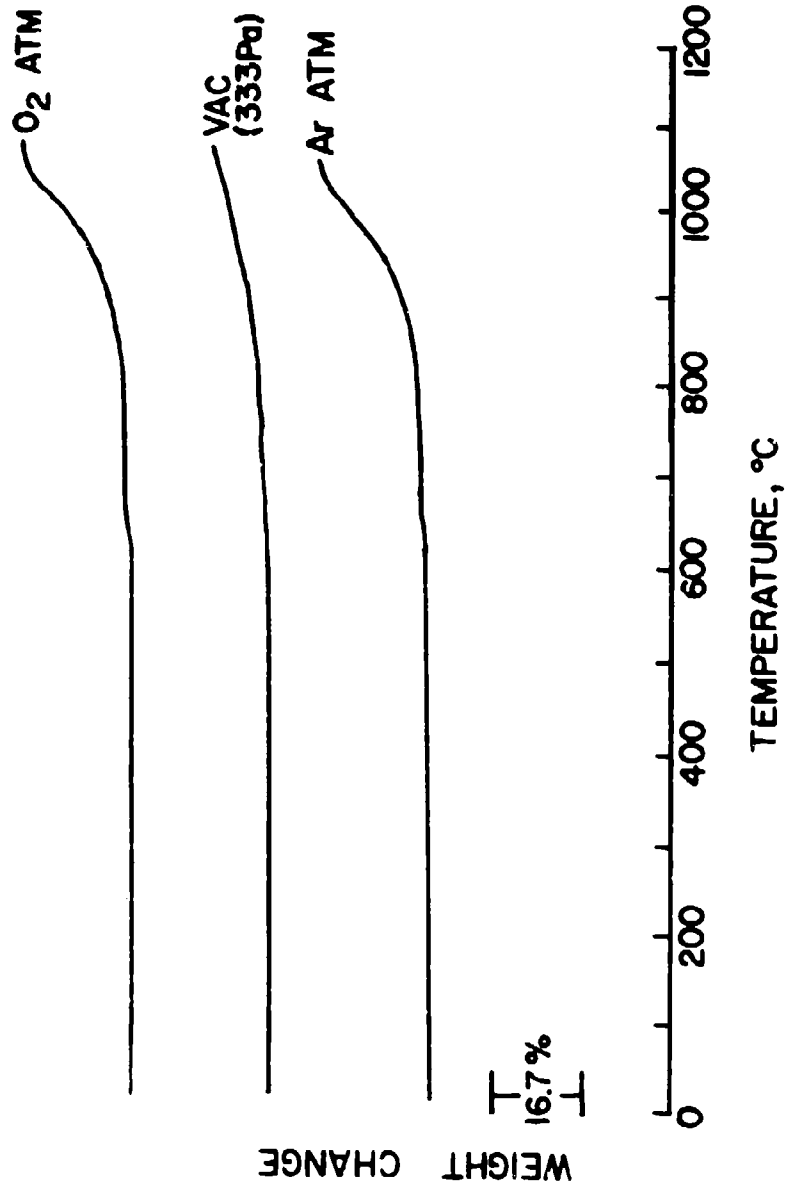


FIGURE 4. Thermogravimetric curves for spherical aluminum powder obtained in different atmospheres at a heating rate of 20°/min.

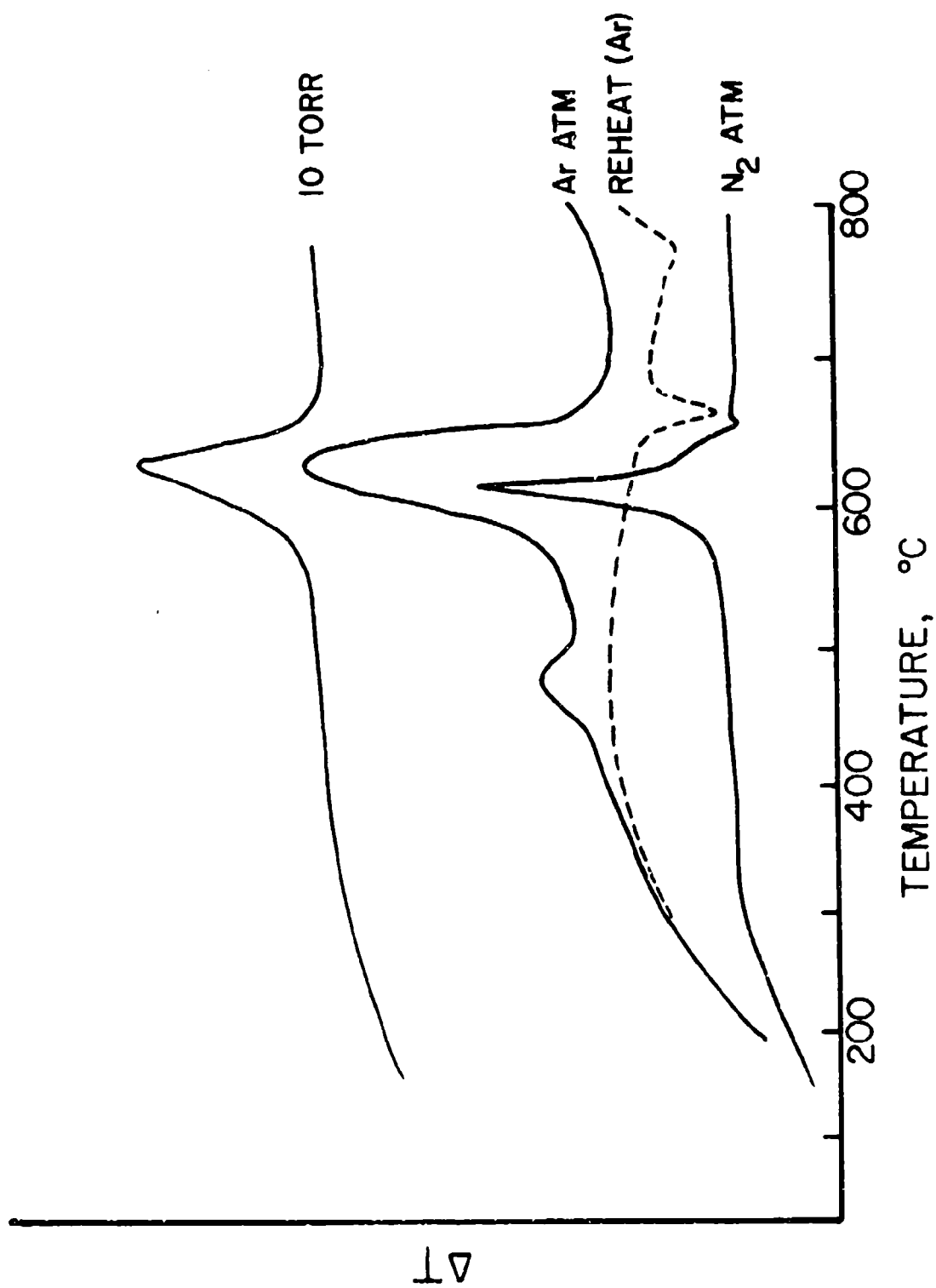


FIGURE 5. DTA curves for spherical aluminum powder.

ratio versus temperature plot presented in Figure 6 which was obtained by AES. Since the oxide coatings remain intact, this increase must be due to diffusion of the metal to the surface rather than an oxide dissolution process as observed for the titanium. The continued increase in oxide thickness opposes the increase in the diffusion rate as the temperature increases. Therefore, this type of process is less likely to kinetically control thermal ignition than a dissolution process.

When aluminum was mixed with Cu_2O to form the thermite blend, thermal reactions for the fine powder were relatively easy to control as indicated by the DTA curve shown in Figure 7. Two strong exotherms are evident but the powder did not ignite. However, when the thermite was consolidated, ignition occurred at 545° . While heat flow differences could produce this behavior, there also seems to be a subtle change in the chemistry for the two conditions. The strong endotherm just prior to ignition of the consolidated material is not present in the powdered form and is an indication of a change in the material due to the hot pressing. The nature of this endotherm is indicated by the DSC of aluminum powder in copper pans as shown in Figure 8; an aluminum-copper alloy forms upon heating the two metals together. The endotherm at 540° is characteristic of a phase change associated with this Al-Cu alloy. Thus, the presence of the endotherm in the DTA curve for consolidated thermite indicates that the Al-Cu alloy was formed during the consolidation process.

Ignition of the thermite powder seems to depend on heat generated by aluminum diffusing to the surface of particles for reaction. However, if the thermite has been consolidated, the high pressures in a nitrogen blanket exclude air while the elevated temperatures generate free aluminum at the particle surface. This aluminum can then alloy with copper from the Cu_2O . Ignition can occur due to heat generated by the oxidation of the alloy rather than aluminum. The phase change at 540° apparently makes the alloy oxidation reaction favorable which can generate the heat to achieve ignition of the thermite reaction which is thought to occur at higher temperatures (perhaps the second exotherm in the DTA of the powder).

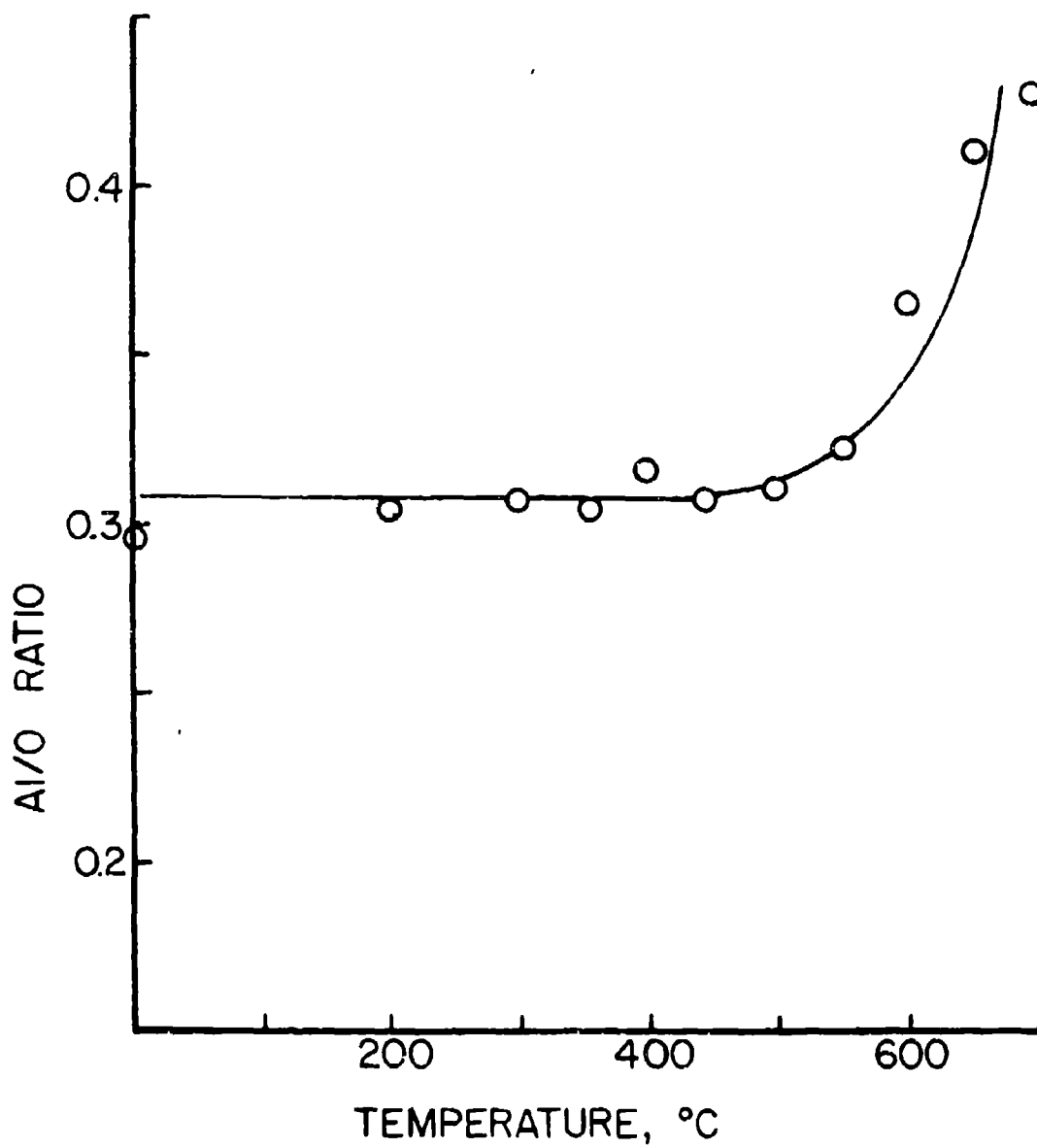


FIGURE 6. Ratio of Al K-LL Auger line to O K-LL line as a function of temperature.

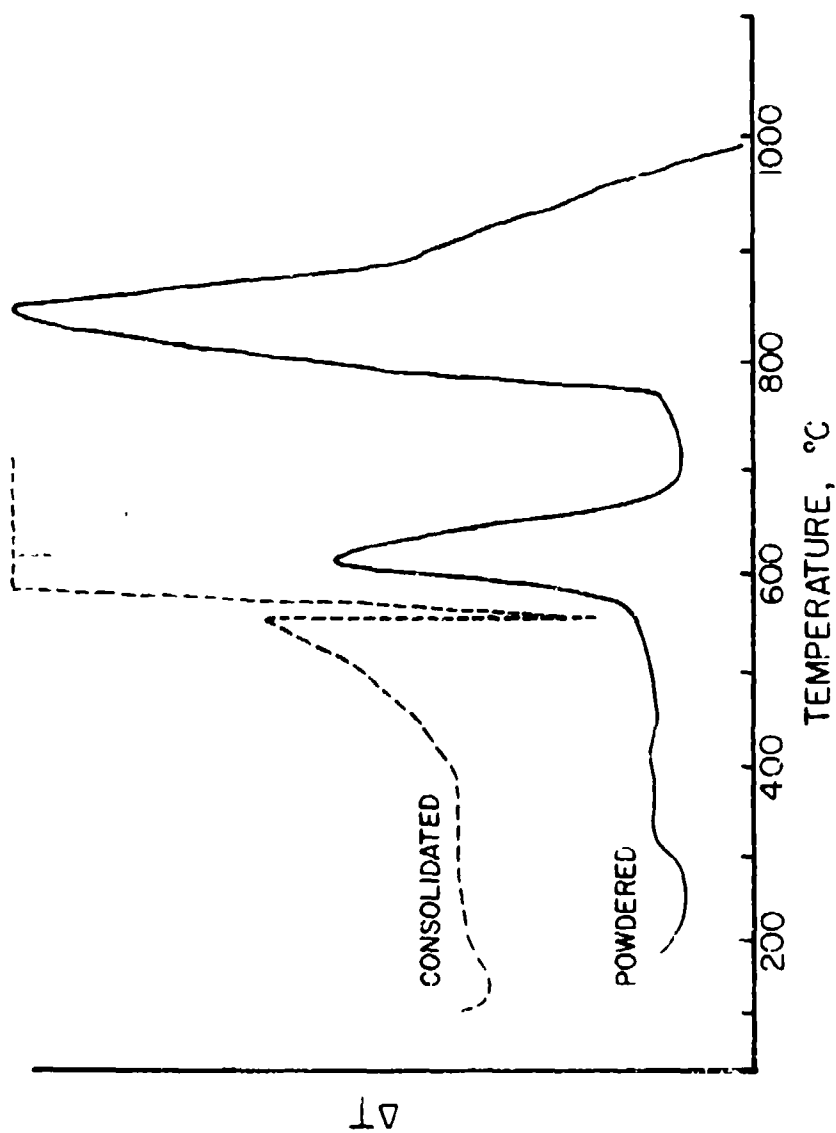


FIGURE 7. DTA curves for Al/Cu₂O thermite powder and consolidated thermite.

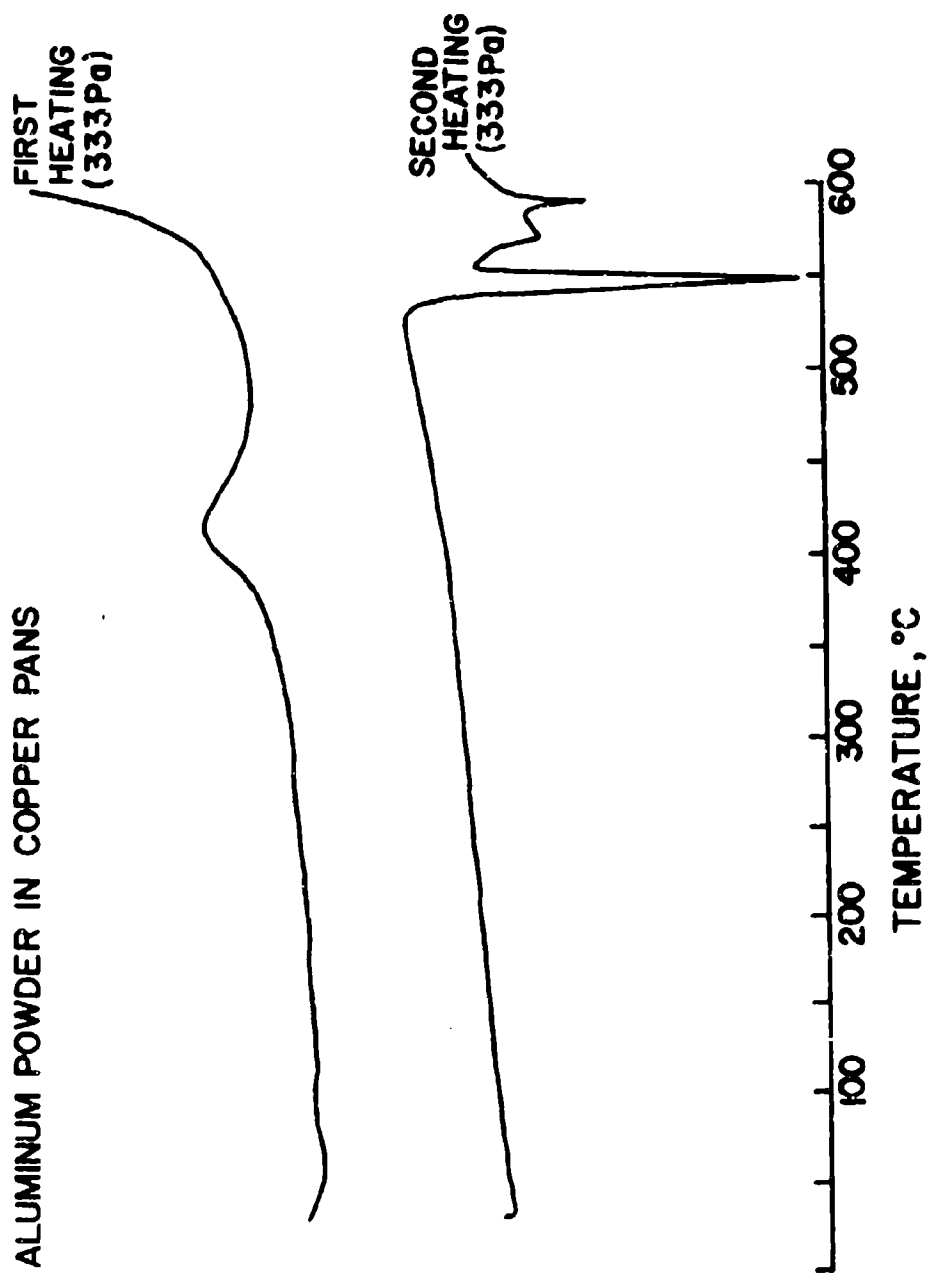


FIGURE 8. DSC curves of spherical aluminum powder in copper pans.

SUMMARY

The surface chemistry of fuels has been shown to play a key role in the ignition of pyrotechnic materials. Since these fuels are usually easily oxidized, the surface must provide protection from undesirable oxidation processes such as pyrophoricity while permitting the desirable pyrotechnic reactions. For both titanium and aluminum, these criteria are met by metal oxide coatings which control the accessibility of the fuel to the oxidizer. However, we have shown that the mechanisms through which this control is exerted are substantially different. The ignition of titanium based pyrotechnics seems to be kinetically controlled by the dissolution of the titanium oxide coating to generate a reactive surface for the pyrotechnic reaction. Reactions of aluminum seem to depend on diffusion of aluminum (or oxygen at higher temperatures) through its oxide coating. It was also shown that the accessibility of aluminum can be improved by alloying.

REFERENCES

1. W. E. Moddeman and W. D. Pardieck, "Surface Chemical Analysis, Surface Integrity of Starting Materials for Pyrotechnic Applications," Technical Report, University of Dayton, VDRI-TR-75-16, May (1975).
2. L. W. Collins, "Thermal Ignition of Titanium Based Pyrotechnics", submitted to Combust. Flame
3. A. Rengan and W. E. Moddeman, "ESCA Studies on the Thermite Mixture of Aluminum and Cuprous Oxide Using Si K α X-Radiation", Technical Report, University of Dayton, UDRI-TR-77-30, June (1977).
4. A. Rengan and W. E. Moddeman, "X-Ray Photoelectron Studies on the Thermite Mixture of Al and Cu₂O. II. Thickness Measurements of Carbon and of Aluminum Oxide on Aluminum, and Changes in Copper Chemistry", University of Dayton, UDRI-TR-78-22, December (1978).
5. A. Rengan, W. E. Moddeman, P. S. Wang and L. D. Haws, Proceedings, 10th Symposium on Explosives and Pyrotechnics, February 14-16, 1979, San Francisco, California.
6. P. S. Wang, L. D. Haws, W. E. Moddeman and A. Rengan, "Aluminum Particle Surface Studies in Al/Cu₂O by Electron Spectroscopy for Analysis and Auger Electron Spectroscopy", MLM-2264, November (1979).
7. P. S. Wang, L. D. Haws and W. E. Moddeman, "Surface Analysis of Consolidated Al/Cu₂O Mixture by Scanning Auger Microscopy", to be published.
8. L. W. Collins, L. D. Haws and A. Gibson, "The Electrostatic Ignition of Non-Dispersed Pyrotechnics", accepted in Combust. and Flame.
9. L. W. Collins, "The Role of Potassium Perchlorate in the Desensitization of Titanium Powder to Electrostatic Ignition", to be published.
10. L. D. Haws, M. D. Kelly and J. H. Mohler, "Consolidated Al/Cu₂O Thermite", Monsanto Research Laboratory, Mound Laboratory Report, MLM-2531, Miamisburg, Ohio 45342.
11. C. G. Pontano and T. N. Wittberg, Appl Surf Sci (in press).
12. T. Porte, M. Demosthenous and T. M. Duc, J Less Common Metals, **56**, 183 (1977).

POWER INDEPENDENT IGNITION ENERGY MEASUREMENTS

Jonathan Mohler
Mound Facility*
Monsanto Research Corporation
Miamisburg, Ohio 45342

ABSTRACT

A portion of the electrical energy supplied to hot-wire ignitable materials is dissipated, largely through thermal conduction, to the unignited portion of the charge and to the containment and igniter system. The remainder of the energy deposited by the igniter wire raises the mass of material required for sustained reaction to the critical reaction temperature. The amount of energy dissipated is a direct function of the time from first application of power, to ignition. Time to ignition can be controlled by altering firing pulse power. Integration of the power pulse from start until ignition yields the ignition energy. Repetition of this procedure at different power levels permits one to plot energy versus firing time. Since conduction losses are time dependent, extrapolation of the resulting curve to zero time yields an ignition energy value that is independent of losses due to thermal conduction.

A key to the success of the procedure is accurate observation of ignition time. It was found that the reaction energy released at ignition causes a discernible deflection in the firing current record. By comparison of light emission and current traces, it was found that the onset of deflagration occurs at the inflection point of the current trace deflection.

This procedure has been successfully applied to hot pressed thermite samples, yielding ignition energies that are in qualitative agreement with the expected sensitivities of the samples.

*Mound Facility is operated by Monsanto Research Corporation for the U.S. Department of Energy under Contract No. DE-AC04-76DP00053.

INTRODUCTION

A portion of the electrical energy supplied to hot-wire ignitable materials is dissipated, largely through thermal conduction, to the un-ignited portion of the charge and to the containment and igniter system. The remainder of the energy deposited by the igniter wire raises the mass of material required for sustained reaction to the critical reaction temperature. The magnitude of these losses is dependent on many variables, such as the thermal properties of the materials involved; the shape of the charge and configuration of the vehicle; but perhaps most importantly, it is dependent on the time to ignition. At low power levels an infinite amount of energy might be applied without ignition, whereas at high power levels the time to ignition is shortened and thermal losses are minimized. The nondissipative part of the ignition energy should be characteristic of the pyrotechnic load for a given wire type and size. We are investigating a procedure for establishing the minimum, power independent ignition energy.

EXPERIMENTAL

Ignition energies are determined by integration of firing pulse power curves, from first application of power to ignition. Firing current and voltage are recorded on a digital transient pulse recorder. The recorded data are transferred to a computer where the power curve is calculated then integrated to yield ignition energy.

Accurate observation of ignition time is a key to successful measurement of hot wire ignition energy. We have found that ignition time can be accurately determined from the shape of either the voltage or current curve. Figure 1 shows current, voltage and light emission records for a bare nichrome wire. The voltage trace is essentially flat prior to rupture. Rupture is marked by a very brief light flash concurrent with cessation of current and recovery of the voltage pulse. A wire loop imbedded in a free-standing hot-pressed thermite (89% Cu_2O ,

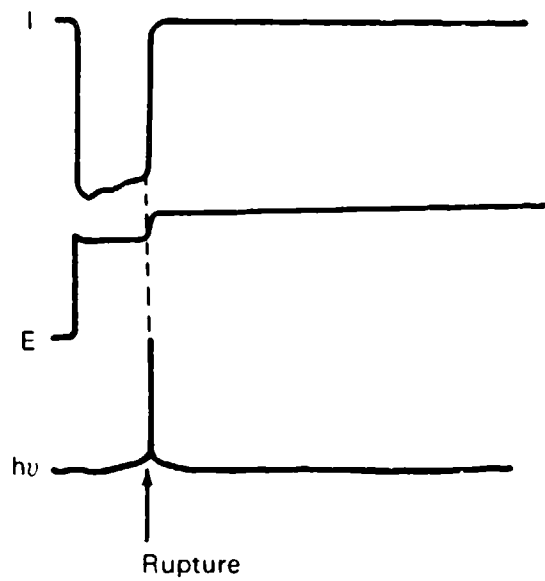


FIGURE 1 - Light emission is virtually concurrent with wire rupture for a bare nichrome wire.

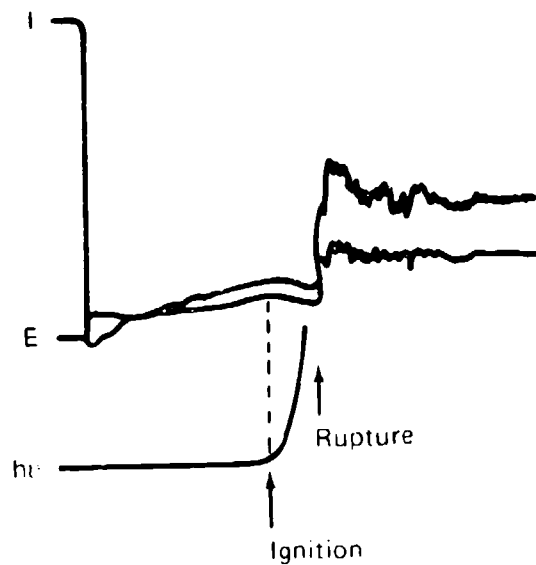
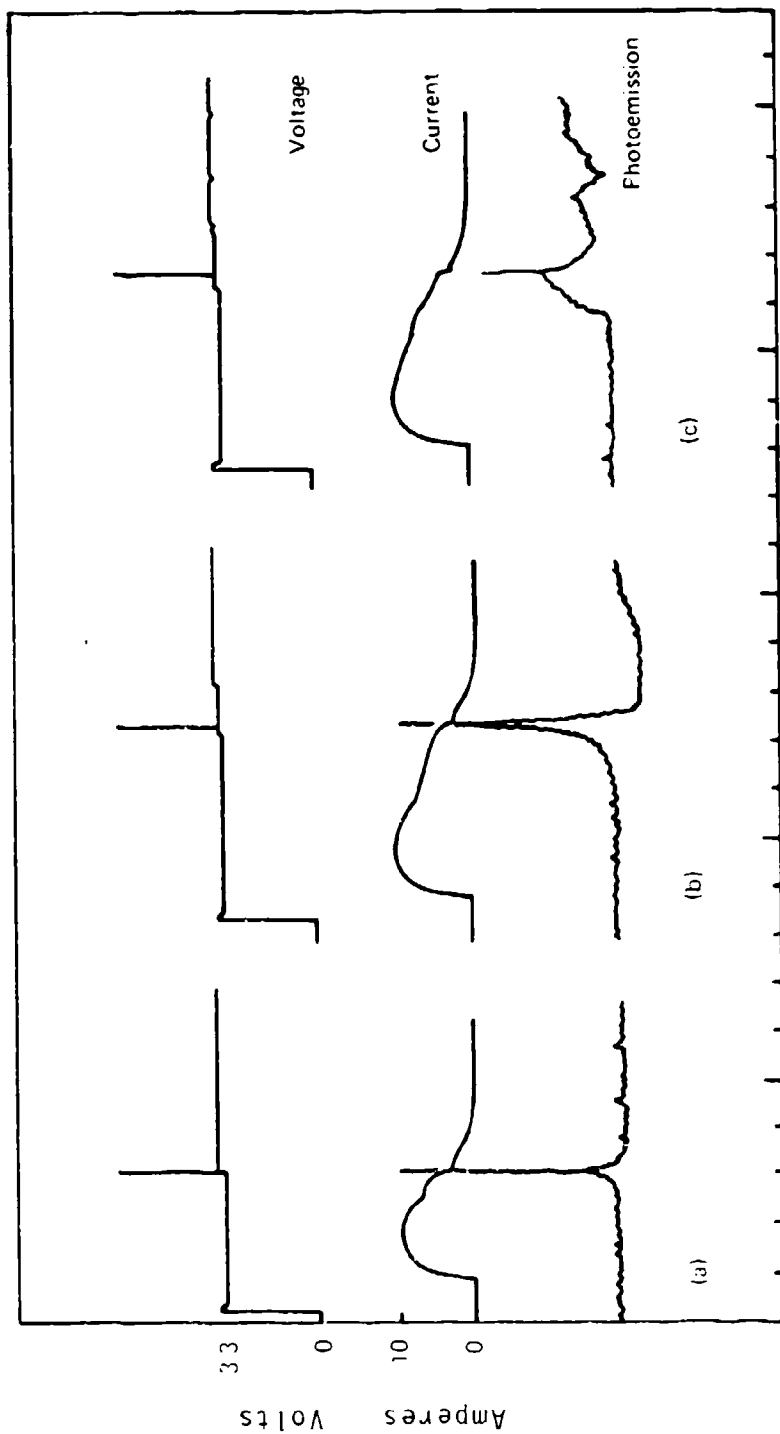


FIGURE 2 - Light emission from a hot-wire fused pellet begins before wire rupture.

11% Al-Si, 87% TMD) pellet shows significantly different behavior. Figure 2 shows the current, voltage and light emission records under these conditions. It is clear that light emission is broader under these conditions, starting approximately 5 msec. before wire rupture. This pre-wire-rupture light is attributed to light emitted by the reaction. A positive voltage inflection and negative current inflection (note that the current trace is inverted in Figures 1 and 2) occur at the time of the first appearance of reaction light emission. This is thought to be a result of a temperature jump in the hot wire as the highly exothermic thermite reaction begins, adjacent to the hot wire ignition source. A similar effect can be seen for B/CaCrO₄ fired in the hot wire mode in an SE-1 detonator. The wire is 1.5 mil by 40 mil gold. The first set of curves (voltage, current and light emission) shown in Figure 3 for a bare wire shows, as before, that rupture and light emission are concurrent. The second set of curves for an inert load of B/CaSO₄ indicates some very low level emission preceding rupture. The live B/CaCrO₄ load shows obvious reaction light more than 100 μ sec before rupture. A drop in current is concurrent with the start of the reaction. These inflections in the current or voltage record can be utilized to determine the time of ignition. Depending on the average slope of the record, the inflection may not form a maximum, so the ignition time becomes even clearer when the second derivative curve is generated. This is illustrated in Figure 4 with the voltage record and the second derivative thereof for a thermite hot wire ignition. In calculating ignition energy from the firing current and voltage data, the upper limit of integration was set by the ignition time taken from the second derivative voltage record.

RESULTS

Ignition energy-ignition time profiles have been determined for three thermite blends having different fuels--pure aluminum, aluminum-12% silicon, aluminum-50% magnesium. In each case, the particles were spherical and sized to pass through a 325 mesh screen. Each blend contained a stoichiometric quantity of Cu₂O. The profiles for these three



Time, 100 μsec/div

FIGURE 3 - Firing voltage, current, and photoemission for: (a) bare bridgewire, (b) B/CaSO₄ inert load, and (c) B/CaCrO₄ pyrotechnic load.

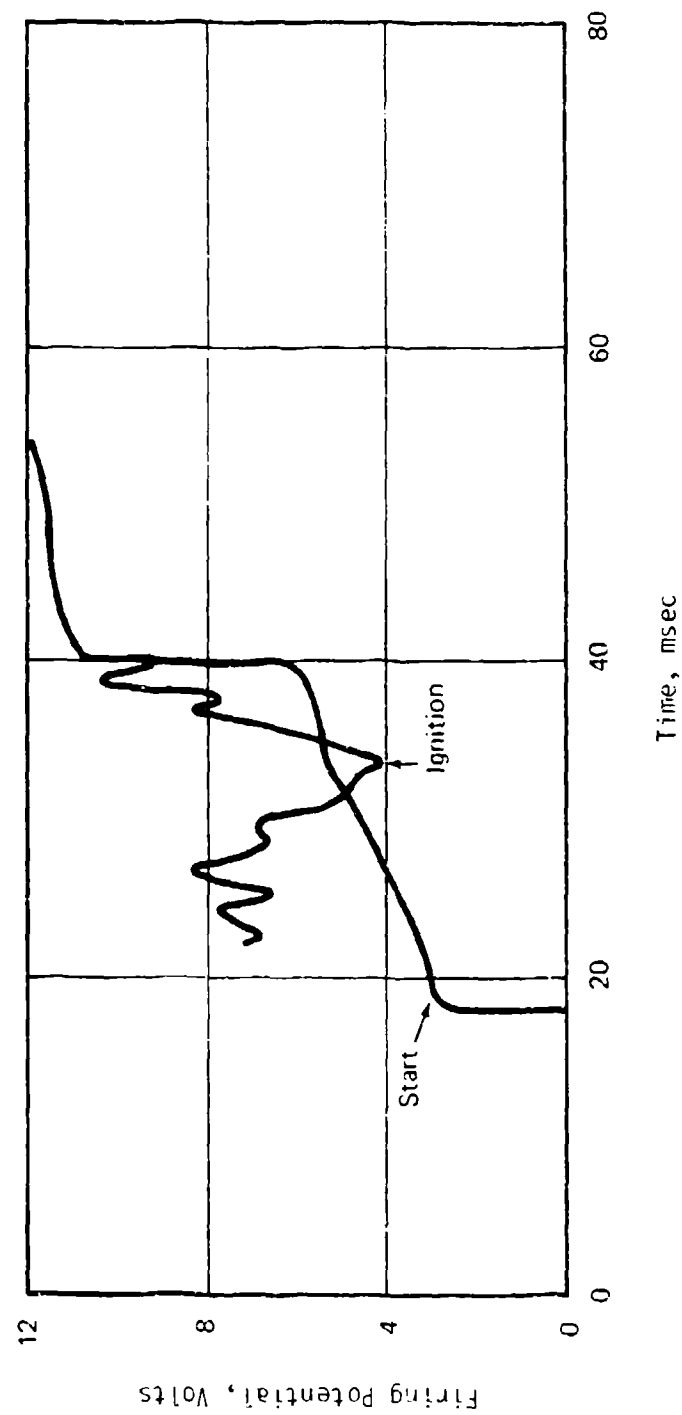


FIGURE 4 - The second derivative of the voltage curve recorded during firing of a hot-wire device exhibits a minimum at ignition.

thermite blends are shown in Figures 5, 6 and 7. Second degree polynomial regressions were made, providing the three parameter E_0 , b and c for the equation

$$E(t) = E_0 + bt + ct^2$$

Where $E(t)$ is the time dependent ignition energy, E_0 , b and c are adjustable parameters. A summary of the parameter values and the R^2 measure of data precision are given in Table 1.

TABLE 1
Second-Degree Polynomial Regression Analysis of Ignition
Energy-Ignition Time Data for Cu_2O Thermites

<u>Fuel</u>	<u>E_0</u>	<u>b</u>	<u>c</u>	<u>R^2</u>
Al	6.60	0.0519	0.0023	0.943
Al-Si	2.81	0.3090	0.0005	0.985
Al-Mg	3.03	0.2770	0.0001	0.932

DISCUSSION

From the form of the above equation, the parameter E_0 is a time independent energy value. It can therefore be thought of as the non-dissipative ignition energy. As previously stated, the nondissipative power independent ignition energy should be a measure of the ignition sensitivity of the pyrotechnic material.

The lattice loosening effect of additives such as silicon or aluminum is expected to increase the sensitivity of Al-Si/ Cu_2O or Al-Mg/ Cu_2O compared to Al/ Cu_2O ¹. The E_0 values listed in Table 1 are consistent with this expectation.

¹A.F.E. Welch, "Chemistry of the Solid State", W. Garner (ed.) Butterworths, London, 1955, pp. 305-309.

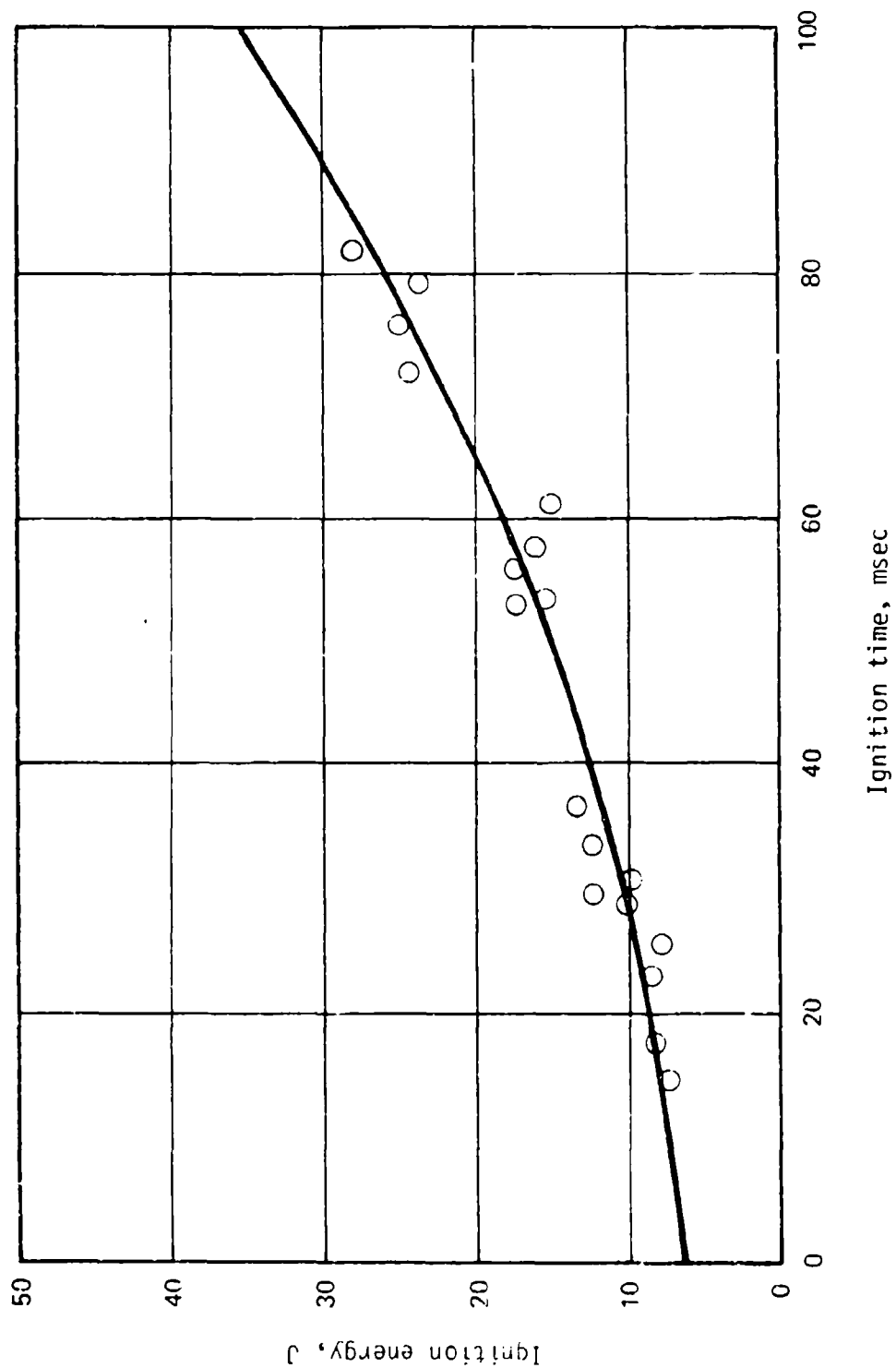


FIGURE 5 - The ignition energy of spherical Al/Cu₂O increases nonlinearly with ignition time.

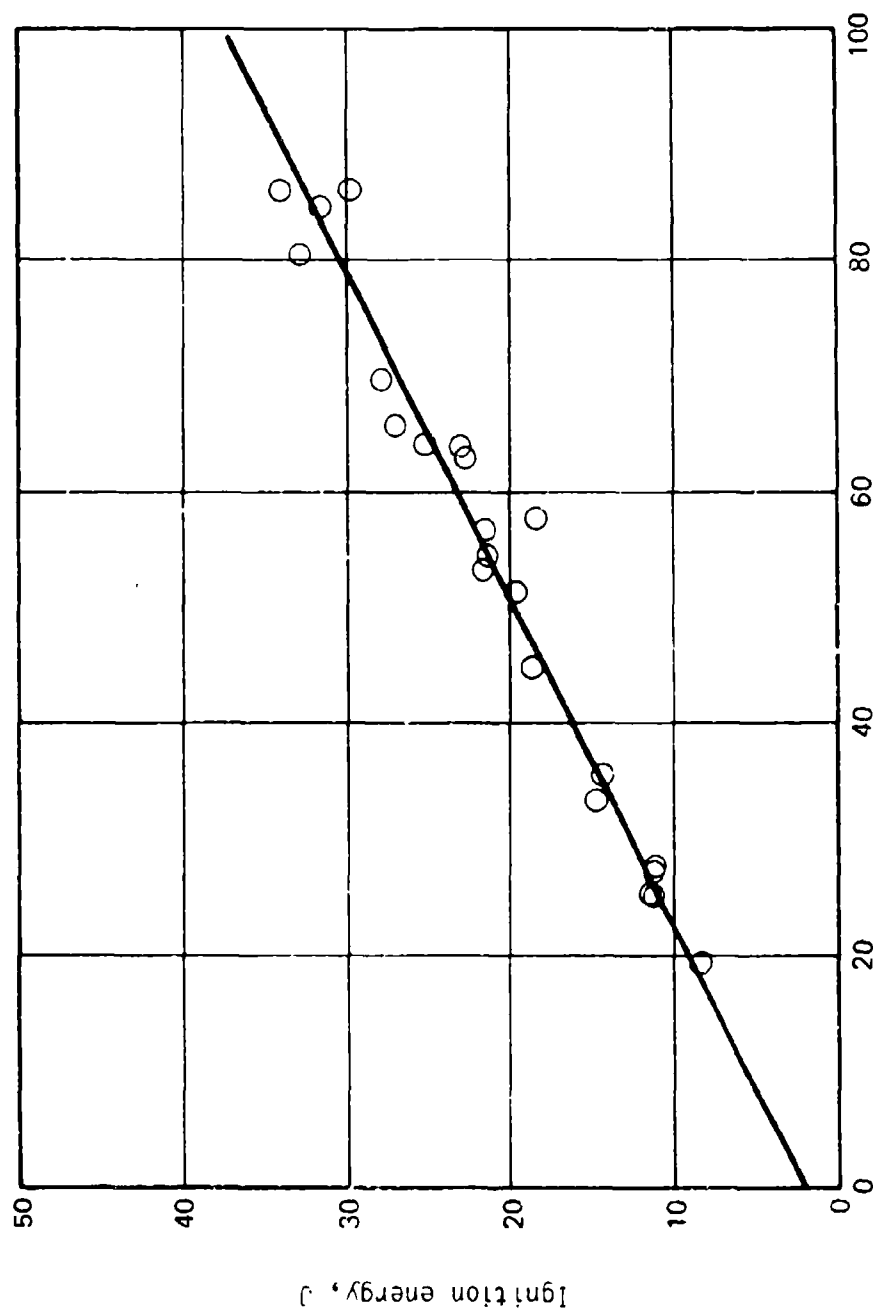


FIGURE 6 - The ignition energy of Al-Si/Cu₂O increases almost linearly with ignition time.

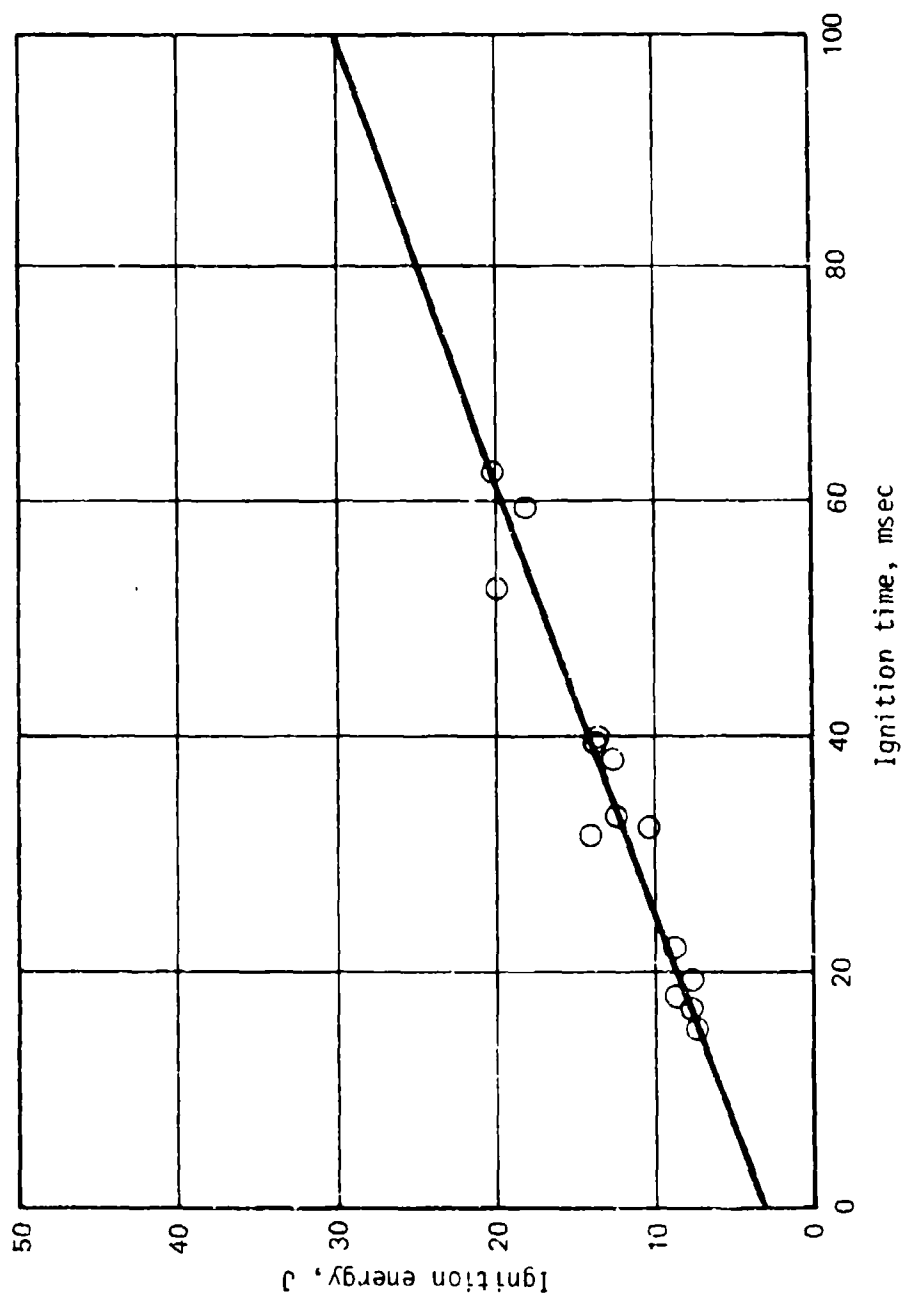


FIGURE 7 The ignition energy of Al-Mg/Cu₂O increases almost linearly with ignition time.

Further work is needed to test this procedure with other pyrotechnics and other igniter configurations. The use of a second degree polynomial to represent the relationship between ignition time and energy is arbitrary and with more experience it may be possible to develop a more realistic function.

THERMAL PROFILE AND REACTION CHARACTERIZATION - COMPUTATIONS AND EXPERIMENTS*

M. R. Birnbaum
C. T. Oien
C. L. Yang
Sandia National Laboratories
Livermore, CA

A. C. Munger
Mound Facility
Miamisburg, OH

ABSTRACT

This paper shows that heat powder output can be tailored to a desired level with the initial design and parameter studies being done by numerical analysis. Experiments can then refine the design and provide confirmation of the computations. The measurement of the physical constants required for computations and long term compatibility studies would continue as experimental endeavours.

*This work supported by Department of Energy.

THERMAL PROFILE AND REACTION CHARACTERIZATION - COMPUTATIONS AND EXPERIMENTS

Introduction

The focus of this work is on an experimental/numerical program to understand and tailor the use of Fe/KClO₄ as a heat source. Surface temperature measurements and calculations show good correlation both as to peak temperature and the time required to reach that temperature. This correspondence was demonstrated for two geometries and a powder mixture of 80/20* compacted to a density of 4000 Kg/M³. These results now permit one to use computations to do the initial design work and parameter studies required to produce desired temperature profiles for particular geometries. Then, experimental verification can be performed to finalize the design parameters. Density determinations were achieved via radiography as well as through the use of compaction curves determined for the powders of interest and direct measurements of the mass and volume of fabricated pellets.

Dynamic radiography proved to be of great value in allowing the viewing of heat powder movement inside its stainless steel shell during functioning. The dynamic radiography showed that the powder does not retain its geometry during the chemical reaction. Compared with the lengths of shell used and the time to achieve peak temperature the reaction time of the powder was quite short.

*This is by weight ratio

It must be noted that analysis does not solve all the problems, some parameters can only be determined experimentally. Long term compatibility, degradation with exposure to temperature and moisture and proper blending and drying conditions are some of the items requiring experimental determination. Also, computations depend on measured physical constants, such as thermal conductivity and calorific output, for their usefulness.

Geometries and Testing Procedure

Two geometrical configurations were considered (Figures 1 and 2). All of the tubes were fabricated from stainless steel. The closure disc was hermetically sealed to the tube via laser welding.

Each heat tube tested was instrumented with two or four Chromel-Alumel thermocouples. The thermocouple juncture was formed by twisting the wire pair together and placing the wire against the tube. The juncture was formed when a laser pulse welded the juncture to the heat tube wall. Thermocouple wire of 0.13 mm was used because a fast response was desired. The 0.13 mm diameter wire was then attached to 0.3 mm diameter standard pair thermocouple lead wire and attached to a differential amplifier for each channel of data collected.

The heat tube was mounted into a test stand that held the thermocouple leads secure and provided a mounting flange for the MAD-1031 ignitor that was used to initiate the heat powder charge.

The MAD-1031 ignitor (Figure 3) contained 38 mg of Titanium Subhydride (0.65)/Potassium Perchlorate in a 33/67 weight mixture ratio. This material generates hot gases and burning particulates that penetrate the thin closure disk of the heat tube and ignite its contents. The output of the ignitor is directed at the heat tube by the use of an orifice plug that is placed on top of the pyrotechnic charge in the ignitor. The MAD-1031 is a test device used by Mound facility as an inexpensive alternative to more costly hardware.

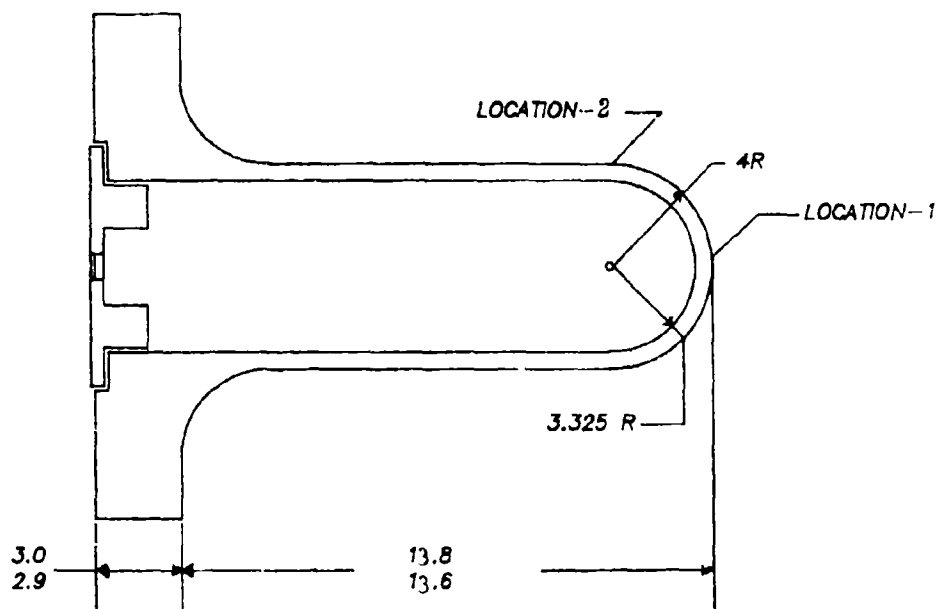


FIGURE 1 - LONG TUBE GEOMETRY, TEMPERATURE MEASUREMENT LOCATIONS NOTED

NOTE: ALL DIMENSIONS ARE IN mm

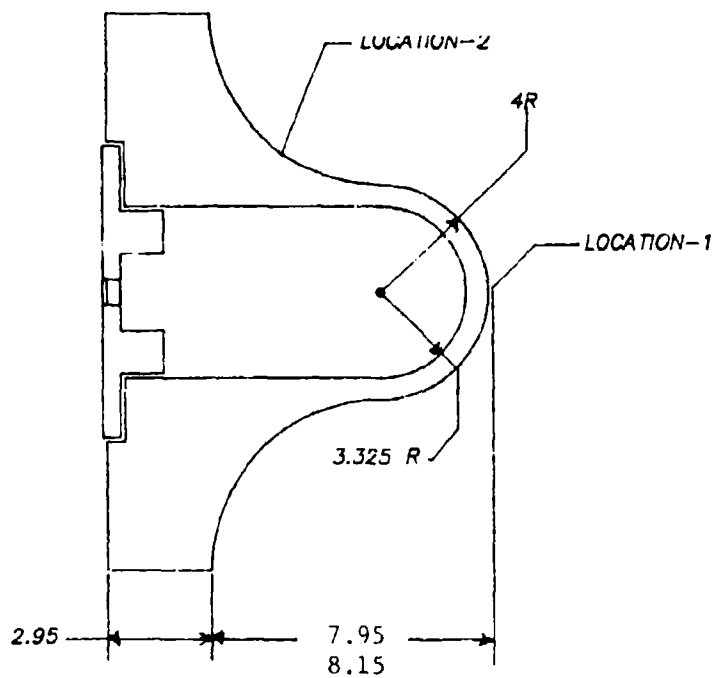
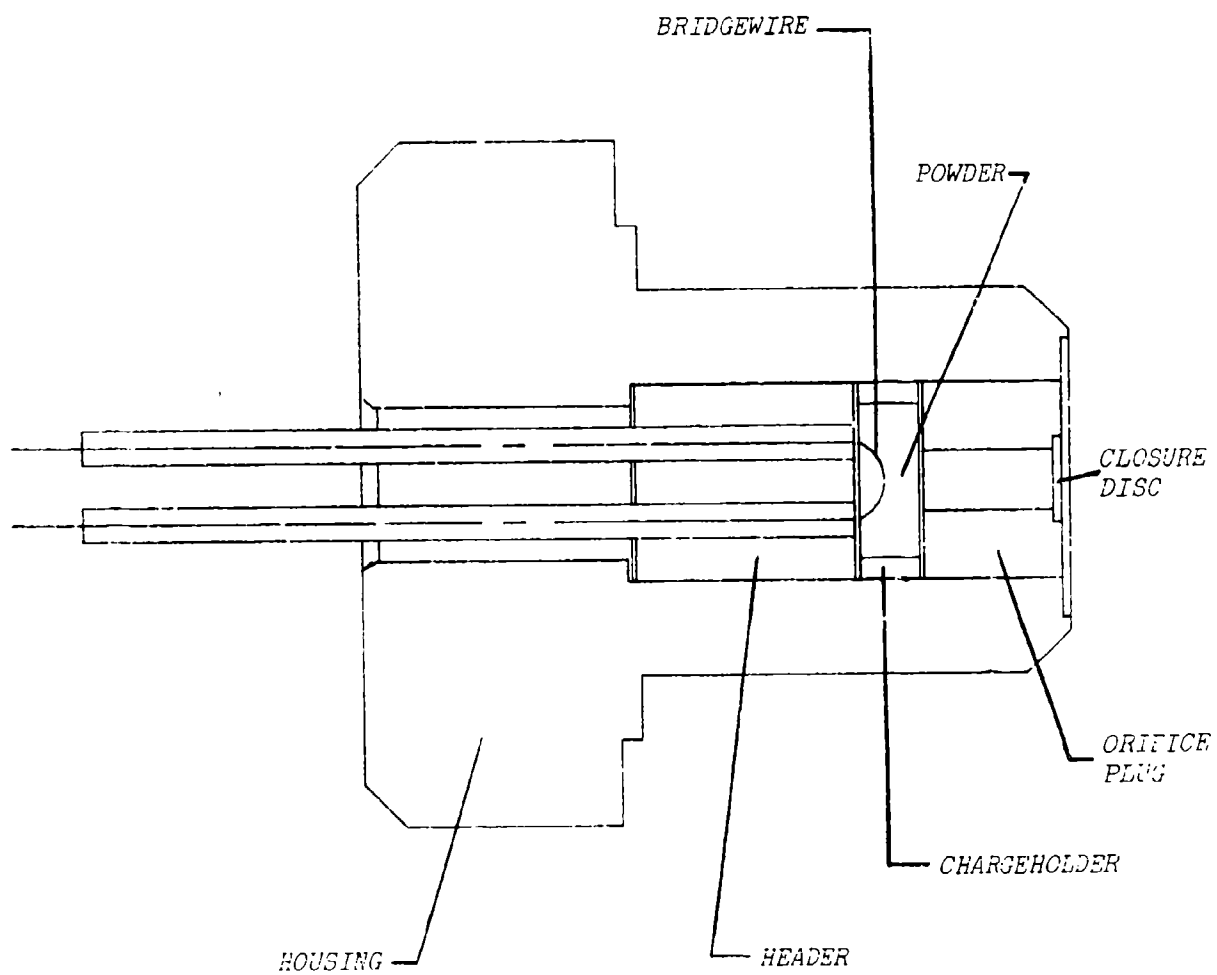


FIGURE 2 - SHORT TUBE GEOMETRY, TEMPERATURE MEASUREMENT LOCATIONS NOTED

NOTE: ALL DIMENSIONS ARE IN mm

FIGURE 3 - IGNITOR / MAD-1031



The MAD-1031 Ignitor was initiated with a 3.5 ampere constant current source. The records of the firing pulse were recorded as oscillographs and retained as part of the shot record. The application of the firing pulse to the ignitor was also used to trigger a Biomation 1015 Waveform Recorder. This unit has a four channel input capability and the thermocouple responses from the differential amplifiers were recorded digitally by the Biomation.

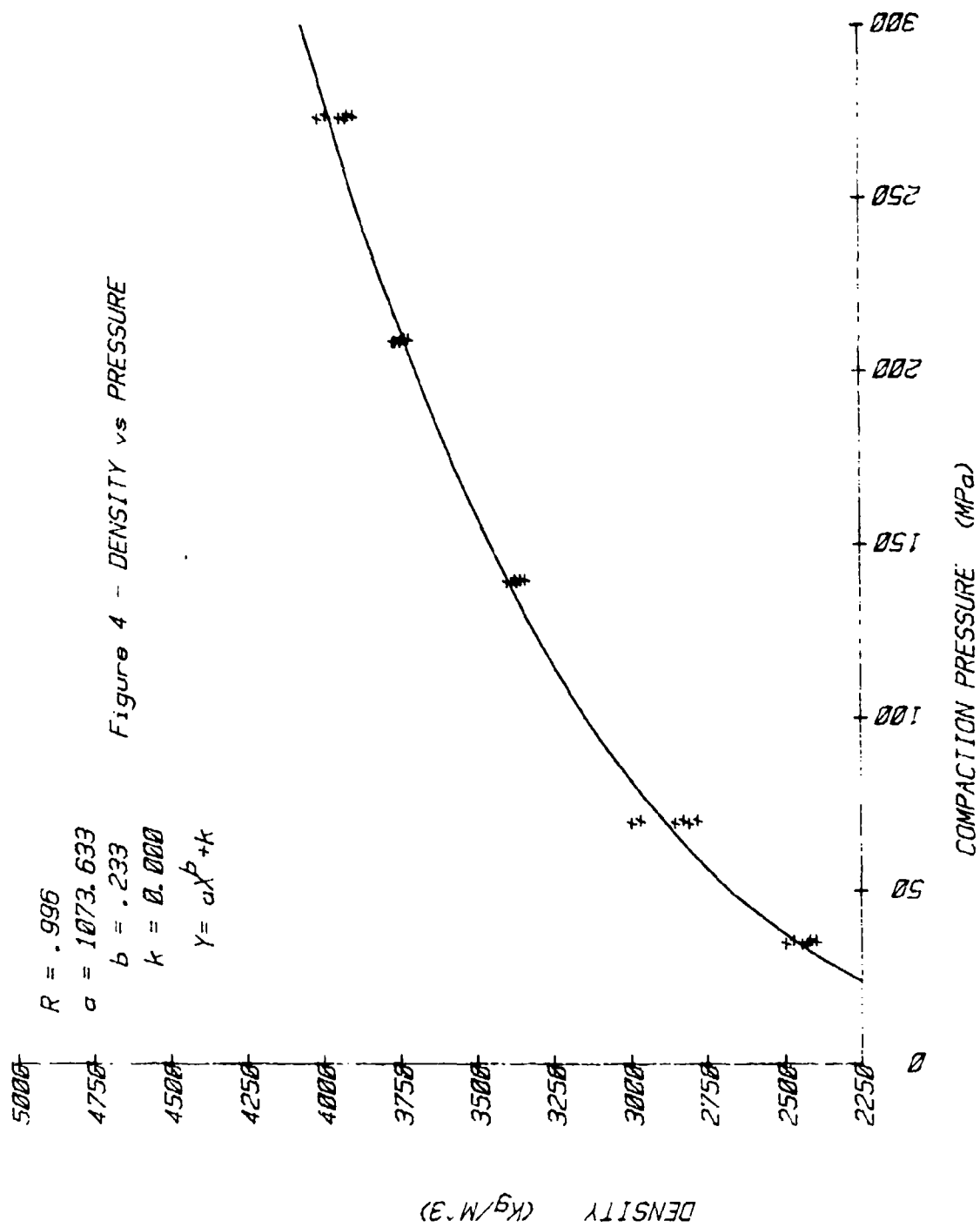
The digital data was obtained from the Biomation by use of a Hewlett-Packard model 9825 desk top computer. The data was then recorded on magnetic tape and transferred to a Hewlett-Packard model 9845 desk top computer. The voltage analogs were manipulated into temperature profiles for each thermocouple location and stored for further processing.

The stored analogs could be manipulated to obtain desired information such as peak temperatures, time to peak temperature and temperatures at various times after ignition of the heat powder.

Compaction Considerations

The density versus pressure relationship was derived for the blend mixture studied. The data for the density dependency was measured on a device that monitored the force applied to and transmitted through a pellet during compaction. When the two forces were equal, the assumption of uniform density was made. The pellets for this study had a mass of 12 mg, and were approximately 0.25 mm thick. An example of the derived relationship is shown in Figure 4.

When the pressure-density relationship is known, the density gradient can be evaluated using the same experimental set-up as above. The desired density variation in the loaded tube was $\pm 100 \text{ Kg/M}^3$. Various loading parameters such as compaction pressure and pressing height were tried and a Length to Diameter (L/D) ratio of 0.22 proved to be satisfactory. The tooling used to



develop the ratio was 4.3 mm in diameter, while the actual part was 6.7 mm in diameter. The L/D ratio was applied to the new diameter, which is common practice with high explosives, and the first part loaded. The results were not as expected, the density achieved was 10-15% lower than the target density of 4000 Kg/M³.

The experimental data was rerun and checked and the same results were obtained. By further experimentation, the correct L/D ratio was obtained. The pellet thickness was nearly the same as used in the preliminary determinations, but because the diameter was larger the L/D ratio was now 0.14. This ratio was found to be appropriate for densities of 3500 to 4500 Kg/M³. For the long tube (Figure 1), twelve pressings were employed and, for the short tube (Figure 2), seven powder pressings were used.

The inability to scale the loading process based upon the L/D ratio indicates that a two dimensional compaction model is needed to predict the behavior of a two component pyrotechnic material. The internal parameters of the mixture, such as particle size distribution and surface configuration, affect the compaction performance as much as the container parameters.

High Temperature Heat Powder Degradation

Differential scanning calorimetry (DSC) was employed to determine the exothermicity of the heat powder as a function of temperature. Heating rates affect this as is seen in Figure 5. Tubes with powders heated to 300°C and held there for 15 minutes were then cooled to ambient conditions and ignited. Temperature measurements on the exterior surface of the tube were significantly lower than unexposed specimens and this agrees with the DSC measurements. The test was then performed at 200°C and no degradation in output noted. The DSC results show an endotherm at ~300°C, indicating a phase change in the KClO₄ with a corresponding degradation in the performance of the powder due to high temperature exposure. This was not noted at 200°C exposure.

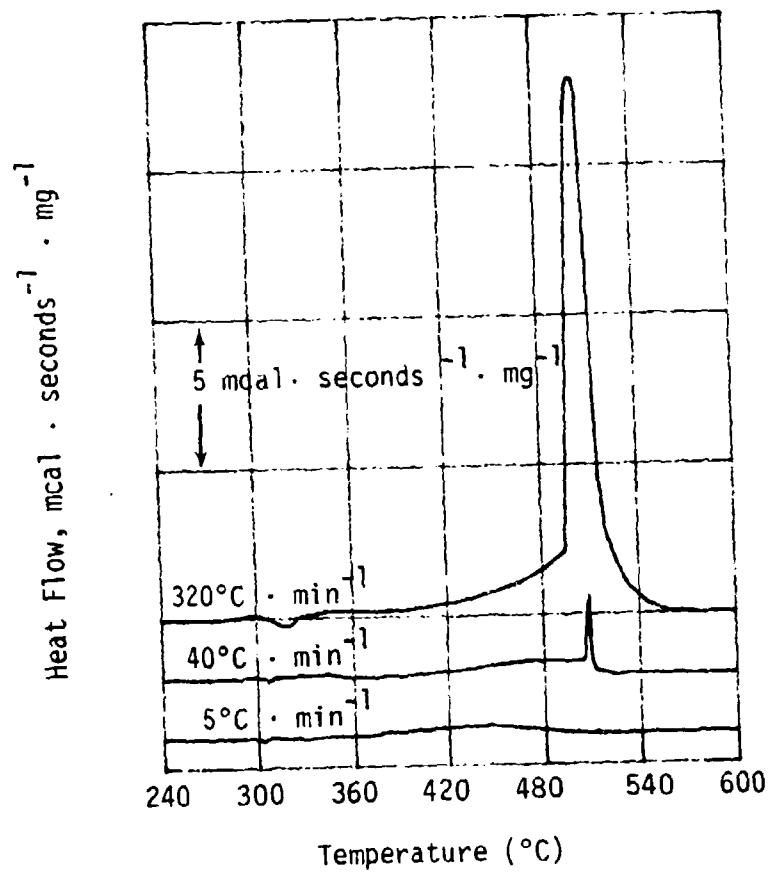


Figure 5 - Differential Scanning Calorimetry Traces for the Heat Powder as a Function of Heating Rate

Long Term Compatibility

Considerable effort has been expended to determine the best methods of handling these heat powders. Due to previous experiences with similar pyrotechnics and their susceptibility to corrosion, this became a point that acquired a great deal of attention. To avoid activation of the iron, it and the $KClO_4$ were not dried until after the heat powders had been blended and pressed into the required form. It was then dried at $75^{\circ}C$ for 7 days at a pressure of less than 0.05 Torr before the system was closed hermetically via laser welding.

It was realized that moisture combines with the free chlorides in the powder which might serve to start corrosion of the steel shell as well as reduce the output from the powder. To demonstrate this, powders were pressed into containers and then exposed to various humidities (0, 55 and 80% relative humidity) before they were sealed. These are stored at $65^{\circ}C$ with samples to be withdrawn over a period of 12 months and the calorific output of the powders examined for degradation. The metal surface that the powder was pressed against will also be examined for signs of corrosion or other anomalies. Samples two months old have given no evidence of problems.

Density Measurements

The pressed powder density and density variations are determined by recording the difference in X-ray transmittance between an empty unit and a loaded unit. Figure 6 is a schematic of the process for determining the pressed powder density variations. The heat tube is radiographed in the empty condition, loaded with heat powder and then reradiographed in the same orientation. These radiographs were scanned using a Joyce-Loebel densitometer line scanner model MK3CS. The difference between the scans of the empty

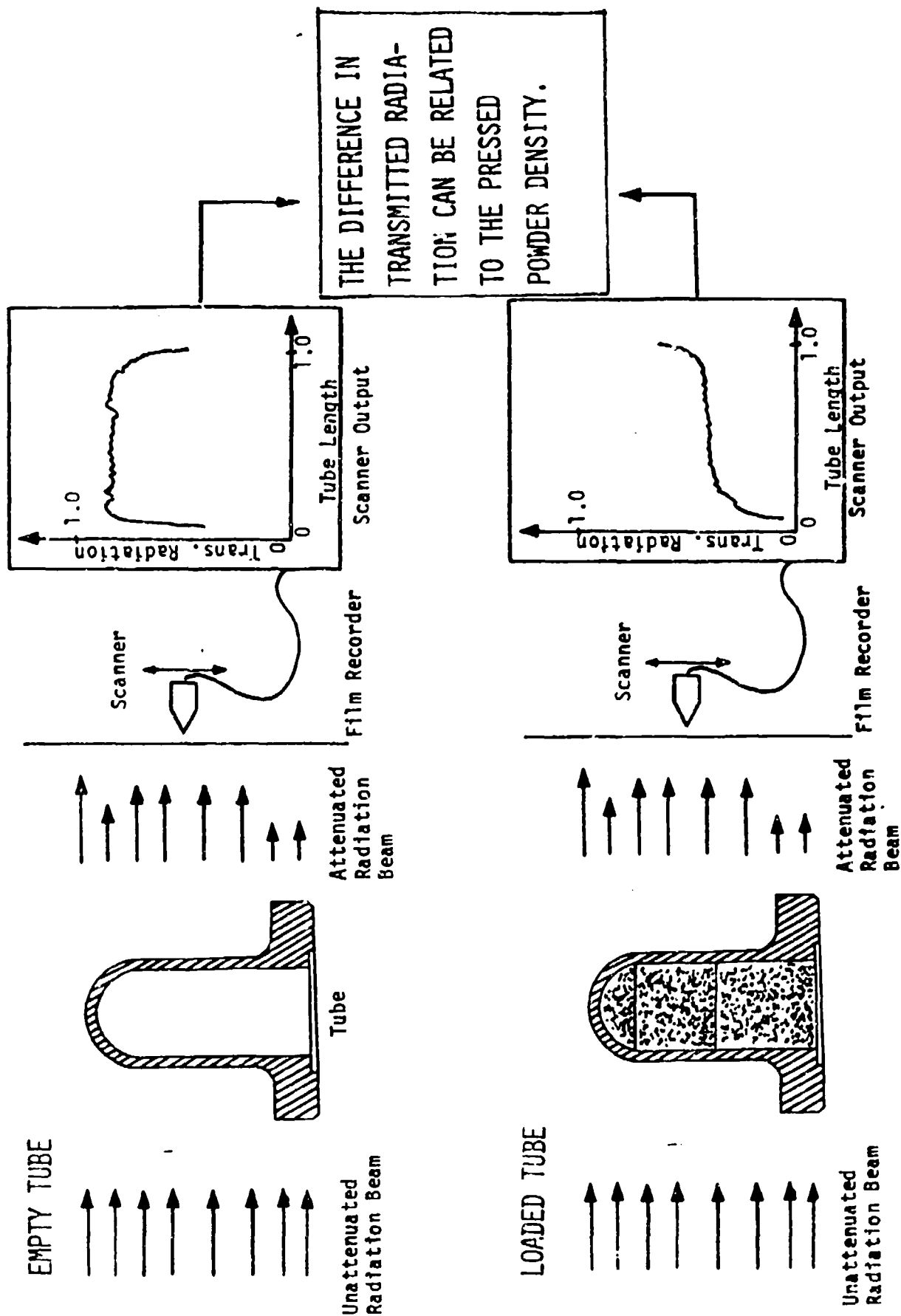


Figure 6 - Radiographic Procedure for Qualitative Determination of Pressed Powder Density Variation

and loaded heat tubes shows the pressed powder density variation. Quantitative densities can be obtained by radiographing a step wedge standard of known composition and density with both the empty and loaded tubes and having the standard also scanned with the densitometer. The empty and loaded tube densitometer scans can then be compared to the scans of the step wedge standard to yield an equivalent standard thickness for the empty and the loaded tubes. The difference in these equivalent thicknesses can then be related to the pressed powder density. Figure 7 is a schematic of this process.

There are several areas where one must be careful in order to yield very accurate results with these processes. The orientation of the tubes for radiography before and after loading is very critical. If the orientation of the tubes is not carefully duplicated for the empty and loaded configuration radiographs small variations in tube wall thickness can cause a several percent error in quantifying the pressed powder density. Also the x-ray energy, film type and film density as well as film processing procedures must be carefully controlled. To date we have analyzed tubes with these procedures and have established an accuracy on the pressed powder density determination at $\pm 3.5\%$ of nominal at 1σ confidence level. Figure 8 shows the pressed powder density as a function of tube axial position for two long tubes as determined with this method. Also plotted on this figure is the density at these same locations as determined from pressing data. The pressing data yields an average density for each pressing by noting the amount of powder pressed into a known volume. There are several areas where the accuracy of these radiographic measurements can be improved. These are where the data is reduced manually and also in the tube fixturing and scanning procedures. Plans are being developed to fully automate these areas to reduce the system type errors if the accuracy as established now is deemed insufficient.

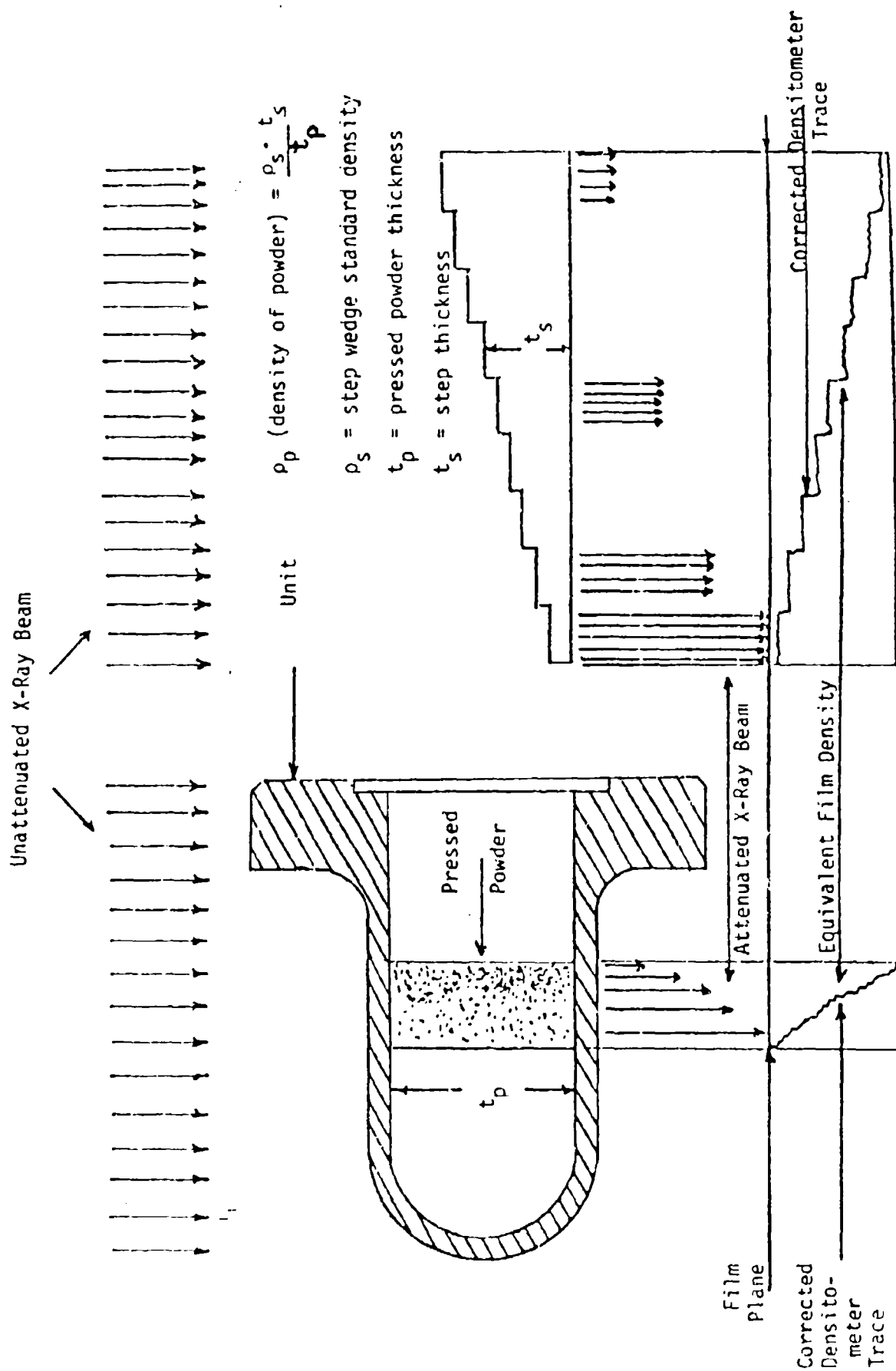


Figure 7 - Radiographic Procedure for Quantitative Pressed Powder Density Measurement

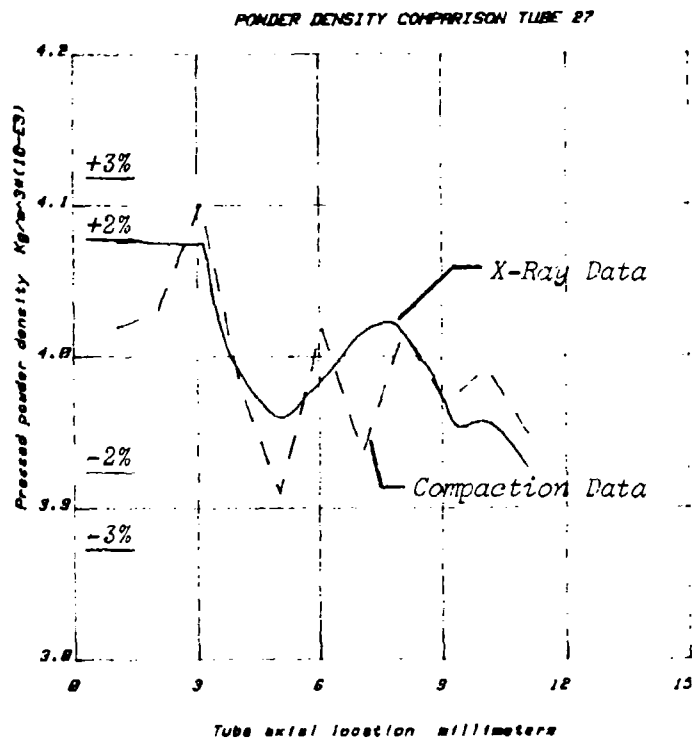
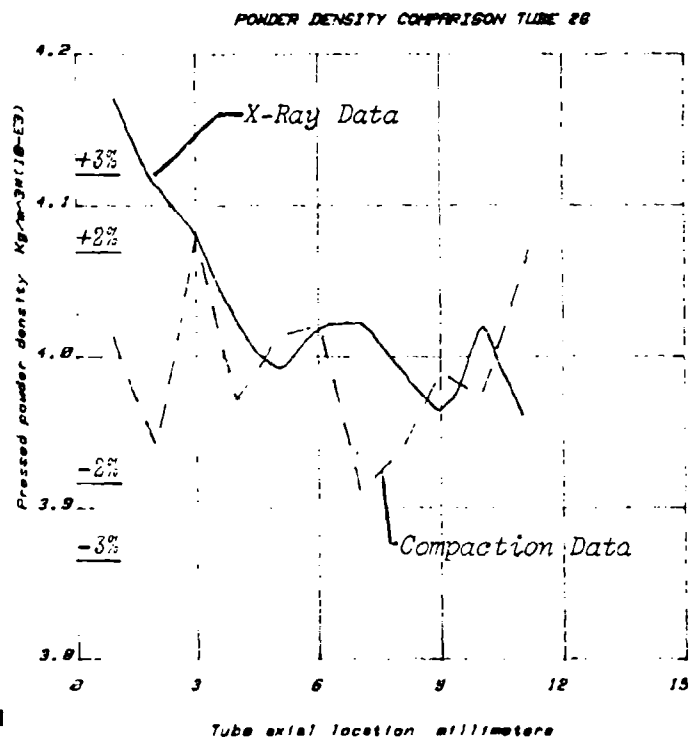


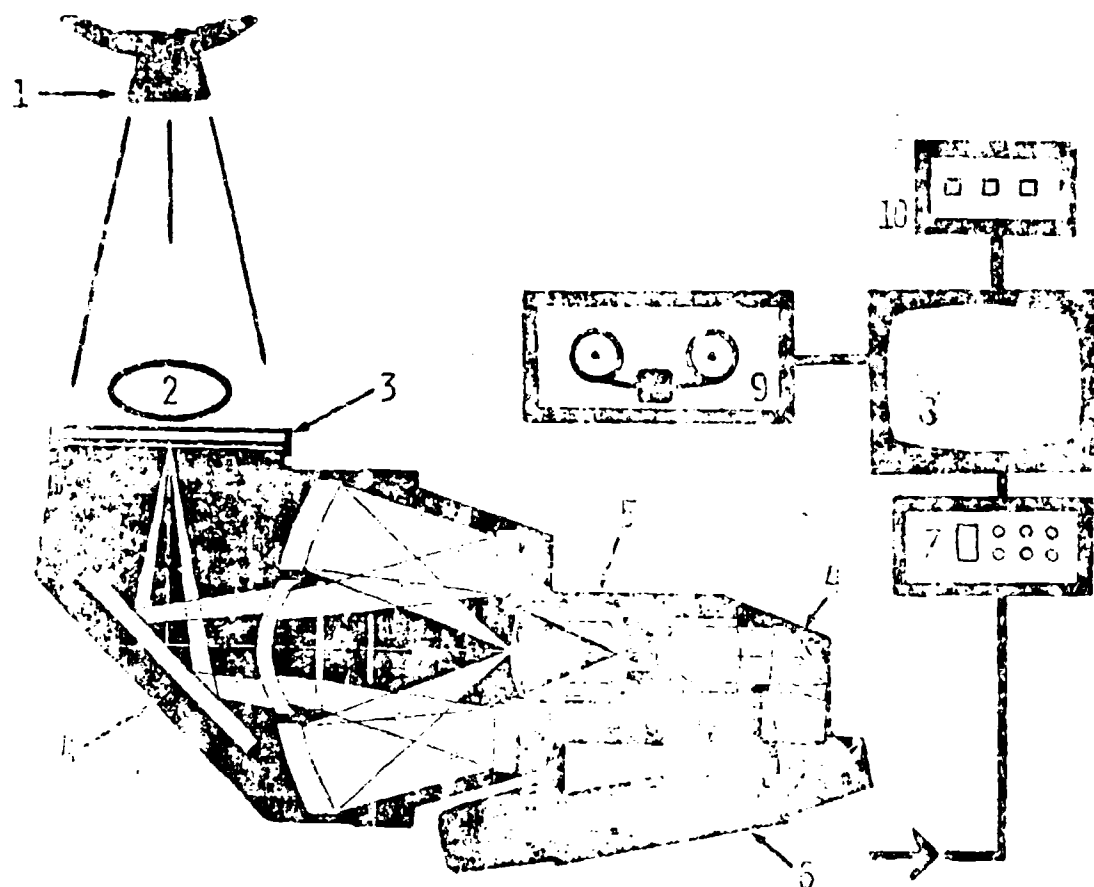
Figure 8 - Pressed Powder Density Measurements -
Radiographic Technique and Direct
Compaction Measurements

Dynamic Radiography

A noninteractive method for viewing a heat powder burn in a sealed tube was used to image the burn of the Fe/KClO_4 heat powder. The method involves the use of the Delcalix* electro-optical radiation imaging system shown in Figure 9. This system essentially converts the spatially modulated radiation beam, after it has passed through the object of interest, into light which is then amplified and converted to a video format. This recorded video signal is then analyzed frame by frame to determine the apparent powder burn rate. This is an apparent burn rate since the system records only a material density change caused by heating and not an actual heat transfer as a series of thermocouples might do. A sample of the frame by frame data available is shown in Figure 10. Four heat tubes were analyzed with this method and the data illustrates several points; (1) the burn characteristics of the four tubes were very similar, (2) the apparent burn for all tubes was complete in less than 0.7 seconds and (3) in all four tubes there was no significant change in the configuration of the reacted powder after the burn was complete. Thermocouples attached to the outside of the tubes indicated that the maximum temperature on the heat tubes occurred at about 3 seconds after initiation. This type of comparison indicates that the powder in the tube fully reacts in the first second and then tube and powder continue to evolve heat for several seconds. Table I lists the material movement front location in the heat tube versus time after initiation and the calculated rate at which this front moves for one of the tested tubes.

*Delcalix is a registered trademark of Old Delft Corporation of America, based in Holland.

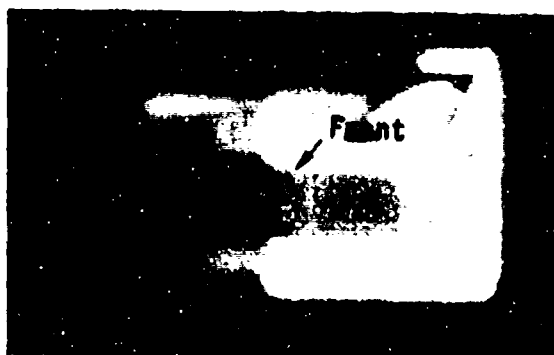
Figure 9 - Delcalix Electro-Optical Radiation Imaging System



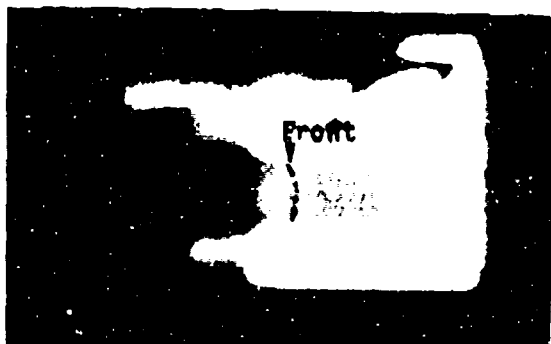
- 1 RADIOGRAPHIC SOURCE (NEUTRON OR X-RAY)
- 2 RADIOGRAPHIC OBJECT
- 3 SCINTILLATOR (32 CM DIAMETER)
- 4 LIGHT FOCUSING OPTICS
- 5 IMAGE INTENSIFIER TUBE
- 6 ICON TV CAMERA TUBE
- 7 DIGITAL IMAGE PROCESSOR
- 8 TV MONITOR
- 9 VIDEO TAPE RECORDER
- 10 DIGITAL STOP WATCH



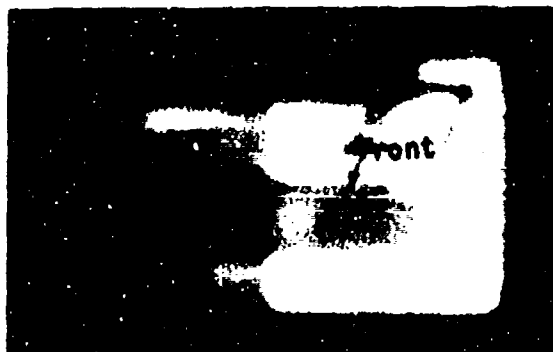
Time = 0.0 sec



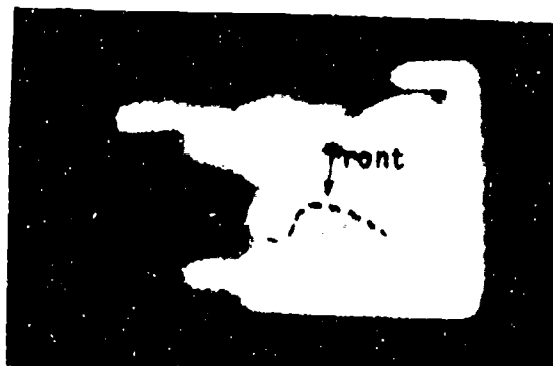
Time = 0.360 sec.



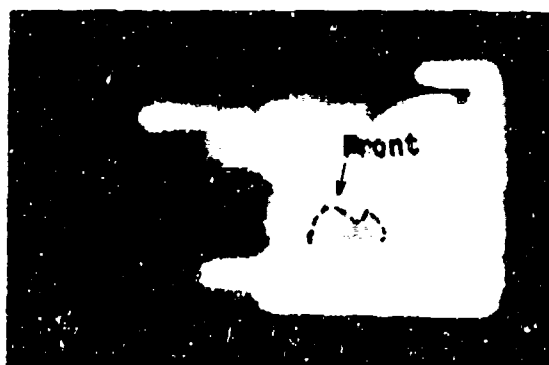
Time = 0.393 sec.



Time = 0.426 sec.



Time = 0.492 sec.



Time = 0.723 sec.

Figure 10. Material Movement Front Location

TABLE I

MATERIAL FRONT MOVEMENT RATE

Elapsed Time (s)	Delta Time (s)	Front Location (mm)	Movement Rate (mm/s)	Comments
0.0	0.0	0.0	0.0	Initial condition
0.360	0.360	8.60	23.9	This is the first indication of the material front movement. The first 8 mm of the heat tube is masked by fixtures.
0.393	0.033	9.60	33.3	This is one video frame later (1/30 sec.) The front appears to be moving uniformly.
0.426	0.033	10.90	36.4	This frame shows the first indication of non-uniform movement. It shows a small jet moving along the top of the tube.
0.459	0.033	11.4	15.2	This frame shows little front progression but rather a mixing behind the jet mentioned in the previous frame.
0.492	0.033	13.7	69.7	This frame shows the front movement jumping rapidly toward the tip of the heat tube.
0.525	0.033	14.9	36.4	This frame shows the front reaching the end of the heat tube and beginning to pull away from the walls.
0.624	0.099	14.9	0.0	This frame shows the material mixing near the tip of the heat tube.
0.723	0.099	14.9	0.0	Subsequent frames to this one show no movement of the heat powder indicating a complete burn.

Thermal Analysis

Calculations to determine temperature response to initiation of heat powder within the two tube configurations were made both to complement and extend experimental work. Several aspects of the process determined experimentally were considered important in terms of modelling. First, there is a discrete point of ignition. That is, the firing of an ignitor is required to start the burning of the heat powder. Consequently, a burn rate can be determined from thermocouple measurements along the tube. Total burn time can then be calculated from this rate and the tube length. Second, a known amount of energy is released. For the 80/20 Fe/KClO₄ mixture, 370 kcal/kg was measured in a Parr Bomb calorimeter. Third, voids develop within the volume occupied by the heat powder. Examination of this volume both during and after firing shows that these voids are neither of uniform size or distribution.

With these points in mind, a model was formulated based on the following assumptions:

- 1) Energy is released at a uniform rate simultaneously throughout the heat powder.
- 2) A 0.2 mm gap exists between the heat powder and the inner surface of the tube.
- 3) The tubes are fired in air with their axis in a horizontal position.
- 4) There is fixturing about the flange.
- 5) The ambient and initial temperatures are 25°C.

The geometrical information required for this analysis was generated using HEATMESH⁽¹⁾. This code takes a 2-dimensional description in the x-y plane and either rotates it about the x-axis to generate an axisymmetric geometry or projects it in the z-direction to produce a constant cross-section geometry. The meshes used for each of the two tube configurations are axisymmetric and shown in Figures 11 and 12.

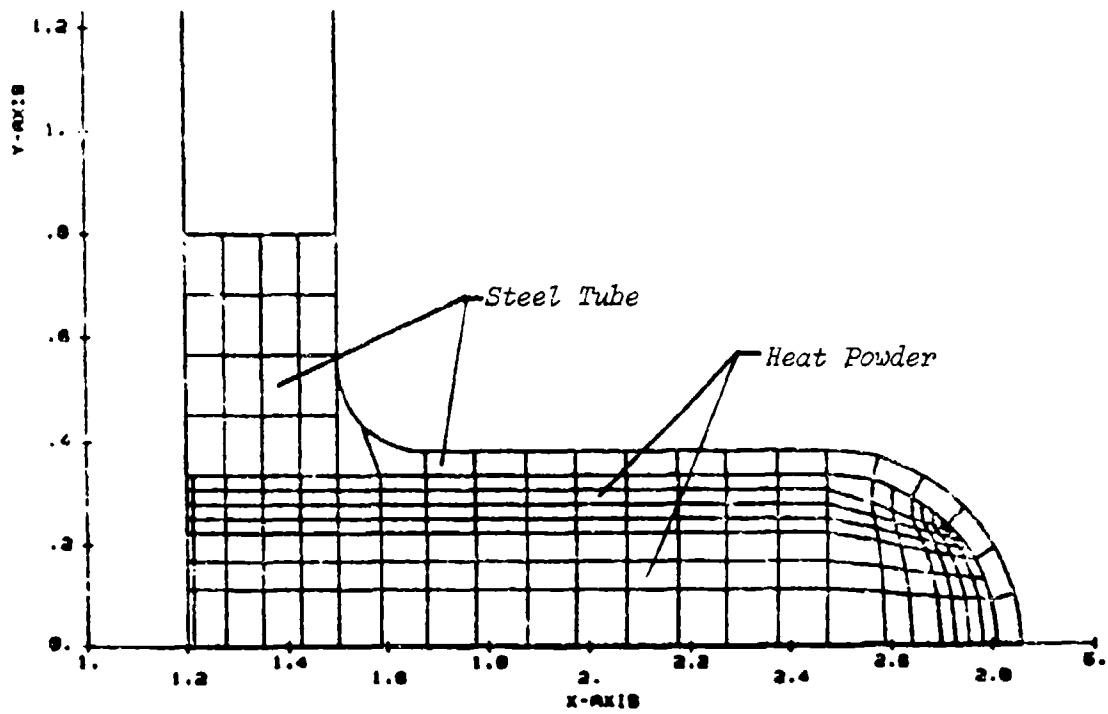


Figure 11 - Mesh Generation for Long Tube - Tube and Heat Powder

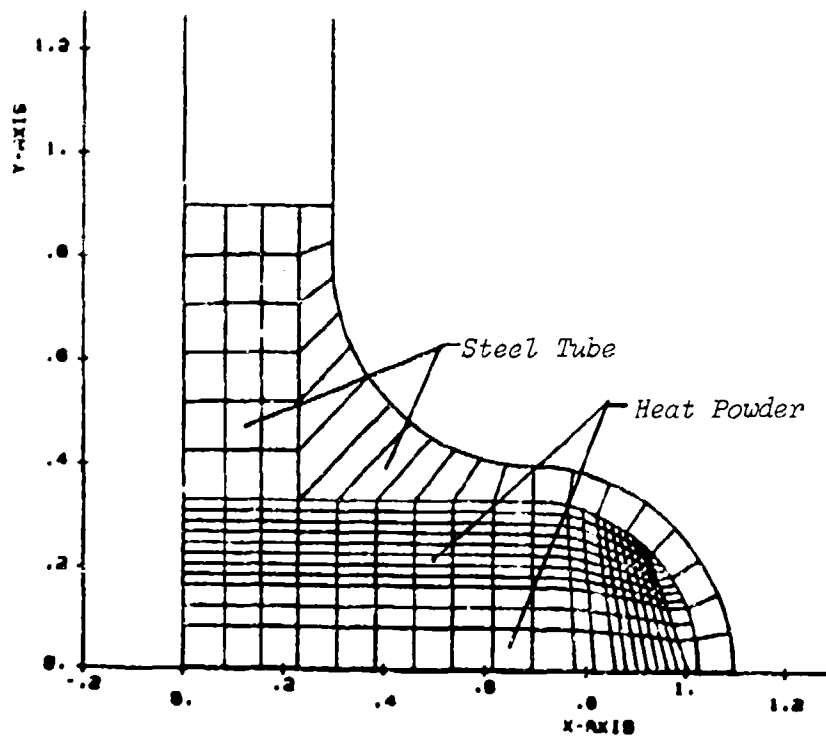


Figure 12 - Mesh Generation for Short Tube - Tube and Heat Powder

Output from HEATMESH was then used as input to SAHARA⁽²⁾, a multi-dimensional, finite difference heat transfer code which employs high speed successive relaxation solution techniques. It treats conduction, convection and radiation. Energy release in the heat powder was specified as a step function of energy rate over a time interval. The 0.2 mm gap was specified as a contact resistance. The convection and radiation boundary conditions applied only to the surface of the tube forward of the fixturing. Convection was described as a function of temperature differential. Initial conditions in the tube were 25°C and specific heat and thermal conductivity were treated as temperature dependent variable properties. The time intervals at which the code calculated temperatures were specified so that an appropriate number of calculations were made when large temperature gradients were seen. This ensured that the numerically calculated transient response closely followed the analytical solution. The convergence criterion was relaxed since the default value was overly conservative for this problem.

Stored output was conveniently examined using an interactive post processor. Plots of temperature as a function of both time and distance were generated and the temperature distribution over various portions of the tube was also examined. Although some transient effects are masked by modelling simultaneous heat release, peak temperatures and time to reach these temperatures match well. The development of any large voids during burning would significantly affect measured temperatures but cannot be taken into account in modelling because they are not predictable. However, the use and value of analysis lies in its ability to predict trends. This, then, makes it possible to formulate a heat powder mixture giving a desired thermal output in a specified geometrical constraint.

Computational and Experimental Results

Surface temperature versus time are plotted in Figures 13a and 13b for the long and short tubes respectively. The data is shown for two physical locations on the tube with the comparisons between the experiments and the calculations. Agreement between the computations and measurements is quite good, with respect to both the maximum temperature and the time required to reach that value.

The calculated maximum internal temperature is 1800°C which is above the melt temperature of iron (1535°C). Figures 14a and 14b show cross sections of fired tubes. The iron in the heat powder indicates melt and resolidification for both tube geometries. Additionally, the Delcalix data described earlier shows the reactants, including molten iron, moving and then resolidifying as the system cools. Thus, the experimental data support the computations.

The thermocouple results were used to measure an effective surface burn rate by noting the time at which each thermocouple first indicated a temperature rise. Most of the data showed a surface burn rate of between 50-70 mm/s. On some samples, however, the apparent burn rate was over 400 mm/s. This is believed due to the jetting actions from the ignitor when it fires into the tube. On several Delcalix tests, the jetting was observed and would account for a much more rapid initiation of the heat powder. Thermocouples inserted into the mixture indicated a burn rate of between 60-78 mm/s, in good agreement with the external thermocouple measurements.

Conclusions

The agreement between the experimental and numerical results demonstrate that analysis can be employed for initial design and parameters studies, assuming that one has the proper values for the needed physical constants. Thus, the heat powder can be tailored to produce a desired temperature profile

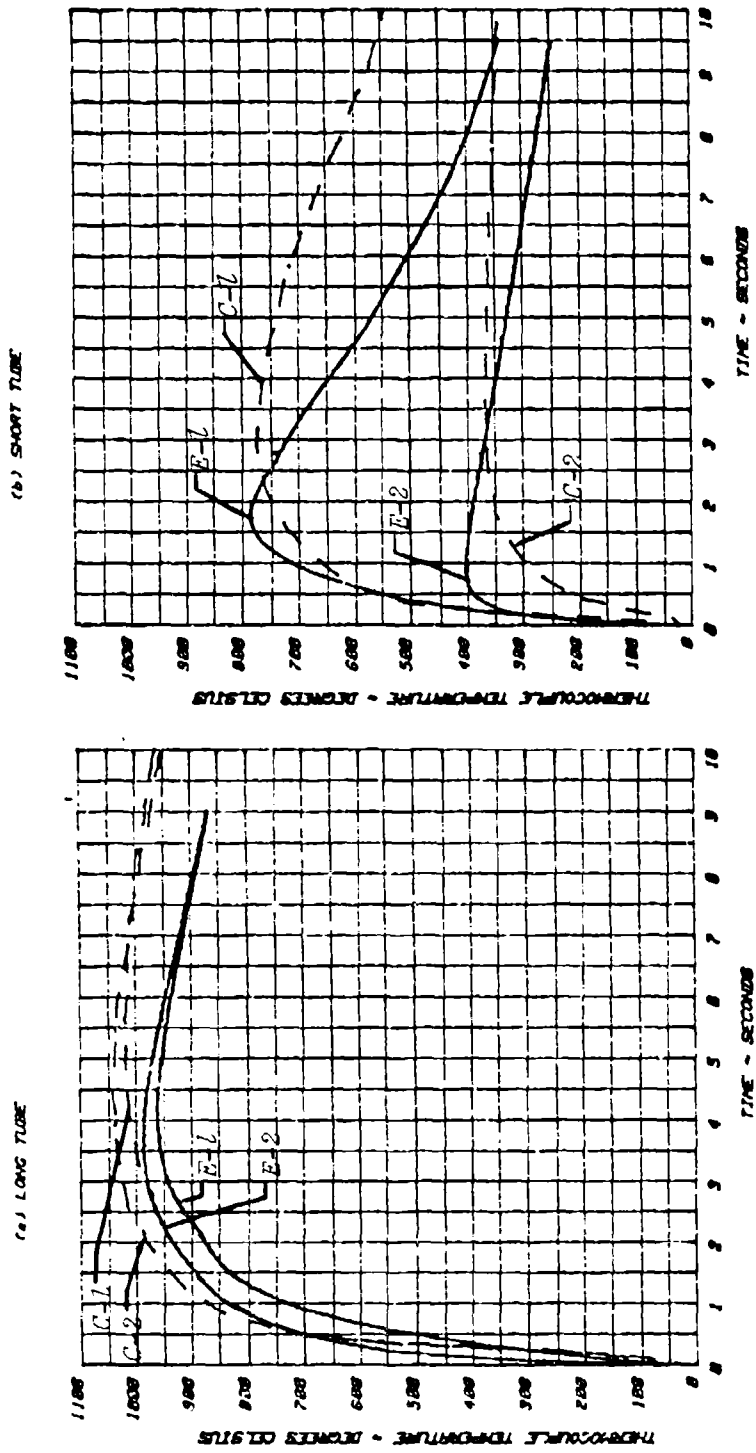


Figure 13 - Temperature versus Time - Calculation (C) and Experiment (E)



10. *Journal of the American Medical Association*, 2000; 283: 2686-2692.



1. *Chlorophyll a* (Chl *a*)

[illegible]

for various geometrical conditions. Numerical studies are then followed by the required number of experiments to refine and finalize the design.

Experimental studies are necessary to establish the long term capability of the heat powder and heat powder/tube interface. Similarly the powder handling and drying procedures must be determined by experimental techniques.

REFERENCES

1. V. K. Gabrielson, "HEATMESH 71: A Computer Code for Generating Geometrical Data for Studies of Heat Transfer in Axisymmetric Structures," Sandia Laboratories, Livermore, Unc., SCL-DR-720004, 1972.
2. V. K. Gabrielson, "SAHARA: A Multidimensional Heat-Transfer Computer Code (User's Manual)," Sandia Laboratories, Livermore, Unc., SCL-DR-720024, 1972.

ELECTROTHERMAL RESPONSE TESTING, A COMPONENT DEVELOPMENT TOOL

A. C. Munger

Mound Facility*
Miamisburg, Ohio

ABSTRACT

The Electrothermal Response Testing (ETR) technique used during the developmental stages of a component measures the thermal response of a bridgewire stimulated with a low level current pulse and thus uncovers flaws in component design or manufacturing procedures that no other NDT method can detect.

The use of the testing technique has uncovered component flaws that x-ray, resistance testing, or visual inspection has not detected. The process of powder compaction is not always predictable; for example, the calculated average density does not necessarily relate to the powder density at the bridgewire due to the length to diameter and side wall friction factors. ETR has detected these changes. Thermal extremes cause the powder to recompact or pull away from the bridgewire in certain component designs. This test has uncovered such conditions. Structural failure of a component may lead to an air gap forming around the bridgewire; this condition has also been detected.

The test is not a panacea and does not predict individual component performance, but rather will indicate the probability of nonfunctional units in a given population. An experienced operator can be invaluable as he can detect "nonclassical" response analogs which may be as important as the numeric data. This testing system has become an integral part of the component development cycle at Mound Facility.

*Mound Facility is operated by the Monsanto Research Corporation for the U. S. Department of Energy under Contract No. DE-AC04-76-DPO0053.

INTRODUCTION

Electrothermal Response Testing (ETR) as a nondestructive quality assurance tool can identify potential product faults. This technique has been instrumental in the development of an actuator for the Department of Energy. The data obtained from the ETR tests performed on this item resulted in the alteration of the component design and the modification of fabrication procedures.

BACKGROUND

Electrothermal Response testing in various forms dates back to the early 1960's. L. A. Rosenthal of Rutgers University and V. J. Minechelli of the Jet Propulsion Laboratory developed the technique of Transient Pulse Testing using a low level constant current source to pulse the bridgewire of an actuator. (1)

The following relationships were developed that describe the electrothermal behavior of a bridgewire as a result of a current pulse:

$$\theta = \Delta R / \alpha R_0 \quad (1)$$

where θ , the temperature rise above ambient of the bridgewire in $^{\circ}\text{C}$, is defined by the change in resistance of the bridgewire divided by the temperature coefficient of resistance of the bridgewire (TCR or α) times the cold resistance of the wire at a specific time along the response.

$$\gamma = \alpha I^2 R^2 / \Delta R \quad (2)$$

or by substituting Equation 1

$$\gamma = I^2 R / \theta \quad (3)$$

where γ is the thermal conductance across the bridgewire/powder interface, expressed in mW/°C, at a specific point in time along the response curve. The value of I is determined by the recorded value of the current pulse used to test the unit.

$$C_\theta = \alpha I^2 R^2 / \text{slope} \quad (4)$$

where C_θ is defined as the thermal capacity of the bridgewire and the surrounding powder, expressed in $\mu\text{J}/^\circ\text{C}$. The slope is determined by $\Delta R / \Delta t$ as shown in Figure 1.

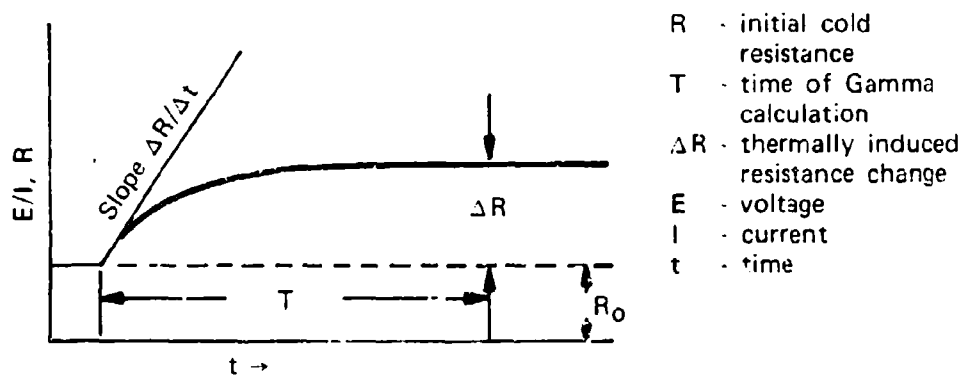


FIGURE 1 - Derivation of ETR parameters.

$$\tau = C_\theta / \gamma \quad (5)$$

where τ is the time constant for the heat transfer expressed in msec. This parameter is analogous to the time constant measured for a discharging capacitor.

Arnold Strasburg of Sandia Albuquerque used the above equations and added computer technology to the test. (2) The use of high-speed analog-to-digital converters and a small

computer enabled the rapid calculation of the response parameters. This new-found speed allowed the test to become an inline test to which all hot wire devices could be subjected. With this inline capability, the data base could be developed as a reference standard for evaluating actuator performance.

This testing technology is used at Mound Facility to evaluate the proposed fabrication processes on all new products and to evaluate component performance under environmental conditions.

CURRENT STATUS

The ETR test is currently used to evaluate pyrotechnic hot-wire devices. These components usually have a bridgewire resistance of 1Ω or greater and a TCR that is sufficiently large to facilitate their testing with low current levels.

The level of current used is generally kept below 1 A and is selected to keep the temperature rise of the bridgewire less than 100°C .

The duration of a square wave current pulse is usually limited to 100 msec.

When a fabrication process is under control, the ETR analog is a smooth and continuous trace and no special consideration need be taken. There are many times, however, when the traces become perturbed by some outside factor; the data as calculated by the computer are of little benefit when this occurs. The operator of the test equipment must be trained to observe the analogs that are displayed and report the occurrence of any unusual ETR response.

When the data from a day's run or some other unique grouping are analyzed, trends in the data may be observed. The primary data analyzed are the γ values. This value is sensitive to the powder compaction process. The magnitude of this value can also be affected by thermal environments that cause the powder column to reconsolidate or otherwise move. Generally, the test will not allow separation of good or bad units, but rather will identify a shift in the quality of the units within a given population.

ETR data that are considered acceptable will show a γ value of 4 to 10 times the magnitude of the γ value of a bare bridgewire. The standard deviation for any ETR data should be less than 10% of the average of the data. Certain types of components have been fabricated with standard deviations as low as 4%.

One caution must be made, however; that is, a loaded unit cannot be evaluated without first having the unloaded condition documented with ETR. This test is relative and the data can only be evaluated as changes induced by the loading process. This is also true when the effects of environmental exposure are evaluated. It is always wise to have "before" and "after" data for a given evaluation. Bare bridgewire data would be the lower limit of expected results for a loaded unit, although the unit would not be considered acceptable.

Discontinuous ETR analogs of bare bridgewires, although yielding no useful numeric data, can be very informative. A trained operator of the test can detect that certain responses are caused by mechanical movement of the bridgewire at the weld juncture.

The zone between the weld and the free wire of a welded bridgewire unit has very little strength. If this zone is

large it tends to peel (open up) when the wire is pulsed. The wire changes length as a result of electrical heating, and the resultant bowing causes the peeling moment. Bridgewires can be welded so that when they are pulsed, they will produce duplicate traces, pulse after pulse. Bridges that are of this type are preferred from the standpoint that whatever irregular traces develop after loading they can be attributed to the loading process. Typically the noise or trace perturbation caused by weld-zone peeling occurs in the first third of the thermal response. Figure 2A shows the effect of the peeling, and Figure 2B shows the same bridgewire when pulsed a second time.

Units that exhibit the peeling irregularities as bare bridgewires will probably show the same phenomenon as loaded units. This is caused by two factors. First the weak zone around the weld is not completely destroyed by one pulse, and the data taken after loading may be a continuation of this process. Secondly, the wire may be pushed down against the conductive feedthrough during loading. The induced movement of the wire during the test may disrupt this contact resistance.

Resistance changes caused by mechanical motion induced by bridgewire heating do not always result in discontinuous traces. The change may occur as a smooth function which is added to the thermal response analog. This can be detected when a second pulse is superimposed over the first; the resistance imbalance causes the second trace to be displaced upward from the first at the beginning of the response. See Figure 3. This displacement is usually caused by mechanically pushing the bridgewire down against the conductive post of the header. This condition has given rise to the practice of applying two separate pulses to each unit and performing the

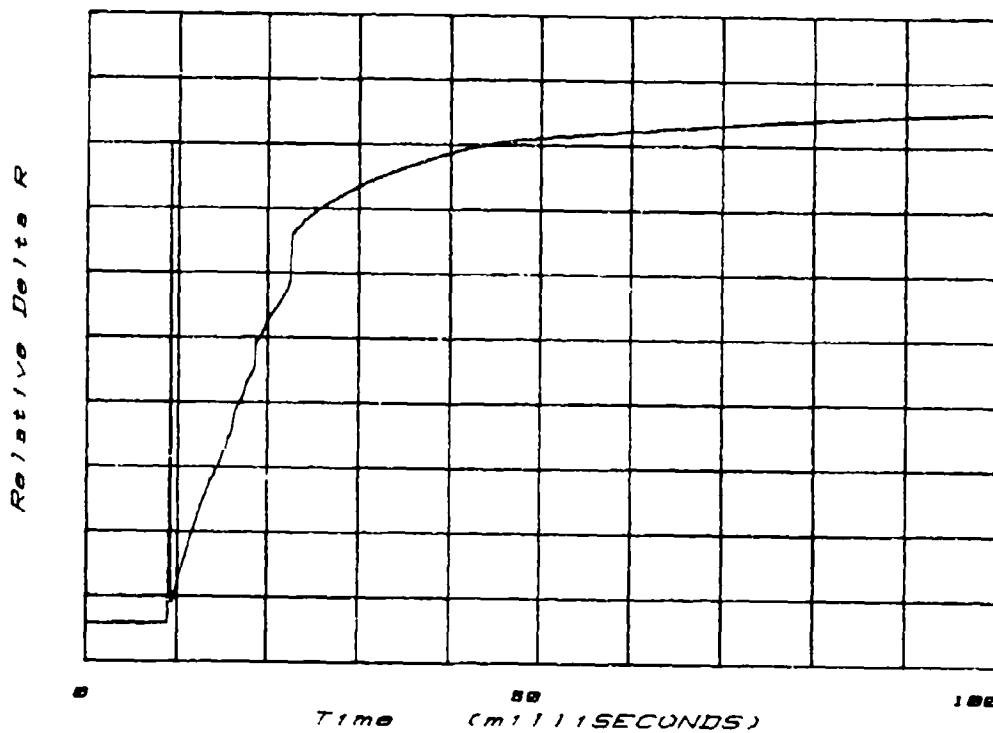


FIGURE 2A - ETR response with 1st pulse.

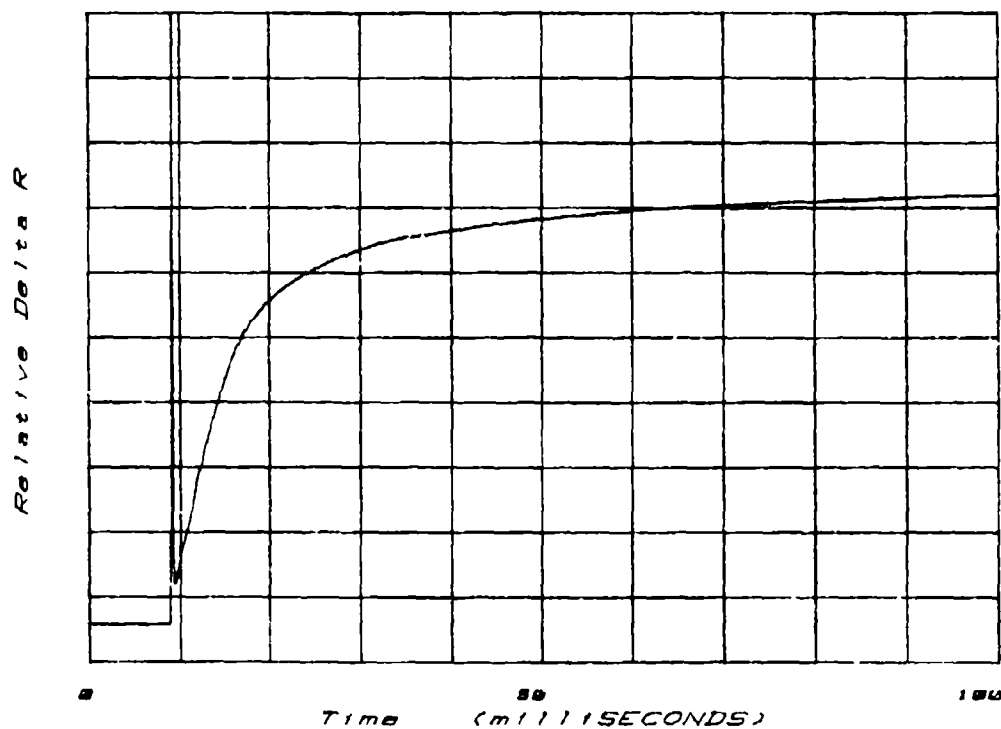


FIGURE 2B - ETR response with 2nd pulse.

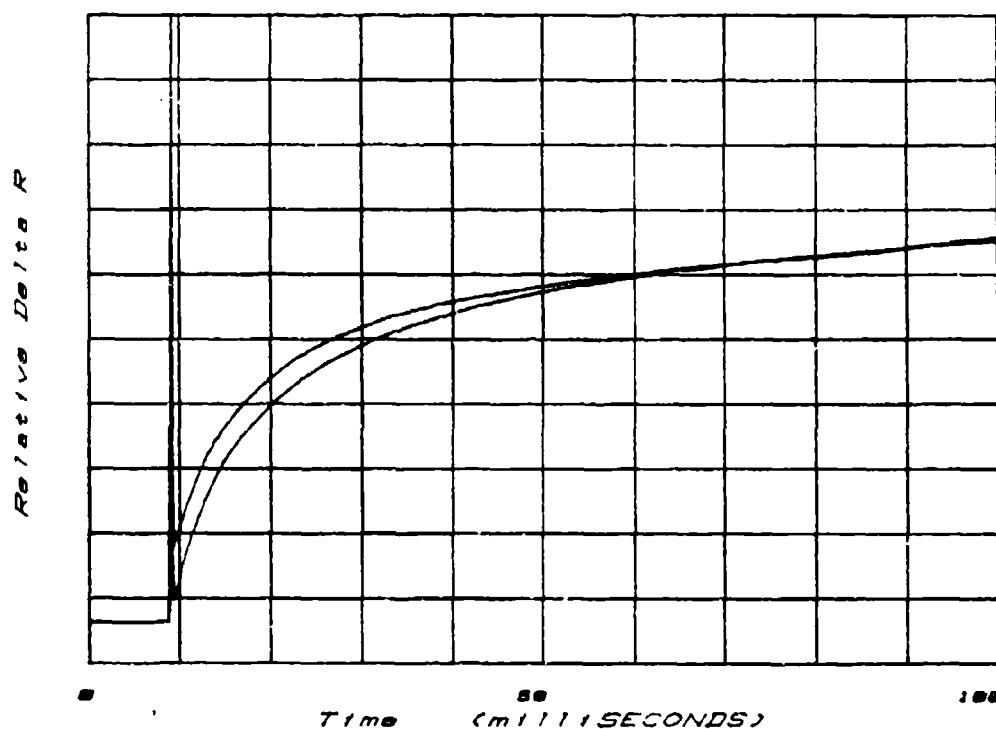


FIGURE 3 - Resistance change due to peeling.

calculations on the second pulse. The second pulse is not exaggerated by the resistance change as a result of mechanical movement, and a more accurate thermal resistance is calculated.

There have been specific cases where the ETR test has shown significant degradation to the powder/bridgewire interface. A test of development actuators was conducted where the units were subjected to very high G-loads. These units were ETR tested before and after the environmental test. The results after the test indicated that many of the units had suffered a complete loss of powder contact with the bridgewire. These data are shown in Table 1. This nondestructive

Table 1
THE EFFECTS OF HIGH G-LOADS ON ETR

Actuator	Bridge	Resistance (ohms)		γ (mW/K)	
		Before	After	Before	After
1	1	0.971	0.989	1.13	0.49
	0	1.025	1.072	1.38	0.43
2	1	0.982	0.984	2.01	0.59
	0	1.062	1.079	1.51	0.42
3	1	1.044	1.067	1.96	0.29
	0	1.051	1.077	1.82	0.66
4	1	0.997	1.005	1.80	1.67
	0	1.020	1.023	2.05	1.78
5	1	1.010	1.016	2.04	1.73
	0	1.016	1.056	1.70	2.05
6	1	1.046	1.057	1.43	0.98
	0	1.027	1.034	2.05	1.20

test suggested that the units would fail during destructive testing. The actuators were destructively tested, and more than 50% of them did fail.

The same effect of failure can be induced in some components by subjecting them to extreme thermal environments. The powder compact expands more than the surrounding chargeholder. This differential in expansion causes the powder to reconsolidate and pull away from the bridgewire when the unit is returned to ambient conditions. ETR data that reflect this fact have been recorded many times. See Table 2.

Table 2

THE EFFECTS OF THERMAL ENVIRONMENTS ON ETR

	<u>Tested</u> <u>Ohms</u>	<u>Y</u> <u>(mW/K)</u>	<u>Tested</u> <u>Ohms</u>	<u>Y</u> <u>(mW/K)</u>
	Actuator 7		Actuator 8	
Before	0.884	7.90	0.790	4.72
After	0.921	6.27	1.013	2.48
	Actuator 9			
Before	0.825	13.39	0.854	12.43
After	0.897	10.32	0.931	9.14

The effectiveness of the test is generally not readily apparent. A data base has to be established for each component, and then the data can be evaluated for trends that are indicative of a change.

When subtle changes in the data obtained are observed, the task of controlling a process has just begun. ETR γ values can go only up or down. The cause for the shift has to be deduced from the assembly records or by other NDT techniques. In some cases the cause is not found for months even with intensive investigation.

The cause of a shift in ETR data may be insignificant; however some have been found to be indicative of total process failure. Excessive friction in a loading tool that is being operated in a constant pressure mode has been detected and corrected before the tooling was broken or uncompacted units were fabricated.

The surface finish of the charge cavity into which the powder is compacted can affect the density of the powder at

the bridgewire and thus the γ value. (3) The density may also be affected by moisture or binders added to the powder. The tap density of the powder, affected by vibration and handling of the loading tool, dictates the final density achieved during the compaction cycle. All of these effects have been observed. Table 3 gives some examples.

The data derived from the ETR test are only as good as the analogs from which they are calculated. If repeatable smooth curves are obtained, the data should be very informative. The data obtained from perturbed analogs are of little value; however, the analogs themselves may be significant and assist in determining the cause of the abnormal response. The meaning of the perturbations in the first third of the trace was discussed earlier. In the last two-thirds of the trace, bridgewire decoupling may be observed. The responses may take many forms; a few are shown in Figures 4 through 7.

Table 3

THE EFFECTS OF CHARGE CAVITY FINISH
ON ETR USING WET AND DRY POWDER

<u>Group</u>	<u>Charge Holder Surface Finish (μM)</u>	<u>Powder Condition</u>	<u>γ (mW/k)</u>
A	<0.2	Dry	3.92
B	0.8 - 1.6	Dry	2.58
C	>3.2	Dry	2.97
D	<0.2	Wet	2.87

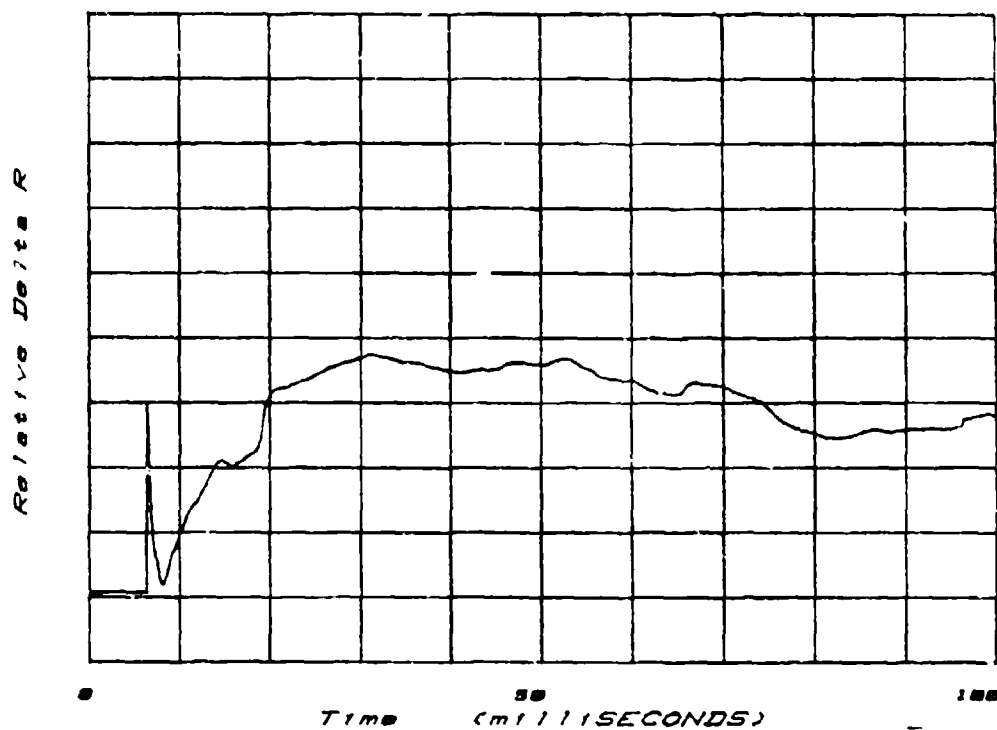


FIGURE 4 - Perturbed ETR responses.

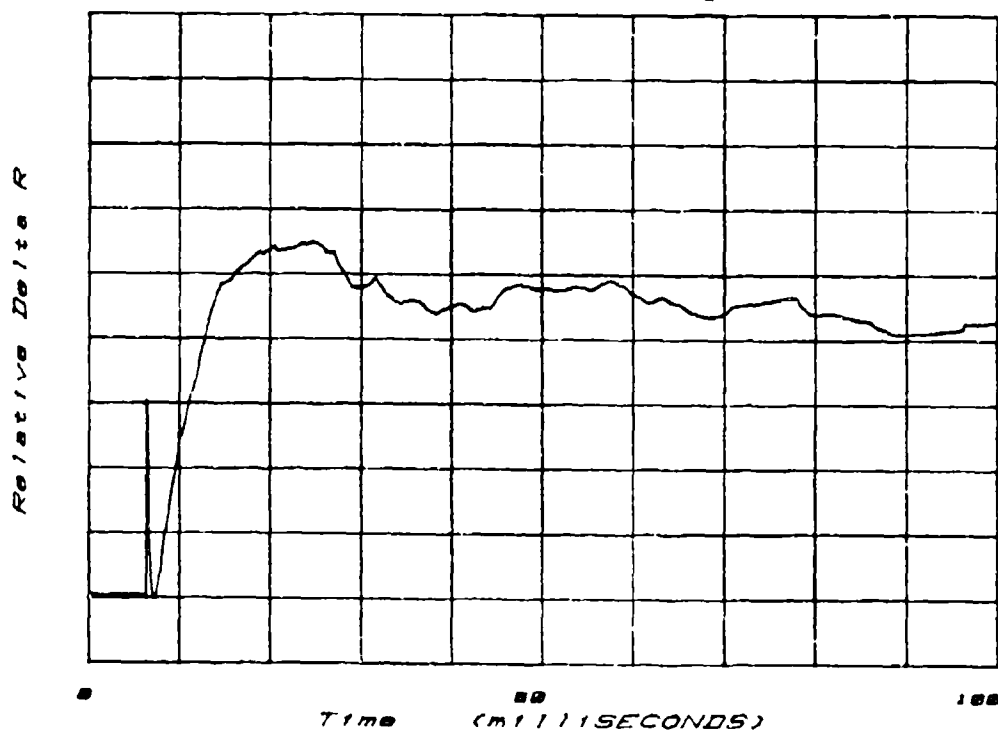


FIGURE 5 - Perturbed ETR responses.

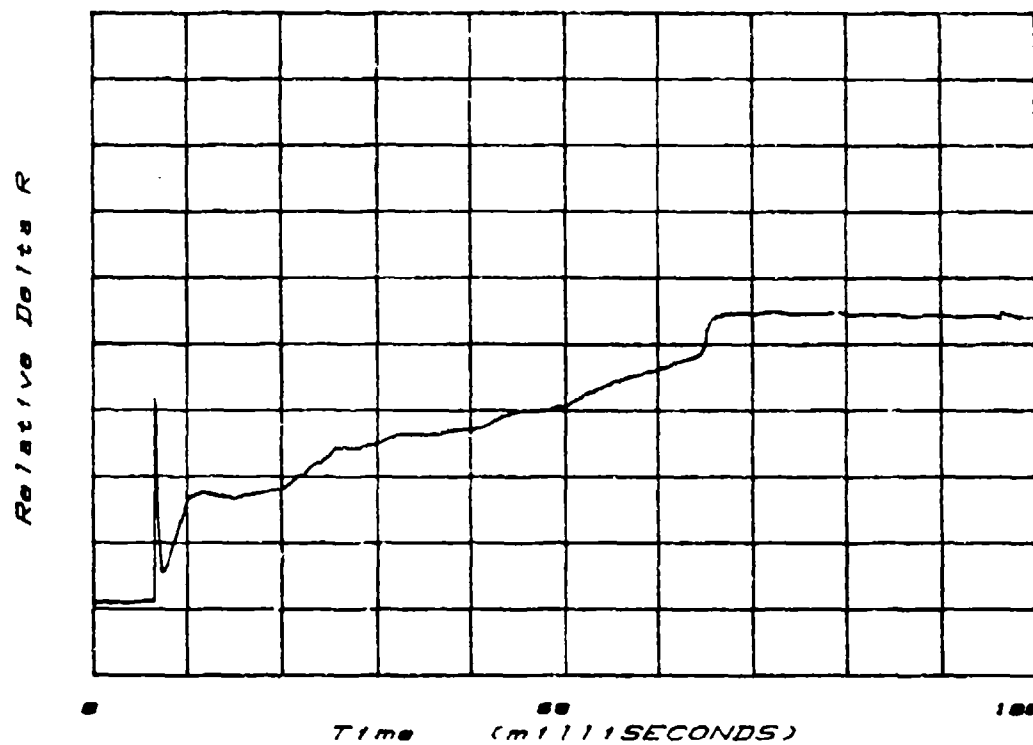


FIGURE 6 - Perturbed ETR responses.

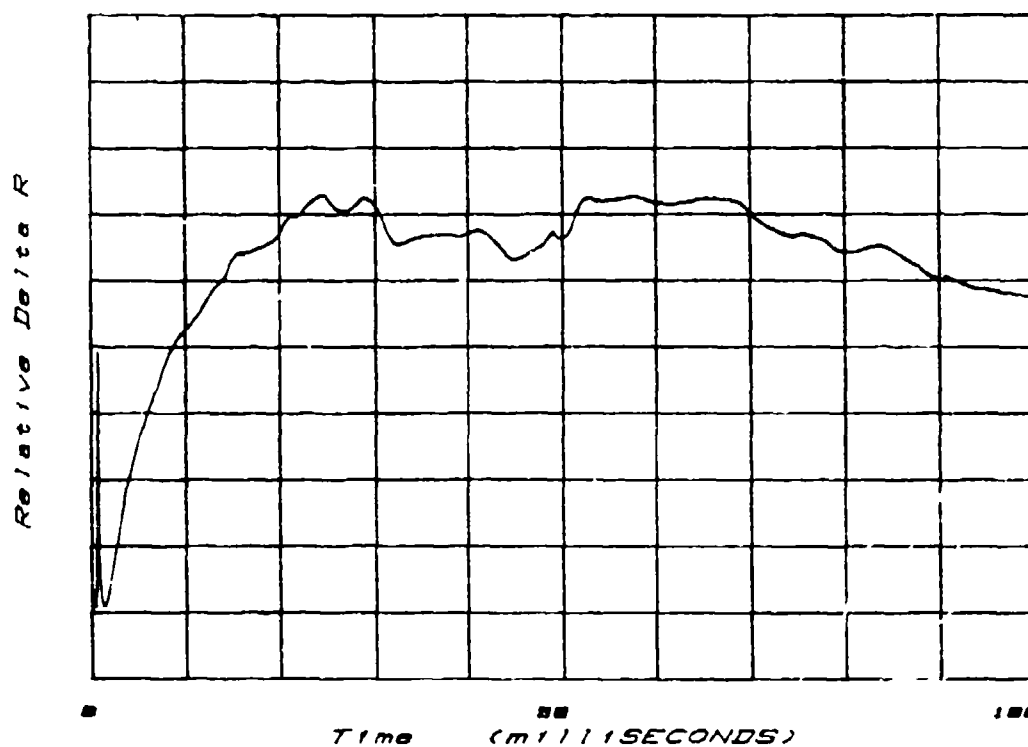


FIGURE 7 - Perturbed ETR responses.

The analog will show erratic heating and cooling or at least an erratic variation of the recorded resistance of the wire during the pulse application. Heating and cooling can be explained by flexing of the bridgewire and subsequent interaction with the powder compact. The wire can be visualized as residing in an irregular tunnel in the powder compact. The wire then interacts with this wall causing the random cooling of the wire.

Resistance changes can be induced in the same manner if the powder is electrically conductive. The resistance in this case is purely electrical and has nothing to do with the heating and cooling of the wire. An example of this type of response is shown in Figure 8. The drop in the observed resistance is so large that the last half of the analog is lost off scale of the recording device.

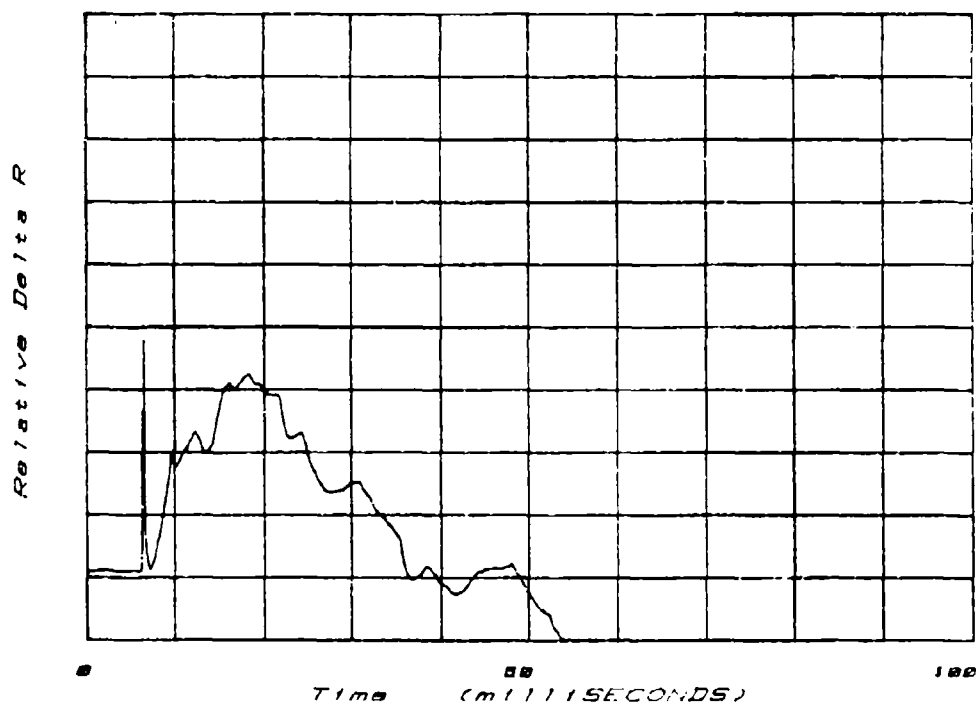


FIGURE 8 - Severe resistance depression.

The tunnel or gap at the powder/bridgewire interface can be the result of flexing of the wire caused by environmental temperature extremes, or by flexing of the wire caused by excessive temperature induced by the ETR test. Mechanical and thermal environment exposure may cause shifting of the powder compact causing a gap to be created at the bridgewire interface. The gap may be large enough that the bridgewire does not interact with the powder when pulsed at the current level required to achieve the nominal 80-100°C temperature rise. When this occurs, a smooth response will be obtained, but the γ values will be significantly lower than a normal unit. In some cases where perturbed traces are being obtained, a lowering of the pulse current will yield smooth traces. Gaps of approximately 0.15 mm or larger tend to yield data comparable to the data obtained from bare bridgewires. Bridgewires of loaded actuators that exhibit this condition may fail to fire as was discussed earlier.

The location of a bridgewire in the powder compact affects the ETR behavior. A bridgewire that is placed tightly against the supporting substrate may not exhibit an ETR response until the energy input is sufficient to overcome the heat-sinking ability of the substrate. In some cases this may be 400 mA or more. The practice of bowing the bridgewire away from the substrate or placing a cavity under the wire causes the response to occur at a lower current level and lowers the γ value. These data and practice can be related to all-fire and no-fire levels for the component.

A question that is encountered many times is "Are the data, in particular γ , independent of the current used to pulse the bridgewire?" Equation 2 shows that $I^2 R^2$ (the resistive heating function) is divided by ΔR (the change in resistance caused by the heating), or Equation 3 shows $I^2 R$ divided

by θ (the temperature change). It is clear that, mathematically, the γ is independent of the test current as long as the TCR is constant. The TCR is known to be constant for most bridgewire alloys up to 100°C. This known relationship is a good reason to limit the upper extremes of temperature experienced by the bridgewire during testing. Data taken from an experimental component that was pulsed with 300 to 600 mA are shown in Table 4. The gamma values vary approximately 4% over the range of current used. The variation of three runs at the same current was about 1%. Other components exhibited up to an 11% change over similar ranges. When the variation of the test current is 100 mA or less, the bias introduced to the data should be inconsequential.

Table 4
THE EFFECTS OF VARIED CURRENTS ON ETR DATA

Milliamperes						
<u>Tested</u>	300	400	500	600	500	500
	γ (mW/K)					
\bar{X}	1.91	1.96	1.97	1.99	1.95	1.97
Sigma	0.16	0.16	0.15	0.15	0.16	0.19
	Tested Ohms					
\bar{X}	0.988	0.989	0.988	0.989	0.989	0.989
Sigma	0.027	0.026	0.028	0.027	0.027	0.027

CONCLUSIONS

The ETR test is not a panacea for detecting all defective components. This test is but one more NDT technique that can be used to evaluate the quality of the components

produced. The test can help identify types of environments that are degrading, or help to evaluate component changes that affect powder density. The variability of loading and weighing processes may be quantified and process changes that affect loading and subsequent compact stability can be evaluated.

The testing technique can be used to monitor the daily variance of an established process. The test can indicate units that are different from the normal, and generally when these "sports" are removed from a given population, the statistical performance of the population is improved. The ignition time and the total function time of an actuator or ignitor is dependent upon the heat transfer from the bridgewire to the pyrotechnic. If this variability is reduced through the use of ETR, generally the variance of the function time is reduced.

The rare occurrence is when the data indicate that a unit or group of units is so severely degraded that the units will fail to function properly. Units of this type have been found and eliminated from the production run at the point of detection, thus avoiding the expenditure of needless labor.

BIBLIOGRAPHY

1. L. A. Rosenthal and V. J. Menichelli, Nondestructive Testing of Insensitive Electroexplosive Devices by Transient Techniques, Technical Report 32-1494, Jet Propulsion Laboratory California Institute of Technology.
2. R. C. Strasburg, Methodology for Computation of Interface Parameters of a Hot-Wire Explosive Device from the Electrothermal Response Analog, SLA-73-1034, Sandia Laboratories, April 1974.

3. J. R. Brinkman, A. C. Munger, N. J. Seubert, "Effect of Powder Compaction Variables on the Performance of a Pyrotechnic Ignitor," Proceedings of 6th International Pyrotechnic seminar, July 17-21, 1978.